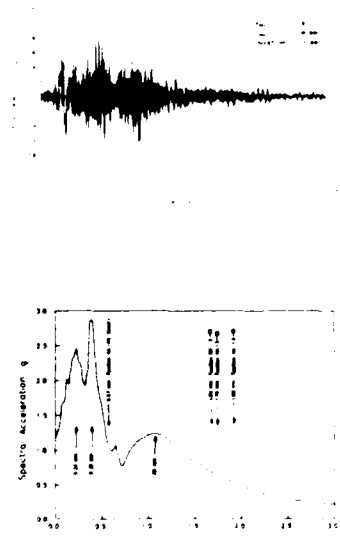


AD-A268 785



US Army Corps  
of Engineers



TECHNICAL REPORT GL-91-22



## SEISMIC STABILITY EVALUATION OF RIRIE DAM AND RESERVOIR PROJECT

### Report 2 STABILITY CALCULATIONS, ANALYSIS, AND EVALUATION

#### Volume II: Appendices A Through E

by

D. W. Sykora, J. P. Koester, M. E. Hynes

Geotechnical Laboratory

DEPARTMENT OF THE ARMY  
Waterways Experiment Station, Corps of Engineers  
3909 Halls Ferry Road, Vicksburg, Mississippi 39180-6199

DTIC  
SELECTED  
AUG 27 1993  
SPD



September 1991

Report 2 of a Series

Approved for Public Release; Distribution Unlimited

93-20034



93 820 062

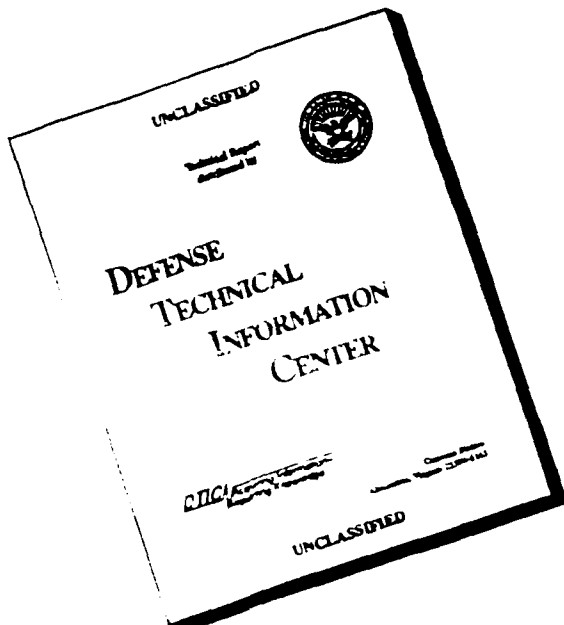
Prepared for US Army Engineer District, Walla Walla  
Walla Walla, Washington 99362-9265

**Destroy this report when no longer needed. Do not return  
it to the originator.**

**The findings in this report are not to be construed as an official  
Department of the Army position unless so designated  
by other authorized documents.**

**The contents of this report are not to be used for  
advertising, publication, or promotional purposes.  
Citation of trade names does not constitute an  
official endorsement or approval of the use of  
such commercial products.**

# **DISCLAIMER NOTICE**



**THIS DOCUMENT IS BEST  
QUALITY AVAILABLE. THE COPY  
FURNISHED TO DTIC CONTAINED  
A SIGNIFICANT NUMBER OF  
PAGES WHICH DO NOT  
REPRODUCE LEGIBLY.**

## CONTENTS

	<u>Page</u>
APPENDIX A: STABILITY ANALYSIS OF RIRIE DAM (Azzouz and Baligh 1989a).....	A1
APPENDIX B: THREE DIMENSIONAL STABILITY ANALYSIS OF RIRIE DAM (Azzouz and Baligh 1989b).....	B1
APPENDIX C: STATIC ANALYSIS OF RIRIE DAM (Woodward-Clyde Consultants 1988).....	C1
APPENDIX D: DYNAMIC RESPONSE ANALYSIS OF RIRIE DAM (Woodward-Clyde Consultants 1989).....	D1
APPENDIX E: PREDICTION OF THE SEISMIC RESPONSE OF THE RIRIE DAM USING SIMPLIFIED NONLINEAR SHEAR BEAM MODELS (Dakoulas 1989a).....	E1

DTIC QUALITY INSPECTED 3

Accession For	
NTIS GRA&I	<input checked="" type="checkbox"/>
DTIC TAB	<input type="checkbox"/>
Unannounced	<input type="checkbox"/>
Justification	
By _____ Distribution/ _____	
Availability Codes Avail and/or	
Dist	Special
A-1	

**APPENDIX A: STABILITY ANALYSIS OF RIRIE DAM**  
**(Azzouz and Baligh 1989a)**

**STABILITY ANALYSES OF RIRIE DAM**

**For**

**U. S. Army Corps of Engineers  
Waterways Experiment Station  
Vicksburg, MS 39180-0631  
(Purchase Order DACW39-86-P-0607)**

**By**

**Amr S. Azzouz, and  
Mohsen M. Baligh  
Consulting Geotechnical Engineers  
Lexington, MA 02173**

**May, 1989**

## SUMMARY

In September, 1988, Mohsen Baligh & Associates (MBA) were contracted by the U. S. Army Corps of Engineers (ACE), Waterways Experiment Station to undertake a study aimed at the evaluation of the stability of the Ririe Dam in Idaho. The work is to be performed in two phases, the first of which is devoted to two-dimensional (2D) analyses, while the second is concerned with the investigation of the influence of the three-dimensional effects on the overall stability of the dam. This report presents results of Phase I of the program.

An extensive number of effective stress stability analyses involving both circular and non-circular failure surfaces were performed using three different methods of stability analyses, namely the modified Bishop, Spencer and MIT methods. Both gravity and earthquake loadings were considered. Circular arc analyses for gravity loading were performed using the computer program STAB3D, whereas the program TSLOPE was utilized for all other analyses.

For gravity loading conditions, results of this study show that the most critical failure mode is non-circular with a factor of safety, FS, of about 2.4, which is only slightly lower than the value of 2.5 corresponding to an infinite slope failure in top gravel fill deposit. Relatively deep circular shear surfaces predict factors of safety in the range of 3.2 to 3.4.

Consideration of the horizontal earthquake loading leads, as expected, to a reduction in the value of FS. The critical value of the seismic coefficient,  $K_c$ , leading to a factor of safety of unity depends on the shear surfaces considered. The minimum values of  $K_c$  for the Ririe Dam are in the range of 0.57 to 0.74 involving both circular as well as non-circular failures.

## TABLE OF CONTENTS

	<u>Page No.</u>
<b>SUMMARY</b>	i
<b>TABLE OF CONTENTS</b>	ii
<b>LIST OF TABLES</b>	iii
<b>LIST OF FIGURES</b>	iv
<b>1. INTRODUCTION</b>	1
1.1. Scope and Objective of Geotechnical Consulting Services	1
1.2 Information Supplied	2
1.3 Scope of Report	2
<b>2. TWO-DIMENSIONAL CIRCULAR ARC STABILITY ANALYSES</b>	3
2.1 Geometry, Soil Properties and Pore Pressures	3
2.2 Stability Analyses - Gravity Loading	4
2.2.1 Approach	4
2.2.2 Results	5
2.3 Stability Analyses - Gravity and Earthquake Loadings	6
2.3.1 Approach	6
2.3.2 Results	7
<b>3. TWO-DIMENSIONAL NON-CIRCULAR ARC STABILITY ANALYSES</b>	9
3.1 Geometry, Soil Properties and Pore Pressures	9
3.2 Stability Analyses - Gravity Loading	9
3.2.1 Approach	9
3.2.2 Results	10
3.3 Stability Analyses - Gravity and Earthquake Loadings	11
3.3.1 Approach	11
3.3.2 Results	11
<b>4. SUMMARY AND CONCLUSIONS</b>	12
<b>REFERENCES</b>	15

LIST OF TABLES

<u>No.</u>	<u>Title</u>	<u>Page</u>
1.1	List of Documents	16
2.1	Soil Properties Utilized in Stability Analyses	17
2.2	Results of 2-D Circular Arc Analysis For Vertical Gravity Loading	18
3.1	Results of Two-Dimensional Non-Circular Arc Stability Analyses for Gravity Loading	19

**LIST OF FIGURES**

<u>No.</u>	<u>Title</u>	<u>Page</u>
2.1	Plan View and Critical Cross Section of the Ririe Dam	20
2.2	Idealized Cross Section, Soil Layers and Water Lines	21
2.3a	Soil Lines and Layers used in STAB3D (X = 800 to 2800 ft)	22
2.3b	Soil Lines and Layers used in STAB3D (X = 900 to 1800 ft)	23
2.3c	Soil Lines and Layers used in STAB3D (X = 1600 to 2400 ft)	24
2.3d	Soil Lines and Layers used in STAB3D (X = 2000 to 2800 ft)	25
2.4	Results of 2D Circular Arc Analysis For Gravity Loading	26
2.5	Results of 2D Circular Arc Analyses for Gravity and Earthquake Loadings	27
3.1a	Locations of Non-Circular Shear Surfaces for 2D Analyses (Surface 1-8)	28
3.1b	Locations of Non-Circular Shear Surfaces for 2D Analyses (Surface 9-11)	29
3.1c	Locations of Non-Circular Shear Surfaces for 2D Analyses (Surface 12-14)	30
3.1d	Locations of Non-Circular Shear Surfaces for 2D Analyses (Surface 15 & 16)	31
3.1e	Locations of Non-Circular Shear Surfaces for 2D Analyses (Surface 17-19)	32
3.2	Results of Non-Circular Arc Stability Analyses for Gravity and Earthquake Loadings	33

## 1. INTRODUCTION

### 1.1 Scope and Objectives of Geotechnical Consulting Services

In June, 1986, Mohsen Baligh & Associates (MBA) submitted a proposal to the Repair, Evaluation, Maintenance and Rehabilitation Research Program (REMR-2) of the U.S. Army Corps of Engineers, Waterways Experiment Station, aimed at evaluating the stability of an earth dam. On September 26, 1986, the U.S. Army Corps of Engineers issued a purchase order DACW39-86-P-0607 that contained a two page scope of work statement. The main objective of the study is to evaluate the stability of the Ririe Dam in Idaho under the combined effect of gravity and earthquake loadings. Specifically, the Consultant is to undertake a two-phase program described as follows:

#### Phase I: Two-Dimensional Analyses

Work in this phase includes the following tasks:

- i) Review existing data and analyses pertaining to the Ririe Dam;
- ii) Perform two-dimensional circular arc analyses for gravity and earthquake loadings;
- iii) Conduct two-dimensional wedge analyses for gravity and earthquake loadings; and
- iv) Prepare an interim report.

#### Phase II: Three-Dimensional Analyses

Work in Phase II includes the following tasks:

- i) Perform three-dimensional circular arc analyses for gravity loading;
- ii) Extend the MIT stability analysis method to consider the effect of horizontal earthquake loading;
- iii) Conduct three-dimensional circular arc analyses for gravity and earthquake loadings; and
- iv) Prepare a final report.

However, work on the project was initiated in September, 1988, after the data related to the project were made available to the Consultant in August, 1988.

The work presented in this report was carried out by Drs. Amr S. Azzouz and Mohsen M. Baligh of Mohsen Baligh & Associates. Assistance in Computer Analyses was provided by Mr. Marawan Shahein, a graduate teaching assistant in the Department of Civil Engineering, Kuwait University.

### 1.2 Information Supplied

Table 1.1 lists the documents sent by Mr. Joseph P. Koester, U.S. Army Engineer, Waterways Experiment Station, to Dr. Azzouz. Items A-G were received on August 1, 1988, whereas items H and I were received on November 15, 1988, and February 10, 1989, respectively.

### 1.3 Scope of Report

This report contains the results obtained in Phase I of the program. Section 2 describes results of the circular arc stability analyses, and Section 3 presents results of the non-circular stability analyses. The main conclusions advanced from the Phase I study are summarized in Section 4.

## 2. TWO-DIMENSIONAL CIRCULAR ARC STABILITY ANALYSES

### 2.1 Geometry, Soil Properties and Pore Pressures

Extensive two-dimensional (2-D) circular arc stability analyses were conducted for the Ririe Dam. In addition to forming the basis for the three-dimensional (3-D) analyses, 2-D analyses provide a convenient tool to conduct sensitivity studies aimed at investigating the influence of various factors and parameters on the stability of the Dam.

Figure 2.1 shows a plan view of the Ririe Dam together with a cross section taken along a curved alignment avoiding direct influence from the canyon walls. A simplified version of this cross-section (Fig. 2.2) was recommended for the stability analysis by the Army Corps of Engineers, ACE (Document D; Table 1.1).

As can be seen in Fig. 2.2, the Dam and its foundation are divided into eight different soil layers. Designations for each of these layers, together with the soil properties provided by the ACE (Document E; Table 1.1) and required for the stability analyses are given in Table 2.1. Since the thickness of the tuffaceous sediments layer(layer 8) is unknown, it was assumed for analysis purposes that a lower boundary with significantly higher friction angle exists below an Elevation of 400 ft. As will be illustrated subsequently, this assumption has no influence on the stability calculations as the critical shear surfaces fall well above the tuffaceous sediments stratum.

Pore pressures within the Dam were defined by the ACE for purposes of stability analyses by the phreatic surface illustrated in Fig. 2.2. The dotted lines in this figure show the phreatic surface at Elevation 1110 ft to extend through the core of the Dam. Immediately to the right of the core, the phreatic surface is located at Elevation 955 ft. In between

these two elevations, the phreatic surface was assumed to coincide with the right boundary of the core (see Fig. 2.2).

## 2.2 Stability Analyses - Gravity Loading

### 2.2.1 Approach

Effective stress circular arc stability analyses for vertical gravity loading were carried out for the Ririe Dam using the Computer Program STAB3D (Azzouz, 1977). A total of 58 soil lines were utilized in STAB3D to specify the geometry of the Dam and its foundation (see Figs. 2.3-a through 2.3-d). The submerged face of the Dam was modelled by considering the water pool in the upstream as an additional layer (layer 9 in Table 2.1) with a unit weight equal to 62.4 lb/ft<sup>3</sup> and zero friction angle.

Table 2.2 lists all the cases considered for evaluating the stability of the Ririe Dam. Basically, these cases were selected to allow an investigation of the influence of variations in soil properties and methods of analyses on the overall stability of the Dam. Analyses were carried out utilizing the saturated and moist unit weights to take into consideration the possible imperfect saturation of the in situ soils. The influence of the value of the effective friction angle of the core material,  $\phi'_{core}$ , on the calculated factor of safety was assessed by performing three stability analyses corresponding to  $\phi'_{core} = 30, 34$  and  $38^\circ$ . Finally, two methods of analyses were considered, the modified Bishop method (Bishop, 1955) and the MIT method (Azzouz and Baligh, 1978).

Statical determinancy in the MIT method is achieved by assuming that, for each slice, the vertical effective stress is a principal stress at failure. Depending on the location of the slice, the horizontal effective stress may then become either a major or a minor principal stress at failure. Knowing the principal stresses and planes, the state of stress on the base of a

slice with any inclination may be easily obtained. Azzouz and Baligh (1978) evaluated the predictions of the MIT method and concluded that it predicts factors of safety that are in close agreement with those predicted by the most widely used modified Bishop method. Moreover, assumptions utilized in the MIT method in two-dimensions allow easy extensions to three-dimensions, which is particularly significant for this project.

For each of the cases considered in Table 2.2, the search for the critical shear surface providing the lowest value of the factor of safety was carried out by varying the center of the shear surface within a rectangular grid having X and Y co-ordinates varying between 1400 to 2600 ft and 1100 to 2300 ft, respectively, in increments of 100 ft. At each of these centers, the tangent to the shear surface was varied between  $Y = 400$  to 1100 ft in increments of 100 ft. Once a critical shear surface was found to exist within the grid specified above, a finer grid was utilized until the most critical shear surface was identified. This process typically resulted in the analysis of about 2,000 circles for each of the cases in Table 2.2. Finally, both clockwise (i.e., upstream) as well as counter-clockwise (i.e., downstream) failures were considered. This required the preparation of a new input data file since STAB3D can only handle counter-clockwise failures.

### 2.2.2 Results

Results of the 2-D circular are stability analyses for gravity loading are summarized in Table 2.2 and Fig. 2.4, where we note:

- 1) The lowest value of the factor of safety corresponds to an infinite-slope failure mode in the gravel fill layer (Layer 2; Fig. 2.2). For this failure mode, the factor of safety, F. S., is given by:

$$F. S. = \frac{\tan \phi'}{\tan i} \quad (1)$$

Noting that the gravel fill layer has an inclination,  $i$ , of  $24^\circ$  and an effective friction angle,  $\phi'$ , of  $48^\circ$ , Eq. (1) yields a factor of safety of about 2.5 (Case 1; Table 2.2).

- 2) Using saturated unit weights for the Dam and its foundation and an effective friction angle for the core material,  $\phi'_{core}$ , of  $30^\circ$ , circular arc analyses yield factors of safety in the order of 3.2 to 3.4 (Cases 2 through 4). The shear surfaces associated with these factors of safety are rather shallow, located in the downstream side of the dam, and mostly pass through the gravel fill layer (Layer 2) and, in some cases (No. 3 & 4), also through the rockfill and random fill layers (see Fig. 2.4).
- 3) Values of the factor of safety and the locations of the corresponding critical shear surfaces are insignificantly affected by changes in  $\phi'_{core}$ , unit weights (i.e., moist vs saturated), or the method of stability analysis (i.e., MIT vs modified Bishop methods) as indicated by the results of Cases 5 through 10 described in Table 2.2.
- 4) Differences between the values of the factor of safety associated with upstream and downstream failures are small. As with downstream failures, the factor of safety for upstream failures decreases as the depth of the failure surface decreases, and ranges between 3.3 and 3.9.

### 2.3 Stability Analyses - Gravity and Earthquake Loadings

#### 2.3.1 Approach

Circular arc stability analyses for gravity and earthquake loadings were performed for the Ririe Dam using the computer program TSLOPE (TAGA Engineering Software Services, 1984) in accordance with the Spencer Method (Spencer, 1967). For each of the slices comprising a failure surface, Spencer's method models the earthquake loading as a horizon-

tal force with a magnitude equals to the product of a seismic coefficient,  $K$ , times the weight of the soil mass enclosed within the slice. The factor of safety is then obtained by satisfying all equations of equilibrium assuming that all inter-slice forces are parallel.

TSLOPE can not perform an automatic search for the critical shear surface providing the lowest value for the factor of safety. As a result, the user must specify the shape and coordinates of all shear surfaces to be analyzed. However, for a given shear surface, TSLOPE automatically searches for the critical seismic coefficient,  $K_c$ , which produces a factor of safety equal to one.

Effective stress circular arc analyses for combined gravity and earthquake loadings were performed for shear surfaces 3 and 4 depicted in Fig. 2.4. The analyses were carried out using the saturated unit weights and an effective friction angle for the core material equals to 30°. Submergence was modelled in TSLOPE by applying hydrostatic pressures along the submerged upstream face of the Dam.

### 2.3.2 Results

Figure 2.5 presents a summary of the results of the circular arc analysis for combined gravity and earthquake loadings, where we note:

- 1) The factor of safety obtained by the Spencer method for the case of gravity loading alone (i.e.,  $K=0$ ) for shear surface 3 is equal to 3.28. This is in close agreement with the value of 3.27 obtained by the modified Bishop method (see Fig. 2.4). Similar results are obtained for shear surface 4, which provide further confirmation as to the insensitivity of the value of the factor of safety to the method used for stability analysis.

2) As expected, increasing the seismic coefficient K results in a decrease in the value of the factor of safety, F.S. The critical seismic coefficients,  $K_c$ , corresponding to F.S. = 1 for both shear surfaces considered herein are equal to 0.57 and 0.61.

### 3. TWO-DIMENSIONAL NON-CIRCULAR ARC STABILITY ANALYSES

#### 3.1 Geometry, Soil Properties and Pore Pressures

Two-dimensional non-circular arc analyses were performed for the Ririe Dam in accordance with the Spencer method implemented in the computer program TSLOPE. The cross-section, soil properties and phreatic surface utilized for the analyses are the same as those used for the circular arc analyses and portrayed in Fig. 2.2 and Table 2.1.

#### 3.2 Stability Analyses - Gravity Loading

##### 3.2.1 Approach

TSLOPE, utilized for the analysis of non-circular shear surfaces, can not perform an automatic search for the critical shear surface providing the lowest value of the factor of safety. Instead, the user has to specify the shapes and coordinates of all shear surfaces to be analyzed. In this project, a total of 26 cases involving 19 different shear surfaces were analyzed (see Fig. 3.1 and Table 3.1). Cases 1 through 19 in Table 3.1 attempt to identify the shear surface with the lowest factor of safety for a non-circular failure of the Ririe Dam, and utilize the saturated soil unit weights. Cases 20 through 25 investigate the sensitivity of the calculated factors of safety to the values of soil unit weights. The first three cases (20-22, Table 3.1) utilize the moist soil unit weights, whereas the last three (23-25, Table 3.1) use moist unit weights above the phreatic surface and saturated unit weights below it. All cases in Table 3.1 were performed using an effective friction angle for the core material equals to 30°.

### 3.2.2 Results

Results of the effective stress non-circular stability analyses for gravity loading are presented in Table 3.1, where we note:

- 1) For the shear surfaces analyzed in Cases 1 through 19, the lowest value of the factor of safety for a non-circular failure is about 2.4, which corresponds to shear surface 16 in Fig. 3.1d. This shear surface consists of 3 wedges: An "active" wedge, which mostly passes through the core material; a central wedge, passing through layers 1, 3, 4 and 7; and a "passive" wedge exiting through layers 7 and 4. In a discussion of an earlier version of this report with Mr. Joseph P. Koester, of the U.S. Army Corps of Engineers, he indicated that there could be an uncertainty as to whether the silt layer (Layer 7 in Fig. 3.1d) was actually encountered in the boring logs performed for the Ririe Dam, and requested that surface 16 be reanalyzed assuming that the silt layer did not exist. This is achieved herein in Case 26 in Table 3.1, in which the shearing resistance along portions ab and bc of shear surface 16 (Fig. 3.1d) was assumed to be provided by layers 5 and 4, respectively, instead of layer 7. Although this modification resulted in a modest increase in the value of factor of safety from 2.378 to 2.519, surface 16 still represents the most critical non-circular shear surface with a factor of safety ranging between 2.4 to 2.5 depending on whether the silt layer (layer 7 in Fig. 3.1d) actually exists.
- 2) The factors of safety are insignificantly affected by the values of soil unit weights utilized in the analyses. For example, using the moist unit weights above the phreatic surface and the saturated unit weights below it for shear surfaces 5, 15, and 16

results in a maximum reduction in F.S. by about 8% compared to the cases which utilize the saturated unit weights everywhere.

### 3.3 Stability Analyses - Gravity and Earthquake Loadings

#### 3.3.1 Approach

Non-Circular arc stability analyses for gravity and earthquake loadings were performed for the Ririe Dam using the same approach described in Section 2.3 of this report. Effective stress analyses were first performed for an infinite slope failure and then for all the shear surfaces depicted in Fig. 3.1a-e using the saturated soil unit weights and an effective friction angle for the core material equals to 30°.

#### 3.3.2 Results

The critical seismic coefficient,  $K_c$ , leading to a factor of safety of unity associated with an infinite slope failure along the downstream face of the dam is about 0.5. Results for the deeper non-circular surfaces providing the lowest values of  $K_c$  are presented in Fig. 3.2. It can be seen from this figure that the critical  $K_c$  values range between 0.67 to 0.74, which are associated with shear surfaces 15, 17, 18, and 19 involving both upstream as well as downstream failures.

#### 4. SUMMARY AND CONCLUSIONS

In September, 1988, Mohsen Baligh & Associates (MBA) were contracted by the U. S. Army Corps of Engineers (ACE), Waterways Experiment Station, to undertake a study aimed at the evaluation of the stability of the Ririe Dam in Idaho under the combined effect of gravity and earthquake loadings. The work is to be undertaken in two phases, the first of which is devoted to two-dimensional (2D) analyses, while the second is concerned with the investigation of the influence of end (i.e., three-dimensional) effects on the stability of the dam. A set of documents containing information on the site, dam geometry, and soil properties were furnished by the ACE to the Consultants (Table 1.1) prior to the initiation of the project. This report presents results of Phase I of the project. The approach and main findings in this phase are summarized herein.

1. Effective stress circular arc analyses for gravity loading were performed using the computer program STAB3D based on the cross-section, soil properties and phreatic surface provided by the ACE. A total of 10 cases were analyzed (Table 2.2), which were basically designed to investigate the influence of variations in soil properties and methods of analyses on the overall stability of the dam. For each of the cases in Table 2.2, an extensive search for the critical circular shear surface providing the lowest value of the factor of safety was undertaken. This process typically resulted in the analysis of about 2,000 shear surfaces for each of the cases in Table 2.2. Results of these analyses indicate the following:

- i) The factor of safety, FS, decreases as the depth of shear surface decreases. In the limit, the minimum factor of safety corresponds to an infinite slope failure in the gravel fill deposit with  $FS = 2.5$ .

- ii) For deeper failures involving circular shear surfaces, the factor of safety ranges between 3.2 and 3.4. The critical shear surfaces are located in the downstream side of the dam and pass through the gravel fill, rockfill and random fill deposits (see Fig. 2.4 and Table 2.2).
- iii) Minor differences exist between the values of the factor of safety associated with upstream and downstream failures.
- iv) Insignificant effects on the stability were obtained due to variations in: the magnitude of the friction angle of the silt core; soil unit weights; and method of stability analysis (modified Bishop vs. MIT).

2. Effective stress non-circular arc analyses for gravity loading were performed in accordance with the Spencer method using the computer program TSLOPE. A total of 26 cases were analyzed (Table 3.1 and Fig. 3.1) in an attempt to identify the non-circular shear surface with the lowest value of the factor of safety and to investigate the influence of variations in soil properties on the overall stability of the dam. Results of these analyses show the following:

- i) For the non-circular shear surfaces analyzed herein, the lowest value of the factor of safety is about 2.4. Although this value is smaller than that associated with the relatively deep critical circular surfaces (3.2 - 3.4), it is only slightly lower than the value of 2.5 corresponding to an infinite slope failure.
- ii) Minor effect on the stability were observed due to variations in the magnitude of soil unit weights.

3. Effective stress circular arc analyses for gravity and earthquake loadings were performed using the computer program TSLOPE in accordance with the Spencer method for shear surfaces 3 and 4 in Fig. 2.4. Results of these analyses indicate the following:

- i) As expected, the magnitude of the factor of safety decreases with increasing the seismic coefficient,  $K (= a_h/g)$ , in which  $a_h$  is the equivalent horizontal earthquake acceleration and  $g$  is the gravitational acceleration.
- ii) The critical seismic coefficient,  $K_c$ , leading to  $FS = 1$  is in the range of 0.57 to 0.61.

4. Effective stress non-circular arc analyses for gravity and earthquake loadings were conducted according to the Spencer method using the computer program TSLOPE. Results of these analyses show the following:

- i) The critical seismic coefficient,  $K_c$ , for an infinite slope failure is about 0.5.
- ii) For deeper non-circular failures, the value of  $K_c$  depends on the shear surfaces considered. The minimum values of  $K_c$  are in the range of 0.67 to 0.74 involving both upstream as well as downstream failures.

REFERENCES

1. Azzouz, A.S. (1977), "Three-Dimensional Analysis of Slopes", Thesis presented to MIT in partial fulfilment for the requirements of the degree Doctor of Science, 383 p.
2. Azzouz, A.S., and Baligh, M.M. (1978), "Three-Dimensional Stability of Slopes", Research Report R78-8, Order No. 595, Department of Civil Engineering, MIT.
3. Bishop, A.W. (1955), "The Use of the Slip Circle in the Stability Analysis of Slopes", Geotechnique, London, England, Vol. 5, No. 1, March, pp. 7-17.
4. Spencer, E. (1967), "A Method of Analysis of the Stability of Embankments Assuming Parallel Inter-Slice Forces", Geotechnique, Vol. 17, No. 1, pp. 11-26.
5. TAGA Engineering Software Services (1984), "TSLOPE/TSTAB User's Manual".

Table 1.1: List of Documents

<u>Designation</u>	<u>Contents/Title</u>
A	Transmittal letter from J. P. Koester dated July 25, 1988 to Consultant
B	Copy of purchase order and accompanying proposal
C	9 Cross-section sheets as determined for the as-built dam from construction documents and site surveys
D	1 slope stability section, taken along a curved alignment through a "maximum" section and along the river channel, avoiding direct influence from the Canyon walls
E	1 table of estimated static and dynamic material parameters (DRAFT - subject to change if warranted later; use to "bracket values for Computer analysis")
F	1 package of general site information (about 34 sheets)
G	1 copy of transmittal letter describing Professor H. Bolton Seed's recommended design ground motions
H	Piezometer data for Ririe Dam
I	Cone Penetration Testing, Ririe Dam

**Table 2.1 . Soil Properties Utilized in Stability Analyses\***

Layer No.	Material	Saturated Unit Weight (Pcf)	Moist Unit Weight (Pcf)	Effective Friction Angle(deg)
1	Impervious Silt Core	125	120	30-38
2	Gravel Fill	145	135	48
3	Rockfill	145	135	48
4	Random Fill	140	130	45
5	Weathered Basalt/Gravel	147	147	50
6	Basalt	170	170	50
7	Silt	120	112	33
8	Tuffaceous Sediments	155	155	45
9	Water	62.4	62.4	0

\* Based on Document E (Table 1.1)

Table 2.2 . Results of 2-D Circular Arc Analysis For Vertical Gravity Loading

Case	Method of Analysis	Unit Weight	$\phi'_{core}$ (deg)	$O_x$ (ft)	$O_y$ (ft)	Critical Shear Surface Radius (ft)	F.S.	Comments
1	Infinite Slope	1	30	$\infty$	$\infty$	$\infty$	2.5	
2	Modified Bishop	30	2000	1300	200	3.168	Surface 2*	
3	Modified Bishop	30	2400	2100	1100	3.27	Surface 3	
4	Modified Bishop	30	2300	1800	800	3.44	Surface 4	
5	Modified Bishop	34	2400	2100	1100	3.275	Surface 3	
6	Modified Bishop	38	2400	2100	1100	3.281	Surface 3	
7	MIT	30	2400	2100	1100	3.293	Surface 3	
8	Modified Bishop	30	2000	1300	200	3.168	Surface 2	
9	Modified Bishop	30	2400	2100	1100	3.269	Surface 3	
10	Modified Bishop	30	2300	1800	800	3.438	Surface 4	

\* (See Fig. 2.4 for location of Shear Surfaces)

Table 3.1: Results of Two-Dimensional Non-Circular Arc Stability Analyses for Gravity Loading  
(see Fig. 3.1 for location of shear surface)

Case	Shear Surface No. (see Fig. 3.1)	F. S.	Comments
1	1	5.426	
2	2	5.343	
3	3	5.063	
4	4	5.744	
5	5	4.916	
6	6	5.28	
7	7	5.545	
8	8	8.00	
9	9	6.785	Using saturated unit weights
10	10	6.326	
11	11	5.662	
12	12	6.553	
13	13	5.473	
14	14	5.273	
15	15	3.806	
16*	16*	2.378	
17	17	3.848	
18	18	3.679	
19	19	5.026	
20	5	4.835	
21*	15*	3.796	Using moist unit weights
22*	16*	2.373	
23	5	4.771	
24*	15*	3.533	Using moist unit weights above phreatic surface and saturated below it
25*	16*	2.371	
26	16	2.519	Using saturated unit weights and assuming the silt layer (layer 7) not to exist.

\* Critical shear surface

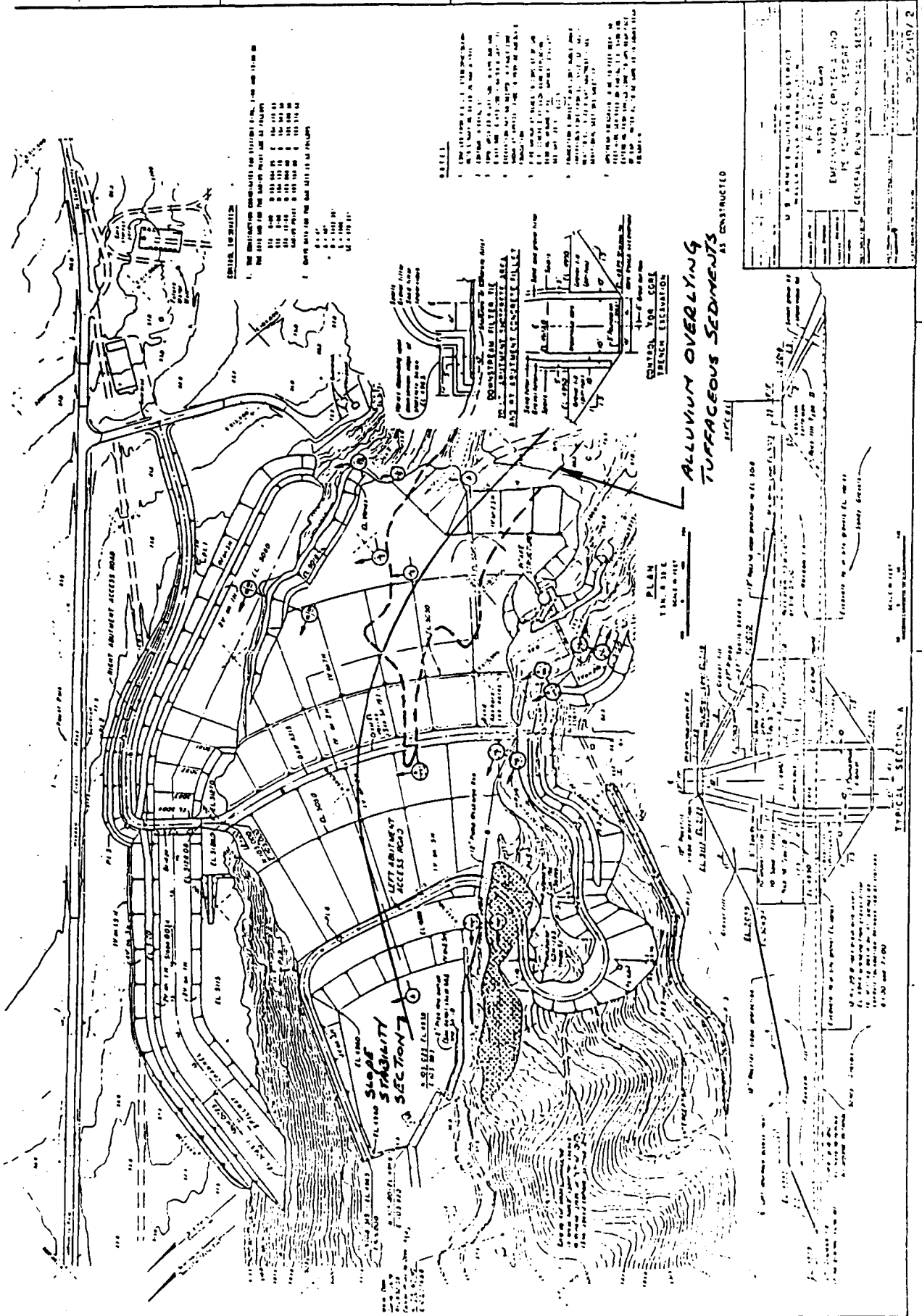


Figure 2.1 Plan View and Critical Cross Section  
of the Ririe Dam

**Figure 2.2 Idealized Cross Section, Soil Layers and Water Lines  
(See Table 2.1 for Soil Properties)**

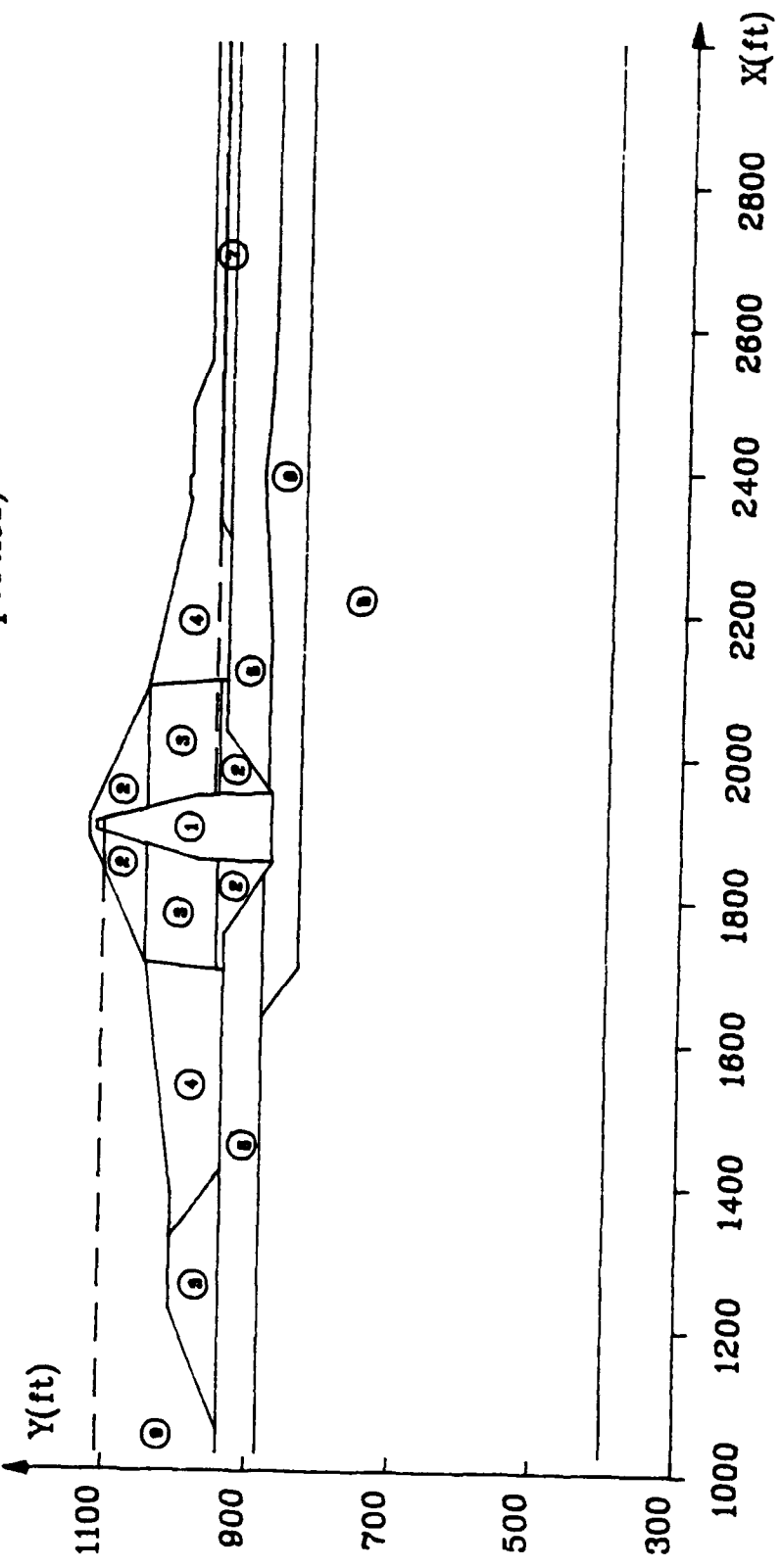


Figure 2.3a Soil Lines and Layers used in STAB3D  
(X=800 to 2800 ft)

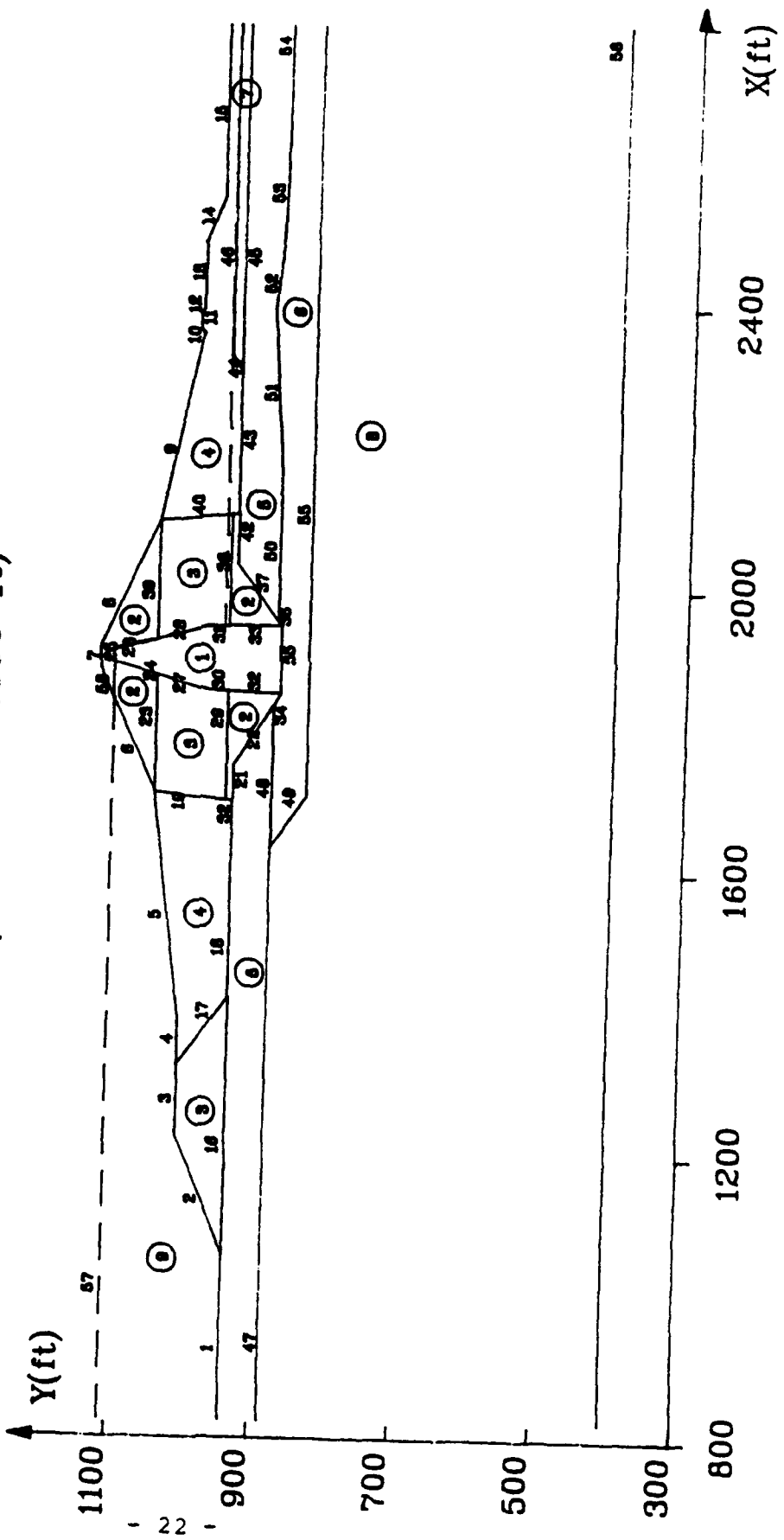


Figure 2.3b Soil Lines and Layers used in STAB3D  
 (X=900 to 1800 ft)

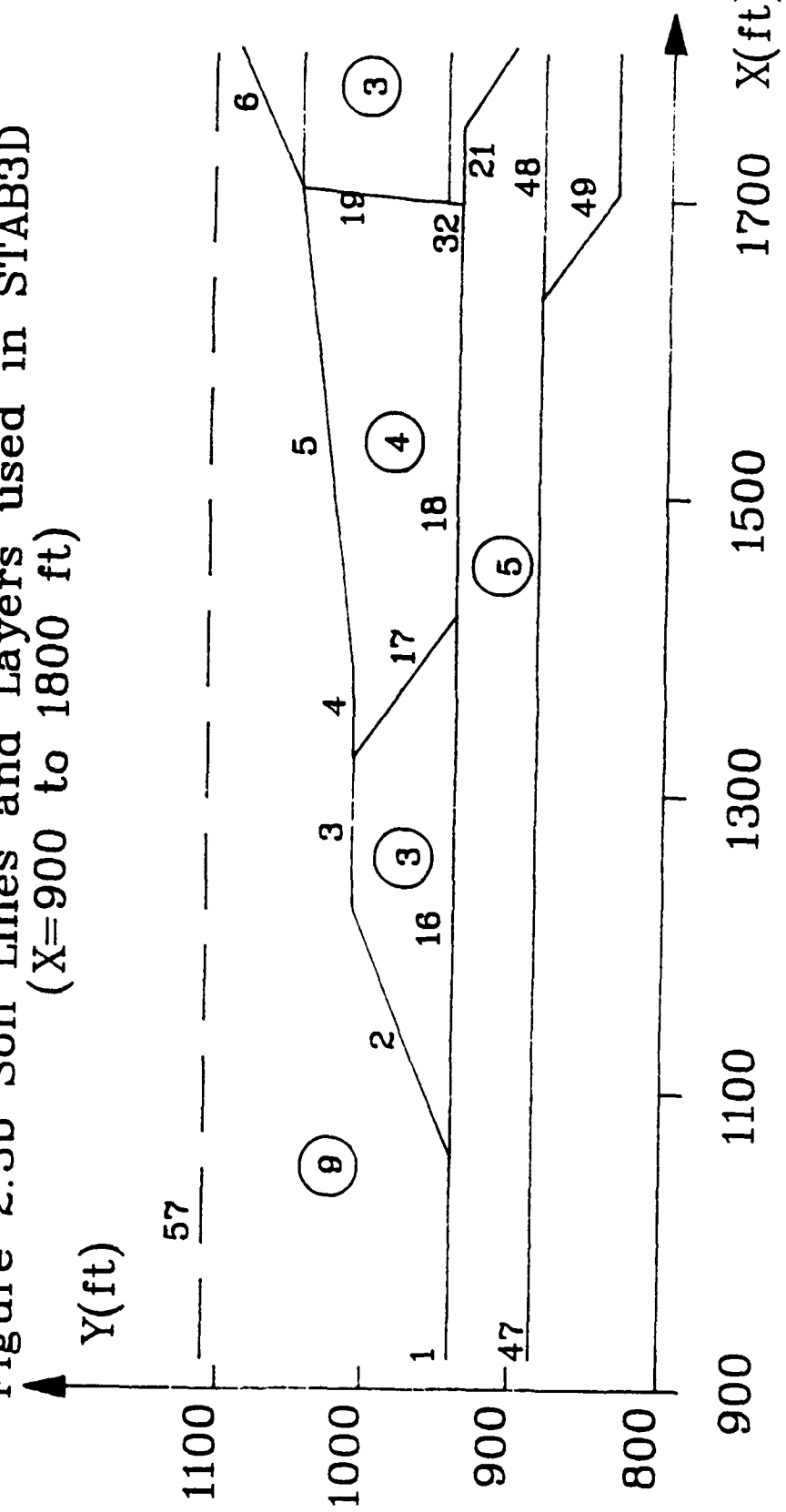


Figure 2.3c Soil Lines and Layers used in STAB3D  
(X=1600 to 2400 ft)

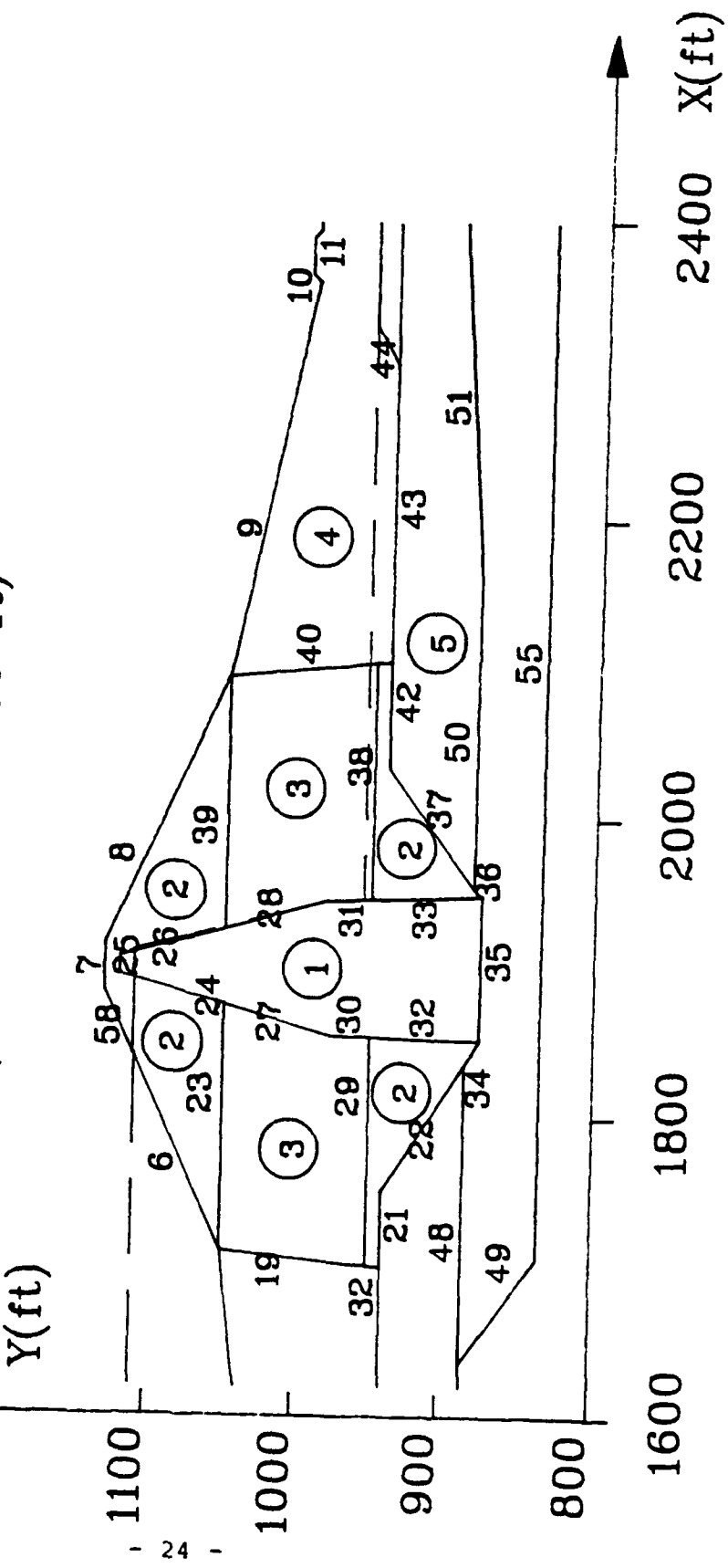


Figure 2.3d Soil Lines and Layers used in STAB3D  
(X=2000 to 2800 ft)

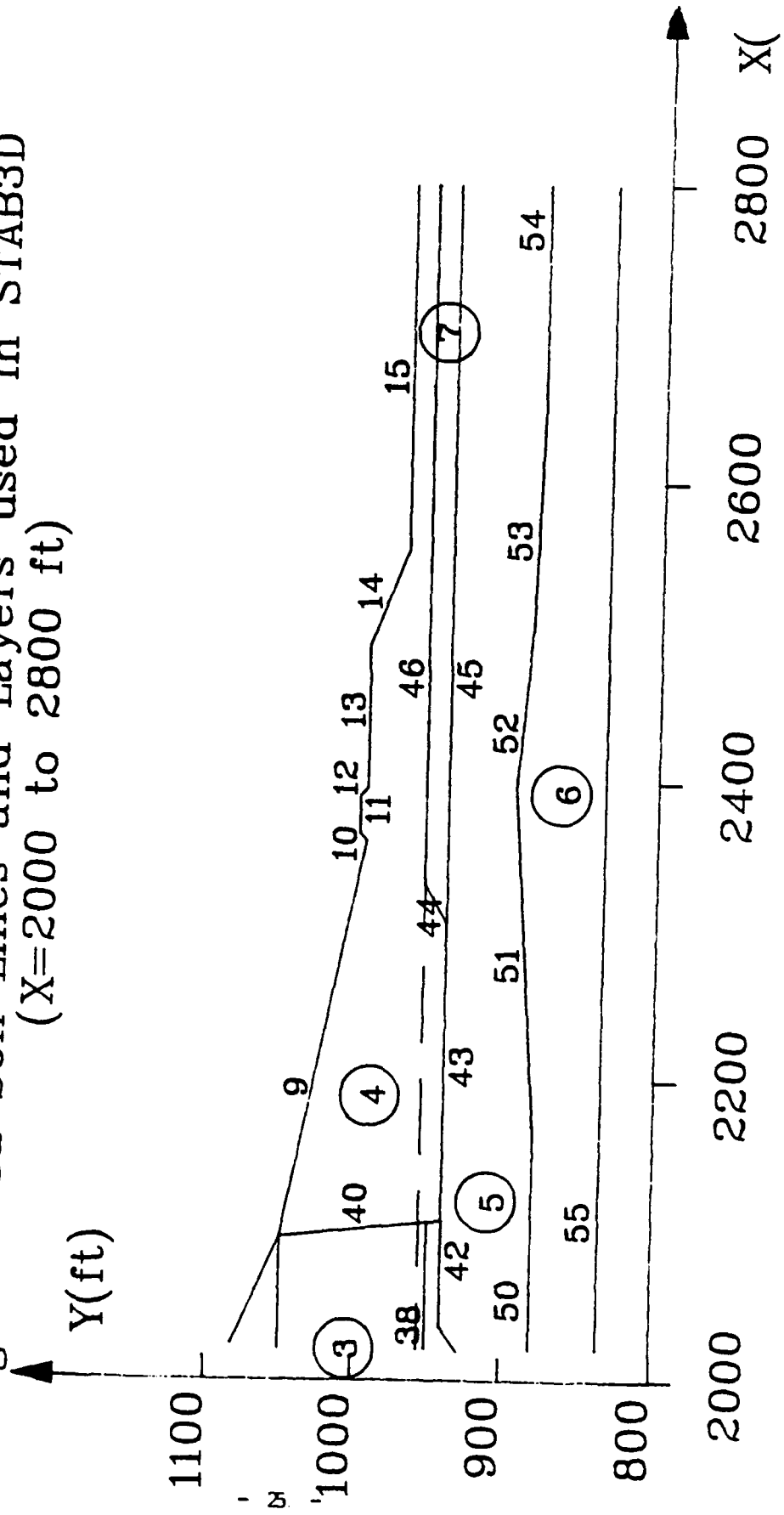


Figure 2.4 Results of 2D Circular Arc Analysis  
For Gravity Loading

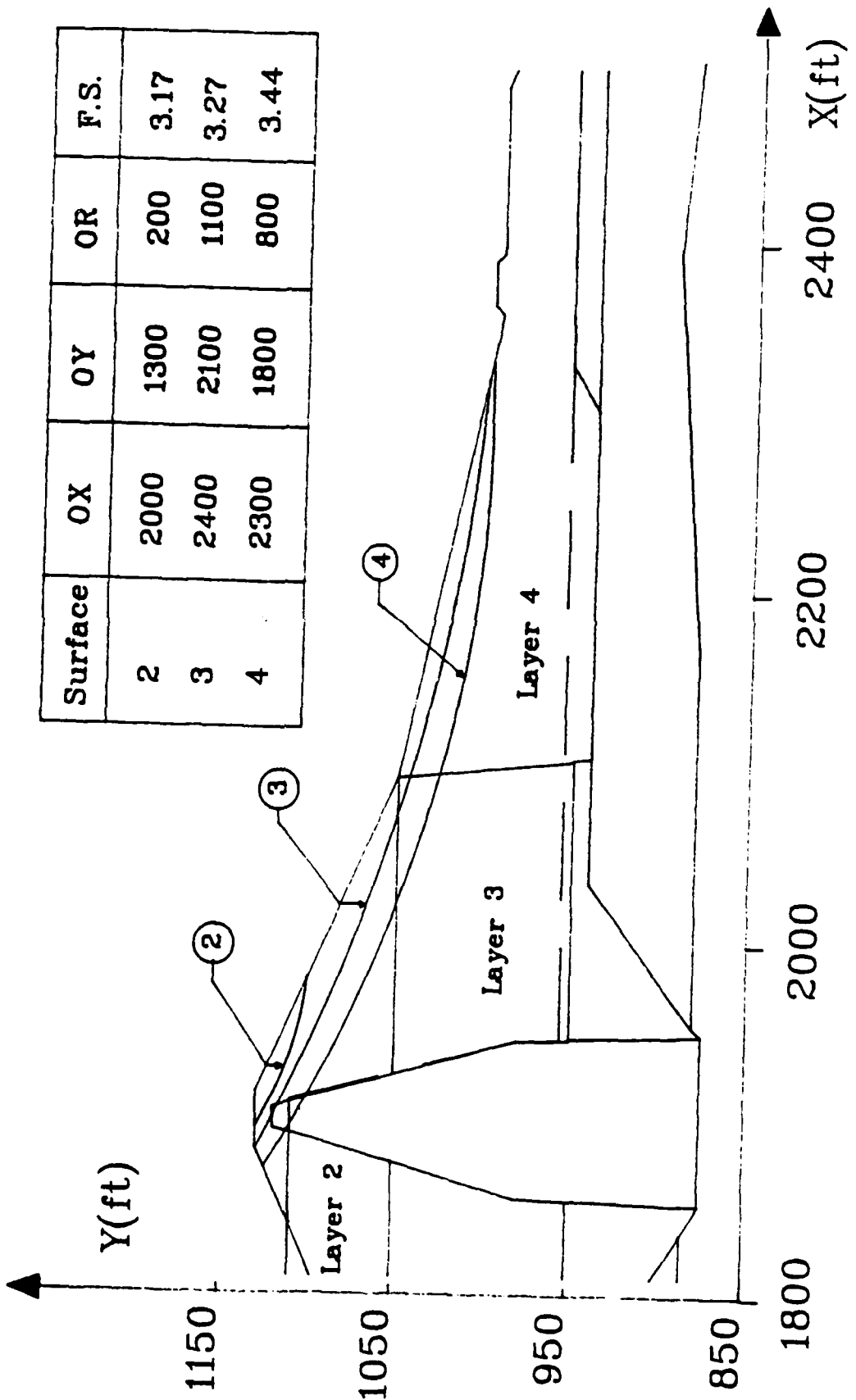


Figure 2.5 Results of 2D Circular Arc Analyses for Gravity and Earthquake Loadings

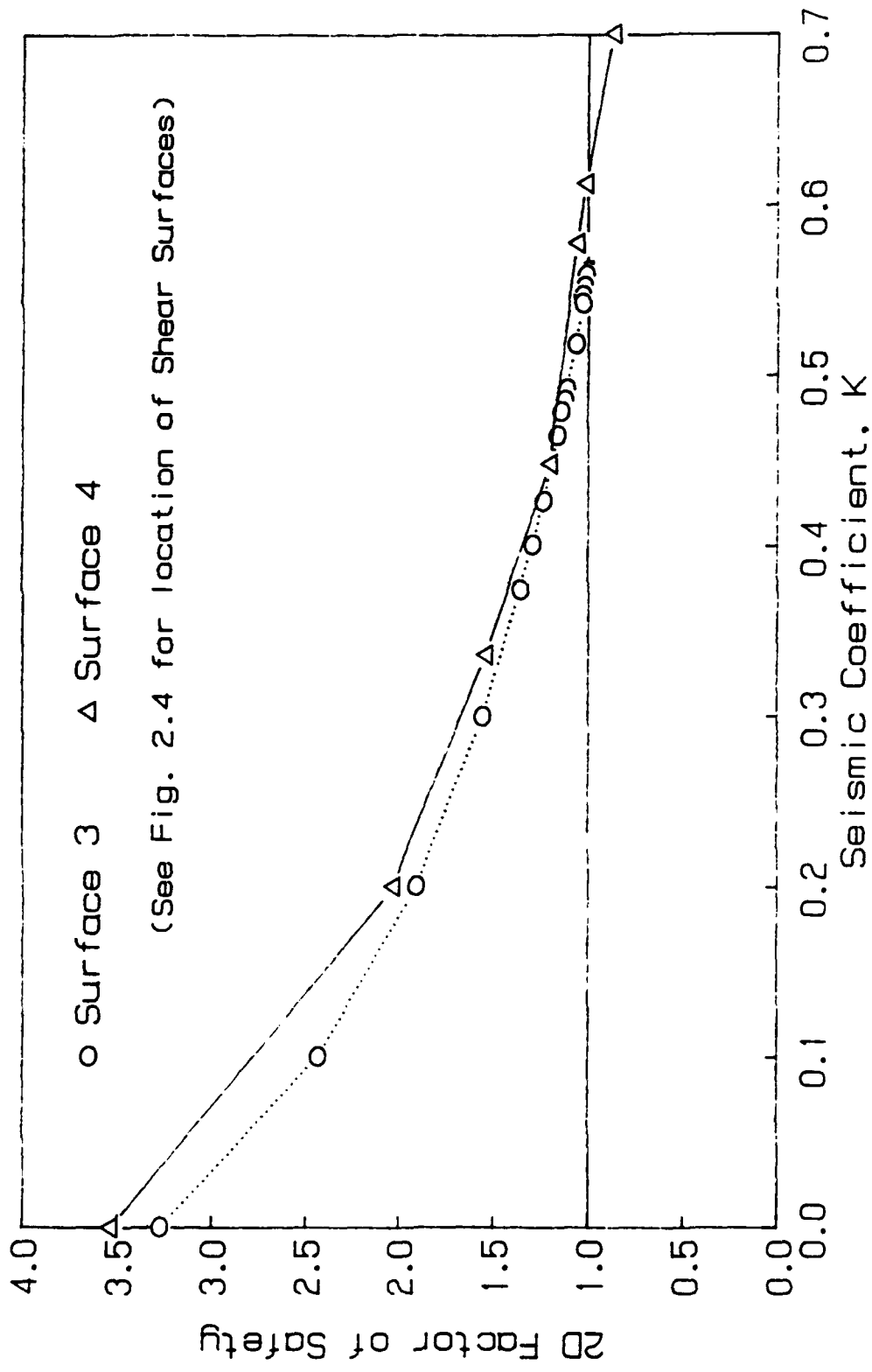


Figure 3.1a Locations of Non-Circular Shear surfaces for 2D Analyses (Surface 1-8)

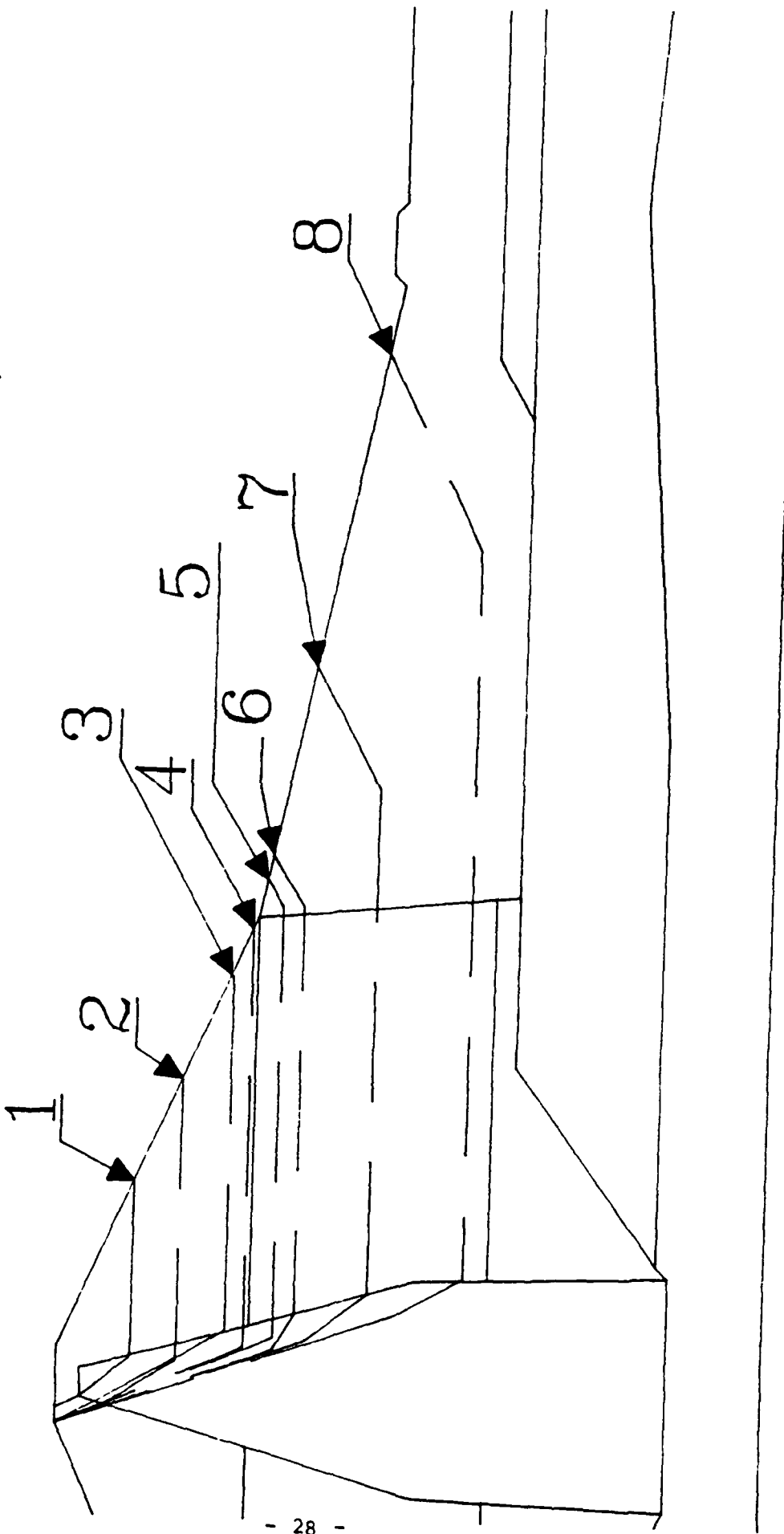


Figure 3.1b Locations of Non-Circular Shear Surfaces  
for 2D Analyses (Surface 9-11)

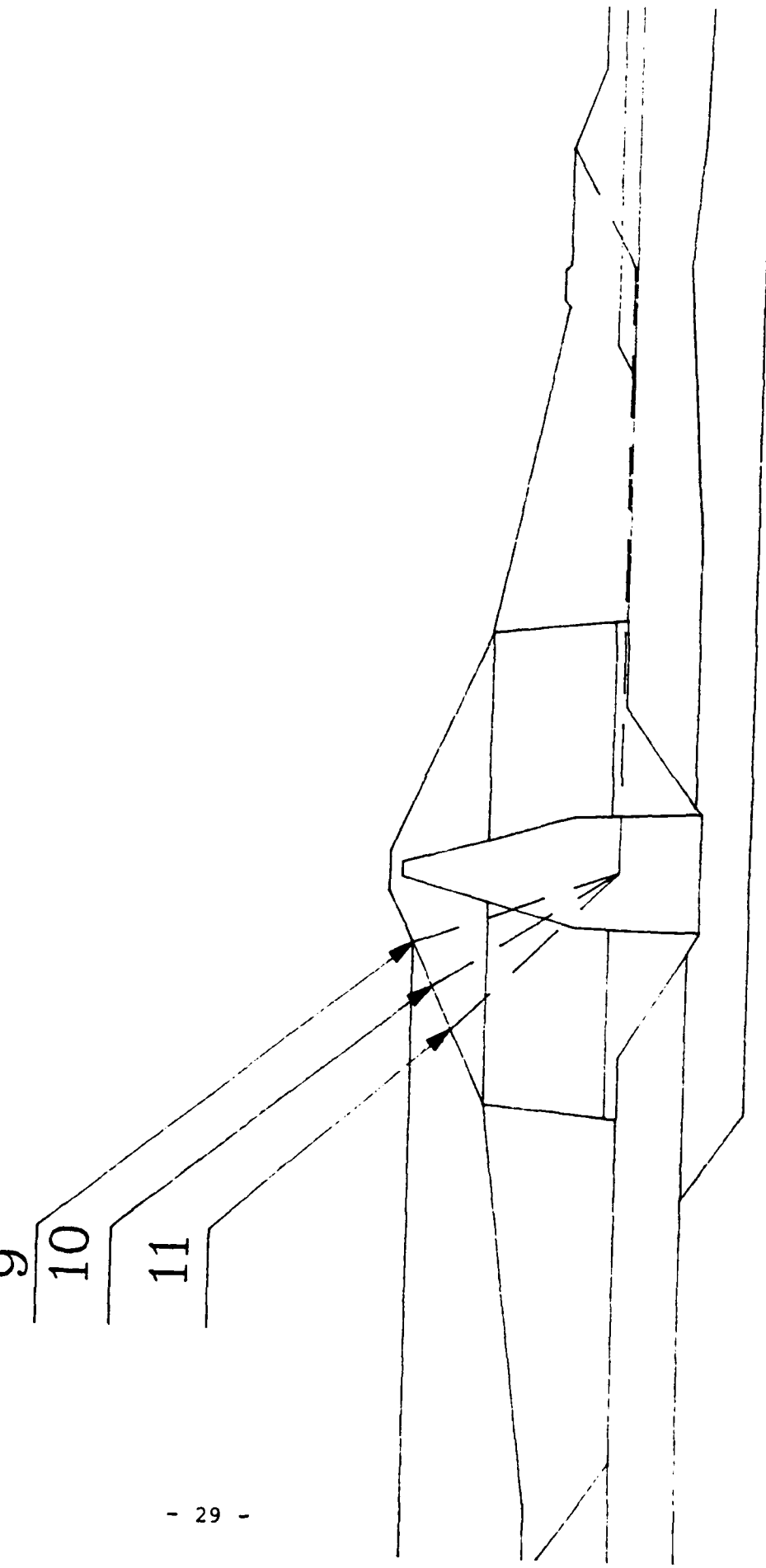


Figure 3.1c Locations of Non-Circular Shear Surfaces  
for 2D Analyses (Surface 12-14)

12

13

14

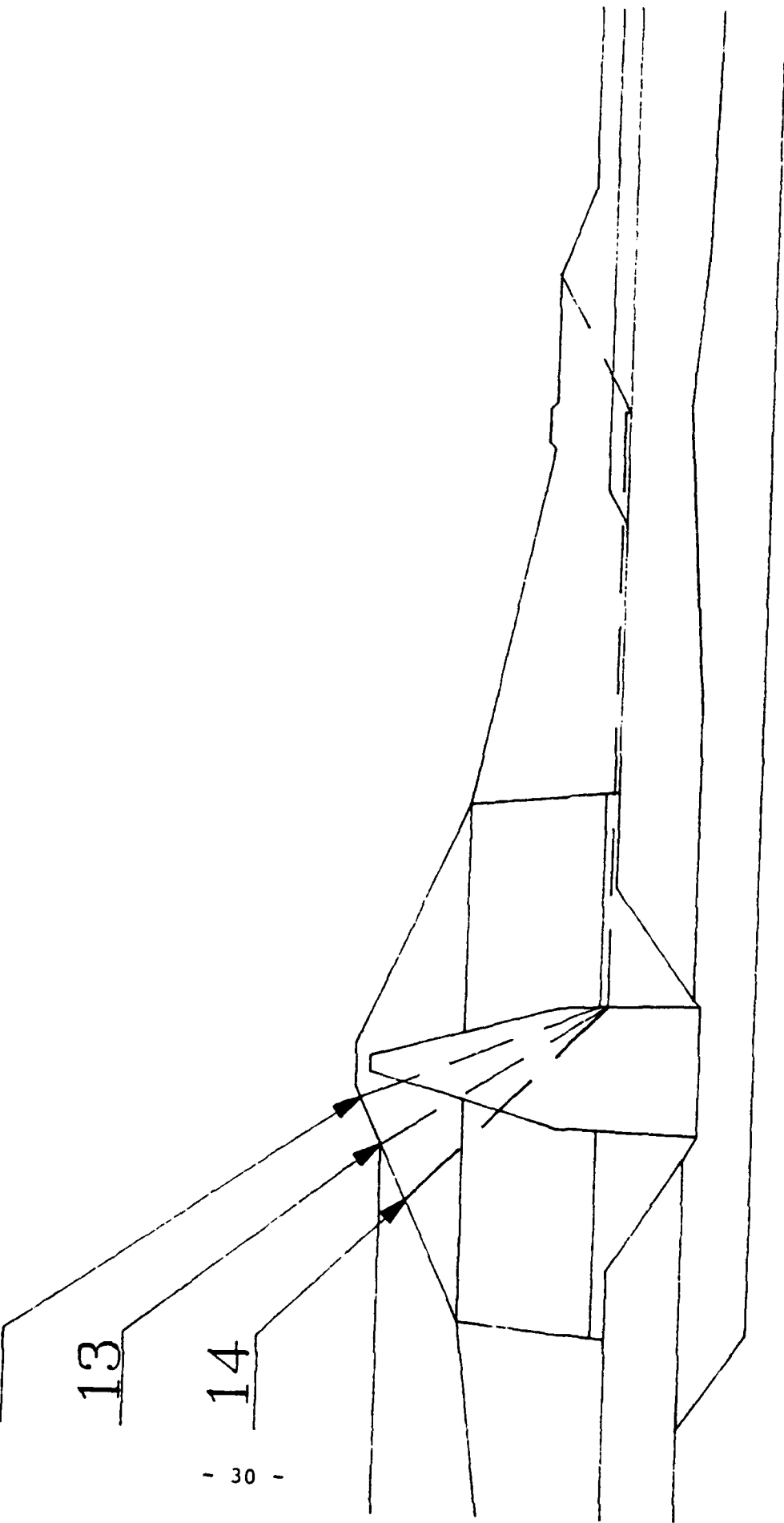


Figure 3.1d Locations of Non-Circular Shear Surfaces  
for 2D Analyses (Surface 15 & 16)

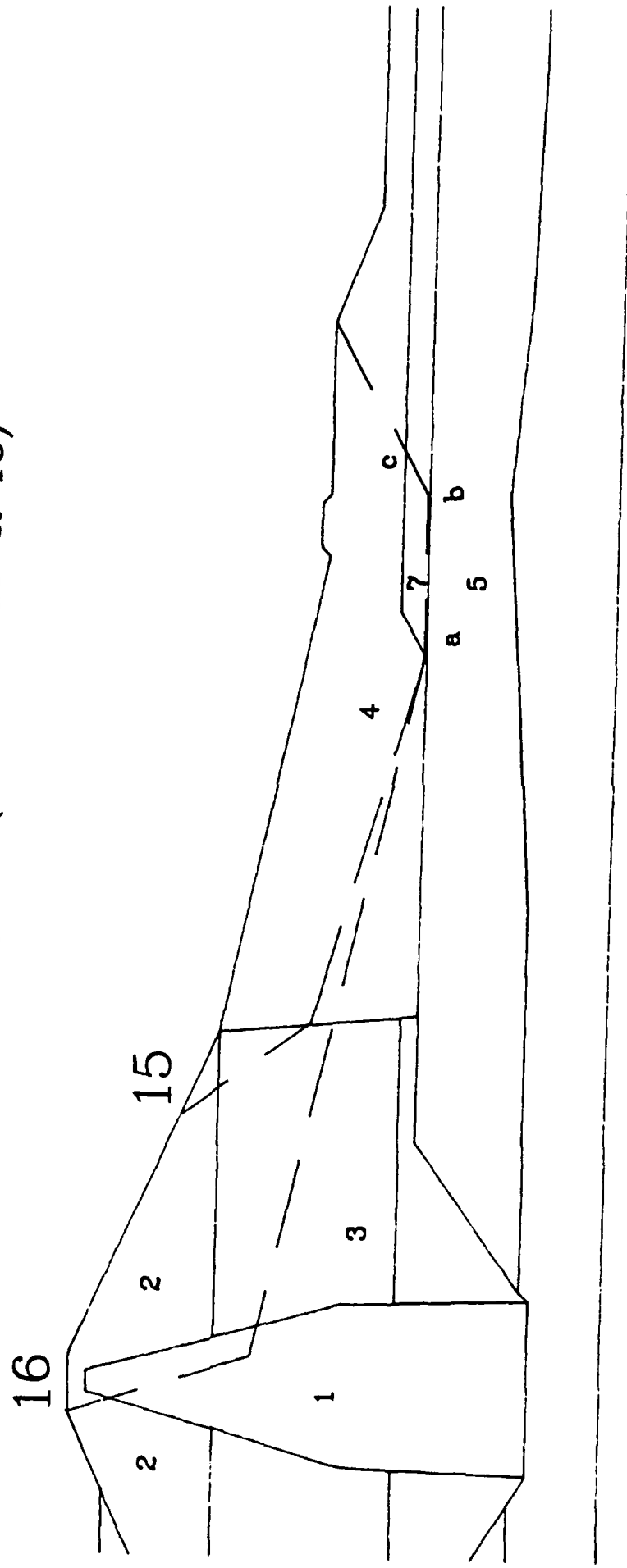


Figure 3.1e Locations of Non-Circular Shear Surfaces  
for 2D analyses (Surface 17-19)

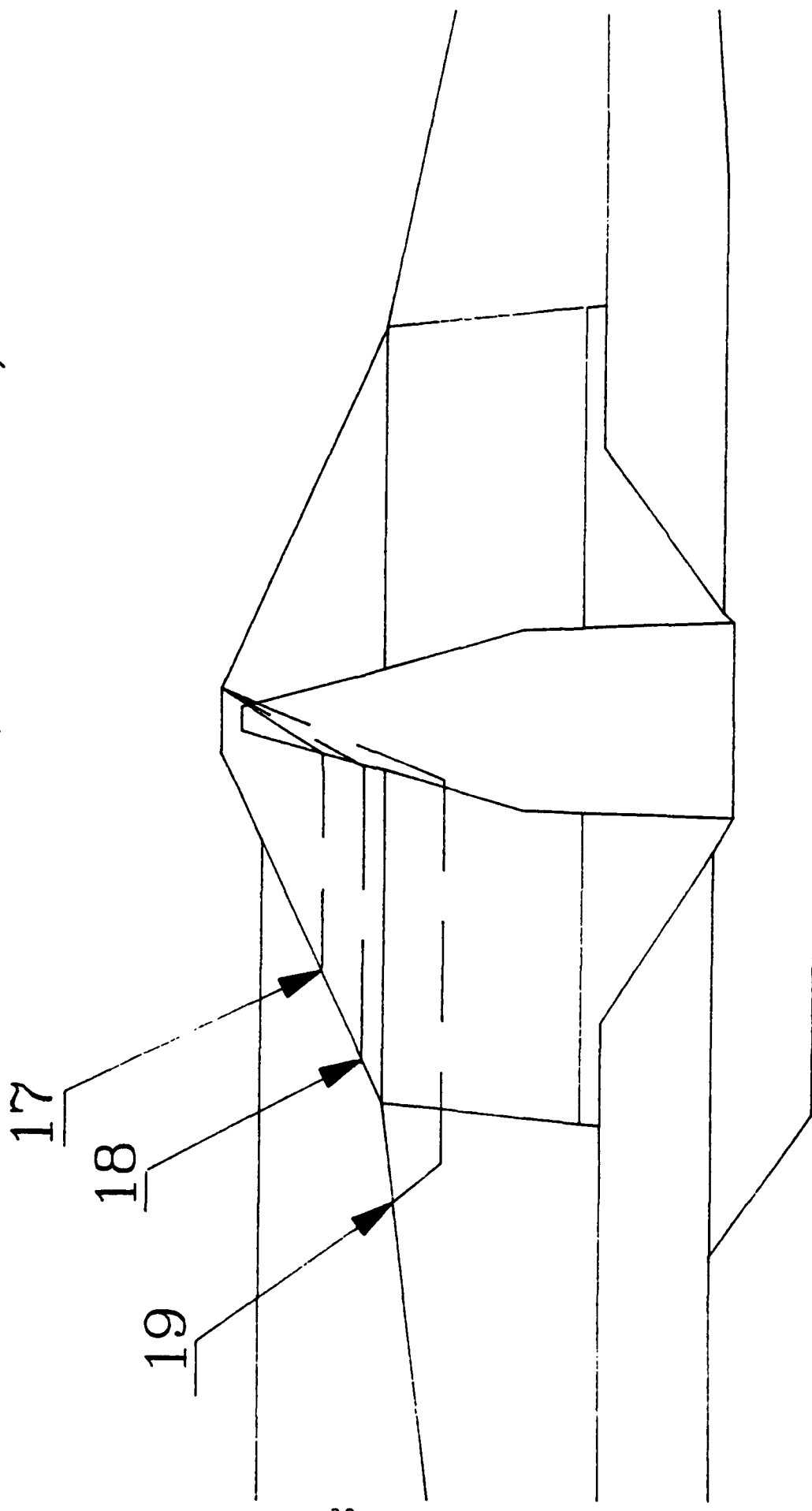
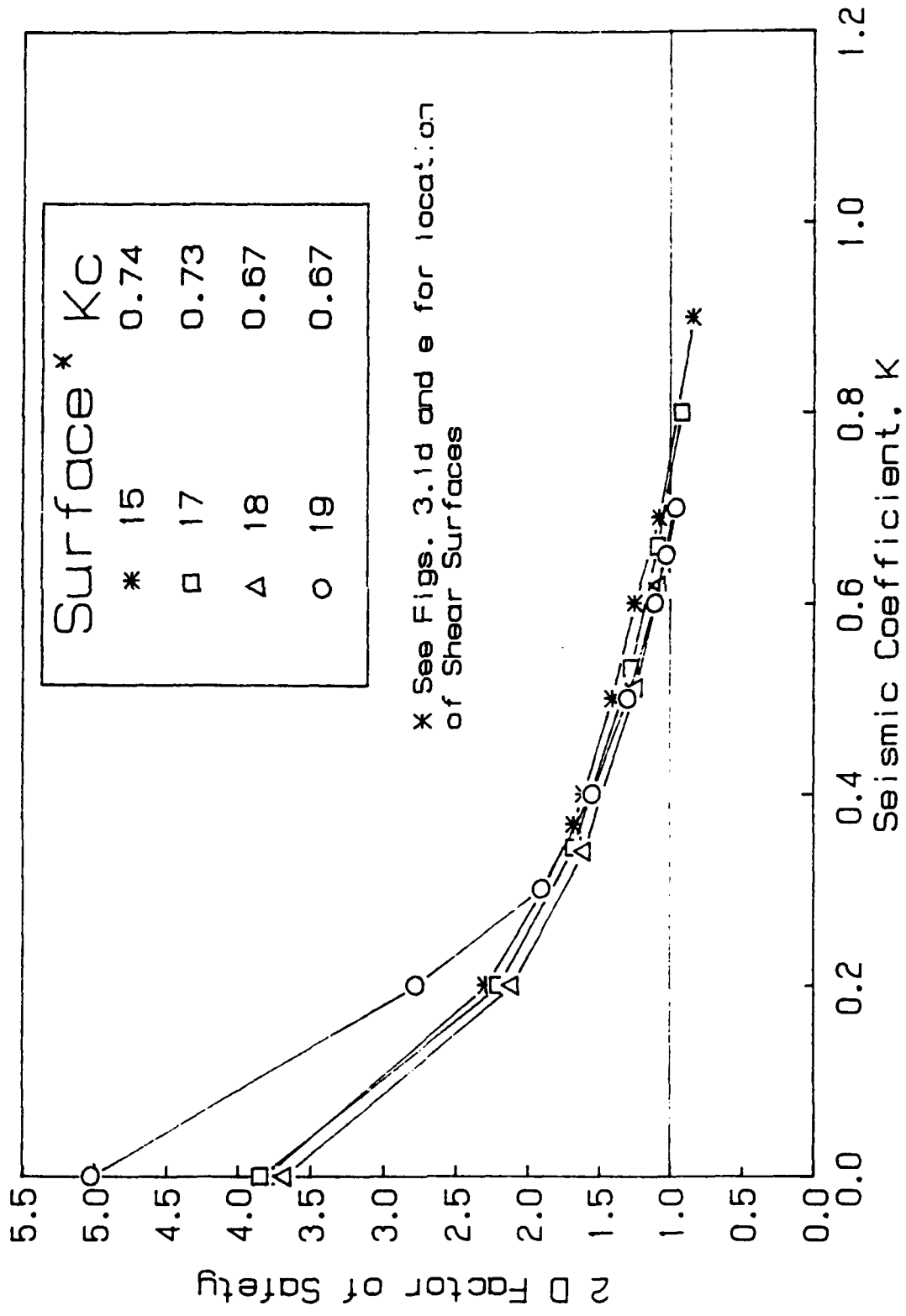


Figure 3.2 Results of Non-Circular Arc Stability Analyses  
for Gravity and Earthquake Loadings



**APPENDIX B: THREE DIMENSIONAL STABILITY ANALYSIS  
OF RIRIE DAM  
(Azzouz and Baligh 1989b)**

**THREE DIMENSIONAL STABILITY ANALYSIS  
OF RIRIE DAM**

**For**

**U. S. Army Corps of Engineers  
Waterways Experiment Station  
Vicksburg, MS 39180-0631  
(Purchase Order DACW39-86-P-0607)**

**By**

**Amr S. Azzouz, and  
Mohsen M. Baligh  
Consulting Geotechnical Engineers  
Lexington, MA-02173**

**July, 1989**

## SUMMARY

In September, 1988, Mohsen Baligh & Associates (MBA) were contracted by the U. S. Army Corps of Engineers (ACE), Waterways Experiment Station to undertake a study aimed at the evaluation of the stability of the Ririe Dam in Idaho. The work is to be performed in two phases, the first of which is devoted to two-dimensional (2D) analyses, while the second is concerned with the investigation of the influence of the three-dimensional (3D) effects on the overall stability of the dam. A final report containing the results of Phase I was submitted by the Consultant in June, 1989. This report presents results of the first task in Phase II dealing with 3-D stability analysis of the Ririe Dam for vertical gravity loading.

Several three-dimensional circular arc effective stress stability analyses for vertical gravity loading were performed using the computer code STAB3D in accordance with the MIT method. Results of the study show that the 3-D factor of safety,  $F$ , decreases as the depth of shear surface decreases and ranges between 3.2 and 3.6. Moreover, end effects increase the plane strain factor of safety,  $F^0$ . However, this increase is rather insignificant with  $F/F^0$  values in the range of 1.008 to 1.045. The small increase in the factor of safety due to end effects is attributed to the fact that the critical shear surfaces are very shallow, thereby resulting in a 3-D failure mode approaching the plane strain mode.

TABLE OF CONTENTS

	<u>Page No.</u>
<b>SUMMARY</b>	i
<b>TABLE OF CONTENTS</b>	ii
<b>LIST OF TABLES</b>	iii
<b>LIST OF FIGURES</b>	iv
<b>1. INTRODUCTION</b>	1
1.1. Scope and Objective of Geotechnical Consulting Services	1
1.2. Scope of Report	2
<b>2. THREE-DIMENSIONAL CIRCULAR ARC STABILITY ANALYSES</b>	3
2.1. Geometry, Soil Properties and Pore Pressures	3
2.2. Stability Analyses	3
2.2.1. Approach	3
2.2.2. Results	6
<b>4. SUMMARY AND CONCLUSIONS</b>	7
<b>REFERENCES</b>	9

LIST OF TABLES

<u>No.</u>	<u>Title</u>	<u>Page</u>
2.1	Soil Properties Utilized in Stability Analyses	10
2.2	Results of 3-D Circular Arc Analysis For Vertical Gravity Loading	11

LIST OF FIGURES

<u>No.</u>	<u>Title</u>	<u>Page</u>
2.1	Plan View and Critical Cross Section of the Ririe Dam	12
2.2	Idealized Cross Section, Soil Layers and Water Lines	13
2.3	Failure Surfaces in Three-dimensional Slope Stability	14
2.4	Shear Surfaces utilized in 3-D Stability Analyses	15

## 1. INTRODUCTION

### 1.1 Scope and Objectives of Geotechnical Consulting Services

In June, 1986, Mohsen Baligh & Associates (MBA) submitted a proposal to the Repair, Evaluation, Maintenance and Rehabilitation Research Program (REMR-2) of the U.S. Army Corps of Engineers, Waterways Experiment Station, aimed at evaluating the stability of an earth dam. On September 26, 1986, the U.S. Army Corps of Engineers issued a purchase order DACW39-86-P-0607 that contained a two page scope of work statement. The main objective of the study is to evaluate the stability of the Ririe Dam in Idaho under the combined effect of gravity and earthquake loadings. Specifically, the Consultant is to undertake a two-phase program described as follows:

#### Phase I: Two-Dimensional Analyses

Work in this phase includes the following tasks:

- i) Review existing data and analyses pertaining to the Ririe Dam;
- ii) Perform two-dimensional circular arc analyses for gravity and earthquake loadings;
- iii) Conduct two-dimensional wedge analyses for gravity and earthquake loadings; and
- iv) Prepare an interim report.

#### Phase II: Three-Dimensional Analyses

Work in Phase II includes the following tasks:

- i) Perform three-dimensional circular arc analyses for gravity loading;
- ii) Extend the MIT stability analysis method to consider the effect of horizontal earthquake loading;

- iii) Conduct three-dimensional circular arc analyses for gravity and earthquake loadings; and
- iv) Prepare a final report.

However, work on the project was initiated in September, 1988, after the data related to the project were made available to the Consultant in August, 1988.

The work presented in this report was carried out by Drs. Amr S. Azzouz and Mohsen M. Baligh of Mohsen Baligh & Associates. Assistance in computer analyses was provided by Mr. Marawan Shahien, a graduate teaching assistant in the Department of Civil Engineering, Kuwait University.

### **1.2 Scope of Report**

A final report containing the results of Phase I was submitted by the Consultant in June, 1989. This report presents the results obtained in the first task of Phase II of the program. Section 2 describes results of the three-dimensional circular arc stability analyses, and Section 3 presents the main conclusions advanced from this study.

## 2. THREE-DIMENSIONAL CIRCULAR ARC STABILITY ANALYSES

### 2.1 Geometry, Soil Properties and Pore Pressures

Three-dimensional (3-D) circular arc stability analyses for vertical gravity loading were conducted for the Ririe Dam. Figure 2.1 shows a plan view of the Ririe Dam together with a cross section taken along a curved alignment avoiding direct influence from the canyon walls. A simplified version of this cross-section (Fig. 2.2) was recommended for the stability analysis by the Army Corps of Engineers, ACE.

As can be seen in Fig. 2.2, the Dam and its foundation are divided into eight different soil layers. Designations for each of these layers, together with the soil properties provided by the ACE and required for the 3-D stability analyses are given in Table 2.1. Since the thickness of the tuffaceous sediments layer(layer 8) is unknown, it was assumed for analysis purposes that a lower boundary with significantly higher friction angle exists below an Elevation of 400 ft. Azzouz and Baligh (1989) show that this assumption has no influence on the stability calculations as the critical shear surfaces fall well above the tuffaceous sediments stratum.

Pore pressures within the Dam were defined by the ACE for purposes of stability analyses by the phreatic surface illustrated in Fig. 2.2. The dotted lines in this figure show the phreatic surface at Elevation 1110 ft to extend through the core of the Dam. Immediately to the right of the core, the phreatic surface is located at Elevation 955 ft. In between these two elevations, the phreatic surface was assumed to coincide with the right boundary of the core (see Fig. 2.2).

### 2.2 Stability Analyses

#### 2.2.1 Approach

Three-dimensional, 3-D, analysis is treated as an extension of the circular arc method (Azzouz and Baligh, 1978). Whereas the basic assumptions regarding this method are retained, the shear surface is not restricted to an infinitely long cylinder,

but is taken as a surface of revolution extending along the ground surface for a finite length,  $2L$ . The rigid body motion at failure still provides an acceptable velocity field which is necessary for obtaining upper-bound solutions.

Let us now consider the surface of revolution shown in Fig. 2.3a, which is symmetric with respect to the plane  $z = 0$ , and has a radius,  $r$ , varying along the  $z$ -axis (embankment axis), i.e.,

$$r = R(z) \quad (1)$$

The three-dimensional resisting and disturbing moments,  $M_r$  and  $M_d$ , respectively, are given by (Azzouz and Baligh, 1978):

$$M_r = \int_{z_1}^{z_2} M_r^o(z) [1 + (\frac{dR}{dz})^2]^{1/2} dz \quad (2)$$

$$M_d = \int_{z_1}^{z_2} M_d^o(z) dz \quad (3)$$

$M_r^o(z)$  and  $M_d^o(z)$  are the two-dimensional (i.e., plane strain) resisting and disturbing moments, respectively, which, for the case of 3-D analysis, are functions of the distance  $z$  along the axis of the embankment. Satisfying the overall moment equilibrium of the sliding mass about the axis of rotation ( $z$ -axis), the 3-D factor of safety,  $F$ , is thus given by:

$$F = \frac{M_r}{M_d} \quad (4)$$

In plane strain solutions,  $r$ ,  $M_r^o$ , and  $M_d^o$  are independent of  $z$ , and the surface of revolution becomes a cylinder. Consequently, the 2-D factor of safety,  $F^o$ , is expressed as follows:

$$F^o = \frac{M_r^o}{M_d^o} \quad (5)$$

The three-dimensional (or end) effects on the stability of the dam can thus be assessed by means of the ratio of the 3-D to the 2-D factors of safety ( $F/F^0$ ).

Three-dimensional analysis for the Ririe dam were carried out using the Computer Program STAB3D (Azzouz, 1977) in accordance with the MIT method (Azzouz and Baligh, 1978). The search for the minimum factor of safety is carried out in STAB3D following the same procedures adopted for the conventional two-dimensional analysis. The location of the z-axis and the function  $R(z)$  are assumed,  $F$  is computed and the process is repeated until  $F_{\min}$  is reached. Arbitrary values of the function  $R(z)$  cannot be treated in numerical computations. Instead, two classes of surfaces of revolution were considered.

The first type of shear surfaces consists of a cone attached to a cylinder (Fig. 2.3b). The cylinder has a radius,  $R_{\max}$  and a length  $2l_c$ . The cone has a height,  $l_n$ , and the total failure length is equal to  $2L$ . The second shear surface considered consists of an ellipsoid attached to a cylinder (Fig. 2.3c). The cylinder has a radius,  $R_{\max}$ , length,  $2l_c$ . The ellipsoid has a semi axis,  $l_e$  and the total failure length is  $2L$ . Knowing the shape of the shear surface, the quantity  $(dR/dz)$  can be determined and used in Eqs. 2 and 3 to estimate the three-dimensional resisting and disturbing moments, and hence the 3-D factor of safety,  $F$ .

Effective stress stability analyses represent statically indeterminate problems in which the normal effective stress along the shear surface,  $\sigma'_N$ , must be assumed in order to calculate the factor of safety. Estimates of  $\sigma'_N$  were achieved in this study by means of the MIT method. In two-dimensions, this method assumes that for each slice, the effective vertical overburden stress is a principal stress at failure. Depending on the location of the slice, the horizontal effective stress may then become either a major or a minor principal stress at failure. In three-dimensions, the longitudinal (out-of-plane) effective stress is also assumed to be a principal stress with a magnitude equals to  $K$  times the effective vertical overburden stress. Knowing the principal stresses and planes,  $\sigma'_N$  can be easily computed.

The geometry of the dam and its foundations were modelled in STAB3D by means of 58 soil lines (Azzouz and Baligh, 1989).

The submerged face of the Dam was modelled by considering the water pool in the upstream as an additional layer (layer 9 in Table 2.1) with a unit weight equal to 62.4 lb/ft<sup>3</sup> and zero friction angle. Analyses were carried out utilizing the saturated soil unit weights and a friction angle for the impervious silt core of 30°. The values of K necessary to estimate the longitudinal (out-of-plane) stress were assumed equal to the at-rest coefficient of earth pressure,  $K_0$  (see Table 2.1).

### 2.2.2 Results

Three-dimensional effective stress analyses for vertical gravity loading were performed for the three shear surfaces illustrated in Fig. 2.4. These are the same surfaces shown by the two-dimensional circular arc analyses to provide the lowest range of values of  $F^o$  (Azzouz and Baligh, 1989). Results of the 3-D analyses are presented in Table 2.2, where we note:

- 1) The three-dimensional factor of safety,  $F$ , decreases as the depth of shear surface decreases, and ranges between 3.2 to 3.6.
- 2) End effects increase the factor of safety of the dam compared to the plane strain analyses. However, this increase is rather insignificant and ranges between 1 and 5%.
- 3) The small increase in the factor of safety due to end effects is essentially due to the fact that the shear surfaces providing the lowest values of  $F^o$  and analyzed herein for 3-D effects are very shallow (Fig. 2.4). For a fixed dam length,  $2L$ , of 960 ft (see Fig. 2.1), this results in very large values of  $2L/DR$  ( $DR$  is the depth of shear surface) approaching the plane strain conditions.

### 3. SUMMARY AND CONCLUSIONS

In September, 1988, Mohsen Baligh & Associates (MBA) were contracted by the U. S. Army Corps of Engineers (ACE), Waterways Experiment Station, to undertake a study aimed at the evaluation of the stability of the Ririe Dam in Idaho under the combined effect of gravity and earthquake loadings. The work is to be undertaken in two phases, the first of which is devoted to two-dimensional (2D) analyses, while the second is concerned with the investigation of the influence of end (i.e., three-dimensional) effects on the stability of the dam. A final report containing the results of Phase I was submitted by the Consultant in June, 1989. This report presents the results of the first task in Phase II dealing with the three-dimensional (3-D) stability analysis of the dam for vertical gravity loading.

Three-dimensional analysis is treated herein as an extension of the circular arc method. Whereas the basic assumptions regarding this method are retained, the shear surface is not restricted to an infinitely long cylinder, but is taken as a surface of revolution extending along the ground surface for a finite length. Two classes of surfaces of revolution are considered. The first consists of a cone attached to a cylinder, whereas the second is composed of an ellipsoid attached to a cylinder.

Three-dimensional analyses were performed by the computer program STAB3D in accordance with the MIT method. Statical determinancy, required for the estimation of the normal effective stress along the shear surface and, hence, the calculation of the factor of safety, is achieved in the MIT method by assuming in two-dimensions that the effective vertical overburden stress is a principal stress at failure. Depending on the location along the shear surface, the horizontal effective stress may then become a major or a minor principal stress at failure. In three-dimensions, the longitudinal (out-of-plane) effective stress is also assumed to be a principal stress with a magnitude equals to K times the vertical effective stress. Knowing the principal stress and planes, the effective normal stress along the shear surface can be easily computed.

Three-dimensional analyses were performed for three circular shear surfaces using the saturated soil unit weights and a fric-

tion angle for the impervious silt core of  $30^\circ$ . Results tabulated in Table 2.2 show the following:

- 1) The three-dimensional factor of safety,  $F$ , decreases as the depth of shear surface decreases, and ranges between 3.2 and 3.6.
- 2) End effects increase the plane strain factor of safety,  $F^0$ . However, the increase is rather insignificant and varies between 1 to 5% (i.e.,  $F/F^0$  values ranging between 1.008 and 1.045).
- 3) The small increase in factor of safety due to end effects is essentially attributed to the fact that the critical shear surfaces are very shallow, thereby resulting in a 3-D failure mode approaching that of a plane strain.

REFERENCES

1. Azzouz, A. S. (1977), "Three-Dimensional Analysis of Slopes", Thesis presented to MIT in partial fulfilment for the requirements of the degree Doctor of Science, 383 p.
2. Azzouz, A. S., and Baligh, M. M. (1978), "Three-Dimensional Stability of Slopes", Research Report R78-8, Order No. 595, Department of Civil Engineering, MIT.
3. Azzouz, A. S., and Baligh, M. M. (1989), "Stability Analyses of Ririe Dam", A report submitted to the U. S. Army Corps of Engineers, Waterways Experiment Station, June, 33p.

**Table 2.1 . Soil Properties Utilized in 3-D Stability Analyses**

Layer No.	Material	Unit Weight (Pcf)	Effective Friction Angle(deg)	K <sup>(1)</sup>
1	Impervious Silt Core	125	30	0.45
2	Gravel Fill	145	48	0.40
3	Rockfill	145	48	0.40
4	Random Fill	140	45	0.40
5	Weathered Basalt/Gravel	147	50	0.40
6	Basalt	170	50	0.35
7	Silt	120	33	0.45
8	Tuffaceous Sediments	155	45	0.45
9	Water	62.4	0	1

(1) Ratio of out-of-plane effective stress to vertical effective stress

Table 2-2 : Results of 3-D Circular Arc Analysis  
for Vertical Gravity Loading

Case	Shear Surface Characteristics <sup>(1)</sup>				$F^o$ <sup>(2)</sup>	(3) DR (ft)	(4) 2L/DR	F	F/F <sup>o</sup>
	No.	OK (ft)	OY (ft)	R <sub>max</sub> (ft)					
1	2	2000	1300	200	3.168	10	96	3.19	1.008
2	3	2400	2100	1100	3.27	11	87.3	3.30	1.009
3	4	2300	1800	800	3.44	20	48	3.61	1.045

(1) See Figure 2.4

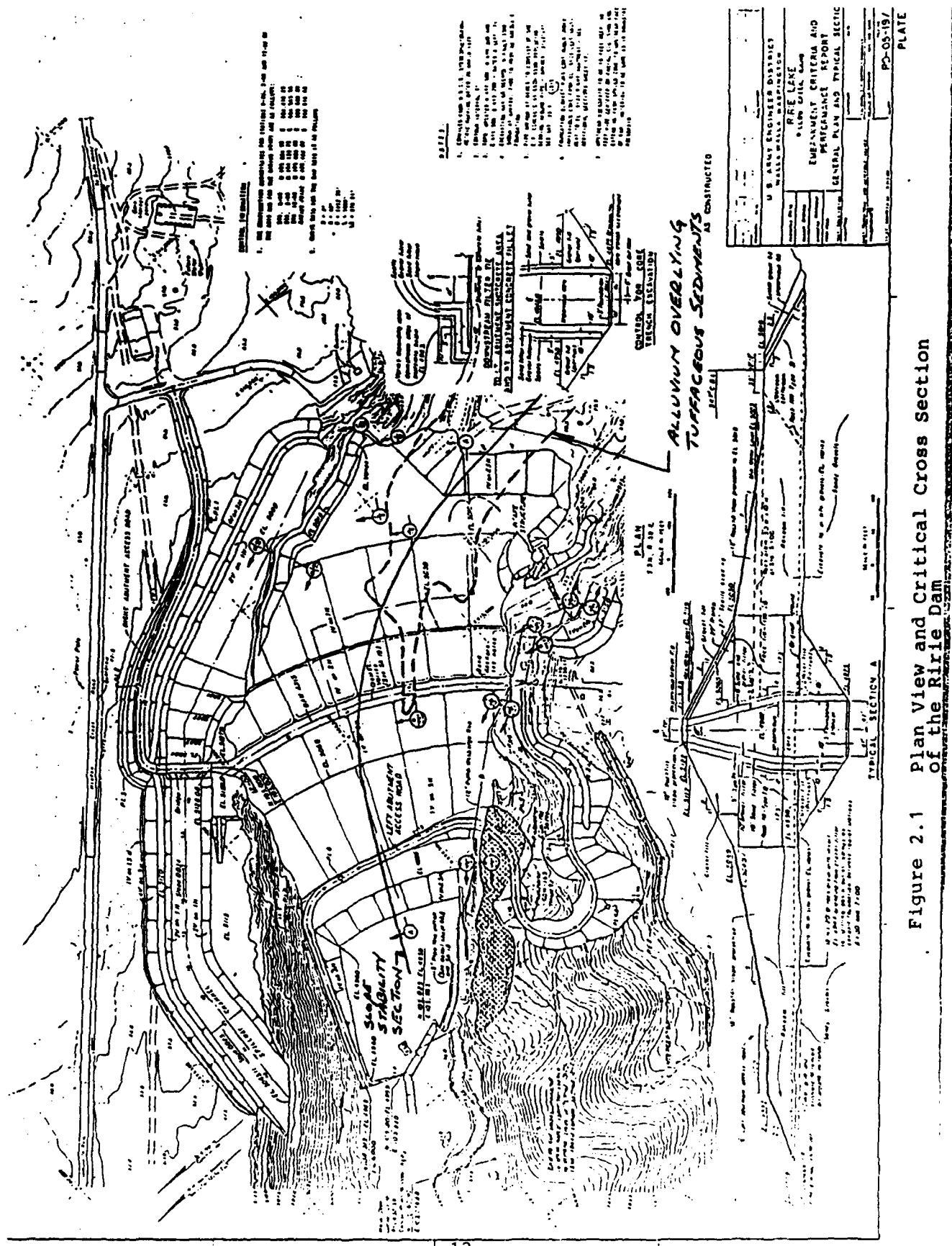
(2) From Azzouz and Baligh (1989)

(3) DR = Depth of shear surface = R<sub>max</sub> - R<sub>min</sub>

R<sub>max</sub> = maximum radius of the shear surface

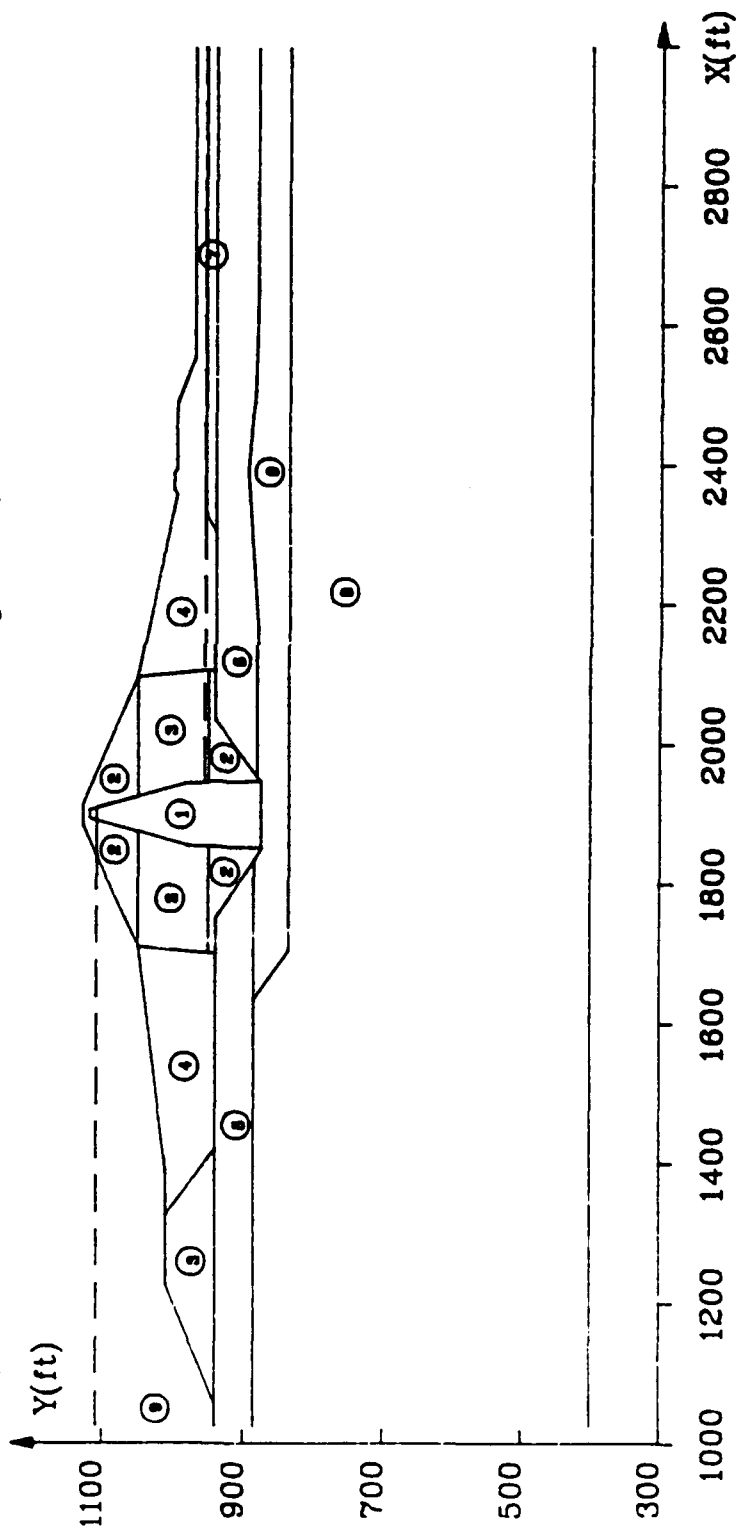
R<sub>min</sub> = minimum radius of the shear surface = radius of  
shear surface at its intersection with ground surface

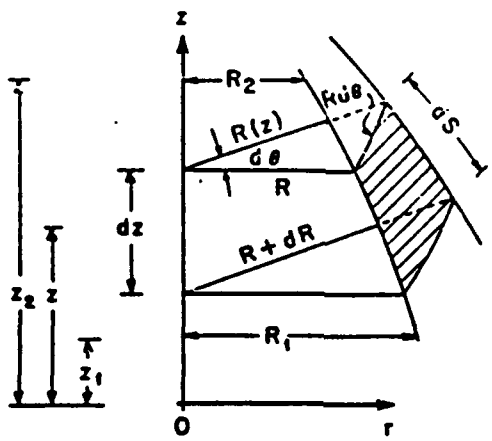
(4) 2L = Total length of dam = 960 ft (see Fig. 2.1)



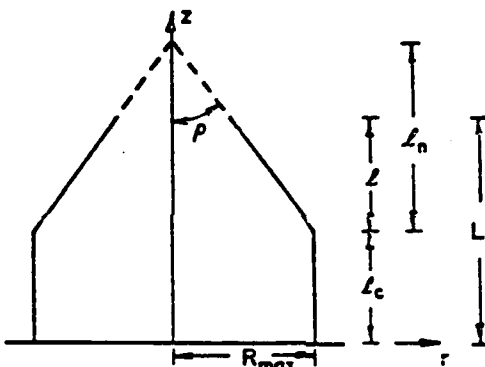
**Figure 2.1** Plan View and Critical Cross Section  
of the Ririe Dam

Figure 2.2 Idealized Cross Section, Soil Layers and Water Lines  
(See Table 2.1 for Soil Properties)

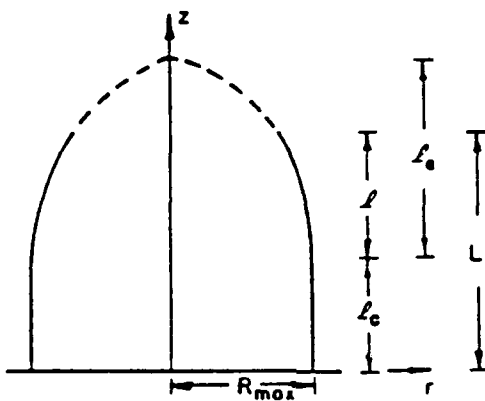




a. General Surface of Revolution



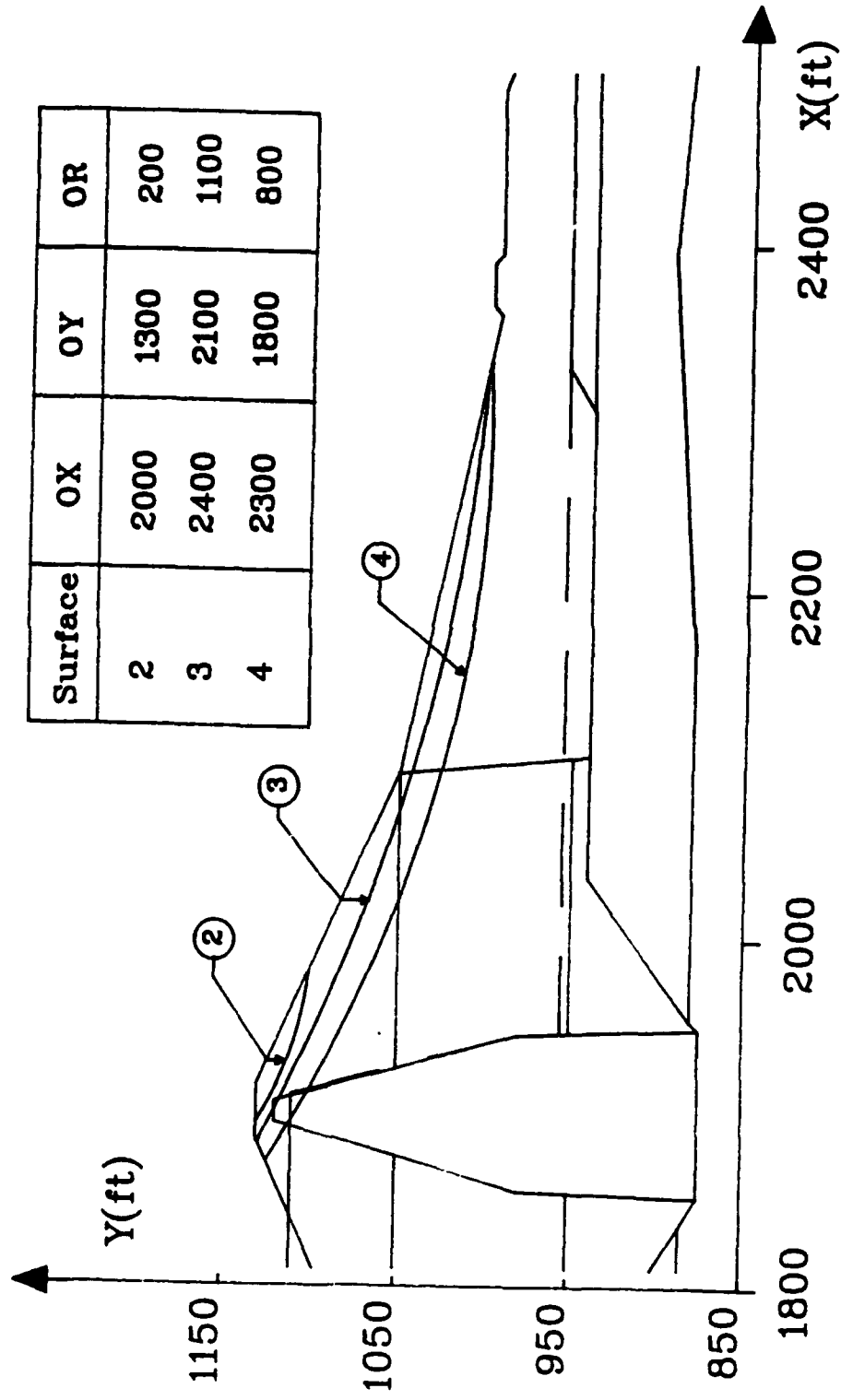
b. Cone Attached to a Cylinder



c. Ellipsoid Attached to a Cylinder

Figure 2.3 Failure Surfaces in Three-Dimensional Slope Stability (Azzouz and Baligh, 1978)

Figure 2.4 Shear Surfaces Considered for 3-D Stability Analyses



**APPENDIX C: STATIC ANALYSIS OF RIRIE DAM**  
**(Woodward-Clyde Consultants 1988)**

**STATIC ANALYSIS OF RIRIE DAM  
Bonneville County, Idaho**

**Prepared for**

**Waterways Experiment Station  
P. O. Box 631  
Vicksburg, Mississippi 39181-0631**

**Prepared by**

**Woodward-Clyde Consultants  
500 12th Street, Suite 100  
Oakland, CA 94607-4014**

**December 20, 1988**

Oakland City Center  
500 12th Street  
Suite 100  
Oakland, CA 94607-4014  
(415) 893-3600

December 20, 1988

Mr. Joseph P. Koester, CEWES-GH-R  
U.S. Army Engineer  
Waterways Experiment Station  
P.O. Box 631  
Vicksburg, Mississippi 39181-0631

Dear Mr. Koester:

**STATIC ANALYSIS OF RIRIE DAM**  
**CONTRACT NO. DACW 39-87-C-0083**  
**Final Report**

We are pleased to transmit herewith one (1) reproduction copy and five (5) additional copies of our final report on the static analysis of Ririe Dam. The report incorporates comments from your review of our draft final report.

As requested, we are transmitting under separate cover the following:

- 1) Input and output computer files on floppy diskette, and
- 2) Finite element meshes with node numbers.

The study was conducted by Ms. Katherine Fung, and Messrs. Frank Tsai and Robert Green under the direction of the undersigned. Dr. I. M. Idriss reviewed the report under the guidelines of our quality assurance program.

We look forward to continue working with you on this interesting project.

Very truly yours,

WOODWARD-CLYDE CONSULTANTS



Lelio H. Mejia, Ph.D.  
Senior Project Engineer

cc: Mr. John W. Turner  
Contracting Officer  
w/o enclosures

8710105AL/MSP

Consulting Engineers, Geologists  
and Environmental Scientists

Offices in Other Principal Cities



## ABSTRACT

This report presents the results of finite element analyses of Ririe Dam performed to evaluate long-term static stresses in the dam and its foundation. These stresses will be used in the seismic stability evaluation of the dam using the Seed-Lee-Idriss procedure and other current methods. The finite element analyses were conducted on two representative cross-sections of the dam using two-dimensional finite element procedures which model construction of the embankment in layer increments. The results of the analyses include vertical and horizontal normal effective stresses, horizontal shear stresses, and values of the ratio between horizontal shear stress and vertical normal stress. These results will be used to evaluate dynamic properties of the dam and foundation materials including pore pressure generation and cyclic strength and deformation characteristics during earthquake shaking.

## PREFACE

This report presents the results of static stress finite element analyses of Ririe Dam. The analyses constitute Phase I of a multi-phase program to analyze the seismic stability of the dam. This work was performed by Woodward-Clyde Consultants (WCC) under contract DACW39-87-C-0083 with the U.S. Army Engineer Waterways Experiment Station (WES). The work was performed by Ms. Katherine Fung, and Messrs. Robert K. Green and Frank Tsai, under the direction of Dr. Lelio H. Mejia of Woodward-Clyde Consultants. This report was reviewed by Dr. I. M. Idriss under the guidelines of WCC's quality assurance program. The report was also reviewed by Dr. Mary Ellen Hynes-Griffin and Messrs. Joseph P. Koester and David Sykora of WES. The contracting officer's representative and project coordinator for WES was Mr. Joseph Koester.

During the course of the work, preliminary results of the study were presented in 4 monthly progress reports and several discussions were held with Dr. Mary Ellen Hynes-Griffin and Mr. Joseph Koester. Previous progress report submittals included finite element meshes for static analysis of the dam and the results of one-dimensional (1-D) dynamic response analyses.

The static finite element analyses were performed using idealized cross-sections of the dam developed by WES. The material properties used in the static finite element analyses were developed on behalf of WES by Professors Tim Stark of the University of California at San Diego and H. Bolton Seed of the University of California at Berkeley. The idealized sections and material properties were transmitted to Woodward-Clyde Consultants on 25 July 1988 by Mr. Joseph Koester.

## CONTENTS

	<u>Page</u>
PREFACE.....	1
INTRODUCTION.....	3
PROJECT DESCRIPTION.....	5
Description of Dam.....	5
Construction History.....	6
ANALYSIS APPROACH.....	7
Overview.....	7
Representative Dam Sections for Analysis.....	8
Material Properties for Static Stress Analysis.....	10
Finite Element Models.....	11
SEEPAGE ANALYSIS.....	12
Methodology.....	12
Results of Seepage Analysis.....	12
STATIC STRESS ANALYSIS.....	14
Section AA.....	14
Section BB.....	16
REFERENCES.....	18
APPENDIX A	
APPENDIX B	

## INTRODUCTION

1. Ririe Dam is a 250-foot high zoned rockfill embankment partially founded on stream alluvium. A plan view of the dam is shown in Figure 1. The dam is located on Willow Creek in southeastern Idaho, about 15 miles northeast of Idaho Falls and 4 miles southeast of the town of Ririe, in Bonneville County. Construction of the dam and related facilities spanned about 10 years and was completed in early 1977.

2. The dam is located in an area which until recently was considered of moderate seismicity. Accordingly, relatively low intensity earthquake motions were considered in design studies for the dam. These studies included pseudo-static stability analyses using a seismic coefficient of about 0.05.\*

3. Local faulting identified near the Ririe Dam site during a recent re-examination of regional seismic hazard was interpreted to be capable of producing  $M_s$  7.0 motions, and the entire near-field (4-10 km) region (specifically the Grand Valley graben) was interpreted as active and capable of producing earthquakes of  $M_s$  7.5 (Krinitzsky and Dunbar, 1987), updating a previous Waterways Experiment Station report on the geology and seismicity of Ririe Dam by Patrick and Whitten (1981). A 7.5 event at a distance of 4 to 10 km could result in rock motions at the dam site with a peak horizontal acceleration of up to 1.2 g (Krinitzsky and Dunbar, 1987). Accordingly, studies have been undertaken to re-evaluate the seismic stability of the dam for these earthquake motions.

4. The seismic stability of the dam will be evaluated using various current methods including the Seed-Lee-Idriss procedure. This procedure can be summarized in the following main steps (Seed, 1983):

a. Selection of the design earthquake motions.

---

\* Personal communication, 4 February 1986, Mary Ellen Hynes-Griffin, U.S. Army Engineer Waterways Experiment Station, Vicksburg, MS.

- b. Evaluation of the static stresses in the dam and its foundation prior to the earthquake. This state of stresses corresponds to long-term conditions after consolidation of the embankment and foundation materials under gravity and reservoir loads.
- c. Computation of the dynamic stresses induced in the dam and its foundation by the selected design earthquake.
- d. Evaluation of the pore pressure generation and cyclic and post-cyclic strength and deformation characteristics of the dam and foundation materials.
- e. Based on the results of steps c and d, evaluation of the overall stability of the dam and of the deformations likely to develop.

5. This report presents the results of finite element analyses performed to evaluate static stresses in Ririe Dam and its foundation in accordance with step b. above. These static stresses will be used to evaluate dynamic properties of the dam and foundation materials such as dynamic shear moduli, and pore pressure generation and cyclic strength and deformation characteristics. Subsequent sections of the report present a description of the project, the analysis approach, and the results of the analyses.

## PROJECT DESCRIPTION

### Description of Dam

6. Ririe Dam is a zoned rockfill with a structural height of about 250 feet and a hydraulic height of about 170 feet. The dam has a crest that is 34 feet wide and 840 feet long at elevation 5128.\* Maximum pool elevation is 5119. Figure 1 shows a plan view of the embankment and related facilities. It may be seen that the longitudinal axis of the dam is curved upstream and that the dam is located in a relatively narrow canyon with a curved stream axis. The spillway is located on the right abutment and consists of a trapezoidal concrete chute. The intake tower and outlet works are located on the left abutment (see Figure 1).

7. A transverse cross-section of the dam representative of the conditions along the stream axis is shown in Figure 2. This section will be designated as section AA herein and is located as shown in Figure 1. Radial cross-sections of the dam at stations 5+00 and 8+00 (see Figure 1) are shown in Figures 3 and 4, respectively. These sections are referred to herein as sections BB and AC, respectively. As shown by these sections the dam is a zoned embankment with a vertical central core. The upstream and downstream shells consist of rockfill, gravel fill, and random fill materials (see Figure 2). Upstream and downstream slopes in the gravel fill are 2:1 while in the random fill they are 7:1 and 5:1, respectively. The upstream cofferdam used for stream diversion during construction was incorporated into the upstream shell (see Figure 2).

8. The stream alluvium was left beneath major portions of the upstream and downstream shells of the dam. The alluvium is approximately 60 to 70 feet thick and consists predominantly of dense sandy gravels with occasional interbedded discontinuous layers of loose gravel and weathered basalt. A core

---

\* All elevations in this report are given in feet (1 ft = 0.3048 m) and refer to mean sea level datum.

trench was used to provide a positive cutoff against seepage through the alluvium. The trench extends the full depth of the alluvium, is about 80 feet wide at the bottom, and has 1.5:1 side slopes (see Figure 2).

9. Figure 5 shows a cross section along the longitudinal axis of the dam. It may be seen that the stream canyon is relatively narrow and has steep side walls. The ratio between crest length and structural height of the dam is about 3. Bedrock consists of a complex sequence of basalt flows with interbedded breccia flows and clay layers, underlain by tuffaceous sediments.

#### Construction History

10. Available records (e.g. U.S. Army Engineers, 1977) indicate that construction of the dam began in July of 1967 with stripping of the right abutment. Various exploration contracts, including excavation of an exploratory adit, were awarded between 1967 and 1972. Excavation of the core trench began in May of 1973 and was completed in November of 1973. Construction of the upstream cofferdam was completed in July of 1974. Filling of the core trench began in August of 1974 and by December of the same year the embankment had reached elevation 4980. The main embankment dam was essentially complete in December of 1975. This sequence of events was used to model "construction" of the dam using incremental finite element procedures as subsequently described.

## ANALYSIS APPROACH

### Overview

11. The approach used to perform the static finite element analyses of Ririe Dam may be summarized in the following steps:

- a. Selection of representative idealized cross-sections of the dam for analysis.
- b. Evaluation of material properties representative of the stress-strain behavior under long-term static loading of the various embankment and foundation materials.
- c. Development of finite element models for the idealized sections selected in step a.
- d. Evaluation of seepage forces due to reservoir loading.
- e. Computation of static stresses in the dam using suitable finite element procedures and input from steps b, c and d.

12. The static stress finite element analyses were conducted using the computer program FEADAM84 (Duncan et al., 1984) which is a modified version of the program FEADAM developed at the University of California at Berkeley (Duncan et al., 1980b). This is an incremental finite element program for two-dimensional plane strain analysis of earth and rockfill dams and slopes. The program allows modeling construction of the dam in layer increments. It uses the nonlinear hyperbolic soil model developed by Duncan et al. (1980a). This soil model incorporates key aspects of the constitutive behavior of soils under static loading such as stress-strain nonlinearity, stress dependency of bulk and elastic moduli, and unloading-reloading behavior.

13. To simulate long term conditions, the stress analysis was conducted using drained material properties. Buoyant unit weights were used to simulate submergence of materials below the phreatic line and seepage forces in the core were used to simulate reservoir loads. This procedure has been previously used successfully in several similar studies (e.g., Marcuson and Krinitzky, 1976; Hynes-Griffin et al., 1988) and has been shown to yield

static stresses in agreement with field measurements and the results of more sophisticated procedures (California Department of Water Resources, 1979; Quigley et al., 1976).

#### Representative Dam Sections for Analysis

14. Ririe Dam is a three-dimensional (3-D) structure located in a relatively narrow canyon with a curved stream axis (see Figures 1 and 5). Thus, 3-D behavior is expected to play a significant role in the seismic stability of the dam. However, in view of the significant expense associated with a full 3-D seismic stability analysis, two-dimensional (2-D) analyses of representative sections of the dam with appropriate corrections for 3-D effects will be used to evaluate the seismic stability of the dam.

15. In current engineering practice, the maximum cross-section of a dam and one or more smaller cross-sections, are typically used to assess the overall dynamic response of the dam. In the case of Ririe Dam, the stream axis of the canyon is curved and the maximum section through the approximate midpoint of the crest, section AC in Figure 1, abuts upstream against the right wall of the canyon (see Figure 4). Because the predominant mode of vibration of the dam is likely to display a tendency to follow the general direction of the stream axis, section AC is not likely to be representative of this mode of deformation. A section likely to be more representative of this deformation mode is the section along the stream axis, section AA on Figure 2.

16. On the above basis, section AA has been selected for seismic stability analysis of Ririe Dam. The quarter section towards the left abutment, section BB, has also been selected to evaluate the seismic stability of the dam. Accordingly, these two sections have been used in the static finite element analyses of the dam. Additional analyses may be performed in the future using other sections if subsequent dynamic analysis results indicate it to be necessary.

17. Cross-sections AA and BB were idealized for analysis as shown in Figures 6 and 7, respectively. It should be noted that these Figures have been transposed with respect to Figures 2 and 3, so the reservoir is on the left hand side of the figure in accordance with current Corps of Engineers practice.\* The layers of basalt, upper tuffaceous sediments, and lower tuffaceous sediments, shown in Figures 6 and 7, were not modeled in the static analysis in view of the fact that under static loading they can be assumed to be rigid when compared to the overlying embankment.

18. The filter and drain zones upstream and downstream of the silt core and upstream of the cofferdam rockfill are expected to have similar material properties to the adjacent rockfill and gravel fill and are not expected to have a significant effect on the overall behavior of the dam. Therefore, they were not modeled as individual zones but were lumped with the adjacent rockfill and gravel fill.

19. The alluvium foundation contains occasional isolated discontinuous layers of loose gravel and weathered basalt. However, the overall static behavior of this zone is likely to be controlled by the dense alluvium gravel. Accordingly, layers of loose gravel and weathered basalt were not modeled in the analyses and material properties for dense gravels were used throughout the foundation.

20. Based on the history of reservoir levels since construction, a reservoir elevation of 5112 will be used for seismic stability evaluation of the dam. This reservoir elevation and a tail water elevation of 4955 were used in the static stress analyses of the dam.

---

\* Personal communication, Joseph P. Koester, Waterways Experiment Station, Vicksburg, Mississippi.

### Material Properties for Static Stress Analysis

21. The nonlinear behavior of the embankment and foundation soils under static loading was modeled using the hyperbolic soil model developed by Duncan et al. (1980a). This model incorporates stress dependent bulk and Young's moduli, accounts for the dependence of Young's modulus on stress level and can be used to simulate unloading-reloading behavior.

22. Table 1 presents the hyperbolic soil parameters used in the static finite element analyses of Ririe Dam. These parameters were evaluated based on 1) laboratory and field data including in situ test data from Becker hammer soundings, SPT borings, and geophysical surveys, and 2) comparisons with a database for over 150 soils published by Duncan et al. (1980a). Table 1 also presents saturated, moist, and buoyant unit weights, and the values of the static stress ratio,  $K_0$ , and of the dynamic modulus factor  $K_{2\max}$ .

23. In addition to the parameters shown in Table 1, the unloading-reloading modulus number,  $K_{ur}$ , was used in the analyses. Values of this parameter were estimated based on data presented by Clough and Duncan (1969) and by Duncan et al. (1980a). The unloading-reloading modulus number,  $K_{ur}$ , was assumed to be 1.5 times the loading value,  $K$ , for the silt core and alluvium silt, and 1.3 times  $K$  for all other embankment and foundation zones. These estimates are reasonable in the absence of any other available data.

24. The hyperbolic parameters shown in Table 1 correspond to drained loading conditions. With the exception of unit weights, the same parameters were used in saturated and unsaturated zones of the dam. That is, no difference was considered in the stress-strain behavior of saturated and dry materials. It is recognized that this is an approximation since the behavior of dry and submerged rockfill and gravel fill can be significantly different, particularly with respect to deformation and compressibility. However, in view of the limited data available, this assumption was considered reasonable and likely to have a relatively small effect on the computed stresses. Although the above assumption could significantly affect computed static

deformations, they are of no particular interest in this study. Buoyant unit weights were used for submerged portions of the embankment and foundation, while moist unit weights were used in the other zones of the dam.

25. The properties for dense sandy gravel shown in Table 1 were used to model the behavior of the foundation alluvium except in the silt layer beneath the downstream toe of the dam where the alluvium silt properties were used. Isolated lenses of loose sandy gravel and weathered basalt were not modeled as discussed above.

#### Finite Element Models

26. The finite element models for the static stress analysis of sections AA and BB are shown in Figures 8 and 9, respectively. The model for section AA has a total of 624 elements and 651 nodes while that for section BB has 414 elements and 446 nodes. A rigid base was assumed at the interface between the alluvium foundation, and the underlying tuffaceous sediments and basalt bedrock. Nodal points on the upstream and downstream end boundaries were constrained to move only vertically.

27. The finite element models were designed to allow proper modeling of the construction sequence of the embankment and to incorporate all significant material zones in the dam. A relatively fine mesh was used near the core trench slopes where significant stress concentrations and gradients were anticipated. The meshes were designed to also be used in the dynamic finite element analysis of the dam. Thus, the design of the meshes was controlled by the need for adequate representation of the predominant modes of vibration of the structure and the need for adequate seismic wave propagation in the range of frequencies of interest to the earthquake response of the dam.

## SEEPAGE ANALYSIS

### Methodology

28. A seepage analysis using the computer program SEEP (Wong and Duncan, 1985) was used to compute seepage forces in the core of Ririe Dam. The program SEEP is a finite element code for the analysis of steady state confined and unconfined flow through porous media. For convenience, the finite element meshes used in the seepage analysis correspond to the meshes used in the core for the static stress analysis. These meshes are shown in Figures 10 and 11 for section AA and BB, respectively.

29. Little data are available on the permeability of the core materials. Laboratory tests on compacted specimens conducted during design yielded permeability values on the order of  $1 \times 10^{-6}$  feet per minute (U.S. Army Engineers, 1978). This value was assumed representative of the vertical coefficient of permeability for the core,  $k_v$ . For embankments of compacted uniform fine grained soils the ratio between horizontal and vertical permeability  $k_h/k_v$  is typically less than about 4 (Sherard et al., 1963). On this basis, a ratio of horizontal to vertical permeability  $k_h/k_v$  of 3 was used in the analyses. It should be noted that parametric analyses using a  $k_h/k_v$  ratio of 1 indicated that the computed seepage forces are not very sensitive to this assumption. In view of the fact that the purpose of the seepage analysis is to evaluate seepage forces as opposed to flow quantities or accurate flow patterns, it can be concluded that the above assumptions regarding  $k_v$  and  $k_h/k_v$  are not critical.

### Results of Seepage Analysis

30. The results of the seepage analysis are summarized in Figures 12 and 13 for sections AA and BB, respectively. These figures show equipotential lines computed from the analysis. For simplicity, flow lines are not shown. However, they can be inferred from the figures since they are normal to the equipotential lines. As shown in Figure 12, the computed seepage pattern corresponds to essentially horizontal flow below elevation 4955 and horizontal

and vertical flow above this elevation. The flow pattern for section BB (see Figure 13) is very similar to that computed for section AA above elevation 4955. Very limited piezometric data are available in the core of the dam to permit a meaningful comparison with the computed results.

31. The computed values of hydraulic head were used to calculate seepage forces in the core using the computer program SFORCE developed at the University of California at Berkeley (Chang, 1975). The computed forces were applied in increments to nodal points in the core after numerical "construction" of the dam as subsequently described.

## STATIC STRESS ANALYSIS

### Section AA

32. The static stress analysis of section AA was conducted in four main steps in order to simulate the construction sequence of the dam. These four steps were as follows:

- a. Evaluation of the stresses in the alluvium foundation after excavation of the core trench. These stresses were evaluated by "building up" the foundation on both sides of the core trench one layer at a time. A total of seven construction increments were used.
- b. Construction of the upstream cofferdam in four increments.
- c. After construction of the cofferdam, the core trench was filled and the embankment shells were placed over the pre-existing foundation in 20 increments.
- d. Application of seepage forces in the core in three increments. Three increments were used in this step because it was found that use of one increment resulted in very large changes in stress in the upstream and downstream shells of the dam and the development of large mobilized strengths in localized zones of the upstream shell.

33. The results of the static stress analyses for section AA are presented in Figures 14 through 17. Figures 14 and 15 show contours of vertical and horizontal normal effective stresses,  $\sigma_y$  and  $\sigma_x$ , respectively. Figure 16 shows contours of horizontal shear stress,  $\tau_{yx}$ , while Figure 17 shows contours of the ratio between horizontal shear stress and vertical normal effective stress,  $\tau_{yx}/\sigma_y$ , also known as the alpha ratio ( $\alpha$ ) (Seed, 1983). Other results, such as principal stresses, principal stress ratios, and stress levels are presented in Table A-1 in Appendix A in accordance with the element numbering system shown in Figure A1.

34. It may be seen from Figure 14 that the calculated vertical effective stresses in the upstream and downstream shells of the dam are approximately equal to the effective overburden pressure at a given point. This result is

typical even for dams with slopes steeper than those of Ririe Dam. Vertical stresses in the upstream shell are lower than those in the downstream shell due to submergence. Vertical stresses in the core are lower than in the adjacent shells due to the tendency for the compressible core to arch between the stiffer shells. It can also be seen that there is a tendency for the more compressible random fill to "hang" from the stiff gravel and rockfill shells.

35. Relatively high stresses, on the order of 24 ksf, are computed at the base of the alluvium foundation downstream of the core trench (see Figure 14). Localized arching appears to occur within the gravel fill at the bottom of the core trench immediately downstream of the core. The reasons for this low stress concentration may include the large difference in compressibility between the gravel fill and the adjacent alluvium dense sandy gravel (see Table 1). This difference in compressibility results in a tendency for the gravel fill to hang from the slope of the core trench as the fill compresses under the weight of the overlying embankment.

36. Figure 15 shows contours of horizontal effective stress,  $\sigma_x$ , throughout the dam. It may be seen that horizontal stresses in the downstream shell of the dam are significantly higher than those in the upstream shell. This is the result of two main factors: 1) the thrust action of seepage forces in the core, and 2) the effects of submergence. The thrust of seepage forces in the core acts to reduce horizontal normal stresses in the upstream shell, and to increase horizontal stresses in the downstream shell. The reduction in horizontal stresses is most pronounced in the gravel fill within the core trench immediately upstream of the core. This reduction is not accompanied by a proportional reduction in vertical effective stresses. As a result, relatively high stress levels (i.e., mobilized strengths) are developed in a significant number of elements in the rockfill and gravel fill immediately upstream of the core.

37. Figure 16 shows contours of horizontal shear stress,  $\tau_{yx}$ . It may be seen that horizontal shear stresses are significantly larger in the downstream shell than in the upstream shell. As is the case with horizontal effective stresses, this is the result of the thrust of seepage forces in the core and

of submergence. A relatively small zone of negative shear stresses develops in the foundation immediately upstream of the core trench. This appears to be the result of the thrust action of the seepage forces in the core in view of the fact that shear stresses in this zone are of positive sign before seepage forces are applied.

38. Contours of the ratio between horizontal shear stress and vertical effective stress,  $\tau_{yx}/\sigma_y$ , are shown in Figure 17. Computed values of this ratio vary between 0 and  $\pm 0.2$  throughout most of the embankment and foundation. Values of 0.3 and 0.4 are obtained in a localized area of the gravel fill slope in the downstream shell of the dam.

#### Section BB

39. The static stress finite element analysis for section BB was conducted in four main steps as follows:

- a. Computation of the static stresses in the foundation prior to placement of the embankment by "building up" the foundation in seven layers.
- b. Placement of the upstream cofferdam in three layers.
- c. Construction of the embankment in 13 layers.
- d. Application of seepage forces in the core in three increments.

40. The results of the analysis are summarized in Figures 18 through 21. Detailed results of the analysis are presented in Table B-1 in accordance with the element numbering scheme shown in Figure B1 in Appendix B.

41. Figure 18 shows contours of vertical effective stress,  $\sigma_y$ . In general, it may be seen from Figures 14 and 18 that there is a striking similarity between computed vertical stresses for sections AA and BB in the embankment above elevation 4955 (i.e., above the foundation). Contours of horizontal normal effective stress,  $\sigma_x$ , are shown in Figure 19. The pattern

of computed horizontal stresses is very similar to that computed for section AA (see Figure 15).

42. Figures 20 and 21 show contours of horizontal shear stresses,  $\tau_{yx}$ , and contours of the ratio between horizontal shear stress and vertical normal effective stress,  $\tau_{yx}/\sigma_y$ . As shown in Figure 20, there is a reversal in the sign and a concentration of shear stresses along the steep bedrock slope on the downstream side of the alluvium foundation. This results from the tendency of the alluvium to hang from the rigid bedrock as the foundation compresses under the weight of the overlying embankment.

43. The stresses presented in Figures 14 through 21 will be used to evaluate dynamic properties including cyclic resistance for seismic stability evaluation of Ririe Dam. The computed effective stresses will be used to compute values of mean effective stress which, together with values of the dynamic modulus factor,  $K_2^{\max}$ , will be used to evaluate dynamic shear moduli of the embankment and foundation materials. Similarly, computed vertical effective stresses and values of the alpha ratio,  $\tau_{yx}/\sigma_y$ , will be used to evaluate pore pressure generation and cyclic strength and deformation characteristics during earthquake shaking.

## REFERENCES

- California Department of Water Resources, 1979. "The August 1, 1975 Oroville Earthquake Investigations," Bulletin No. 203-78, Department of Water Resources, California.
- Chang, C. S. 1975. "Users Guide for Program SFORCE," Department of Civil Engineering, University of California, Berkeley, CA, July.
- Clough, G. W., and Duncan, J. M. 1969. "Finite Element Analyses of Port Allen and Old River Locks," Report No. TE69-13, University of California, Berkeley, CA.
- Duncan, J. M., Byrne, P., Wong, K. S., and Mabry, P. 1980a. "Strength, Stress-Strain and Bulk Modulus Parameters for Finite Element Analyses of Stresses and Movements in Soil Masses," Report No. UCB/GT/80-01, Department of Civil Engineering, University of California, Berkeley, CA.
- Duncan, J. M., Wong, K. S., and Ozawa, Y. 1980b. "FEADAM: A Computer Program for Finite Element Analysis of Dams," Report No. UCB/GT/80-02, Department of Civil Engineering, University of California, Berkeley, CA.
- Duncan, J. M., Seed, R. B., Wong, K. S., and Ozawa, Y. 1984. "FEADAM84: A Computer Program for Finite Element Analysis of Dams," Research Report No. SU/GT/84-03, Stanford University, Stanford, CA.
- Hynes-Griffin, M. E., Wahl, R. E., Donaghe, R. T., and Tsuchida, T. 1988. "Seismic Stability Evaluation of Folsom Dam and Reservoir Project," Technical Report GL-87-14, U. S. Army Engineer Waterways Experiment Station, Vicksburg, Mississippi.
- Krinitzsky, E. L., and Dunbar, J. B. 1987. "Geological and Seismological Evaluation of Earthquake Hazards at Ririe Dam, Idaho," Draft report to U.S. Army Engineer District, Walla Walla, U.S. Army Engineer Waterways Experiment Station, Vicksburg, Mississippi.
- Marcuson, W. F., III and Krinitzsky, E. L. 1976. "Dynamic Analyses of Fort Peck Dam," Technical Report S-76-1, U. S. Army Engineer Waterways Experiment Station, Vicksburg, Mississippi.
- Patrick, D.M. and Whitten, C.B., 1981. "Geological and Seismological Investigations at Ririe Dam, Idaho," Miscellaneous Paper GL-81-7, U.S. Army Engineer Waterways Experiment Station (WES), Vicksburg, MS.
- Quigley, D. W., Duncan, J. M., Caronna, S., Moroux, P. J., and Chang, C. S. 1976. "Three-dimensional Finite Element Analyses of New Melones Dam," Report No. TE 76-3, Department of Civil Engineering, University of California, Berkeley, California.
- Seed, H. B. 1983. "Earthquake Resistant Design of Earth Dams," Proceedings of ASCE symposium on seismic design of embankments and caverns, 41-64, Philadelphia.

Sherard, J. L., Woodward, R. J., Gizienski, S. F., and Clevenger, W. A. 1963. Earth and Earth Rock Dams, 725 pp., Wiley, New York.

U. S. Army Corps of Engineers. 1977. "Historical Report on Construction of Ririe Lake, Idaho," Walla Walla District, April.

U.S. Army Corps of Engineers. 1978. "Embankment Criteria and Performance Report, Rire Dam," Walla Walla District, April.

Wong, K. S., and Duncan, J. M. 1985. "SEEP: A Computer Program for Seepage Analysis of Saturated Free Surface or Confined Steady Flow," Department of Civil Engineering, Virginia Tech, Blacksburg, Virginia.

**Table I**  
**Estimated Material Properties for Static Analysis of Ririe Dam**

Material Location	Saturated/ Dry unit weight (pcf)	Young's Modulus (psi)	Young's Modulus/ Unit Weight (pcf)	Unloading Exponent	K	n	Rf	Rb	m	Change in f Per Lag			Static Stress Ratio	Shear Modulus	
										Bulk Modulus	Cohesion	Friction Angle	(k <sub>0</sub> ) (k <sub>1</sub> )	(degrees)	k <sub>0</sub>
In pervious Silt Core	125/63	120	700	0.65	0.6	520	0.3	0	0	35	5	35	0.45	55	
Gravel Fill	145/83	135	1400	0.45	0.7	500	0.3	0	0	45	6	6	0.4	120	
Rockfill	165/83	135	1000	0.35	0.7	500	0.3	0	0	45	6	6	0.4	120	
Random Fill	140/73	130	700	0.45	0.7	255	0.3	0	0	45	6	6	0.4	65	(H1)60<=25
Alluvium															
I.) Silt	120/58	112	425	0.5	0.7	205	0.3	0	0	33	6	33	0.45	50	(H1)60<=20
II.) Coarse Sandy Gravel	135/73	135	500	0.5	0.8	255	0.3	0	0	43	6	6	0.4	80	(H1)60<=16
III.) Dense Sandy Gravel	144/82	144	1400	0.5	0.7	1300	0.3	0	0	48	6	6	0.4	100	(H1)60<=30
IV.) Weathered Basalt/ Gravel	167/75	147	1600	0.5	0.7	1300	0.3	0	0	50	6	6	0.4	150	(H1)60<=30
Bedrock	170/108	170	2000	0.4	0.7	1400	0.3	0	0	50	0	0	0.35	N/A	v <sub>0</sub> =3000 f <sub>0</sub>
Turfaceous Sediments	155/73	155	1000	0.45	0.9	520	0.3	0	0	45	6	6	0.45	N/A	v <sub>0</sub> =1600 & 2500

Estimated Material Parameters for Static and Dynamic Analyses of Ririe Dam by Woodard-Clyde Consultants  
 T.O. Stark 7/25/88 Edited by H.S. Seed 7/22/88

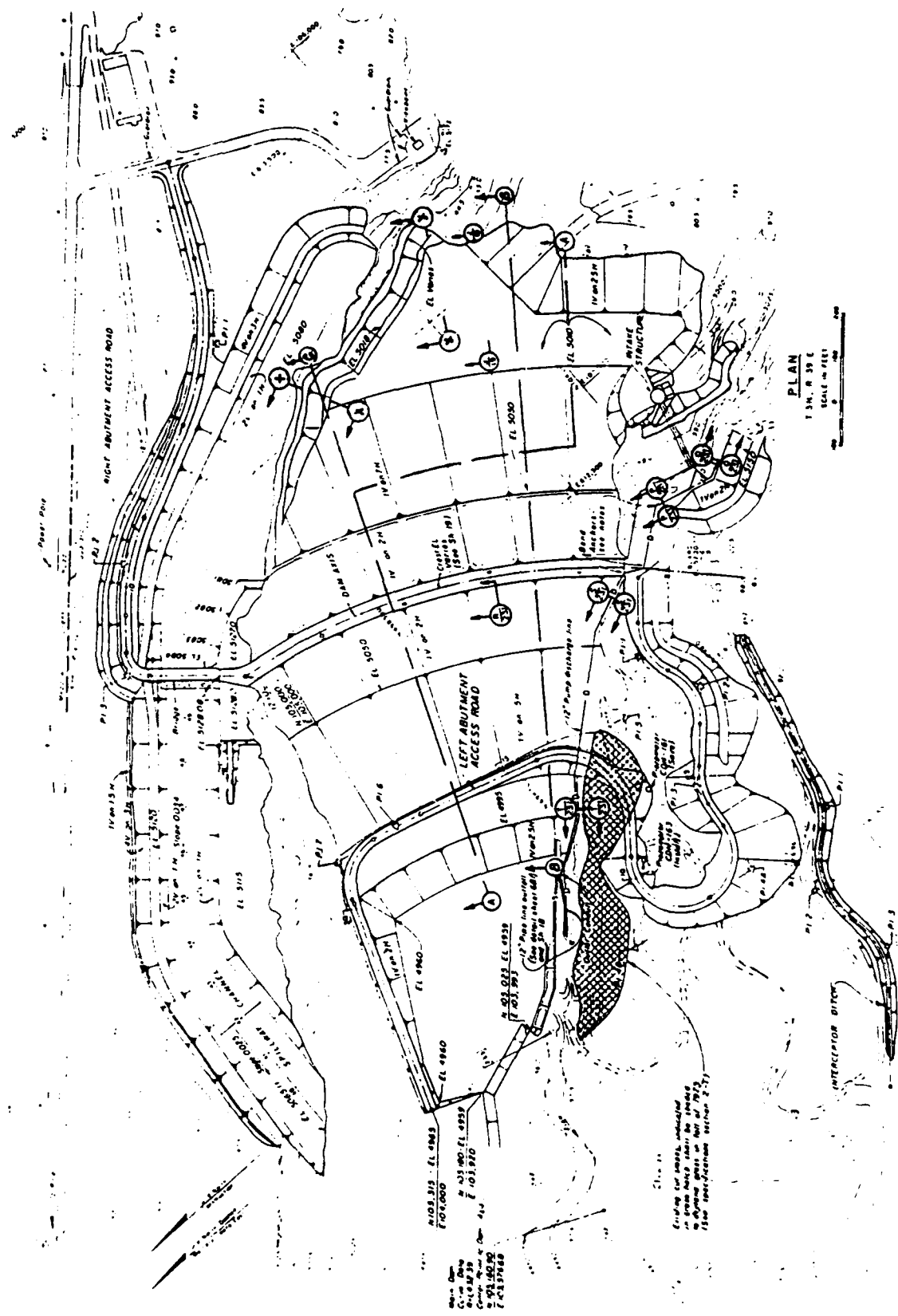


Figure 1. Plan view of Ririe Dam

**SECTION AA**

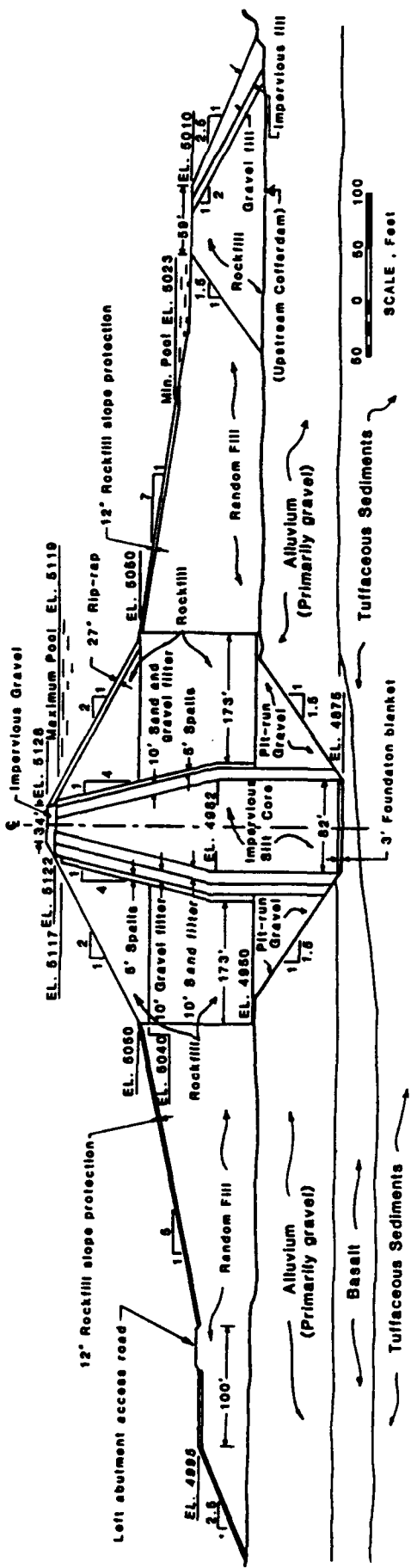


Figure 2. Cross-section of dam along stream axis

SECTION 88

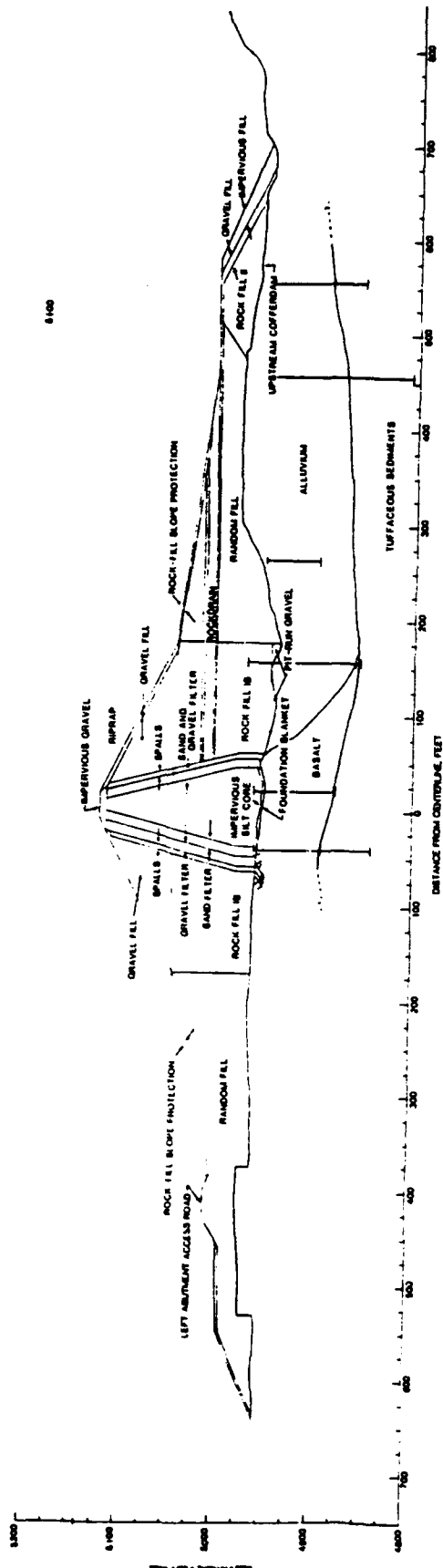


Figure 3. Radial cross-section of dam at station 5+00

SECTION AC

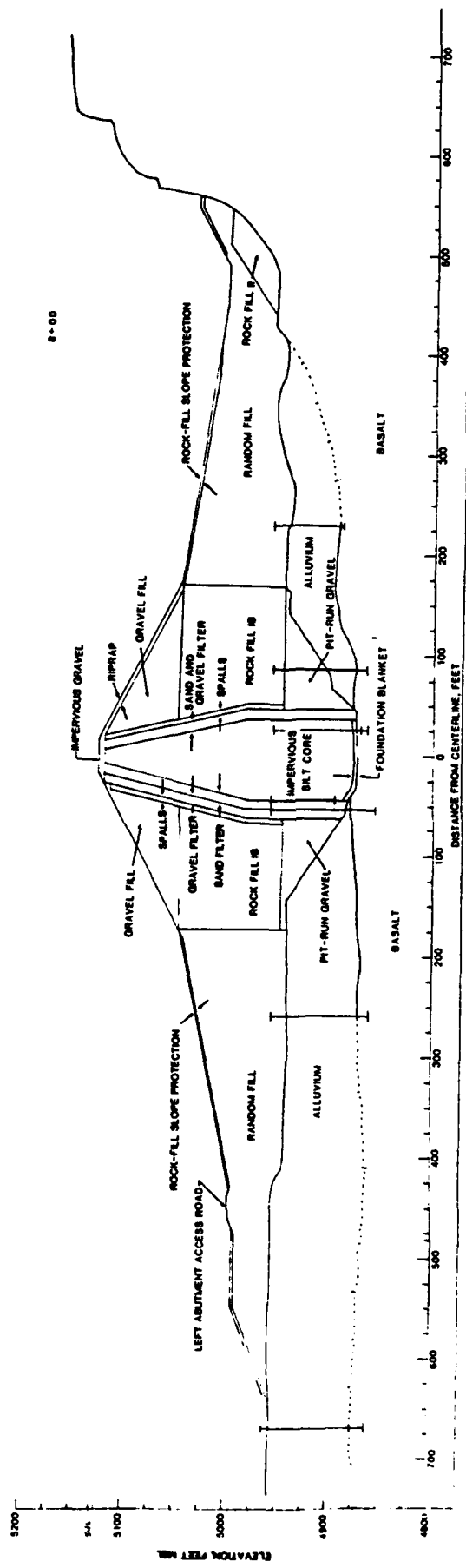


Figure 4. Radial cross-section of dam at station 8+00

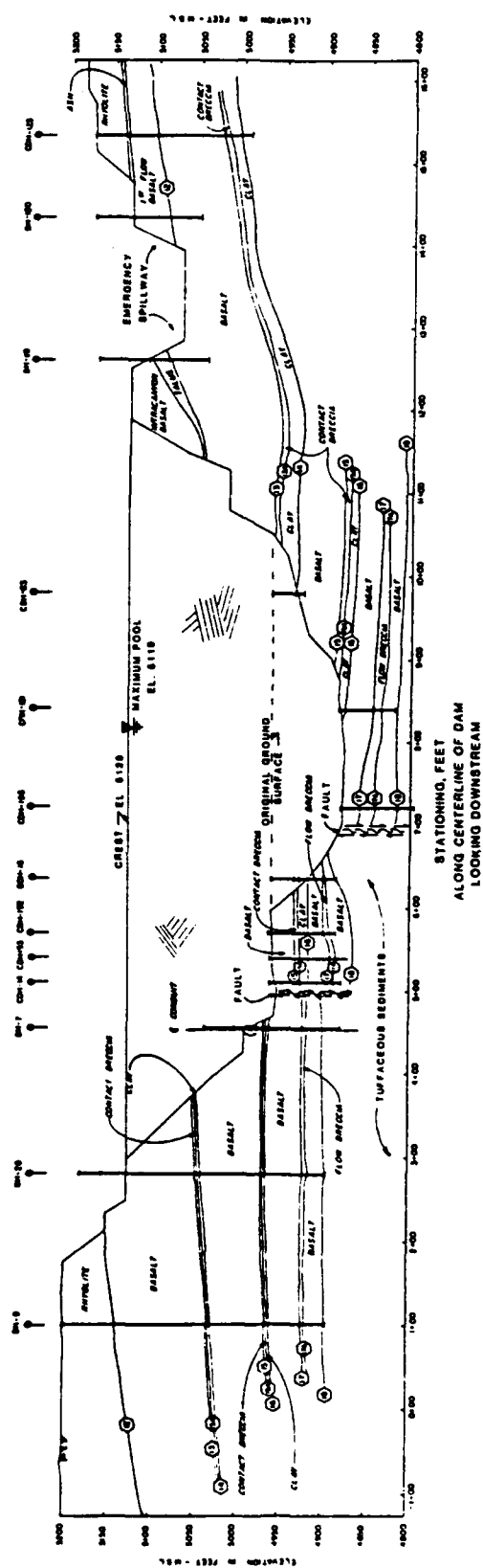
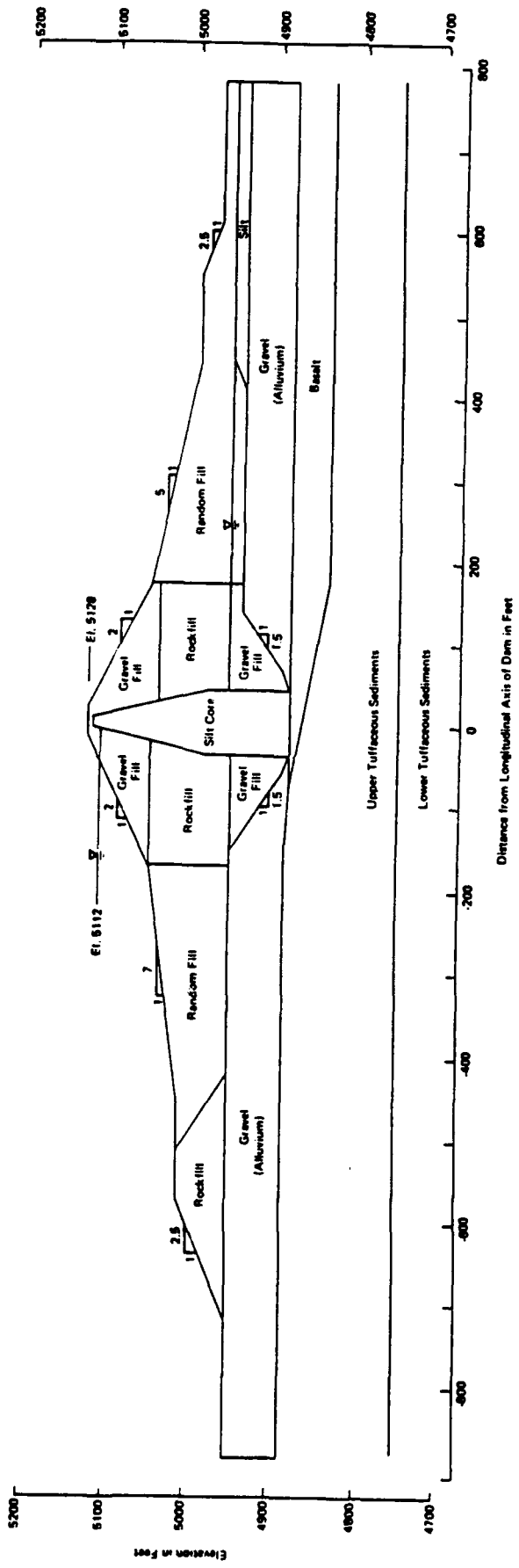


Figure 5. Cross-section along longitudinal axis of dam



**Figure 6.** Idealized section AA for analysis

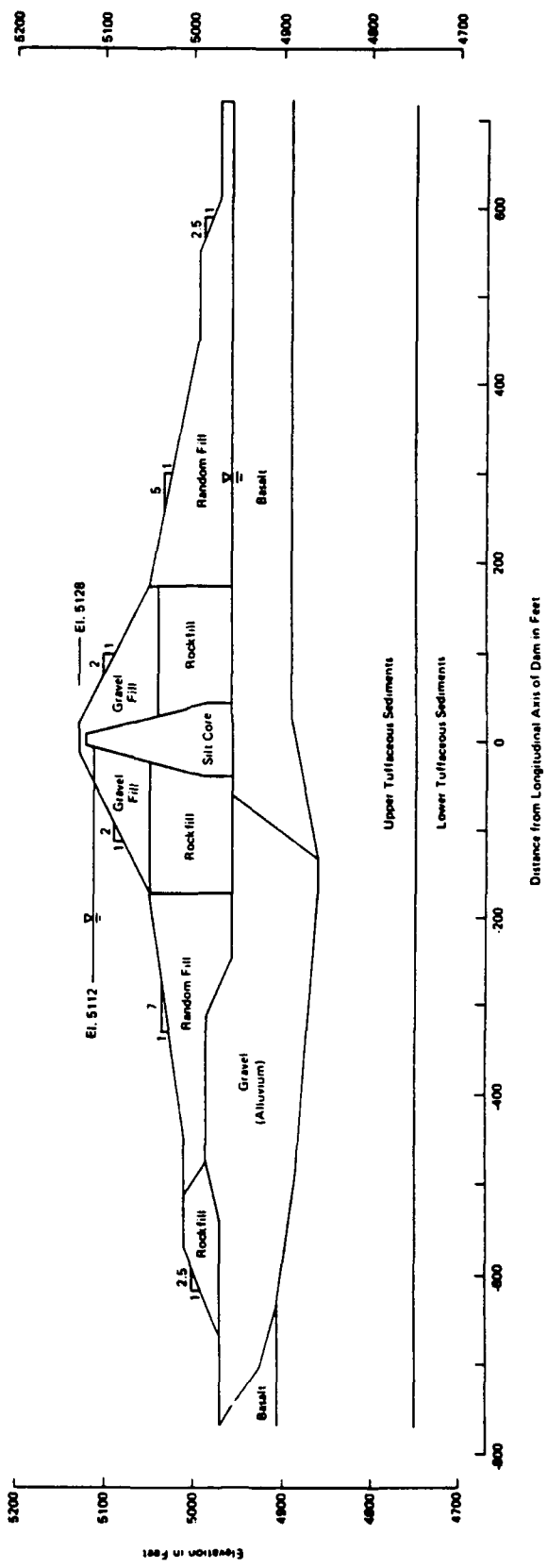


figure 7. Idealized section BB for analysis

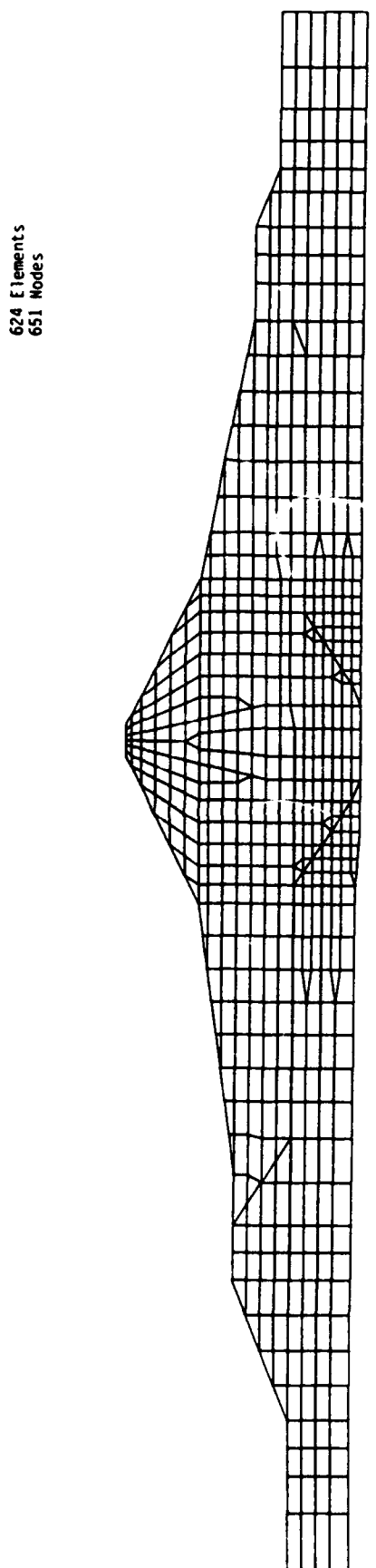


Figure 8. Finite element mesh for static analysis of section AA

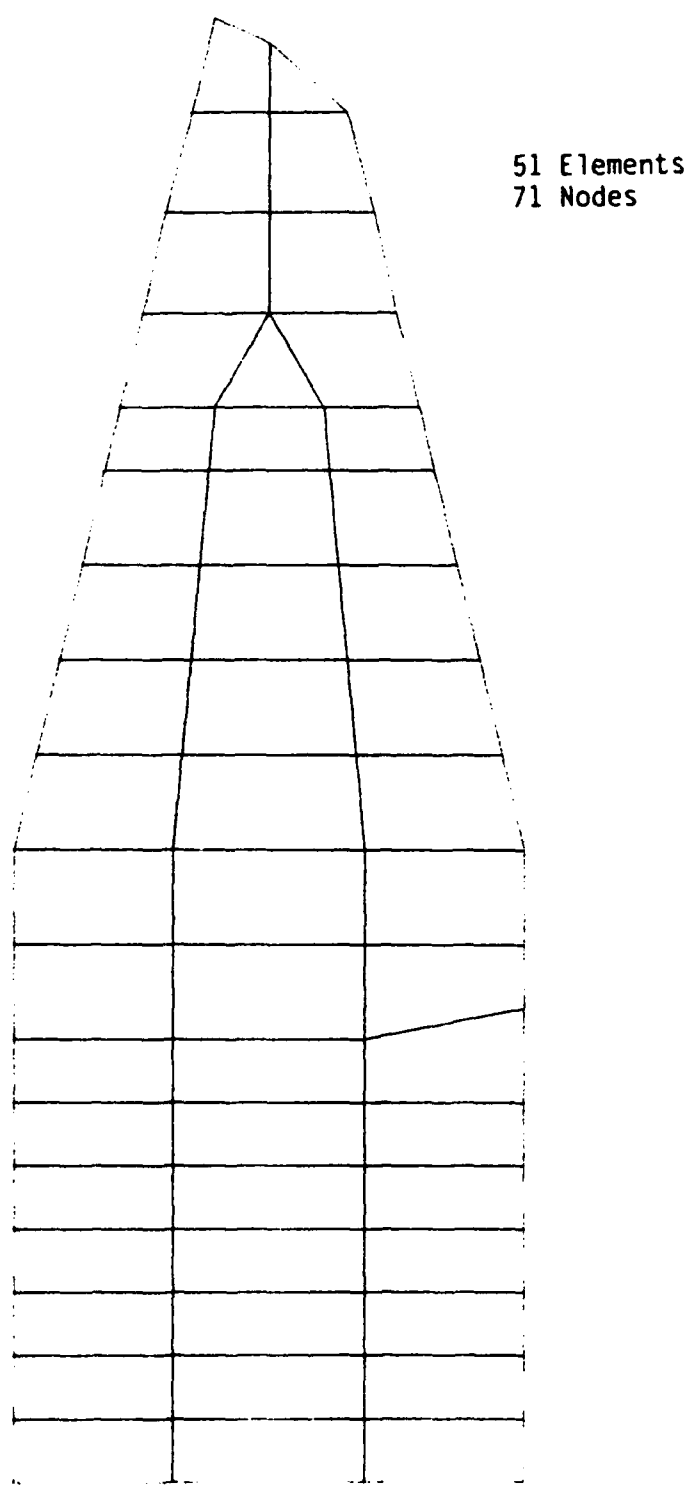


Figure 10. Finite element mesh for seepage analysis of section AA

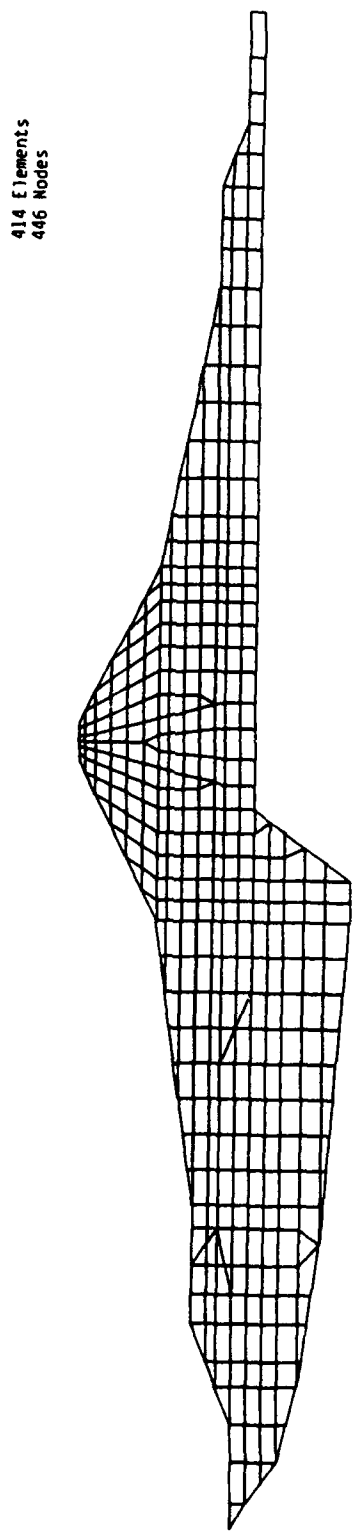


Figure 9. Finite element mesh for static analysis of section 88

30 Elements  
43 Nodes

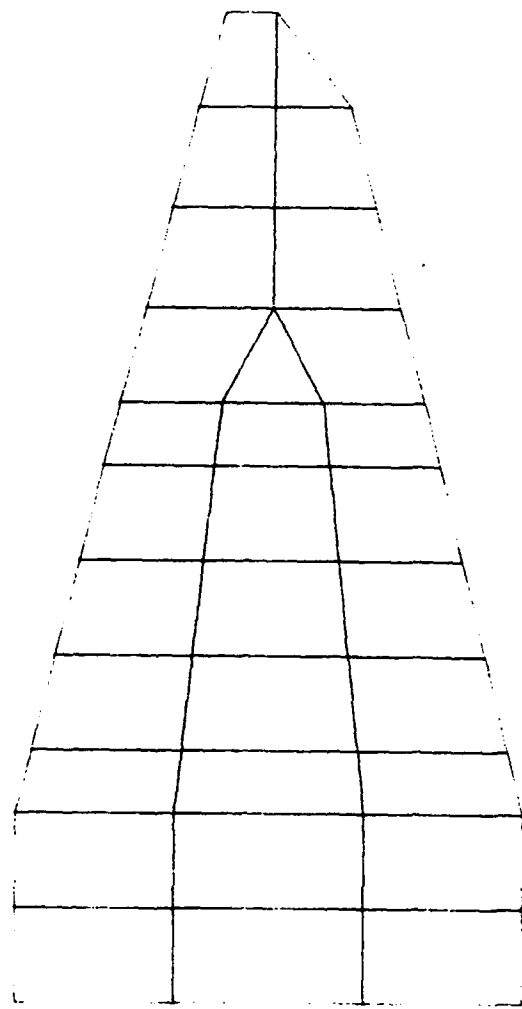
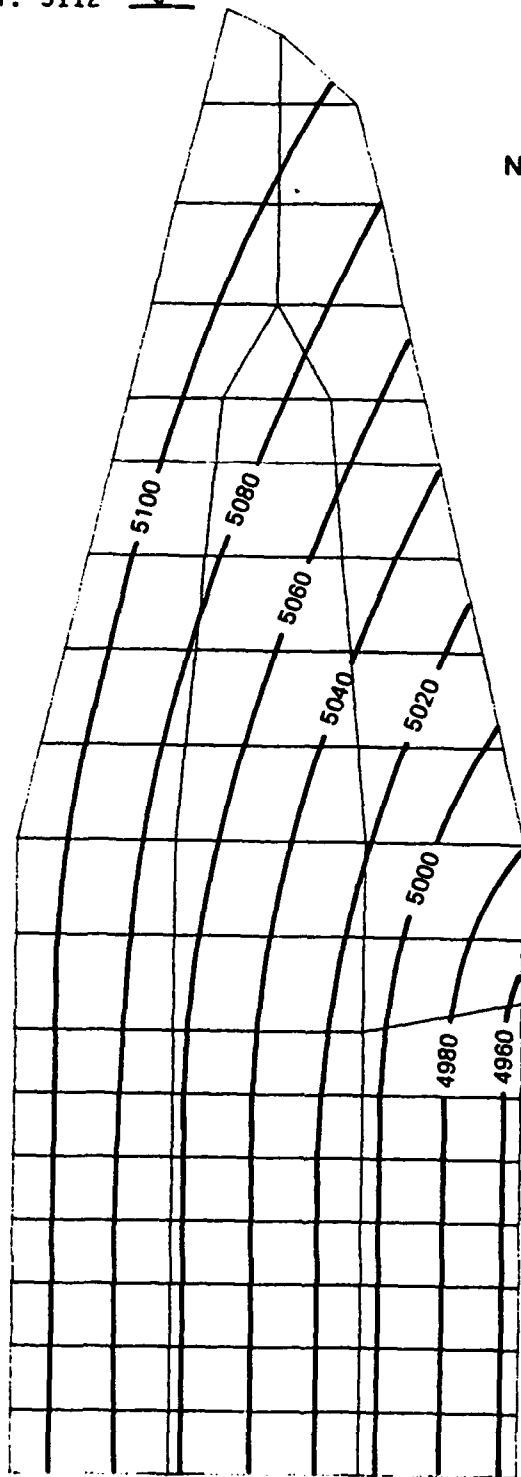


Figure 11. Finite element mesh for seepage analysis of section BB

E1. 5112



Note: Contours of hydraulic head are in feet

E1. 4955

Figure 12. Computed equi-potential lines for section AA

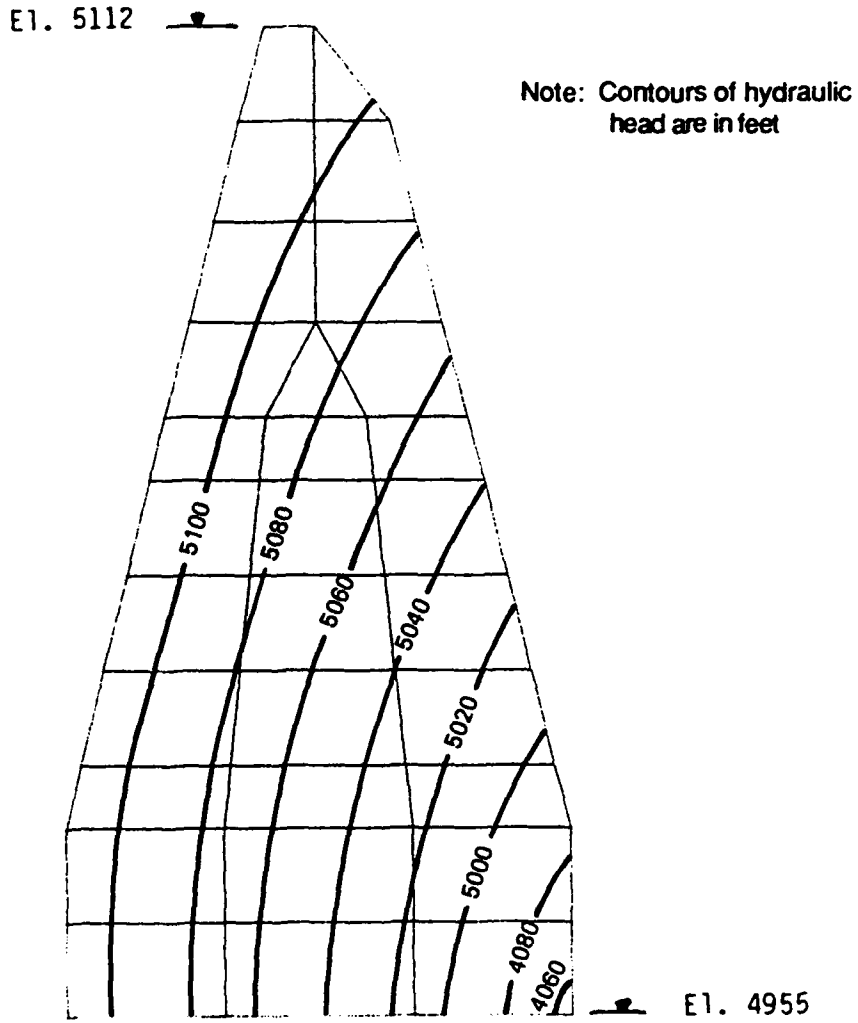


Figure 13. Computed equi-potential lines for section BB

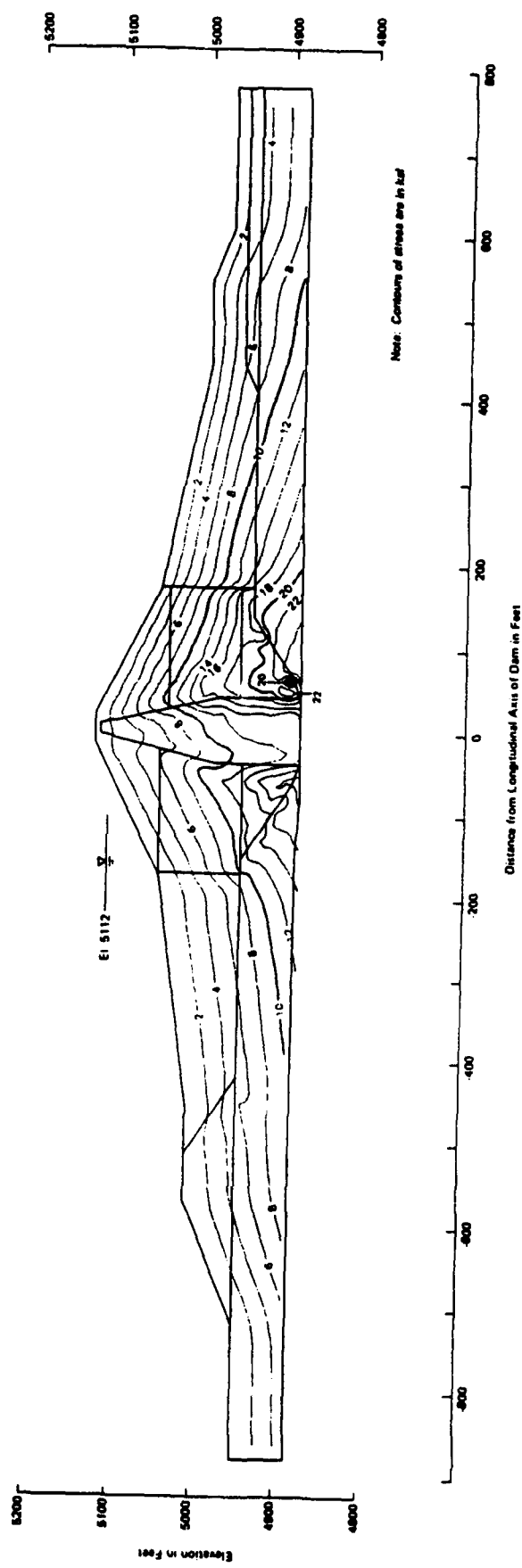


Figure 14. Computed static vertical effective stresses,  $\sigma_y$ ,  
for section AA

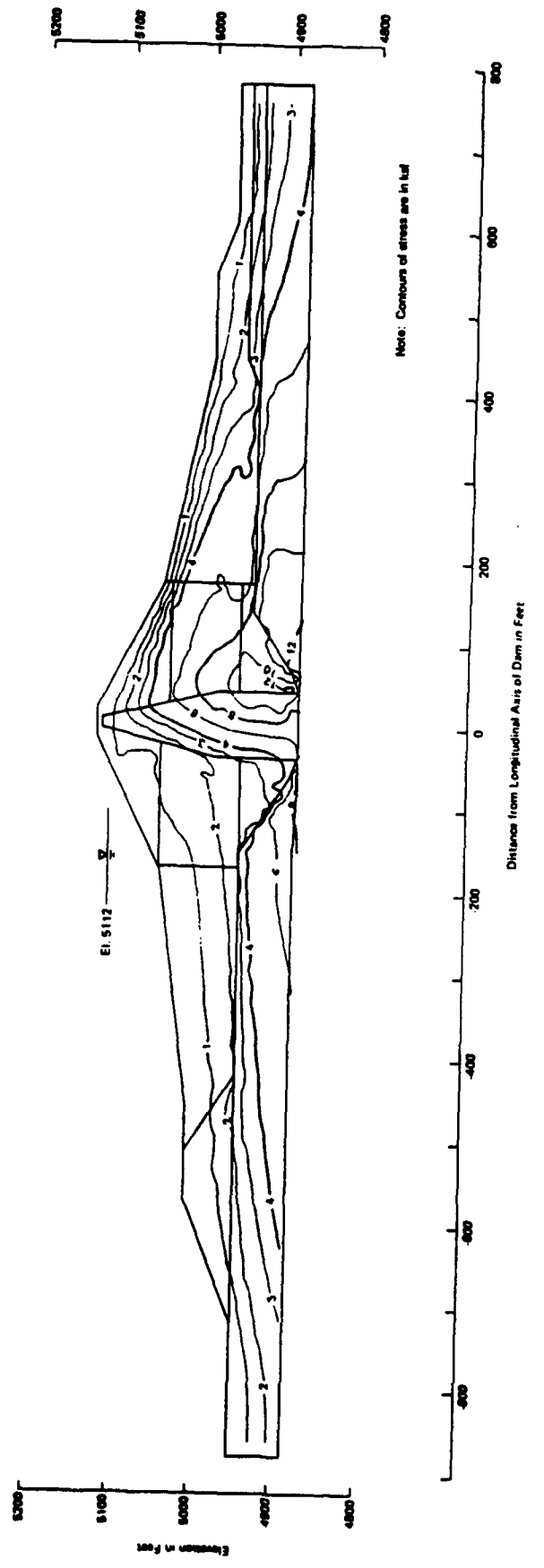
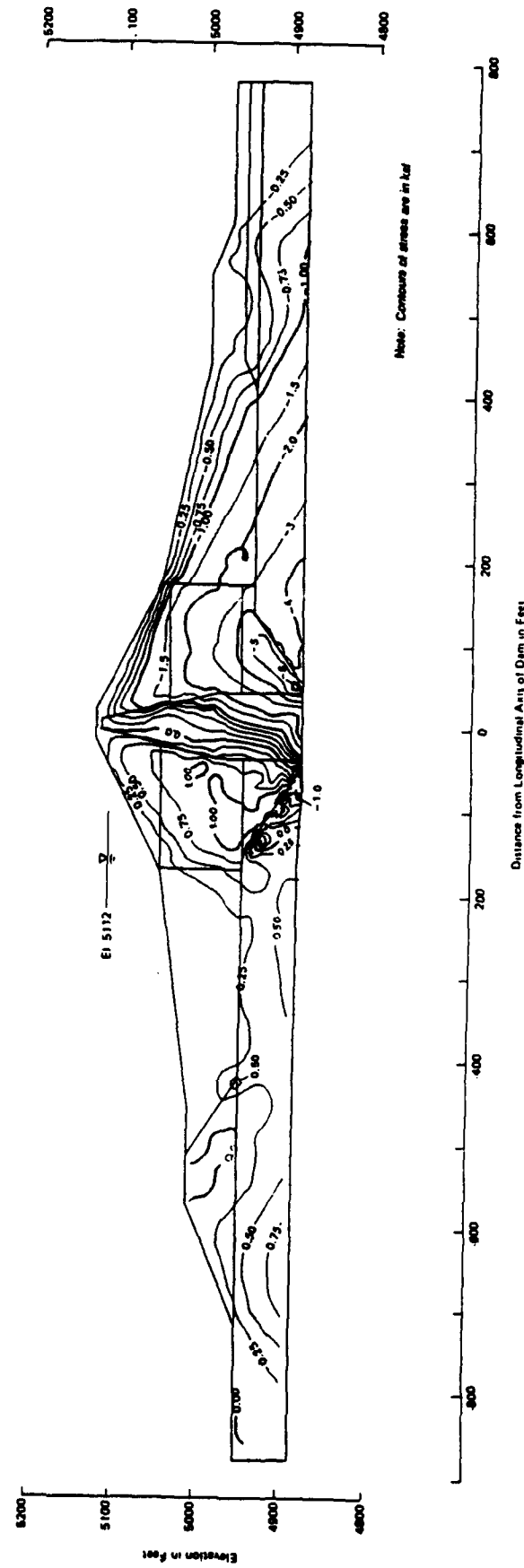


Figure 15. Computed static horizontal effective stresses,  $\sigma_x$ , for section AA



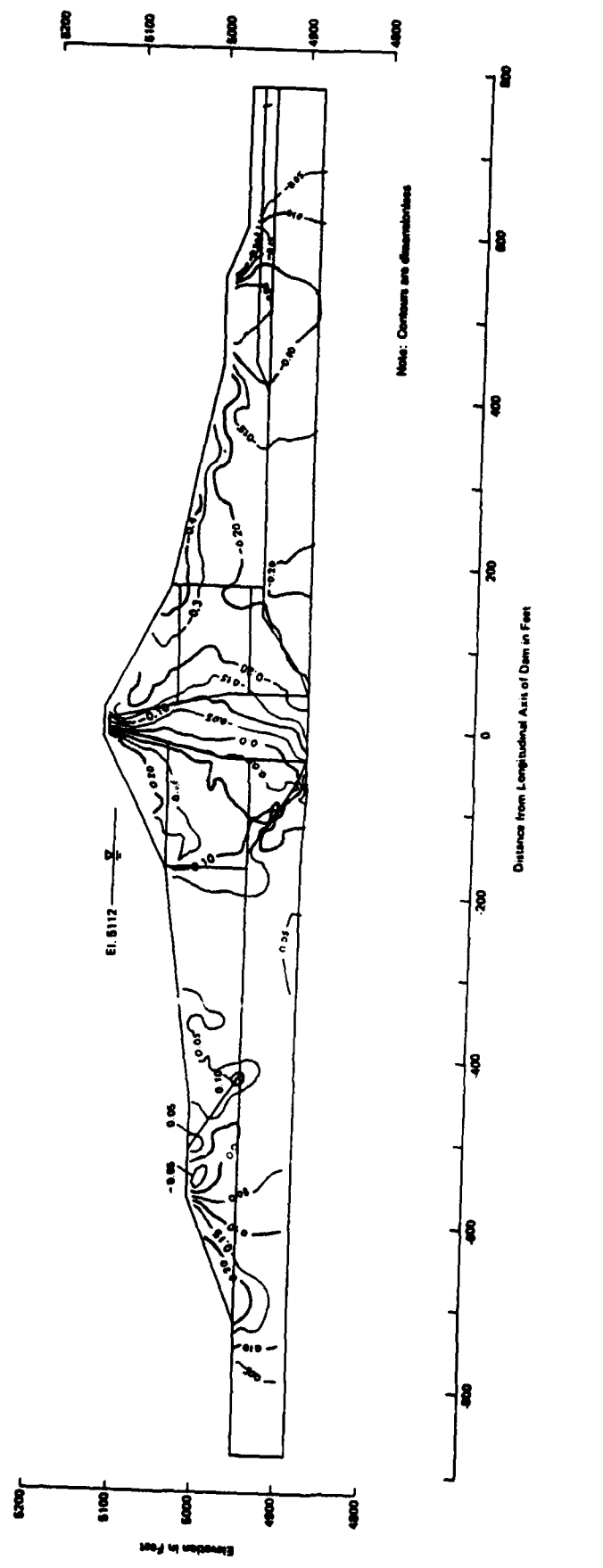


Figure 17. Computed values of the ratio between horizontal shear stress and vertical effective stress,  $\sigma_x/\sigma_y$ , for section AA

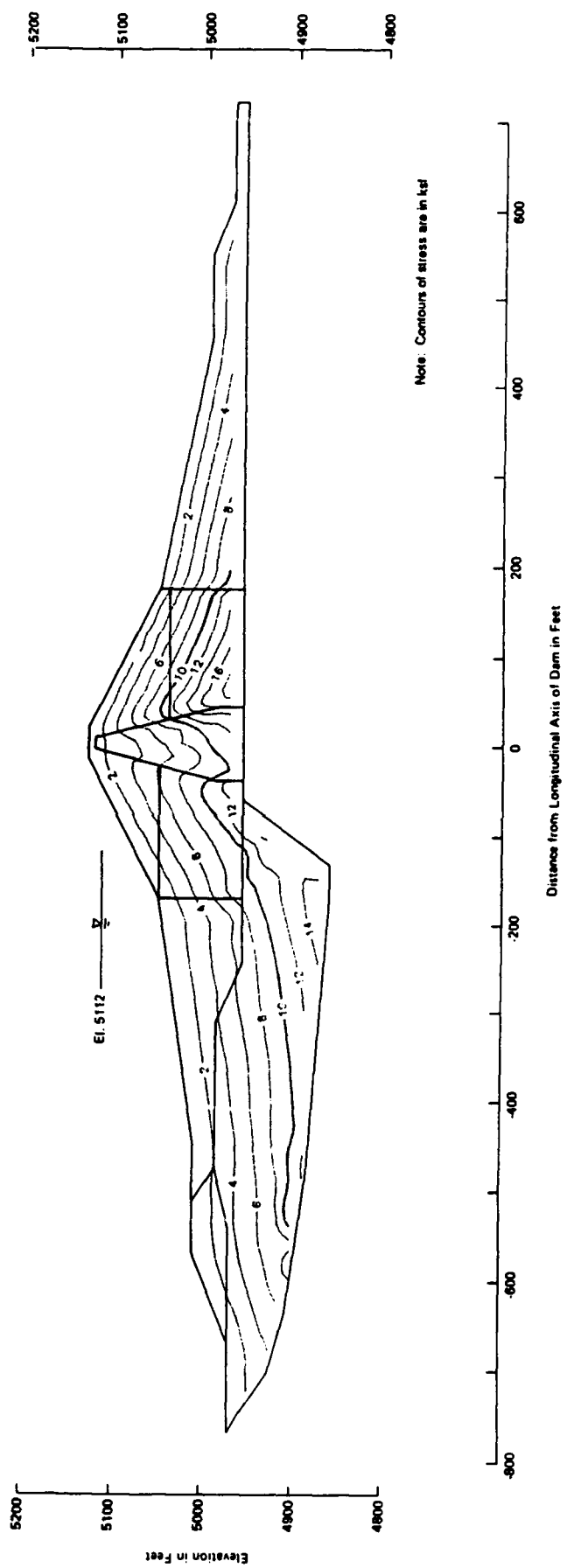


Figure 18. Computed static vertical effective stresses,  $\sigma_y$ , for section BB

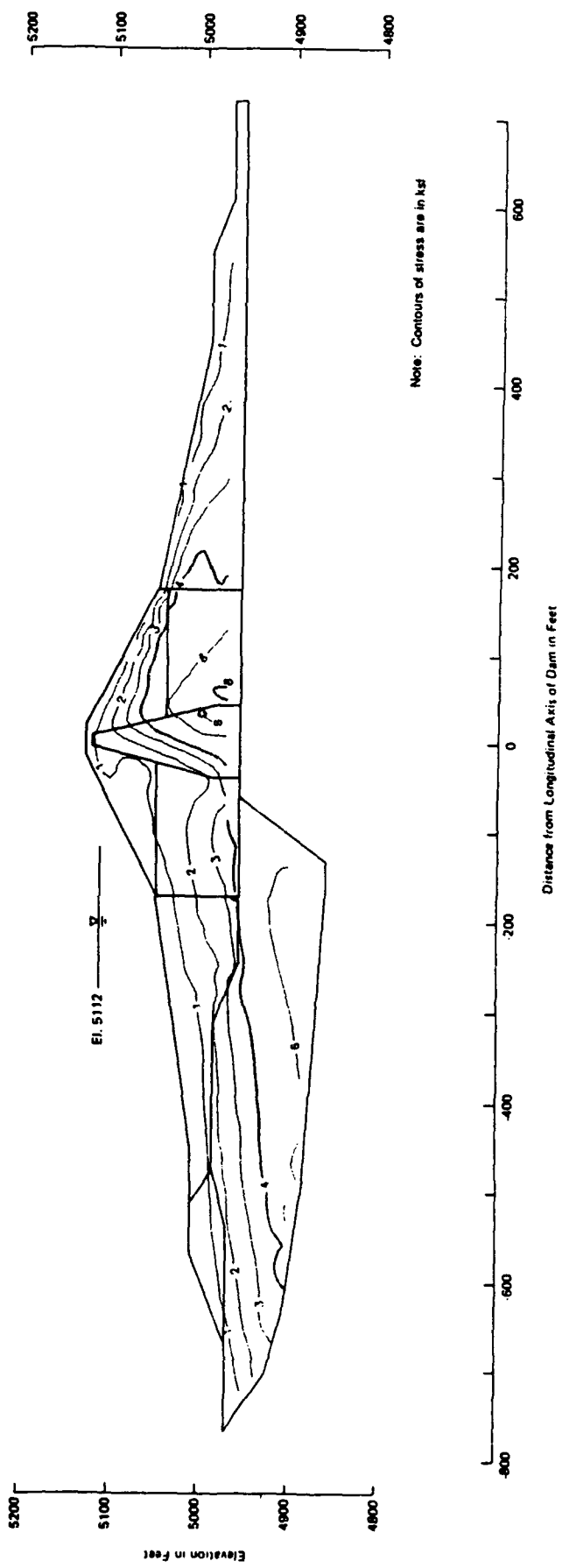


Figure 19. Computed static horizontal effective stresses,  $\sigma_x$ , for section 88

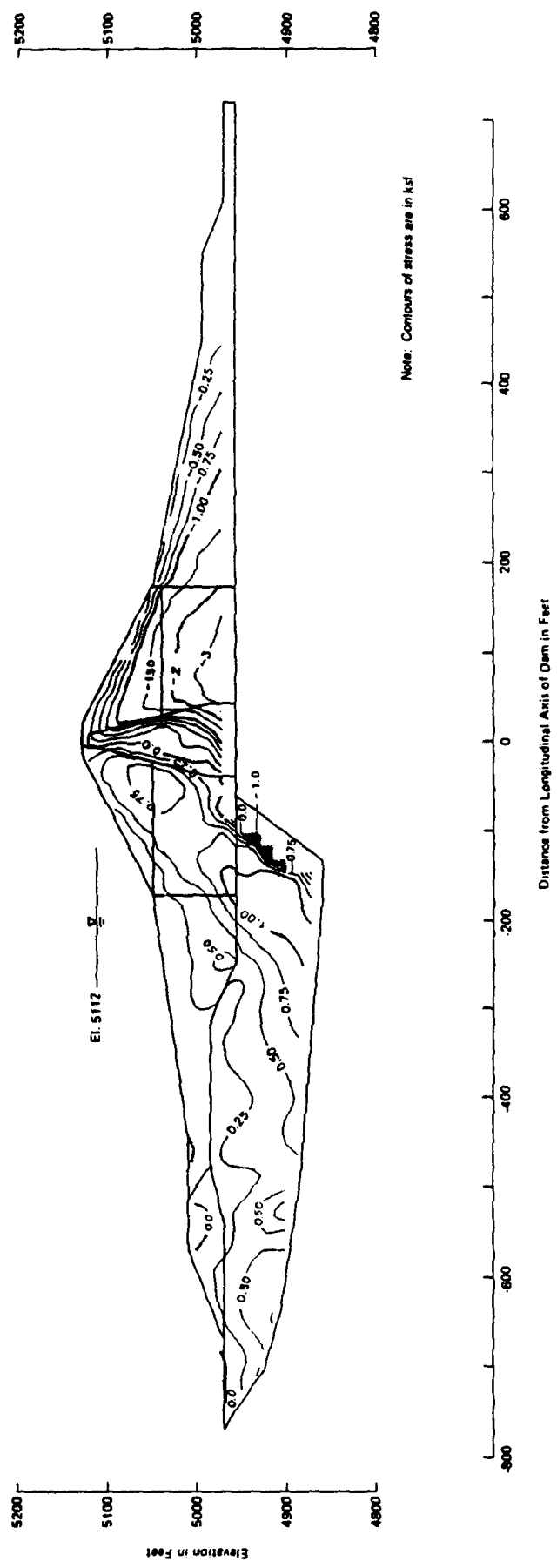


Figure 20. Computed static horizontal shear stresses,  $\tau_{yx}$ , for section BB

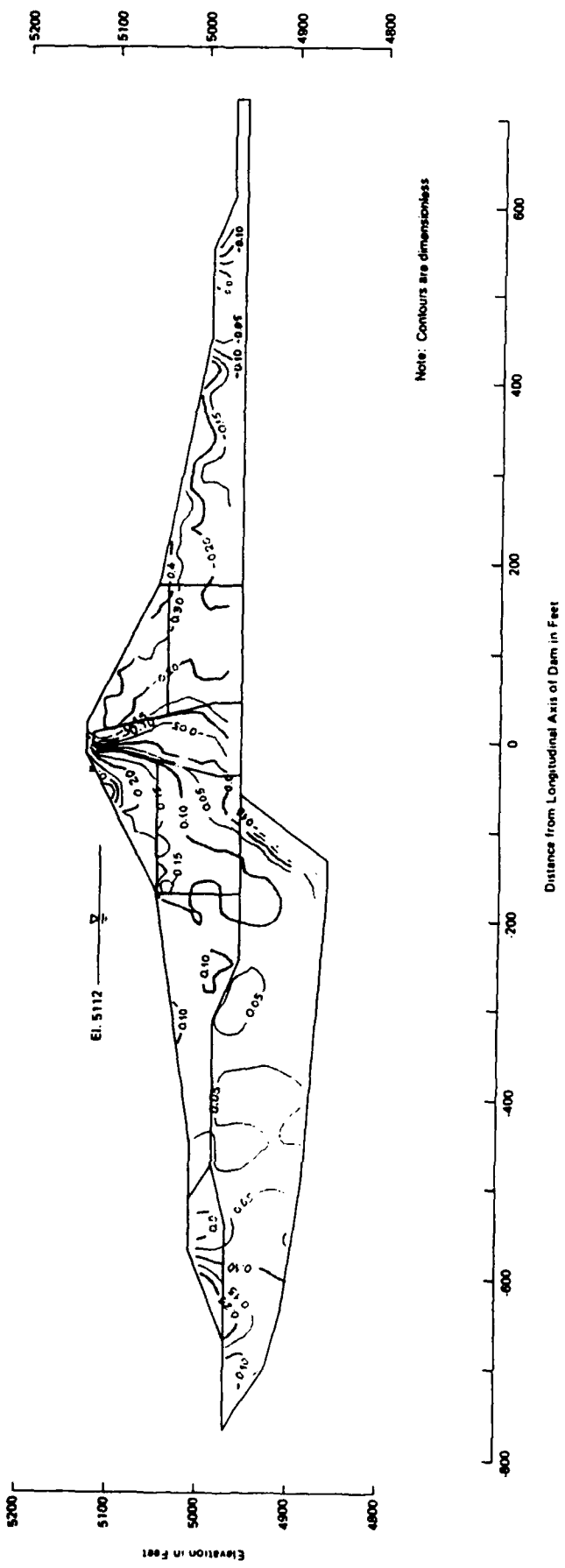


Figure 21. Computed values of the ratio between horizontal shear stress and vertical effective stress,  $\tau_{xy}/\alpha_y$ , for section BB

**APPENDIX A**

TABLE A - 1  
COMPUTED LONG-TERM STATIC STRESSES FOR SECTION AA

ELE	SIG-1 (KSF)	SIG-2 (KSF)	TAU-XY (KSF)	SIG-1 (KSF)	SIG-3 (KSF)	TAU-MAX (KSF)	THETA	SIG1/SIG3	TAUXY/SIGY	SLOP <sup>**</sup>	SUPES	ELE
1	6.666	15.671	.446	15.697	6.040	6.829	3.342	1.952	.028	.212	.203	1
2	7.826	18.037	.164	18.041	7.823	4.109	1.141	2.050	.010	.229	.223	2
3	8.631	18.976	.026	18.976	8.031	4.473	.165	2.114	.002	.237	.237	3
4	7.367	17.107	-.265	17.115	7.959	4.570	-1.657	2.150	-.015	.245	.245	4
5	8.453	17.845	-.923	17.935	8.373	4.781	-5.566	2.142	-.052	.245	.245	5
6	8.557	18.342	-1.052	18.454	8.446	5.004	-6.065	2.185	-.057	.255	.255	6
7	8.823	18.975	-1.470	19.164	8.614	5.285	-9.076	2.227	-.077	.264	.264	7
8	4.486	15.467	.287	16.414	4.473	5.970	1.376	3.869	.018	.519	.519	8
9	6.382	13.429	-1.311	13.664	6.146	3.759	-10.202	2.223	-.098	.521	.521	9
10	6.876	13.511	-2.369	14.271	6.119	4.076	-17.771	2.332	-.175	.567	.567	10
11	8.563	15.290	-2.946	16.398	7.455	4.472	-20.607	2.200	-.193	.524	.524	11
12	8.583	19.351	-6.058	22.072	5.882	6.105	-24.186	3.785	-.313	.561	.561	12
13	10.987	22.552	-4.223	23.930	9.809	7.100	-18.070	2.490	-.187	.327	.327	13
14	12.514	24.441	-4.235	25.794	11.162	7.316	-17.701	2.311	-.173	.294	.294	14
15	12.964	25.795	-4.187	27.032	11.718	7.657	-16.573	2.307	-.162	.295	.295	15
16	12.205	24.526	-3.979	25.698	11.031	7.333	-16.429	2.330	-.182	.295	.295	16
17	12.235	24.515	-4.061	25.737	11.016	7.360	-16.745	2.336	-.168	.293	.293	17
18	11.922	23.860	-4.132	25.150	10.631	7.280	-17.346	2.366	-.173	.304	.304	18
19	11.642	23.163	-4.285	24.900	10.225	7.187	-18.299	2.406	-.185	.311	.311	19
20	11.162	21.345	-4.379	23.499	9.808	6.946	-19.542	2.446	-.200	.317	.317	20
21	10.563	20.582	-4.298	23.161	9.057	6.551	-20.490	2.447	-.209	.314	.314	21
22	10.039	19.313	-6.693	20.282	6.560	5.861	-20.807	2.370	-.207	.295	.295	22
23	9.300	17.422	-6.262	18.631	8.091	5.270	-19.795	2.303	-.192	.278	.278	23
24	8.593	16.193	-2.863	17.151	7.626	4.762	-18.479	2.249	-.177	.264	.264	24
25	7.992	15.097	-2.487	15.845	7.205	4.320	-17.575	2.199	-.165	.251	.251	25
26	7.466	14.009	-2.140	14.647	6.829	3.909	-16.597	2.145	-.152	.239	.239	26
27	6.913	12.975	-1.619	13.479	6.409	3.535	-15.483	2.103	-.140	.227	.227	27
28	5.373	11.591	-1.554	12.289	5.970	3.160	-14.735	2.059	-.131	.215	.215	28
29	5.925	10.938	-1.240	11.285	5.638	2.824	-13.001	2.002	-.113	.202	.202	29
30	5.595	10.513	-1.033	10.727	5.377	2.675	-11.364	1.995	-.098	.199	.199	30
31	5.262	10.062	-1.004	10.265	5.079	2.593	-11.395	2.021	-.100	.203	.203	31
32	4.901	9.103	-1.031	9.467	4.672	2.397	-12.637	2.026	-.111	.201	.201	32
33	4.533	8.226	-.857	8.545	4.314	2.115	-13.147	1.981	-.113	.190	.190	33
34	4.260	7.749	-.734	7.899	4.131	1.883	-11.473	1.912	-.095	.175	.175	34
35	4.103	7.441	-.560	7.513	4.028	1.743	-9.344	1.885	-.087	.166	.166	35
36	3.993	7.302	-.279	7.324	3.960	1.682	-4.779	1.850	-.038	.165	.165	36
37	3.907	7.226	-.056	7.230	3.904	1.663	-1.481	1.852	-.012	.165	.162	37
38	2.462	4.564	.057	4.565	2.460	1.052	1.558	1.856	.012	.157	.152	38
39	2.531	4.635	.169	4.629	2.514	1.055	5.160	1.939	.041	.158	.149	39
40	2.641	4.592	.257	4.743	2.591	1.081	9.541	1.939	.076	.155	.149	40
41	2.779	4.084	.542	4.997	2.647	1.175	13.735	1.888	.111	.159	.159	41
42	3.077	5.508	.774	5.732	2.851	1.440	16.256	2.010	.141	.164	.163	42
43	3.515	6.564	.903	6.811	3.267	1.772	15.324	2.085	.138	.203	.201	43
44	3.952	7.620	.879	7.820	3.756	2.031	12.816	2.081	.115	.205	.205	44
45	4.346	8.466	.727	8.513	4.216	2.198	9.863	2.043	.086	.202	.201	45
46	4.810	9.041	.561	9.111	4.540	2.286	7.107	2.007	.082	.199	.198	46
47	4.777	9.353	.452	9.397	4.733	2.332	5.597	1.985	.048	.200	.193	47
48	4.667	9.543	.373	9.572	4.657	2.358	4.551	1.977	.039	.195	.191	48
49	5.001	9.570	.343	9.596	4.974	2.311	4.253	1.929	.038	.195	.184	49
50	5.227	9.779	.419	9.810	5.189	2.315	5.219	1.892	.043	.195	.178	50
51	5.434	10.261	.465	10.225	5.389	2.455	5.445	1.916	.045	.197	.163	51
52	5.579	10.564	.517	10.637	5.526	2.555	5.836	1.925	.049	.193	.166	52
53	5.765	10.873	.555	10.933	5.705	2.614	6.132	1.916	.051	.195	.165	53
54	6.095	11.444	.512	11.513	6.026	2.744	6.442	1.911	.053	.200	.186	54
55	6.453	11.217	.503	12.294	6.391	2.952	6.691	1.924	.051	.205	.190	55
56	6.774	13.076	.569	13.129	6.723	3.203	5.113	1.953	.043	.210	.198	56

57	7.074	14.275	.376	14.295	7.055	3.621	2.995	2.027	.026	.226	.214	57
59	7.376	15.191	.392	15.211	7.356	3.927	2.865	2.068	.026	.227	.225	59
59	7.132	15.582	.156	15.584	7.129	4.228	1.056	2.186	.010	.248	.248	59
60	7.137	16.054	-.006	16.054	7.137	4.459	-.041	2.249	.000	.201	.201	60
61	7.576	17.019	-.441	17.039	7.555	4.742	-2.689	2.255	-.026	.265	.265	61
62	7.499	17.052	-.962	17.148	7.403	4.873	-5.693	2.316	-.056	.277	.277	62
63	7.795	17.504	-1.132	17.634	7.685	4.985	-6.563	2.301	-.065	.275	.275	63
64	4.121	15.927	1.241	16.056	3.992	6.032	5.934	4.022	.079	.578	.578	64
65	4.498	17.958	.086	17.959	4.497	6.731	.366	3.993	.005	.583	.583	65
66	4.825	12.065	-.753	12.142	4.750	3.695	-5.877	2.556	-.062	.641	.641	66
67	6.890	13.967	-1.457	14.256	6.802	3.827	-11.189	2.159	-.104	.499	.499	67
68	8.586	13.754	-2.830	15.002	7.337	3.833	-23.799	2.045	-.208	.455	.455	68
69	12.427	23.212	-.6157	26.005	9.835	8.185	-24.394	2.899	-.285	.372	.372	69
70	8.116	16.451	-.5005	18.796	5.770	6.513	-25.110	3.257	-.304	.467	.457	70
71	13.606	25.166	-3.918	26.368	12.403	6.993	-17.066	2.126	-.156	.257	.257	71
72	12.035	23.992	-3.813	25.105	10.923	7.091	-16.264	2.298	-.159	.290	.290	72
73	12.112	24.294	-3.905	25.438	10.968	7.235	-16.331	2.319	-.181	.295	.295	73
74	11.722	23.409	-3.904	24.593	10.538	7.028	-16.872	2.334	-.187	.298	.298	74
75	11.546	23.258	-3.945	24.463	10.341	7.061	-16.982	2.386	-.170	.303	.303	75
76	11.175	22.352	-4.059	23.670	9.957	6.907	-17.935	2.401	-.182	.306	.306	76
77	10.872	21.223	-4.162	22.689	9.406	6.641	-19.401	2.412	-.196	.308	.308	77
78	10.485	19.529	-4.064	21.087	8.929	6.079	-20.974	2.362	-.208	.295	.295	78
79	10.199	18.423	-3.885	19.969	8.654	5.657	-21.687	2.308	-.211	.282	.282	79
80	5.781	10.719	.536	10.777	5.723	2.527	6.127	1.883	.050	.189	.179	80
81	5.977	11.169	.498	11.217	5.929	2.644	5.432	1.892	.045	.191	.191	81
82	6.160	12.135	.484	12.174	6.121	3.026	4.802	1.989	.040	.208	.202	82
83	6.154	13.254	.373	13.274	6.134	3.570	2.998	2.164	.026	.238	.238	83
84	6.252	14.213	.243	14.220	6.245	3.987	1.744	2.277	.017	.252	.262	84
85	6.314	14.655	.064	14.656	6.313	4.171	.442	2.321	.004	.271	.271	85
86	6.723	15.829	-.141	15.831	6.721	4.555	-.884	2.355	-.009	.281	.281	86
87	6.636	16.105	-.508	16.132	6.609	4.762	-3.061	2.441	-.032	.298	.298	87
88	7.072	16.893	-1.003	16.985	6.971	5.007	-5.776	2.437	-.059	.300	.300	88
89	2.645	12.662	.657	12.898	2.609	5.145	3.390	4.944	.047	.705	.705	89
90	4.702	17.283	1.034	17.369	4.617	6.375	4.667	3.761	.060	.540	.540	90
91	3.541	16.832	.414	16.845	3.529	6.653	1.763	4.775	.025	.709	.708	91
92	4.551	11.935	-.368	11.955	4.553	3.711	-2.848	2.637	-.031	.671	.671	92
93	7.054	13.380	-1.104	13.567	6.976	3.345	-9.635	1.973	-.083	.448	.421	93
94	11.171	14.659	-2.733	16.207	9.623	3.293	-29.011	1.684	-.191	.423	.329	94
95	11.466	22.886	-4.969	24.745	9.606	7.570	-20.517	2.576	-.217	.419	.345	95
96	9.563	23.032	-5.603	25.059	7.537	9.760	-19.879	3.325	-.243	.501	.491	96
97	9.467	22.560	-6.915	24.837	7.191	8.923	-21.051	3.454	-.262	.514	.514	97
98	11.719	23.774	-3.865	24.997	10.595	7.160	-16.335	2.353	-.163	.301	.301	98
99	11.699	22.993	-3.970	24.249	10.443	6.903	-17.555	2.322	-.172	.293	.293	99
100	11.844	22.912	-3.689	24.012	10.543	8.735	-16.810	2.278	-.161	.284	.284	100
101	11.220	22.256	-3.772	23.422	10.054	6.884	-17.178	2.330	-.169	.293	.293	101
102	11.054	21.726	-3.893	22.998	9.812	6.593	-18.095	2.344	-.179	.295	.295	102
103	10.765	20.393	-3.979	21.827	9.352	6.238	-19.819	2.334	-.195	.291	.291	103
104	10.428	18.614	-3.913	20.184	8.859	5.682	-21.054	2.278	-.210	.277	.277	104
105	10.089	17.189	-3.502	18.626	8.653	4.997	-22.307	2.153	-.204	.249	.249	105
106	9.153	15.958	-3.007	17.096	8.015	4.541	-20.731	2.133	-.188	.241	.241	106
107	8.337	14.800	-2.605	15.720	7.417	4.151	-19.446	2.119	-.176	.236	.236	107
108	7.748	13.707	-2.262	14.469	6.985	3.742	-18.598	2.071	-.165	.223	.223	108
109	7.154	12.625	-1.915	13.228	6.550	3.339	-17.499	2.019	-.152	.211	.211	109
110	6.567	11.643	-1.599	12.101	6.129	2.956	-16.070	1.974	-.136	.199	.199	110
111	6.043	10.535	-1.364	10.917	5.661	2.629	-15.632	1.929	-.129	.187	.187	111
112	5.547	9.674	-1.053	9.932	5.289	2.322	-13.630	1.878	-.110	.181	.175	112
113	5.042	9.273	-.653	9.395	4.664	2.251	-11.132	1.922	-.093	.194	.182	113
114	4.656	8.845	-.930	9.033	4.467	2.253	-10.810	2.002	-.094	.204	.195	114
115	4.325	7.998	-.878	8.196	4.126	2.035	-12.753	1.986	-.110	.193	.190	115
116	4.093	7.029	-.798	7.231	3.991	1.675	-14.222	1.863	-.114	.165	.164	116
117	3.621	6.413	-.631	6.562	3.742	1.410	-13.295	1.754	-.098	.154	.143	117

113	3.635	6.117	-.425	6.195	3.613	1.289	-9.663	1.713	-.036	.155	.134	115
119	3.494	6.006	-.229	6.027	3.463	1.282	-5.147	1.740	-.038	.157	.138	119
120	3.352	5.955	-.070	5.957	3.350	1.303	-1.541	1.778	-.012	.158	.145	120
121	1.747	3.097	.049	3.098	1.746	.676	1.697	1.775	.013	.150	.130	121
122	1.667	3.116	.125	3.129	1.654	.637	5.802	1.687	.041	.147	.116	122
123	2.082	3.153	.245	3.205	2.028	.589	12.306	1.581	.078	.144	.100	123
124	2.335	3.301	.437	3.453	2.168	.651	21.087	1.601	.132	.142	.104	124
125	2.545	4.000	.624	4.231	2.317	.957	20.340	1.828	.198	.154	.145	125
126	2.838	5.102	.718	5.310	2.627	1.341	16.189	2.021	.141	.186	.183	126
127	3.177	6.224	.701	6.376	3.023	1.677	12.360	2.110	.113	.211	.203	127
128	3.507	7.135	.573	7.224	3.419	1.903	8.763	2.113	.080	.226	.208	128
129	3.783	7.593	.433	7.728	3.738	1.996	8.259	2.069	.058	.234	.202	129
130	3.976	7.955	.363	7.991	3.943	2.024	5.172	2.027	.046	.234	.196	130
131	4.143	8.134	.323	8.160	4.123	2.018	4.802	1.979	.040	.215	.188	131
132	4.418	8.115	.240	8.131	4.403	1.864	3.897	1.847	.030	.172	.164	132
133	4.611	8.345	.346	8.377	4.579	1.899	5.245	1.829	.041	.168	.162	133
134	4.702	8.005	.394	8.042	4.685	2.089	5.432	1.896	.045	.183	.175	134
135	4.871	9.123	.436	9.167	4.828	2.170	5.789	1.899	.048	.184	.177	135
136	5.095	9.455	.433	9.498	5.053	2.222	5.616	1.880	.046	.185	.174	136
137	5.373	9.255	.451	9.337	5.326	2.265	5.510	1.881	.047	.183	.172	137
139	5.530	10.305	.427	10.345	5.490	2.428	5.190	1.884	.042	.185	.178	138
139	5.644	11.307	.467	11.345	5.606	2.870	4.686	2.024	.041	.206	.206	139
140	5.800	12.615	.429	12.636	5.574	3.531	3.485	2.267	.034	.255	.255	140
141	5.476	13.306	.183	13.310	5.472	3.919	1.316	2.433	.014	.265	.288	141
142	5.883	14.306	-.154	14.311	5.880	4.225	-1.047	2.442	-.011	.293	.293	142
143	5.874	14.742	-.149	14.747	5.871	4.438	-.954	2.512	-.010	.307	.307	143
144	6.427	16.077	-.667	16.127	6.377	4.875	-4.111	2.529	-.043	.314	.314	144
145	3.518	14.395	1.536	14.611	3.305	5.653	7.883	4.420	.107	.635	.635	145
146	3.494	15.486	1.232	15.611	3.368	6.122	5.808	4.635	.080	.676	.676	146
147	3.967	16.651	.745	16.904	3.924	6.490	3.297	4.309	.044	.631	.631	147
148	3.349	16.619	.183	16.621	3.346	6.638	.790	4.967	.011	.738	.738	148
149	4.326	11.303	.022	11.303	4.320	3.491	.179	2.616	.002	.655	.656	149
150	7.267	15.122	-1.070	15.311	7.077	3.117	-10.042	1.881	-.082	.449	.382	150
151	10.099	15.273	-2.944	16.605	6.766	3.920	-24.344	1.894	-.193	.444	.399	151
152	9.738	20.599	-4.323	22.109	8.227	6.941	-19.263	2.687	-.210	.447	.361	152
153	10.169	21.697	-5.337	23.023	8.044	7.890	-21.531	2.962	-.245	.469	.418	153
154	8.904	20.515	-5.305	22.575	6.846	7.865	-21.206	3.298	-.259	.499	.478	154
155	11.955	23.133	-3.916	23.401	10.594	6.403	-18.291	2.209	-.172	.285	.269	155
156	11.459	21.614	-3.539	22.725	10.348	6.188	-17.434	2.196	-.164	.288	.265	156
157	11.362	21.924	-3.679	22.079	10.207	6.436	-17.427	2.261	-.168	.291	.273	157
158	11.069	20.792	-3.760	22.071	9.791	6.140	-18.025	2.254	-.180	.279	.276	158
159	10.857	19.640	-3.827	21.074	9.424	5.825	-20.536	2.236	-.195	.270	.270	159
160	10.552	17.664	-3.761	19.264	8.932	5.176	-23.302	2.159	-.213	.251	.251	160
161	10.227	15.693	-3.131	17.283	8.837	4.223	-23.930	1.956	-.197	.207	.207	161
162	9.055	14.539	-2.655	15.613	7.982	3.815	-22.027	1.956	-.182	.209	.204	162
163	6.261	13.499	-2.339	14.394	7.386	3.504	-20.940	1.949	-.173	.205	.200	163
164	7.532	12.264	-2.007	13.018	6.798	3.110	-20.093	1.915	-.163	.199	.190	164
165	6.995	11.301	-1.692	11.556	6.412	2.737	-19.089	1.854	-.150	.182	.176	165
166	6.376	10.276	-1.346	10.695	5.956	2.376	-17.313	1.796	-.131	.183	.182	166
167	5.793	9.249	-1.164	9.604	5.438	2.083	-16.982	1.766	-.126	.173	.154	167
168	5.134	6.295	-.621	8.495	4.933	1.781	-13.734	1.722	-.099	.182	.143	168
169	4.438	7.955	-.665	8.063	4.394	1.834	-9.889	1.835	-.076	.197	.182	169
170	4.035	7.540	-.654	7.760	3.978	1.891	-10.277	1.951	-.057	.209	.182	170
171	3.831	6.721	-.751	6.964	3.618	1.673	-13.526	1.925	-.112	.191	.174	171
172	3.611	6.733	-.720	5.954	3.390	1.282	-17.079	1.756	-.126	.156	.141	172
173	3.448	5.073	-.523	5.226	3.294	.966	-16.383	1.586	-.103	.145	.109	173
174	3.176	4.653	-.101	4.651	3.117	.672	-16.567	1.560	-.065	.147	.103	174
175	2.915	4.725	-.161	4.739	2.904	.918	-5.049	1.632	-.034	.149	.115	175
176	2.753	4.694	-.047	4.695	2.752	.971	-1.378	1.708	-.010	.151	.127	176
177	1.032	1.851	.022	1.852	1.031	.410	1.507	1.798	.012	.161	.123	177
178	1.145	1.655	.087	1.265	1.139	.363	5.341	1.638	.036	.157	.100	176
179	1.333	1.866	.122	1.893	1.307	.293	12.353	1.449	.006	.151	.072	179

180	1.651	1.649	.267	2.106	1.493	.304	30.715	1.406	.137	.146	.066	180
181	2.017	2.765	.534	3.000	1.726	.637	28.536	1.738	.197	.154	.123	181
182	2.266	3.655	.595	4.053	2.068	.992	19.402	1.960	.154	.189	.165	182
183	2.599	5.636	.562	5.165	2.464	1.350	12.443	2.096	.113	.212	.194	183
184	2.853	5.965	.466	6.033	2.784	1.624	8.339	2.167	.078	.244	.211	184
185	3.086	6.560	.300	6.526	3.059	1.733	4.989	2.133	.046	.259	.208	185
186	3.384	6.737	.283	6.757	3.344	1.707	4.429	2.021	.039	.256	.190	186
187	3.596	6.945	.245	6.983	3.579	1.692	4.169	1.946	.035	.221	.178	187
188	3.845	6.866	.147	6.875	3.838	1.519	2.775	1.791	.021	.166	.150	188
189	3.972	7.094	.334	7.130	3.936	1.597	6.037	1.811	.047	.166	.155	189
190	4.079	7.523	.318	7.552	4.050	1.751	5.234	1.865	.042	.180	.168	190
191	4.321	7.915	.342	7.947	4.289	1.829	5.308	1.853	.043	.177	.185	191
192	4.527	8.234	.371	8.271	4.491	1.890	5.659	1.842	.045	.179	.164	192
193	4.845	8.792	.371	8.827	4.811	2.008	5.327	1.835	.042	.179	.164	193
194	5.126	9.475	.353	9.504	5.098	2.203	4.812	1.864	.037	.179	.172	194
195	5.202	10.504	.513	10.553	5.153	2.700	5.481	2.048	.049	.208	.209	195
196	4.992	11.690	.466	11.712	4.960	3.376	3.985	2.361	.040	.269	.269	196
197	5.144	13.199	.166	13.202	5.141	4.031	1.183	2.568	.013	.312	.312	197
198	5.005	13.203	-.271	13.211	4.996	4.108	-1.892	2.644	-.021	.326	.326	198
199	5.416	13.971	-.264	13.976	5.411	4.285	-1.355	2.553	-.016	.317	.317	199
200	3.076	12.863	1.417	13.061	2.875	5.093	8.077	4.543	.110	.643	.643	200
201	3.176	13.914	1.144	14.035	3.056	5.489	6.014	4.593	.082	.658	.658	201
202	2.697	14.262	.753	14.311	2.547	5.732	3.774	5.026	.053	.730	.730	202
203	3.305	15.233	.691	16.340	3.269	6.536	3.032	4.999	.042	.741	.741	203
204	4.070	16.655	.129	16.655	4.067	3.296	1.213	2.521	.013	.655	.655	204
205	7.106	16.825	-.963	12.471	6.960	3.256	-8.804	1.935	-.072	.460	.405	205
206	3.915	14.655	-2.511	15.655	6.817	3.420	-23.627	1.776	-.173	.458	.346	206
207	11.054	21.023	-4.012	22.437	9.840	6.399	-19.415	2.328	-.191	.428	.291	207
208	9.264	19.947	-5.035	21.859	7.251	7.304	-21.789	3.015	-.254	.489	.423	208
209	10.520	22.103	-5.650	24.407	9.228	8.089	-22.149	2.966	-.256	.476	.421	209
210	8.560	17.043	-4.541	19.016	6.588	6.214	-23.478	2.887	-.265	.479	.390	210
211	11.756	21.346	-3.347	22.399	10.704	5.847	-17.457	2.093	-.157	.294	.243	211
212	11.547	20.916	-3.633	22.155	10.310	5.923	-18.057	2.149	-.173	.294	.265	212
213	11.243	20.113	-3.523	21.405	9.952	5.726	-19.623	2.151	-.180	.281	.254	213
214	11.217	18.627	-2.777	20.392	9.662	5.365	-22.377	2.111	-.201	.251	.244	214
215	10.904	16.764	-3.551	18.438	9.229	4.604	-25.238	1.992	-.212	.217	.217	215
216	10.269	14.933	-3.056	16.485	6.766	3.859	-26.180	1.880	-.204	.201	.190	216
217	4.413	6.125	.246	8.142	4.397	1.873	3.799	1.852	.030	.181	.165	217
218	4.663	8.724	.230	8.750	4.661	2.045	4.646	1.877	.038	.178	.172	218
219	4.551	9.498	.508	9.551	4.598	2.476	5.915	2.077	.053	.210	.210	219
220	4.679	11.349	.605	11.404	4.824	3.390	5.143	3.465	.053	.287	.297	220
221	4.315	12.039	.159	12.042	4.312	3.865	1.175	2.793	.013	.347	.347	221
222	4.929	13.426	-.434	13.448	4.907	4.271	-2.917	2.740	-.032	.344	.344	222
223	1.895	9.720	.557	9.760	1.855	3.952	4.050	5.260	.057	.721	.721	223
224	3.350	13.299	1.514	13.524	3.125	5.199	8.464	4.328	.114	.612	.612	224
225	2.575	12.564	1.211	12.710	2.530	5.090	6.892	5.023	.096	.716	.716	225
226	2.934	14.297	.692	14.238	2.894	5.722	3.423	4.955	.048	.719	.719	226
227	2.715	14.926	.767	14.874	2.666	6.105	3.611	5.575	.052	.821	.821	227
228	4.042	10.626	.259	10.636	4.032	3.302	2.245	2.638	.024	.661	.661	228
229	6.955	12.997	-.844	13.084	6.639	3.123	-7.844	1.913	-.085	.467	.394	229
230	10.336	14.656	-2.359	15.720	9.302	3.209	-23.865	1.890	-.161	.458	.310	230
231	10.824	20.330	-3.555	21.512	9.642	5.935	-18.398	2.231	-.175	.437	.270	231
232	10.600	19.780	-4.618	21.710	8.690	6.515	-22.571	2.501	-.233	.463	.324	232
233	10.666	21.575	-5.197	23.745	8.616	7.564	-21.699	2.755	-.240	.480	.378	233
234	9.506	20.252	-4.925	22.176	7.591	7.293	-21.243	2.921	-.243	.503	.406	234
235	9.703	19.317	-5.242	21.623	7.396	7.113	-23.743	2.923	-.271	.484	.405	235
236	11.335	19.655	-5.565	21.665	10.692	5.407	-20.630	2.076	-.183	.295	.237	236
237	12.535	19.733	-3.942	21.471	10.797	5.337	-23.801	1.989	-.200	.279	.221	237
238	13.742	17.815	-3.774	19.926	10.732	4.547	-28.049	1.847	-.212	.247	.189	238
239	12.479	16.700	-3.335	17.793	10.385	3.704	-32.112	1.713	-.212	.208	.150	239
240	10.631	13.651	-2.266	14.919	9.212	2.854	-26.277	1.620	-.164	.203	.135	240

241	3.232	13.352	-2.313	14.369	8.195	3.097	-24.156	1.756	-173	.206	.162	241
242	8.246	12.000	-2.000	12.937	7.300	2.775	-23.149	1.751	-166	.199	.150	242
243	7.502	11.001	-1.730	11.712	6.791	2.461	-22.340	1.725	-157	.192	.151	243
244	6.796	9.899	-1.483	10.415	6.100	2.118	-22.223	1.605	-151	.176	.140	244
245	6.393	9.083	-1.109	9.493	5.995	1.743	-19.757	1.582	-122	.164	.110	245
246	5.636	7.813	-.895	8.126	5.313	1.407	-19.494	1.530	-113	.159	.106	246
247	4.557	6.953	-.486	7.047	4.479	1.284	-10.651	1.573	-067	.172	.112	247
248	3.996	6.719	-.427	6.784	3.931	1.427	-8.896	1.726	-083	.197	.138	248
249	3.669	6.488	-.488	6.570	3.597	1.492	-9.542	1.832	-075	.203	.156	249
250	3.305	5.579	-.647	5.750	3.134	1.308	-14.810	1.835	-116	.163	.154	250
251	3.066	4.434	-.844	4.890	2.810	.940	-21.836	1.869	-145	.146	.121	251
252	2.851	3.700	-.398	3.857	2.693	.582	-21.575	1.432	-108	.131	.078	252
253	2.595	3.511	-.105	3.547	2.559	.494	-11.091	1.306	-053	.123	.069	253
254	2.299	3.457	-.079	3.482	2.294	.584	-3.882	1.509	-023	.137	.059	254
255	2.142	3.446	-.026	3.447	2.142	.653	-1.150	1.609	-008	.140	.106	255
256	.365	.614	.008	.614	.365	.125	1.460	1.884	.010	.165	.089	256
257	.440	.819	.019	.821	.438	.091	8.030	1.417	.031	.157	.056	257
258	.567	.816	.032	.630	.542	.044	23.948	1.162	.053	.149	.022	258
259	.778	.634	.074	.808	.602	.103	88.943	1.342	.117	.145	.048	259
260	1.292	1.007	.343	1.654	.566	.344	42.709	1.713	.257	.146	.103	260
261	1.555	2.566	.451	2.906	1.835	.636	24.574	1.776	.179	.162	.129	261
262	2.023	3.782	.470	3.900	1.905	.997	14.045	2.047	.124	.206	.176	262
263	2.304	4.926	.359	4.876	2.254	1.312	7.947	2.184	.074	.247	.203	263
264	2.471	5.346	.230	5.356	2.453	1.453	4.565	2.184	.043	.273	.210	264
265	2.639	5.449	.073	5.450	2.637	1.407	1.405	2.067	.013	.200	.191	265
266	3.143	5.917	.145	5.825	3.135	1.345	3.097	1.859	.025	.217	.158	266
267	3.199	5.561	.130	5.569	3.191	1.199	3.109	1.752	.023	.193	.139	267
268	3.233	5.776	.289	5.803	3.201	1.304	6.394	1.815	.050	.169	.150	268
269	3.533	6.343	.213	6.259	3.522	1.419	4.315	1.805	.034	.172	.151	269
270	3.671	6.646	.273	6.571	3.646	1.512	5.203	1.930	.041	.174	.156	270
271	3.953	7.023	.286	7.057	3.829	1.815	5.100	1.944	.041	.175	.160	271
272	4.055	7.433	.263	7.453	4.034	1.709	4.424	1.847	.035	.173	.163	272
273	5.870	7.642	.246	7.663	3.954	1.855	3.864	1.930	.032	.160	.178	273
274	4.267	8.945	.542	8.909	4.203	2.352	6.666	2.119	.051	.216	.216	274
275	3.814	10.136	.776	10.289	3.721	3.284	6.832	2.765	.076	.334	.334	275
276	4.189	12.122	.063	12.123	4.169	3.967	.594	2.894	.007	.365	.365	276
277	2.715	11.228	1.299	11.422	2.521	4.450	8.456	4.530	.116	.628	.628	277
278	2.552	11.986	1.040	12.099	2.456	4.922	6.229	4.927	.087	.695	.695	278
279	2.897	13.752	1.173	12.890	2.760	5.065	6.594	4.671	.092	.652	.652	279
280	2.555	12.341	.866	12.421	2.475	4.973	5.133	5.019	.072	.711	.712	280
281	2.497	13.575	.737	13.136	2.437	5.349	4.295	5.389	.041	.775	.776	281
282	2.466	14.225	.755	14.273	2.420	5.927	3.661	5.899	.053	.865	.865	282
283	3.847	10.206	.303	10.221	3.832	3.194	2.780	2.657	.031	.653	.663	283
284	6.865	12.627	-.769	12.726	6.767	2.979	-7.379	1.881	-.000	.471	.380	284
285	10.241	14.729	-2.004	15.406	9.475	3.005	-20.915	1.634	-135	.453	.286	285
286	11.307	19.835	-3.389	21.017	10.124	6.447	-19.235	2.076	-171	.444	.233	286
287	10.619	19.405	-4.595	21.362	9.862	6.350	-23.115	2.466	-236	.474	.316	287
288	9.351	19.367	-4.546	20.267	7.481	6.393	-22.674	2.709	-246	.453	.332	288
289	8.676	18.050	-4.662	19.974	6.752	6.611	-22.424	2.958	-258	.500	.406	289
290	7.371	17.506	-3.896	18.824	8.053	6.386	-18.741	3.110	-222	.479	.430	290
291	6.572	18.250	-3.557	19.341	5.581	6.880	-15.568	3.465	-194	.505	.457	291
292	5.276	12.801	-2.263	13.429	4.848	4.391	-15.511	2.889	-177	.442	.442	292
293	5.669	13.009	-2.056	13.507	4.510	4.498	-13.815	2.995	-159	.454	.454	293
294	4.773	11.951	-1.961	12.490	4.270	4.110	-14.406	2.926	-165	.444	.444	294
295	4.377	10.793	-1.773	11.250	3.914	3.668	-14.450	2.874	-164	.430	.427	295
296	3.937	9.671	-1.492	10.038	3.563	3.238	-13.723	2.816	-154	.420	.409	296
297	3.531	8.615	-1.286	8.910	3.226	2.842	-13.159	2.782	-146	.403	.393	297
298	3.116	7.490	-1.039	7.724	2.882	2.421	-12.706	2.880	-139	.390	.385	298
299	2.829	7.084	-.750	7.213	2.700	2.256	-9.709	2.671	-106	.385	.380	299
300	3.299	6.482	-.409	6.525	3.246	1.844	-7.209	2.012	-063	.482	.482	300
301	3.122	5.895	-.354	5.946	3.070	1.439	-7.734	1.937	-065	.452	.415	301

301	.611	5.666	-.309	5.702	2.975	1.363	-6.555	1.916	-.055	.446	.464	312
303	2.764	5.520	-.319	5.557	2.728	1.414	-6.527	2.037	-.058	.476	.451	303
304	2.323	4.567	-.459	4.657	2.233	1.212	-11.126	2.086	-.101	.460	.450	304
305	1.946	3.286	-.456	3.424	1.708	.858	-16.466	2.004	-.142	.416	.406	305
306	1.547	2.540	-.284	2.615	1.471	.572	-14.905	1.779	-.112	.389	.308	306
307	1.265	2.367	-.038	2.292	1.259	.587	-3.976	1.900	-.053	.414	.348	307
308	1.195	2.392	-.037	2.400	1.194	.603	-1.740	2.010	-.015	.425	.397	308
309	1.181	2.399	-.011	2.399	1.160	.614	-.492	2.059	-.004	.431	.404	309
310	.359	.363	.146	.507	.216	.146	44.639	2.351	.401	.179	.160	310
311	.752	1.312	.295	1.439	.625	.407	23.266	2.301	.225	.216	.185	311
312	1.209	2.681	.379	2.773	1.117	.828	13.628	2.483	.141	.253	.231	312
313	1.314	3.542	.279	3.576	1.279	1.148	7.034	2.795	.079	.322	.286	313
314	1.562	4.249	.141	4.256	1.555	1.351	2.987	2.738	.053	.339	.286	314
315	1.579	4.247	.068	4.249	1.577	1.336	1.457	2.694	.016	.345	.279	315
316	1.780	4.524	-.093	4.527	1.777	1.375	-1.941	2.547	-.021	.294	.260	316
317	2.305	5.465	.107	5.469	2.301	1.584	1.940	2.376	.020	.257	.241	317
318	1.810	4.692	.804	4.814	1.688	1.583	11.364	2.851	.129	.362	.370	318
319	1.728	4.816	.140	4.823	1.722	1.551	2.597	2.801	.029	.379	.361	319
320	1.883	5.133	.181	5.143	1.873	1.635	3.170	2.746	.035	.371	.355	320
321	1.883	5.414	.123	5.423	1.924	1.753	3.654	2.822	.142	.392	.372	321
322	2.069	5.930	.205	5.841	2.058	1.892	3.114	2.839	.036	.393	.379	322
323	2.206	6.266	.202	6.276	2.196	2.040	2.846	2.858	.032	.397	.367	323
324	2.331	6.834	.259	6.849	2.316	2.265	3.275	2.957	.038	.411	.411	324
325	2.404	7.101	.405	7.136	2.369	2.384	4.905	3.012	.057	.424	.424	325
326	2.899	10.100	.716	10.170	2.827	3.671	5.625	3.597	.071	.470	.470	326
327	3.921	9.890	1.116	10.062	2.649	3.706	8.762	3.795	.113	.501	.501	327
328	2.737	10.275	1.094	10.430	2.592	3.924	8.095	4.040	.106	.542	.542	328
329	2.977	11.413	1.114	11.555	2.832	4.363	7.397	4.081	.098	.559	.559	329
330	2.807	12.256	.871	12.335	2.728	4.804	5.225	4.522	.071	.634	.634	330
331	2.624	12.784	.739	12.937	2.571	5.133	4.137	4.994	.056	.712	.712	331
332	3.816	10.074	.406	10.161	3.789	3.156	3.895	2.666	.040	.667	.667	332
333	6.553	12.192	-.651	12.272	6.479	2.997	-6.491	1.894	-.033	.482	.384	333
334	9.704	14.365	-.196	15.019	9.056	2.985	-19.336	1.660	-.136	.466	.295	334
335	10.437	18.875	-.303	19.840	9.533	5.154	-17.814	2.091	-.133	.396	.237	335
336	9.524	19.290	-.404	19.935	7.969	5.933	-21.222	2.469	-.219	.409	.317	336
337	8.410	17.254	-.407	16.846	6.818	6.014	-21.336	2.764	-.236	.421	.367	337
338	7.413	16.432	-.392	17.906	5.940	5.983	-20.543	3.015	-.239	.435	.410	338
339	6.699	16.128	-.336	17.189	5.638	5.775	-17.640	3.049	-.207	.431	.413	339
340	5.746	15.466	-.353	16.105	5.126	5.491	-13.766	3.142	-.154	.449	.426	340
341	5.469	11.749	-.107	12.332	4.646	3.773	-16.972	2.557	-.179	.400	.367	341
342	5.298	11.032	-.114	11.981	4.719	3.631	-17.005	2.539	-.197	.426	.361	342
343	5.230	10.345	-.184	10.941	4.633	3.154	-17.914	2.362	-.178	.414	.318	343
344	4.730	9.129	-.154	9.620	4.239	2.690	-17.572	2.269	-.170	.394	.293	344
345	4.122	8.005	-.129	8.400	3.728	2.336	-16.085	2.253	-.162	.391	.283	345
346	3.563	6.954	-.105	7.253	3.264	1.995	-15.993	2.222	-.151	.369	.271	346
347	3.036	5.943	-.085	6.192	2.701	1.705	-15.862	2.227	-.149	.369	.265	347
348	2.440	5.009	-.514	5.108	2.341	1.383	-10.896	2.182	-.103	.335	.249	348
349	2.233	4.634	-.345	4.390	2.177	1.106	-9.094	2.016	-.090	.340	.211	349
350	1.924	4.317	-.145	4.326	1.916	1.205	-3.455	2.258	-.034	.362	.257	350
351	1.534	4.044	-.155	4.053	1.524	1.264	-3.513	2.659	-.035	.402	.327	351
352	1.423	3.270	-.346	3.323	1.360	.987	-10.277	2.451	-.106	.331	.281	352
353	1.239	1.779	-.359	1.958	1.060	.449	-26.517	1.847	-.202	.281	.157	353
354	.869	1.014	-.039	1.024	.660	.082	-14.096	1.191	-.033	.195	.034	354
355	.657	.966	-.029	.969	.655	.157	-5.366	1.480	-.031	.209	.063	355
356	.547	.979	-.016	.980	.547	.217	-2.084	1.792	-.016	.219	.133	356
357	.489	.975	-.003	.975	.489	.243	-.351	1.992	-.003	.225	.163	357
358	.333	.346	.102	.437	.232	.103	41.842	1.954	.035	.176	.105	358
359	.652	1.311	.258	1.400	.563	.418	19.006	2.485	.196	.233	.207	359
360	.970	2.507	.210	2.535	.949	.793	7.874	2.670	.084	.285	.254	360
361	1.014	2.859	.049	2.661	1.012	.924	1.530	2.825	.017	.330	.280	361
362	1.525	3.267	.016	3.267	1.325	.971	.296	2.466	.033	.320	.235	362

363	1.193	3.203	-.042	3.206	1.197	1.005	-1.209	2.679	-.012	.320	.265	363
364	1.782	3.755	.254	3.787	1.750	1.018	7.226	2.164	.088	.221	.195	364
365	1.280	3.284	.270	3.320	1.224	1.048	7.473	2.712	.082	.354	.326	365
366	1.449	3.725	.040	3.727	1.448	1.140	.997	2.575	.011	.334	.309	366
367	1.483	3.868	.186	3.882	1.468	1.207	4.445	2.844	.048	.352	.322	367
368	1.562	4.275	.176	4.286	1.551	1.368	3.703	2.764	.041	.366	.348	368
369	1.675	4.665	.148	4.672	1.668	1.502	2.836	2.802	.032	.376	.360	369
370	1.795	5.090	.145	5.097	1.789	1.654	2.523	2.949	.029	.388	.373	370
371	1.934	5.564	.224	5.578	1.890	1.844	3.487	2.951	.040	.398	.397	371
372	2.047	6.046	.323	6.072	2.021	2.026	4.589	3.005	.053	.412	.412	372
373	2.087	8.265	.572	8.258	2.034	3.112	5.291	4.061	.070	.526	.526	373
374	2.256	8.534	1.025	8.698	2.093	3.302	9.042	4.156	.120	.545	.545	374
375	2.365	9.129	1.075	9.296	2.198	3.549	8.820	4.230	.118	.562	.562	375
376	2.459	10.177	1.074	10.324	2.312	4.006	7.777	4.465	.105	.608	.608	376
377	2.360	10.956	.940	11.060	2.258	4.401	6.169	4.899	.088	.681	.681	377
378	2.454	11.973	.885	12.055	2.372	4.841	5.289	5.081	.074	.719	.719	378
379	3.293	9.026	.391	9.054	3.267	2.894	3.878	2.772	.043	.898	.898	379
380	6.280	11.996	-.411	11.926	6.250	2.838	-4.167	1.908	-.035	.490	.388	380
381	8.499	12.937	-1.592	13.449	7.988	2.732	-17.023	1.684	-.123	.493	.301	381
382	10.124	16.171	-2.779	19.037	9.257	4.830	-17.317	2.057	-.163	.391	.230	382
383	6.765	16.400	-3.297	17.620	7.485	5.087	-20.295	2.354	-.201	.419	.285	383
384	8.025	15.755	-3.658	17.211	6.569	5.321	-21.713	2.620	-.232	.415	.335	384
385	7.000	14.499	-6.340	15.771	5.728	5.022	-20.847	2.753	-.230	.423	.355	385
386	6.242	13.888	-2.928	14.821	5.310	4.755	-18.245	2.791	-.204	.433	.358	386
387	5.371	13.427	-2.321	14.090	5.307	4.392	-15.954	2.855	-.173	.434	.331	387
388	5.700	10.155	-2.056	10.958	4.898	3.031	-21.353	2.239	-.202	.371	.292	388
389	5.745	9.552	-1.928	10.415	4.900	2.759	-23.063	2.126	-.265	.392	.255	389
390	6.231	8.555	-1.694	9.303	4.526	2.388	-22.587	2.055	-.197	.387	.246	390
391	4.560	7.403	-1.330	7.930	4.035	1.948	-21.532	1.965	-.180	.362	.221	391
392	3.840	5.269	-1.076	6.694	3.435	1.630	-20.656	1.949	-.171	.365	.212	392
393	3.253	5.267	-.992	5.823	2.917	1.353	-20.827	1.928	-.159	.331	.202	393
394	2.561	4.215	-.633	4.430	2.346	1.042	-18.895	1.888	-.150	.338	.197	394
395	2.085	3.273	-.445	3.427	1.940	.743	-18.385	1.766	-.136	.282	.157	395
396	1.634	2.703	-.195	2.743	1.600	.571	-9.954	1.714	-.072	.293	.142	396
397	1.214	2.457	-.060	2.490	1.211	.640	-2.697	2.056	-.024	.321	.201	397
398	1.269	3.553	-.042	2.683	1.267	.708	-1.717	2.117	-.016	.301	.214	398
399	.817	1.531	-.293	1.689	.719	.495	-18.601	2.349	-.184	.295	.236	399
400	.376	.463	-.098	.504	.301	.102	-37.346	1.676	-.226	.005	.103	400
401	.235	.370	.073	.401	.203	.099	23.622	1.981	.197	.162	.115	401
402	.467	1.221	.165	1.255	.432	.411	11.821	2.933	.135	.267	.254	402
403	.673	1.871	-.037	1.813	.577	.569	-1.979	2.573	-.021	.269	.241	403
404	.675	1.943	-.091	1.953	.670	.642	-3.630	2.915	-.042	.309	.275	404
405	.826	2.337	.044	2.306	.825	.742	1.111	2.800	.019	.299	.267	405
406	.654	1.797	.120	1.810	.642	.584	5.942	2.820	.067	.357	.313	406
407	.897	2.095	.096	2.103	.880	.612	4.594	2.391	.047	.282	.251	407
408	1.037	2.351	.124	2.373	.995	.689	5.191	2.384	.053	.297	.255	408
409	1.070	2.704	.140	2.716	1.059	.829	4.854	2.567	.052	.332	.291	409
410	1.184	3.132	.132	3.141	1.175	.963	3.890	2.674	.042	.337	.315	410
411	1.269	3.501	.105	3.506	1.285	1.121	2.676	2.773	.030	.352	.339	411
412	1.350	3.895	.101	3.899	1.356	1.271	2.277	2.975	.026	.370	.363	412
413	1.488	4.265	.159	4.377	1.480	1.449	3.148	2.958	.036	.384	.384	413
414	1.611	4.840	.277	4.863	1.567	1.638	4.886	3.064	.057	.409	.409	414
415	1.655	5.552	.545	6.710	1.597	2.557	6.157	4.202	.082	.529	.529	415
416	1.739	7.061	.869	7.199	1.601	2.795	9.043	4.497	.123	.576	.576	416
417	1.892	7.892	1.002	8.055	1.722	3.163	9.236	4.660	.127	.613	.613	417
418	2.003	8.927	.976	8.984	1.867	3.549	7.992	4.802	.111	.644	.644	418
419	2.213	10.021	1.130	10.180	2.058	4.081	8.021	4.946	.113	.679	.679	419
420	1.990	10.567	.866	10.657	1.900	4.379	5.937	5.609	.084	.783	.783	420
421	2.203	8.859	.139	8.881	3.200	2.831	1.410	2.769	.016	.893	.893	421
422	5.663	10.571	-.356	10.598	5.556	2.521	-4.179	1.907	-.035	.490	.382	422
423	8.447	12.669	-.910	13.040	8.267	2.386	-11.202	1.577	-.071	.496	.256	423

424	.662	16.237	-2.313	16.340	6.376	4.361	-15.215	2.065	-.137	.424	.231	424
425	8.616	15.364	-3.320	16.724	7.256	4.734	-22.272	2.305	-.216	.406	.274	425
426	7.503	13.217	-2.883	14.419	6.301	4.059	-22.629	2.288	-.218	.392	.264	426
427	6.745	12.327	-2.775	13.475	5.597	3.939	-22.440	2.407	-.225	.408	.284	427
428	6.319	11.508	-2.492	12.511	5.316	3.598	-21.923	2.354	-.217	.404	.271	428
429	5.990	10.861	-2.030	11.696	5.255	3.171	-19.908	2.207	-.187	.400	.241	429
430	6.034	8.455	-1.969	9.555	4.932	2.311	-29.205	1.937	-.233	.342	.221	430
431	5.457	7.833	-1.830	8.827	4.463	2.192	-28.502	1.978	-.234	.386	.227	431
432	4.874	6.841	-1.441	7.602	4.113	1.745	-27.045	1.848	-.211	.353	.195	432
433	4.079	5.661	-1.067	6.214	3.526	1.344	-26.974	1.763	-.192	.523	.171	433
434	3.337	4.619	-.834	5.031	2.925	1.053	-26.227	1.720	-.181	.326	.157	434
435	2.652	3.553	-.694	3.930	2.275	.827	-28.515	1.727	-.195	.299	.152	435
436	2.056	2.564	-.406	2.789	1.830	.479	-28.995	1.924	-.159	.262	.106	436
437	1.352	1.573	-.277	1.760	1.165	.298	-34.139	1.511	-.176	.229	.096	437
438	.808	.984	-.045	.995	.797	.099	-13.555	1.248	-.046	.199	.044	438
439	.641	.972	-.014	.973	.641	.166	-2.349	1.518	-.014	.210	.009	439
440	.589	.972	-.029	.974	.567	.204	-4.022	1.720	-.029	.217	.121	440
441	.331	.498	-.183	.571	.250	.156	-28.950	2.213	-.266	.252	.180	441
442	.119	.313	.051	.326	.106	.110	13.837	3.068	.163	.246	.216	442
443	.197	.605	-.006	.607	.163	.212	-4.532	3.001	-.006	.001	.265	443
444	.111	.695	-.006	.695	.111	.292	-.794	6.278	-.012	.655	.556	444
445	.218	.917	.087	.928	.266	.360	6.977	4.465	.095	.442	.408	445
446	.265	.602	-.008	.602	.264	.169	-1.407	2.278	-.014	.219	.190	446
447	.356	.794	.058	.802	.351	.226	7.488	2.285	.073	.231	.200	447
448	.541	1.203	.056	1.214	.537	.339	4.744	2.261	.046	.241	.211	448
449	.667	1.543	.072	1.549	.552	.444	4.664	2.342	.047	.273	.232	449
450	.771	1.961	.101	1.971	.763	.604	4.803	2.592	.051	.287	.279	450
451	.851	2.343	.067	2.346	.848	.749	2.552	2.765	.028	.318	.317	451
452	.941	2.721	.062	2.723	.929	.892	1.992	2.899	.023	.348	.345	452
453	1.027	3.159	.101	3.162	1.023	1.070	2.710	3.093	.032	.357	.397	453
454	1.171	3.617	.212	3.636	1.153	1.241	4.938	3.154	.059	.406	.406	454
455	1.279	5.127	.522	5.191	1.214	1.993	7.308	4.276	.098	.516	.518	455
456	1.367	5.881	.765	5.790	1.227	2.291	10.069	4.717	.139	.539	.559	456
457	1.554	6.605	.896	6.766	1.353	2.703	9.620	4.993	.135	.643	.643	457
458	1.672	7.837	.912	7.773	1.536	3.119	8.504	5.062	.119	.667	.667	458
459	1.764	8.557	.870	8.662	1.653	3.492	6.706	5.186	.095	.697	.697	459
460	2.032	10.057	.993	10.176	1.911	4.133	6.954	5.326	.099	.736	.736	460
461	1.866	9.862	.896	9.951	1.757	4.102	6.307	5.669	.091	.764	.794	461
462	2.760	7.714	.233	7.735	2.749	2.488	2.689	2.810	.030	.696	.696	462
463	5.095	9.855	-.263	9.843	5.069	2.387	-.425	1.942	-.029	.506	.391	463
464	7.072	10.987	-.931	11.197	6.295	2.164	-12.735	1.630	-.095	.516	.272	464
465	8.194	15.886	-1.052	15.313	7.767	4.273	-12.920	2.100	-.117	.427	.233	465
466	8.555	16.693	-2.292	17.316	8.242	4.533	-15.116	2.099	-.137	.416	.235	466
467	7.664	12.640	-2.070	13.399	6.916	3.238	-19.879	1.936	-.164	.566	.195	467
468	6.863	11.332	-2.426	12.446	5.902	3.319	-23.490	2.143	-.213	.384	.232	468
469	6.376	10.169	-2.426	11.352	5.193	3.080	-25.992	2.185	-.239	.390	.236	469
470	5.976	9.197	-2.199	10.312	4.881	2.728	-26.892	2.122	-.239	.367	.221	470
471	5.926	9.853	-1.950	9.574	4.912	2.381	-27.464	1.990	-.228	.355	.195	471
472	5.465	6.459	-1.724	7.756	4.167	1.795	-36.957	1.861	-.267	.310	.196	472
473	5.004	5.753	-1.476	6.901	3.856	1.523	-37.075	1.790	-.257	.307	.180	473
474	4.097	4.678	-1.074	5.500	3.275	1.113	-37.435	1.879	-.230	.203	.151	474
475	3.297	3.837	-.806	4.290	2.643	.824	-39.056	1.623	-.222	.267	.134	475
476	2.472	2.575	-.493	3.013	2.027	.496	-42.026	1.489	-.192	.254	.101	476
477	1.616	1.601	-.383	1.933	1.227	.382	-45.564	1.637	-.243	.232	.121	477
478	.892	.759	-.178	1.015	.635	.190	-55.282	1.598	-.234	.200	.103	478
479	.396	.263	-.116	.461	.189	.136	-60.014	2.450	-.459	.204	.204	479
480	.176	.033	.007	.101	.073	.014	15.890	1.396	.076	.163	.049	480
481	.135	.231	.023	.295	.131	.082	8.318	2.245	.080	.197	.165	481
482	.198	.487	.024	.489	.195	.146	4.653	2.494	.049	.220	.212	482
483	.317	.802	.049	.806	.312	.247	5.690	2.586	.061	.242	.242	483
484	.430	1.132	.027	1.193	.423	.382	2.021	2.782	.023	.257	.257	484

465	.512	1.544	.030	1.545	.511	.517	1.637	3.021	.015	.325	.335	465
466	.578	1.963	.062	1.966	.575	.695	2.508	3.419	.032	.408	.408	466
467	.716	2.392	.119	2.401	.708	.847	4.056	3.393	.050	.417	.417	467
468	.864	3.579	.425	3.644	.800	1.422	8.686	4.559	.119	.526	.526	468
469	1.047	4.289	.872	4.423	.914	1.755	11.204	4.842	.157	.580	.580	469
470	1.247	5.320	.771	5.461	1.108	2.178	10.369	4.940	.145	.614	.614	470
471	1.425	6.439	.805	6.565	1.300	2.633	8.901	5.052	.125	.648	.648	471
472	1.491	7.205	.895	7.343	1.353	2.995	8.729	5.426	.125	.712	.712	472
473	1.776	8.192	1.002	8.345	1.623	3.361	8.674	5.142	.122	.698	.698	473
474	1.864	8.518	.741	8.597	1.585	3.506	8.097	5.424	.067	.730	.730	474
475	2.417	6.849	.127	6.852	2.414	2.219	1.843	2.039	.019	.695	.695	475
476	4.364	8.725	-.192	8.733	4.355	2.189	-2.521	2.005	-.022	.533	.410	476
477	6.255	9.650	-.577	9.746	6.160	1.793	-9.384	1.582	-.060	.527	.248	477
478	7.419	13.504	-.441	13.816	7.108	3.354	-12.441	1.944	-.104	.399	.197	478
479	7.501	12.713	-.284	13.572	6.641	3.465	-20.619	2.044	-.180	.376	.216	479
480	8.344	10.708	-.042	11.515	5.537	2.989	-21.548	2.079	-.191	.392	.217	480
481	6.182	9.512	-.079	10.510	5.184	2.863	-25.653	2.027	-.218	.357	.205	481
482	5.898	8.062	-.216	9.313	4.446	2.433	-30.453	2.095	-.284	.345	.213	482
483	5.506	7.028	-.990	8.397	4.137	2.130	-34.536	2.030	-.283	.322	.198	483
484	5.147	6.168	-.107	7.439	3.675	1.782	-36.677	1.920	-.277	.301	.176	484
485	4.757	4.451	-.140	6.018	3.192	1.412	-48.112	1.885	-.315	.258	.195	485
486	3.980	3.525	-.105	4.834	2.672	1.081	-51.074	1.909	-.300	.245	.174	486
487	3.079	2.920	-.622	3.512	2.107	.662	-55.128	1.605	-.237	.223	.125	487
488	1.904	1.623	-.421	2.207	1.320	.443	-54.255	1.672	-.269	.227	.129	488
489	1.069	.758	-.239	1.198	.628	.285	-61.519	1.908	-.315	.205	.155	489
490	.475	.275	-.142	.549	.201	.174	-62.531	2.729	-.517	.248	.248	490
491	.623	.103	.005	.103	.032	.035	4.359	3.191	.052	.231	.261	491
492	.070	.291	.007	.292	.070	.111	1.829	4.175	.024	.405	.405	492
493	.095	.483	-.002	.483	.096	.193	-.329	5.045	-.005	.516	.516	493
494	.151	.803	.032	.604	.149	.328	2.822	5.393	.040	.595	.595	494
495	.211	1.175	.025	1.176	.211	.483	1.466	5.585	.021	.657	.657	495
496	.414	2.052	.306	2.106	.358	.875	10.323	5.890	.153	.632	.632	496
497	.733	2.957	.428	3.036	.654	1.191	10.490	4.643	.144	.521	.521	497
498	1.061	4.060	.637	5.193	.931	1.629	11.516	4.500	.157	.530	.530	498
499	1.209	5.053	.717	5.183	1.080	2.052	10.233	4.799	.142	.599	.599	499
500	1.370	6.039	.857	6.185	1.224	2.480	9.859	5.052	.139	.642	.642	500
501	1.436	6.743	.858	6.879	1.301	2.789	8.957	5.289	.127	.686	.686	501
502	1.646	7.812	.984	7.735	1.523	3.108	8.078	5.078	.114	.669	.669	502
503	2.010	5.762	.106	5.763	2.009	1.877	1.042	2.869	.012	.690	.690	503
504	3.886	7.746	-.094	7.749	3.878	1.935	-1.385	1.995	-.012	.526	.401	504
505	5.140	7.890	-.086	7.835	5.092	1.423	-7.455	1.559	-.046	.532	.232	505
506	6.636	12.109	-.152	12.579	5.166	3.207	-15.713	2.040	-.156	.371	.213	506
507	5.962	10.402	-.173	11.001	5.363	2.819	-19.015	2.051	-.167	.376	.210	507
508	5.669	8.937	-.182	9.749	4.857	2.446	-24.044	2.007	-.204	.343	.199	508
509	5.076	7.359	-.178	6.335	4.097	2.120	-28.718	2.035	-.242	.323	.199	509
510	4.811	6.110	-.195	7.436	3.485	1.975	-35.402	2.134	-.305	.293	.211	510
511	4.109	4.792	-.165	6.134	2.767	1.863	-39.152	2.216	-.344	.273	.219	511
512	4.029	3.821	-.146	5.425	2.425	1.500	-46.989	2.237	-.392	.240	.219	512
513	3.176	2.253	-.803	3.641	1.788	.927	-59.949	2.037	-.357	.209	.209	513
514	2.043	1.451	-.492	2.321	1.173	.574	-80.515	1.980	-.339	.209	.185	514
515	1.255	.799	-.269	1.396	.658	.369	-84.131	2.120	-.362	.200	.193	515
516	.541	.258	-.129	.591	.208	.192	-88.029	2.042	-.500	.263	.263	516
517	.076	.117	.004	.117	.076	.021	6.144	1.540	.037	.205	.069	517
518	.152	.253	.009	.259	.151	.054	4.901	1.716	.036	.190	.097	518
519	.115	.835	.113	.853	.098	.377	8.748	8.717	.136	.806	.806	519
520	.637	2.002	.143	2.016	.623	.697	5.917	3.238	.071	.317	.317	520
521	.783	2.747	.625	3.373	.552	1.113	14.056	4.415	.191	.485	.485	521
522	1.129	4.110	.624	4.236	1.003	1.616	11.357	4.221	.152	.494	.494	522
523	1.217	4.824	.760	4.978	1.083	1.958	11.423	4.683	.158	.570	.570	523
524	1.409	5.879	.659	5.038	1.250	2.394	10.509	4.832	.146	.603	.603	524
525	1.389	6.395	.627	6.529	1.256	2.636	9.146	5.197	.129	.657	.657	525

546	2.007	6.533	.083	5.540	2.005	1.767	1.351	2.762	.015	.651	.651	546
547	3.001	6.035	-.068	6.036	3.000	1.518	-1.291	2.012	-.011	.552	.393	547
548	5.099	7.545	-.272	7.575	5.069	1.253	-6.285	1.494	-.038	.501	.205	548
549	5.509	10.226	-1.511	10.069	5.066	2.801	-16.324	2.105	-.148	.455	.219	549
550	5.614	9.026	-1.005	9.064	4.978	2.343	-21.618	1.941	-.178	.403	.186	550
551	4.988	7.014	-1.589	7.006	4.117	1.084	-28.741	1.915	-.227	.373	.176	551
552	5.017	5.912	-1.551	7.079	3.850	1.615	-36.957	1.839	-.262	.317	.159	552
553	3.949	4.145	-1.557	5.007	2.487	1.560	-43.198	2.254	-.376	.325	.223	553
554	4.032	3.265	-1.225	4.932	2.364	1.284	-53.693	2.086	-.375	.202	.191	554
555	1.888	1.580	-.913	2.660	.808	.926	-49.778	3.291	-.578	.339	.339	555
556	1.214	.623	-.357	1.382	.455	.464	-64.799	3.039	-.573	.331	.331	556
557	.515	.149	-.074	.530	.135	.197	-79.014	3.921	-.494	.389	.389	557
558	.134	.262	-.011	.263	.133	.065	-4.851	1.979	-.042	.208	.107	558
559	.193	.839	.120	.881	.171	.345	10.158	5.031	.143	.459	.459	559
560	.651	2.165	.329	2.233	.582	.826	11.736	3.835	.152	.397	.397	560
561	.766	2.936	.595	3.088	.814	1.237	14.374	5.032	.203	.570	.570	561
562	.927	4.062	.873	4.200	.789	1.708	11.614	5.326	.186	.638	.638	562
563	1.007	4.795	.747	4.939	.865	2.037	10.748	5.712	.156	.705	.705	563
564	1.062	5.696	.785	5.730	.930	2.400	9.545	6.162	.140	.782	.782	564
565	1.667	4.633	.123	4.633	1.821	1.429	2.473	2.560	.026	.559	.571	565
566	2.854	5.761	-.042	5.762	2.853	1.454	-.826	2.020	-.007	.543	.394	566
567	3.818	5.925	-.354	5.934	3.760	1.112	-9.275	1.592	-.080	.493	.237	567
568	4.679	6.801	-1.443	9.347	4.233	2.557	-17.177	2.208	-.162	.428	.233	568
569	4.505	7.304	-1.400	7.884	3.925	1.979	-22.506	2.008	-.192	.368	.192	569
570	4.329	6.027	-1.310	6.739	3.618	1.561	-28.525	1.863	-.217	.313	.162	570
571	3.363	4.219	-1.281	5.142	2.441	1.351	-35.761	2.107	-.304	.298	.198	571
572	3.118	3.001	-1.095	4.250	2.069	1.099	-43.916	2.054	-.340	.223	.182	572
573	1.295	1.396	-.610	1.958	.733	.812	-42.834	2.876	-.437	.243	.243	573
574	1.060	.557	-.352	1.241	.376	.433	-62.784	3.303	-.632	.319	.300	574
575	.072	.295	.000	.295	.072	.112	-.036	4.119	.000	.339	.326	575
576	.376	.991	.232	1.060	.298	.381	18.722	3.582	.236	.321	.321	576
577	.634	3.065	.503	2.443	.677	.693	17.376	3.810	.220	.375	.375	577
578	.854	2.915	.649	3.102	.666	1.218	16.105	4.857	.223	.524	.524	578
579	.988	3.926	.646	3.986	.949	1.558	12.228	4.671	.169	.548	.548	579
580	1.065	4.564	.619	4.670	.958	1.856	9.741	4.872	.136	.589	.589	580
581	1.538	3.695	.030	3.699	1.525	1.052	.795	2.409	.009	.539	.503	581
582	2.832	4.662	-.389	4.761	2.754	1.003	-11.417	1.729	-.083	.459	.280	582
583	2.714	7.044	-.239	7.454	3.303	2.076	-18.331	2.257	-.176	.367	.233	583
584	3.331	5.945	-.152	6.300	2.948	1.720	-21.023	2.167	-.194	.331	.213	584
585	2.715	4.123	-1.055	4.692	2.153	1.270	-28.096	2.180	-.256	.302	.205	585
586	2.539	3.293	-.766	3.762	2.060	.951	-32.050	1.826	-.233	.217	.142	586
587	1.077	1.435	-.491	1.779	.733	.523	-34.986	2.425	-.342	.230	.208	587
588	.585	.453	-.123	.659	.380	.140	-59.143	1.735	-.271	.276	.096	588
589	.164	.332	.111	.388	.109	.140	26.450	3.568	.335	.270	.270	589
590	.654	1.085	.380	1.307	.433	.437	30.205	3.020	.350	.275	.269	590
591	.998	2.170	.556	2.393	.775	.809	21.786	3.088	.257	.311	.307	591
592	.949	2.663	.577	2.839	.772	1.033	16.982	3.876	.217	.399	.393	592
593	1.029	3.479	.461	3.563	.945	1.309	10.304	3.772	.132	.421	.421	593
594	1.326	2.692	-.037	2.893	1.327	.783	-1.361	2.180	-.013	.465	.413	594
595	2.039	3.406	-.290	3.509	1.936	.786	-14.845	1.813	-.114	.393	.299	595
596	2.533	5.135	-.969	5.457	2.212	1.622	-18.343	2.467	-.189	.311	.255	596
597	2.091	3.854	-.874	4.214	1.731	1.242	-22.381	2.435	-.227	.290	.240	597
598	1.924	3.116	-.603	3.654	1.596	.884	-21.514	2.114	-.194	.236	.184	598
599	.644	1.691	-.691	1.586	.633	.474	-27.701	2.485	-.282	.222	.211	599
600	.269	.494	.026	.497	.266	.115	8.821	1.867	.054	.216	.107	600
601	.392	.222	.230	.589	.126	.231	48.086	4.872	.692	.396	.396	601
602	.522	1.104	.429	1.420	.522	.449	26.414	2.719	.386	.244	.237	602
603	1.100	2.032	.404	2.156	.945	.605	20.920	2.281	.202	.236	.195	603
604	1.111	2.397	.318	2.472	1.037	.717	13.181	2.384	.133	.253	.213	604
605	1.138	2.135	-.045	2.139	1.136	.501	-2.601	1.882	-.021	.341	.303	605
606	1.328	2.255	-.150	2.372	1.211	.551	-18.512	1.959	-.155	.339	.332	606

607	.435	3.051	-.608	3.261	1.286	.986	-19.016	2.536	-.193	.247	.245	607
608	.180	2.480	-.430	2.591	1.048	.772	-16.952	2.472	-.175	.227	.227	608
609	.644	1.284	-.275	1.385	.542	.421	-20.329	2.554	-.214	.215	.215	609
610	.120	.473	.017	.474	.127	.173	2.838	3.720	.036	.294	.294	610
611	.412	.354	.103	.589	.198	.186	49.486	2.879	.518	.226	.219	611
612	.891	1.011	.220	1.123	.579	.272	26.980	1.939	.218	.166	.132	612
613	.774	1.340	.115	1.362	.751	.308	11.055	1.814	.086	.183	.119	613
614	.861	1.383	-.005	1.383	.861	.261	-.503	1.607	-.003	.262	.201	614
615	.892	1.440	-.178	1.493	.839	.327	-16.510	1.780	-.124	.264	.256	615
616	.635	1.473	-.201	1.518	.590	.404	-12.801	2.575	-.136	.221	.221	616
617	.384	.939	-.120	.963	.340	.312	-11.352	2.833	-.128	.235	.235	617
618	.063	.358	-.013	.358	.062	.148	-2.526	5.743	-.036	.496	.496	618
619	.222	.364	.119	.431	.155	.138	29.529	2.786	.326	.249	.200	619
620	.241	.388	.003	.388	.240	.074	1.227	1.814	.008	.153	.074	620
621	.208	.397	-.039	.405	.200	.103	-11.285	2.028	-.099	.160	.120	621
622	.141	.416	-.032	.420	.138	.141	-6.622	3.052	-.076	.225	.225	622
623	.107	.417	.000	.417	.107	.155	.021	3.890	.000	.303	.303	623
624	.077	.346	-.070	.363	.089	.152	-13.687	6.074	-.201	.530	.530	624

## **APPENDIX B**

TABLE B - 1  
COMPUTED LONG-TERM STATIC STRESSES FOR SECTION BB

ELE	SIG-7 (KSF)	SIG-1 (KSF)	TAU-IV (KSF)	SIG-1 (KSF)	SIG-3 (KSF)	TAU-MAX (KSF)	THETA	SIG1/SIG3	TAUXY/SIGY	SICRIT	SLPRES	ELE
1	5.590	10.597	.145	10.601	5.586	2.508	1.660	1.898	.014	.185	.181	1
2	6.022	11.206	.553	11.254	5.974	2.640	5.492	1.884	.045	.180	.180	2
3	6.018	11.392	.592	11.459	5.951	2.754	6.282	1.926	.053	.189	.189	3
4	6.305	11.835	.635	11.907	6.237	2.835	6.504	1.909	.054	.188	.186	4
5	6.539	12.278	.805	12.389	6.426	2.980	7.838	1.927	.066	.193	.191	5
6	6.802	12.771	.936	12.915	6.656	3.129	8.724	1.940	.073	.198	.195	6
7	7.124	13.338	1.024	13.503	6.960	3.272	9.122	1.940	.077	.202	.196	7
8	7.476	14.164	1.095	14.337	7.303	3.517	9.009	1.963	.077	.207	.202	8
9	7.583	14.801	.947	14.922	7.441	3.741	7.333	2.005	.064	.216	.212	9
10	7.371	15.160	.552	15.199	7.333	3.933	4.034	2.073	.036	.230	.225	10
11	6.231	13.108	-.309	13.128	6.210	3.459	-3.219	2.114	-.030	.232	.229	11
12	6.255	10.929	-2.946	12.353	4.831	3.761	-25.787	2.557	-.270	.311	.306	12
13	3.602	6.215	.715	6.398	3.420	1.489	14.342	1.870	.115	.162	.162	13
14	4.565	6.973	.567	9.106	4.753	2.176	10.043	1.916	.063	.181	.180	14
15	3.754	7.079	.249	7.097	3.725	1.681	4.254	1.900	.065	.189	.170	15
16	7.130	12.185	1.004	13.349	6.968	3.190	9.176	1.916	.076	.191	.191	16
17	5.451	10.742	.275	10.756	5.437	2.660	2.989	1.978	.026	.206	.196	17
18	6.079	11.246	.446	11.279	6.040	2.619	4.898	1.867	.040	.192	.177	18
19	5.271	9.986	.595	10.057	5.198	2.430	6.978	1.935	.055	.190	.186	19
20	5.447	10.290	.446	10.331	5.406	2.463	5.256	1.911	.044	.190	.183	20
21	6.671	10.499	.582	10.563	5.807	2.476	6.557	1.884	.054	.185	.178	21
22	9.872	10.856	.699	10.952	5.775	2.588	7.835	1.896	.064	.188	.181	22
23	6.112	11.253	.797	11.374	6.006	2.684	8.635	1.894	.071	.190	.192	23
24	6.436	11.700	.545	11.832	6.304	2.764	8.635	1.877	.072	.187	.180	24
25	6.657	12.402	.951	12.565	6.503	3.031	9.441	1.932	.079	.200	.192	25
26	6.654	13.160	1.075	13.303	6.481	3.426	9.139	2.057	.082	.223	.219	26
27	6.357	13.177	1.092	13.344	6.189	3.578	8.798	2.156	.065	.246	.237	27
28	5.273	13.995	.547	14.033	6.235	3.899	4.033	2.251	.039	.267	.256	28
29	5.199	11.229	-.229	11.963	4.456	3.753	-18.211	2.695	-.195	.237	.237	29
30	2.532	4.096	.544	4.267	2.362	.953	17.413	1.807	.133	.159	.142	30
31	3.395	5.463	.742	5.707	3.156	1.275	17.795	1.807	.136	.151	.149	31
32	3.539	6.331	.697	6.467	3.372	1.548	13.390	1.916	***	.174	.171	32
33	3.745	6.951	.694	7.104	3.605	1.749	11.515	1.971	.095	.195	.182	33
34	3.947	7.509	.477	7.570	3.766	1.892	7.305	2.000	.064	.214	.189	34
35	4.405	7.942	.753	8.095	4.256	1.926	11.540	1.903	.095	.195	.174	35
36	4.192	7.583	.294	7.587	4.158	1.714	4.764	1.924	.039	.177	.159	36
37	4.853	8.534	.405	8.577	4.759	1.969	6.129	1.803	.048	.175	.158	37
38	4.497	8.492	.388	8.520	4.480	2.030	5.512	1.910	.045	.195	.177	38
39	4.704	8.635	.255	8.661	4.674	1.994	5.049	1.853	.041	.195	.167	39
40	4.664	8.775	.448	8.926	4.813	2.006	6.446	1.834	.051	.183	.164	40
41	5.001	8.159	.565	9.236	5.004	2.116	7.745	1.845	.062	.183	.167	41
42	5.385	9.597	.624	9.667	5.275	2.206	6.212	1.837	.065	.195	.167	42
43	5.720	9.964	.653	10.082	5.822	2.230	8.518	1.793	.065	.178	.160	43
44	6.014	10.652	.884	10.814	5.851	2.482	10.421	1.848	.083	.190	.172	44
45	6.057	11.407	1.180	11.649	5.845	2.902	11.785	1.893	.102	.215	.201	45
46	6.062	11.987	1.083	12.179	5.871	3.154	10.042	2.075	.092	.234	.218	46
47	5.913	12.047	.953	12.192	5.774	3.209	8.651	2.112	.079	.243	.225	47
48	5.526	13.511	-.127	13.709	5.329	4.190	-8.872	2.572	-.095	.331	.314	48
49	3.980	10.121	-.243	10.969	3.131	3.919	-19.209	3.503	-.241	.503	.486	49
50	2.139	3.257	.542	3.471	1.919	.776	22.143	1.953	.167	.177	.139	50
51	2.173	3.247	.030	3.377	2.049	.654	15.171	1.848	.121	.159	.111	51
52	2.665	4.023	.573	4.235	2.473	.801	20.292	1.712	.142	.144	.126	52
53	2.795	4.812	.574	4.992	2.615	1.174	14.632	1.899	.119	.175	.100	53
54	2.907	5.579	.559	5.693	2.953	1.420	11.584	1.995	.102	.211	.180	54
55	3.208	6.184	.415	6.241	3.149	1.546	7.791	1.952	.067	.224	.181	55
56	3.349	6.287	.471	6.361	3.275	1.543	8.092	1.942	.075	.213	.174	56

57	3.766	6.470	.251	6.493	3.765	1.364	5.294	1.725	.039	.166	.137	57
58	3.733	6.663	.314	6.697	3.899	1.499	6.052	1.810	.047	.180	.153	58
59	4.039	7.253	.376	7.293	3.996	1.849	6.585	1.825	.052	.183	.150	59
60	3.973	7.114	.279	7.139	3.948	1.595	5.027	1.808	.039	.151	.154	60
61	4.132	7.294	.354	7.333	4.091	1.821	6.303	1.792	.049	.181	.152	61
62	4.332	7.694	.448	7.753	4.274	1.740	7.464	1.814	.059	.182	.157	62
63	4.588	8.147	.460	8.205	4.529	1.838	7.254	1.812	.057	.185	.158	63
64	5.026	8.511	.427	8.563	4.974	1.794	6.876	1.721	.050	.171	.143	64
65	5.457	9.013	.762	9.170	5.300	1.935	11.598	1.731	.085	.163	.146	65
66	5.677	9.661	1.123	10.162	5.396	2.383	14.050	1.893	.114	.192	.177	66
67	5.736	10.760	1.241	11.050	5.446	2.802	13.144	2.029	.115	.224	.206	67
68	5.540	10.540	.829	10.673	5.406	2.634	9.169	1.974	.079	.214	.195	68
69	6.169	13.809	1.003	13.938	6.040	3.949	7.354	2.359	.072	.293	.287	69
70	3.282	9.513	-1.752	9.972	2.823	3.574	-14.679	3.532	-.184	.524	.459	70
71	1.198	1.909	.245	1.995	1.122	.432	17.273	1.770	.126	.190	.120	71
72	1.625	1.984	.172	2.053	1.556	.248	21.899	1.319	.087	.148	.053	72
73	1.895	2.692	.476	2.915	1.673	.621	25.069	1.742	.177	.154	.123	73
74	2.109	3.624	.513	3.791	1.951	.915	17.086	1.938	.142	.159	.160	74
75	2.341	4.462	.428	4.493	2.251	1.121	11.509	1.995	.100	.218	.174	75
76	2.563	4.926	.337	4.973	2.516	1.229	7.971	1.977	.069	.232	.174	76
77	2.828	5.233	.319	5.246	2.786	1.230	7.519	1.883	.061	.220	.159	77
78	2.997	5.149	.134	5.157	2.988	1.084	3.550	1.726	.026	.176	.132	78
79	3.247	5.569	.345	5.615	3.197	1.210	8.273	1.757	.062	.175	.140	79
80	2.906	5.234	.295	5.271	2.670	1.251	6.903	1.672	.056	.197	.158	80
81	3.402	5.982	.197	5.977	5.387	1.295	4.370	1.765	.033	.177	.142	81
82	2.508	6.033	.324	6.050	3.467	1.307	7.175	1.754	.054	.176	.141	82
83	3.613	6.336	.329	6.394	3.574	1.410	6.752	1.763	.052	.183	.148	83
84	4.146	7.046	.307	7.077	4.016	1.531	5.783	1.763	.044	.178	.146	84
85	4.213	7.193	.257	7.212	4.290	1.461	5.074	1.591	.036	.164	.132	85
86	4.863	7.569	.501	7.655	4.773	1.441	10.173	1.604	.066	.147	.119	86
87	5.534	8.583	1.053	8.309	5.206	1.052	17.321	1.711	.123	.155	.142	87
88	5.403	9.390	1.322	9.636	4.996	2.350	17.106	1.941	.142	.204	.195	88
89	5.559	10.623	.859	10.765	5.417	2.674	9.366	1.997	.081	.214	.199	89
90	4.846	9.390	.651	9.464	4.751	2.366	8.116	1.996	.070	.225	.195	90
91	6.917	16.850	-.556	16.891	6.896	4.998	-3.195	2.452	-.033	.341	.302	91
92	2.319	6.333	-1.249	6.729	1.986	2.387	-15.775	3.429	-.196	.769	.415	92
93	.335	.665	.041	.592	.329	.132	9.013	1.803	.070	.169	.102	93
94	.491	.619	.029	.629	.476	.075	11.197	1.816	.046	.154	.043	94
95	.693	.817	.067	.724	.596	.069	61.835	1.235	.093	.146	.033	95
96	1.147	1.346	.302	1.564	.929	.310	35.872	1.594	.224	.141	.104	96
97	1.625	2.456	.393	2.639	1.473	.563	21.202	1.722	.156	.163	.129	97
98	1.760	3.164	.353	3.255	1.677	.795	13.198	1.346	.111	.209	.155	98
99	2.073	3.763	.177	3.782	2.055	.863	5.927	1.840	.047	.216	.145	99
100	2.287	3.979	.237	4.011	2.235	.966	7.736	1.795	.060	.212	.139	100
101	2.443	4.024	.663	4.026	2.440	.793	2.234	1.551	.015	.170	.115	101
102	2.343	3.644	.373	3.744	2.249	.747	14.993	1.665	.102	.155	.116	102
103	2.690	4.099	.235	4.137	2.642	.748	9.175	1.555	.057	.138	.101	103
104	2.719	4.412	.141	4.424	2.707	.953	4.733	1.634	.032	.156	.114	104
105	2.862	4.748	.245	4.779	2.830	.974	7.300	1.888	.052	.171	.125	105
106	3.121	5.310	.275	5.344	3.087	1.128	7.041	1.731	.052	.174	.134	106
107	3.251	5.641	.178	5.654	3.235	1.208	4.223	1.748	.022	.175	.138	107
108	3.807	6.290	.070	6.292	3.805	1.244	1.613	1.654	.011	.162	.124	108
109	2.316	5.853	.731	5.957	2.163	1.922	11.835	2.925	.129	.391	.350	109
110	2.523	6.422	.431	6.526	2.477	2.026	6.139	2.936	.066	.370	.347	110
111	2.857	6.523	.725	6.654	2.526	2.064	10.276	2.934	.111	.373	.348	111
112	3.551	7.161	1.126	7.451	3.332	3.034	11.017	2.521	.124	.353	.339	112
113	3.551	6.916	1.050	9.115	3.291	2.862	10.756	2.998	.116	.340	.314	113
114	3.722	9.453	.926	9.599	3.576	3.011	8.954	2.884	.098	.349	.316	114
115	4.029	10.579	.496	10.616	3.991	3.313	4.309	2.951	.047	.337	.317	115
116	3.070	11.164	-.486	11.193	3.041	4.076	-3.421	3.551	-.044	.510	.491	116
117	4.139	13.700	.350	13.793	4.126	4.033	2.079	3.343	.025	.453	.450	117

115	4.666	10.580	-1.670	10.655	4.611	3.023	-6.423	2.311	-1.064	.538	.633	115
116	5.604	11.581	-1.581	11.955	5.211	3.372	-13.982	2.294	-1.137	.540	.541	116
120	7.359	13.632	-2.377	14.431	6.580	3.936	-18.576	2.200	-1.174	.515	.515	120
121	7.695	19.077	-3.826	20.244	6.532	6.856	-16.965	3.099	-1.201	.433	.433	121
122	7.671	19.246	-3.881	20.427	6.490	6.968	-16.920	3.147	-1.202	.443	.443	122
123	8.791	17.234	-3.537	18.320	5.706	6.307	-17.056	3.211	-1.205	.447	.447	123
124	8.428	16.113	-3.446	17.214	5.327	5.944	-17.721	3.232	-1.214	.446	.446	124
125	5.932	15.215	-3.184	16.202	4.945	5.829	-17.229	3.276	-1.209	.450	.450	125
126	5.642	15.937	-2.943	16.719	4.860	5.930	-14.879	3.440	-1.185	.481	.481	126
127	4.177	11.260	-1.950	11.761	3.676	4.042	-14.417	3.199	-1.173	.496	.496	127
128	4.032	11.193	-1.739	11.593	3.632	3.980	-12.950	3.192	-1.155	.493	.493	128
129	3.739	10.302	-1.544	10.647	3.394	3.627	-12.601	3.137	-1.150	.476	.476	129
130	3.334	9.108	-1.281	9.380	3.063	3.150	-11.980	3.062	-1.141	.452	.452	130
131	2.921	7.971	-1.011	8.166	2.726	2.720	-10.910	2.996	-1.127	.430	.430	131
132	2.542	6.891	-.804	7.035	2.398	2.318	-10.147	2.934	-1.117	.408	.408	132
133	2.155	5.849	-.598	5.942	2.064	1.939	-8.957	2.880	-1.102	.388	.388	133
134	1.859	4.915	-.411	4.970	1.805	1.582	-7.525	2.754	-1.084	.357	.354	134
135	1.619	4.323	-.185	4.335	1.006	1.385	-3.905	2.899	-1.043	.350	.337	135
136	1.539	4.264	-.055	4.265	1.538	1.383	-1.164	2.773	-1.013	.356	.349	136
137	1.336	4.678	-.157	4.083	1.588	1.347	-2.529	2.940	-1.034	.377	.376	137
138	1.228	3.400	-.263	2.436	1.191	1.123	-7.313	2.865	-1.063	.357	.357	138
139	.780	1.869	-.276	1.935	.714	.611	-13.427	2.711	-1.148	.293	.299	139
140	.459	.997	-.046	1.001	.454	.273	-4.868	2.205	-1.046	.229	.196	140
141	.399	.976	.001	.976	.389	.293	.084	2.510	.001	.239	.239	141
142	.390	.975	.000	.975	.390	.292	-.004	2.499	.000	.238	.238	142
143	.303	.363	.118	.454	.212	.121	37.900	2.146	.324	.181	.135	143
144	.571	1.107	.232	1.194	.490	.352	20.671	2.435	.210	.221	.165	144
145	.889	2.677	.243	2.124	.842	.641	11.083	2.524	.117	.264	.227	145
146	1.043	2.560	.059	2.552	1.041	.761	2.226	2.462	.023	.282	.225	146
147	1.243	2.628	.025	2.628	1.244	.692	1.026	2.112	.009	.244	.177	147
148	1.043	2.382	.023	2.383	1.042	.670	1.392	2.286	.014	.240	.195	148
149	1.995	3.515	.135	3.526	1.986	.770	5.031	1.775	.039	.216	.133	149
150	1.626	2.653	.072	2.659	1.623	.517	3.997	1.637	.027	.165	.106	150
151	1.631	2.608	.135	2.632	1.825	.402	9.852	1.440	.052	.123	.074	151
152	2.043	2.970	.144	2.895	2.023	.436	9.637	1.431	.050	.115	.074	152
153	2.143	3.195	.144	3.215	2.123	.546	7.644	1.514	.045	.134	.063	153
154	2.166	3.509	.155	3.535	2.160	.887	7.644	1.636	.053	.165	.110	154
155	2.355	4.050	.215	4.077	2.329	.874	7.106	1.750	.052	.151	.132	155
156	2.610	4.517	.125	4.526	2.801	.962	3.830	1.740	.026	.174	.132	156
157	1.734	4.321	.482	4.338	1.857	1.370	9.841	2.853	.105	.275	.330	157
158	2.085	4.754	.493	4.841	1.965	1.437	10.038	2.460	.104	.343	.299	158
159	2.264	5.176	.480	5.248	2.213	1.517	8.822	2.371	.089	.332	.286	159
160	2.463	5.431	.534	5.524	2.399	1.567	9.967	2.312	.098	.307	.277	160
161	2.781	7.417	.709	7.523	2.855	2.434	8.482	2.834	.096	.345	.329	161
162	3.135	7.788	.982	7.979	2.945	2.517	11.234	2.709	.124	.332	.311	162
163	3.295	5.439	.790	8.555	3.179	2.889	8.440	2.691	.092	.317	.312	163
164	3.246	9.436	.904	9.496	3.286	3.105	5.609	2.889	.064	.350	.350	164
165	2.951	10.553	-.092	10.604	2.951	3.827	-.687	3.593	-.069	.472	.472	165
166	2.695	12.315	.063	12.315	2.898	4.009	.373	4.585	.005	.640	.640	166
167	3.282	9.356	.063	9.357	3.281	3.039	.596	2.852	.007	.728	.728	167
168	5.323	11.492	-.609	11.552	5.283	3.144	-5.589	2.195	-.053	.499	.499	168
169	6.760	11.973	-2.008	12.855	6.078	3.209	-18.709	2.082	-1.168	.485	.485	169
170	8.559	19.192	-3.544	19.352	7.378	5.987	-18.146	2.823	-1.195	.383	.341	170
171	6.776	16.407	-3.255	17.404	5.779	5.813	-17.030	3.012	-1.198	.414	.407	171
172	6.564	15.519	-3.295	16.001	5.482	5.559	-18.174	3.028	-1.212	.407	.407	172
173	5.702	13.759	-2.985	14.733	4.729	5.002	-18.177	3.115	-1.215	.415	.415	173
174	5.037	13.146	-2.743	13.995	4.196	4.895	-17.037	3.334	-1.209	.449	.449	174
175	4.290	12.858	-2.016	13.118	3.830	4.644	-12.882	3.425	-1.159	.460	.460	175
176	3.944	9.490	-1.709	9.975	3.459	3.256	-15.821	2.883	-1.190	.421	.421	176
177	3.993	9.072	-1.840	9.532	3.233	3.150	-15.886	2.949	-1.181	.431	.431	177
178	3.456	6.249	-1.414	6.036	3.072	2.702	-15.275	2.611	-1.171	.408	.397	178

179	3.063	7.047	-1.097	7.329	2.781	2.274	-14.421	2.636	-.156	.364	.353	179
180	2.598	5.925	-.849	6.129	2.394	1.867	-13.520	2.560	-.143	.361	.329	180
181	2.175	4.858	-.639	5.002	2.030	1.486	-12.744	2.464	-.132	.349	.301	181
182	1.755	3.831	-.440	3.920	1.665	1.127	-11.488	2.354	-.115	.340	.273	182
183	1.355	2.884	-.302	2.942	1.297	.822	-10.790	2.267	-.105	.292	.243	183
184	1.070	2.317	-.085	2.323	1.064	.629	-3.860	2.183	-.036	.292	.220	184
185	.845	2.252	-.034	2.253	.845	.704	-1.394	2.067	-.015	.319	.299	185
186	.820	2.275	-.030	2.276	.819	.728	-1.189	2.770	-.013	.326	.317	186
187	.805	1.555	-.199	1.596	.565	.515	-11.386	2.825	-.120	.311	.307	187
188	.283	.427	-.084	.486	.244	.111	-24.837	1.908	-.198	.233	.133	188
189	.218	.258	.080	.320	.158	.082	37.993	2.053	.309	.175	.118	189
190	.439	1.017	.158	1.057	.399	.329	14.317	2.849	.155	.244	.217	190
191	.704	1.652	-.013	1.652	.703	.474	-.803	2.349	-.008	.220	.195	191
192	.765	1.650	-.030	1.651	.764	.444	-1.956	2.162	-.018	.234	.170	192
193	.978	2.193	-.017	2.193	.978	.602	-.790	2.243	-.008	.225	.190	193
194	.875	1.663	.142	1.883	.855	.514	8.019	2.588	.085	.316	.270	194
195	.661	1.638	.020	1.638	.880	.479	1.219	2.409	.012	.297	.244	195
196	.753	1.803	.097	1.812	.744	.534	5.253	2.438	.054	.282	.252	196
197	.871	2.179	.126	2.191	.859	.666	5.467	2.552	.059	.316	.279	197
198	1.012	2.549	.149	2.563	.998	.783	5.492	2.570	.066	.366	.269	198
199	1.127	2.984	.156	2.978	1.112	.933	5.109	2.679	.056	.347	.314	199
200	1.395	3.356	.334	3.411	1.340	1.036	9.412	2.546	.100	.355	.296	200
201	1.746	3.771	.389	3.836	1.881	1.077	10.006	2.282	.096	.320	.256	201
202	2.021	4.179	.399	4.251	1.949	1.151	10.143	2.181	.095	.302	.241	202
203	2.255	4.482	.441	4.567	2.183	1.192	10.871	2.092	.099	.279	.227	203
204	2.436	6.148	.556	6.230	2.256	1.937	8.344	2.644	.090	.323	.289	204
205	2.644	6.695	.782	6.832	2.498	2.167	10.570	2.735	.117	.313	.308	205
206	2.791	7.517	.771	7.840	2.669	2.486	9.038	2.863	.103	.334	.334	206
207	2.803	8.464	.498	8.507	2.759	2.874	4.986	3.083	.059	.375	.375	207
208	2.700	10.036	.452	10.064	2.672	3.096	3.512	3.766	.045	.496	.496	208
209	1.990	11.051	.264	11.059	1.992	4.538	1.669	5.580	.024	.783	.783	209
210	2.920	9.024	-.053	9.025	2.919	3.053	-.500	3.031	-.006	.910	.910	210
211	5.110	10.269	-.382	10.296	5.092	2.607	-4.215	2.026	-.037	.492	.426	211
212	8.329	12.743	-1.319	13.113	7.985	2.574	-15.419	1.846	-.103	.433	.365	212
213	7.517	16.197	-2.710	16.973	6.740	5.117	-15.990	2.518	-.167	.433	.315	213
214	6.985	15.627	-3.511	16.874	5.739	5.567	-19.547	2.940	-.225	.406	.392	214
215	5.814	13.081	-2.899	13.974	4.921	4.526	-18.304	2.840	-.206	.376	.363	215
216	5.078	12.140	-2.516	12.944	4.273	4.336	-17.735	3.029	-.207	.331	.332	216
217	4.403	11.033	-2.193	11.695	3.737	3.979	-16.773	3.130	-.199	.403	.403	217
218	4.068	10.495	-1.837	10.986	3.580	3.703	-14.870	3.069	-.175	.401	.389	218
219	4.051	7.932	-1.618	8.495	3.488	2.503	-20.133	2.435	-.205	.343	.321	219
220	4.020	7.436	-1.577	8.054	3.403	2.326	-21.351	2.367	-.212	.366	.305	220
221	3.645	6.493	-1.257	6.965	3.169	1.899	-20.715	2.199	-.194	.367	.264	221
222	3.017	5.322	-.927	5.648	2.691	1.479	-19.407	2.099	-.174	.337	.236	222
223	2.394	4.231	-.657	4.441	2.174	1.133	-17.723	2.043	-.155	.341	.217	223
224	1.826	3.153	-.514	3.329	1.652	.839	-18.902	2.015	-.163	.337	.202	224
225	1.345	2.171	-.265	2.249	1.269	.491	-16.322	1.774	-.122	.271	.148	225
226	.769	1.189	-.170	1.250	.708	.271	-19.486	1.764	-.143	.222	.133	226
227	.368	.638	.003	.639	.368	.135	.091	1.733	.005	.204	.115	227
228	.322	.652	-.013	.653	.321	.165	-2.251	2.031	-.020	.311	.158	228
229	.281	.650	-.003	.650	.281	.185	-.467	2.313	-.005	.219	.197	229
230	.136	.325	-.063	.345	.117	.114	-15.918	2.943	-.195	.259	.252	230
231	.150	.220	-.059	.333	.133	.103	17.415	2.557	.184	.204	.170	231
232	.241	.601	-.011	.601	.240	.181	-1.821	2.504	-.019	.221	.181	232
233	.207	.679	-.018	.680	.207	.237	-2.150	3.291	-.026	.340	.289	233
234	.419	.750	.069	.764	.405	.179	11.242	1.694	.091	.105	.117	234
235	.285	.588	.004	.588	.284	.152	.746	2.066	.007	.205	.160	235
236	.300	.582	.000	.582	.300	.141	.034	1.939	.000	.208	.143	236
237	.397	.808	.061	.817	.388	.214	8.237	2.103	.075	.219	.175	237
238	.550	1.207	.069	1.214	.543	.336	5.829	2.235	.055	.254	.207	238
239	.704	1.555	.098	1.566	.693	.437	6.494	2.260	.063	.285	.219	239

240	.828	1.967	.131	1.982	.813	.584	6.494	2.437	.067	.307	.255	240
241	1.041	2.374	.206	2.404	1.012	.896	8.352	2.375	.084	.325	.254	241
242	1.378	2.762	.254	2.807	1.333	.737	10.087	2.106	.092	.290	.213	242
243	1.676	3.185	.303	3.247	1.617	.815	11.127	2.006	.097	.270	.200	243
244	1.932	3.522	.340	3.591	1.864	.884	11.590	1.927	.097	.254	.188	244
245	2.097	4.931	.470	5.007	2.021	1.493	9.176	2.477	.095	.296	.253	245
246	2.216	5.567	.666	5.695	2.091	1.802	10.841	2.723	.120	.298	.297	246
247	2.338	6.522	.719	6.642	2.216	2.213	9.482	2.998	.110	.346	.348	247
248	2.329	7.587	.589	7.652	2.261	2.896	8.305	3.384	.078	.416	.416	248
249	2.173	8.886	.317	8.901	2.158	3.371	2.701	4.124	.036	.542	.542	249
250	1.884	10.304	.617	10.349	1.839	4.255	4.189	5.627	.000	.782	.782	250
251	1.704	10.503	.756	10.568	1.639	4.464	4.872	6.446	.072	.903	.903	251
252	2.548	7.839	.116	7.838	2.543	2.648	1.251	3.082	.015	.792	.792	252
253	4.932	9.804	-.343	9.829	4.906	2.461	-4.011	2.003	-.035	.518	.415	253
254	6.714	10.914	-1.271	11.269	6.359	2.455	-15.592	1.772	-.118	.529	.330	254
255	7.308	16.012	-2.296	16.581	6.739	4.921	-13.907	2.480	-.143	.480	.303	255
256	7.783	18.855	-2.525	17.332	7.115	5.109	-14.812	2.438	-.152	.425	.300	256
257	6.535	12.969	-2.285	13.898	5.807	3.948	-17.692	2.359	-.176	.365	.275	257
258	5.456	11.805	-2.307	12.375	4.687	3.844	-18.440	2.640	-.199	.383	.321	258
259	4.947	10.239	-2.229	11.053	4.133	3.460	-20.055	2.874	-.216	.376	.322	259
260	4.721	9.182	-1.998	9.948	3.966	2.991	-20.956	2.509	-.210	.361	.288	260
261	4.662	8.497	-1.718	9.155	4.004	2.575	-20.930	2.286	-.202	.352	.246	261
262	4.480	8.306	-1.546	7.188	3.599	1.795	-29.716	1.993	-.245	.306	.224	262
263	4.101	5.697	-1.394	5.495	3.301	1.598	-30.020	1.968	-.243	.312	.215	263
264	3.338	4.735	-.962	5.242	2.831	1.206	-27.287	1.852	-.207	.318	.185	264
265	2.578	3.593	-.735	3.979	2.192	.893	-27.700	1.815	-.205	.287	.170	265
266	1.929	2.533	-.419	2.751	1.716	.518	-26.982	1.603	-.165	.263	.121	266
267	1.202	1.545	-.292	1.715	1.036	.339	-29.749	1.655	-.189	.229	.121	267
268	.632	.751	-.123	.829	.556	.136	-32.123	1.490	-.163	.208	.082	268
269	.233	.257	-.082	.328	.161	.083	-40.929	2.032	-.321	.186	.141	269
270	.092	.099	.009	.105	.095	.010	34.842	1.232	.094	.165	.030	270
271	.173	.234	.034	.302	.164	.069	14.690	1.847	.116	.186	.116	271
272	.264	.489	.038	.495	.258	.119	9.455	1.822	.079	.206	.127	272
273	.414	.807	.070	.619	.402	.208	9.794	2.035	.057	.236	.165	273
274	.505	1.202	.070	1.212	.595	.308	7.282	2.027	.065	.254	.176	274
275	.855	-1.561	.130	1.571	.835	.366	9.542	1.881	.078	.243	.158	275
276	1.135	1.990	.187	2.029	1.096	.467	11.803	1.852	.094	.229	.159	276
277	1.412	2.359	.226	2.410	1.351	.525	12.753	1.771	.096	.219	.149	277
278	1.560	3.471	.366	3.540	1.511	1.015	10.638	2.343	.106	.259	.220	278
279	1.731	4.241	.571	4.365	1.808	1.379	12.223	2.715	.135	.264	.284	279
280	1.848	5.266	.651	5.377	1.727	1.825	10.455	3.113	.124	.353	.353	280
281	1.914	6.534	.609	6.613	1.835	2.389	7.386	3.604	.093	.440	.440	281
282	1.691	7.437	.663	7.513	1.615	2.949	6.501	4.653	.099	.604	.604	282
283	1.739	8.519	.791	8.610	1.848	3.451	6.563	5.224	.093	.701	.701	283
284	1.473	8.851	.642	8.906	1.418	2.744	4.937	6.253	.073	.856	.856	284
285	2.217	6.899	.036	6.899	2.217	2.341	.436	3.112	.005	.790	.790	285
286	4.163	8.734	-.259	8.749	4.148	2.300	-3.229	2.109	-.020	.552	.449	286
287	5.871	9.545	-.671	9.664	5.752	1.956	-10.040	1.880	-.070	.556	.287	287
288	6.896	13.784	-.1598	14.117	6.543	3.787	-12.463	2.158	-.118	.418	.239	288
289	6.627	12.865	-2.361	13.701	6.015	3.843	-18.971	2.278	-.193	.388	.280	289
290	5.537	10.831	-2.090	11.557	4.811	3.373	-19.149	2.402	-.193	.394	.276	290
291	5.402	9.665	-2.009	10.463	4.605	2.929	-21.658	2.272	-.208	.354	.249	291
292	5.059	6.105	-.199	9.091	4.076	2.807	-26.274	2.232	-.246	.339	.236	292
293	4.076	6.987	-1.855	8.066	3.797	2.135	-30.179	2.124	-.266	.321	.213	293
294	4.490	6.075	-1.510	6.988	3.578	1.705	-31.150	1.953	-.248	.296	.179	294
295	4.144	4.356	-.1254	5.545	2.983	1.289	-42.617	1.870	-.295	.260	.180	295
296	3.476	3.507	-.1017	4.508	2.473	1.017	-44.547	1.822	-.391	.247	.175	296
297	2.460	2.654	-.586	3.243	2.070	.588	-45.135	1.587	-.221	.231	.117	297
298	1.636	1.821	-.401	2.030	1.228	.401	-45.515	1.653	-.247	.223	.124	298
299	.571	.793	-.181	1.007	.632	.189	-52.042	1.594	-.235	.202	.102	299
300	.330	.256	-.112	.412	.176	.118	-53.960	2.335	-.434	.186	.186	300

301	.109	.098	.014	.119	.088	.015	55.613	1.352	.148	.163	.045	301
302	.184	.295	.031	.303	.176	.063	14.427	1.717	.103	.183	.100	302
303	.280	.486	.032	.490	.255	.117	7.919	1.921	.066	.206	.136	303
304	.426	.811	.068	.822	.415	.204	9.654	1.982	.083	.194	.157	304
305	.712	1.171	.080	1.184	.698	.243	9.805	1.695	.088	.174	.121	305
306	.926	2.049	.296	2.122	.853	.635	13.915	2.489	.145	.222	.222	306
307	1.144	2.877	.371	2.953	1.069	.942	11.578	2.764	.129	.273	.273	307
308	1.451	4.038	.566	4.155	1.333	1.412	11.817	3.118	.140	.340	.340	308
309	1.496	5.141	.624	5.244	1.392	1.926	9.446	3.767	.121	.447	.447	309
310	1.523	6.292	.756	6.409	1.406	2.501	8.791	4.558	.120	.576	.576	310
311	1.415	7.009	.790	7.118	1.305	2.906	7.890	5.454	.113	.712	.712	311
312	1.532	7.901	.867	8.016	1.416	3.300	7.818	5.861	.110	.755	.755	312
313	1.811	8.739	.001	5.739	1.811	1.964	.019	3.169	.000	.790	.790	313
314	3.675	7.763	-.120	7.766	3.671	2.048	-1.876	2.115	-.015	.563	.445	314
315	4.819	7.768	-.379	7.816	4.771	1.522	-7.208	1.838	-.049	.588	.263	315
316	6.208	12.445	-1.772	12.918	5.815	3.552	-14.960	2.222	-.142	.406	.248	316
317	5.518	10.553	-1.770	11.113	4.958	3.078	-17.559	2.241	-.169	.395	.245	317
318	5.243	9.050	-1.850	9.801	4.492	2.855	-22.092	2.182	-.204	.349	.230	318
319	4.692	7.430	-1.772	8.300	3.822	2.239	-26.155	2.172	-.238	.328	.222	319
320	4.512	6.127	-1.798	7.289	3.350	1.969	-32.693	2.176	-.293	.292	.219	320
321	3.809	4.697	-1.457	5.776	2.730	1.523	-36.528	2.116	-.310	.267	.201	321
322	3.775	3.743	-1.353	5.112	2.406	1.353	-45.345	2.125	-.381	.233	.198	322
323	3.655	2.226	-.760	3.506	1.776	.865	-53.262	1.974	-.341	.198	.198	323
324	1.983	1.448	-.480	2.286	1.166	.550	-59.584	1.943	-.332	.199	.178	324
325	1.145	.761	-.272	1.289	.626	.231	-62.346	2.058	-.354	.199	.181	325
326	.408	.216	-.112	.460	.164	.148	-65.234	2.798	-.520	.247	.247	326
327	.042	.101	.002	.101	.042	.030	1.878	2.418	.019	.195	.181	327
328	.096	.290	-.001	.280	.098	.092	-.191	2.920	-.002	.248	.245	328
329	.187	.835	.160	.872	.150	.361	13.148	5.819	.192	.536	.536	329
330	.766	1.925	.102	1.934	.757	.598	4.986	2.555	.053	.226	.228	330
331	.928	2.722	.463	2.935	.813	1.011	13.631	3.486	.170	.368	.368	331
332	1.323	4.240	.567	4.346	1.217	1.555	10.612	3.572	.134	.407	.332	332
333	1.272	5.007	.761	5.156	1.122	2.017	11.098	4.594	.152	.561	.561	333
334	1.412	6.195	.662	6.346	1.261	2.542	8.915	5.032	.139	.641	.641	334
335	1.297	6.598	.895	6.746	1.150	2.798	8.332	5.868	.136	.763	.763	335
336	1.937	5.513	.054	5.503	1.827	1.838	.842	3.013	.010	.734	.734	336
337	2.812	5.977	-.066	5.978	2.810	1.594	-1.198	2.127	-.011	.596	.434	337
338	4.705	7.291	-.240	7.402	4.714	1.344	-6.135	1.570	-.032	.541	.235	338
339	5.294	10.460	-1.568	10.918	4.856	3.021	-15.592	2.248	-.160	.491	.246	339
340	5.313	9.204	-1.628	9.794	4.323	2.555	-19.944	2.074	-.177	.425	.211	340
341	4.731	7.074	-1.656	7.931	3.874	2.028	-27.355	2.047	-.234	.355	.193	341
342	4.808	6.004	-1.550	7.057	3.744	1.662	-34.449	1.888	-.258	.316	.168	342
343	3.587	4.072	-1.484	5.333	2.326	1.504	-40.358	2.293	-.364	.325	.227	343
344	3.917	3.160	-1.088	4.825	2.352	1.137	-53.401	1.987	-.344	.201	.170	344
345	1.970	1.589	-.861	2.601	.859	.871	-49.652	3.029	-.541	.303	.303	345
346	1.158	.599	-.310	1.296	.461	.418	-66.017	2.811	-.518	.295	.295	346
347	.432	.154	-.090	.458	.128	.185	-73.507	3.589	-.583	.341	.341	347
348	.122	.254	-.023	.258	.118	.070	-9.791	2.185	-.092	.209	.126	348
349	.137	.844	.098	.857	.123	.387	7.731	5.942	.116	.638	.638	349
350	.572	2.096	.207	2.124	.544	.795	7.589	3.904	.099	.402	.402	350
351	.761	3.020	.583	3.162	.819	1.271	13.851	5.104	.193	.581	.581	351
352	.932	4.337	.688	4.471	.799	1.836	11.003	5.599	.159	.679	.679	352
353	.984	4.982	.812	5.141	.606	2.157	10.999	6.378	.163	.795	.795	353
354	.935	5.813	.872	5.972	.845	2.563	9.939	7.064	.150	.904	.904	354
355	1.637	4.544	.149	4.552	1.630	1.461	2.933	2.793	.033	.654	.645	355
356	2.661	5.550	-.019	5.650	2.661	1.494	-.252	2.123	-.003	.572	.430	356
357	3.554	6.785	-.307	5.800	5.522	1.143	-.793	1.849	-.053	.526	.266	357
358	4.513	9.083	-1.482	9.521	4.075	2.723	-10.483	2.337	-.163	.468	.256	358
359	4.294	7.487	-.1404	8.018	3.765	2.126	-20.861	2.129	-.187	.401	.214	359
360	4.107	6.119	-.1405	8.840	3.385	1.727	-27.204	2.021	-.230	.349	.190	360
361	3.130	4.141	-.1299	5.020	2.250	1.385	-34.299	2.231	-.311	.316	.215	361
362	2.975	3.239	-.1027	4.142	2.072	1.035	-41.334	1.999	-.317	.225	.172	362

363	1.165	1.386	-.591	1.877	.674	.602	-39.704	2.785	-.427	.274	.256	363
364	.803	.459	-.249	.933	.328	.303	-62.345	2.844	-.543	.289	.235	364
365	.124	.267	-.012	.268	.123	.073	-4.928	2.189	-.047	.210	.120	365
366	.214	.943	.139	.973	.188	.392	10.409	5.188	.147	.482	.482	366
367	.639	2.379	.455	2.492	.574	.980	14.161	4.343	.191	.487	.467	367
368	.781	3.086	.890	3.258	.589	1.334	15.559	5.530	.225	.636	.636	368
369	.913	4.062	.734	4.225	.750	1.738	12.503	5.635	.181	.677	.677	369
370	.971	4.889	.732	4.828	.832	1.998	10.747	5.801	.156	.714	.714	370
371	1.444	3.887	.100	3.671	1.440	1.116	2.582	2.560	.027	.579	.549	371
372	2.889	4.957	-.322	4.611	2.636	.988	-9.500	1.750	-.071	.504	.287	372
373	3.587	7.202	-1.281	7.809	3.179	2.215	-17.861	2.394	-.178	.414	.257	373
374	3.290	6.065	-1.172	6.494	2.881	1.816	-20.095	2.270	-.193	.371	.230	374
375	2.587	4.300	-1.069	4.813	2.074	1.369	-25.646	2.320	-.249	.343	.227	375
376	2.441	3.285	-.870	3.830	1.898	.967	-32.067	2.021	-.265	.256	.173	376
377	1.036	1.391	-.470	1.718	.712	.502	-34.648	2.411	-.338	.244	.204	377
378	.581	.539	-.118	.880	.440	.120	-49.971	1.544	-.219	.306	.073	378
379	.071	.319	.021	.321	.069	.126	4.795	4.655	.086	.382	.382	379
380	.514	1.104	.354	1.270	.348	.481	25.117	3.851	.321	.341	.341	380
381	.853	2.399	.617	2.534	.527	.954	20.155	4.043	.287	.432	.432	381
382	.858	2.803	.650	3.001	.661	1.170	16.889	4.542	.232	.507	.507	382
383	.276	3.592	.580	3.721	.856	1.433	11.941	4.349	.161	.500	.500	383
384	1.253	2.779	.063	2.762	1.251	.766	2.341	2.225	.022	.499	.426	384
385	2.015	3.311	-.301	3.404	1.921	.742	-14.576	1.772	-.109	.420	.284	385
386	2.555	5.283	-1.021	5.623	2.215	1.704	-18.413	2.538	-.193	.349	.268	386
387	2.095	4.001	-.890	4.352	1.745	1.304	-21.526	2.494	-.222	.324	.250	387
388	1.657	3.217	-.546	3.475	1.599	.938	-21.778	2.173	-.201	.259	.194	388
389	.631	1.478	-.412	1.679	.630	.524	-25.945	2.684	-.279	.264	.236	389
390	.312	.457	-.015	.459	.311	.074	-5.842	1.476	-.033	.279	.060	390
391	.200	.361	.224	.557	.104	.225	41.078	5.351	.621	.455	.455	391
392	.839	1.186	.472	1.501	.503	.499	35.443	2.983	.405	.271	.271	392
393	1.110	2.076	.479	2.275	.913	.881	22.344	2.491	.230	.257	.225	393
394	1.151	2.409	.397	2.524	1.036	.744	16.134	2.435	.165	.281	.221	394
395	1.191	2.079	-.012	2.079	1.191	.444	-.761	1.746	-.006	.365	.258	395
396	1.390	2.247	-.367	2.382	1.254	.584	-20.292	1.899	-.163	.359	.313	396
397	1.533	3.104	-.663	3.354	1.349	1.003	-20.689	2.487	-.214	.259	.239	397
398	1.271	2.525	-.493	2.695	1.101	.797	-19.081	2.448	-.195	.239	.225	398
399	.699	1.310	-.307	1.436	.562	.437	-22.335	2.558	-.235	.219	.217	399
400	.182	.495	.010	.496	.182	.157	1.824	2.728	.020	.229	.199	400
401	.495	.366	.243	.694	.180	.252	52.599	3.805	.865	.322	.322	401
402	.866	1.028	.285	1.243	.651	.295	37.081	1.911	.277	.166	.130	402
403	.395	1.357	.125	1.396	.956	.220	17.281	1.480	.092	.157	.070	403
404	1.059	1.328	-.023	1.330	1.057	.137	-4.891	1.259	-.018	.249	.088	404
405	1.089	1.411	-.221	1.523	.977	.273	-26.945	1.559	-.156	.254	.188	405
406	.816	1.521	-.252	1.603	.735	.434	-17.794	2.180	-.166	.174	.172	406
407	.470	.968	-.169	1.020	.418	.301	-17.091	2.439	-.175	.191	.191	407
408	.096	.353	-.029	.356	.093	.131	-6.378	3.817	-.082	.294	.294	408
409	.331	.329	.137	.467	.193	.137	45.280	2.425	.418	.194	.166	409
410	.383	.371	.021	.398	.355	.022	53.215	1.122	.056	.139	.016	410
411	.386	.390	-.050	.429	.326	.051	-38.140	1.316	-.128	.142	.040	411
412	.274	.412	-.050	.429	.258	.086	-17.963	1.864	-.122	.151	.081	412
413	.202	.419	-.025	.422	.199	.112	-6.500	2.120	-.060	.161	.131	413
414	.097	.294	-.055	.308	.083	.113	-14.672	3.716	-.188	.284	.284	414

**APPENDIX D: DYNAMIC RESPONSE ANALYSIS OF RIRIE DAM**  
**(Woodward-Clyde Consultants 1989)**

**DYNAMIC RESPONSE ANALYSIS  
OF RIRIE DAM  
CONTRACT NO. DACW 39-87-C-0083  
Final Report**

Prepared for  
**U.S. Army Engineer  
Waterways Experiment Station  
Vicksburg, Mississippi**

**September 1989**

Prepared by  
**Woodward-Clyde Consultants  
500 12th Street, Suite 100  
Oakland, CA 94607-4014**

500 12th Street  
Suite 100  
Oakland, CA 94607-4014  
(415) 893-3600

September 14, 1989

Mr. Joseph P. Koester, CEWES-GH-R  
U.S. Army Engineer  
Waterways Experiment Station  
P.O. Box 631  
Vicksburg, Mississippi 39181-0631

Dear Mr. Koester:

DYNAMIC RESPONSE ANALYSIS OF RIRIE DAM  
CONTRACT NO. DACW 39-87-C-0083  
Final Report

We are pleased to transmit herewith one (1) reproduction copy and five (5) additional copies of our final report on the dynamic response analysis of Ririe Dam. The report incorporates comments from your review of our draft final report.

The study was conducted by Ms. Katherine Fung under the direction of the undersigned. Mr. Robert K. Green reviewed the report under the guidelines of our quality assurance program.

We look forward to continue being of service to you and the Waterways Experiment Station on this and other projects.

Very truly yours,

WOODWARD-CLYDE CONSULTANTS

*Lelio H. Mejia*  
Lelio H. Mejia, Ph.D.  
Senior Project Engineer

cc: Mr. John W. Turner  
Contracting Officer  
w/o Enclosures

Consulting Engineers, Geologists  
and Environmental Scientists

Offices in Other Principal Cities



## ABSTRACT

This report presents the results of plane strain finite element analyses of Ririe Dam performed to evaluate the dynamic response of the dam and its foundation to the design earthquake motions specified by WES for seismic stability evaluation of the dam. The computed dynamic response parameters will be used in the seismic stability evaluation of the dam using the Seed-Lee-Idriss procedure and other current methods. The finite element analyses were conducted on two representative cross-sections of the dam using two-dimensional finite element procedures. The results of the analyses include peak ground accelerations and peak dynamic shear stresses, and acceleration and shear stress time histories. These results together with the cyclic strength and deformation characteristics of the dam and foundation materials will be used to evaluate the seismic stability of the dam.

## PREFACE

This report presents the results of dynamic finite element analyses of Ririe Dam. The analyses constitute part of a multi-phase program to analyze the seismic stability of the dam. This work was performed by Woodward-Clyde Consultants (WCC) during the period May 1988 through September 1989 under contract DACW 39-87-C-0083 with the U.S. Army Engineer Waterways Experiment Station (WES). The work was performed by Ms. Katherine Fung under the direction of Dr. Lelio H. Mejia of Woodward-Clyde Consultants. This report was reviewed by Mr. Robert K. Green under the guidelines of WCC's quality assurance program. The report was also reviewed by Drs. Mary Ellen Hynes and Paul Hadala and Messrs. Joseph Koester, David Sykora, and Ron Wahl, of WES. The contracting officer's representative and project coordinator for WES was Mr. Joseph Koester.

The dynamic finite element analyses were performed using idealized cross-sections of the dam developed by WES. The material properties used in the analyses were developed by WES and Professor H. Bolton Seed of the University of California at Berkeley. Minor modifications to the properties estimated by WES and Seed were made based on comparisons with field measurements of shear wave velocities. These modifications were discussed with WES prior to their use in the dynamic analyses of the dam.

The dynamic response of the dam was analyzed for the ground motions recorded at the damsite during the 1983 Borah Peak earthquake and for the design earthquake motions specified by Dr. E. Krinitzky and Mr. J. Dunbar of WES. Acceleration time histories for the 1983 Borah Peak earthquake were provided by WES. An input acceleration time history meeting the requirements of Dr. Krinitzky and Mr. Dunbar was developed by Professor H. Bolton Seed and was provided by WES.

## CONTENTS

	<u>Page</u>
INTRODUCTION.....	3
DESCRIPTION OF DAM.....	5
ANALYSIS APPROACH.....	6
General.....	6
Representative Dam Sections for Analysis.....	7
Finite Element Models.....	9
Dynamic Material Properties.....	9
DYNAMIC RESPONSE OF RIRIE DAM TO THE 1983 BORAH PEAK EARTHQUAKE.....	13
Earthquake Motions Recorded at Dam Site.....	13
Assessment of 3-D Effects on the Recorded Crest Motions.....	14
Computed Response Using 2-D Finite Element Model of Section AA.....	15
DYNAMIC RESPONSE OF RIRIE DAM TO DESIGN EARTHQUAKE MOTIONS.....	18
Dynamic Response of Section AA.....	18
Dynamic Response of Section BB.....	20
Estimated Effects of 3-D Behavior.....	21
REFERENCES.....	24
APPENDIX A	
APPENDIX B	
APPENDIX C	
APPENDIX D	

## INTRODUCTION

1. Ririe Dam is a 250-foot-high zoned rockfill embankment partially founded on stream alluvium. A plan view of the dam is shown in Figure 1. The dam is located on Willow Creek in southeastern Idaho, about 15 miles northeast of Idaho Falls and 4 miles southeast of the town of Ririe, in Bonneville County. Construction of the dam and related facilities was completed in early 1977.

2. The dam is located in an area which until recently was considered of moderate seismicity. Accordingly, relatively low intensity earthquake motions were considered in design studies for the dam. These studies included pseudo-static stability analyses using a seismic coefficient of about 0.05.\*

3. The dam was shaken by the 1983 Borah Peak earthquake ( $M_s$  7.3) which was centered approximately 180 km west to northwest of the dam site. Although the earthquake resulted in ground motions at the site with a peak acceleration on rock less than about 0.02 g, reliable records of the motion were obtained at the dam crest, the left abutment, the contact between the downstream berm and the left abutment slope, and the intake tower. The location of the instruments which recorded the motion at the dam site is shown in Figure 1.

4. Local faulting identified near the dam site during a recent re-examination of regional seismic hazard was interpreted to be capable of producing an  $M_s$  7.0 earthquake. Similarly, the near-field region within 4 to 10 km of the dam (specifically the Grand Valley graben) was interpreted as active and capable of producing earthquakes of  $M_s$  7.5 (Krinitzky and Dunbar, 1987), thus updating a previous WES report on the geology and seismicity of the region by Patrick and Whitten (1981). A magnitude 7.5 event at a distance of 4 to 10 km could result in rock motions at the dam site with a peak

---

\* Personal communication, 4 February 1986, Mary Ellen Hynes, U.S. Army Engineer Waterways Experiment Station, Vicksburg, MS.

horizontal acceleration of up to 1.2 g (Krinitzky and Dunbar, 1987). Accordingly, studies have been undertaken to re-evaluate the seismic stability of the dam for these earthquake motions.

5. An accelerogram representative of the rock motions specified by Krinitzky and Dunbar (1987) for seismic stability evaluation of the dam was developed by Professor H. B. Seed of the University of California at Berkeley and is shown in Figure 31. The corresponding acceleration response spectrum for 5% damping is shown in Figure 32.

6. The seismic stability of the dam is being evaluated using various current methods including the Seed-Lee-Idriss procedure. This procedure may be summarized in the following main steps (Seed, 1983):

- a. Selection of the design earthquake motions.
- b. Evaluation of the long-term static stresses in the dam and its foundation prior to the earthquake. These stresses were previously evaluated by Woodward-Clyde Consultants (1988).
- c. Computation of the dynamic stresses induced in the dam and its foundation by the selected design earthquake.
- d. Evaluation of the pore pressure generation and cyclic and post-cyclic strength and deformation characteristics of the dam and foundation materials.
- e. Based on the results of steps c and d, evaluation of the overall stability of the dam and of the deformations likely to develop.

7. This report presents the results of finite element analyses performed to evaluate the dynamic stresses induced in Ririe Dam and its foundation by the design earthquake in accordance with step c above. The computed dynamic stresses together with the cyclic resistance of the dam and foundation materials will be used to evaluate the seismic stability and deformations of the dam. Subsequent sections of this report present a description of the dam, the general approach to the dynamic response analyses, and the results of the analyses.

#### DESCRIPTION OF DAM

8. Ririe Dam is a zoned rockfill with a structural height of about 250 feet and a hydraulic height of about 170 feet. The crest of the dam is 34 feet wide and 840 feet long. The crest elevation is 5128.\* Maximum pool elevation is 5119. Figure 1 shows a plan view of the embankment and related facilities. It may be seen that the longitudinal axis of the dam is curved upstream and that the dam is located in a relatively narrow canyon with a curved stream axis.

9. A transverse cross-section of the dam representative of the conditions along the stream axis is shown in Figure 2. This section will be designated as section AA herein and is located as shown in Figure 1. Radial cross-sections of the dam at stations 5+00 and 8+00 (see Figure 1) are shown in Figures 3 and 4, respectively. The dam is a zoned embankment with a vertical central core. The upstream and downstream shells consist of rockfill, gravel fill, and random fill materials. Upstream and downstream slopes in the gravel fill are 2:1 while in the random fill they are 7:1 and 5:1, respectively.

10. The stream alluvium was left beneath major portions of the upstream and downstream shells of the dam. The alluvium is approximately 60 to 70 feet thick and consists predominantly of medium dense to dense sandy gravels with occasional interbedded discontinuous layers of loose gravel and weathered basalt.

11. Figure 5 shows a cross section along the longitudinal axis of the dam. The stream canyon is relatively narrow and has steep sidewalls. The ratio between crest length and structural height of the dam is about 3.4. Bedrock consists of a complex sequence of basalt flows with interbedded breccia flows and clay layers, underlain by tuffaceous sediments.

---

\* All elevations in this report are given in feet (1 ft = 0.3048 m) and refer to mean sea level datum.

## ANALYSIS APPROACH

### General

12. The approach used to evaluate the dynamic response of Ririe Dam and its foundation to the design earthquake consisted of the following steps:

- a. Selection of representative idealized cross-sections of the dam.
- b. Development of finite element models of the idealized sections selected in step a.
- c. Evaluation of dynamic material properties.
- d. Computation of the dynamic response of the dam to the rock motions recorded at the dam site during the 1983 Borah Peak earthquake to assess the adequacy of the selected dynamic material properties and finite element models to simulate the recorded dynamic behavior of the dam.
- e. Computation of the dynamic response of the dam to the design earthquake using two-dimensional finite element procedures and input from steps b, c, and d above; and
- f. Assessment of the effects of three-dimensional behavior on the computed dynamic shear stresses and other dynamic response parameters.

13. The dynamic finite element analyses were performed using the computer program SUPERFLUSH (Earthquake Engineering Technology, 1983) which is a modified version of the program FLUSH developed at the University of California at Berkeley (Lysmer et al., 1975). SUPERFLUSH is a two-dimensional finite element program for the dynamic response analysis of earth structures such as earth and rockfill dams, and the analysis of dynamic soil-structure interaction. The program uses the method of complex response to solve the equations of motion of a soil-structure system in the frequency domain. The non-linear dynamic behavior of soils is modeled using the equivalent-linear method as proposed by Seed and Idriss (1970). The program allows the use of a finite element model with energy-transmitting lateral boundaries and a compliant base. The lateral boundaries represent the exact dynamic effect of

the free-field on the sides of the finite element model (Lysmer et al., 1975). The compliant base prevents the total reflection of energy which occurs at a rigid base (Earthquake Engineering Technology, 1983).

#### Representative Dam Sections for Analysis

14. Ririe Dam is a three-dimensional (3-D) structure located in a relatively narrow canyon with a curved stream axis (see Figures 1 and 5). Thus, 3-D behavior is expected to play a significant role in the dynamic response of the dam. However, in view of the significant expense associated with a full 3-D dynamic response analysis, two-dimensional (2-D) analyses of representative sections of the dam with appropriate corrections for 3-D effects are being used to evaluate the seismic stability of the dam.

15. In current engineering practice, the maximum cross-section of a dam and one or more smaller sections, are typically used to assess the overall dynamic response of the dam. In the case of Ririe Dam, the stream axis of the canyon is curved and the maximum section through the approximate midpoint of the crest, section AC in Figure 1, abuts upstream against the right wall of the canyon (see Figure 4). Because the predominant mode of vibration of the dam is likely to display a tendency to follow the general direction of the stream axis, section AC is not likely to be representative of this mode of deformation. A section likely to be more representative of this deformation mode is the section along the stream axis, section AA in Figure 2.

16. On the above basis, section AA has been selected for seismic stability analysis of Ririe Dam. The quarter section towards the left abutment, section BB (see Figure 3), has also been selected to evaluate the seismic stability of the dam. Accordingly, these two sections have been used in the dynamic finite element analyses presented herein. They were also used for the static finite element analyses previously conducted by Woodward-Clyde Consultants (1988).

17. Cross-sections AA and BB were idealized for analysis as shown in Figures 6 and 7, respectively. It should be noted that these Figures have been transposed with respect to Figures 2 and 3, so the reservoir is on the left side of the figure in accordance with current Corps of Engineers' practice.\*

18. The filter and drain zones upstream and downstream of the silt core and upstream of the cofferdam rockfill (see Figure 2) are likely to have similar material properties to the adjacent rockfill and gravel fill and are not expected to have a significant effect on the overall dynamic behavior of the dam. Therefore, they were not modeled as individual zones but were lumped with the adjacent rockfill and gravel fill.

19. The alluvium foundation contains occasional isolated discontinuous layers of loose gravel and weathered basalt. However, the overall dynamic behavior of this zone is likely to be controlled by the medium dense to dense alluvium gravel. Accordingly, discontinuous layers of loose gravel and weathered basalt were not modeled in the analyses and material properties for medium dense to dense gravels were used throughout the foundation.

20. Based on the history of reservoir levels since construction, a reservoir elevation of 5112 will be used for seismic stability evaluation of the dam. This reservoir elevation and a tail water elevation of 4955 were used in the static and dynamic analyses of the dam. A tailwater elevation of 4955, five feet above the design elevation 4950, was used for convenience. The effect of this slightly higher assumed tail water elevation is expected to be negligible.

---

\* Personal communication, Joseph P. Koester, Waterways Experiment Station, Vicksburg, Mississippi

Finite Element Models

21. The finite element models for dynamic response analysis of sections AA and BB are shown in Figures 8 and 9, respectively. The model for section AA has a total of 782 elements and 781 nodes while that for section BB has 619 elements and 632 nodes. As shown in Figures 8 and 9, a compliant base was assumed at the interface between the upper and lower tuffaceous sediments, and energy-transmitting boundaries were used at the upstream and downstream lateral end boundaries.

22. The finite element models were designed to incorporate all significant material zones in the dam and to provide adequate representation of the predominant modes of vibration of the structure and seismic wave propagation in the range of frequencies of interest to the earthquake response of the dam. Assuming low-strain shear moduli the lowest cutoff frequency of the mesh is about 12 Hz. The portions of the meshes representing the embankment and foundation alluvium are identical to the finite element meshes used in the static analysis of the dam. Although the upper tuffaceous sediments and basalt rock were not modeled in the static analyses, they were modeled in the dynamic analyses in view of the fact that one-dimensional dynamic response analyses indicated that the computed response of the embankment would be affected by the presence of these materials in the foundation.

Dynamic Material Properties

23. The non-linear dynamic behavior of the embankment and foundation materials was modeled using the equivalent-linear method proposed by Seed and Idriss (1970). In this method the dynamic stress-strain behavior of soils is represented by that of a viscoelastic material with elastic modulus and viscous damping which are compatible with the amplitude of induced dynamic shear strain. The analysis is performed in iterations until the shear moduli and damping used in the analysis are compatible with the computed shear strains.

24. The parameters required for the viscoelastic soil model are the total unit weight,  $\gamma$ ; the shear modulus,  $G$ ; the fraction of critical damping,  $\beta$ ; and Poisson's ratio,  $\nu$ . The shear modulus of the embankment and foundation soils was assumed to depend on the effective confining pressure in accordance with following equation proposed by Seed and Idriss (1970).

$$G = 1000 K_2 (\sigma'_m)^{1/2}$$

where  $G$  = shear modulus in psf,  
 $\sigma'_m$  = mean effective confining pressure in psf,  
and  $K_2$  = a factor which depends on shear strain, relative density, maximum particle size, gradation, and other parameters.

25. The variation of  $K_2$  with shear strain is typically defined by the value of  $K_2$  at small strains,  $K_{2\max}$ , and the variation of the ratio  $K_2/K_{2\max}$  (or  $G/G_{\max}$ ) with strain, also known as the modulus reduction relationship. The mean effective confining pressure was computed using the following equation:

$$\sigma'_m = (\sigma'_1 + \sigma'_2 + \sigma'_3)/3$$

The values of  $\sigma'_1$  and  $\sigma'_3$  were obtained from the results of the static stress analyses of the dam. The value of  $\sigma'_2$  was assumed to be as follows:

$$\sigma'_2 = 0.35 (\sigma'_1 + \sigma'_3)$$

but not less than  $\sigma'_3$ , i.e.,  $\sigma'_2 \geq \sigma'_3$ . This assumed value of the intermediate principal effective stress,  $\sigma'_2$ , is based on an estimated average static Poisson's ratio for the embankment and alluvium foundation and on the amount of confinement likely to be imposed by the dam abutments.

26. Values of total unit weight,  $\gamma$ , and of  $K_{2\max}$  for the embankment and foundation materials were estimated by WES and Professor H. B. Seed of the

University of California at Berkeley, based on laboratory and field data including in-situ test data from Becker hammer soundings. These properties were selected for dynamic analysis of the dam. The  $K_{2\max}$  values for the rockfill, the alluvium gravel, and the silt core (see Figures 6 and 7) were, however, modified slightly based on the results of field measurements of shear wave velocities in these materials.

27. A summary of material properties used in the dynamic response analyses of the dam is presented in Table 1. This table summarizes estimated values of total unit weight,  $K_{2\max}$ , modulus reduction and damping relationships, and Poisson's ratio. The modulus reduction and damping relationships for sands by Seed and Idriss (1970) are shown in Figures 10 and 12, respectively. The modulus reduction relationship for gravels by Seed et al. (1984) is shown in Figure 11. Figure 13 shows the modulus reduction and damping relationships for rock by Schnabel (1973).

28. The maximum shear modulus of the tuffaceous sediments and basalt rock at small strains was assumed to be independent of confining pressure and to be given by the values of shear wave velocity estimated for these materials by WES and Seed (see Table 1). The values of Poisson's ratio were estimated from the results of seismic wave velocity measurements in the embankment and foundation.

29. Figures 14 through 17 show comparisons between shear wave velocities used in the dynamic analyses and field measurements at the toe of the dam, the downstream berm, the downstream shell, and in the core of the dam, respectively. The shear wave velocities used in the analyses were computed using the estimated values of total unit weight and  $K_{2\max}$  shown in Table 1, and the results of the static stress analyses of the dam as discussed above. Also shown in these figures are the shear wave velocities computed using the  $K_{2\max}$  values suggested by WES and Seed for the silt core, the rockfill, and the alluvium gravel. It may be seen that the values of  $K_{2\max}$  shown in Table 1 for these materials result in shear wave velocities which are in better agreement with the field measurements than the shear wave velocities computed

using the values of  $K_{2\max}$  estimated by WES and Seed. It may also be noted that the selected values of  $K_{2\max}$  are consistent with published data for similar materials (Seed et al., 1984).

## DYNAMIC RESPONSE OF RIRIE DAM TO THE 1983 BORAH PEAK EARTHQUAKE

Earthquake Motions Recorded at Dam Site

30. The earthquake motions from the 1983 Borah Peak earthquake were recorded by five strong motion accelerographs at the dam site. These instruments are located on the dam crest, on the left abutment, near the contact between the downstream berm and the left abutment slope, and at the base and top of the intake tower, as shown in Figure 1. The abutment and downstream instruments are located on rock. The horizontal components of the downstream instrument are oriented at 140° and 237°. The horizontal components of the other instruments are oriented at 025° and 295° which correspond to the approximate directions of the longitudinal and transverse axes of the dam, respectively.

31. The acceleration time histories recorded during the earthquake were digitized using a time step of 0.005 seconds and were baseline-corrected by WES (Chang, 1985). WES later re-digitized the motions using a time step of 0.01 seconds and rotated the motions recorded by the downstream instrument to coincide with the orientations of the other instruments at the dam site (i.e., 025° and 295°).

32. Of special interest in the evaluation of the dynamic response of the dam to the 1983 Borah Peak earthquake are the motions recorded by the downstream, abutment, and crest instruments in the direction of the transverse axis of the dam (295° component). This direction coincides with the approximate direction of motion at the crest in the fundamental mode of vibration of the dam. Thus, the crest record is likely to display the characteristics of the predominant mode of vibration of the dam more clearly in this direction than in other directions. In addition, the 295° component of the crest motions shows a larger amplification of the rock motions recorded by the abutment and downstream instruments than the other components.

33. Careful examination of the instrument records from the earthquake indicated that the motions recorded at the abutment are more representative of the rock free-field motions at the dam site than the motions recorded at the downstream berm. The acceleration time history for the 295° component of the abutment motions is shown in Figure 18. The corresponding acceleration response spectrum for 5% damping is shown in Figure 19. The Fourier amplitude spectrum, smoothed using a triangular weighting function with an aperture of 1 Hz, is shown in Figure 20. It may be seen that the motions have a peak acceleration of 0.017 g and a predominant period of about 0.4 seconds.

34. The acceleration time history recorded at the crest in the direction of the transverse axis of the dam (295° component) is shown in Figure 21. The corresponding acceleration response spectrum for 5% damping is shown in Figure 22. Figure 23 shows the Fourier amplitude spectrum, smoothed using a triangular weighting function with an aperture of 1 Hz. The peak ground acceleration recorded at the crest is about 0.041 g and the predominant period of the motions is between about 0.4 and 0.5 seconds.

35. The amplification ratio between the Fourier amplitude spectra of the crest and of the abutment motions is shown in Figure 24. The amplification ratio has a large peak at a frequency of 1.76 Hz corresponding to the fundamental mode of vibration of the dam. The corresponding predominant period of vibration is 0.57 seconds. Other peaks in the amplification ratio, corresponding to higher modes of vibration of the structure, occur at frequencies of about 4, 6, 8 and 13 Hz. Beyond 13 Hz the amplification factor between the crest and the abutment motions is less than 1.0.

#### Assessment of 3-D Effects on the Recorded Crest Motions

36. In evaluating the dynamic response of the dam to the 1983 Borah Peak earthquake, it is important to recognize that the dam is located in a relatively narrow canyon with steep sidewalls. Since the dam has a crest length to structural height ratio, L/H, of about 3.4, the 3-D behavior of the structure is likely to have a significant effect on the motions at the crest

of the dam. Therefore, it is desirable to assess the effects of 3-D behavior on the recorded crest motions to allow a meaningful comparison with the computed response from a 2-D dynamic analysis.

37. Previous studies by Mejia and Seed (1983) have shown that the natural frequencies of vibration of dams in narrow canyons are generally higher than the corresponding frequencies of 2-D structures of identical cross-section. For most rock motions the higher natural frequencies of vibration of a 3-D structure result in peak accelerations at the crest which are higher than the crest accelerations of a 2-D structure.

38. A comparison between fundamental frequencies of vibration computed from 2-D and 3-D analyses of dams in triangular and rectangular canyons is shown in Figure 25 (Mejia and Seed, 1983). From this figure it is estimated that the fundamental frequency of vibration of Ririe Dam ( $L/H = 3.4$ ) is likely to be between 1.15 and 1.3 times higher than the frequency of a 2-D model representative of the dam's main section. Considering that the observed fundamental frequency of vibration of the dam during the 1983 Borah Peak earthquake is about 1.76 Hz, it may be concluded that a 2-D model representative of the dynamic characteristics of the dam should have a natural frequency of vibration between about 1.35 and 1.55 Hz. Thus, the predominant period of vibration of the 2-D model should be between about 0.65 and 0.75 seconds.

39. On the above basis and considering the shape of the acceleration response spectrum for the abutment motions (see Figure 19), it may be concluded that a 2-D model representative of the dynamic characteristics of the dam should result in a computed peak acceleration at the dam crest lower than that recorded during the 1983 Borah Peak earthquake.

#### Computed Response Using 2-D Finite Element Model of Section AA

40. The dynamic response of the dam to the 1983 Borah Peak earthquake was computed using the computer program SUPERFLUSH and the finite element

model for section AA together with the dynamic material properties presented in Table 1. The abutment record shown in Figure 18 was used as the input motion. The record was input as an outcrop motion on the lower tuffaceous sediments with a shear-wave velocity of about 2500 feet per second. A maximum frequency of 12 Hz was used in the analysis.

41. The computed acceleration time history at the crest of the dam is shown in Figure 26. It may be seen that the character of the computed motion is very similar to that of the motion recorded at the crest of the dam. In addition, the computed peak acceleration (0.033 g) is consistent with that expected from a 2-D analysis as discussed above. A comparison between the computed and the recorded acceleration response spectra at the crest of the dam is shown in Figure 27. For periods greater than about 0.6 seconds there is good agreement between the spectra. For lower periods the computed spectrum is lower than that recorded at the crest. However, the difference is consistent with the expected difference between 2-D and 3-D accelerations at the crest of the dam.

42. A comparison between the computed and the recorded Fourier amplification ratios at the crest of the dam is shown in Figure 28. In general there is good agreement in the shape of the computed and recorded amplification ratios. As shown by the computed ratio, the fundamental frequency of vibration of the 2-D model of the dam is about 1.55 Hz. This corresponds to a predominant period of vibration of about 0.65 seconds. This value is within the range of periods estimated for the 2-D model of the dam based on the recorded response of the dam and the estimated effects of 3-D behavior.

43. On the above basis, it may concluded that the 2-D finite element model of section AA and the dynamic material properties presented in Table 1 provide a reasonable analytical representation of the recorded dynamic response of Ririe Dam during the 1983 Borah Peak earthquake. Accordingly, it may be assumed that this model will provide an adequate means for evaluating the dynamic response of the dam to the design earthquake motions.

44. The dynamic response of the dam to the 1983 Borah Peak earthquake was also computed using the  $K_{2\max}$  values estimated by Stark and Seed for the rockfill, the alluvium gravel, and the silt core. A comparison between the acceleration response spectrum computed at the crest of the dam using these  $K_{2\max}$  values and the recorded spectrum is shown in Figure 29. A comparison between the computed and the recorded Fourier amplification ratios is shown in Figure 30. It may be seen that the estimates of  $K_{2\max}$  suggested by Stark and Seed for the rockfill, alluvium gravel, and silt core, do not result in a better match of the recorded response than the values presented in Table 1. In fact, the degree of agreement between the computed and recorded motions is slightly lower than for the properties presented in Table 1.

## DYNAMIC RESPONSE OF RIRIE DAM TO DESIGN EARTHQUAKE MOTIONS

45. The dynamic response of Ririe Dam to the design earthquake motions specified by Krinitzky and Dunbar (1987) was computed using the computer program SUPERFLUSH together with the finite element models of sections AA and BB and the material properties presented in Table 1. The acceleration time history used in the analyses is shown in Figure 31. The corresponding acceleration response spectrum for 5% damping is shown in Figure 32. These motions were assumed to be representative of an outcrop of the lower tuffaceous sediments with a shear wave velocity of about 2500 fps. Accordingly, the motions were input at the surface of an outcrop of the lower tuffaceous sediments. The computer program SUPERFLUSH automatically deconvolves the input motions and obtains the motions in the free field and throughout the finite element model including the compliant base. A maximum frequency of 12 Hz was used in the analyses.

46. To evaluate the effects of a maximum frequency of 12 Hz on the computed stresses and accelerations, the results of the SUPERFLUSH analyses were compared with the results of analyses using the computer program SHAKE (Schnabel et al., 1972) and a maximum frequency of 25 Hz. The computed peak accelerations and peak shear stresses in the free-field downstream of the dam are shown in Figures 33 and 34, respectively. Figure 33 shows that using a maximum frequency of 12 Hz as opposed to 25 Hz has a small effect on the computed peak ground accelerations particularly in the soil portion of the profile above approximate elevation 4890 (see Figure 6). As shown in Figure 34 the effects of using a maximum frequency of 12 Hz as opposed to 25 Hz on the computed shear stresses are negligible.

Dynamic Response of Section AA

47. The results of the dynamic response analysis for section AA are summarized in Figures 35 through 38 and Appendices A and B. Figure 35 shows the computed Fourier acceleration amplification ratio between the computed

crest motions and the input rock outcrop motions. The fundamental frequency of vibration of the dam during the design earthquake is about 0.52 Hz. The corresponding predominant period of vibration is about 1.9 seconds. The change in the period of vibration of the dam with respect to that recorded during the 1983 Borah Peak earthquake is due to the degradation in the stiffness of the materials under the strong shaking induced by the design earthquake. The corresponding increase in damping results in damping-out of the motions with frequencies above 4 Hz (see Figure 35).

48. Figure 36 shows the peak horizontal accelerations computed at various points throughout the dam and the foundation. The peak horizontal acceleration computed at the crest of the dam is 0.77 g. The peak accelerations at the base of the finite element model are on the order of 0.58 g. The reduction in peak acceleration from the rock outcrop motions to the base of the model is mainly due to compliance of the lower tuffaceous sediments. It is interesting to note that while the ground motions at the base of the model are relatively uniform, there is a significant difference between the motions computed upstream and downstream of the core trench at the contact between the alluvium and the underlying upper tuffaceous sediments and basalt (see Figure 6).

49. The acceleration time history computed at the crest of the dam is shown in Figure 37. It may be seen that the peak acceleration at the crest is associated with the long period acceleration pulse present in the input time history after about 3 seconds of motion. Acceleration time histories computed at other points throughout the dam and the foundation are presented in Appendix A in accordance with Figure A-1.

50. Figure 38 shows contours of computed peak horizontal shear stresses,  $\tau_{yx}$  (same as  $\tau_{xy}$ ). In general, the stresses computed downstream of the core in the shells of the dam and foundation alluvium are higher than those computed upstream. The shear stresses computed in the core are significantly lower than those computed in the adjacent rockfill and

gravelfill. A table of computed dynamic stresses and strains for section AA is presented in Appendix B in accordance with the element numbering system shown in Figure B-1. Computed shear stress time histories at various points throughout the dam and the foundation are presented in Appendix A in accordance with Figure A-1.

#### Dynamic Response of Section BB

51. The results of the dynamic response analysis for section BB for the design earthquake are summarized in Figures 39 through 42 and Appendices C and D. Figure 39 shows the acceleration amplification ratio computed at the crest of the dam. This ratio indicates that section BB has a predominant period of vibration of about 1.7 seconds for the design earthquake motions. As in the case of section AA, there is a deamplification of the motions for frequencies above 1 Hz and essentially zero response for frequencies above 4 Hz.

52. Figure 40 shows the peak horizontal ground accelerations computed at various points throughout the dam and the foundation. The peak ground acceleration at the crest is 0.92 g. The peak accelerations at the base of the finite element model are on the order of 0.7 g. It is interesting to note that the motions at the base of the model are fairly uniform.

53. The acceleration time history computed at the dam crest is shown in Figure 41. As in the case of section AA, the peak acceleration occurs in response to the long period acceleration pulse in the input motion at about 3 seconds. Acceleration time histories computed at various points throughout the dam and the foundation are presented in Appendix C in accordance with Figure C-1.

54. Figure 42 shows contours of the computed peak horizontal shear stresses throughout the dam and the foundation ( $\tau_{yx}$ ). As in the case of section AA, the stresses in the dam shells downstream of the core are

typically higher than those upstream. In addition, the stresses in the core are significantly lower than in the adjacent rockfill shells. It may be seen that there is a concentration of low shear stresses in the foundation alluvium at the contact with the basalt just upstream of the core. This is likely due to the fact that the low shear strains induced in the rock restrain the development of large shear strains in the adjacent alluvium. A table of dynamic stresses and strains computed from the analysis is presented in Appendix D in accordance with Figure D-1. Shear stress time histories computed at various points throughout the dam and the foundation are presented in Appendix C in accordance with Figure C-1.

#### Estimated Effects of 3-D Behavior

55. Ririe Dam is a complex three-dimensional structure with a crest length to structural height ratio, L/H, of about 3.4. The crest length to height ratio excluding the foundation alluvium is about 4.7. The shape of the cross-section of the canyon is somewhere between rectangular and triangular (see Figure 5). In addition, the transverse axis of the dam is curved in the upstream-downstream direction as shown in Figure 1.

56. Previous studies by Mejia and Seed (1983) have shown that 3-D behavior can have a significant effect on the dynamic response of earth and rockfill dams in narrow canyons, and therefore, may need to be considered in assessing the seismic stability of these dams. The main effects of 3-D behavior typically include an increase in the natural frequencies of vibration of the structure and a reduction in the earthquake-induced shear stresses on horizontal planes,  $\tau_{yx}$ , due to the constraint imposed by the canyon walls.

57. A comparison between the fundamental frequencies computed from 2-D and 3-D dynamic analyses of dams in rigid triangular and rectangular canyons is shown in Figure 25 (Mejia and Seed, 1983). Because of the higher natural frequencies of vibration of the structure, 3-D dynamic behavior typically results in ground accelerations at the dam crest which are higher than those corresponding to 2-D conditions.

58. Based on the geometry of Ririe Dam it is estimated that the ratio between its fundamental frequency of vibration and the frequency of a 2-D model of the main section of the dam,  $f_{3D}/f_{2D}$ , will be about 1.15 for the design earthquake (see Figure 25). Since the fundamental frequency computed using a 2-D model of section AA is about 0.52 Hz (see Figure 35), it is estimated that the natural frequency of the prototype structure will be about 0.60 Hz. The corresponding predominant period of vibration will be about 1.67 seconds.

59. Because the natural frequencies of vibration of the dam will be higher than those of a 2-D model of the structure, the peak ground acceleration at the crest near the dam midsection is likely to be higher than that computed using the 2-D model of section AA. Based on 1) the peak acceleration computed at the crest of section AA (about 0.8 g), 2) the acceleration response spectrum for the design earthquake motions, and 3), the level of damping induced by the shaking in the embankment and foundation materials, a conservative estimate of the peak ground acceleration at the crest near the midsection of the dam is about 1.05 g. Based on the studies by Mejia and Seed (1981) it is estimated that the crest acceleration at the location of section BB in the prototype structure is not likely to be significantly higher than that computed using the 2-D model of section BB (say 0.95 g).

60. For dams in triangular canyons 3-D effects typically result in a reduction in horizontal shear stresses,  $\tau_{yx}$ , at the base of the canyon of about 10 to 20% for dams with a crest length to height ratio, L/H, of 6, and up to about 75% for dams with a ratio, L/H, of 2. For dams in rectangular canyons 3-D effects are somewhat smaller than for dams in triangular canyons (Mejia and Seed, 1983). In view of the fact that 3-D effects on the  $\tau_{yx}$  stresses depend on several other factors including the geometry of the river canyon, the internal zoning of the dam, the difference in stiffness between the upstream and downstream shells, and the intensity of the ground motions, a

reasonable amount of conservatism needs to be exercised in estimating 3-D effects for Ririe Dam, to account for these factors.

61. The effects of 3-D behavior on the computed dynamic shear stresses on horizontal planes,  $\tau_{yx}$ , were estimated based on published results for dams in triangular canyons by Makdisi (1976) and Mejia and Seed (1983), and for dams in rectangular canyons by Ambraseys (1960). Consideration was given to the complex shape of the river canyon at the dam site and the fact that the alluvium underlies the embankment and extends upstream and downstream beyond the toes of the dam.

62. The correction factors recommended to estimate 3-D horizontal shear stresses ( $\tau_{xy3D}$ ) from computed 2-D horizontal shear stresses ( $\tau_{xy2D}$ ) for Ririe Dam are shown in Figure 43. The correction factors vary between 0.75 and 1.0 and depend on the location within the dam section as shown in Figure 43. At a given point, the correction factor depends on the ratio ( $y/h$ ) between the height of the point above the base of the alluvium directly below the point ( $y$ ) and the combined thickness of the embankment and the alluvium along a vertical section through the point ( $h$ ). The recommended correction factors may be used in the foundation alluvium upstream and downstream of the dam and are applicable to sections AA and BB.

63. In applying the above correction factors to the evaluation of earthquake-induced pore pressures and liquefaction potential, the effects of complementary horizontal shear stresses on vertical planes,  $\tau_{zx}$ , and the effects of multidirectional shaking should be considered. Based on the results of Mejia and Seed (1981), it is estimated that for Ririe Dam the ratio  $\tau_{xy}/\tau_{max}$  will be between about 0.85 and 1.0, which is only slightly lower than under typical 2-D conditions (about 0.9 and 1.0). Accordingly, it may be concluded that the effects of the complementary shear stresses,  $\tau_{zx}$ , on the liquefaction potential of the Ririe Dam materials are likely to be small. Thus, it seems reasonable to assume that correction factors commonly used to account for multidirectional shaking in two-dimensional dams are likely to be adequate for Ririe Dam.

REFERENCES

- Ambraseys, N. N. 1960. "On the Shear Response of a Two-Dimensional Wedge Subjected to an Arbitrary Disturbance," Bulletin of the Seismological Society of America, Vol. 50, pp. 45-56, January.
- Chang, F. K. 1985. "Analysis of Strong-Motion Data from the Mount Borah, Idaho, Earthquake of 28 October 1983," Miscellaneous Paper GL-85-12, U.S. Army Engineers Waterways Experiment Station, Vicksburg, Mississippi.
- Davenport and Hadley, Ltd. 1987. "Cross-Hole and Down-Hole Seismic Surveys, Ririe Dam," Report prepared for U.S. Army Engineer Waterways Experiment Station, January.
- Donovan, N. C. 1969. "Research Brief - Soil Dynamics Specialty Session," 7th International Conference on Soil Mechanics and Foundation Engineering, Mexico City.
- Drnevich, V. P., Hall, J. R., Jr., and Richard, F. E., Jr. 1966. "Large Amplitude Vibration Effects on the Shear Modulus of Sand," University of Michigan Report to Waterways Experiment Station, Corps of Engineers, U.S. Army, Contract DA-22-079-eng-340, October 1966.
- Earth Technology Corporation. 1985. "Cone Penetrometer Testing, Ririe Dam," Report to U.S. Army Engineer Waterways Experiment Station, January.
- Earthquake Engineering Technology Corp. 1983. "SUPERFLUSH: User's Manual," Vols. 1-3, May.
- Hardin, B. O. 1965. "The Nature of Damping in Sands," Journal of the Soils Mechanics and Foundations Division, ASCE, Vol. 91, No. SMI, pp. 63-67, January 1965.
- Hardin, B. O. and Drnevich, V. P. 1970. "Shear Modulus and Damping in Soils: I. Measurement and Parameter Effects, II. Design and Equations and Curves," Technical Reports UKY 27-70-CE 2 and 3, College of Engineering, University of Kentucky, Lexington, Kentucky, July.
- Kishida, H. and Takano, A. 1970. "The Damping in the Dry Sand," Proceedings of the 3rd Japan Earthquake Engineering Symposium, Tokyo, Japan.
- Krinitzky, E. L. and Dunbar, J. B. 1987. "Geological and Seismological Evaluation of Earthquake Hazards at Ririe Dam, Idaho," Draft report to U.S. Army Engineer District, Walla Walla, U.S. Army Engineer Waterways Experiment Station, Vicksburg, MS.

Lysmer, J., Uda, T., Tsai, C., and Seed, H. B. 1975. "FLUSH: A Computer Program for Approximate 3-D Analysis of Soil Structure Interaction Problems," Report No. EERC 75-30, University of California, Berkeley, November.

Makdisi, F. I. 1976. "Performance and Analysis of Earth Dams during Strong Earthquakes," Ph.D. Thesis, University of California, Berkeley.

Matsushita, K., Kishida, H. and Kyo, K. 1967. "Experiments on Damping of Sands," Transactions of the Architectural Institute of Japan, Summaries of Technical Papers, p. 166.

Mejia, L. H. and Seed, H. B. 1981. "Three-Dimensional Dynamic Response Analysis of Earth Dams," Report No. UCB-EERC-81/15, University of California, Berkeley, September.

Mejia, L. H. and Seed, H. B. 1983. "Comparison of 2-D and 3-D Dynamic Analyses of Earth Dams," Journal of Geotechnical Engineering, ASCE, Vol. 109, No. 11, pp. 1383-1398, November.

Patrick, D. M. and Whitten, C. B. 1981. "Geological and Seismological Investigations at Ririe Dam, Idaho," Miscellaneous Paper GL-81-7, U.S. Army Engineer Waterways Experiment Station (WES), Vicksburg, MS.

Schnabel, P. B. 1973. "Effects of Local Geology and Distance from Source on Earthquake Ground Motions," Ph.D. Thesis, University of California, June.

Schnabel, P. B., Lysmer, J., and Seed, H. B. 1972. "SHAKE: A Computer Program for Earthquake Response Analysis of Horizontally Layered Sites," Report No. EERC 72-12, University of California, Berkeley, December.

Seed, H. B., 1983. "Earthquake Resistant Design of Earth Dams," Proceedings of ASCE Symposium on Seismic Design of Embankments and Caverns, pp. 41-64, Philadelphia.

Seed, H. B. and Idriss, I. M. 1970. "Soil Moduli in Damping Factors for Dynamic Response Analysis," Report No. EERC 70-10, University of California, Berkeley, December.

Seed, H. B., Wong, R. T., Idriss, I. M., and Tokimatsu, K. 1984. "Moduli and Damping Factors for Dynamic Analyses of Cohesionless Soils," Report No. UCB/EERC-84-14, University of California, Berkeley, September.

Severn, R. T., Jeary, A. P., Ellis, B. R. and Dungar, R. 1979. "Prototype Dynamic Studies on a Rockfill Dam and on a Buttress Dam," Proceedings of the Thirteenth International Congress on Large Dams, Q. 51, R. 16, New Delhi, 1979.

Silver, M. L. and Seed, H. B. 1969. "The Behavior of Sands under Seismic Loading Conditions," Report No. EERC 69-16, University of California, Berkeley.

Weissman, G. F. and Hart, R. R. 1961. "The Damping Capacity of Some Granular Soils," Symposium of Soil Dynamics, ASTM Special Technical Publication No. 305, June 1961, pp. 45-54.

Woodward-Clyde Consultants. 1988. "Static Analysis of Ririe Dam," Report to U.S. Army Engineer Waterways Experiment Station, December.

Table 1. DYNAMIC MATERIAL PROPERTIES USED IN ANALYSIS

	$\gamma$ (pcf)	$K_2^{\max}$	Modulus Reduction	Damping	Poisson's Ratio
Core	125	45	Sands <sup>(1)</sup>	Sands <sup>(2)</sup>	0.48
Gravel Fill - Saturated	145	120	Gravels <sup>(3)</sup>	Sands	0.40
- Unsaturated	135	120	Gravels	Sands	0.35
Rockfill - Saturated	145	100	Gravels	Sands	0.40
- Unsaturated	135	100	Gravels	Sands	0.35
Random Fill - Saturated	140	85	Gravels	Sands	0.45
- Unsaturated	130	85	Gravels	Sands	0.35
Alluvium Silt	120	50	Sands	Sands	0.45
Alluvium Gravel	144	140	Gravels	Sands	0.40
Tuffaceous Sediments	155	Vs=1600fps	Rock <sup>(4)</sup>	Rock <sup>(5)</sup>	0.45
Basalt	170	Vs=3000fps	Rock	Rock	0.40

Note: (1) Modulus reduction relationship for sands by Seed and Idriss (1970).

(2) Damping relationship for sands by Seed and Idriss (1970).

(3) Modulus reduction relationship for gravels by Seed et al. (1984).

(4) Modulus reduction relationship for rock by Schnabel (1973).

(5) Damping relationship for rock by Schnabel (1973).

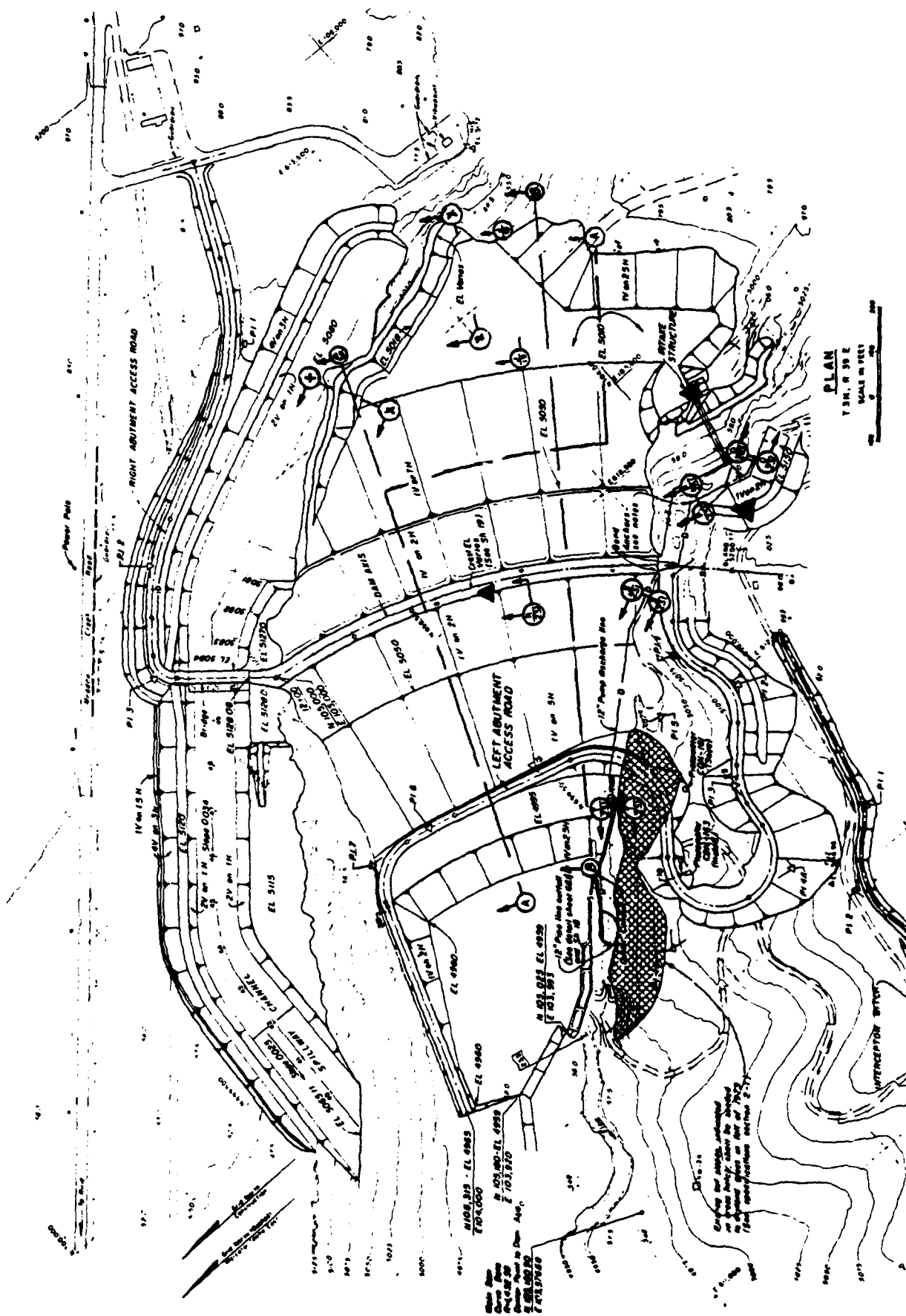


Figure 1. Plan view of Ririe Dam

SECTION AA

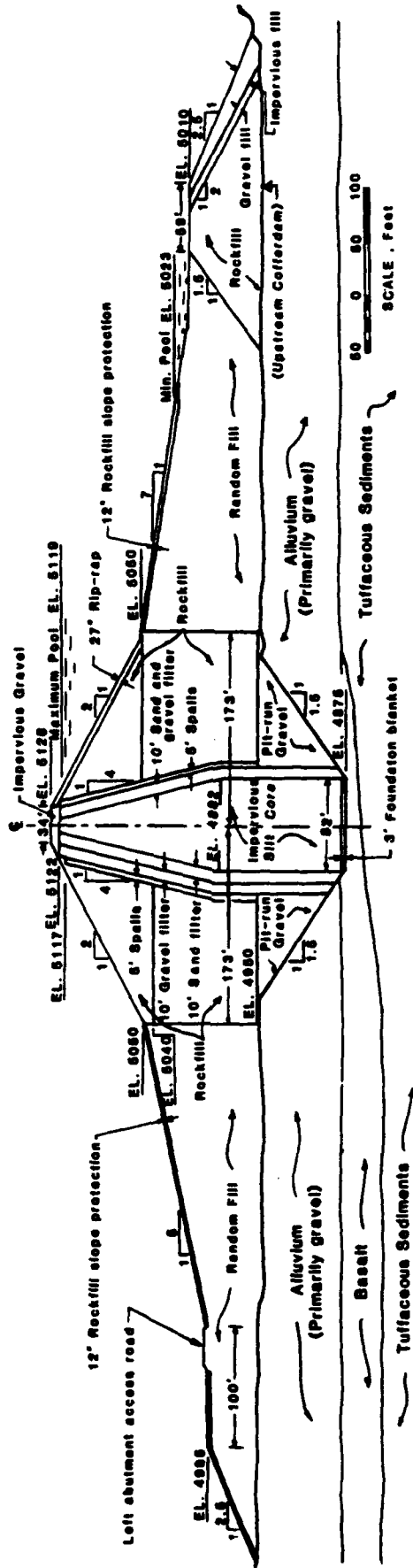


Figure 2. Cross-section of dam along stream axis

**SECTION BB**

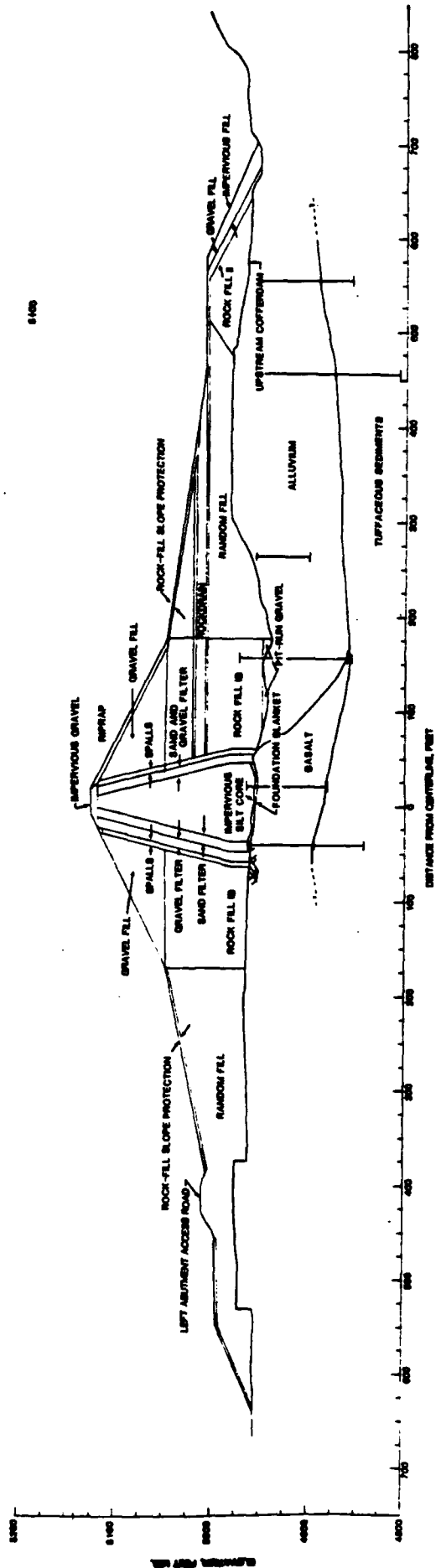


Figure 3. Radial cross-section of dam at station 5+00

SECTION AC

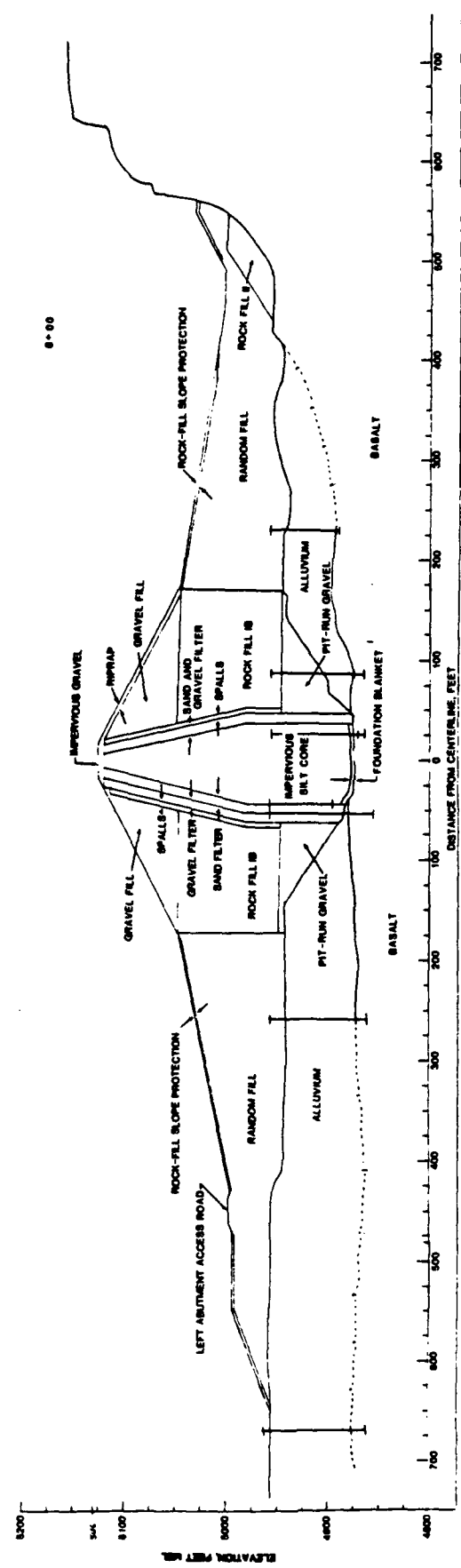


Figure 4. Radial cross-section of dam at station 8+00

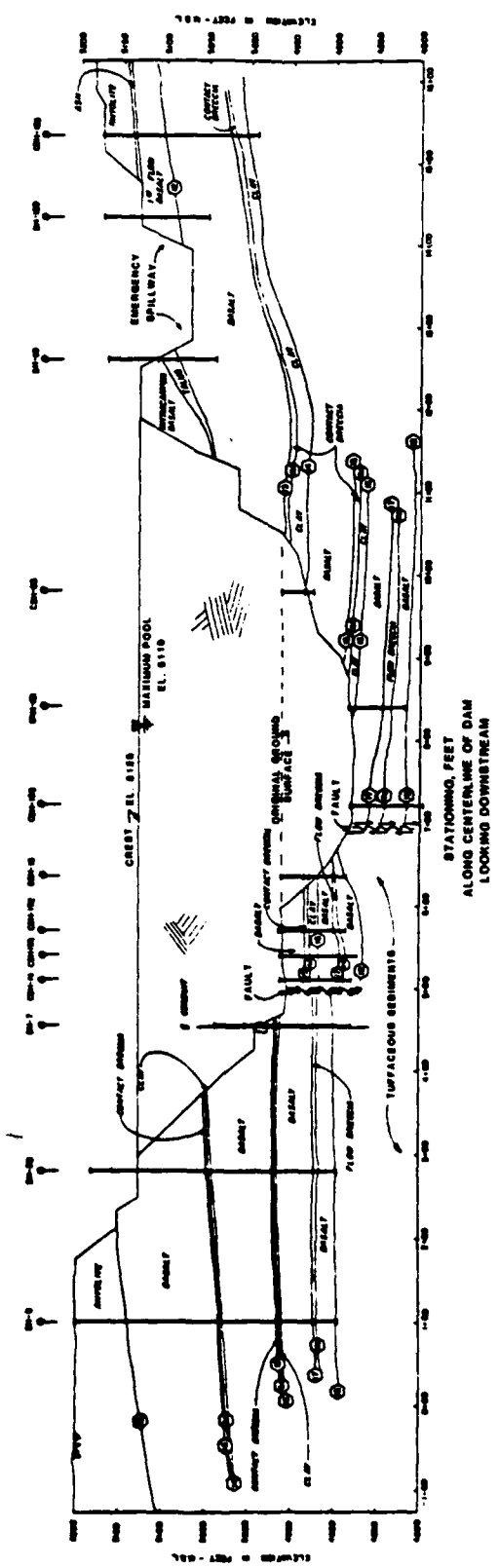


Figure 5. Cross-section along longitudinal axis of dam

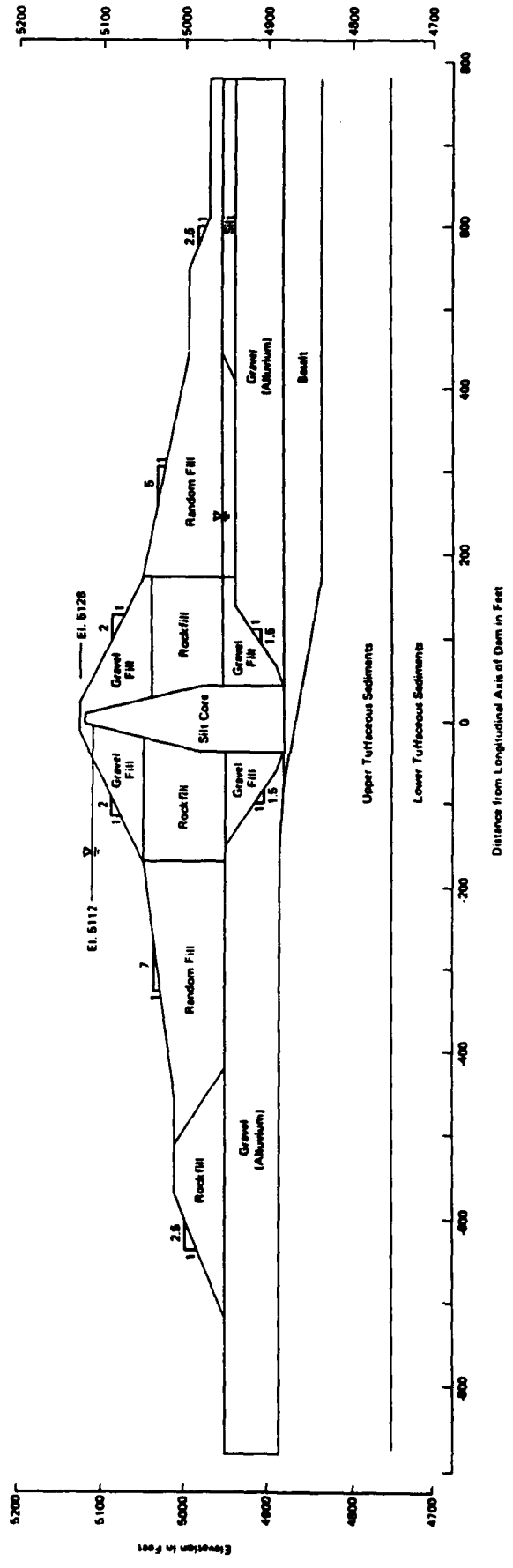


figure 6. Idealized section AA for analysis

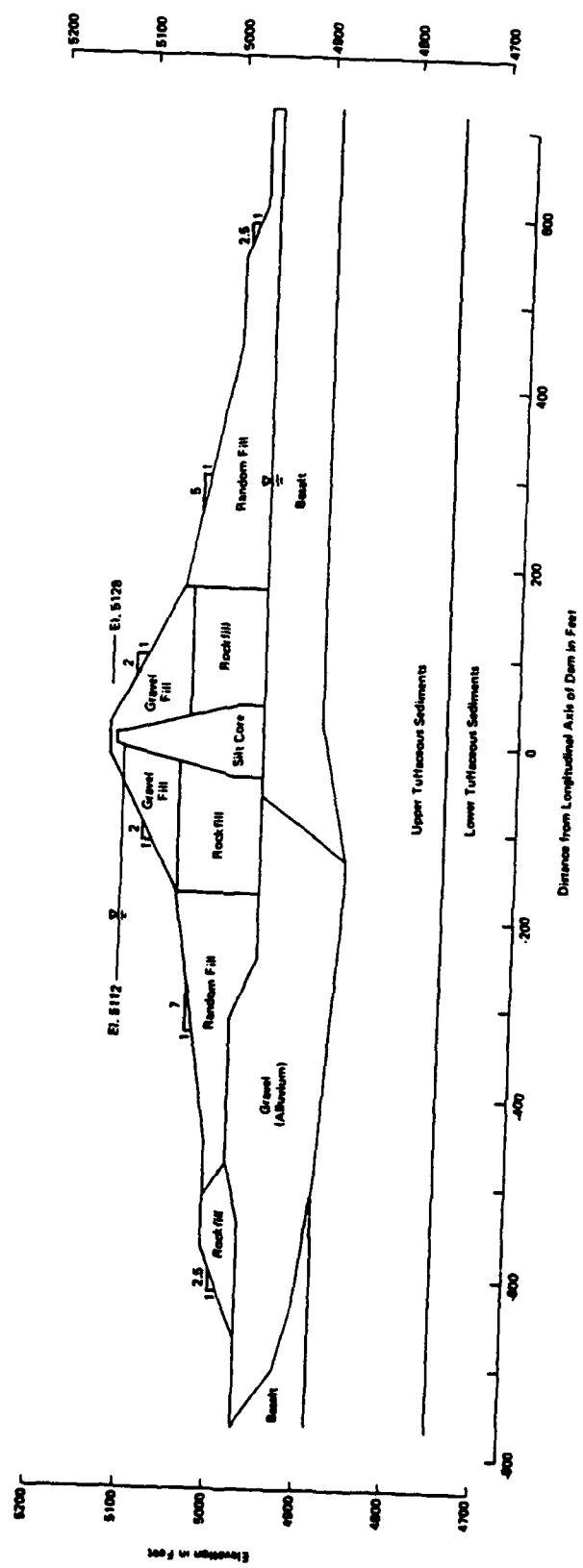


Figure 7. Idealized section BB for analysis

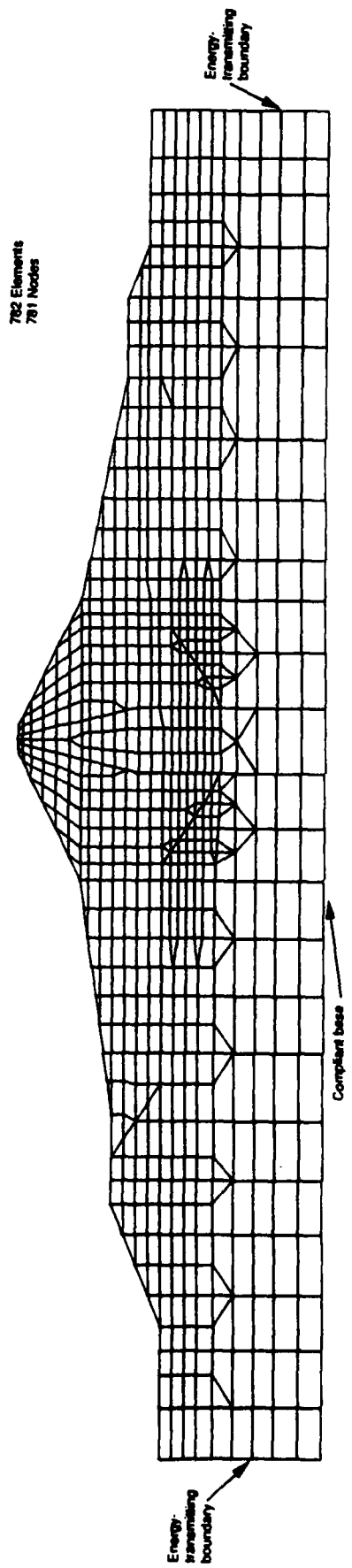


Figure 8. Finite element model for dynamic response analysis of section AA

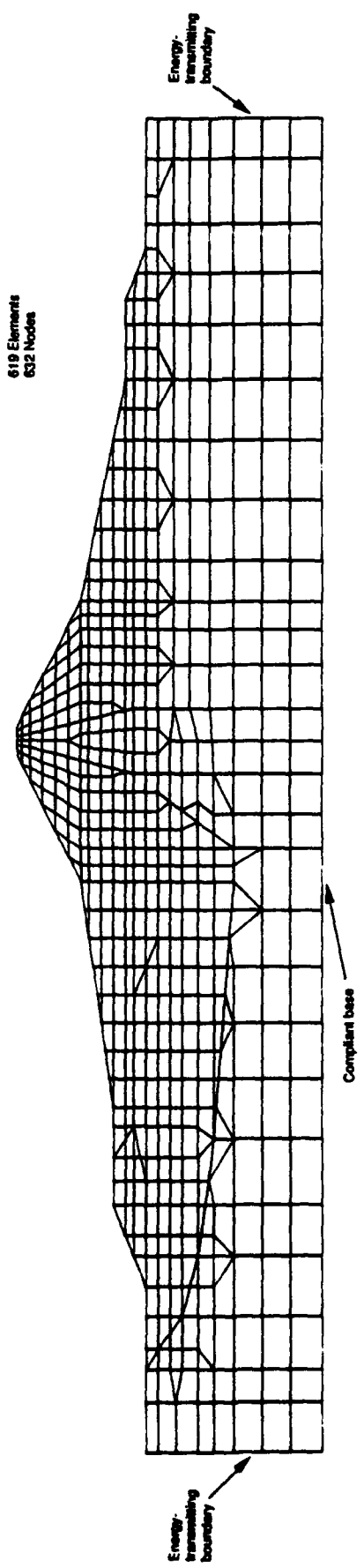
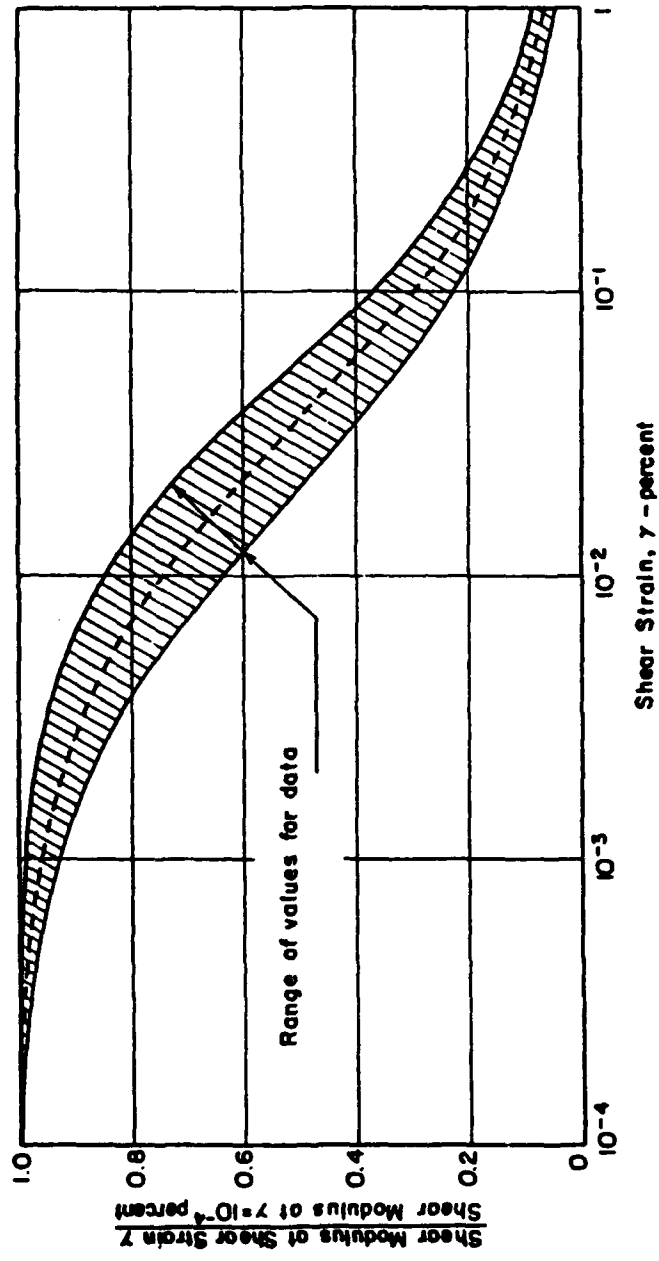


Figure 9. Finite element model for dynamic response analysis of section 88

Figure 10. Modulus reduction relationship for sands by Seed and Idriss (1975)



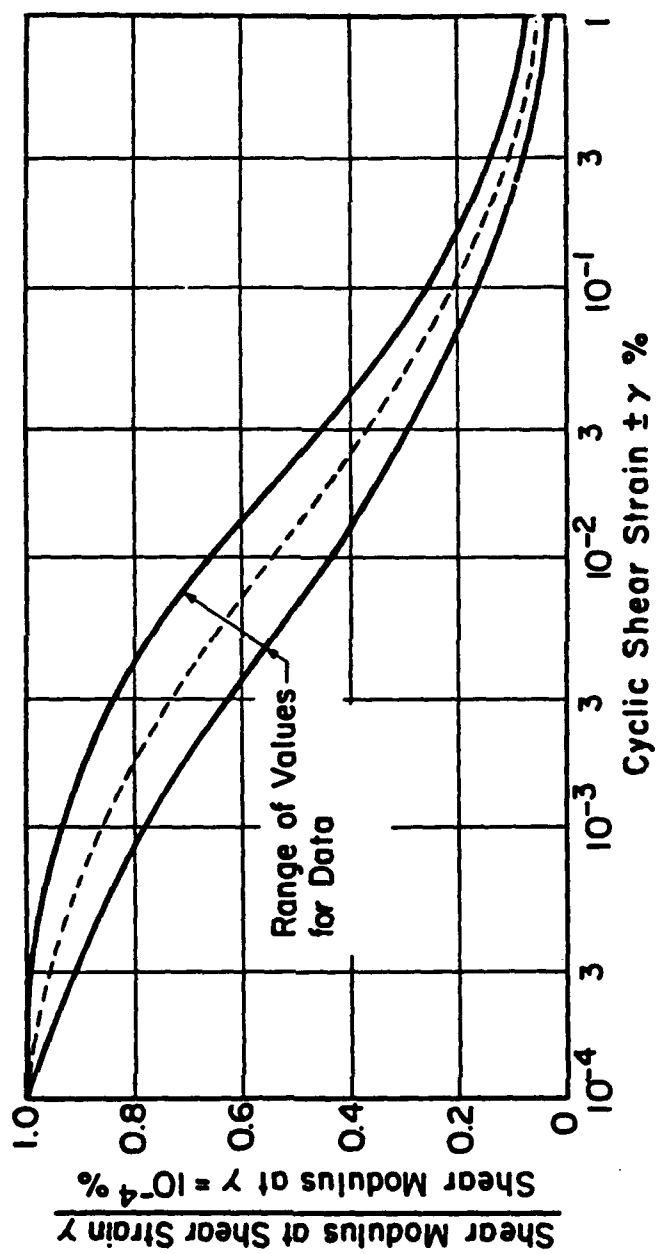


Figure 11. Modulus reduction relationship for gravels by Seed et al. (1984)

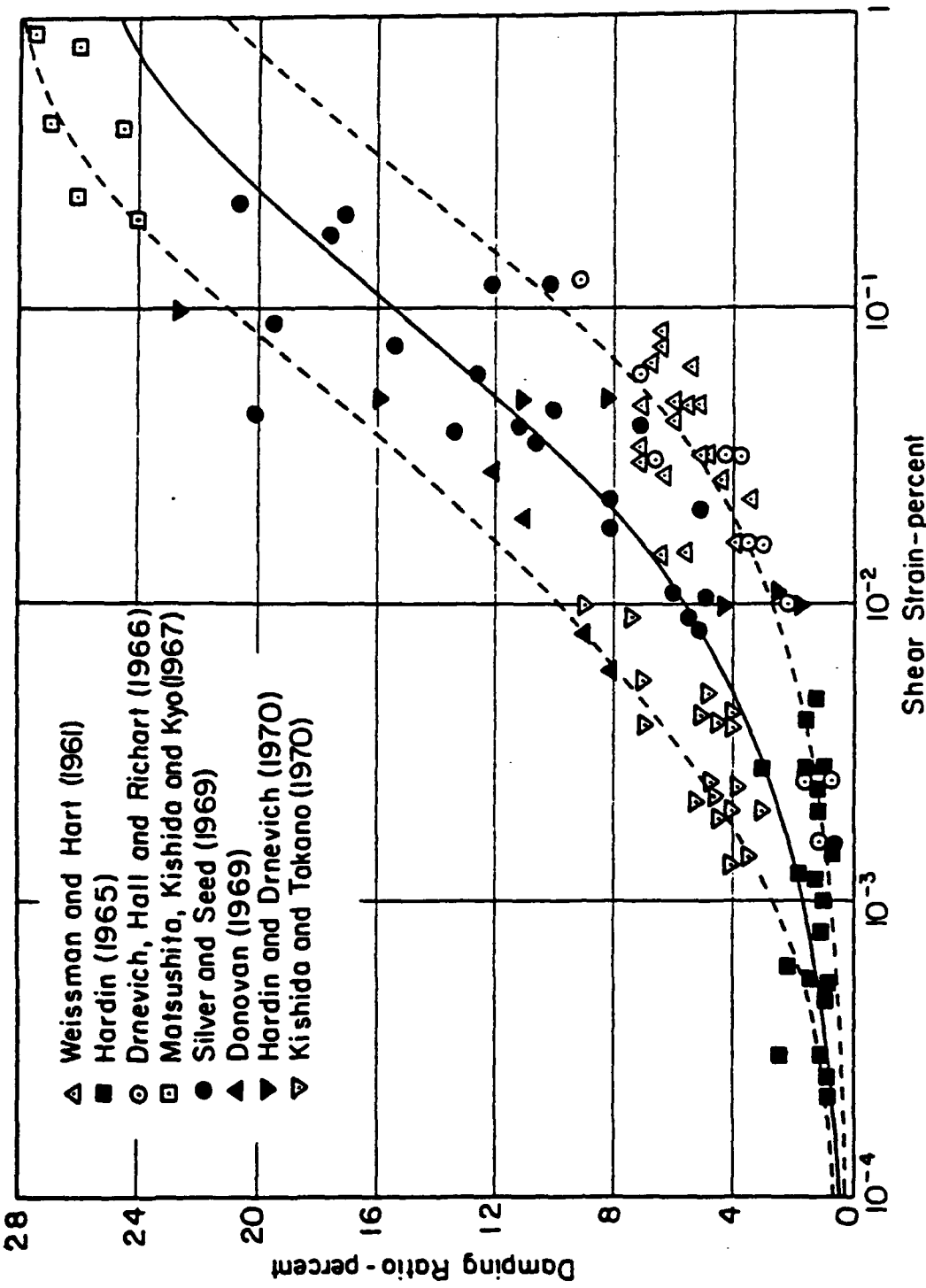


Figure 12. Damping relationship for sands by Seed and Idriss (1970)

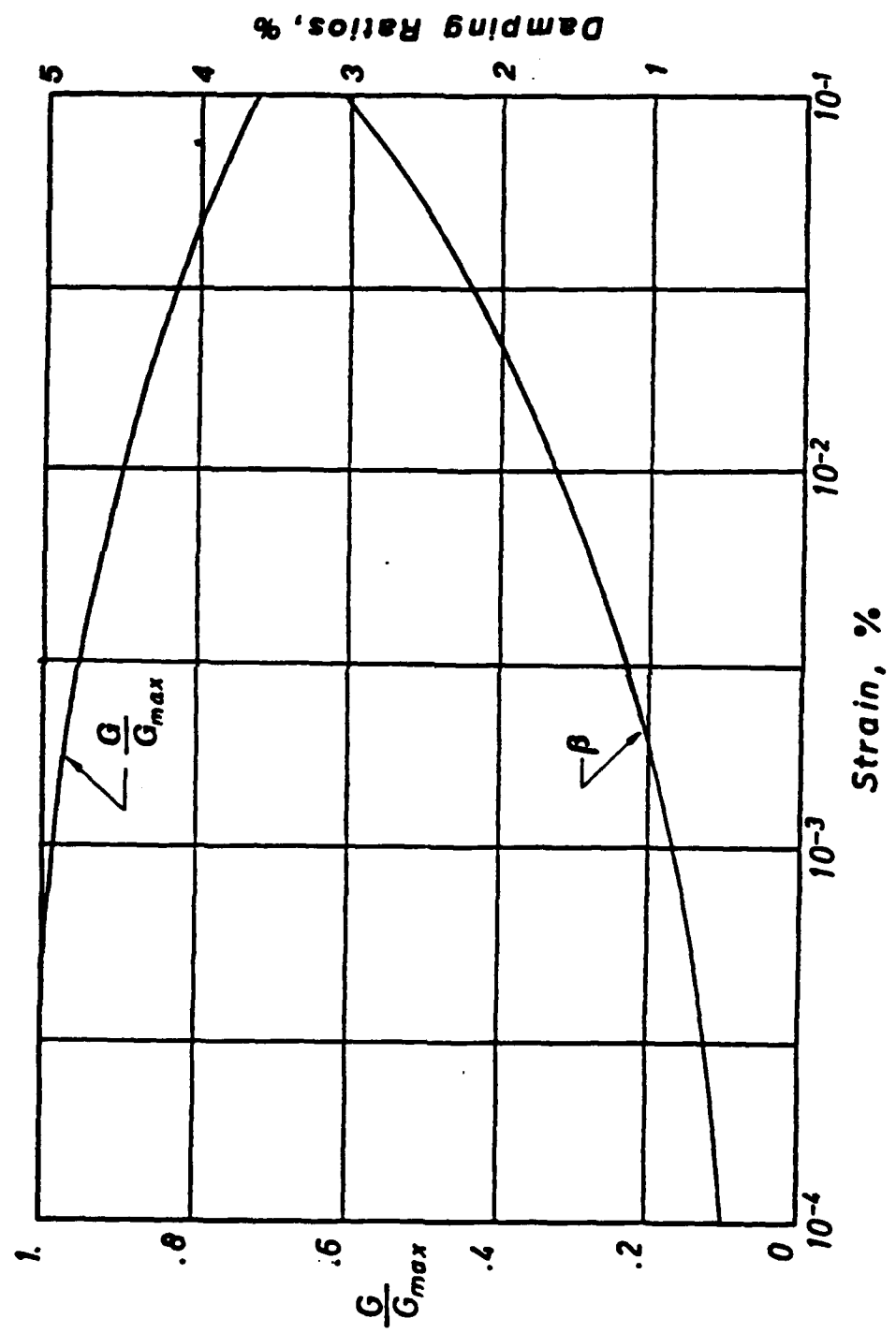


Figure 13. Modulus reduction and damping relationships for rock by Schnabe1 (1973)

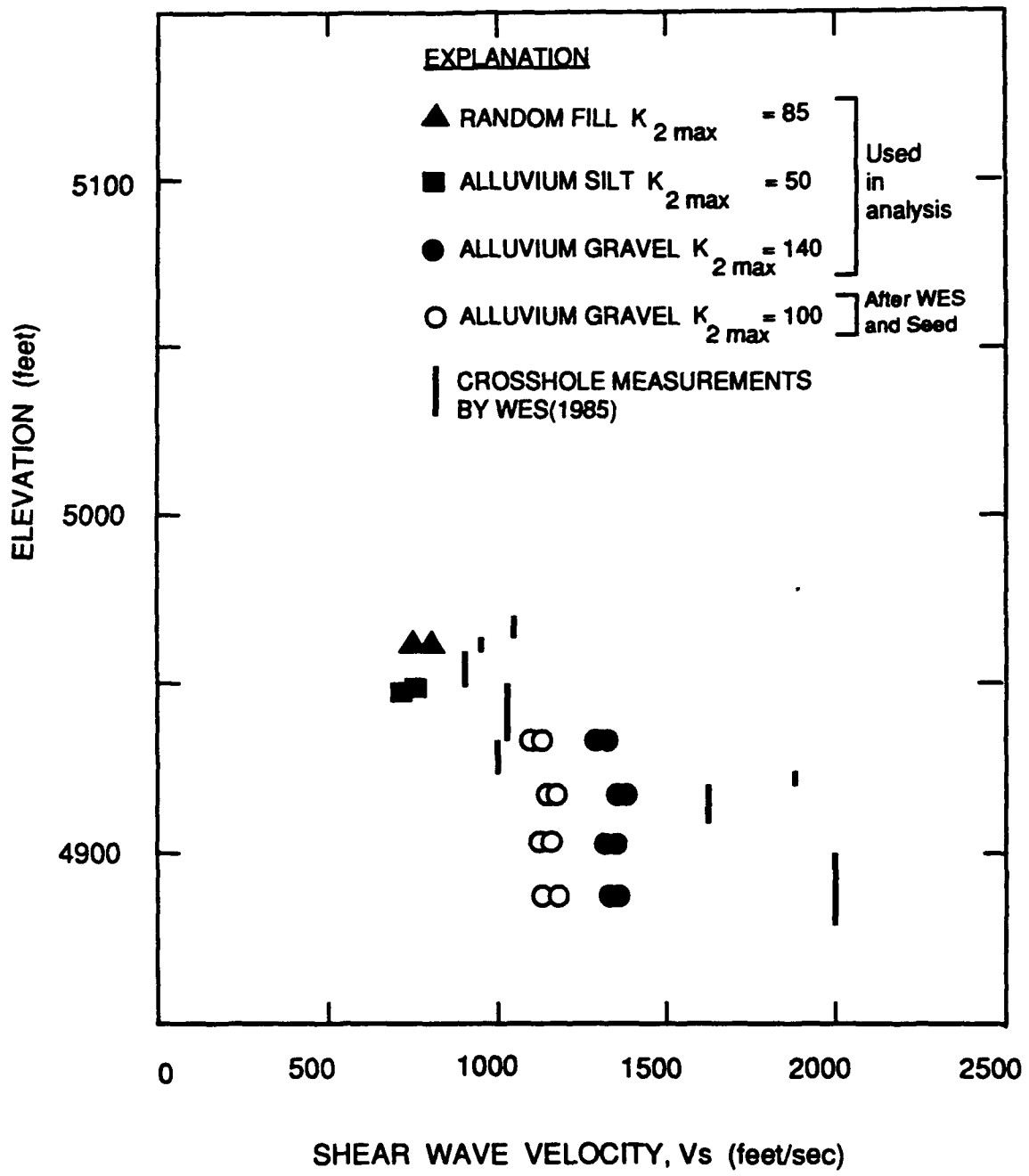
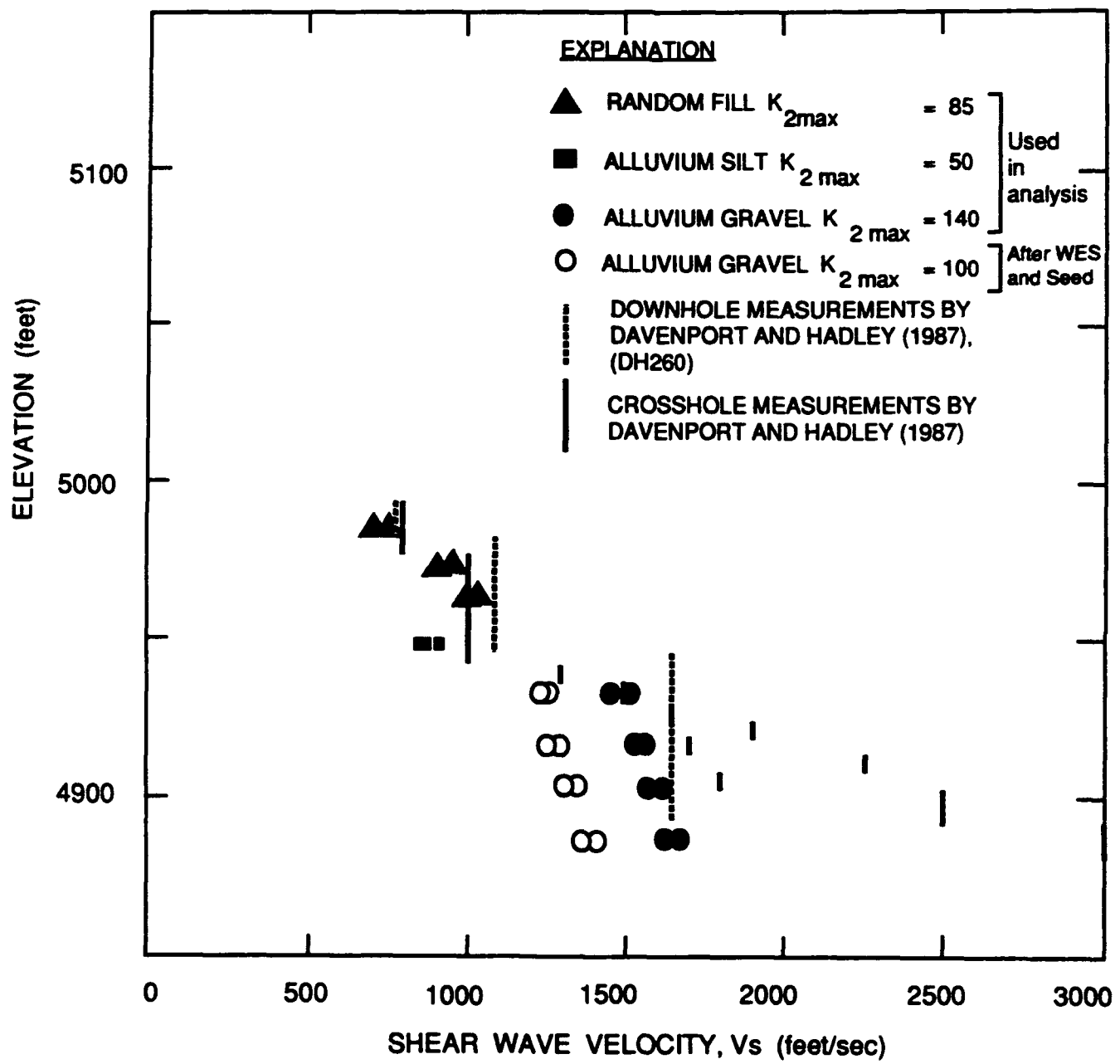


Figure 14. Comparison between shear wave velocities used in analysis and field measurements at toe of dam



**Figure 15.** Comparison between shear wave velocities used in analysis and field measurements at downstream berm

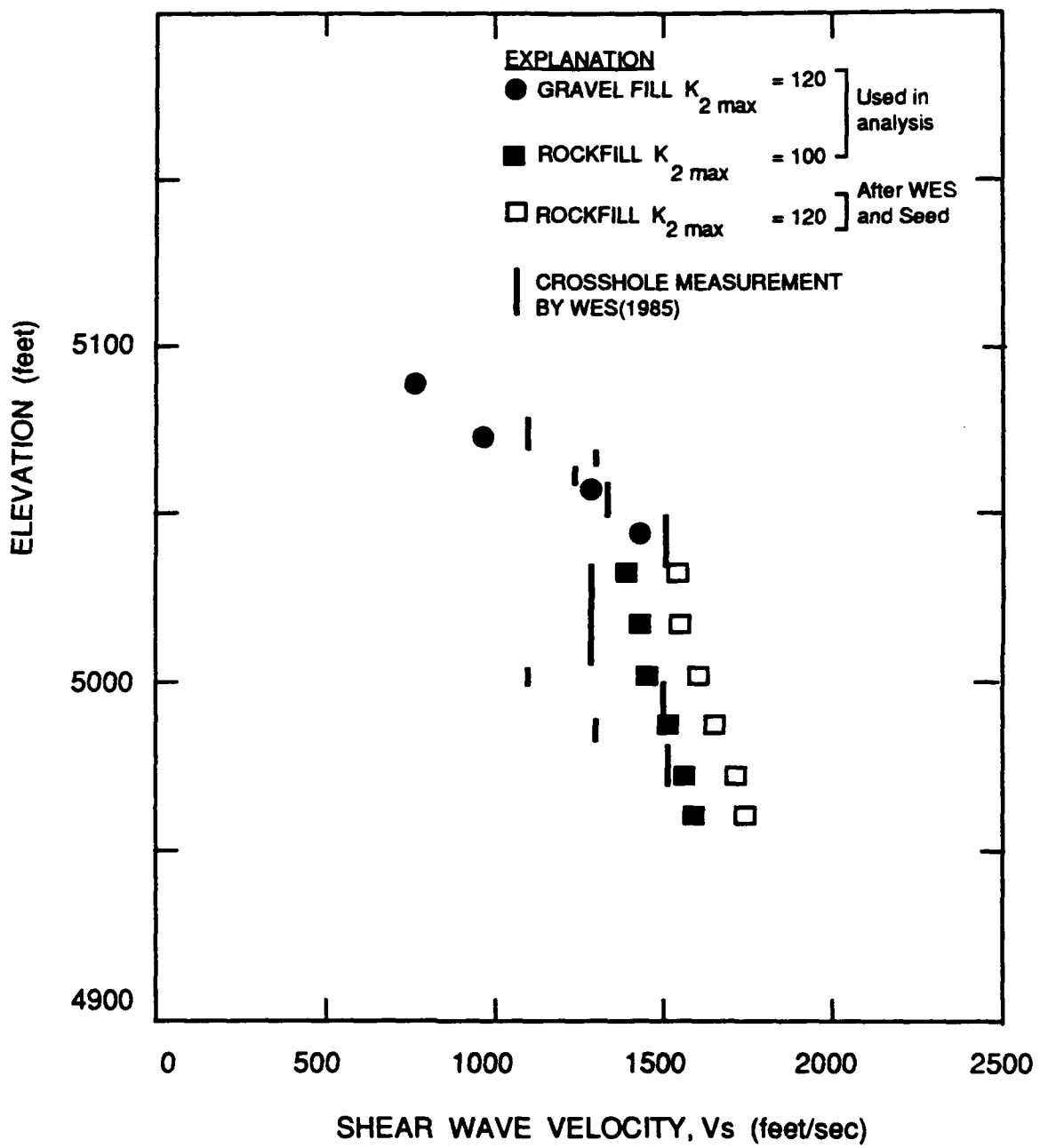


Figure 16. Comparison between shear wave velocities used in analysis and field measurements in downstream shell

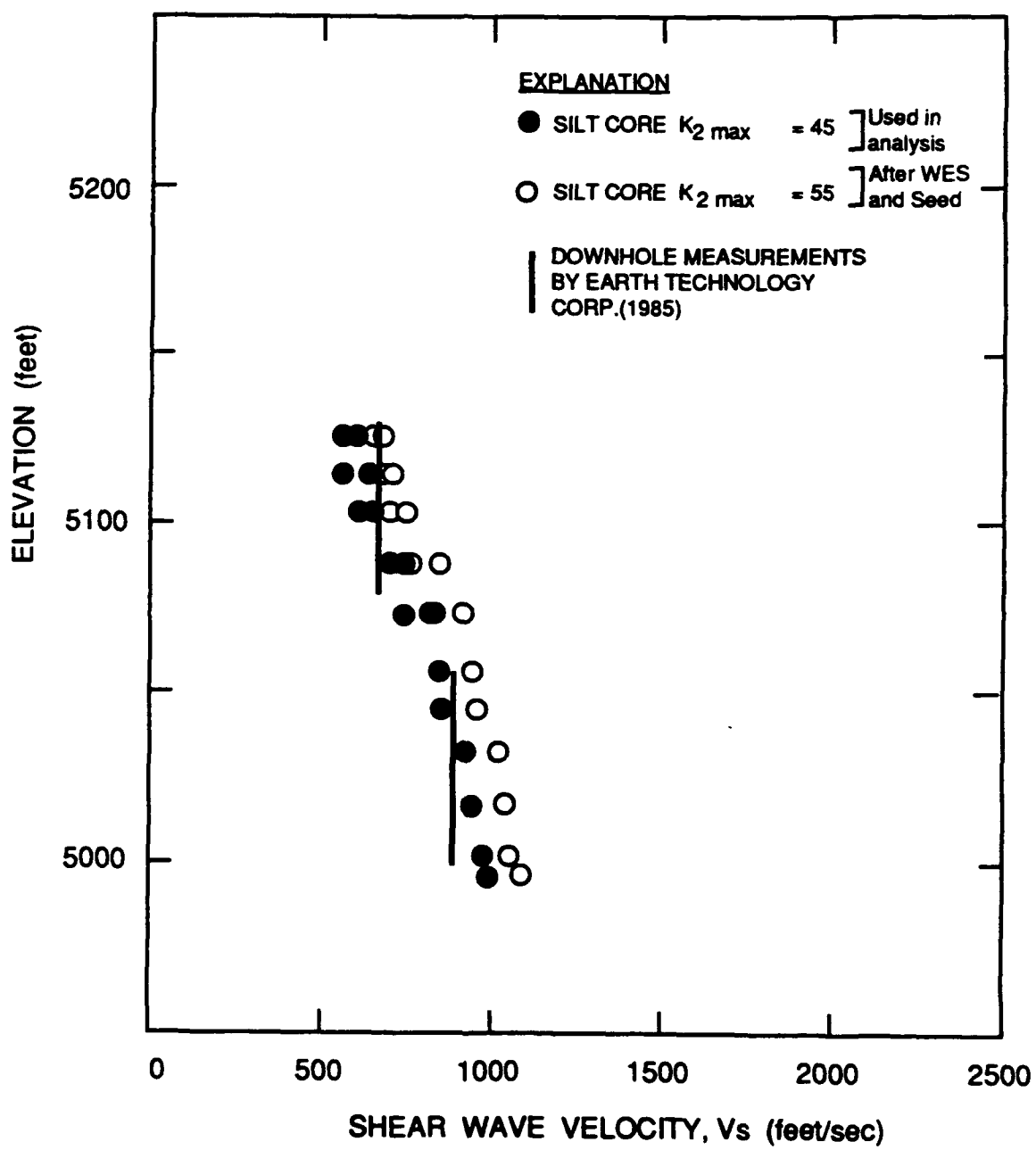


Figure 17. Comparison between shear wave velocities used in analysis and field measurements in core of dam

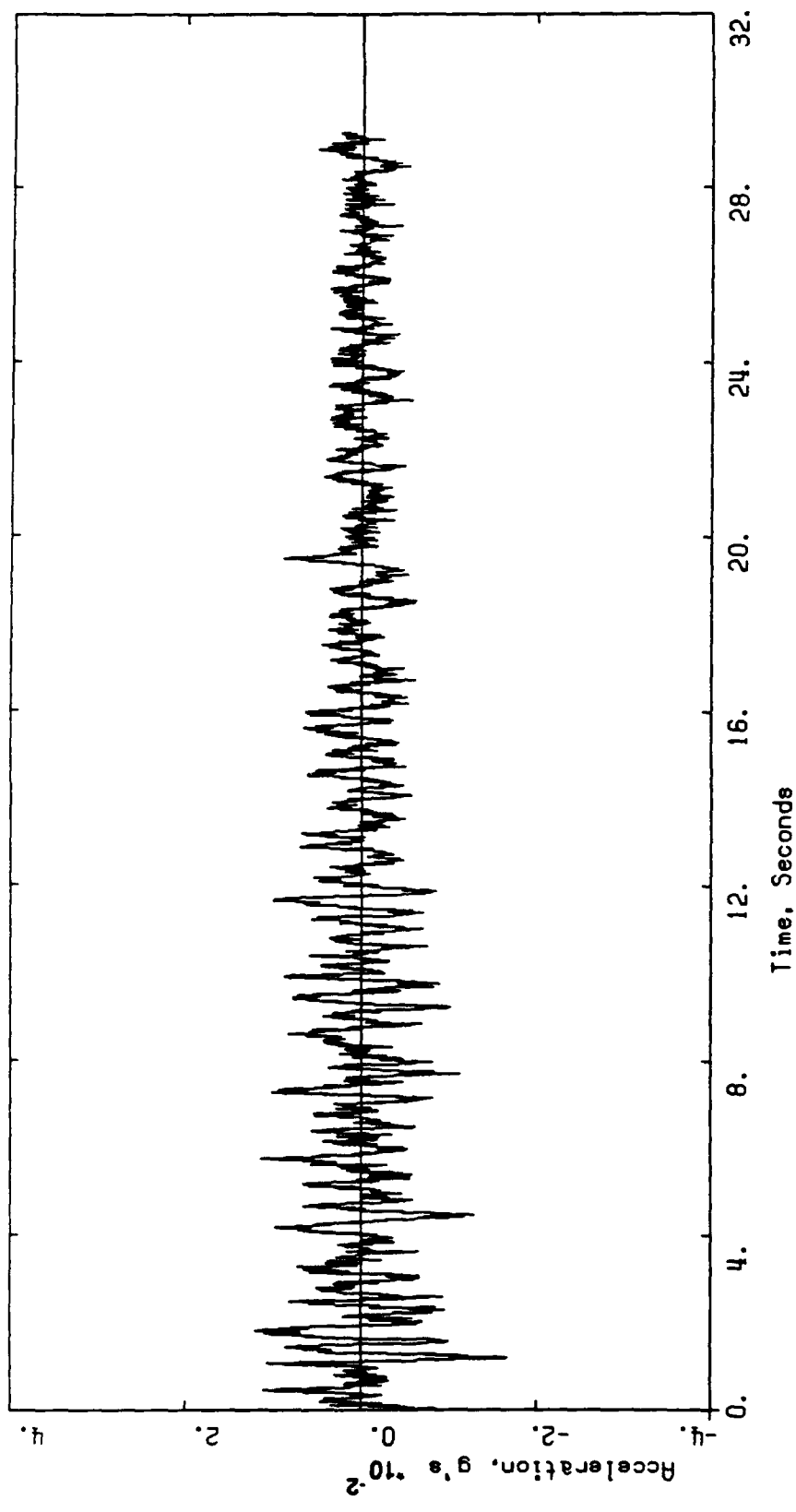


Figure 18. Acceleration time history recorded on abutment (295° component)

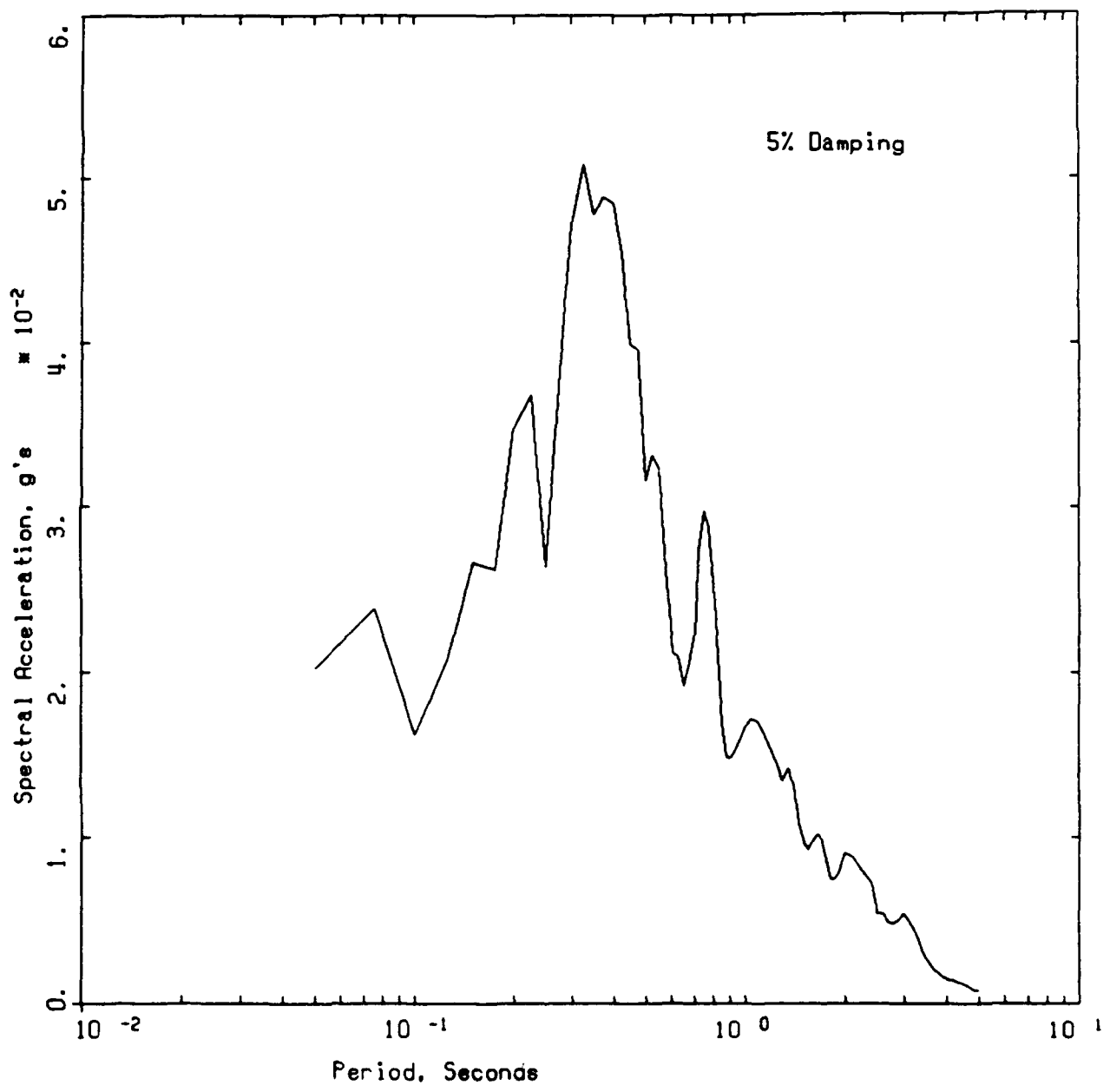


Figure 19. Acceleration response spectrum for abutment record

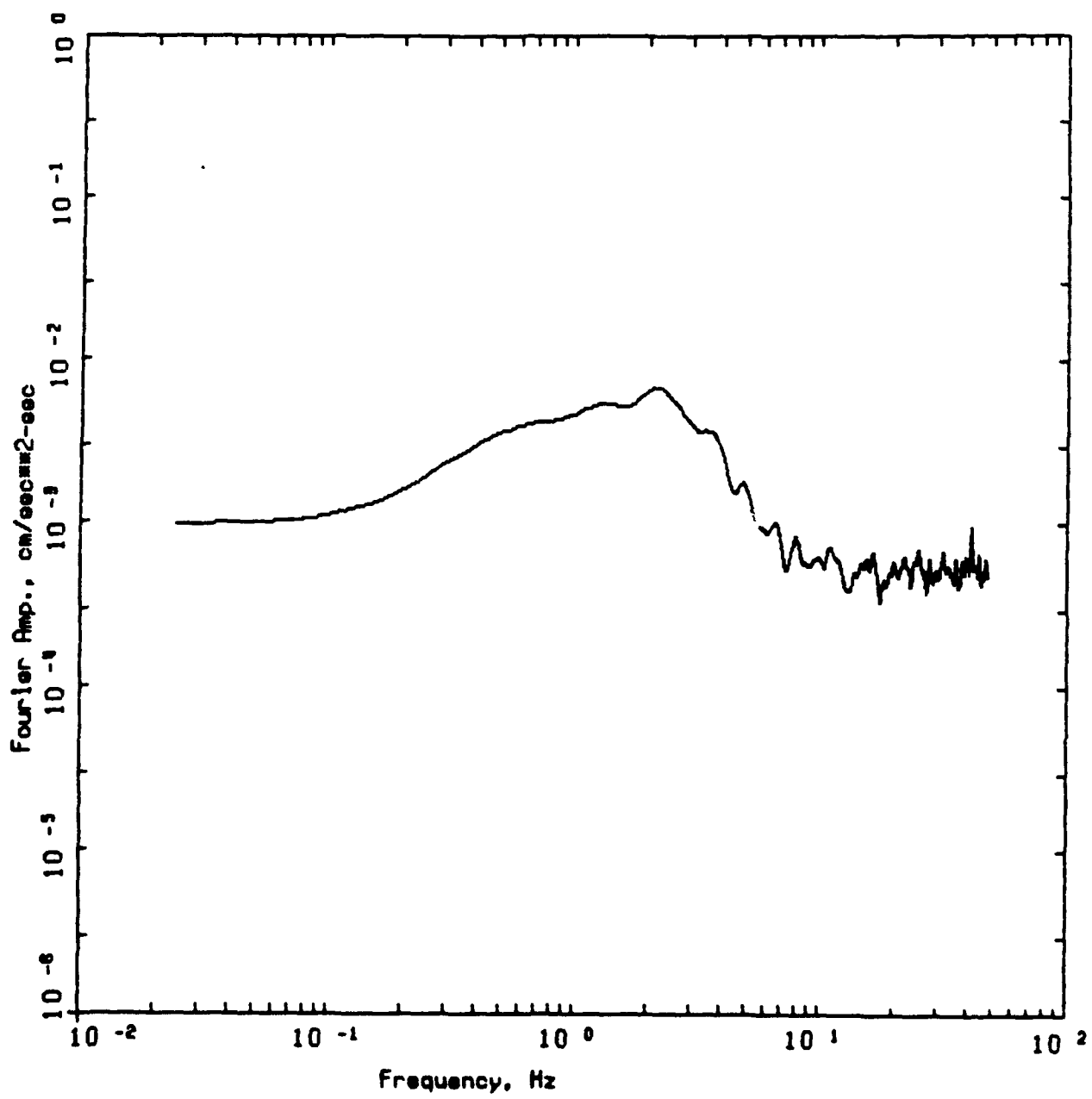


Figure 20. Fourier amplitude spectrum for abutment record

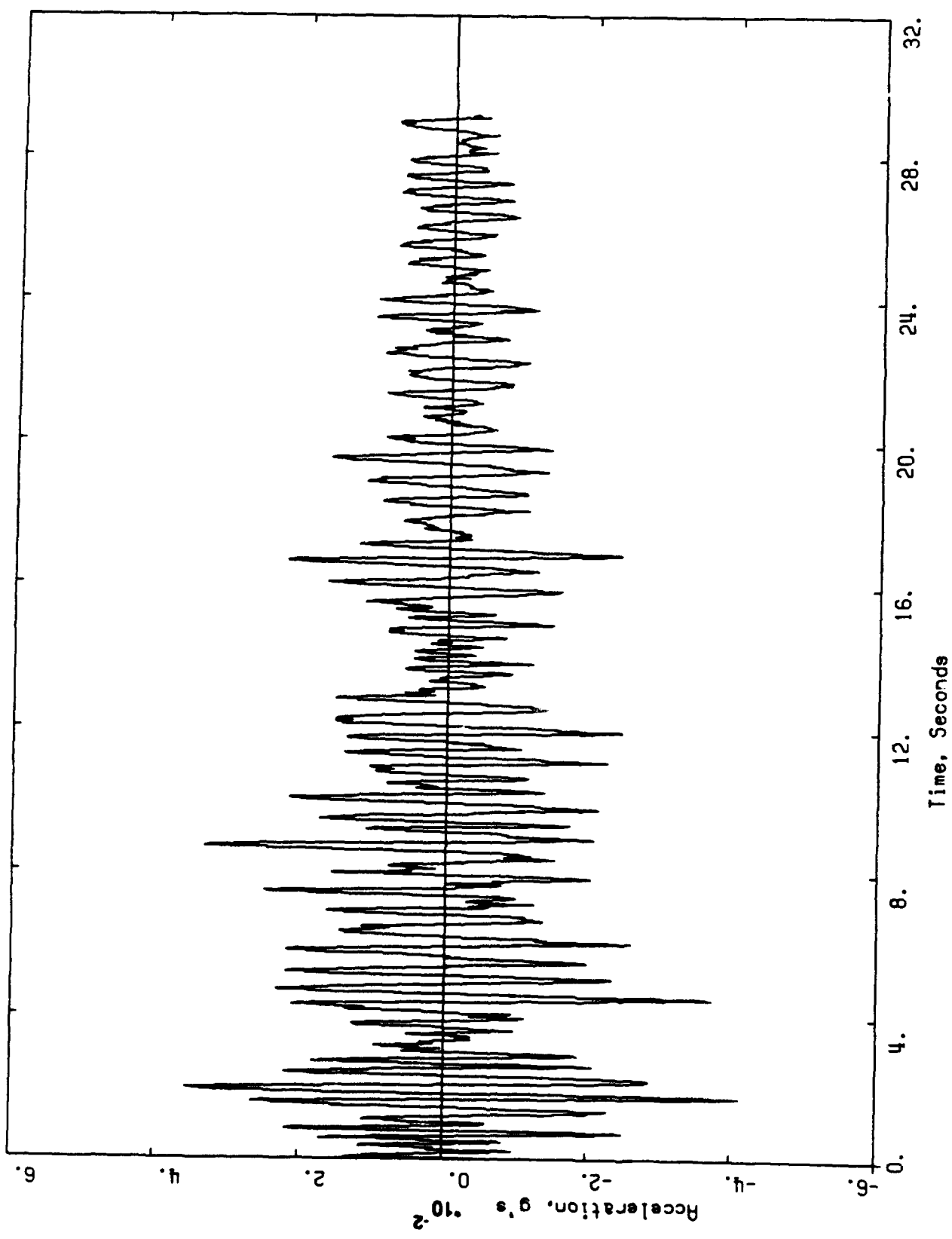


Figure 21. Acceleration time history recorded on dam crest (295° component)

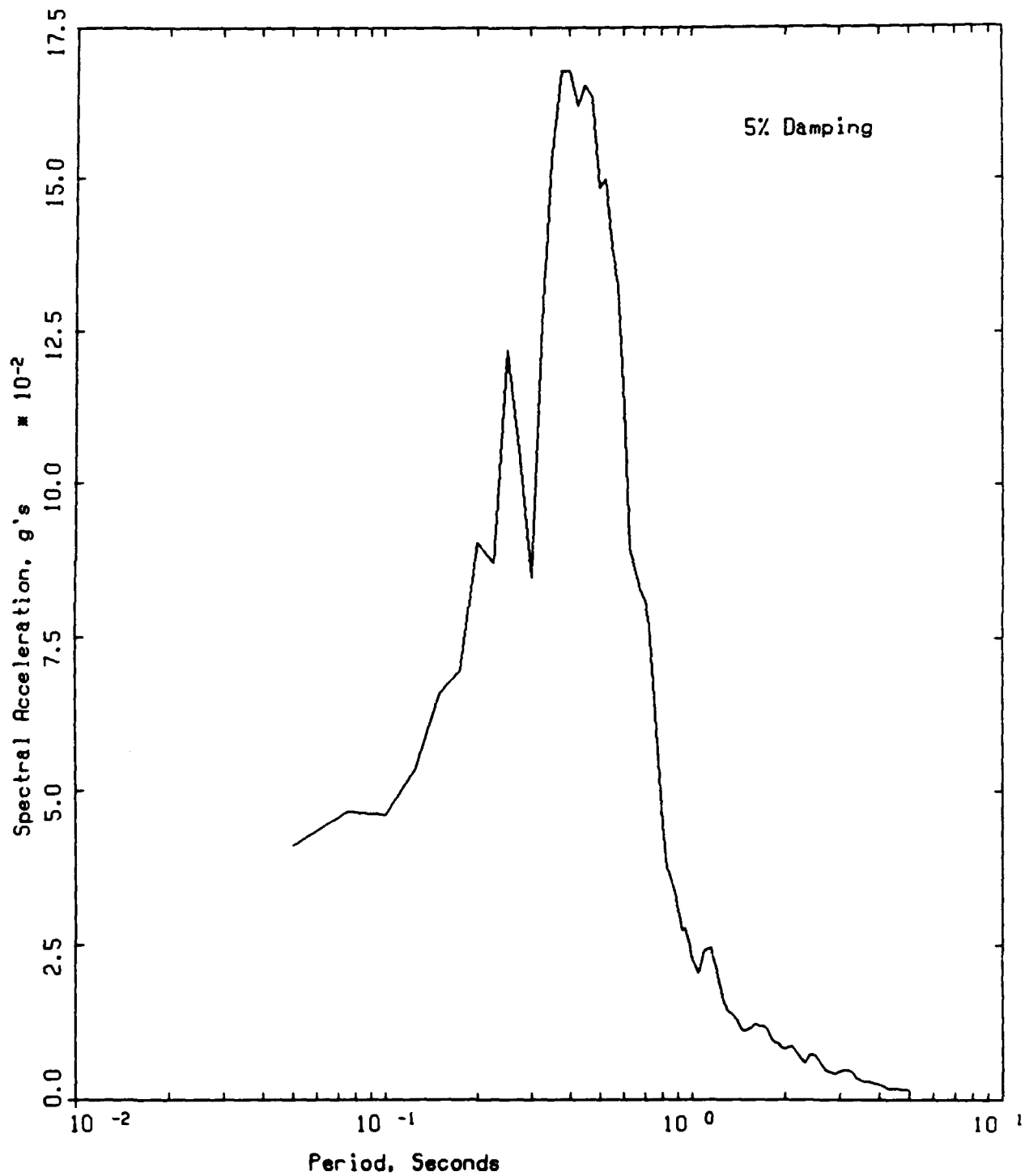


Figure 22. Acceleration response spectrum for crest record

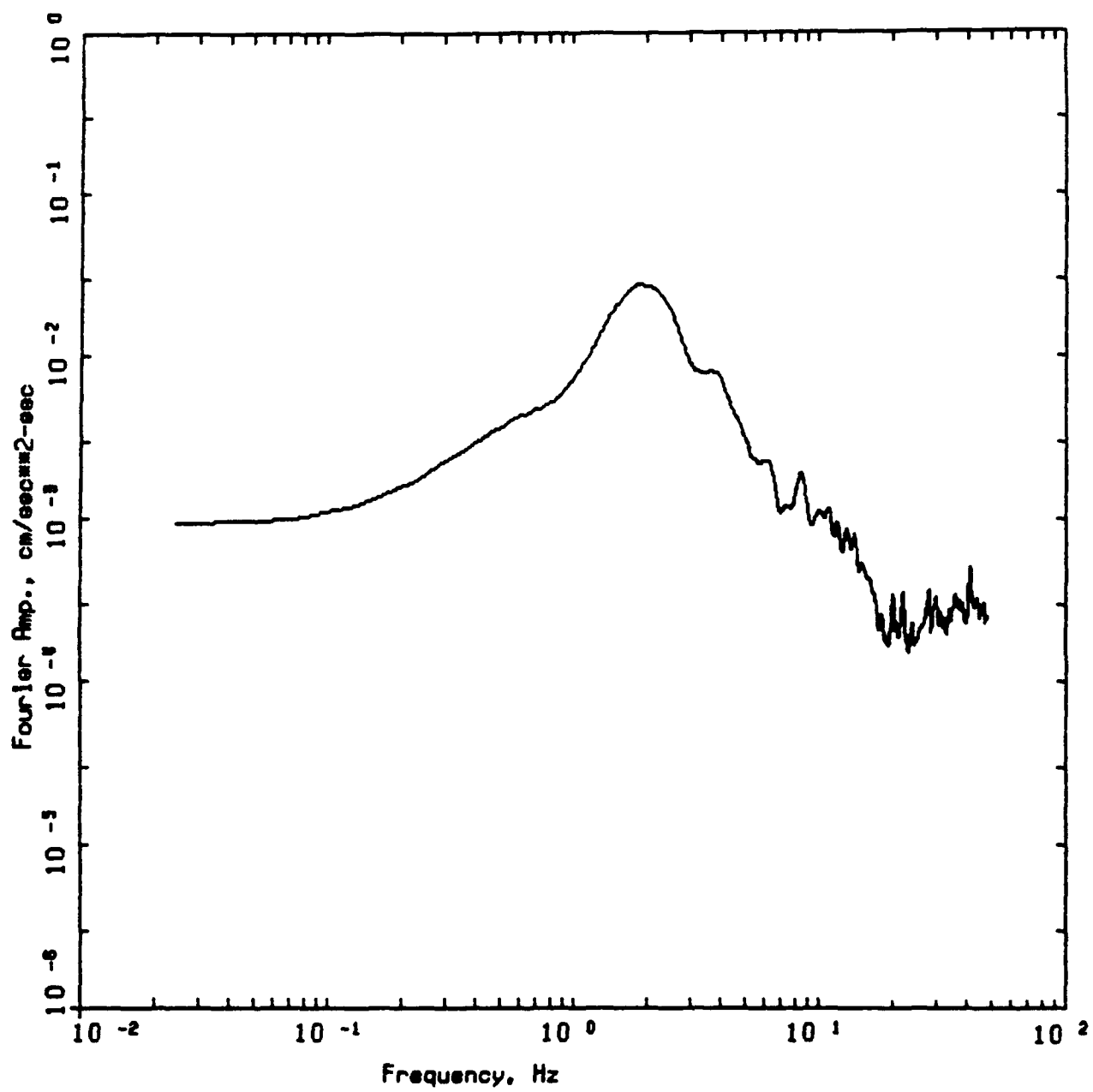


Figure 23. Fourier amplitude spectrum for crest record

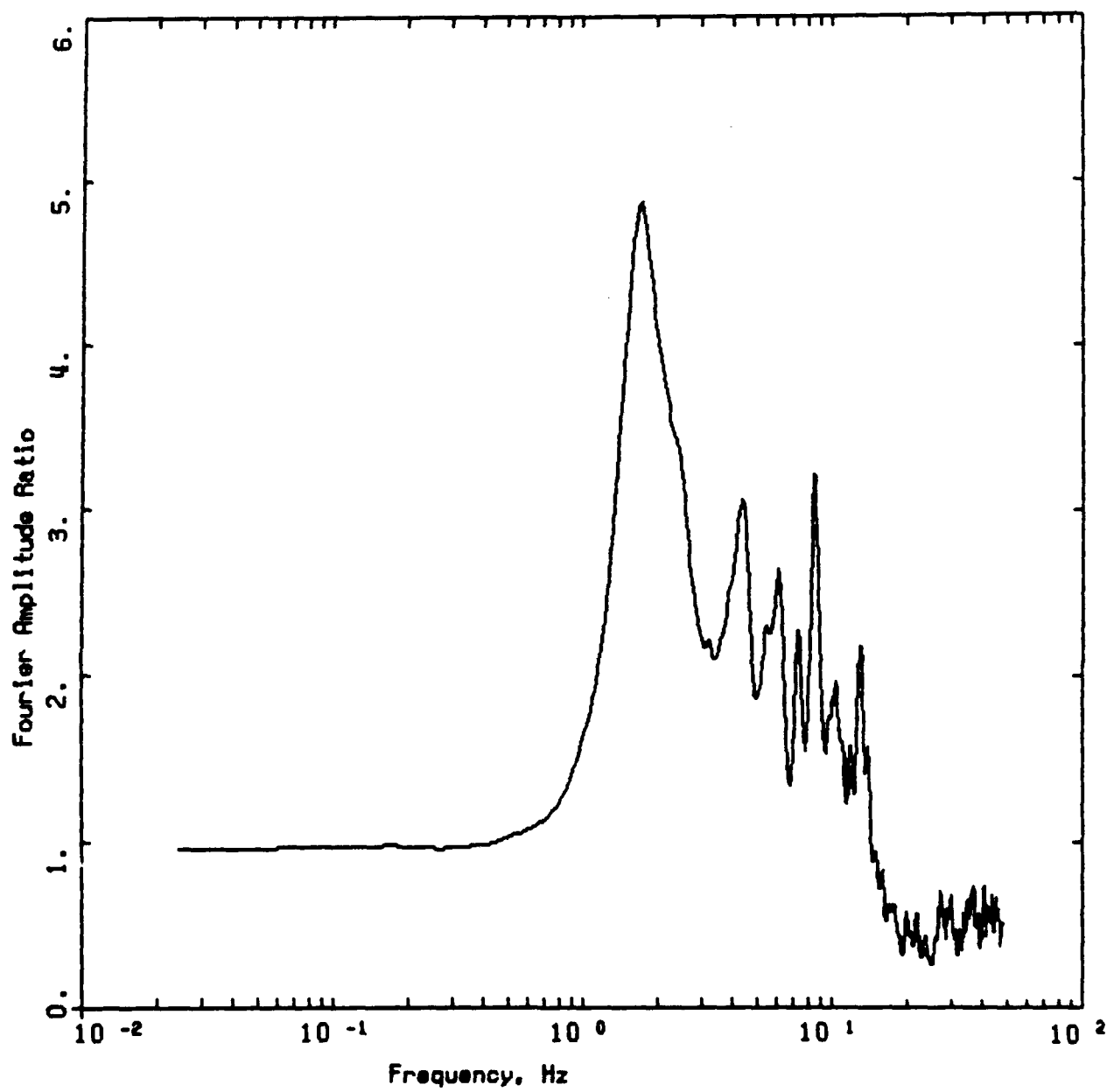


Figure 24. Fourier amplitude ratio between crest and abutment records

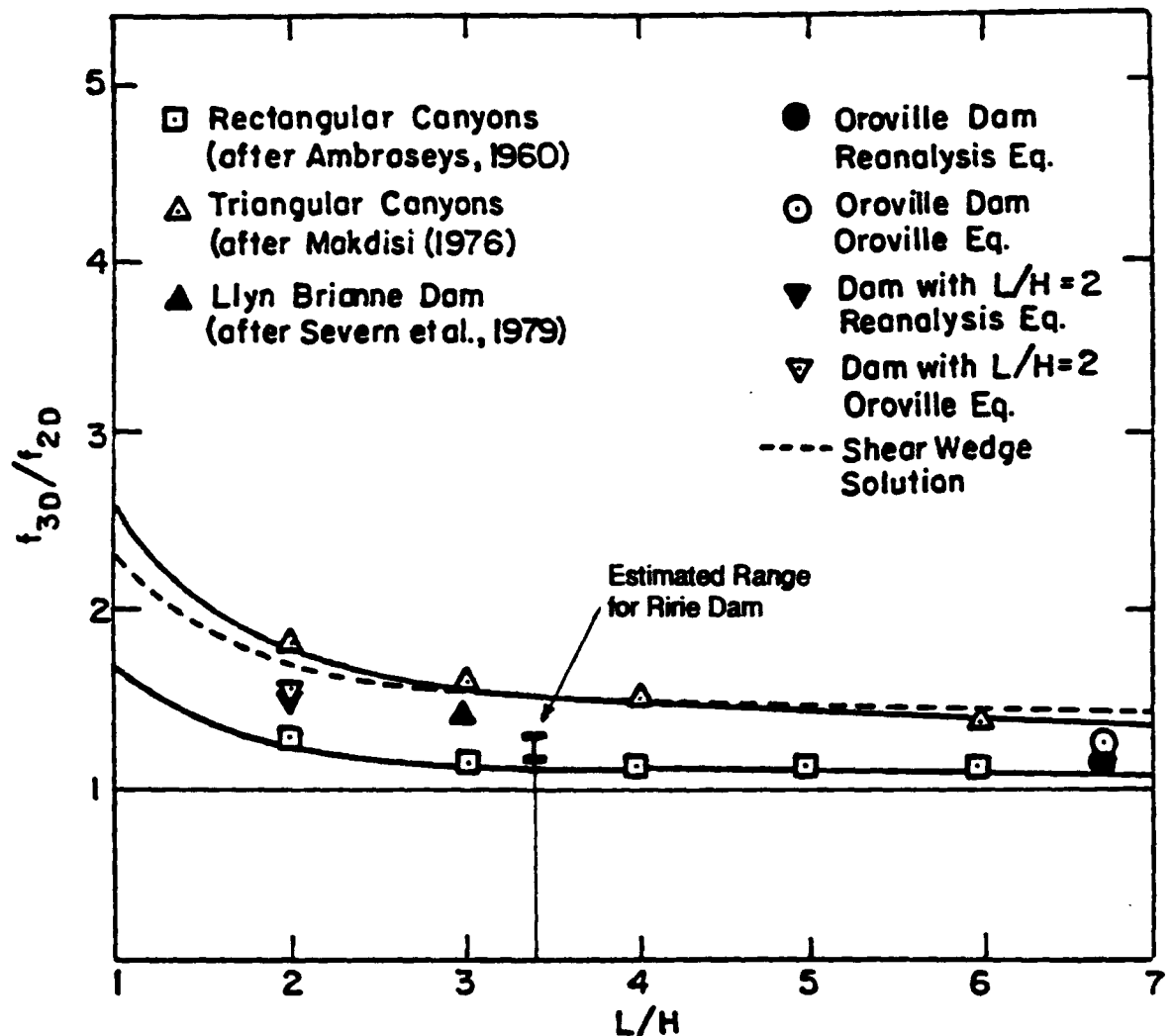


Figure 25. Comparison between fundamental frequencies computed from 2-D and 3-D analyses of dams in triangular and rectangular canyons (after Mejia and Seed, 1983)

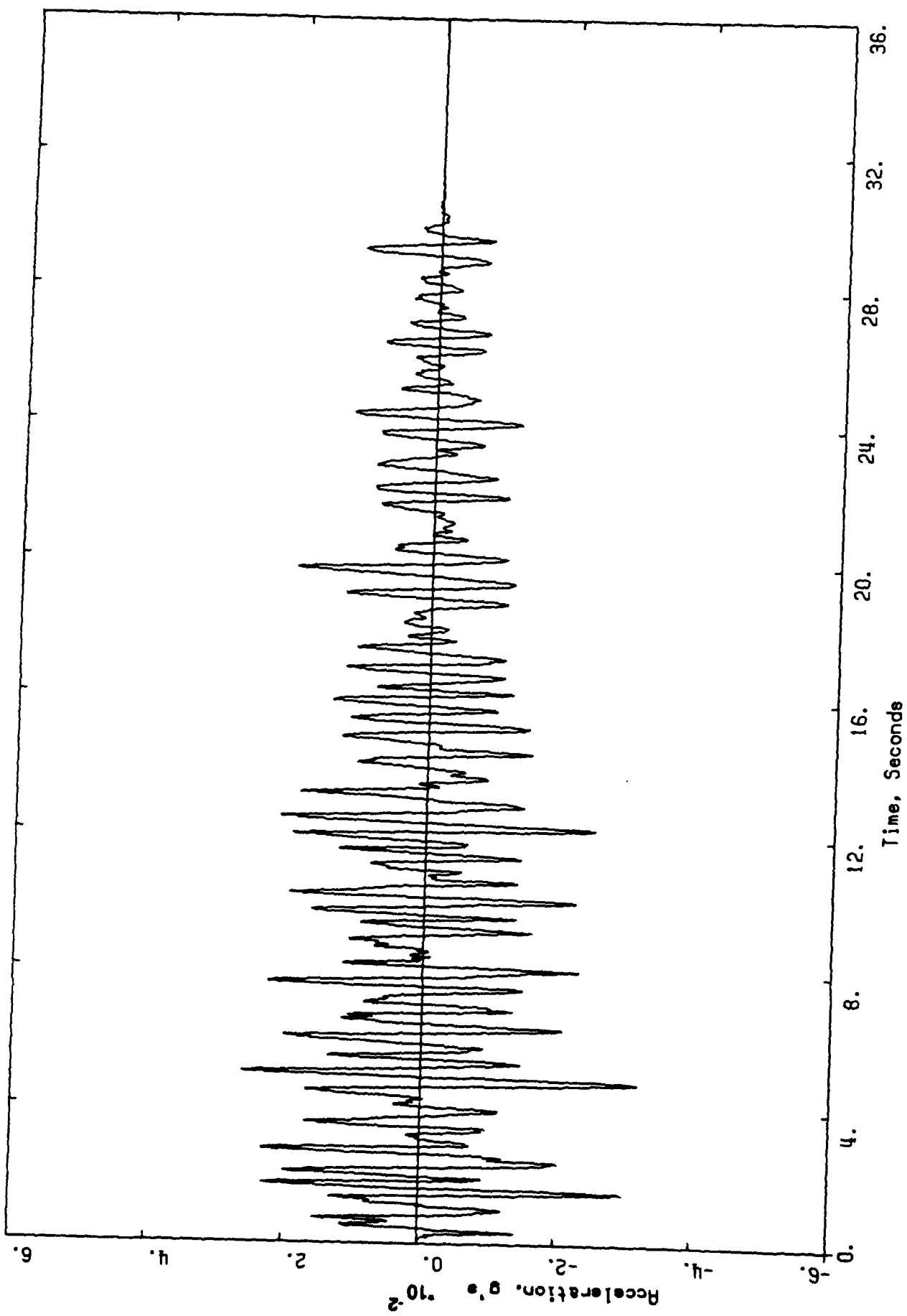


Figure 26. Computed acceleration time history at dam crest

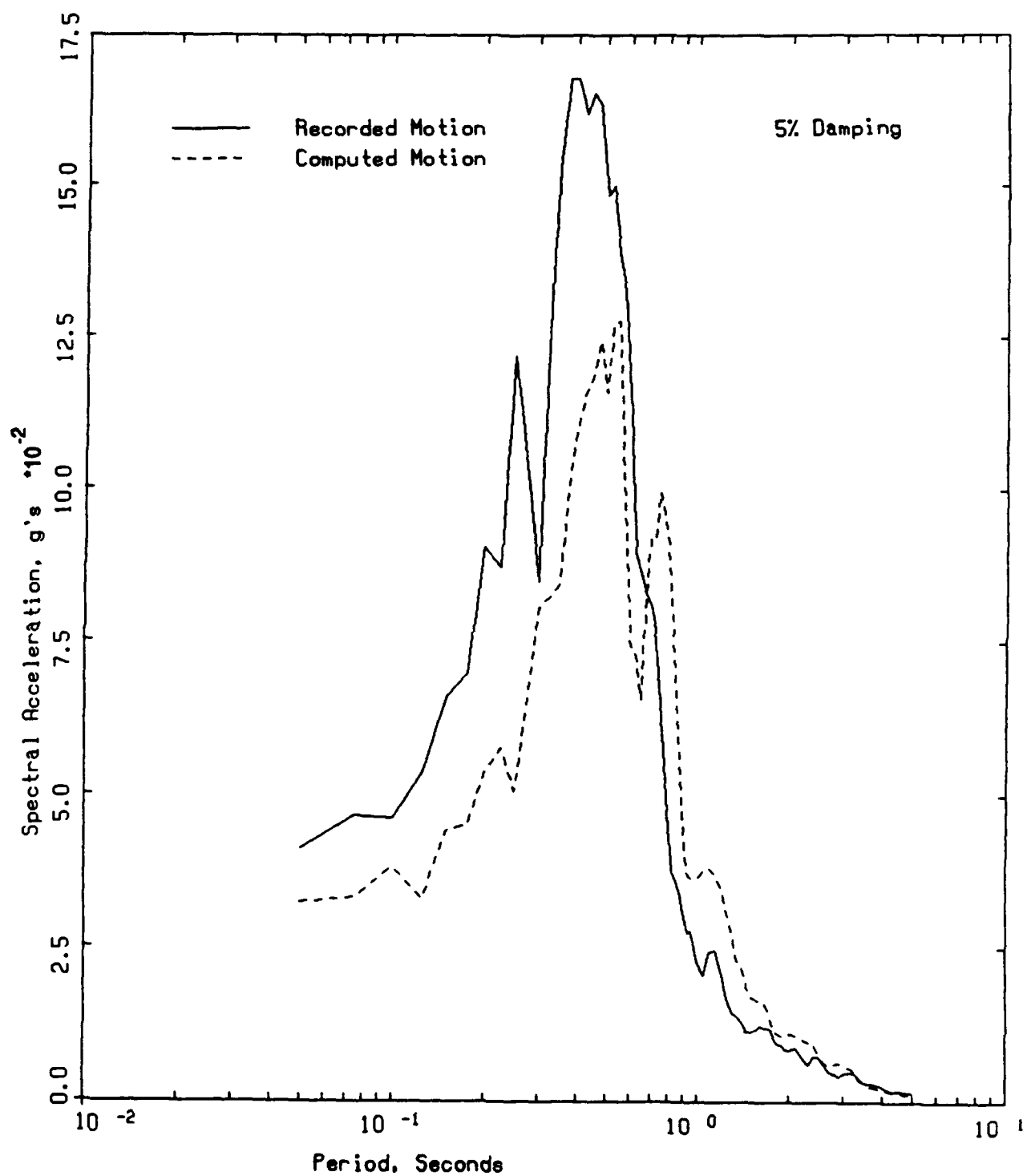


Figure 27. Comparison between computed and recorded acceleration response spectra at dam crest

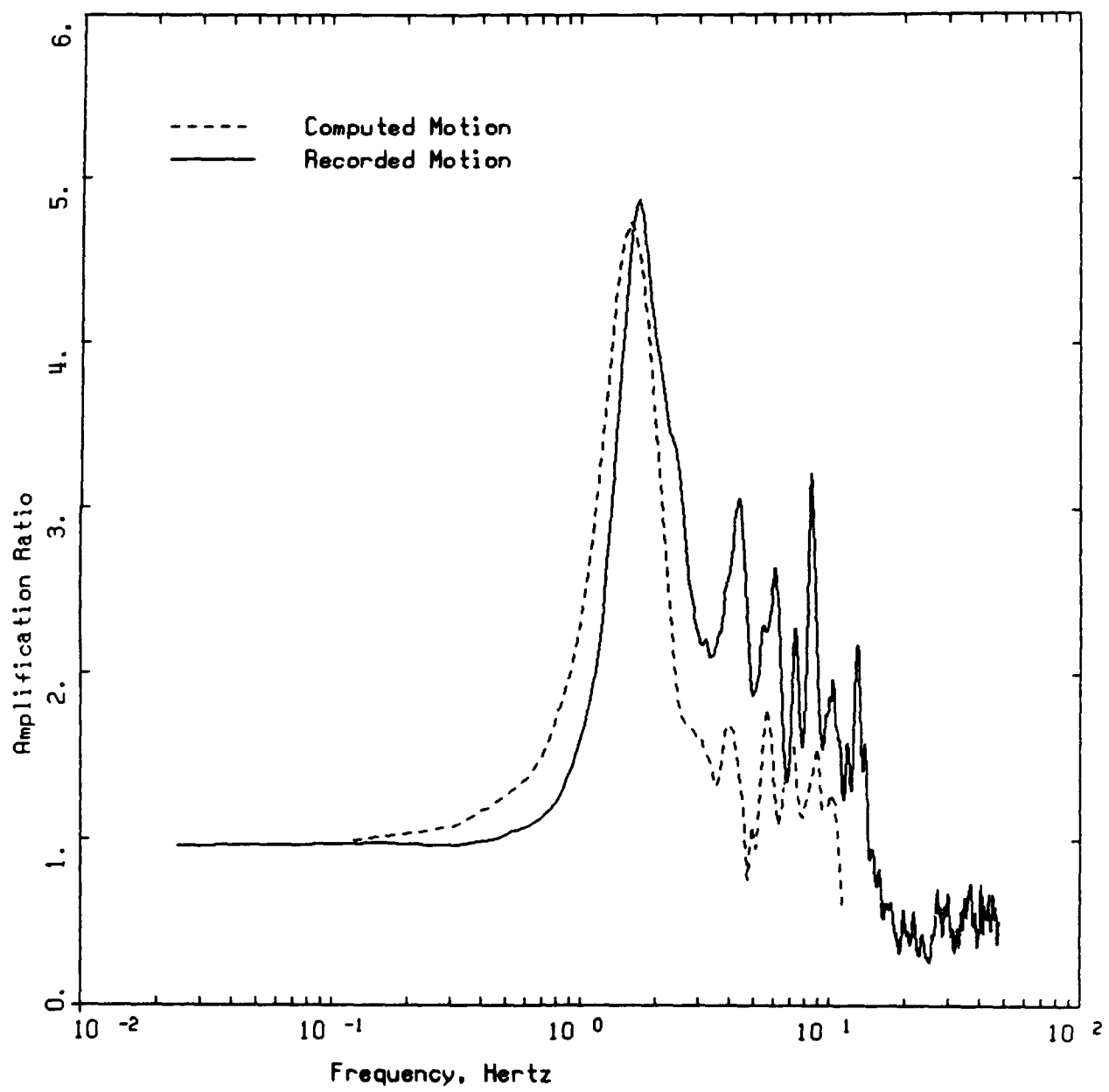


Figure 28. Comparison between computed and recorded amplification ratios at dam crest

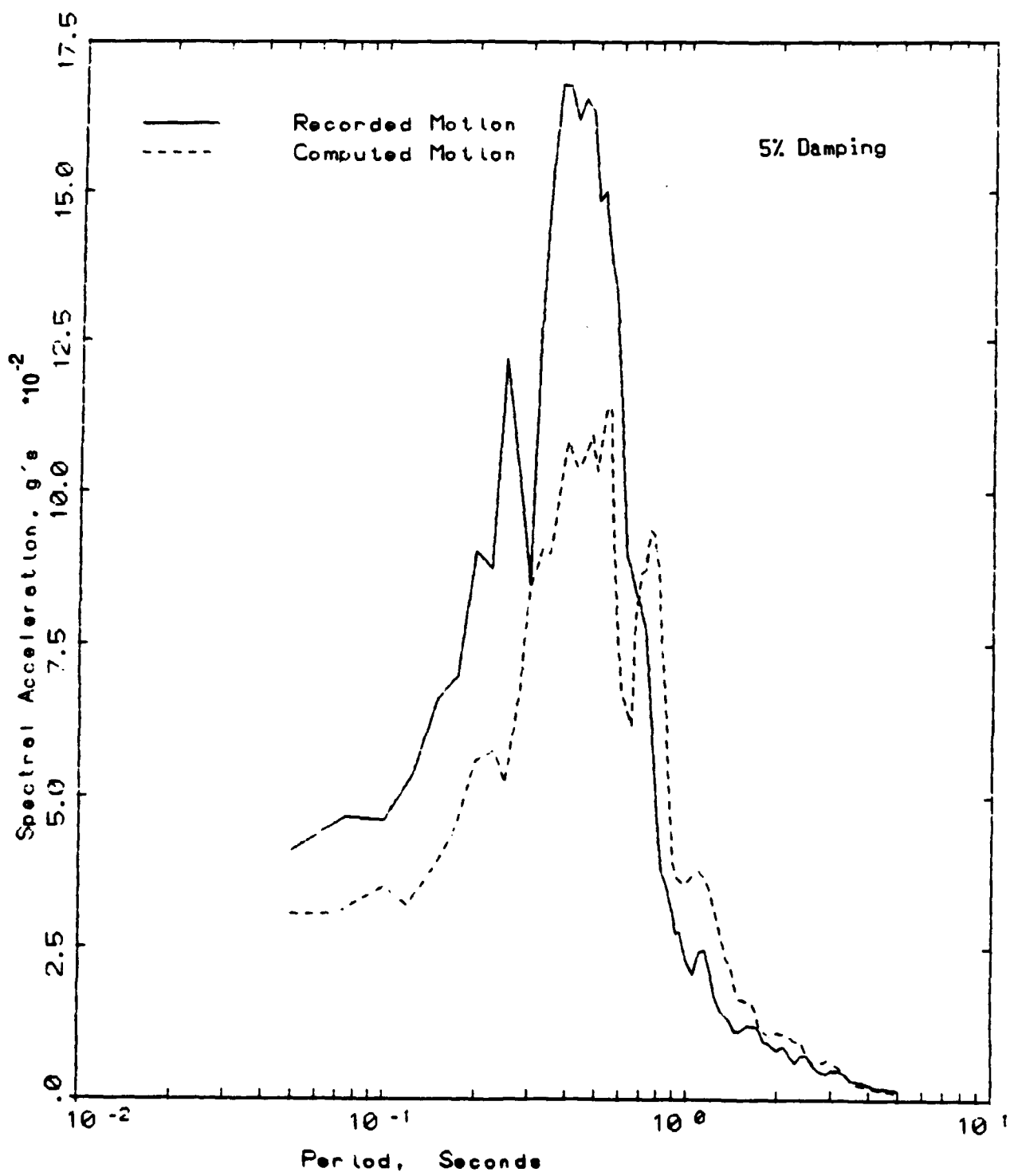


Figure 29. Comparison between computed and recorded acceleration response spectra at dam crest for  $K_{2\max}$  values estimated by Stark and Seed

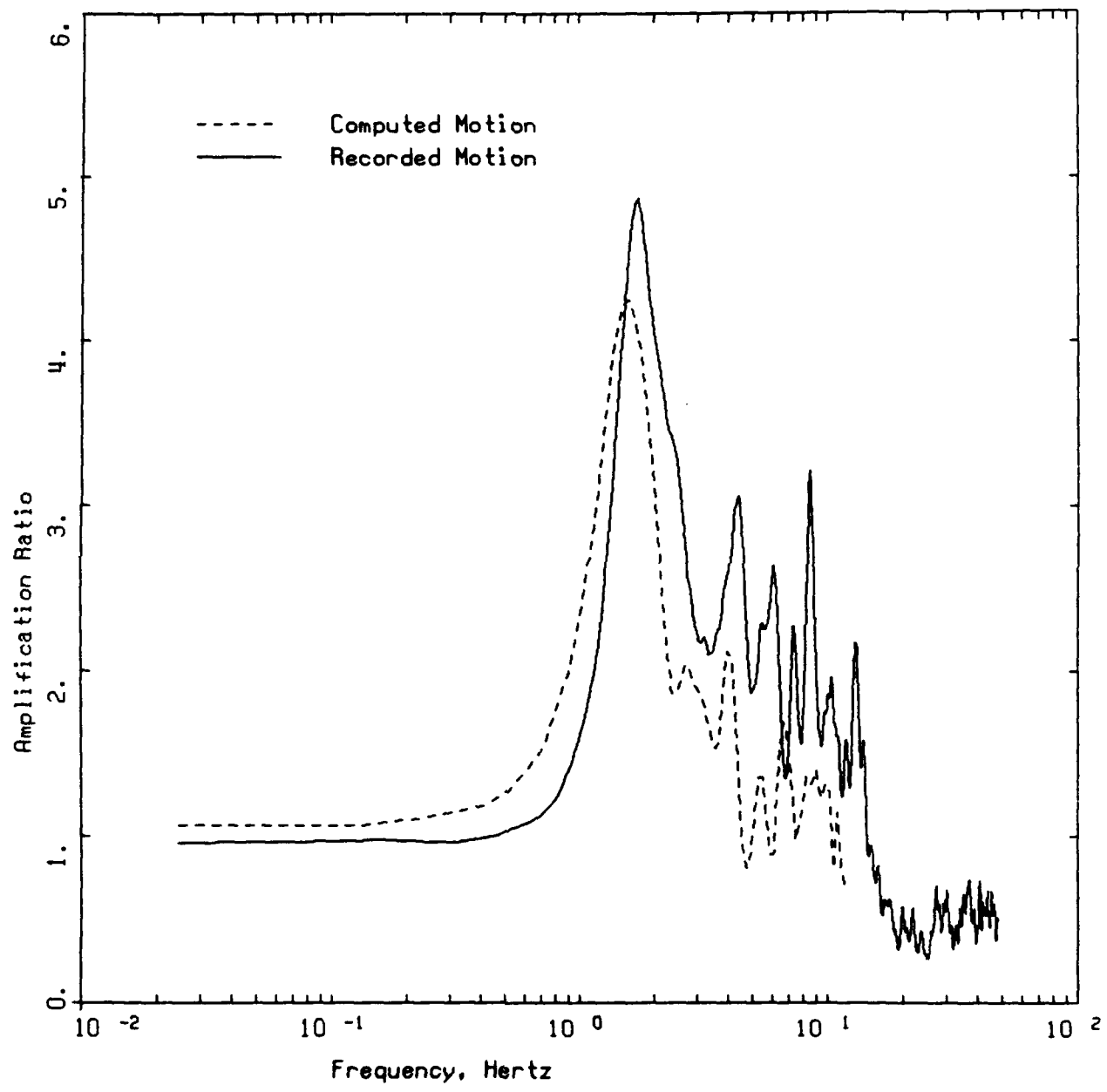


Figure 30. Comparison between computed and recorded amplification ratios at dam crest for  $K_{2\max}$  values estimated by Stark and Seed

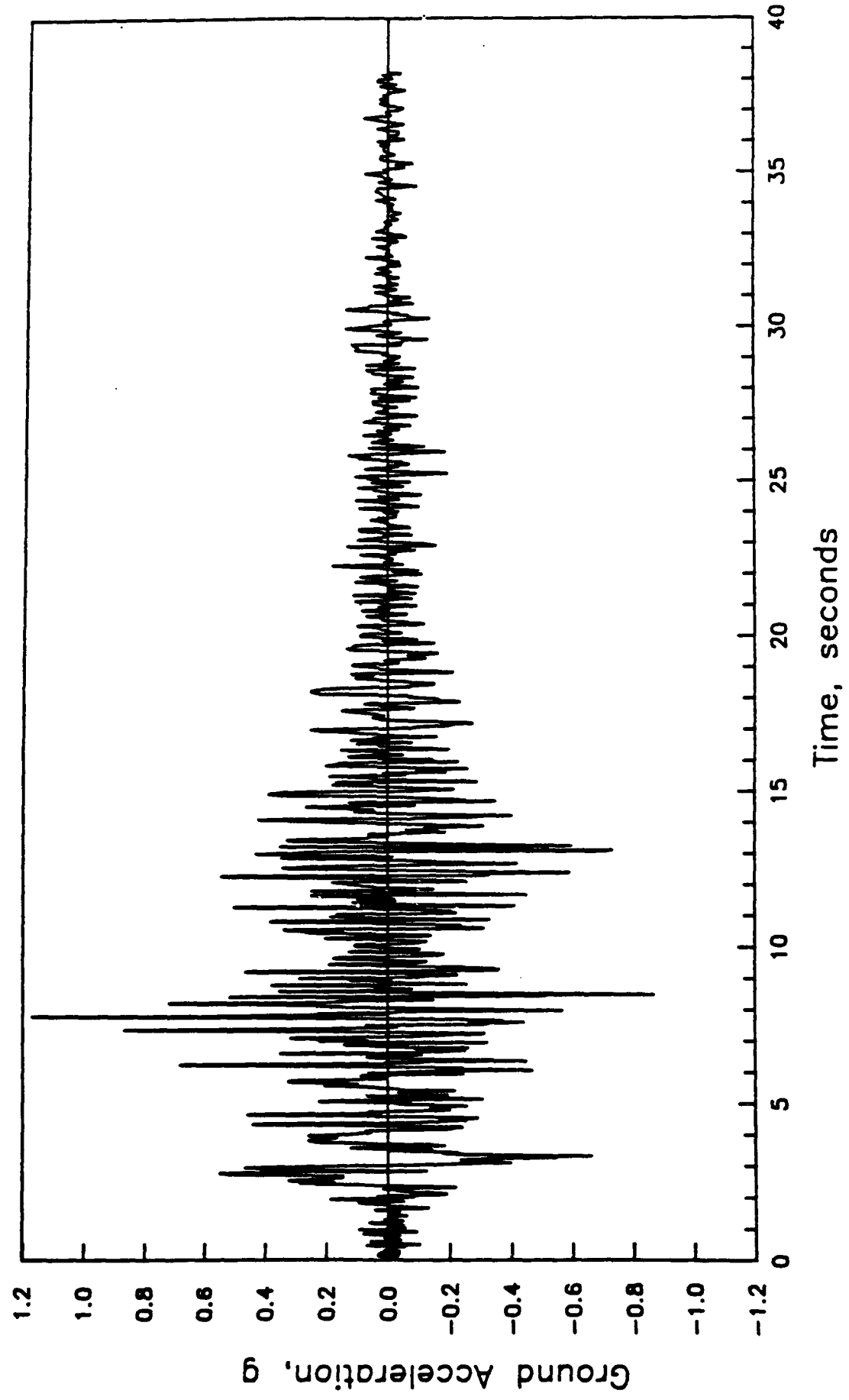


Figure 31. Acceleration time history specified for dynamic response analysis of Ririe Dam

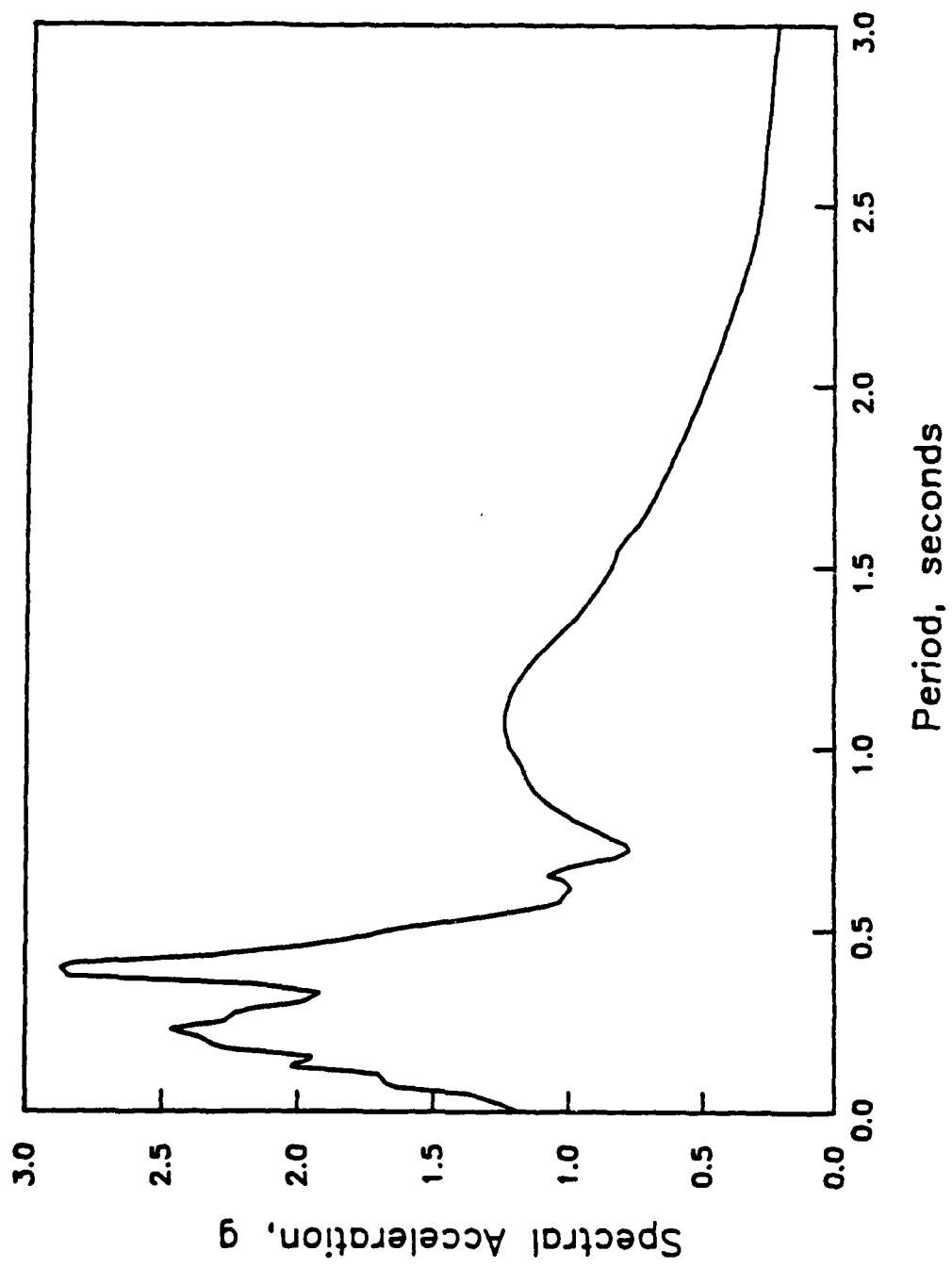
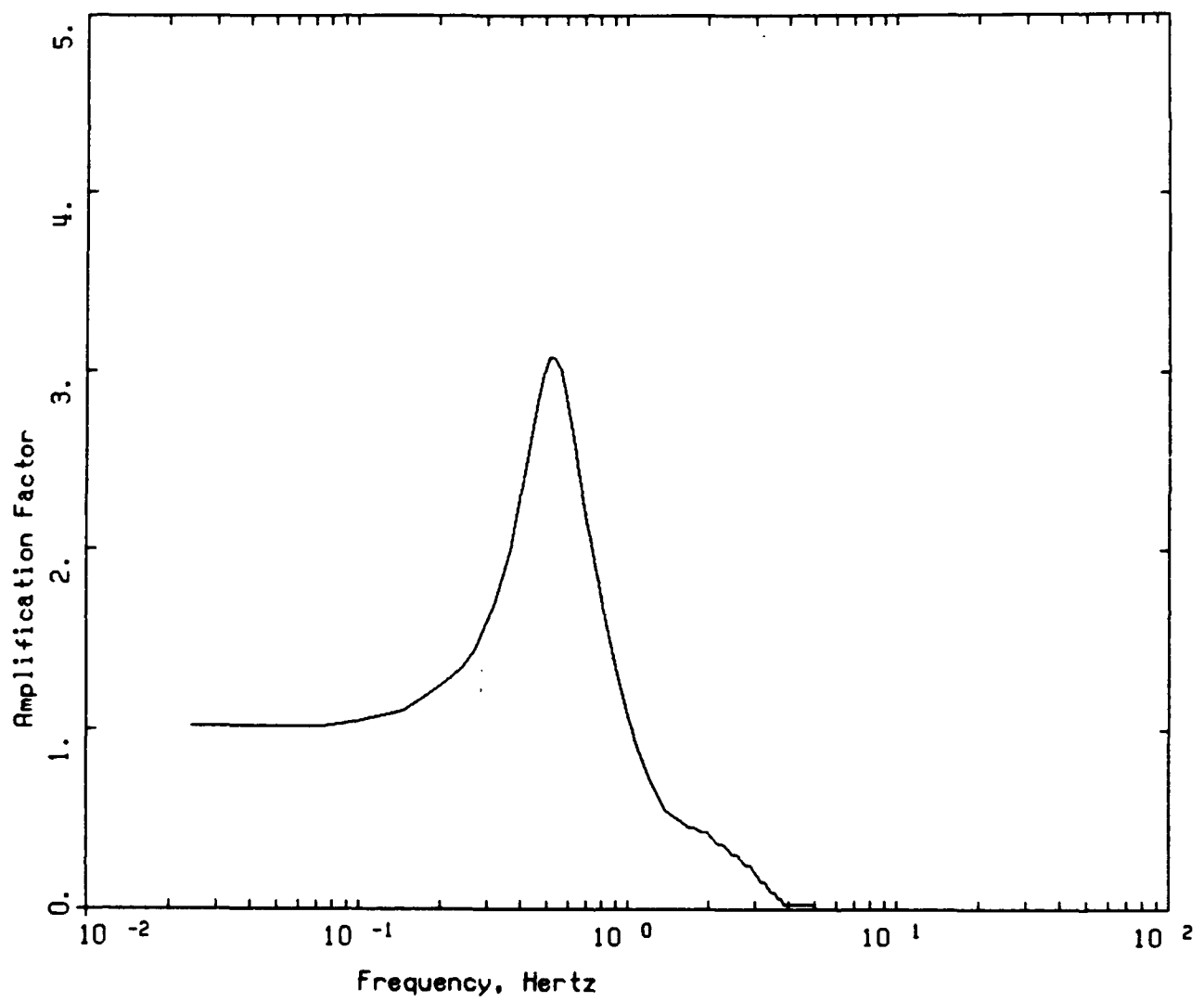


Figure 32. Acceleration response spectrum for specified time history



**Figure 35. Computed acceleration amplification function at crest of dam for section AA**

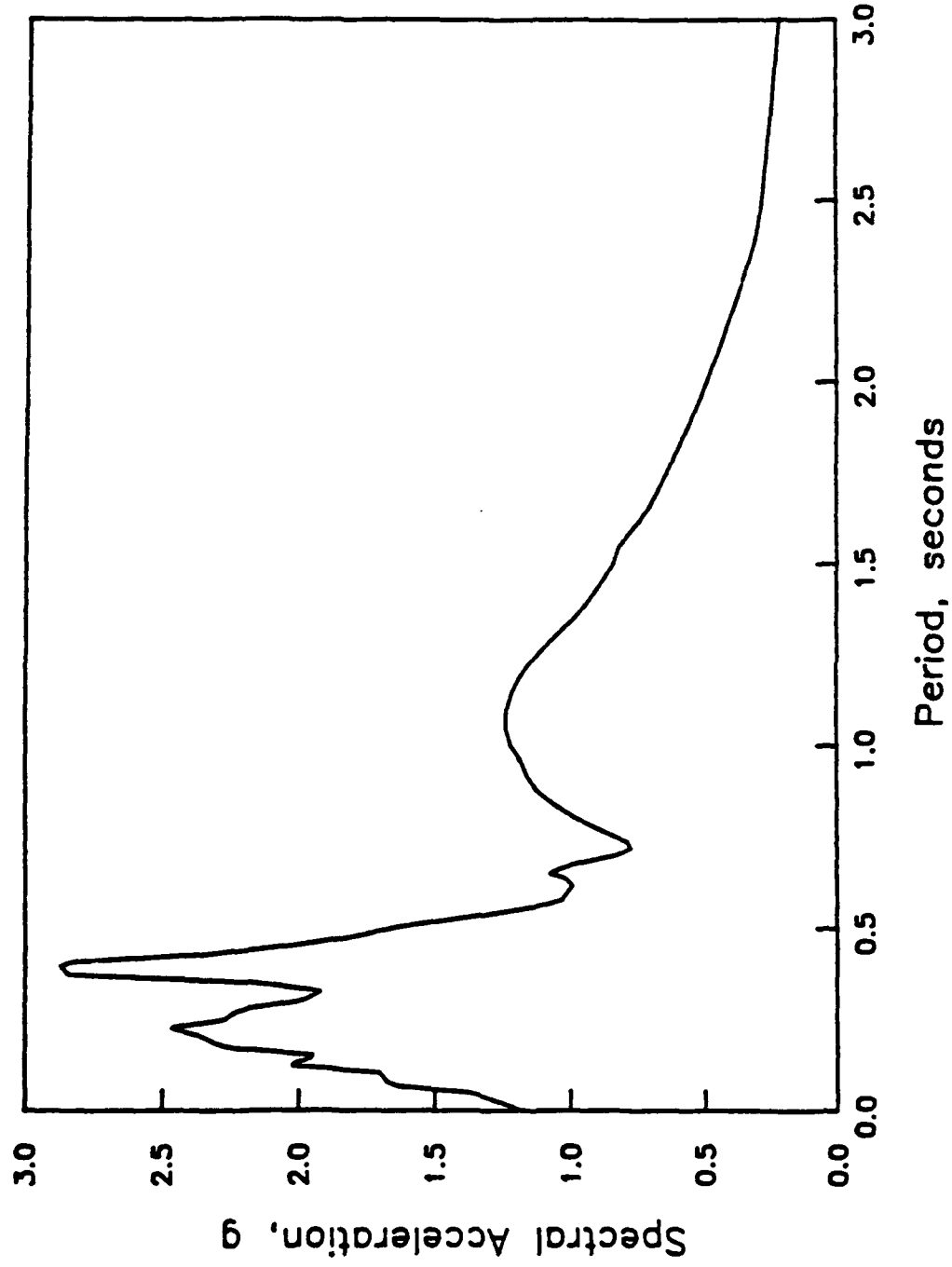


Figure 32. Acceleration response spectrum for specified time history

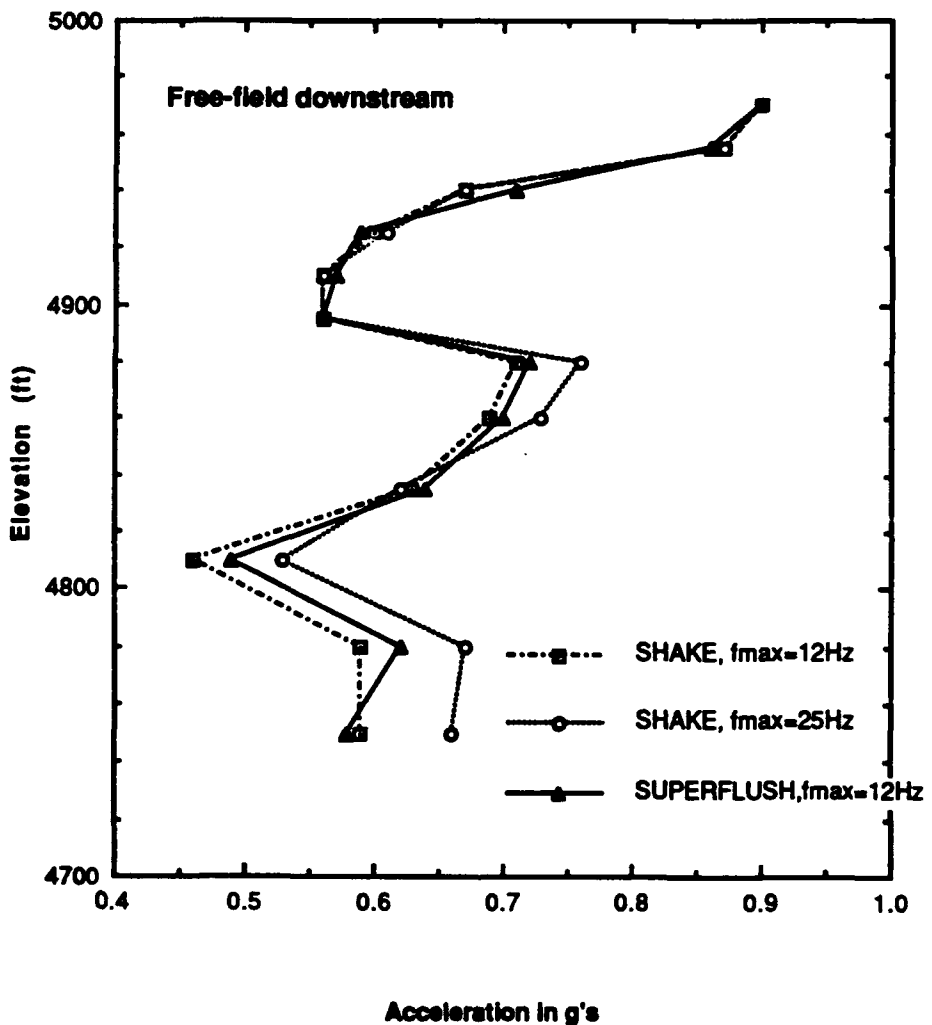


Figure 33. Peak ground accelerations computed using SHAKE and SUPERFLUSH

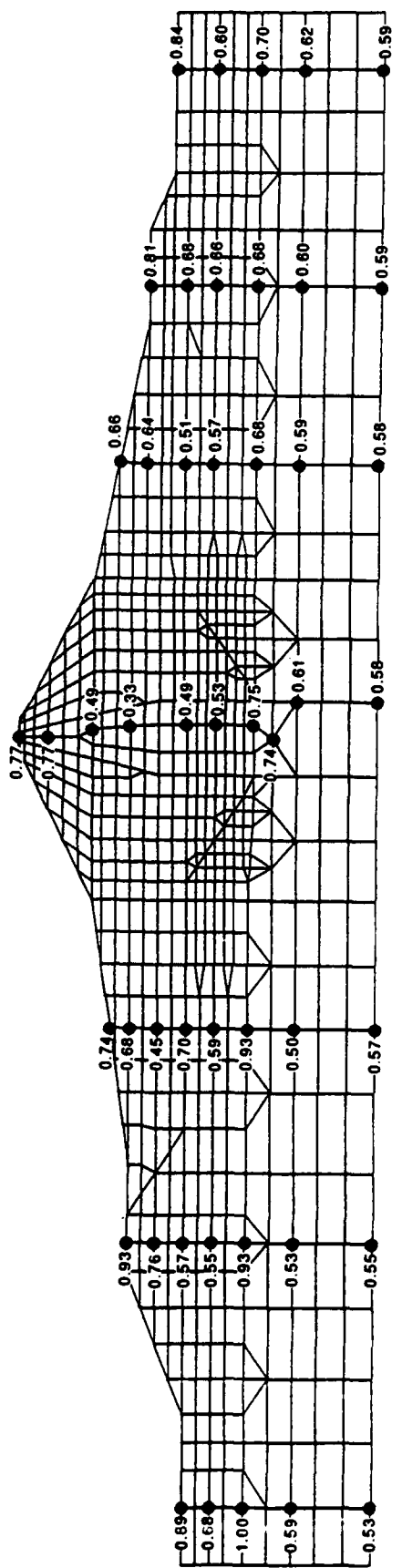


Figure 36. Computed peak horizontal ground accelerations for section AA

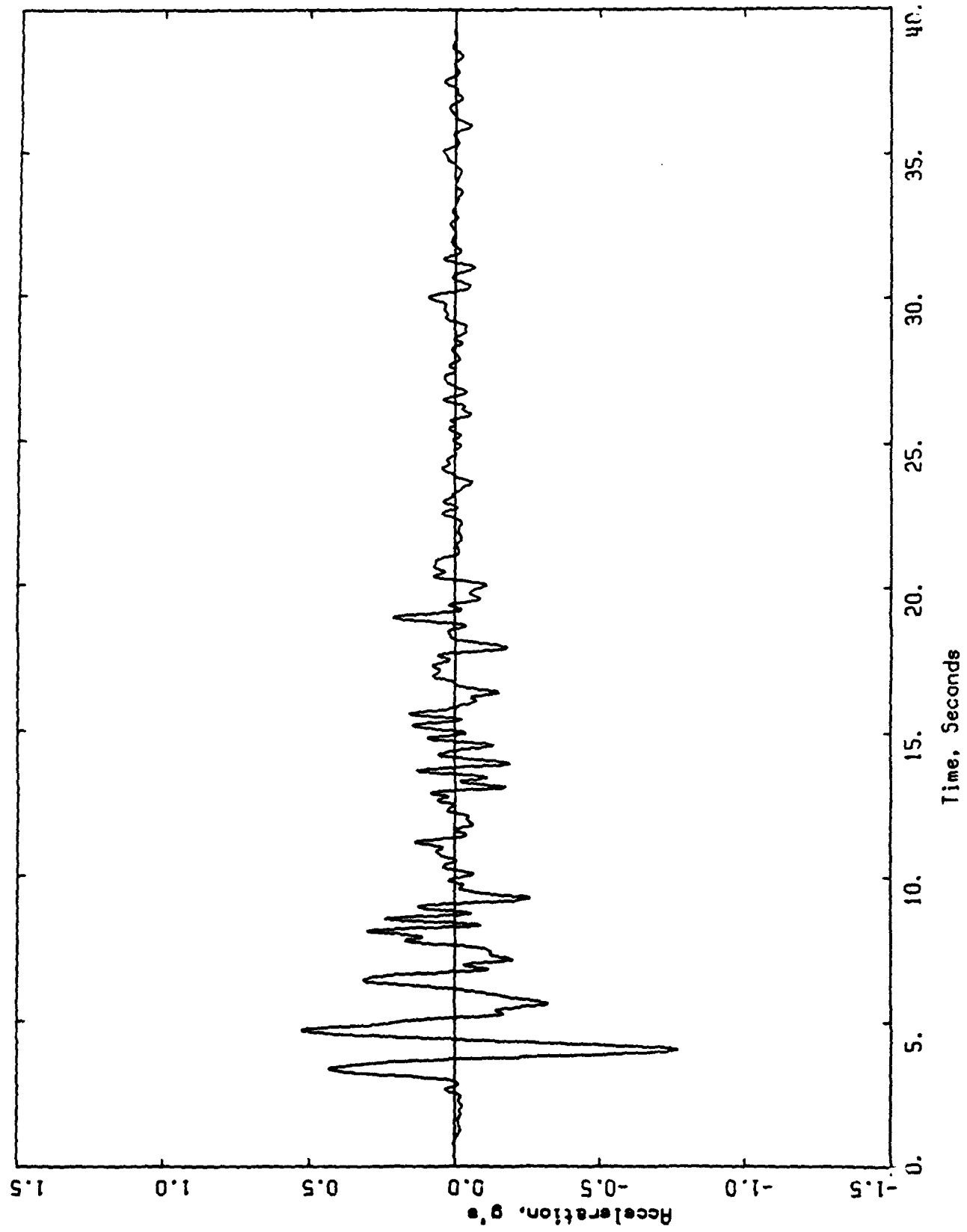


Figure 37. Computed acceleration time history at dam crest for section AA

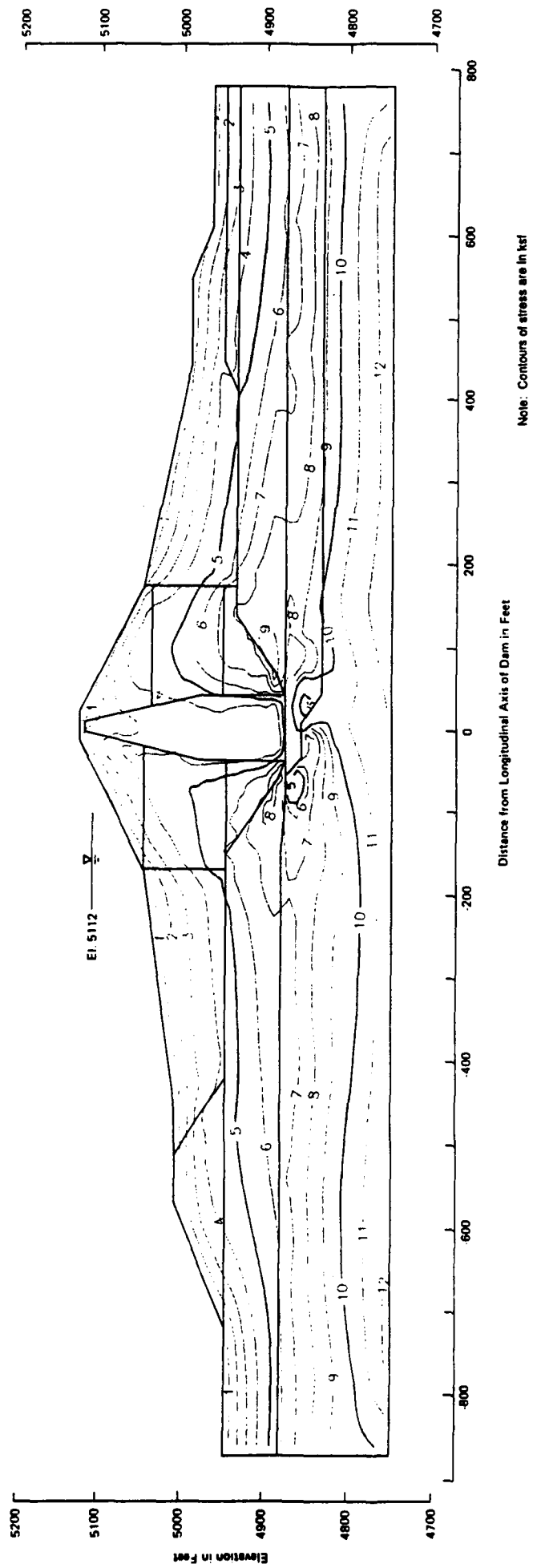


Figure 38. Computed peak horizontal dynamic shear stresses for section AA

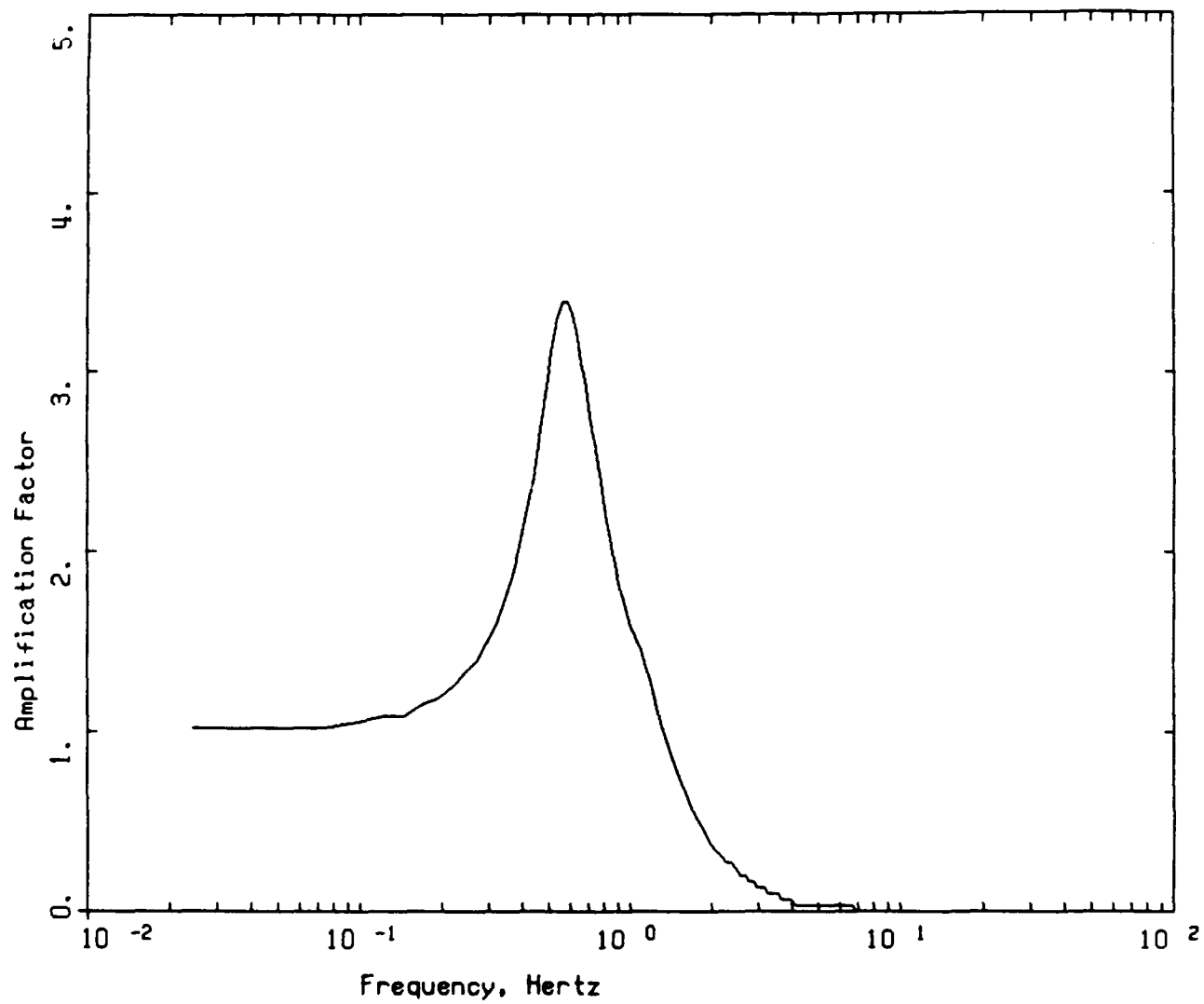


Figure 39. Computed acceleration amplification function at crest of dam for section BB

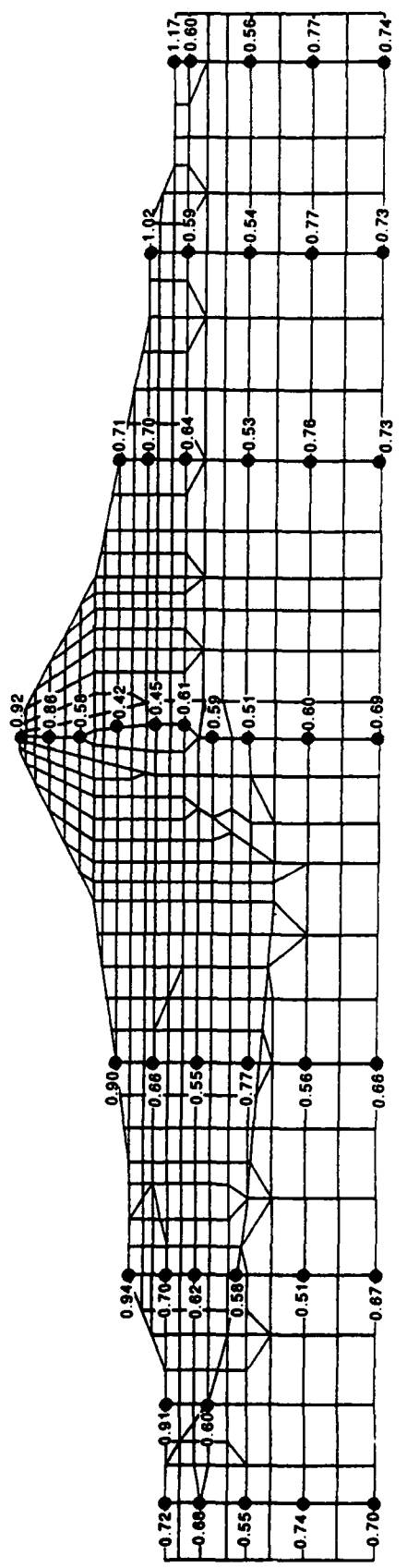


Figure 40. Computed peak horizontal ground accelerations for section BB

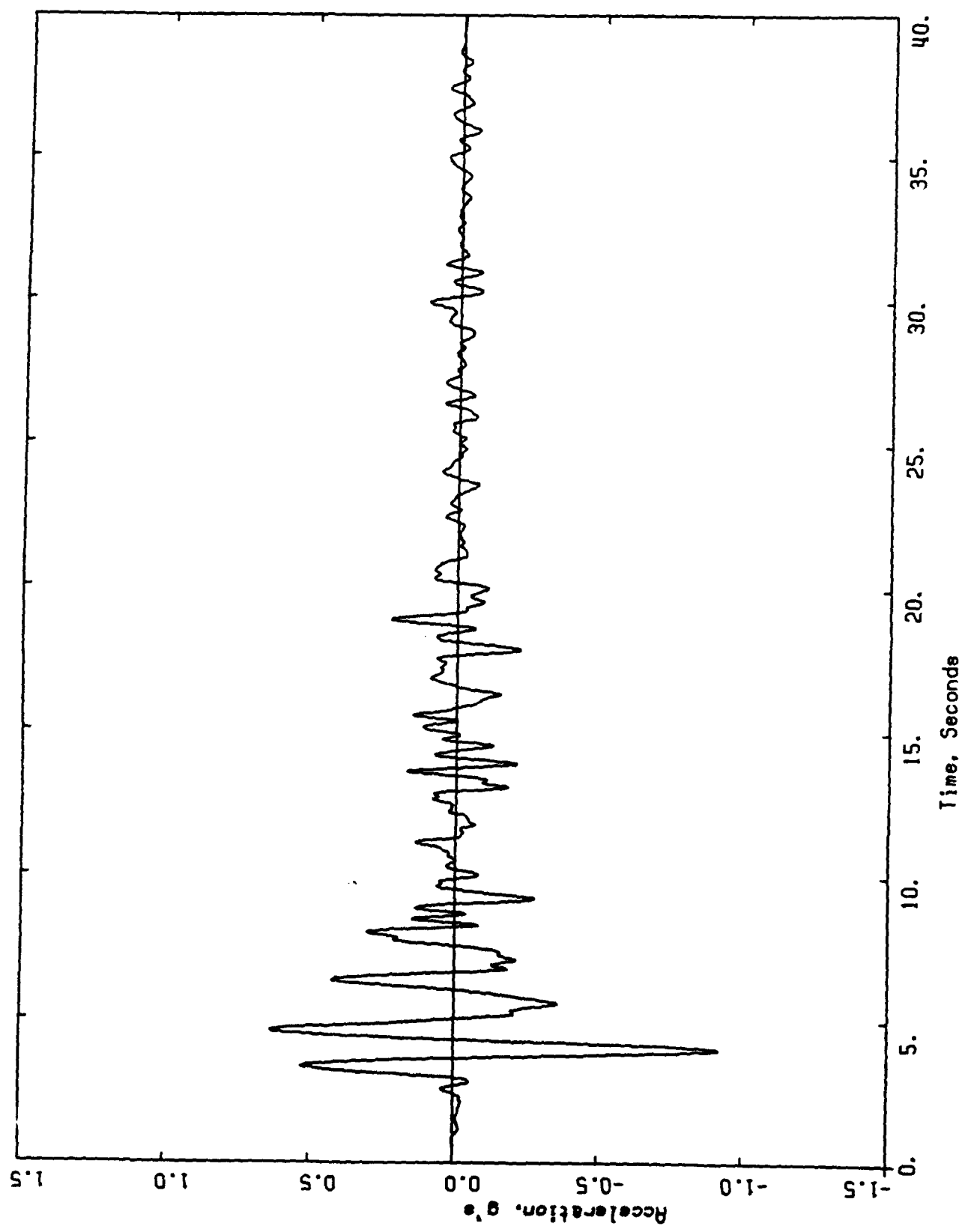


Figure 41. Computed acceleration time history at dam crest for section BB

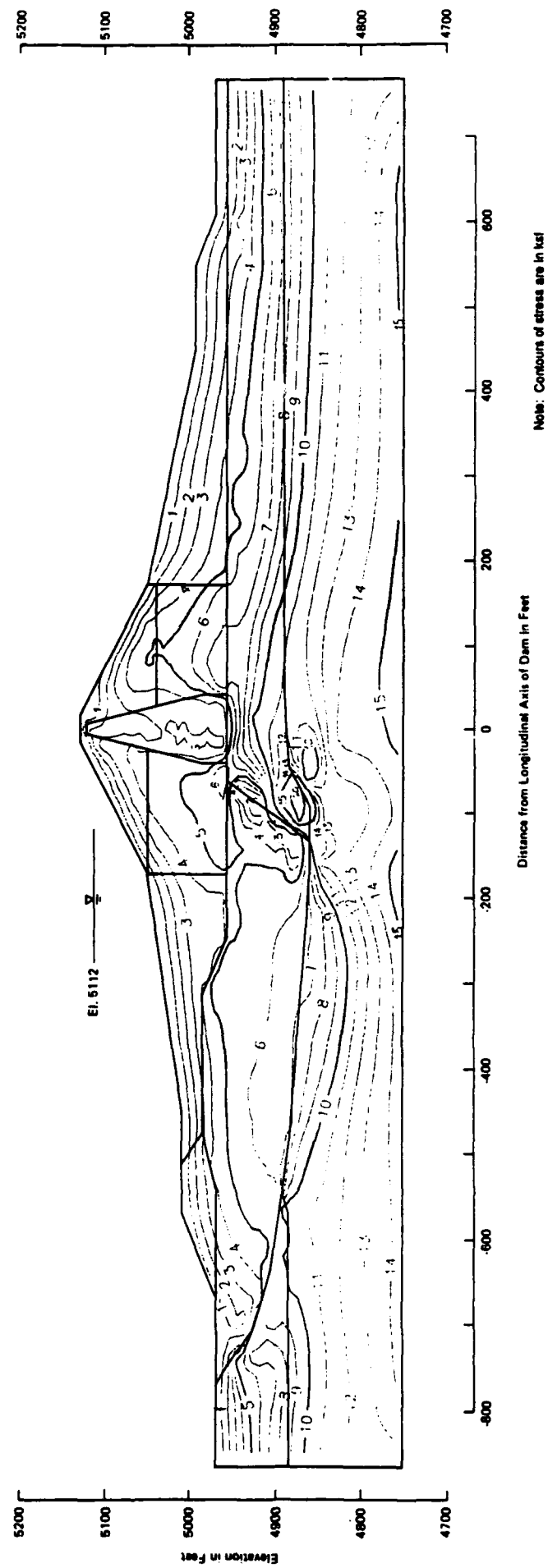
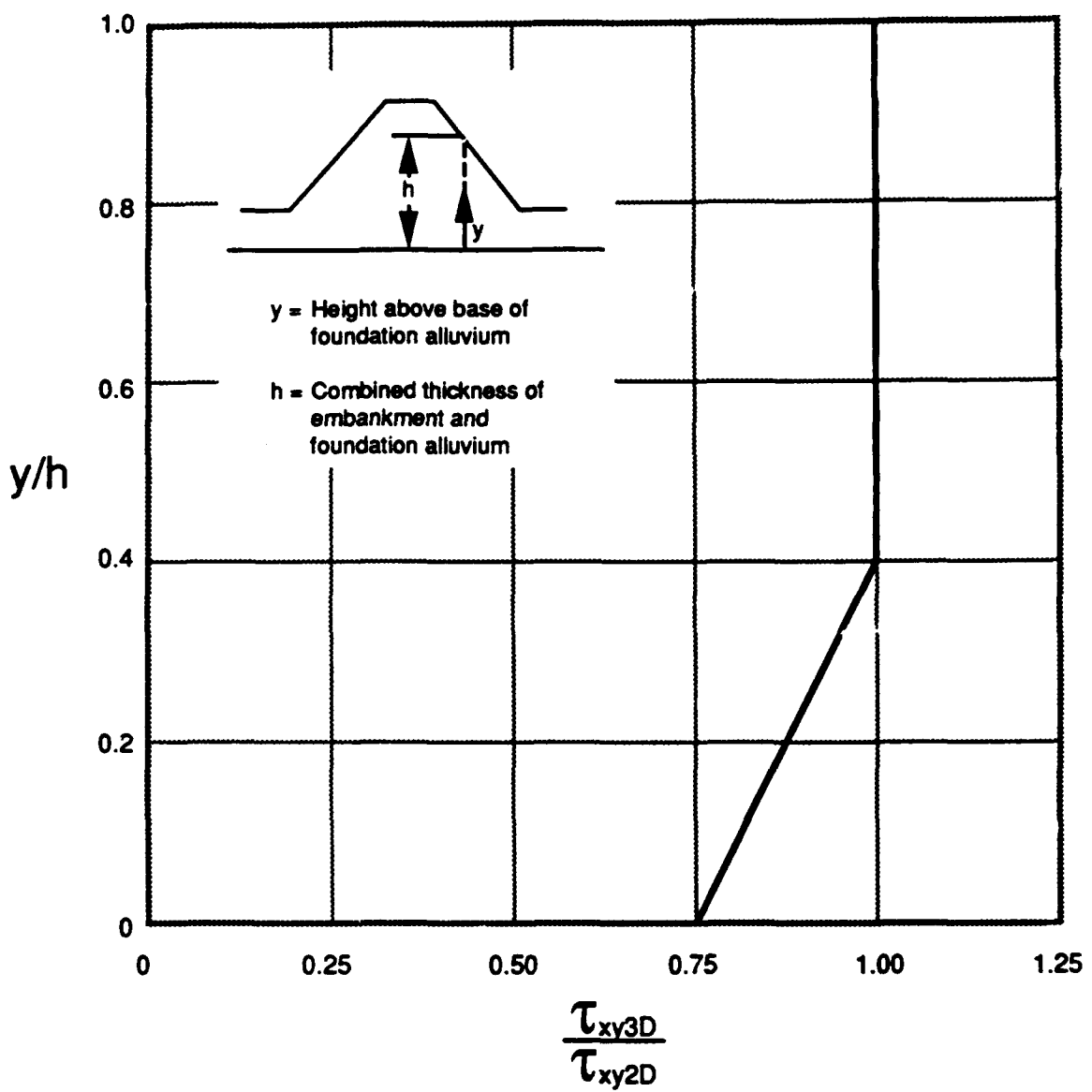
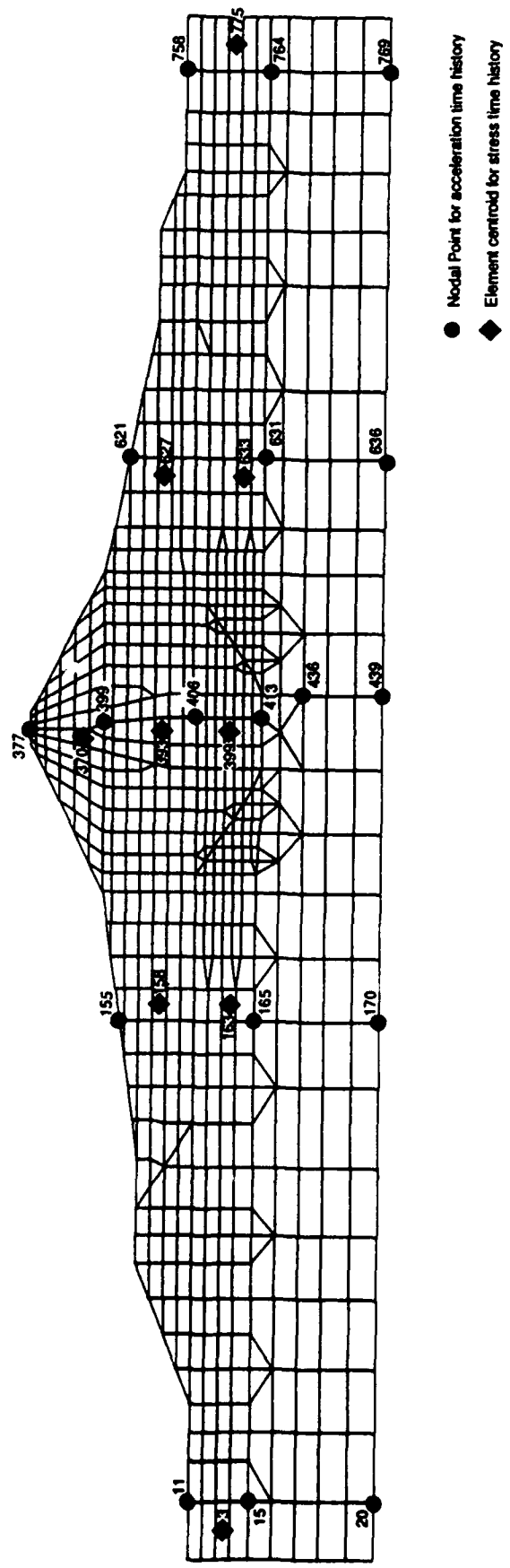


Figure 42. Computed peak horizontal dynamic shear stresses for section 88



**Figure 43.** Recommended correction factor to estimate 3-D horizontal shear stresses ( $\tau_{xy3D}$ ) from computed 2-D horizontal shear stresses ( $\tau_{xy2D}$ ) for Ririe Dam

**APPENDIX A**



**Figure A-1.** Location of nodal points and element centroids in section AA for time history output

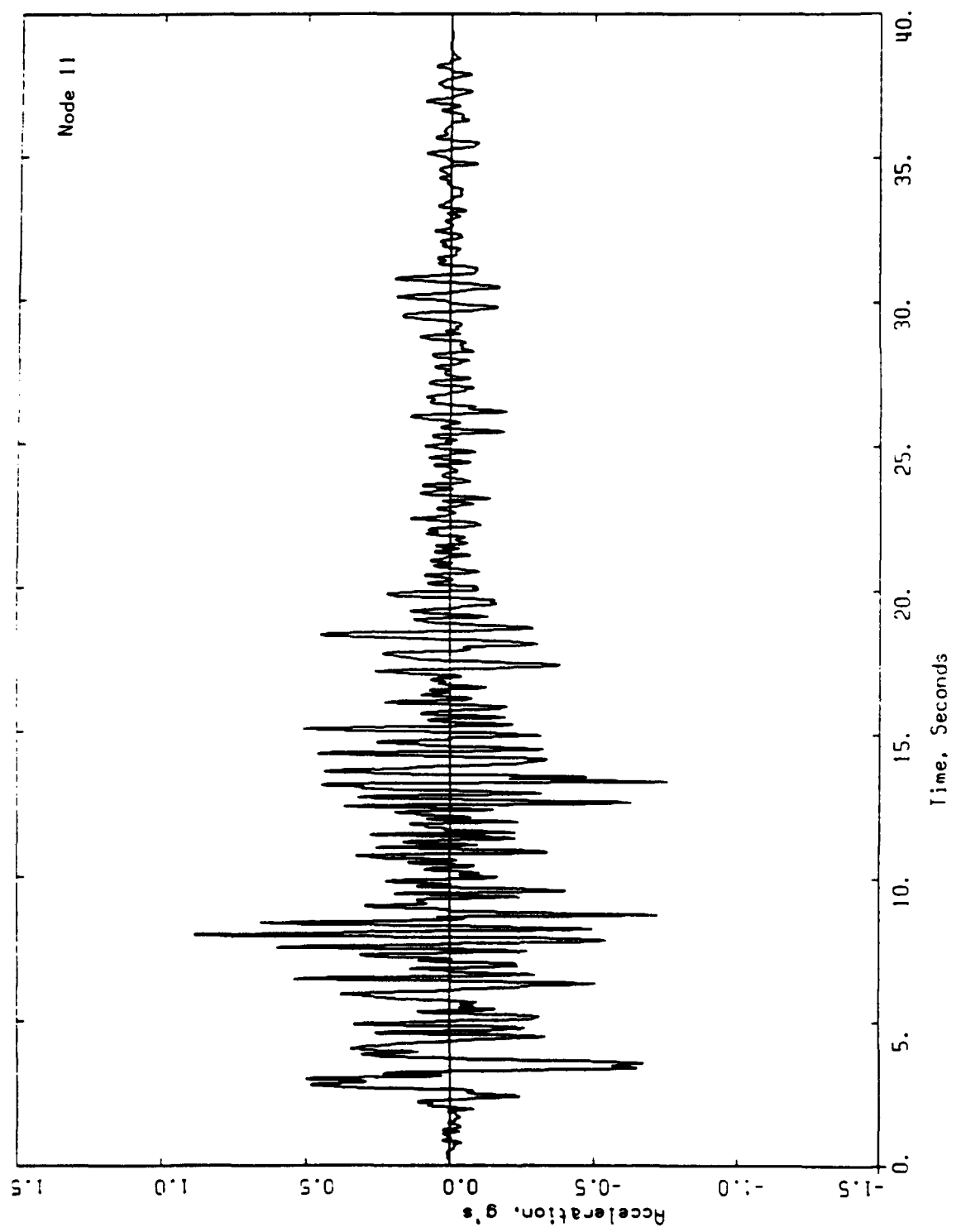


Figure A-2. Acceleration time history at nodal point 11

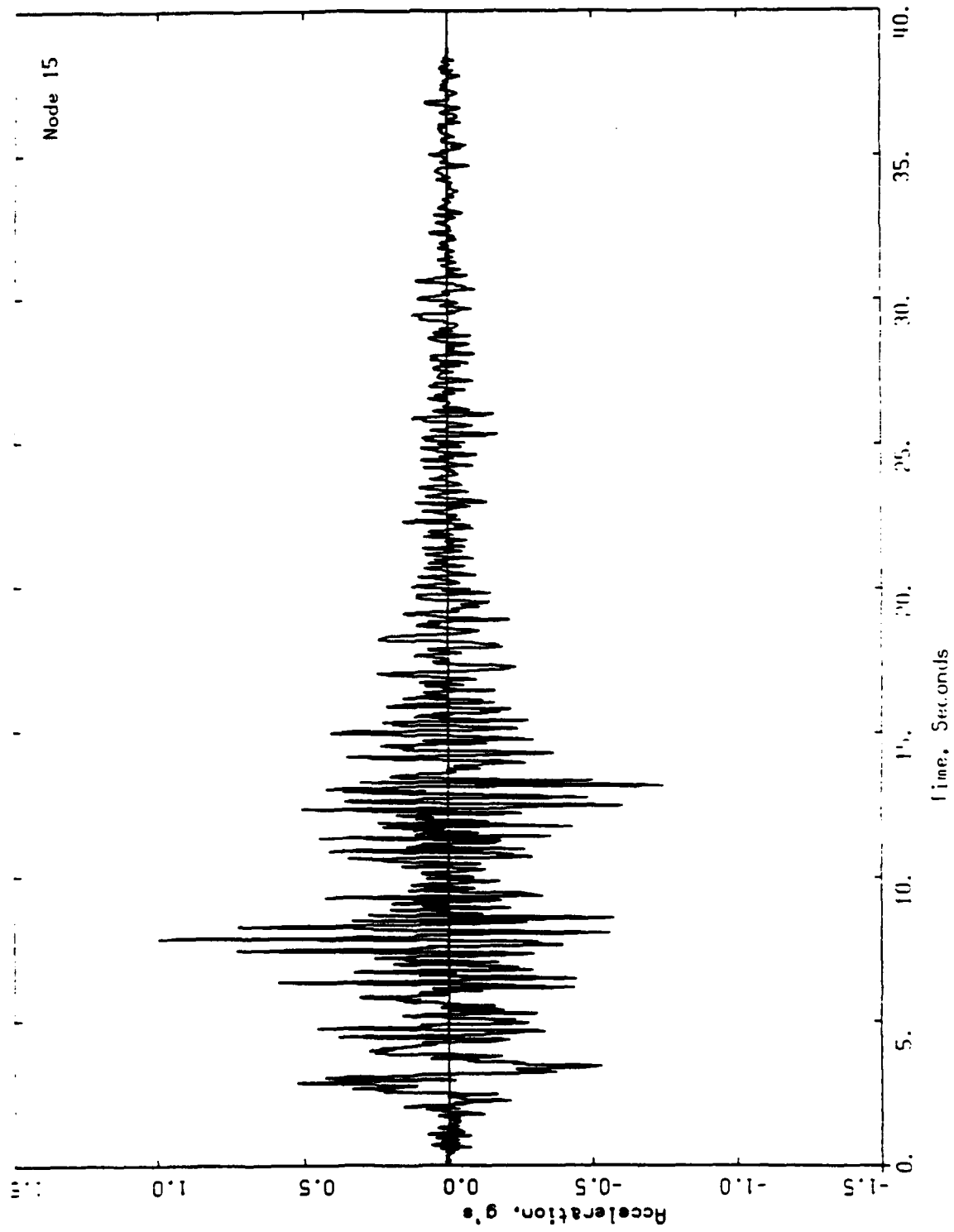


Figure A-3. Acceleration time history at nodal point 15

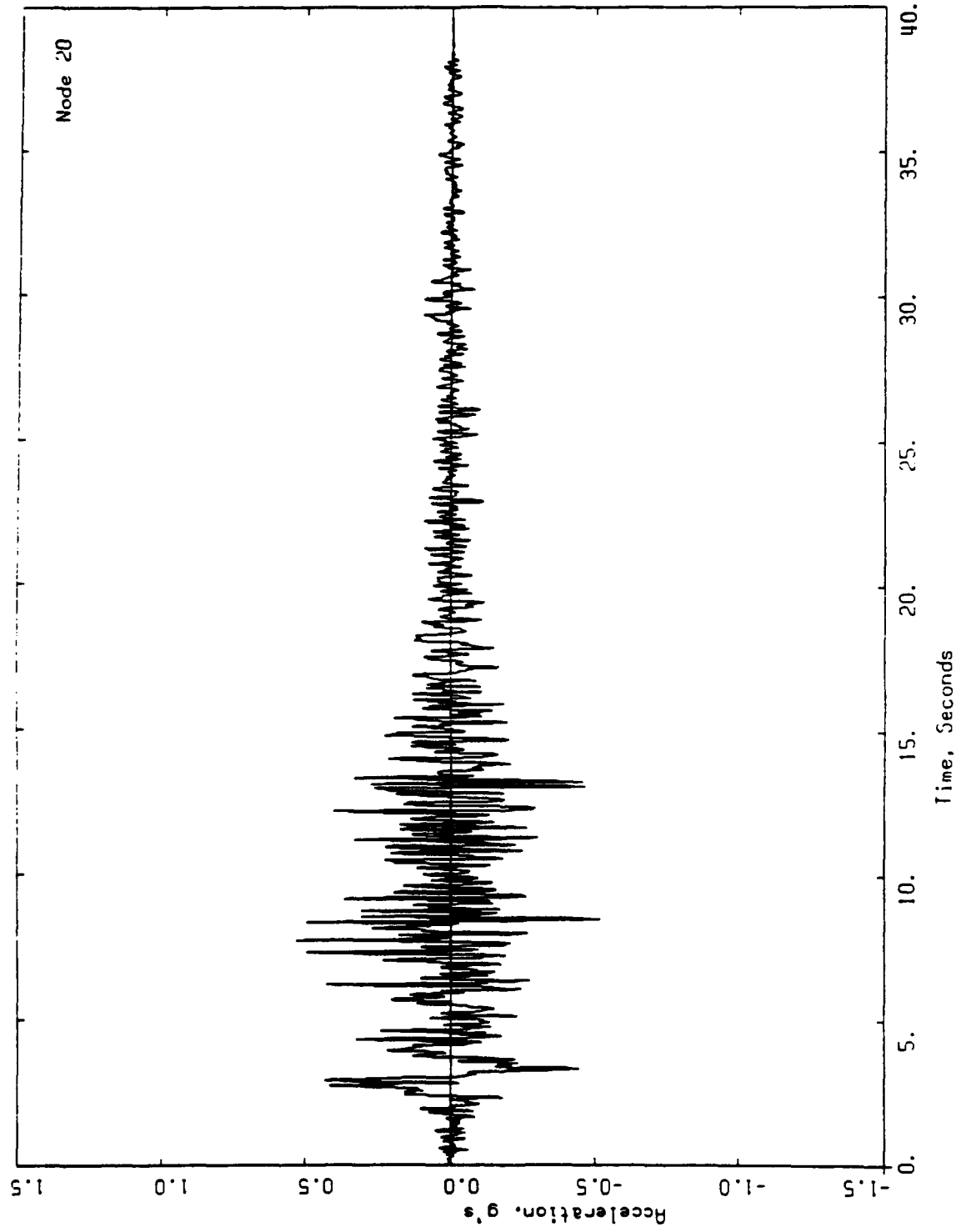


Figure A-4. Acceleration time history at nodal point 20

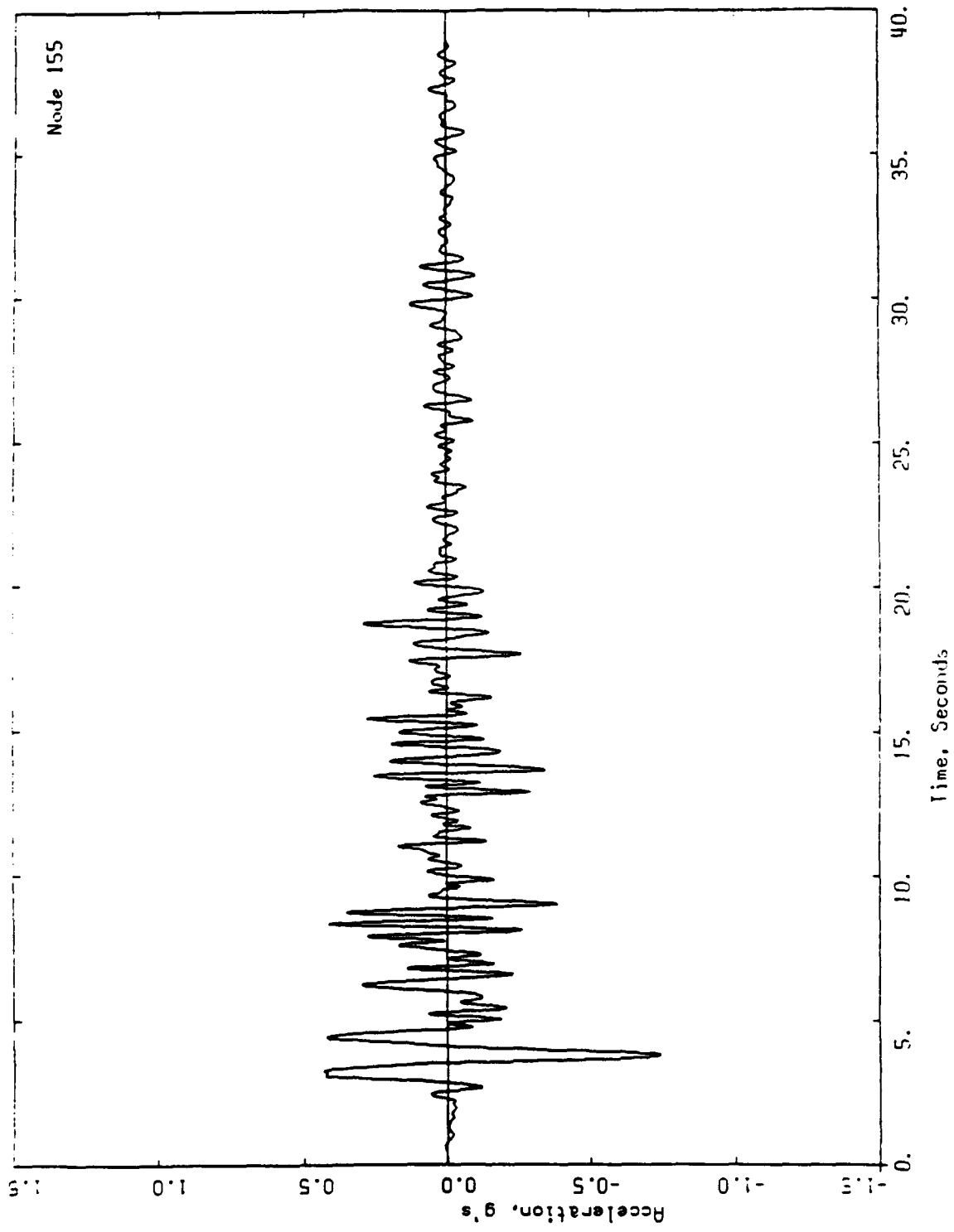


Figure A-5. Acceleration time history at nodal point 155

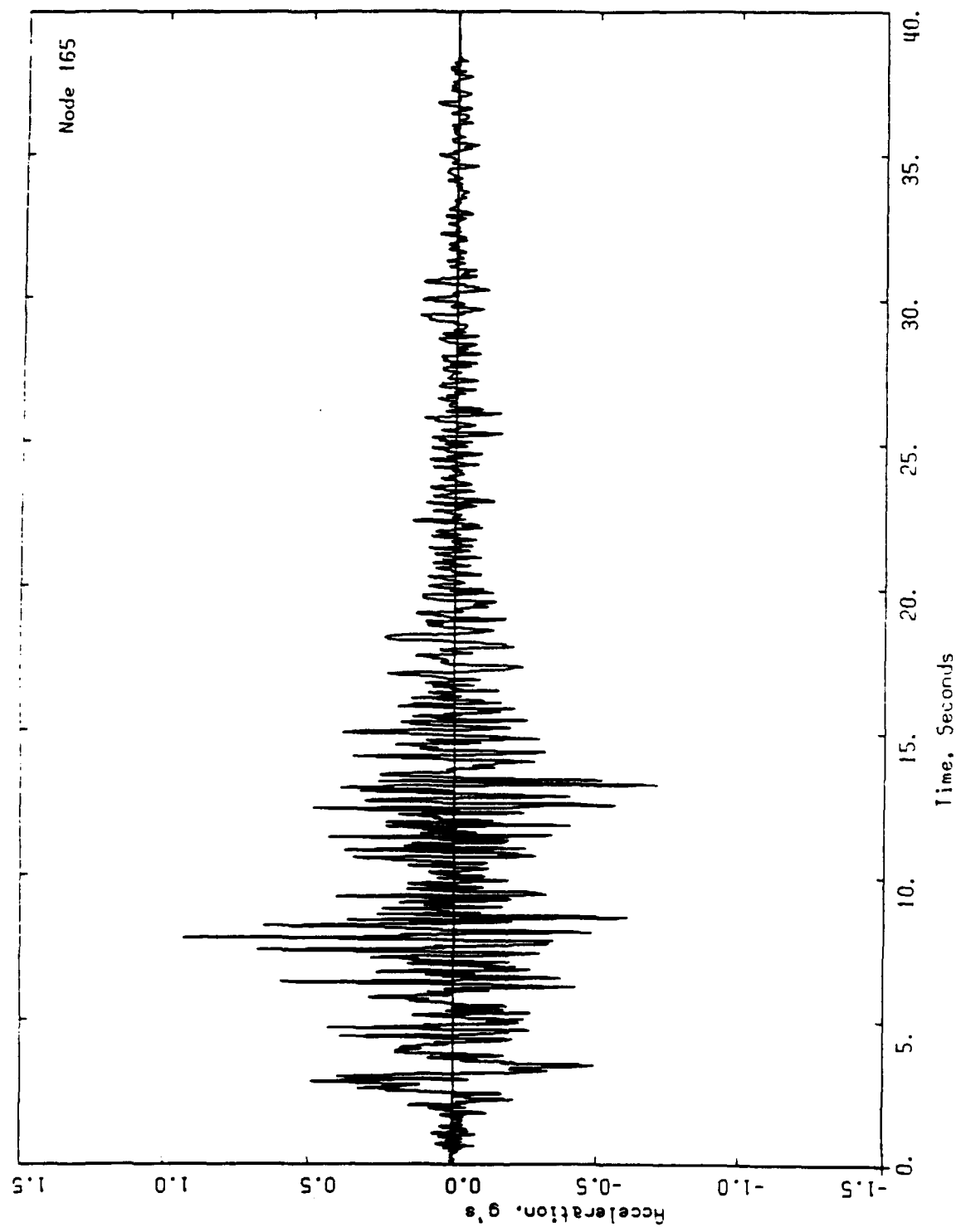


Figure A-6. Acceleration time history at nodal point 165

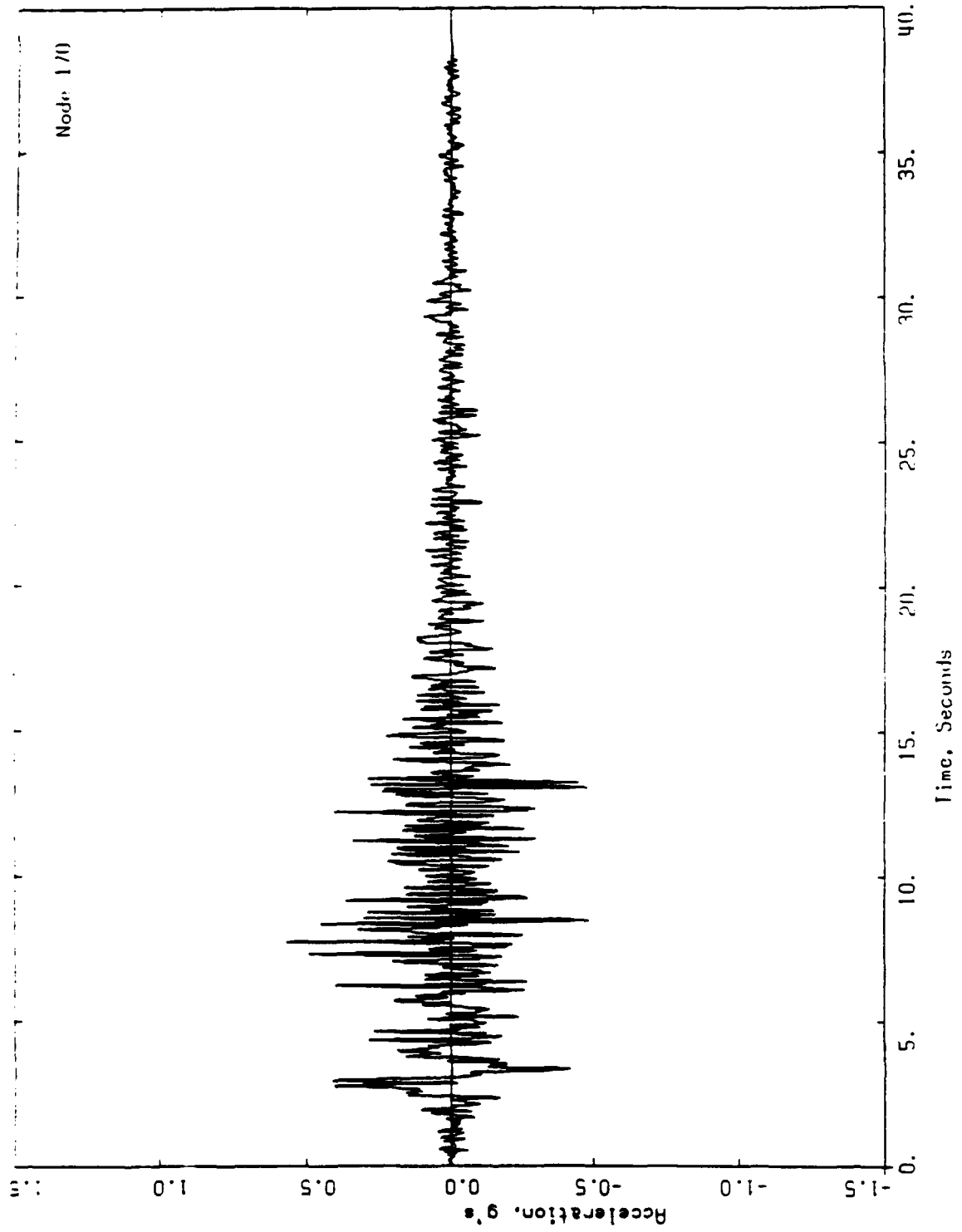


Figure A-7. Acceleration time history at nodal point 170

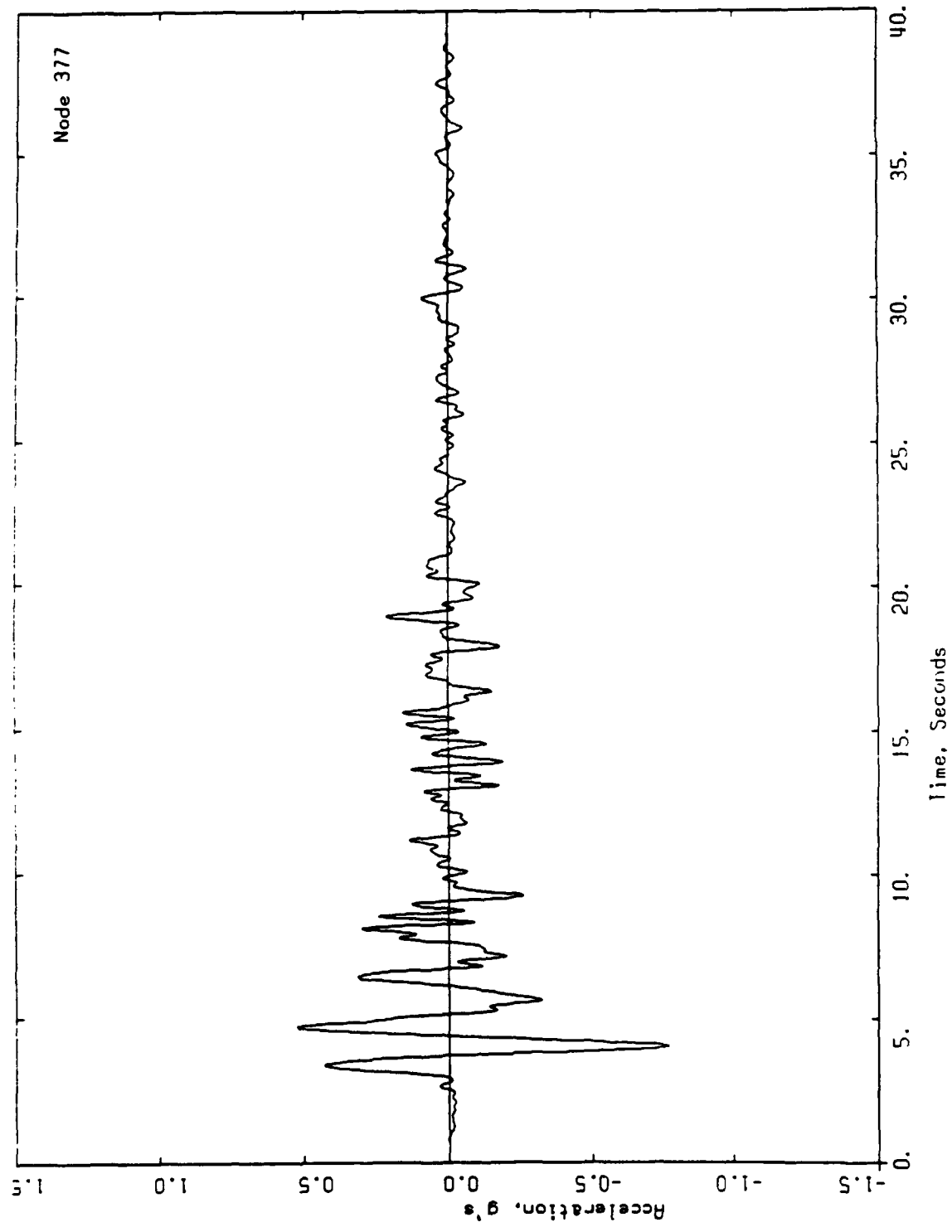


Figure A-8. Acceleration time history at nodal point 377

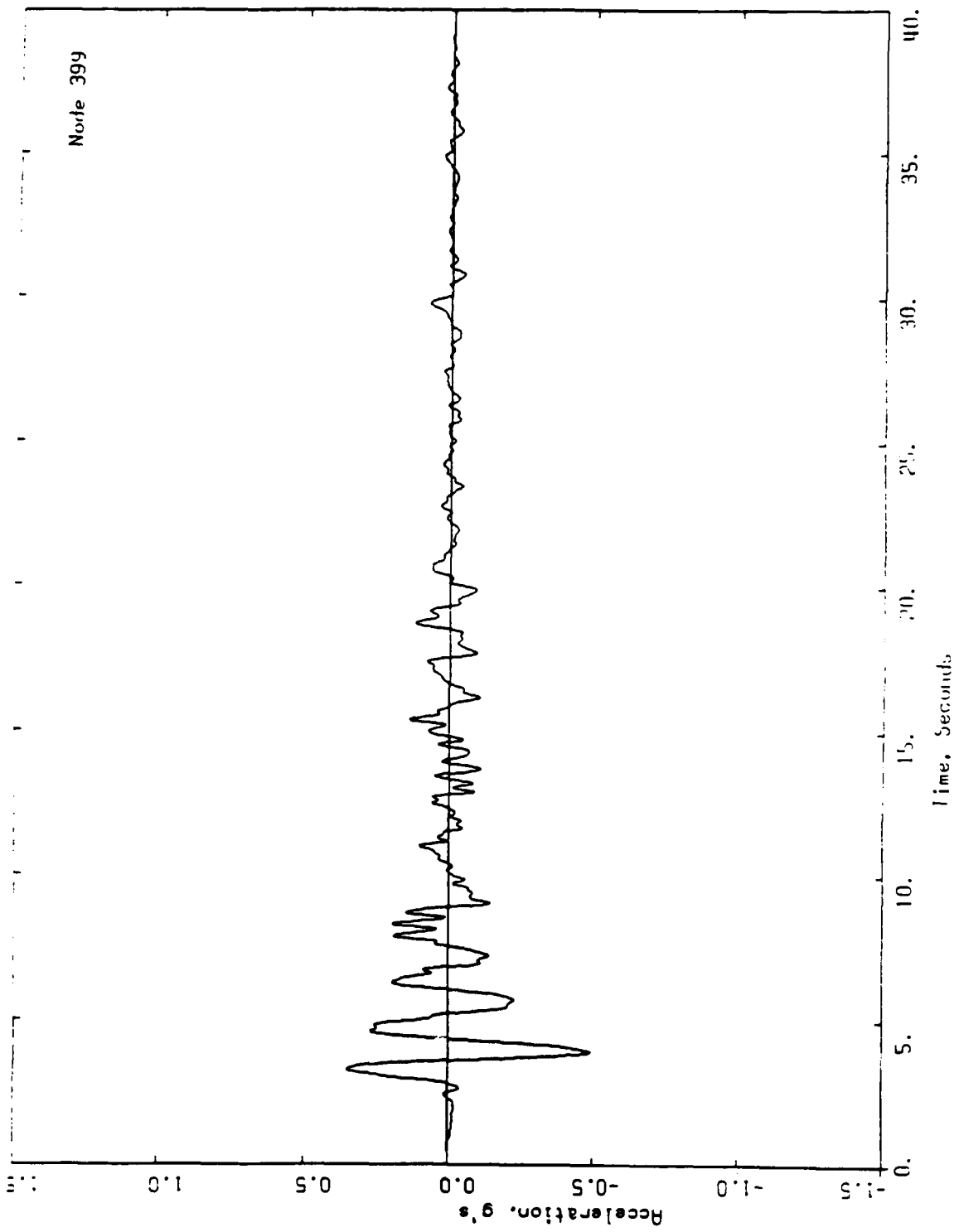


Figure A-9. Acceleration time history at nodal point 399

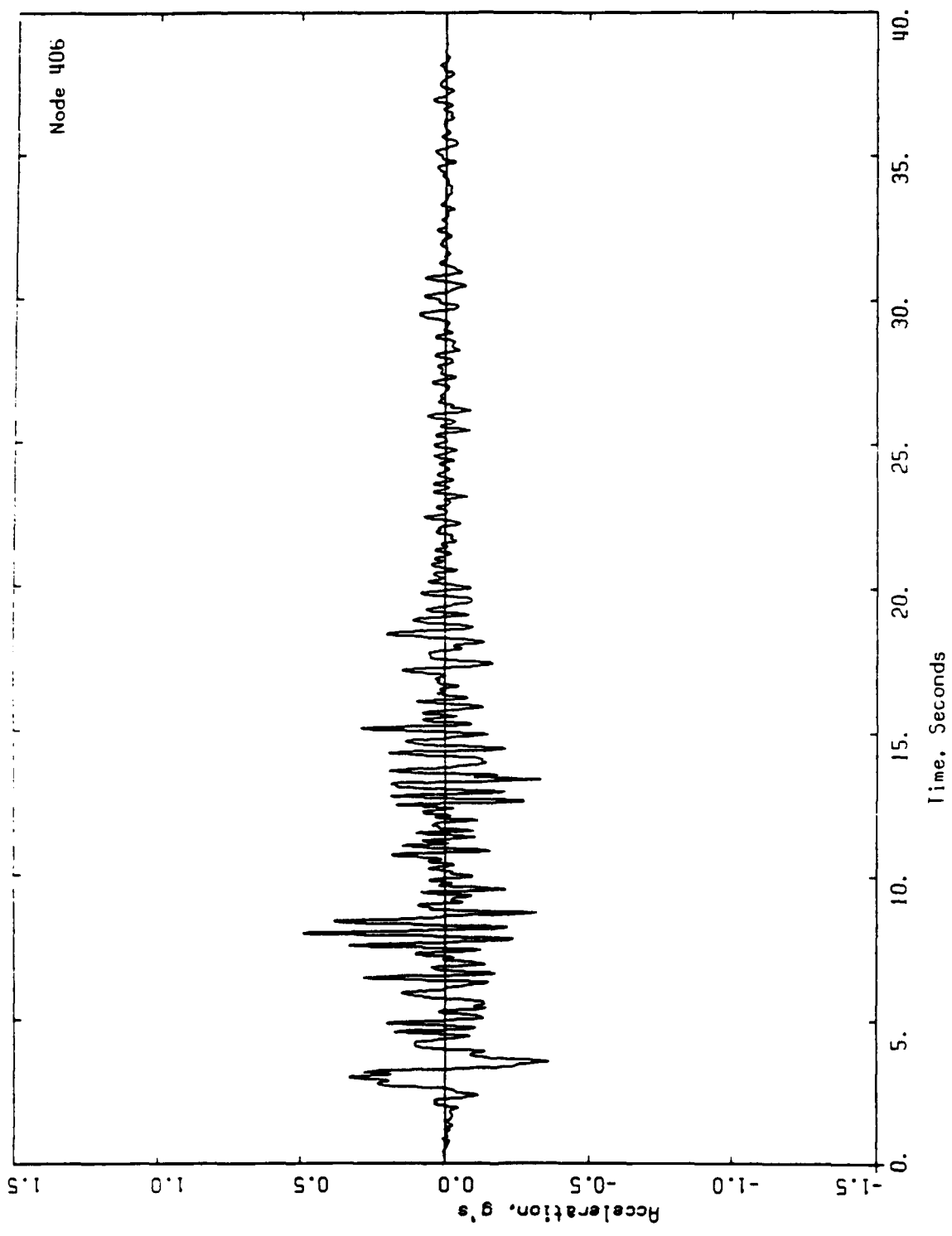


Figure A-10. Acceleration time history at nodal point 406

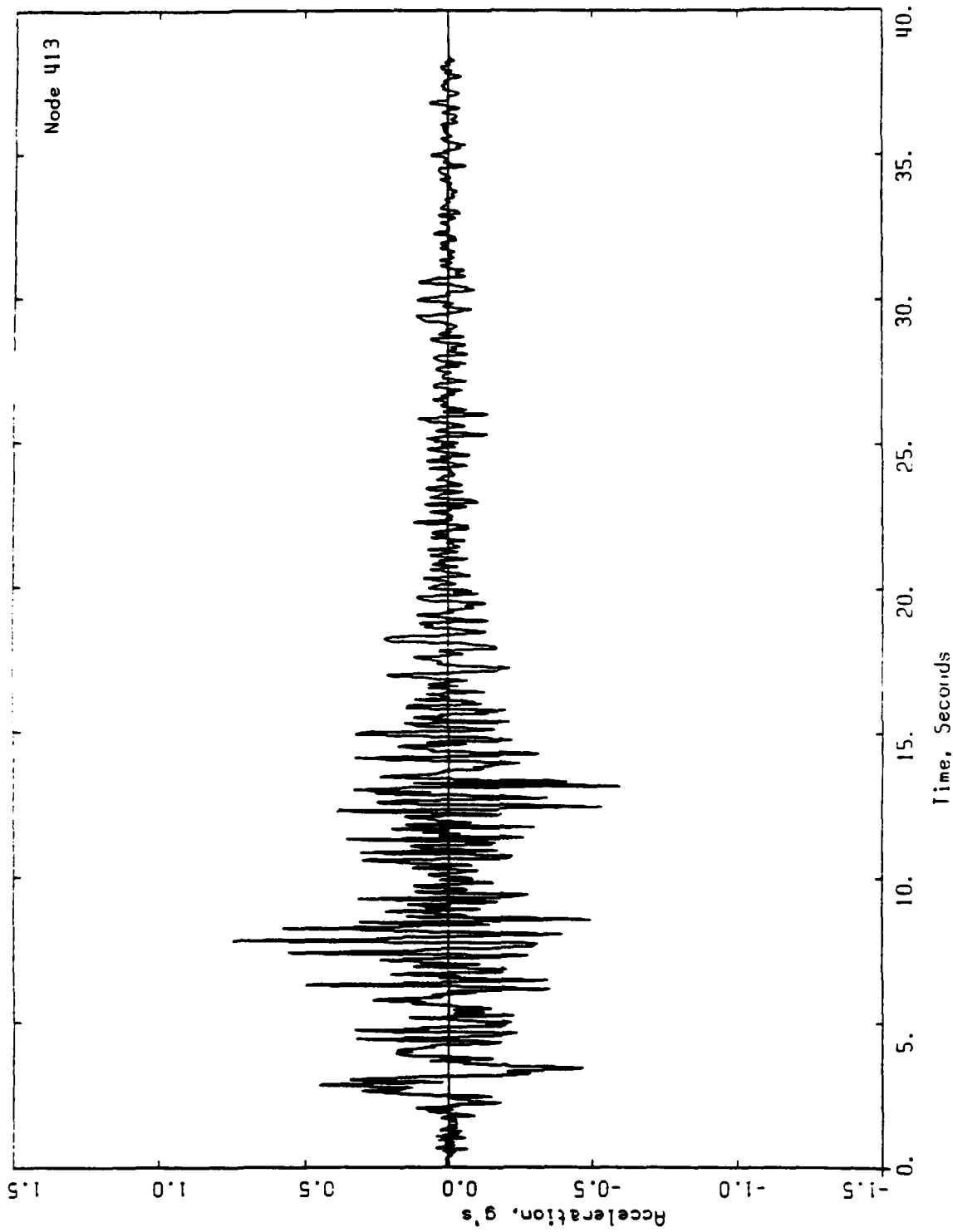


Figure A-11. Acceleration time history at nodal point 413

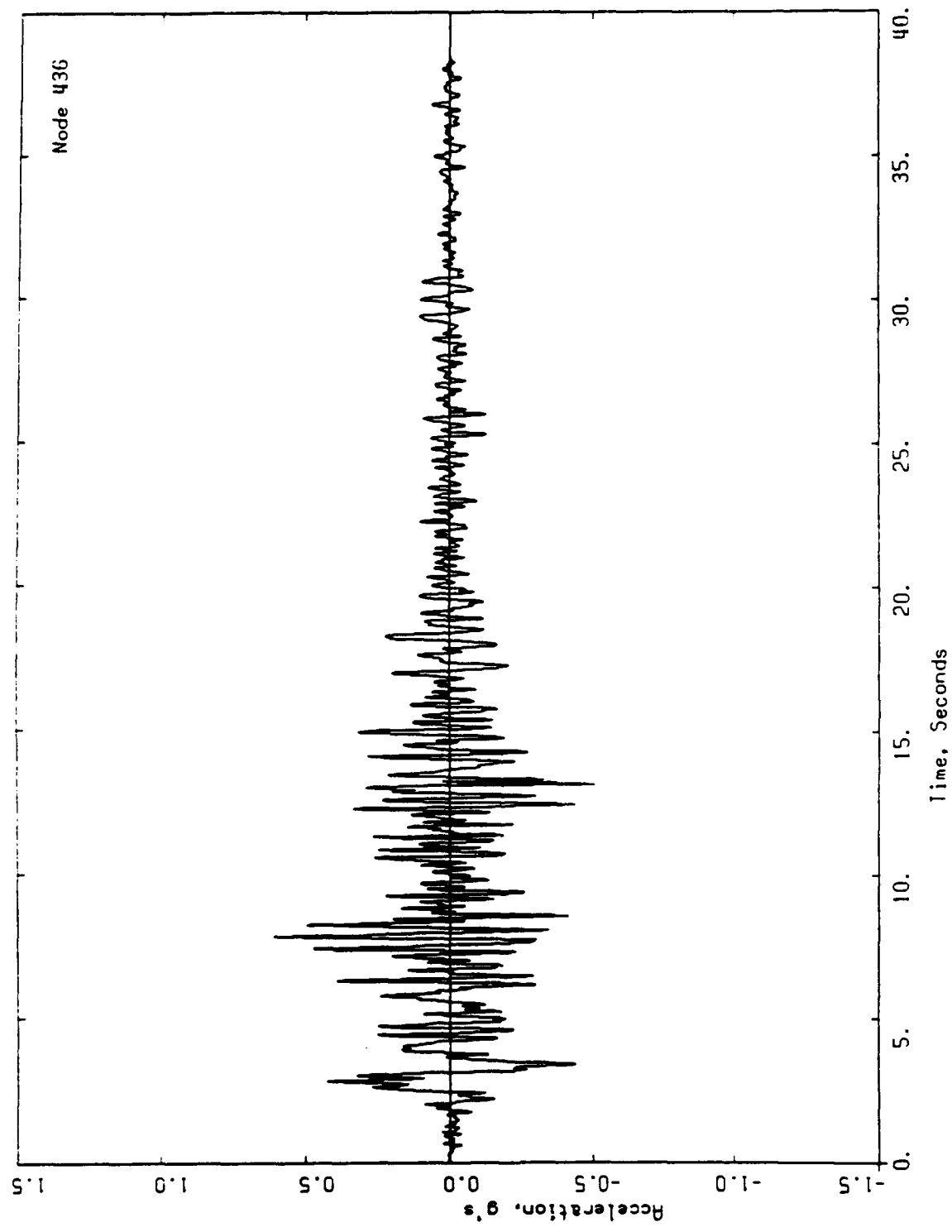


Figure A-12. Acceleration time history at nodal point 436

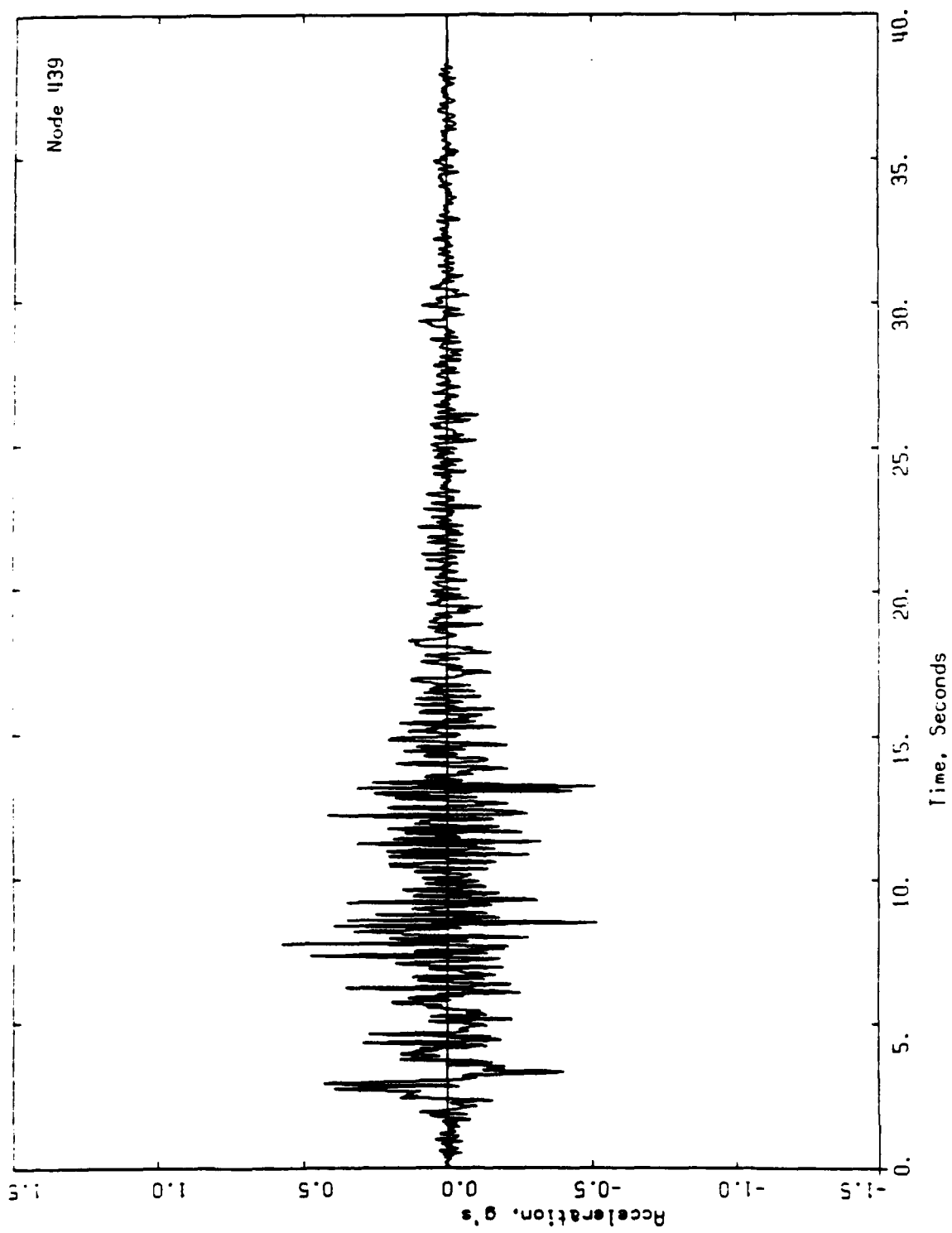


Figure A-13. Acceleration time history at nodal point 439

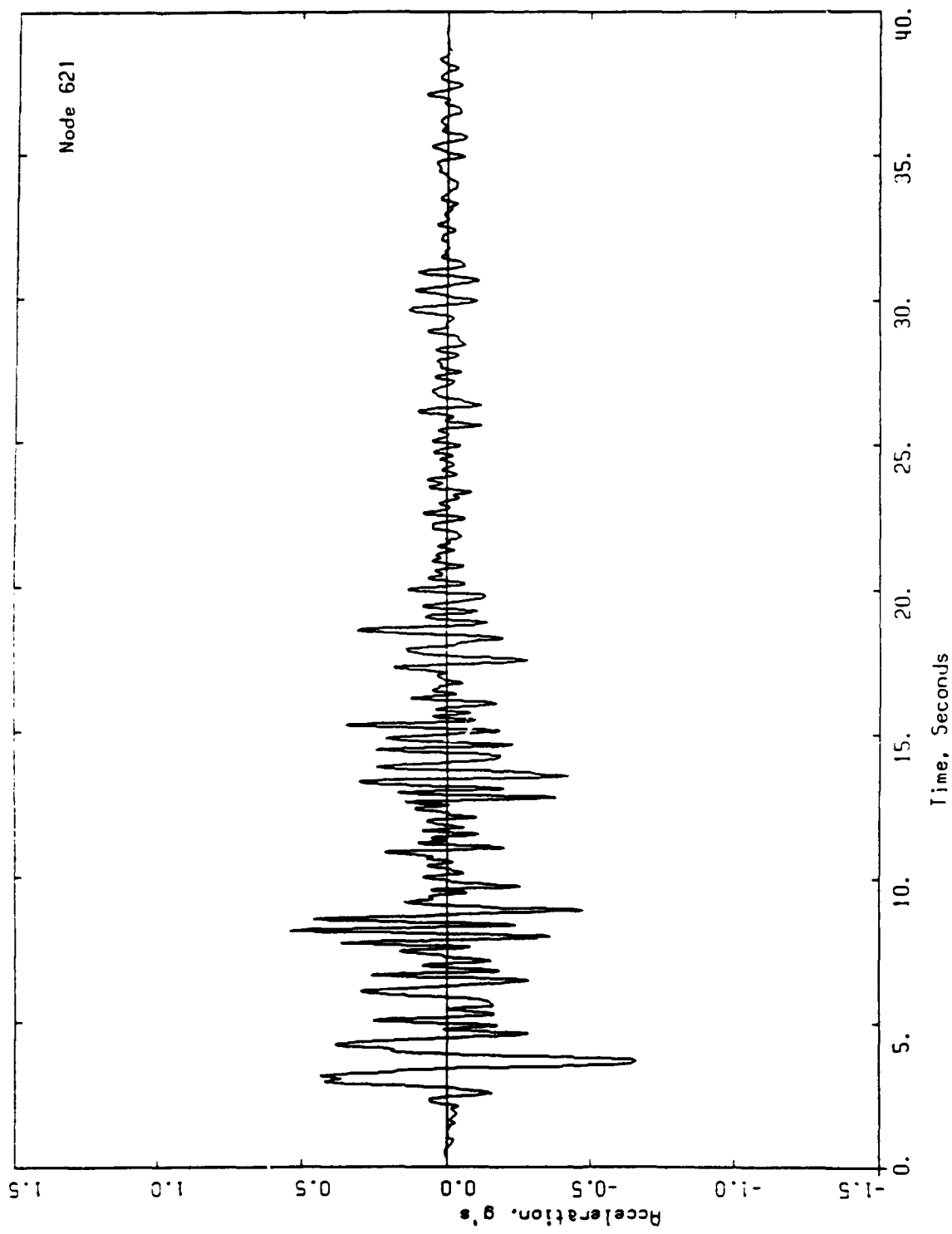


Figure A-14. Acceleration time history at nodal point 621

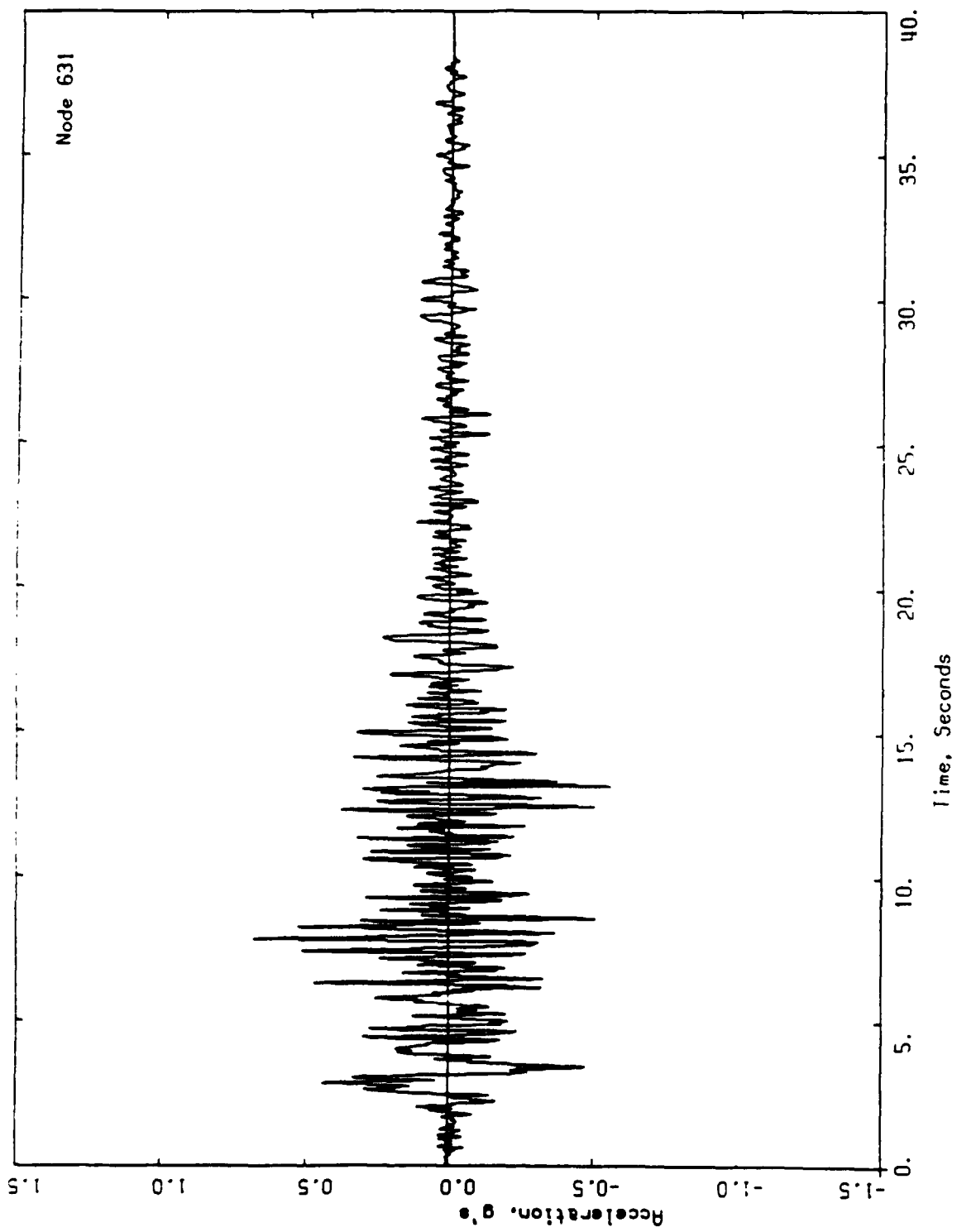


Figure A-15. Acceleration time history at nodal point 631

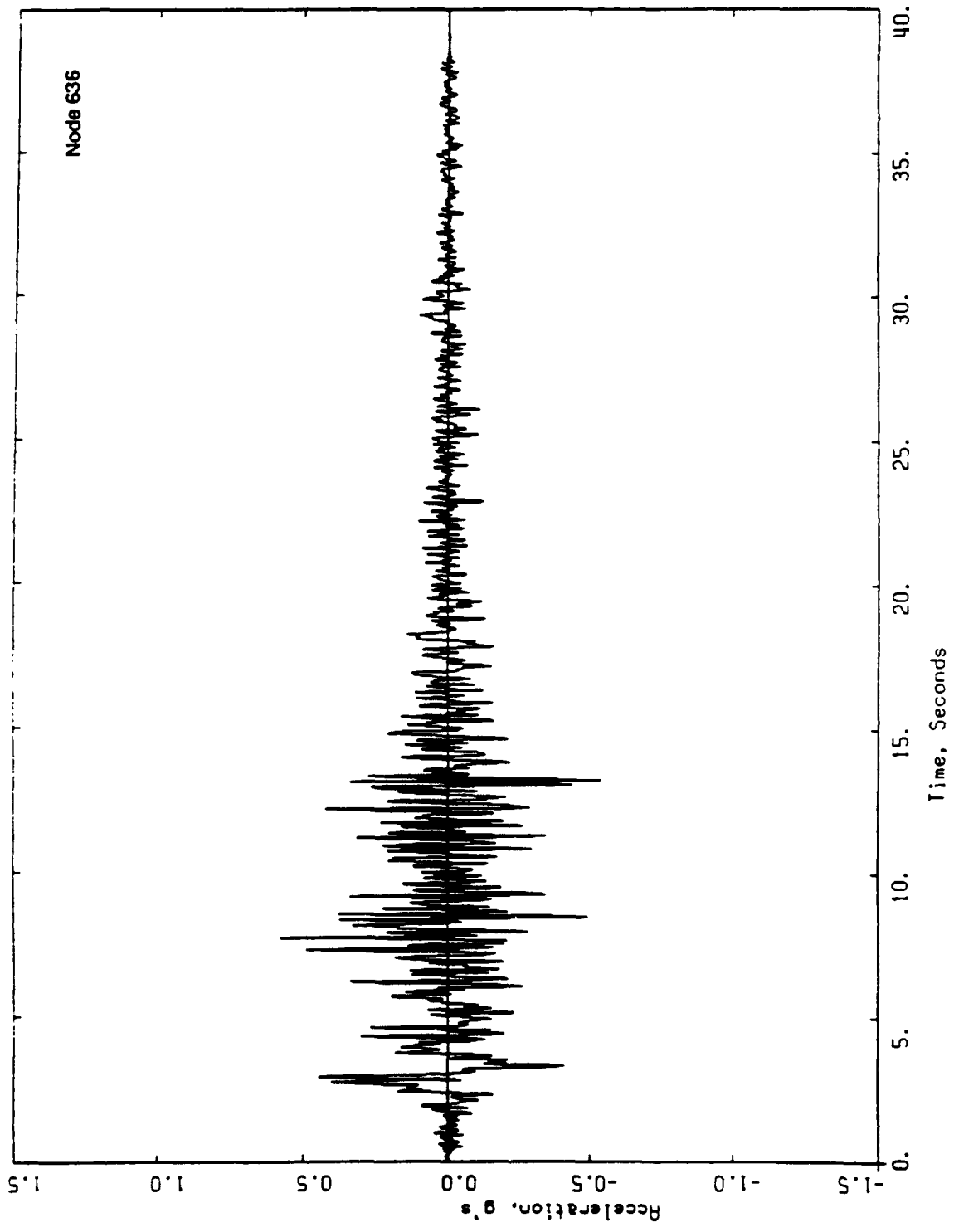


Figure A-16. Acceleration time history at nodal point 636

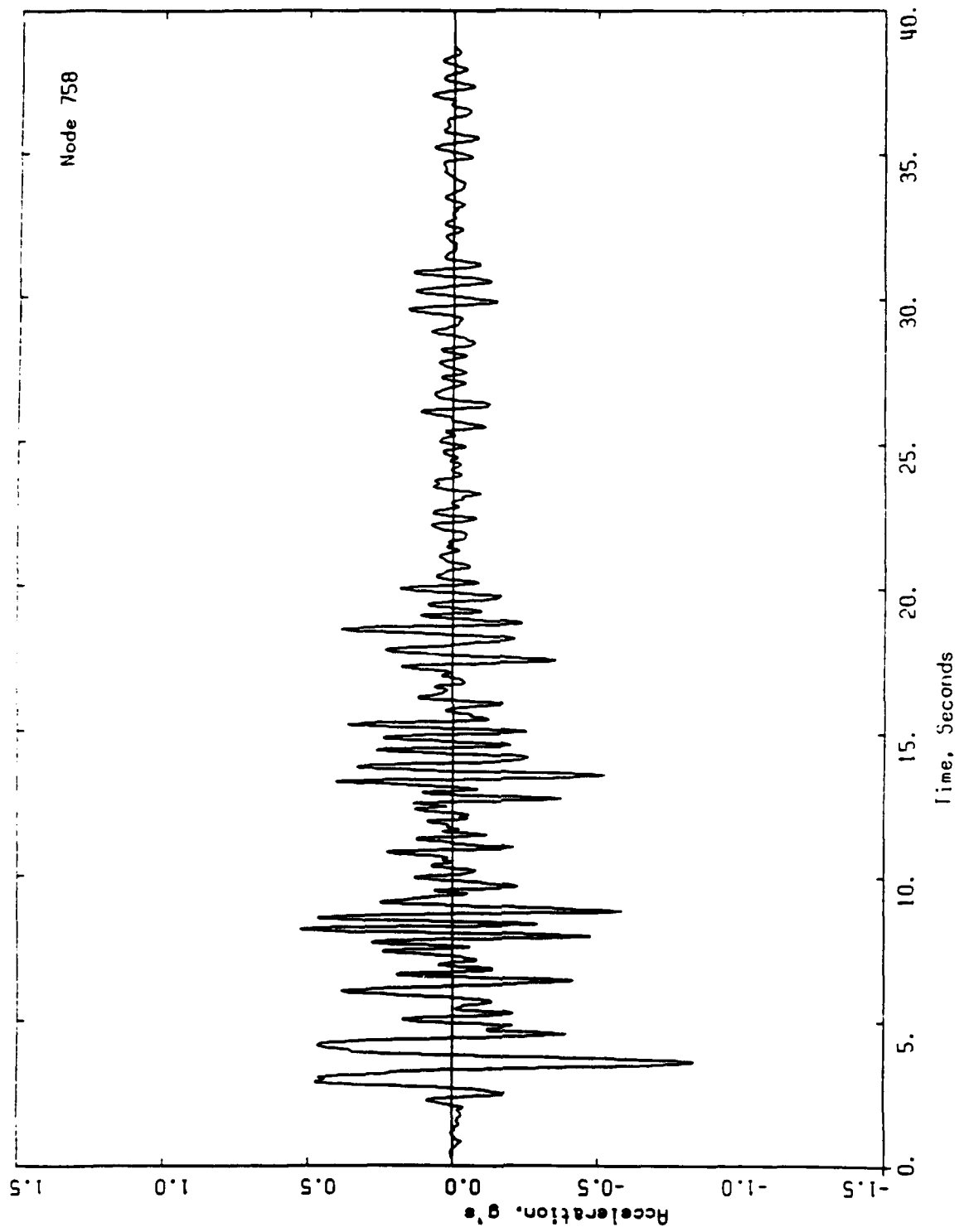


Figure A-17. Acceleration time history at nodal point 758

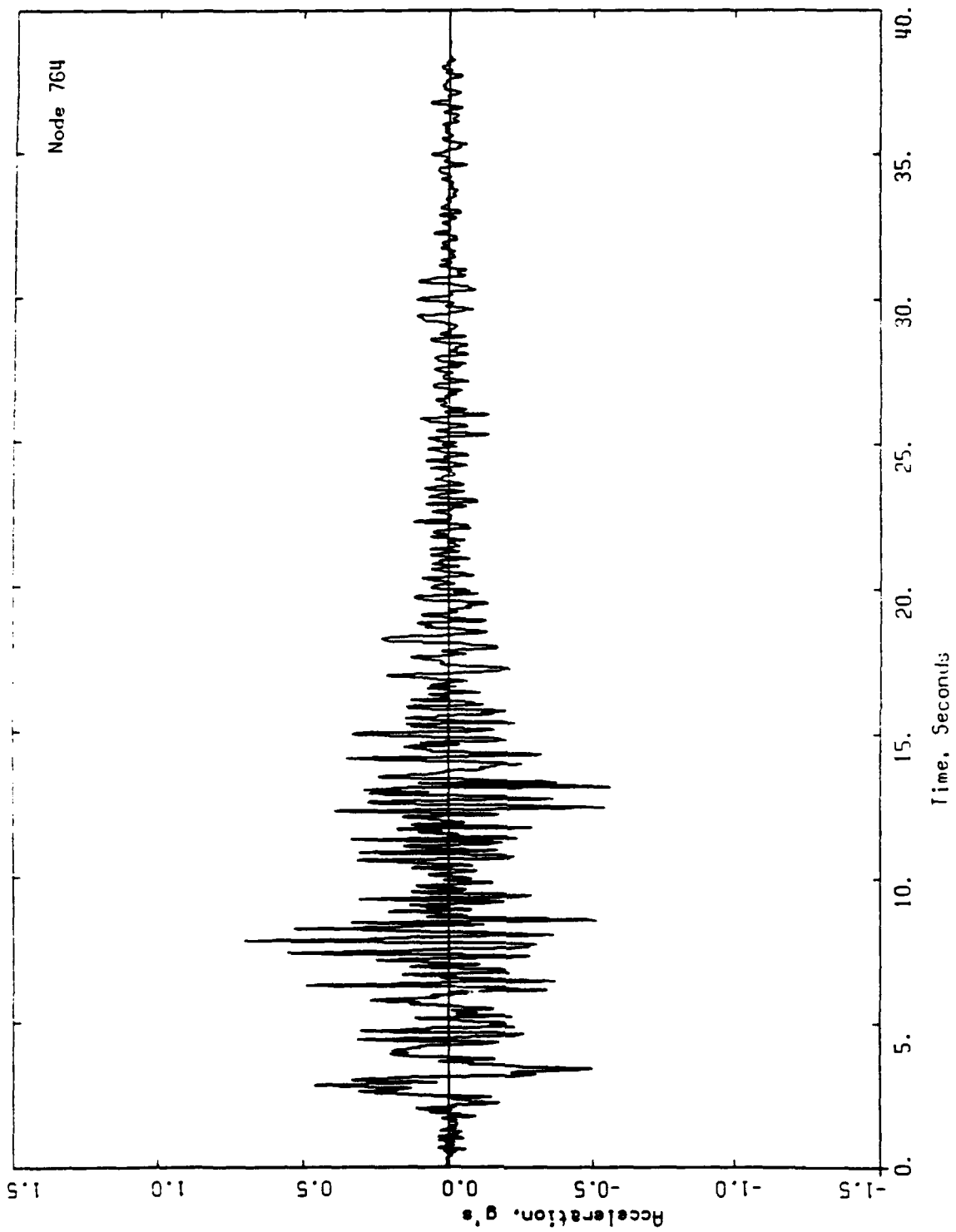


Figure A-18. Acceleration time history at nodal point 764

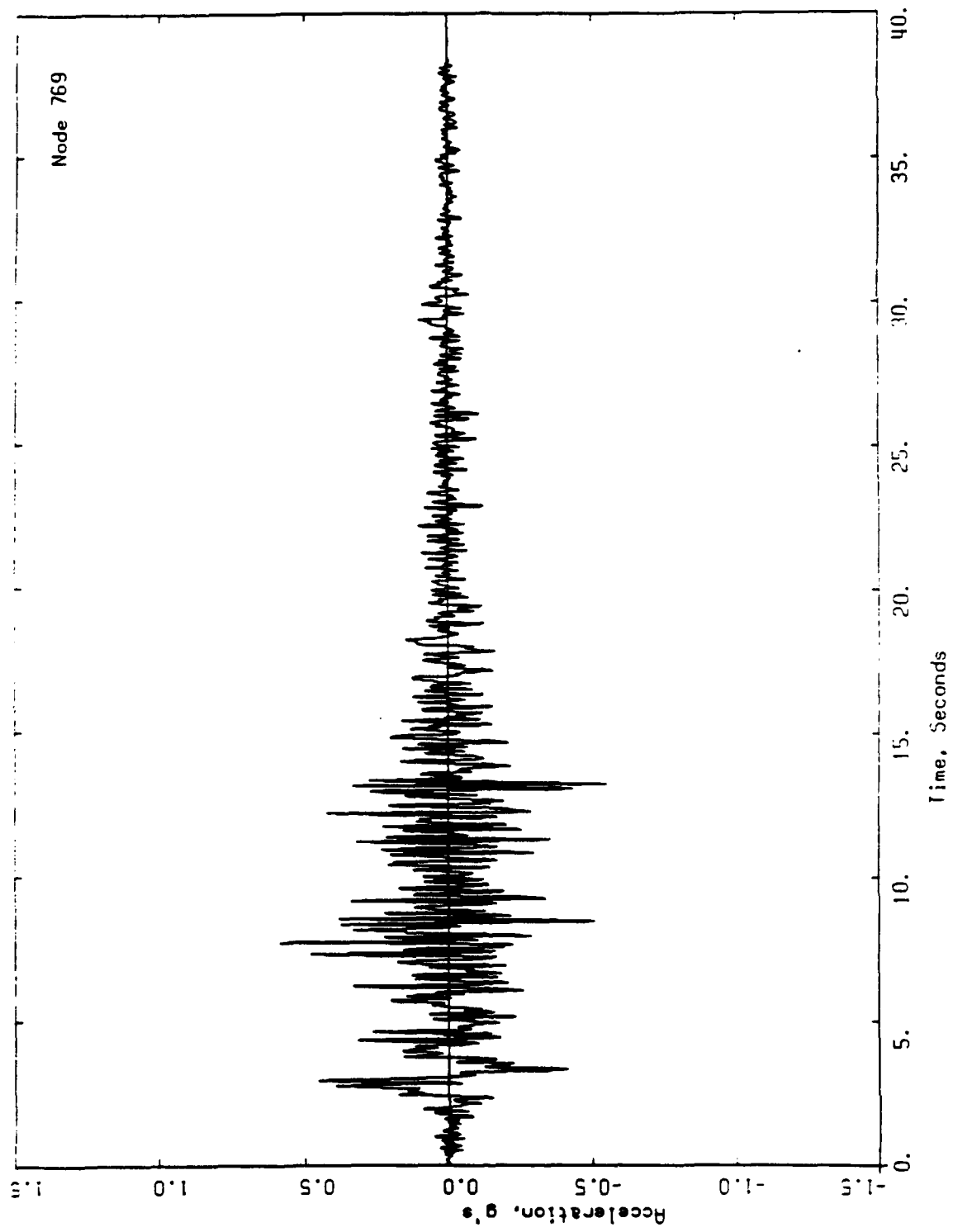


Figure A-19. Acceleration time history at nodal point 769

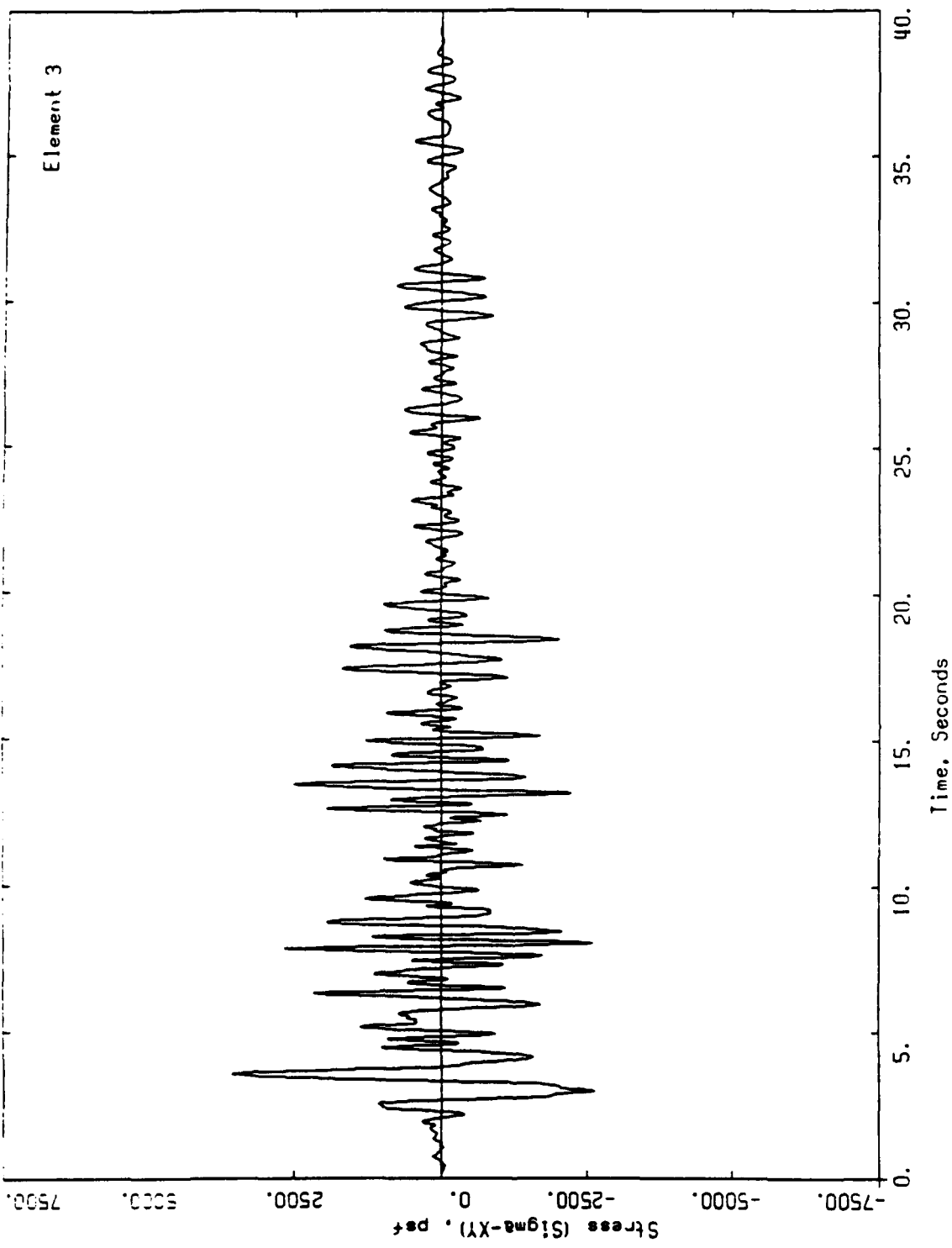


Figure A-20. Time history of horizontal shear stress in element 3

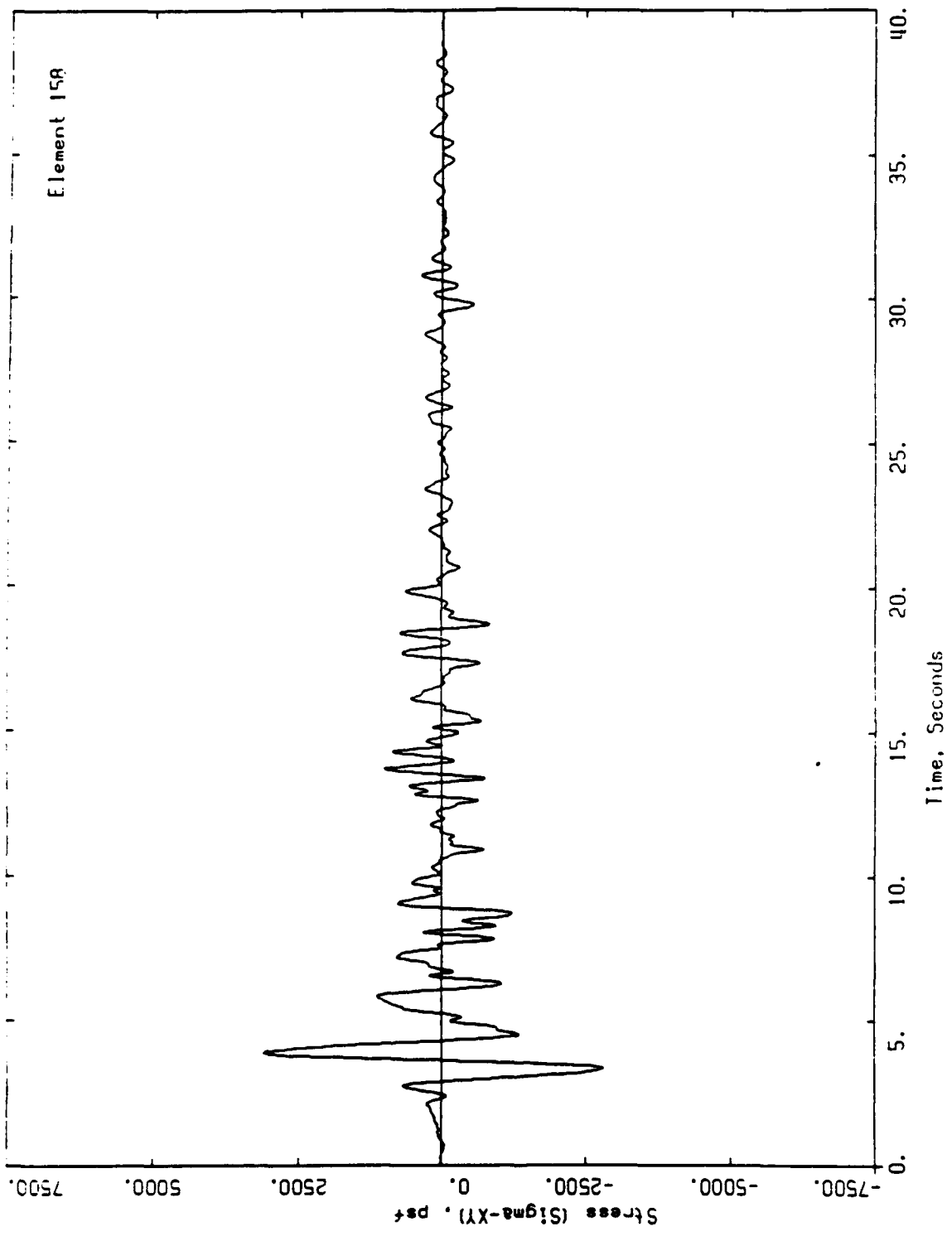


Figure A-21. Time history of horizontal shear stress in element 158

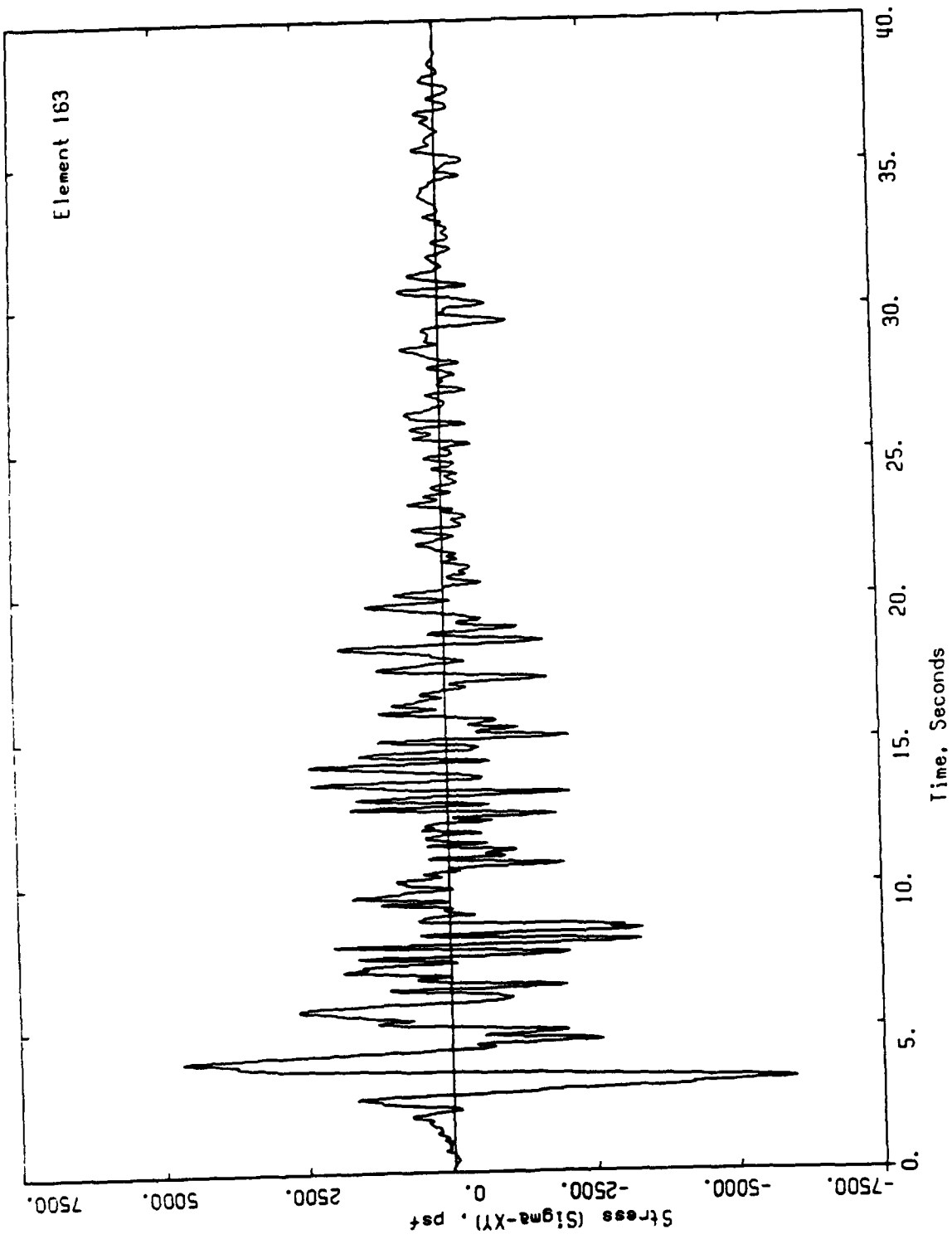


Figure A-22. Time history of horizontal shear stress in element 163

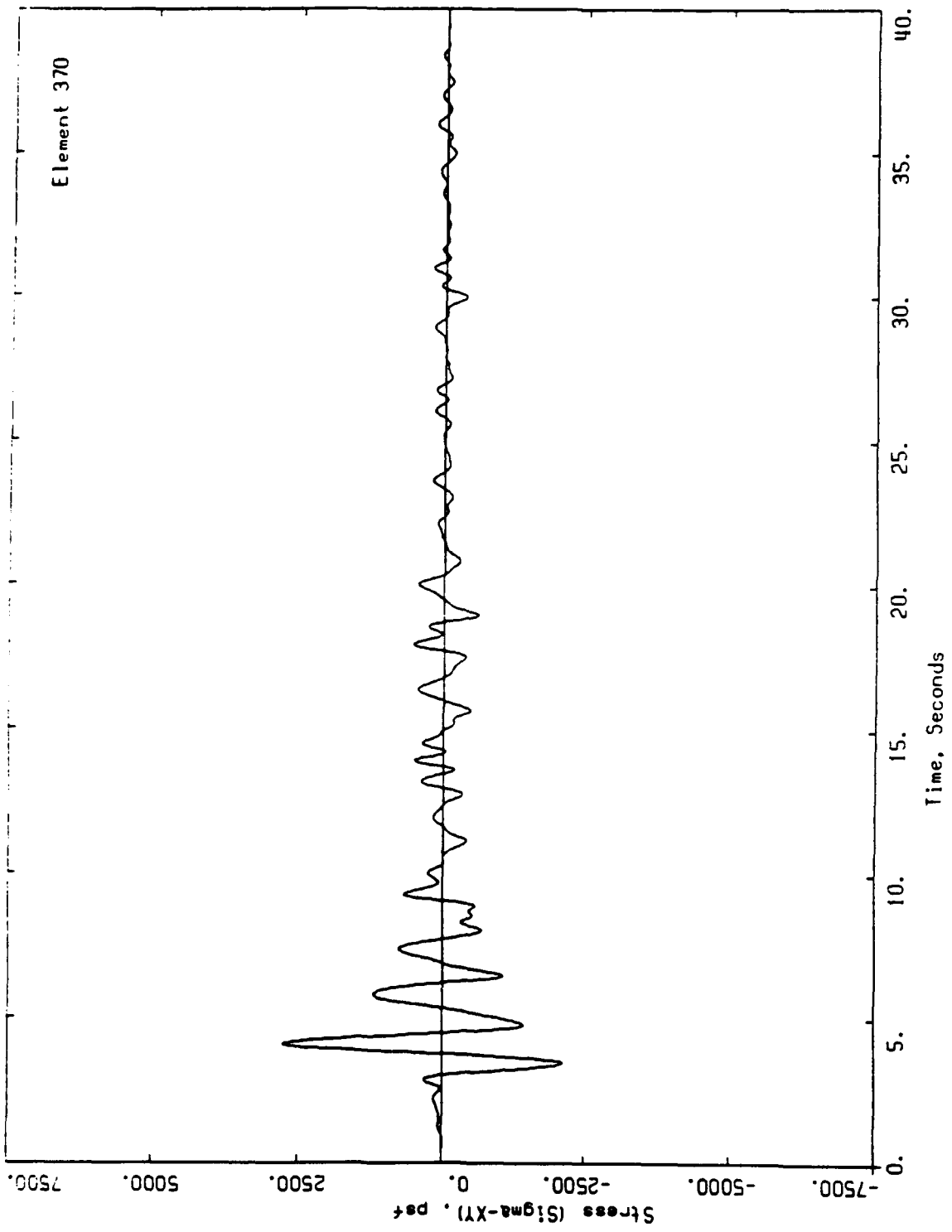


Figure A-23. Time history of horizontal shear stress in element 370

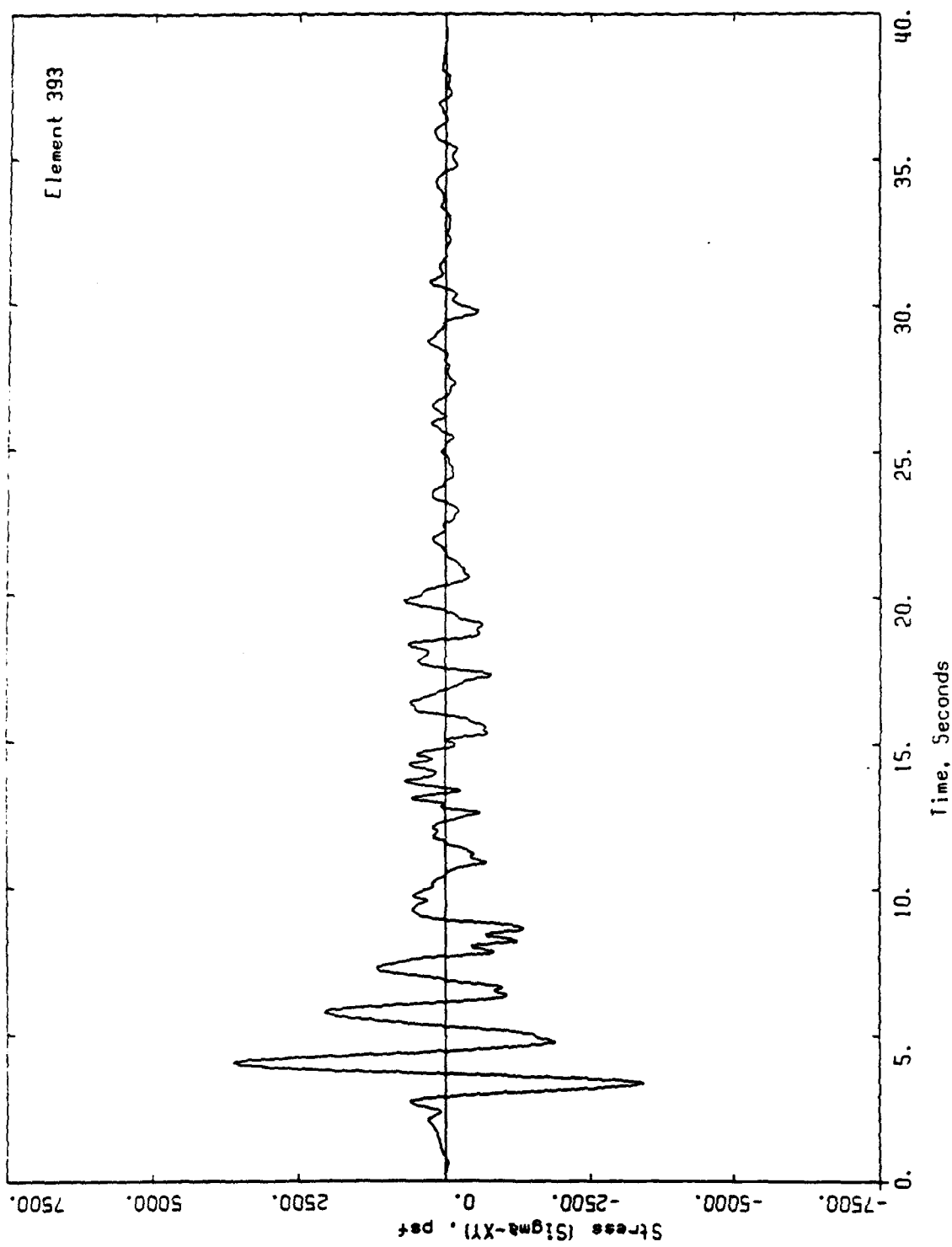


Figure A-24. Time history of horizontal shear stress in element 393

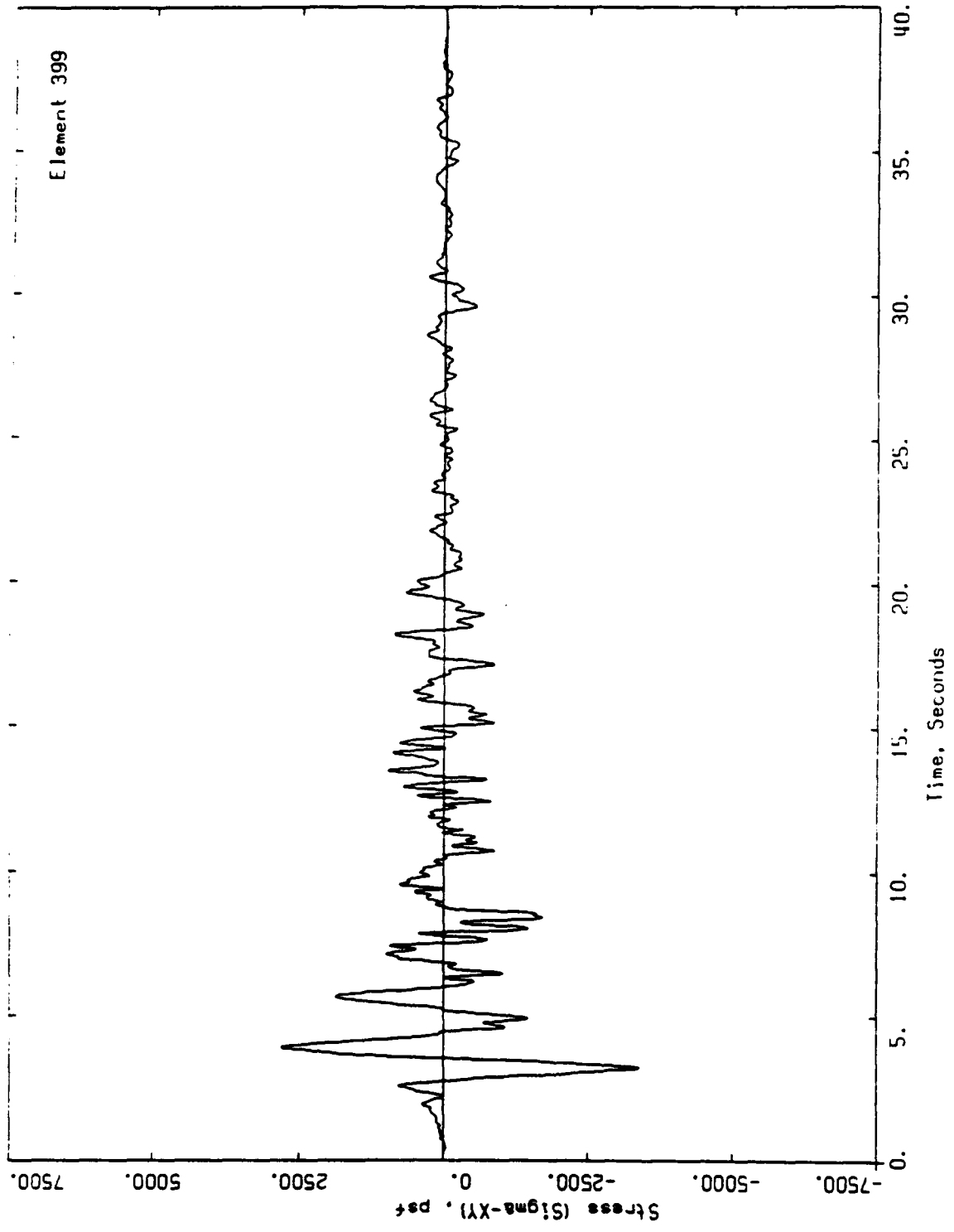


Figure A-25. Time history of horizontal shear stress in element 399

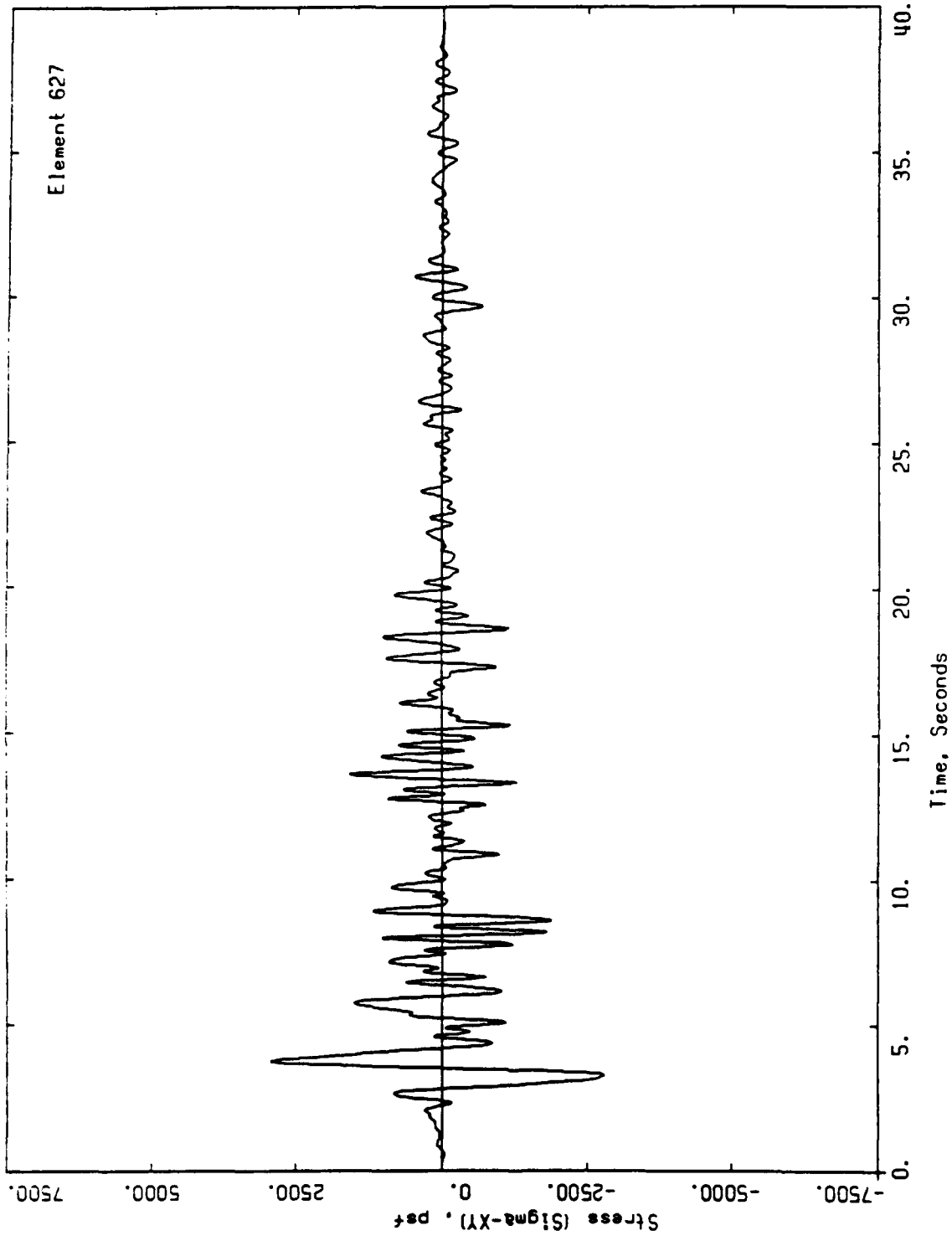


Figure A-26. Time history of horizontal shear stress in element 627

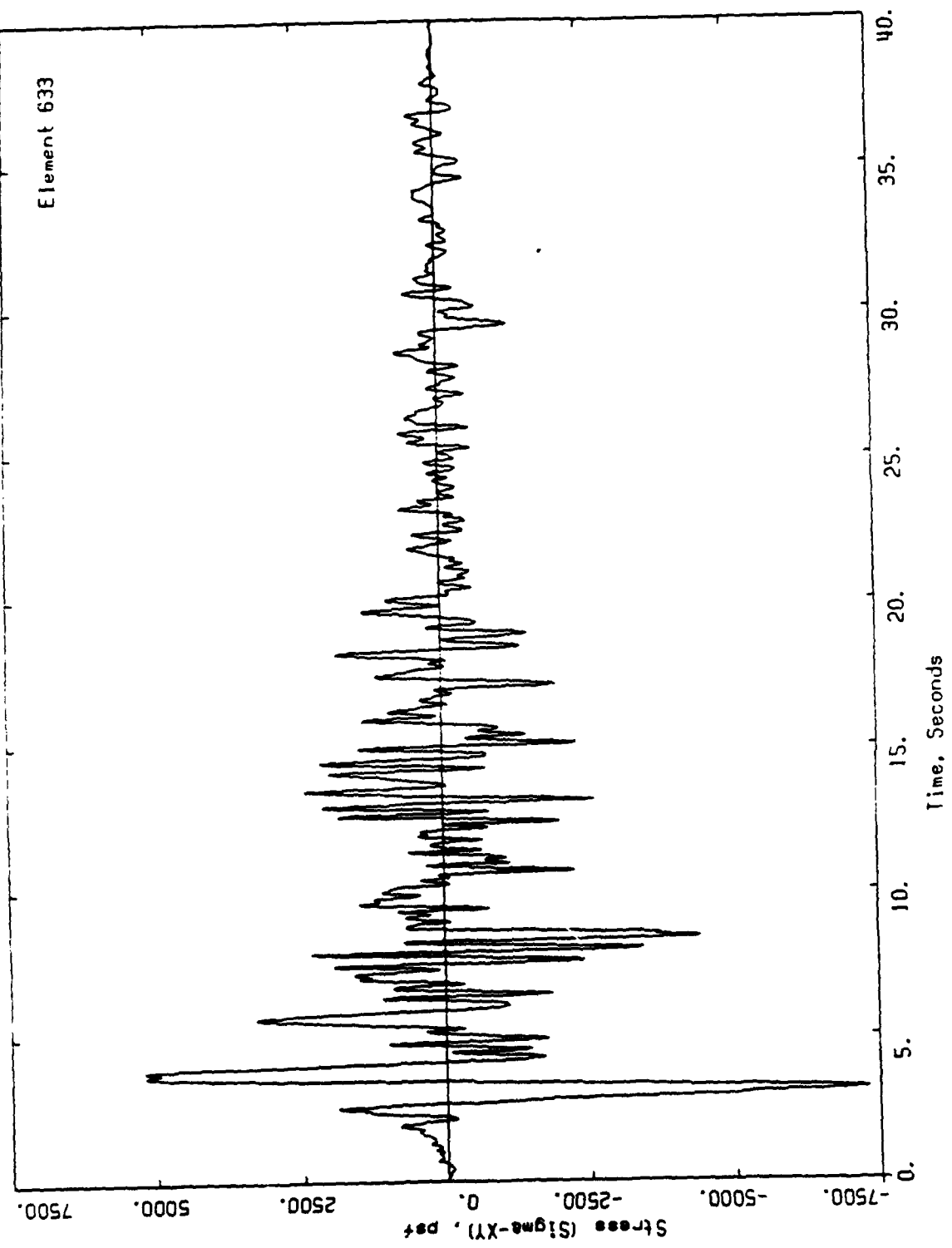


Figure A-27. Time history of horizontal shear stress in element 633

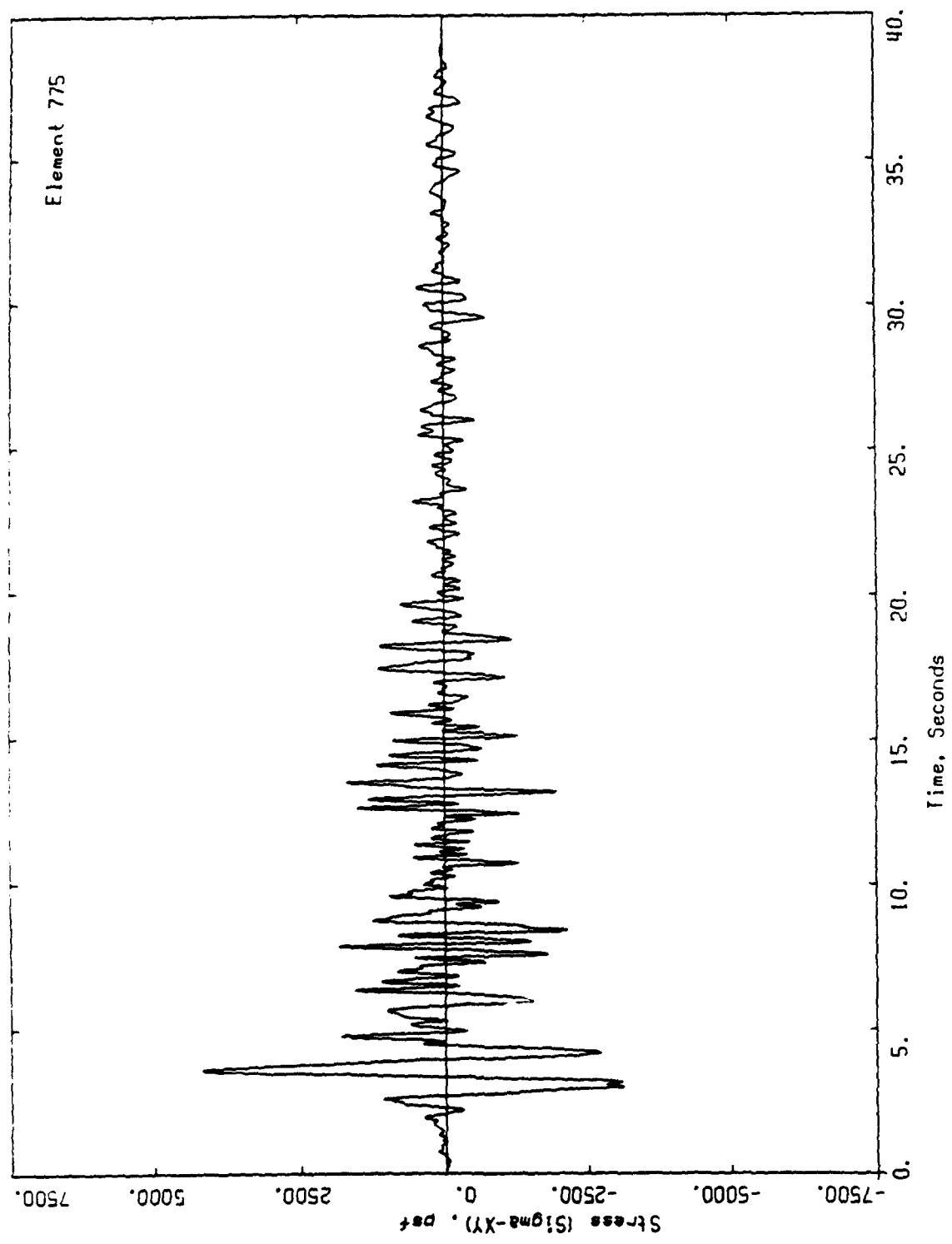
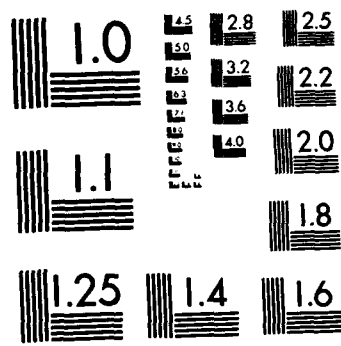


Figure A-28. Time history of horizontal shear stress in element 775

## **APPENDIX B**



MICROCOPY RESOLUTION TEST CHART  
NATIONAL BUREAU OF STANDARDS-1963-A

(1)

1	12	15	24	34	41	49	52	75
2	11	16	25	35	42	50	53	75
3	12	17	26	36	43	51	54	77
4	13	19	27	37	44	52	55	79
5	14	18	29	38	45	53	56	83
6	20		23		54		57	
7	21		30		55		58	
8	22		31		56		59	
9	23		32		57		60	

(2)

59	71	90	93	93	105	120	130	141	155	172	194	195	197	
59	72	91	92	91	105	122	132	143	158	173	197	201		
59	73	92	93	93	105	123	133	144	159	174	198	202		
51	74	93	94	94	110	124	134	145	159	175	199	203		
52	75	94	95	95	111	125	135	146	151	176	190	204		
53	75	95	95	95	112	125	135	147	152	178	192	205		
54	77	96	97	97	113	127	137	148	153	179	193	207		
55	78	97	98	98	114	128	138	149	154	180	194	208		
59	79	98	99	99	115	129	139	143	155	181	195	210		
59	80	99	99	99	115	129	139	150	182	196	197	198	211	
59	100				115			151		186	196		211	
59	101				117			152		187			212	
59	102				119			153		188			213	
70	103				119			154		189			214	

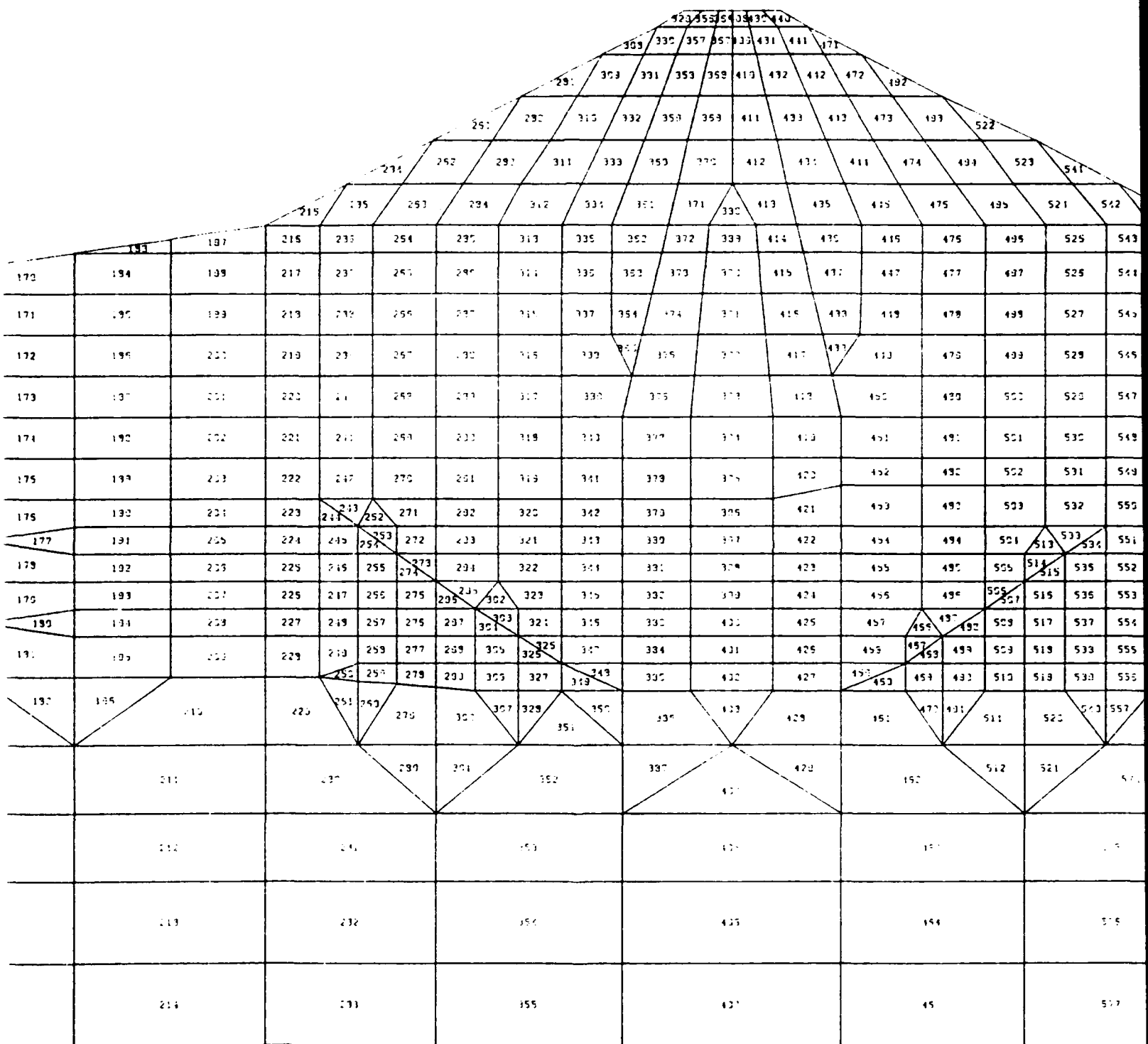


Figure B-1. Element numbering of dynamic finite element mesh for section AA

on AA



577	541	701	73	722					
578	542	702	75	723	735				
579	543	702	711	724	736	743	750	751	72
580	544	703	712	725	737	744	751	752	73
581	545	704	713	726	738	745	752	753	74
582	546	705	714	727	739	746	753	754	75
583	547	706	715	728	740	747	754	755	756
584	548	707	716	729	741	748	755	756	757
585	549	708	717	730	742	749	756	757	758
586	550	709	718	731	743	750	757	758	759
587		719		732		751	758	759	760
588		720		733		752	759	760	761
589		721		734		753	760	761	762

\*\*\*\*\*  
TABLE B-1  
SUMMARY OF SHEAR STRAIN AND STRESS  
SECTION AA'

\*\*\*\*\*

SOLID ELEMENTS

MAXIMUM SHEAR STRAIN COMPUTED FROM ITS TIME HISTORY

COMPARISON BETWEEN MAXIMUM SHEAR STRAINS

ELEM.	SIG-X LB/FT <sup>**2</sup>	SIG-Y LB/FT <sup>**2</sup>	SIG-XY LB/FT <sup>**2</sup>	EFF. SHEAR STRN PERCENT	TIME DOMAIN	FREQ DOMAIN
					MAX. SHEAR STRN PERCENT	MAX. SHEAR STRN PERCENT
1	.1109E+04	.3465E+02	.7817E+03	.8063E-01	.1240E+00	.2275E+00
2	.1011E+04	.1086E+03	.2287E+04	.2200E+00	.3385E+00	.5476E+00
3	.8467E+03	.1695E+03	.3546E+04	.3335E+00	.5131E+00	.7735E+00
4	.6229E+03	.2594E+03	.6846E+04	.4273E+00	.6574E+00	.9069E+00
5	.4184E+04	.2809E+03	.6269E+04	.4267E-01	.6564E-01	.8374E-01
6	.4323E+04	.4597E+03	.7823E+04	.5437E-01	.8365E-01	.1112E+00
7	.4773E+04	.8275E+03	.8904E+04	.6260E-01	.9631E-01	.1372E+00
8	.5576E+04	.1295E+04	.9704E+04	.6897E-01	.1061E+00	.1611E+00
9	.1006E+05	.2602E+04	.1012E+05	.7344E-01	.1130E+00	.1840E+00
10	.1555E+04	.6242E+02	.8390E+03	.7596E-01	.1169E+00	.2321E+00
11	.1384E+04	.1406E+03	.2316E+04	.2111E+00	.3248E+00	.5280E+00
12	.1159E+04	.2217E+03	.3551E+04	.3221E+00	.4955E+00	.7484E+00
13	.9232E+03	.2961E+03	.4756E+04	.4054E+00	.6236E+00	.8704E+00
14	.5694E+04	.1238E+04	.6098E+04	.4167E-01	.6611E-01	.8481E-01
15	.1939E+04	.4544E+02	.8568E+03	.9058E-01	.1394E+00	.2523E+00
16	.1944E+04	.2564E+03	.2450E+04	.2171E+00	.3339E+00	.5331E+00
17	.1591E+04	.3390E+03	.3663E+04	.3220E+00	.4953E+00	.7342E+00
18	.1130E+04	.5695E+03	.4763E+04	.3969E+00	.6106E+00	.8510E+00
19	.5600E+04	.1127E+04	.6465E+04	.4580E-01	.7045E-01	.9057E-01
20	.5547E+04	.1079E+04	.7559E+04	.5370E-01	.8261E-01	.1134E+00
21	.5515E+04	.1336E+04	.8723E+04	.6248E-01	.9612E-01	.1396E+00
22	.6185E+04	.1464E+04	.9881E+04	.7168E-01	.1103E+00	.1650E+00
23	.6164E+04	.2273E+04	.1146E+05	.8508E-01	.1309E+00	.1900E+00
24	.2551E+04	.1749E+03	.1113E+04	.1261E+00	.1941E+00	.3328E+00
25	.2535E+04	.5906E+03	.2740E+04	.2461E+00	.3786E+00	.5759E+00
26	.2098E+04	.8559E+03	.3849E+04	.3318E+00	.5104E+00	.7368E+00
27	.1496E+04	.1123E+04	.4825E+04	.3919E+00	.6030E+00	.8332E+00
28	.6823E+04	.1628E+04	.6599E+04	.4796E-01	.7378E-01	.9508E-01
29	.6186E+04	.2453E+04	.7818E+04	.5660E-01	.8707E-01	.1189E+00
30	.5820E+04	.2500E+04	.9073E+04	.6573E-01	.1011E+00	.1436E+00
31	.5354E+04	.2765E+04	.1033E+05	.7488E-01	.1152E+00	.1676E+00
32	.4762E+04	.3010E+04	.1172E+05	.8552E-01	.1316E+00	.1891E+00
33	.1123E+04	.4569E+03	.1164E+04	.5247E+00	.8073E+00	.1105E+01
34	.3970E+04	.1126E+04	.1980E+04	.2058E+00	.3167E+00	.4745E+00
35	.3184E+04	.1395E+04	.3218E+04	.2806E+00	.4317E+00	.6144E+00
36	.2586E+04	.1714E+04	.4131E+04	.3392E+00	.5218E+00	.7261E+00
37	.1988E+04	.2018E+04	.5018E+04	.3800E+00	.5847E+00	.7993E+00
38	.7806E+04	.2801E+04	.6430E+04	.4793E-01	.7374E-01	.9881E-01
39	.1744E+04	.6314E+03	.1259E+04	.7730E+00	.1189E+01	.1487E+01
40	.2718E+04	.1225E+04	.2169E+04	.6483E+00	.9973E+00	.1267E+01
41	.6145E+04	.1569E+04	.3076E+04	.2812E+00	.4326E+00	.5849E+00
42	.3477E+04	.2065E+04	.3772E+04	.3077E+00	.4734E+00	.6619E+00
43	.2889E+04	.2419E+04	.4530E+04	.3392E+00	.5219E+00	.7107E+00
44	.2442E+04	.2776E+04	.5261E+04	.3584E+00	.5515E+00	.7611E+00
45	.7727E+04	.2376E+04	.6513E+04	.4844E-01	.7452E-01	.9876E-01
46	.1959E+04	.8289E+03	.1239E+04	.8639E+00	.1329E+01	.1605E+01

47	.2837E+04	.1113E+04	.2322E+04	.8539E+00	.1314E+01	.1583E+01
48	.2677E+04	.1497E+04	.3343E+04	.8393E+00	.1291E+01	.1551E+01
49	.3930E+04	.1960E+04	.3790E+04	.3292E+00	.5064E+00	.6509E+00
50	.3395E+04	.2292E+04	.4347E+04	.3270E+00	.5031E+00	.6719E+00
51	.2908E+04	.2605E+04	.4912E+04	.3369E+00	.5183E+00	.7080E+00
52	.2552E+04	.2898E+04	.5477E+04	.3408E+00	.5243E+00	.7373E+00
53	.7617E+04	.3248E+04	.6612E+04	.4920E-01	.7569E-01	.1024E+00
54	.6662E+04	.2896E+04	.8033E+04	.5861E-01	.9016E-01	.1223E+00
55	.5817E+04	.3063E+04	.9353E+04	.6766E-01	.1041E+00	.1452E+00
56	.5128E+04	.3153E+04	.1054E+05	.7589E-01	.1167E+00	.1675E+00
57	.4284E+04	.3209E+04	.1165E+05	.8421E-01	.1296E+00	.1869E+00
58	.1477E+04	.5686E+03	.7898E+03	.4650E+00	.7154E+00	.9041E+00
59	.2018E+04	.5784E+03	.2097E+04	.7591E+00	.1168E+01	.1422E+01
60	.2366E+04	.9809E+03	.3293E+04	.9273E+00	.1427E+01	.1680E+01
61	.2127E+04	.1321E+04	.3887E+04	.9402E+00	.1446E+01	.1709E+01
62	.3383E+04	.1607E+04	.4349E+04	.3496E+00	.5378E+00	.6805E+00
63	.3074E+04	.1920E+04	.4709E+04	.3322E+00	.5111E+00	.6805E+00
64	.2742E+04	.2184E+04	.5188E+04	.3315E+00	.5099E+00	.6990E+00
65	.2403E+04	.2448E+04	.5660E+04	.3320E+00	.5108E+00	.7204E+00
66	.7314E+04	.2676E+04	.6804E+04	.5034E-01	.7745E-01	.1038E+00
67	.6525E+04	.2533E+04	.8100E+04	.5858E-01	.9013E-01	.1228E+00
68	.5854E+04	.2682E+04	.9451E+04	.6780E-01	.1043E+00	.1450E+00
69	.5168E+04	.2891E+04	.1058E+05	.7573E-01	.1165E+00	.1665E+00
70	.4480E+04	.3073E+04	.1157E+05	.8313E-01	.1279E+00	.1849E+00
71	.1074E+04	.1551E+03	.1040E+04	.3679E+00	.5660E+00	.7541E+00
72	.1701E+04	.3659E+03	.2549E+04	.7187E+00	.1106E+01	.1350E+01
73	.1664E+04	.5320E+03	.3542E+04	.9797E+00	.1507E+01	.1758E+01
74	.1568E+04	.7865E+03	.4334E+04	.1003E+01	.1544E+01	.1812E+01
75	.2879E+04	.9763E+03	.4615E+04	.3585E+00	.5516E+00	.6942E+00
76	.2761E+04	.1189E+04	.4917E+04	.3324E+00	.5114E+00	.6820E+00
77	.2540E+04	.1481E+04	.5321E+04	.3260E+00	.5016E+00	.6939E+00
78	.2090E+04	.1752E+04	.5872E+04	.3354E+00	.5160E+00	.7144E+00
79	.7987E+04	.1980E+04	.6700E+04	.4936E-01	.7593E-01	.1043E+00
80	.1412E+04	.9559E+02	.1045E+04	.3498E+00	.5381E+00	.7750E+00
81	.1555E+04	.2392E+03	.2640E+04	.7252E+00	.1116E+01	.1361E+01
82	.1366E+04	.3755E+03	.3905E+04	.1020E+01	.1569E+01	.1818E+01
83	.1165E+04	.4038E+03	.4366E+04	.1035E+01	.1592E+01	.1862E+01
84	.2648E+04	.5611E+03	.4745E+04	.3657E+00	.5625E+00	.7078E+00
85	.2639E+04	.7947E+03	.5043E+04	.3331E+00	.5125E+00	.6897E+00
86	.2322E+04	.9756E+03	.5447E+04	.3307E+00	.5088E+00	.6998E+00
87	.1848E+04	.1208E+04	.6043E+04	.3422E+00	.5265E+00	.7167E+00
88	.7667E+04	.1529E+04	.6944E+04	.5033E-01	.7743E-01	.1057E+00
89	.1857E+04	.2176E+03	.8653E+03	.3648E+00	.5612E+00	.8700E+00
90	.1779E+04	.2681E+03	.1194E+04	.3234E+00	.4975E+00	.7521E+00
91	.2247E+04	.7055E+03	.2202E+04	.7530E+00	.1158E+01	.1481E+01
92	.1766E+04	.2103E+03	.2869E+04	.7066E+00	.1087E+01	.1330E+01
93	.1323E+04	.2091E+03	.3854E+04	.1047E+01	.1611E+01	.1872E+01
94	.1160E+04	.2675E+03	.4505E+04	.9814E+00	.1510E+01	.1782E+01
95	.2656E+04	.4590E+03	.4899E+04	.3527E+00	.5425E+00	.6911E+00
96	.2440E+04	.5396E+03	.5090E+04	.3271E+00	.5032E+00	.6781E+00
97	.2125E+04	.6731E+03	.5573E+04	.3351E+00	.5155E+00	.6950E+00
98	.1641E+04	.8359E+03	.6152E+04	.3469E+00	.5337E+00	.7152E+00
99	.7256E+04	.1476E+04	.6770E+04	.4825E-01	.7423E-01	.1036E+00
100	.6469E+04	.1789E+04	.7964E+04	.5684E-01	.8745E-01	.1229E+00
101	.5841E+04	.2110E+04	.9313E+04	.6614E-01	.1017E+00	.1447E+00
102	.5249E+04	.2431E+04	.1045E+05	.7432E-01	.1143E+00	.1658E+00
103	.4835E+04	.2784E+04	.1150E+05	.8221E-01	.1265E+00	.1837E+00
104	.9621E+03	.2381E+03	.2267E+03	.4040E+00	.6215E+00	.8080E+00
105	.2191E+04	.2981E+03	.1111E+04	.3929E+00	.6045E+00	.9695E+00
106	.1861E+04	.3573E+03	.2690E+04	.8135E+00	.1252E+01	.1566E+01
107	.1738E+04	.7369E+03	.3375E+04	.1086E+01	.1671E+01	.1987E+01
108	.1266E+04	.2923E+03	.4357E+04	.1075E+01	.1655E+01	.1922E+01
109	.2204E+04	.1269E+04	.3838E+04	.9399E+00	.1446E+01	.1795E+01
110	.1356E+04	.2657E+03	.4923E+04	.9179E+00	.1412E+01	.1702E+01
111	.2775E+04	.3541E+03	.4660E+04	.3297E+00	.5073E+00	.6647E+00
112	.2518E+04	.5250E+03	.5153E+04	.3272E+00	.5033E+00	.6673E+00

113	.2135E+04	.6682E+03	.5672E+04	.3387E+00	.5210E+00	.6900E+00
114	.1660E+04	.8500E+03	.6269E+04	.3529E+00	.5430E+00	.7166E+00
115	.6688E+04	.9778E+03	.6592E+04	.4639E-01	.7168E-01	.1042E+00
116	.6375E+04	.1702E+04	.7664E+04	.5281E-01	.8125E-01	.1229E+00
117	.5773E+04	.1933E+04	.8904E+04	.6244E-01	.9606E-01	.1443E+00
118	.5601E+04	.2239E+04	.1011E+05	.7127E-01	.1096E+00	.1648E+00
119	.5203E+04	.2523E+04	.1134E+05	.8059E-01	.1240E+00	.1828E+00
120	.1338E+04	.1879E+03	.4800E+03	.3905E+00	.6008E+00	.8811E+00
121	.2169E+04	.3441E+03	.1557E+04	.4911E+00	.7555E+00	.1137E+01
122	.1820E+04	.5911E+03	.2708E+04	.8842E+00	.1360E+01	.1699E+01
123	.1644E+04	.7093E+03	.3532E+04	.1043E+01	.1605E+01	.1956E+01
124	.1405E+04	.6812E+03	.3850E+04	.9564E+00	.1471E+01	.1864E+01
125	.3341E+04	.7506E+03	.4481E+04	.2985E+00	.4593E+00	.6273E+00
126	.2832E+04	.8424E+03	.5227E+04	.3248E+00	.4997E+00	.6563E+00
127	.2360E+04	.9457E+03	.5777E+04	.3374E+00	.5191E+00	.6801E+00
128	.1772E+04	.1090E+04	.6334E+04	.3516E+00	.5609E+00	.7083E+00
129	.7261E+04	.2004E+04	.6336E+04	.4451E-01	.6648E-01	.1020E+00
130	.1620E+04	.2485E+03	.6963E+03	.3758E+00	.5781E+00	.9378E+00
131	.2202E+04	.4797E+03	.1835E+04	.5625E+00	.8654E+00	.1266E+01
132	.1894E+04	.7057E+03	.2846E+04	.8786E+00	.1352E+01	.1712E+01
133	.1719E+04	.8288E+03	.3526E+04	.9704E+00	.1493E+01	.1867E+01
134	.1483E+04	.9650E+03	.3976E+04	.9409E+00	.1448E+01	.1895E+01
135	.3518E+04	.1091E+04	.4533E+04	.2741E+00	.4217E+00	.5758E+00
136	.3020E+04	.1125E+04	.5228E+04	.3116E+00	.4794E+00	.6289E+00
137	.2527E+04	.1184E+04	.5817E+04	.3289E+00	.5059E+00	.6616E+00
138	.1904E+04	.1309E+04	.6418E+04	.3442E+00	.5296E+00	.6930E+00
139	.6639E+04	.1140E+04	.6471E+04	.4295E-01	.6608E-01	.1024E+00
140	.7136E+03	.1109E+03	.1962E+03	.3983E+00	.6128E+00	.8875E+00
141	.2105E+04	.3049E+03	.9888E+03	.3851E+00	.5924E+00	.1008E+01
142	.2318E+04	.5892E+03	.2111E+04	.6253E+00	.9619E+00	.1376E+01
143	.2122E+04	.8113E+03	.3017E+04	.8506E+00	.1309E+01	.1693E+01
144	.1962E+04	.9753E+03	.3600E+04	.9012E+00	.1387E+01	.1807E+01
145	.1586E+04	.1078E+04	.4093E+04	.9552E+00	.1470E+01	.1904E+01
146	.3717E+04	.1128E+04	.4595E+04	.2682E+00	.4126E+00	.5634E+00
147	.3158E+04	.1198E+04	.5317E+04	.3048E+00	.4690E+00	.6152E+00
148	.2648E+04	.1284E+04	.5888E+04	.3238E+00	.4982E+00	.6508E+00
149	.1985E+04	.1420E+04	.6458E+04	.3377E+00	.5195E+00	.6810E+00
150	.6282E+04	.2131E+04	.6599E+04	.4354E-01	.6699E-01	.1012E+00
151	.5550E+04	.1895E+04	.7841E+04	.5272E-01	.8111E-01	.1215E+00
152	.5294E+04	.2295E+04	.8950E+04	.6115E-01	.9407E-01	.1429E+00
153	.5012E+04	.2459E+04	.9822E+04	.6855E-01	.1055E+00	.1633E+00
154	.5109E+04	.2719E+04	.1123E+05	.7940E-01	.1221E+00	.1820E+00
155	.1250E+04	.1736E+03	.3871E+03	.4203E+00	.6466E+00	.9709E+00
156	.2550E+04	.3943E+03	.1349E+04	.4142E+00	.6372E+00	.1123E+01
157	.2548E+04	.6737E+03	.2282E+04	.6520E+00	.1003E+01	.1460E+01
158	.2451E+04	.8678E+03	.3106E+04	.8000E+00	.1231E+01	.1662E+01
159	.2237E+04	.1005E+04	.3661E+04	.8340E+00	.1283E+01	.1763E+01
160	.1736E+04	.1103E+04	.4248E+04	.9519E+00	.1466E+01	.1899E+01
161	.3850E+04	.1213E+04	.4690E+04	.2644E+00	.4068E+00	.5577E+00
162	.3301E+04	.1324E+04	.5406E+04	.3008E+00	.4628E+00	.6094E+00
163	.2729E+04	.1448E+04	.5994E+04	.3215E+00	.4946E+00	.6470E+00
164	.2132E+04	.1705E+04	.6529E+04	.3347E+00	.5149E+00	.6774E+00
165	.4777E+04	.1582E+04	.6690E+04	.4416E-01	.6794E-01	.1015E+00
166	.4813E+04	.2058E+04	.7891E+04	.5304E-01	.8160E-01	.1199E+00
167	.4127E+04	.2782E+04	.8926E+04	.6092E-01	.9372E-01	.1409E+00
168	.4034E+04	.2884E+04	.9719E+04	.6701E-01	.1031E+00	.1615E+00
169	.4086E+04	.2878E+04	.1118E+05	.7858E-01	.1209E+00	.1813E+00
170	.1564E+04	.2074E+03	.5875E+03	.4466E+00	.6871E+00	.1079E+01
171	.2836E+04	.4836E+03	.1611E+04	.4793E+00	.7374E+00	.1243E+01
172	.2863E+04	.7418E+03	.2528E+04	.6744E+00	.1038E+01	.1498E+01
173	.2865E+04	.9857E+03	.3189E+04	.7418E+00	.1141E+01	.1622E+01
174	.2508E+04	.1117E+04	.3799E+04	.8300E+00	.1277E+01	.1752E+01
175	.2011E+04	.1253E+04	.4393E+04	.9389E+00	.1446E+01	.1894E+01
176	.3858E+04	.1365E+04	.4809E+04	.2616E+00	.6024E+00	.5549E+00
177	.3832E+04	.1694E+04	.5207E+04	.2794E+00	.4298E+00	.5814E+00
178	.3260E+04	.1568E+04	.5611E+04	.3023E+00	.4651E+00	.6163E+00

179	.2864E+04	.1763E+04	.6123E+04	.3202E+00	.4927E+00	.6469E+00
180	.2789E+04	.2166E+04	.6450E+04	.3278E+00	.5044E+00	.6661E+00
181	.2116E+04	.1999E+04	.6730E+04	.3363E+00	.5173E+00	.6820E+00
182	.5424E+04	.3343E+04	.6728E+04	.4444E-01	.6837E-01	.1005E+00
183	.7197E+03	.3931E+03	.1696E+03	.5334E+00	.8206E+00	.1069E+01
184	.2085E+04	.2954E+03	.8793E+03	.5128E+00	.7889E+00	.1255E+01
185	.3098E+04	.6323E+03	.1899E+04	.5213E+00	.8020E+00	.1352E+01
186	.3200E+04	.1021E+04	.2692E+04	.6444E+00	.9914E+00	.1507E+01
187	.3110E+04	.1337E+04	.3296E+04	.6985E+00	.1075E+01	.1595E+01
188	.2800E+04	.1580E+04	.3911E+04	.8086E+00	.1244E+01	.1728E+01
189	.2351E+04	.1637E+04	.4519E+04	.9181E+00	.1413E+01	.1902E+01
190	.3859E+04	.1844E+04	.4866E+04	.2666E+00	.4101E+00	.5738E+00
191	.3507E+04	.2012E+04	.5453E+04	.2927E+00	.4503E+00	.6104E+00
192	.3208E+04	.2286E+04	.5939E+04	.3160E+00	.4861E+00	.6454E+00
193	.2996E+04	.2511E+04	.6319E+04	.3280E+00	.5046E+00	.6662E+00
194	.2656E+04	.2529E+04	.6649E+04	.3340E+00	.5139E+00	.6766E+00
195	.2351E+04	.2732E+04	.7033E+04	.3435E+00	.5284E+00	.6971E+00
196	.3837E+04	.1880E+04	.6734E+04	.4452E-01	.6848E-01	.1016E+00
197	.1846E+04	.5273E+03	.6698E+03	.8194E+00	.1261E+01	.1705E+01
198	.2807E+04	.8391E+03	.1427E+04	.7264E+00	.1118E+01	.1712E+01
199	.3405E+04	.1347E+04	.2375E+04	.6759E+00	.1040E+01	.1658E+01
200	.3286E+04	.1815E+04	.3062E+04	.7346E+00	.1130E+01	.1722E+01
201	.3028E+04	.2254E+04	.3573E+04	.7843E+00	.1207E+01	.1771E+01
202	.2823E+04	.2691E+04	.4101E+04	.8439E+00	.1298E+01	.1833E+01
203	.3070E+04	.3239E+04	.4561E+04	.9072E+00	.1396E+01	.1926E+01
204	.3660E+04	.3447E+04	.5636E+04	.3203E+00	.4928E+00	.6844E+00
205	.3232E+04	.3571E+04	.6026E+04	.3333E+00	.5127E+00	.6968E+00
206	.2904E+04	.3636E+04	.6430E+04	.3398E+00	.5228E+00	.6981E+00
207	.2641E+04	.3656E+04	.6725E+04	.3439E+00	.5291E+00	.6985E+00
208	.2519E+04	.3735E+04	.6989E+04	.3442E+00	.5295E+00	.6965E+00
209	.2461E+04	.3729E+04	.7300E+04	.3477E+00	.5349E+00	.7021E+00
210	.3084E+04	.3901E+04	.7013E+04	.4641E-01	.7140E-01	.1035E+00
211	.2661E+04	.2947E+04	.7747E+04	.5189E-01	.7984E-01	.1175E+00
212	.2505E+04	.3177E+04	.8663E+04	.5887E-01	.9057E-01	.1378E+00
213	.2651E+04	.2979E+04	.9639E+04	.6635E-01	.1021E+00	.1598E+00
214	.3069E+04	.2855E+04	.1122E+05	.7868E-01	.1210E+00	.1812E+00
215	.2037E+04	.3298E+03	.9747E+03	.8105E+00	.1247E+01	.1588E+01
216	.2379E+04	.7170E+03	.1492E+04	.8904E+00	.1370E+01	.1793E+01
217	.3314E+04	.1323E+04	.2437E+04	.7281E+00	.1120E+01	.1563E+01
218	.3399E+04	.1948E+04	.3243E+04	.6036E+00	.9287E+00	.1352E+01
219	.3034E+04	.2596E+04	.3887E+04	.5973E+00	.9189E+00	.1335E+01
220	.2749E+04	.3196E+04	.4406E+04	.6171E+00	.9493E+00	.1371E+01
221	.2647E+04	.3704E+04	.5060E+04	.6563E+00	.1010E+01	.1443E+01
222	.3119E+04	.4161E+04	.5919E+04	.7161E+00	.1102E+01	.1531E+01
223	.3922E+04	.4620E+04	.5680E+04	.3060E+00	.4708E+00	.6457E+00
224	.2809E+04	.4445E+04	.6162E+04	.3075E+00	.4730E+00	.6400E+00
225	.2450E+04	.4400E+04	.6401E+04	.3188E+00	.4905E+00	.6549E+00
226	.2284E+04	.4415E+04	.6765E+04	.3259E+00	.5014E+00	.6640E+00
227	.2208E+04	.4339E+04	.7038E+04	.3305E+00	.5084E+00	.6682E+00
228	.2664E+04	.4328E+04	.7509E+04	.3426E+00	.5271E+00	.6864E+00
229	.2184E+04	.3304E+04	.6816E+04	.4506E-01	.6932E-01	.1015E+00
230	.1496E+04	.2981E+04	.7159E+04	.4750E-01	.7307E-01	.1104E+00
231	.1153E+04	.2450E+04	.8235E+04	.5558E-01	.8551E-01	.1329E+00
232	.1886E+04	.2608E+04	.9753E+04	.6720E-01	.1034E+00	.1591E+00
233	.2841E+04	.2509E+04	.1144E+05	.8043E-01	.1237E+00	.1830E+00
234	.1304E+04	.3553E+03	.9023E+03	.4560E+00	.7015E+00	.8794E+00
235	.2335E+04	.9763E+03	.1696E+04	.5386E+00	.8287E+00	.1066E+01
236	.2852E+04	.1587E+04	.2664E+04	.7205E+00	.1108E+01	.1474E+01
237	.3101E+04	.2130E+04	.3122E+04	.6739E+00	.1037E+01	.1427E+01
238	.3073E+04	.2709E+04	.3683E+04	.6343E+00	.9759E+00	.1377E+01
239	.2698E+04	.3093E+04	.4183E+04	.6443E+00	.9913E+00	.1415E+01
240	.2458E+04	.3374E+04	.4639E+04	.6506E+00	.1001E+01	.1654E+01
241	.2492E+04	.3639E+04	.5233E+04	.6710E+00	.1032E+01	.1692E+01
242	.2813E+04	.3744E+04	.5743E+04	.6873E+00	.1057E+01	.1484E+01
243	.3949E+04	.4135E+04	.5532E+04	.4004E+00	.6160E+00	.8447E+00
244	.2691E+04	.3294E+04	.6619E+04	.3517E+00	.5411E+00	.7410E+00

245	.2572E+04	.3939E+04	.6485E+04	.3341E+00	.5140E+00	.6921E+00
246	.2184E+04	.4062E+04	.6833E+04	.3284E+00	.5053E+00	.6708E+00
247	.2020E+04	.4049E+04	.6909E+04	.3280E+00	.5047E+00	.6660E+00
248	.2045E+04	.4110E+04	.7202E+04	.3271E+00	.5033E+00	.6566E+00
249	.2171E+04	.4026E+04	.7623E+04	.3340E+00	.5138E+00	.6637E+00
250	.3264E+04	.3987E+04	.7607E+04	.3067E+00	.4719E+00	.6007E+00
251	.2999E+04	.3770E+04	.6985E+04	.4703E-01	.7236E-01	.1067E+00
252	.3430E+04	.3746E+04	.5722E+04	.4113E+00	.6327E+00	.8646E+00
253	.3366E+04	.3648E+04	.5184E+04	.4208E+00	.6474E+00	.8661E+00
254	.1920E+04	.3543E+04	.7144E+04	.3591E+00	.5524E+00	.7399E+00
255	.1876E+04	.3612E+04	.7044E+04	.3505E+00	.5392E+00	.7110E+00
256	.1785E+04	.3697E+04	.7310E+04	.3410E+00	.5245E+00	.6845E+00
257	.1793E+04	.3627E+04	.7602E+04	.3365E+00	.5177E+00	.6690E+00
258	.1927E+04	.3629E+04	.7575E+04	.3278E+00	.5044E+00	.6462E+00
259	.2034E+04	.3430E+04	.7483E+04	.3078E+00	.4736E+00	.6000E+00
260	.2842E+04	.3232E+04	.6653E+04	.4467E-01	.6872E-01	.1017E+00
261	.1277E+04	.5222E+03	.8101E+03	.2350E+00	.3615E+00	.4631E+00
262	.1781E+04	.8899E+03	.1738E+04	.3856E+00	.5932E+00	.7684E+00
263	.2669E+04	.1648E+04	.2772E+04	.4703E+00	.7235E+00	.9335E+00
264	.2428E+04	.1772E+04	.3095E+04	.6837E+00	.1052E+01	.1395E+01
265	.2621E+04	.2206E+04	.3695E+04	.6661E+00	.1025E+01	.1398E+01
266	.2493E+04	.2626E+04	.4103E+04	.6432E+00	.9896E+00	.1386E+01
267	.2270E+04	.3005E+04	.4477E+04	.6350E+00	.9769E+00	.1402E+01
268	.2129E+04	.3271E+04	.4814E+04	.6205E+00	.9546E+00	.1410E+01
269	.2152E+04	.3440E+04	.5302E+04	.6385E+00	.9823E+00	.1426E+01
270	.2360E+04	.3511E+04	.5664E+04	.6474E+00	.9960E+00	.1400E+01
271	.2867E+04	.3496E+04	.5966E+04	.4068E+00	.6259E+00	.8557E+00
272	.2661E+04	.3604E+04	.6217E+04	.4165E+00	.6408E+00	.8565E+00
273	.2738E+04	.3433E+04	.5978E+04	.4032E+00	.6203E+00	.8107E+00
274	.1536E+04	.3346E+04	.7333E+04	.3562E+00	.5479E+00	.7205E+00
275	.1531E+04	.3233E+04	.7425E+04	.3441E+00	.5294E+00	.6861E+00
276	.1591E+04	.3314E+04	.7666E+04	.3357E+00	.5164E+00	.6630E+00
277	.1652E+04	.3171E+04	.7544E+04	.3181E+00	.4894E+00	.6228E+00
278	.1862E+04	.3117E+04	.7547E+04	.2987E+00	.4595E+00	.5780E+00
279	.2486E+04	.3055E+04	.6320E+04	.4205E-01	.6469E-01	.9625E-01
280	.2173E+04	.2882E+04	.6742E+04	.4462E-01	.6864E-01	.1059E+00
281	.1271E+04	.1242E+04	.4611E+03	.6543E-01	.1007E+00	.1483E+00
282	.1097E+04	.6909E+03	.1617E+04	.2312E+00	.3558E+00	.4497E+00
283	.1724E+04	.1272E+04	.2639E+04	.3707E+00	.5703E+00	.7204E+00
284	.1927E+04	.1552E+04	.3135E+04	.4406E+00	.6778E+00	.8758E+00
285	.1877E+04	.1814E+04	.3727E+04	.6560E+00	.1009E+01	.1338E+01
286	.1906E+04	.2086E+04	.4062E+04	.6560E+00	.1009E+01	.1371E+01
287	.1818E+04	.2410E+04	.4467E+04	.6358E+00	.9781E+00	.1367E+01
288	.1684E+04	.2653E+04	.4735E+04	.6098E+00	.9382E+00	.1353E+01
289	.1644E+04	.2882E+04	.4936E+04	.5771E+00	.8878E+00	.1325E+01
290	.1648E+04	.3016E+04	.5402E+04	.5943E+00	.9143E+00	.1325E+01
291	.1819E+04	.3072E+04	.5749E+04	.5971E+00	.9187E+00	.1283E+01
292	.2436E+04	.2986E+04	.5860E+04	.4156E+00	.6394E+00	.8659E+00
293	.2232E+04	.2887E+04	.5963E+04	.4204E+00	.6467E+00	.8552E+00
294	.2117E+04	.2860E+04	.6297E+04	.4176E+00	.6424E+00	.8323E+00
295	.2153E+04	.2632E+04	.6271E+04	.3940E+00	.6062E+00	.7723E+00
296	.1431E+04	.3079E+04	.7862E+04	.3533E+00	.5436E+00	.6996E+00
297	.1361E+04	.2742E+04	.7836E+04	.3467E+00	.5335E+00	.6785E+00
298	.1441E+04	.2804E+04	.7883E+04	.3258E+00	.5012E+00	.6332E+00
299	.1642E+04	.2686E+04	.7483E+04	.2875E+00	.4423E+00	.5535E+00
300	.3340E+04	.2312E+04	.5958E+04	.3969E-01	.6106E-01	.8947E-01
301	.1970E+04	.1977E+04	.7074E+04	.4705E-01	.7238E-01	.1078E+00
302	.2626E+04	.2935E+04	.6415E+04	.3889E+00	.5983E+00	.7618E+00
303	.1572E+04	.2087E+04	.5895E+04	.4058E+00	.6243E+00	.7820E+00
304	.1253E+04	.2561E+04	.8099E+04	.3511E+00	.5402E+00	.6850E+00
305	.1421E+04	.2240E+04	.7971E+04	.3325E+00	.5115E+00	.6421E+00
306	.1884E+04	.2297E+04	.7665E+04	.2870E+00	.4416E+00	.5514E+00
307	.7748E+04	.2405E+04	.5329E+04	.4068E-01	.6259E-01	.9385E-01
308	.7166E+03	.1132E+04	.6252E+03	.9801E-01	.1508E+00	.1801E+00
309	.8569E+03	.5568E+03	.1284E+04	.1263E+00	.1943E+00	.2498E+00
310	.1123E+04	.1503E+04	.2321E+04	.2828E+00	.4351E+00	.5639E+00

311	.9173E+03	.1559E+04	.3049E+04	.4149E+00	.6383E+00	.8042E+00
312	.1091E+04	.1770E+04	.3651E+04	.4487E+00	.6902E+00	.8902E+00
313	.1147E+04	.1844E+04	.3966E+04	.6510E+00	.1002E+01	.1324E+01
314	.1128E+04	.2027E+04	.4361E+04	.6447E+00	.9918E+00	.1346E+01
315	.1068E+04	.2165E+04	.4616E+04	.6119E+00	.9414E+00	.1312E+01
316	.1083E+04	.2334E+04	.4827E+04	.5612E+00	.8634E+00	.1244E+01
317	.1069E+04	.2426E+04	.5043E+04	.5213E+00	.8020E+00	.1196E+01
318	.1062E+04	.2460E+04	.5268E+04	.5279E+00	.8121E+00	.1174E+01
319	.1320E+04	.2615E+04	.5498E+04	.5158E+00	.7936E+00	.1099E+01
320	.1940E+04	.2366E+04	.5654E+04	.3787E+00	.5826E+00	.7786E+00
321	.1892E+04	.2369E+04	.5907E+04	.3753E+00	.5774E+00	.7543E+00
322	.1876E+04	.2276E+04	.5955E+04	.3838E+00	.5905E+00	.7565E+00
323	.1539E+04	.2632E+04	.6397E+04	.3696E+00	.5687E+00	.7176E+00
324	.1541E+04	.2573E+04	.6730E+04	.3805E+00	.5854E+00	.7306E+00
325	.1254E+04	.3224E+04	.6436E+04	.3813E+00	.5867E+00	.7257E+00
326	.1956E+04	.2800E+04	.7888E+04	.3176E+00	.6886E+00	.6089E+00
327	.2686E+04	.3318E+04	.7715E+04	.2814E+00	.4330E+00	.5355E+00
328	.1198E+05	.4699E+04	.3174E+04	.3088E+01	.4751E+01	.7537E+01
329	.5338E+03	.9674E+03	.2830E+03	.7533E+01	.1159E+00	.1381E+00
330	.7089E+03	.3014E+03	.1365E+04	.1467E+00	.2257E+00	.2845E+00
331	.9478E+03	.1526E+04	.2334E+04	.2811E+00	.4325E+00	.5310E+00
332	.4670E+03	.1868E+04	.2970E+04	.4361E+00	.6709E+00	.8265E+00
333	.3826E+03	.2395E+04	.3657E+04	.5120E+00	.7876E+00	.9834E+00
334	.4452E+03	.2395E+04	.3942E+04	.4938E+00	.7597E+00	.9731E+00
335	.5073E+03	.2358E+04	.4237E+04	.6568E+00	.1010E+01	.1326E+01
336	.4852E+03	.2340E+04	.4355E+04	.6077E+00	.9349E+00	.1264E+01
337	.5286E+03	.2566E+04	.4597E+04	.5402E+00	.8312E+00	.1162E+01
338	.5010E+03	.2699E+04	.4680E+04	.4553E+00	.7005E+00	.1017E+01
339	.6583E+03	.2961E+04	.4333E+04	.3775E+00	.5808E+00	.8885E+00
340	.6148E+03	.2186E+04	.4502E+04	.3627E+00	.5579E+00	.8155E+00
341	.8419E+03	.2637E+04	.4598E+04	.3704E+00	.5698E+00	.7896E+00
342	.1516E+04	.3756E+04	.4760E+04	.2802E+00	.4311E+00	.5821E+00
343	.1470E+04	.4306E+04	.4807E+04	.2830E+00	.6353E+00	.5757E+00
344	.1576E+04	.4945E+04	.5148E+04	.3022E+00	.4650E+00	.6040E+00
345	.1732E+04	.5156E+04	.5331E+04	.3213E+00	.4943E+00	.6347E+00
346	.1324E+04	.5801E+04	.5777E+04	.3599E+00	.5536E+00	.7015E+00
347	.1266E+04	.6209E+04	.6512E+04	.3958E+00	.6089E+00	.7581E+00
348	.1695E+04	.7747E+04	.6872E+04	.4618E+00	.7104E+00	.8739E+00
349	.2995E+04	.4437E+04	.8119E+04	.3095E+00	.4761E+00	.5896E+00
350	.2049E+05	.1297E+05	.8681E+04	.1487E+01	.2288E+01	.3447E+01
351	.2944E+04	.3032E+04	.3332E+04	.2116E+01	.3256E+01	.4980E+01
352	.1888E+04	.2425E+04	.6762E+04	.4493E+01	.6913E+01	.1004E+00
353	.1785E+04	.1854E+04	.8915E+04	.6119E+01	.9613E+01	.1378E+00
354	.1932E+04	.1721E+04	.1028E+05	.7159E+01	.1101E+00	.1671E+00
355	.2630E+04	.1709E+04	.1161E+05	.8191E+01	.1260E+00	.1876E+00
356	.1008E+04	.6972E+02	.4174E+03	.6707E+01	.1032E+00	.1461E+00
357	.1291E+04	.1491E+04	.2249E+04	.3777E+00	.5810E+00	.7080E+00
358	.4233E+03	.2092E+04	.3306E+04	.5525E+00	.8499E+00	.1033E+01
359	.2379E+03	.3189E+04	.3770E+04	.6616E+00	.1010E+01	.1247E+01
360	.1096E+04	.2992E+04	.4190E+04	.6795E+00	.1045E+01	.1301E+01
361	.1293E+04	.3514E+04	.4304E+04	.6282E+00	.9665E+00	.1232E+01
362	.9424E+03	.2969E+04	.4268E+04	.7190E+00	.1107E+01	.1469E+01
363	.9311E+03	.2903E+04	.4537E+04	.6487E+00	.9980E+00	.1353E+01
364	.7832E+03	.2838E+04	.4582E+04	.5674E+00	.8730E+00	.1237E+01
365	.9007E+03	.3013E+04	.4589E+04	.4809E+00	.7398E+00	.1106E+01
366	.1117E+04	.4884E+03	.2038E+04	.1392E+01	.2141E+01	.2626E+01
367	.1130E+04	.4579E+03	.2026E+04	.1901E+01	.2925E+01	.3579E+01
368	.6897E+03	.6533E+03	.2369E+04	.1850E+01	.2847E+01	.3490E+01
369	.2044E+04	.1489E+04	.2585E+04	.1785E+01	.2747E+01	.3381E+01
370	.1727E+04	.8969E+03	.2745E+04	.1660E+01	.2554E+01	.3176E+01
371	.3585E+04	.3021E+04	.2948E+04	.1525E+01	.2346E+01	.2950E+01
372	.1829E+04	.1441E+04	.3235E+04	.1591E+01	.2447E+01	.3129E+01
373	.1925E+04	.1737E+04	.3127E+04	.1443E+01	.2220E+01	.2902E+01
374	.1716E+04	.1790E+04	.3244E+04	.1309E+01	.2014E+01	.2703E+01
375	.1503E+04	.1797E+04	.3227E+04	.1160E+01	.1784E+01	.2452E+01
376	.1894E+04	.2300E+04	.3235E+04	.1035E+01	.1593E+01	.2251E+01

377	.3869E+03	.8599E+03	.3185E+04	.9604E+00		.1447E+01	.2058E+01
378	.6303E+03	.1105E+04	.3370E+04	.8661E+00		.1333E+01	.1836E+01
379	.6552E+03	.9143E+03	.3279E+04	.7365E+00		.1133E+01	.1526E+01
380	.8406E+03	.9890E+03	.3274E+04	.6786E+00		.1044E+01	.1378E+01
381	.1046E+04	.1026E+04	.3212E+04	.6358E+00		.9782E+00	.1266E+01
382	.1151E+04	.1158E+04	.3213E+04	.5925E+00		.9115E+00	.1160E+01
383	.1240E+04	.1383E+04	.3190E+04	.5569E+00		.8567E+00	.1076E+01
384	.8853E+03	.1948E+04	.3172E+04	.5404E+00		.8314E+00	.1031E+01
385	.2867E+04	.4087E+04	.3694E+04	.5994E+00		.9221E+00	.1126E+01
386	.7601E+04	.1687E+04	.8910E+04	.1409E-01		.2168E-01	.3184E-01
387	.3296E+04	.4530E+04	.7585E+04	.5076E-01		.7807E-01	.1062E+00
388	.2160E+04	.9621E+03	.2946E+04	.1382E+01		.2127E+01	.2686E+01
389	.3545E+04	.1323E+04	.3063E+04	.1336E+01		.2055E+01	.2627E+01
390	.2681E+04	.7445E+03	.3367E+04	.1228E+01		.1889E+01	.2452E+01
391	.2408E+04	.7518E+03	.3397E+04	.1111E+01		.1710E+01	.2266E+01
392	.2274E+04	.8823E+03	.3500E+04	.9882E+00		.1520E+01	.2058E+01
393	.1839E+04	.9976E+03	.3608E+04	.8853E+00		.1362E+01	.1894E+01
394	.1666E+04	.1033E+04	.3755E+04	.7798E+00		.1200E+01	.1706E+01
395	.1054E+04	.1156E+04	.3729E+04	.6721E+00		.1034E+01	.1441E+01
396	.1036E+04	.1066E+04	.3573E+04	.5553E+00		.8543E+00	.1166E+01
397	.6561E+03	.1174E+04	.3499E+04	.5065E+00		.7793E+00	.1041E+01
398	.6568E+03	.1222E+04	.3455E+04	.4717E+00		.7257E+00	.9461E+00
399	.6526E+03	.1232E+04	.3376E+04	.4443E+00		.6836E+00	.8738E+00
400	.6891E+03	.1262E+04	.3292E+04	.4176E+00		.6425E+00	.8081E+00
401	.8820E+03	.1301E+04	.3421E+04	.4476E+00		.6886E+00	.8512E+00
402	.1031E+04	.1217E+04	.3881E+04	.6525E+00		.1004E+01	.1221E+01
403	.6257E+04	.2082E+04	.6273E+04	.9864E-02		.1517E-01	.2487E-01
404	.6747E+04	.5067E+04	.6498E+04	.4295E-01		.6608E-01	.9087E-01
405	.4509E+04	.2241E+04	.1032E+05	.7174E-01		.1104E+00	.1566E+00
406	.2571E+04	.1415E+04	.1107E+05	.7759E-01		.1194E+00	.1749E+00
407	.2379E+04	.1250E+04	.1162E+05	.8196E-01		.1261E+00	.1900E+00
408	.2111E+04	.3759E+03	.1526E+04	.8368E+00		.1287E+01	.1600E+01
409	.5062E+03	.3652E+03	.1675E+04	.1186E+01		.1824E+01	.2215E+01
410	.1705E+04	.5347E+03	.1953E+04	.1230E+01		.1893E+01	.2287E+01
411	.2546E+04	.5680E+03	.2388E+04	.1336E+01		.2055E+01	.2503E+01
412	.4093E+04	.1488E+04	.2758E+04	.1355E+01		.2085E+01	.2574E+01
413	.3507E+04	.4728E+03	.3108E+04	.1379E+01		.2122E+01	.2667E+01
414	.3641E+04	.7462E+03	.3401E+04	.1302E+01		.2004E+01	.2564E+01
415	.3487E+04	.1055E+04	.3424E+04	.1274E+01		.1959E+01	.2556E+01
416	.3022E+04	.1729E+04	.3561E+04	.1153E+01		.1774E+01	.2364E+01
417	.2665E+04	.2071E+04	.3609E+04	.1006E+01		.1547E+01	.2109E+01
418	.2147E+04	.2445E+04	.3901E+04	.8498E+00		.1307E+01	.1845E+01
419	.2380E+04	.1936E+04	.4038E+04	.7689E+00		.1183E+01	.1688E+01
420	.2343E+04	.1739E+04	.4235E+04	.7137E+00		.1098E+01	.1524E+01
421	.1573E+04	.2035E+04	.4114E+04	.6050E+00		.9308E+00	.1257E+01
422	.1607E+04	.1724E+04	.4023E+04	.5726E+00		.8809E+00	.1166E+01
423	.1191E+04	.1986E+04	.3895E+04	.5505E+00		.8469E+00	.1100E+01
424	.1097E+04	.2405E+04	.3888E+04	.5343E+00		.8221E+00	.1050E+01
425	.1204E+04	.2505E+04	.3819E+04	.5025E+00		.7731E+00	.9752E+00
426	.1114E+04	.3602E+04	.3523E+04	.5043E+00		.7758E+00	.9628E+00
427	.4816E+04	.6229E+04	.3991E+04	.5762E+00		.8865E+00	.1073E+01
428	.6030E+04	.4316E+04	.1003E+05	.1590E-01		.2446E-01	.3390E-01
429	.9756E+04	.3646E+04	.1865E+05	.3119E-01		.4799E-01	.6363E-01
430	.2020E+04	.1231E+03	.4186E+03	.3564E+00		.5483E+00	.6994E+00
431	.6652E+03	.1766E+04	.6964E+03	.1128E+00		.1736E+00	.2469E+00
432	.2201E+04	.1927E+04	.1768E+04	.1125E+00		.1730E+00	.2461E+00
433	.3734E+04	.2624E+04	.2747E+04	.1941E+00		.2906E+00	.3964E+00
434	.4373E+04	.3180E+04	.3325E+04	.2634E+00		.4053E+00	.5369E+00
435	.4991E+04	.3672E+04	.3744E+04	.2925E+00		.4500E+00	.6080E+00
436	.5139E+04	.4491E+04	.3643E+04	.2866E+00		.4409E+00	.6051E+00
437	.3830E+04	.4935E+04	.3887E+04	.3484E+00		.5360E+00	.7569E+00
438	.4009E+04	.5526E+04	.4102E+04	.3521E+00		.5417E+00	.7802E+00
439	.3514E+04	.7535E+04	.4175E+04	.3607E+00		.5242E+00	.7687E+00
440	.8752E+03	.4542E+03	.5795E+03	.2844E+00		.4376E+00	.5699E+00
441	.1236E+04	.4952E+03	.4532E+03	.4524E-01		.6960E-01	.1235E+00
442	.2204E+04	.8384E+03	.9895E+03	.1135E+00		.1746E+00	.2243E+00

443	.3591E+04	.1184E+04	.2362E+04	.2726E+00	.6194E+00	.5162E+00
444	.5160E+04	.1334E+04	.3434E+04	.3592E+00	.5527E+00	.6939E+00
445	.5947E+04	.1348E+04	.6000E+04	.3770E+00	.5801E+00	.7646E+00
446	.6315E+04	.1467E+04	.4385E+04	.3424E+00	.5575E+00	.7318E+00
447	.4551E+04	.1984E+04	.4385E+04	.4026E+00	.6194E+00	.8486E+00
448	.4376E+04	.2679E+04	.4531E+04	.3562E+00	.5480E+00	.7824E+00
449	.4060E+04	.3608E+04	.4891E+04	.2929E+00	.6506E+00	.6712E+00
450	.3161E+04	.4793E+04	.4917E+04	.2902E+00	.6464E+00	.6774E+00
451	.2414E+04	.5717E+04	.5411E+04	.3215E+00	.4945E+00	.7247E+00
452	.2133E+04	.5525E+04	.5752E+04	.3414E+00	.5252E+00	.7401E+00
453	.3041E+04	.5838E+04	.6016E+04	.2560E+00	.3938E+00	.5515E+00
454	.2162E+04	.5898E+04	.6134E+04	.2614E+00	.6021E+00	.5498E+00
455	.1979E+04	.6056E+04	.6425E+04	.2806E+00	.4317E+00	.5750E+00
456	.1637E+04	.6198E+04	.6506E+04	.3080E+00	.4738E+00	.6162E+00
457	.1225E+04	.7625E+04	.7009E+04	.3223E+00	.4958E+00	.6328E+00
458	.1588E+04	.8010E+04	.7696E+04	.3539E+00	.5445E+00	.6773E+00
459	.2834E+04	.9617E+04	.7634E+04	.4297E+00	.6611E+00	.8074E+00
460	.4383E+04	.5889E+04	.8533E+04	.2773E+00	.4266E+00	.5175E+00
461	.9872E+04	.7482E+04	.5539E+04	.8806E-02	.1355E-01	.2039E-01
462	.8021E+04	.4255E+04	.9136E+04	.1490E-01	.2292E-01	.3406E-01
463	.2985E+04	.1673E+04	.9942E+04	.6884E-01	.1059E+00	.1546E+00
464	.3205E+04	.2318E+04	.1091E+05	.7632E-01	.1174E+00	.1717E+00
465	.4027E+04	.2811E+04	.1202E+05	.8510E-01	.1309E+00	.1883E+00
466	.2168E+04	.2536E+04	.7665E+04	.3286E+00	.5056E+00	.6201E+00
467	.1008E+04	.3783E+04	.6780E+04	.3453E+00	.5312E+00	.6520E+00
468	.2583E+04	.3562E+04	.9588E+04	.3066E+00	.4718E+00	.5713E+00
469	.3125E+04	.4357E+04	.8893E+04	.2715E+00	.4177E+00	.5091E+00
470	.1005E+05	.3180E+04	.7119E+04	.1182E-01	.1819E-01	.2701E-01
471	.3904E+03	.4067E+03	.4972E+03	.1190E+00	.1831E+00	.2960E+00
472	.1840E+04	.3082E+03	.1174E+04	.1472E+00	.2265E+00	.2929E+00
473	.4009E+04	.4446E+03	.2576E+04	.3416E+00	.5256E+00	.6384E+00
474	.5331E+04	.5848E+03	.3449E+04	.4281E+00	.6585E+00	.8120E+00
475	.6648E+04	.7202E+03	.4362E+04	.4449E+00	.6844E+00	.8601E+00
476	.6918E+04	.7885E+03	.4588E+04	.4214E+00	.6482E+00	.8351E+00
477	.5318E+04	.8618E+03	.4845E+04	.4741E+00	.7295E+00	.9810E+00
478	.5154E+04	.8919E+03	.4860E+04	.4108E+00	.6320E+00	.8954E+00
479	.4763E+04	.8743E+03	.5226E+04	.3691E+00	.5678E+00	.8228E+00
480	.3934E+04	.7436E+03	.5960E+04	.3900E+00	.6000E+00	.8366E+00
481	.3034E+04	.7255E+03	.6352E+04	.4141E+00	.6370E+00	.8537E+00
482	.2699E+04	.9209E+03	.6785E+04	.4260E+00	.6553E+00	.8526E+00
483	.3697E+04	.1059E+04	.7130E+04	.3202E+00	.4927E+00	.6310E+00
484	.3058E+04	.1172E+04	.7226E+04	.3228E+00	.4966E+00	.6221E+00
485	.2325E+04	.1348E+04	.7287E+04	.3373E+00	.5189E+00	.6404E+00
486	.1777E+04	.1671E+04	.7778E+04	.3442E+00	.5295E+00	.6466E+00
487	.1357E+04	.2148E+04	.7670E+04	.3330E+00	.5123E+00	.6241E+00
488	.1169E+04	.1293E+04	.9102E+04	.2994E+00	.4606E+00	.5562E+00
489	.1427E+04	.1898E+04	.9179E+04	.2991E+00	.4601E+00	.5569E+00
490	.1539E+04	.1800E+04	.9130E+04	.2720E+00	.4185E+00	.5095E+00
491	.9080E+04	.2191E+04	.7671E+04	.1225E-01	.1884E-01	.2726E-01
492	.1738E+04	.2272E+03	.7029E+03	.2940E+00	.4523E+00	.5816E+00
493	.3427E+04	.8232E+03	.2169E+04	.4568E+00	.7028E+00	.8532E+00
494	.5726E+04	.1000E+04	.3584E+04	.5103E+00	.7850E+00	.9623E+00
495	.6551E+04	.1399E+04	.4111E+04	.5050E+00	.7769E+00	.9685E+00
496	.7561E+04	.1689E+04	.4725E+04	.4612E+00	.7095E+00	.9020E+00
497	.5799E+04	.1769E+04	.4785E+04	.5146E+00	.7917E+00	.1047E+01
498	.5873E+04	.1843E+04	.4917E+04	.4294E+00	.6607E+00	.9190E+00
499	.5253E+04	.1934E+04	.5175E+04	.3820E+00	.5877E+00	.8482E+00
500	.4313E+04	.2035E+04	.5756E+04	.4047E+00	.6227E+00	.8616E+00
501	.3560E+04	.2122E+04	.6456E+04	.4404E+00	.6775E+00	.9025E+00
502	.3180E+04	.2142E+04	.6919E+04	.4682E+00	.7204E+00	.9302E+00
503	.4259E+04	.2016E+04	.7332E+04	.3490E+00	.5370E+00	.6794E+00
504	.3739E+04	.1510E+04	.7674E+04	.3327E+00	.5118E+00	.6362E+00
505	.2978E+04	.1514E+04	.7903E+04	.3460E+00	.5292E+00	.6455E+00
506	.2488E+04	.9410E+03	.7510E+04	.3420E+00	.5261E+00	.6364E+00
507	.1556E+04	.1818E+04	.8978E+04	.3066E+00	.4716E+00	.5692E+00
508	.1137E+04	.1215E+04	.9031E+04	.3008E+00	.4627E+00	.5570E+00

509	.1226E+04	.1452E+04	.9191E+04	.2946E+00	.4532E+00	.5466E+00
510	.1221E+04	.1380E+04	.8951E+04	.2759E+00	.4245E+00	.5156E+00
511	.8120E+04	.1213E+04	.7509E+04	.1217E-01	.1872E-01	.2721E-01
512	.8820E+04	.3682E+04	.8069E+04	.1300E-01	.2000E-01	.2996E-01
513	.4263E+04	.3197E+04	.7407E+04	.3341E+00	.5140E+00	.6360E+00
514	.3912E+04	.2528E+04	.7012E+04	.3464E+00	.5329E+00	.6500E+00
515	.2469E+04	.2889E+04	.8767E+04	.3012E+00	.4634E+00	.5643E+00
516	.2090E+04	.2603E+04	.8823E+04	.3037E+00	.4672E+00	.5639E+00
517	.1893E+04	.2762E+04	.9001E+04	.2985E+00	.4593E+00	.5527E+00
518	.1750E+04	.2689E+04	.8982E+04	.2908E+00	.4474E+00	.5400E+00
519	.1863E+04	.2711E+04	.8999E+04	.2781E+00	.4278E+00	.5193E+00
520	.8626E+04	.2873E+04	.8066E+04	.1292E-01	.1988E-01	.2821E-01
521	.8264E+04	.3551E+04	.9613E+04	.1526E-01	.2347E-01	.3206E-01
522	.2183E+04	.1513E+03	.1327E+04	.6076E+00	.9344E+00	.1140E+01
523	.4426E+04	.1179E+04	.2479E+04	.5736E+00	.8825E+00	.1091E+01
524	.6559E+04	.1640E+04	.3923E+04	.5621E+00	.8648E+00	.1081E+01
525	.7475E+04	.2130E+04	.4147E+04	.4951E+00	.7617E+00	.9651E+00
526	.6253E+04	.2393E+04	.4577E+04	.5612E+00	.8327E+00	.1090E+01
527	.6335E+04	.2649E+04	.4670E+04	.4362E+00	.6710E+00	.9223E+00
528	.5777E+04	.2930E+04	.4937E+04	.3746E+00	.5763E+00	.8363E+00
529	.4687E+04	.3133E+04	.5545E+04	.4018E+00	.6182E+00	.8561E+00
530	.3846E+04	.3325E+04	.6218E+04	.4477E+00	.6887E+00	.9170E+00
531	.3441E+04	.3454E+04	.6839E+04	.4887E+00	.7519E+00	.9709E+00
532	.4700E+04	.3519E+04	.7526E+04	.3714E+00	.5713E+00	.7214E+00
533	.5121E+04	.3522E+04	.7231E+04	.3296E+00	.5070E+00	.6282E+00
534	.3649E+04	.3485E+04	.8312E+04	.2886E+00	.4440E+00	.5485E+00
535	.3364E+04	.3680E+04	.8535E+04	.2874E+00	.4421E+00	.5393E+00
536	.2719E+04	.3762E+04	.8720E+04	.2898E+00	.4458E+00	.5390E+00
537	.2416E+04	.3776E+04	.8790E+04	.2920E+00	.4492E+00	.5413E+00
538	.2401E+04	.3827E+04	.8922E+04	.2890E+00	.4446E+00	.5370E+00
539	.2555E+04	.3751E+04	.8921E+04	.2809E+00	.4322E+00	.5236E+00
540	.9333E+04	.3552E+04	.7830E+04	.1259E-01	.1937E-01	.2831E-01
541	.2743E+04	.4503E+03	.1645E+04	.6506E+00	.1001E+01	.1251E+01
542	.4757E+04	.1378E+04	.2558E+04	.5924E+00	.9113E+00	.1150E+01
543	.7533E+04	.2013E+04	.3903E+04	.5242E+00	.8064E+00	.1026E+01
544	.6252E+04	.2377E+04	.4045E+04	.5473E+00	.8420E+00	.1101E+01
545	.6715E+04	.2905E+04	.4309E+04	.4221E+00	.6495E+00	.8918E+00
546	.6055E+04	.3285E+04	.4596E+04	.3532E+00	.5434E+00	.7963E+00
547	.4960E+04	.3661E+04	.5244E+04	.3842E+00	.5910E+00	.8205E+00
548	.4019E+04	.3974E+04	.5960E+04	.4401E+00	.6771E+00	.9012E+00
549	.3533E+04	.4176E+04	.6740E+04	.4972E+00	.7649E+00	.9860E+00
550	.4674E+04	.4282E+04	.7531E+04	.3931E+00	.6048E+00	.7614E+00
551	.5250E+04	.4426E+04	.8120E+04	.2590E+00	.3985E+00	.4938E+00
552	.3896E+04	.4537E+04	.8103E+04	.2600E+00	.4000E+00	.4888E+00
553	.3265E+04	.4691E+04	.8355E+04	.2745E+00	.4223E+00	.5117E+00
554	.2965E+04	.4789E+04	.8605E+04	.2847E+00	.4380E+00	.5291E+00
555	.2922E+04	.4777E+04	.8734E+04	.2886E+00	.4440E+00	.5370E+00
556	.3162E+04	.4722E+04	.8864E+04	.2861E+00	.4602E+00	.5320E+00
557	.1051E+05	.4886E+04	.7705E+04	.1244E-01	.1914E-01	.2831E-01
558	.3744E+04	.6904E+03	.1930E+04	.6671E+00	.1026E+01	.1306E+01
559	.5753E+04	.1179E+04	.2568E+04	.5899E+00	.9076E+00	.1155E+01
560	.6528E+04	.2001E+04	.3474E+04	.5368E+00	.8258E+00	.1082E+01
561	.6715E+04	.2597E+04	.3760E+04	.3911E+00	.6018E+00	.8358E+00
562	.6242E+04	.3193E+04	.4203E+04	.3176E+00	.4886E+00	.7296E+00
563	.5116E+04	.3759E+04	.4836E+04	.3461E+00	.5325E+00	.7441E+00
564	.4078E+04	.4311E+04	.5591E+04	.4047E+00	.6226E+00	.8284E+00
565	.3511E+04	.4865E+04	.6297E+04	.4716E+00	.7255E+00	.9365E+00
566	.4663E+04	.4961E+04	.7760E+04	.4128E+00	.6351E+00	.7973E+00
567	.6204E+04	.5568E+04	.7200E+04	.2036E+00	.3133E+00	.3890E+00
568	.4393E+04	.5581E+04	.7684E+04	.2403E+00	.3697E+00	.4516E+00
569	.3692E+04	.5554E+04	.8027E+04	.2659E+00	.4091E+00	.4961E+00
570	.3353E+04	.5499E+04	.8337E+04	.2842E+00	.4372E+00	.5283E+00
571	.3318E+04	.5482E+04	.8575E+04	.2938E+00	.4520E+00	.5462E+00
572	.3608E+04	.5370E+04	.8768E+04	.2985E+00	.4592E+00	.5527E+00
573	.1102E+05	.4736E+04	.7760E+04	.1283E-01	.1974E-01	.2845E-01
574	.8512E+04	.3988E+04	.9504E+04	.1530E-01	.2353E-01	.3202E-01

575	.3470E+04	.2901E+04	.1055E+05	.7345E-01	.1130E+00	.1567E+00
576	.3234E+04	.2968E+04	.1159E+05	.8169E-01	.1257E+00	.1774E+00
577	.3210E+04	.2875E+04	.1232E+05	.8732E-01	.1346E+00	.1914E+00
578	.3759E+04	.8655E+03	.1288E+04	.7797E+00	.1200E+01	.1563E+01
579	.5732E+04	.1374E+04	.2284E+04	.6583E+00	.1013E+01	.1356E+01
580	.6454E+04	.2039E+04	.3100E+04	.5176E+00	.7962E+00	.1141E+01
581	.6216E+04	.2528E+04	.3797E+04	.4351E+00	.6694E+00	.1017E+01
582	.5229E+04	.2943E+04	.4415E+04	.4700E+00	.7231E+00	.1019E+01
583	.4287E+04	.3349E+04	.6884E+04	.5306E+00	.8163E+00	.1088E+01
584	.3341E+04	.3508E+04	.9256E+04	.5731E+00	.8817E+00	.1133E+01
585	.4480E+04	.4384E+04	.5678E+04	.5883E+00	.9052E+00	.1128E+01
586	.6206E+04	.6904E+04	.7379E+04	.2325E+00	.3577E+00	.4644E+00
587	.4805E+04	.4849E+04	.7733E+04	.2740E+00	.4215E+00	.5127E+00
588	.4125E+04	.4991E+04	.8024E+04	.2937E+00	.4518E+00	.5437E+00
589	.3776E+04	.5107E+04	.8319E+04	.3086E+00	.4748E+00	.5696E+00
590	.3542E+04	.5002E+04	.8540E+04	.3135E+00	.4823E+00	.5782E+00
591	.3686E+04	.5119E+04	.8837E+04	.3208E+00	.4935E+00	.5912E+00
592	.1308E+05	.5465E+04	.8189E+04	.1272E-01	.1957E-01	.3129E-01
593	.9616E+04	.3567E+04	.8949E+04	.1473E-01	.2267E-01	.3328E-01
594	.3416E+04	.3531E+04	.1031E+05	.7154E-01	.1101E+00	.1566E+00
595	.3007E+04	.3264E+04	.1143E+05	.8035E-01	.1236E+00	.1774E+00
596	.2391E+04	.3013E+04	.1222E+05	.8667E-01	.1333E+00	.1917E+00
597	.1574E+04	.2657E+03	.4339E+03	.5410E+00	.8323E+00	.1064E+01
598	.6081E+04	.3652E+03	.1212E+04	.4740E+00	.7292E+00	.9919E+00
599	.5534E+04	.9170E+03	.2291E+04	.4187E+00	.6441E+00	.9536E+00
600	.5915E+04	.1518E+04	.3159E+04	.3537E+00	.5441E+00	.8789E+00
601	.5130E+04	.2048E+04	.3898E+04	.4011E+00	.6171E+00	.9009E+00
602	.4388E+04	.2448E+04	.4463E+04	.4513E+00	.6943E+00	.9434E+00
603	.3722E+04	.2829E+04	.4907E+04	.5031E+00	.7740E+00	.9985E+00
604	.3984E+04	.2939E+04	.5509E+04	.5988E+00	.9212E+00	.1143E+01
605	.5809E+04	.3214E+04	.6318E+04	.1953E+00	.3004E+00	.3756E+00
606	.5323E+04	.4057E+04	.7099E+04	.2463E+00	.3789E+00	.4624E+00
607	.4449E+04	.3711E+04	.7443E+04	.2664E+00	.4099E+00	.4939E+00
608	.3873E+04	.3958E+04	.8001E+04	.3005E+00	.4623E+00	.5531E+00
609	.3936E+04	.4601E+04	.8328E+04	.3122E+00	.4804E+00	.5750E+00
610	.3357E+04	.4124E+04	.8593E+04	.3263E+00	.5020E+00	.6006E+00
611	.1539E+05	.3031E+04	.7859E+04	.1421E-01	.2187E-01	.3435E-01
612	.2627E+04	.1830E+03	.7097E+03	.3397E+00	.5226E+00	.7079E+00
613	.4338E+04	.4558E+03	.1534E+04	.3115E+00	.4793E+00	.7344E+00
614	.5165E+04	.8095E+03	.2441E+04	.2720E+00	.4185E+00	.7300E+00
615	.4598E+04	.1151E+04	.3366E+04	.3455E+00	.5316E+00	.8205E+00
616	.4102E+04	.1469E+04	.4030E+04	.4082E+00	.6280E+00	.8836E+00
617	.3546E+04	.1773E+04	.4644E+04	.4813E+00	.7405E+00	.9704E+00
618	.3467E+04	.2075E+04	.5344E+04	.6046E+00	.9302E+00	.1153E+01
619	.5648E+04	.2392E+04	.6028E+04	.1920E+00	.2954E+00	.3735E+00
620	.4540E+04	.2759E+04	.6919E+04	.2518E+00	.3873E+00	.4701E+00
621	.3701E+04	.3009E+04	.7650E+04	.2970E+00	.4570E+00	.5478E+00
622	.3064E+04	.3275E+04	.8254E+04	.3248E+00	.4997E+00	.5987E+00
623	.1590E+05	.3583E+04	.8393E+04	.1356E-01	.2086E-01	.3496E-01
624	.1372E+04	.1045E+03	.3817E+03	.2530E+00	.3892E+00	.5204E+00
625	.3072E+04	.3018E+03	.9519E+03	.2296E+00	.3532E+00	.5382E+00
626	.4305E+04	.5817E+03	.2036E+04	.2143E+00	.3296E+00	.6001E+00
627	.3731E+04	.8383E+03	.2921E+04	.3203E+00	.4928E+00	.7676E+00
628	.3454E+04	.1002E+04	.3599E+04	.3845E+00	.5915E+00	.8623E+00
629	.3042E+04	.1207E+04	.4303E+04	.4599E+00	.7075E+00	.9610E+00
630	.2810E+04	.1380E+04	.5073E+04	.6000E+00	.9231E+00	.1161E+01
631	.5325E+04	.1641E+04	.5692E+04	.1903E+00	.2928E+00	.3782E+00
632	.4216E+04	.1895E+04	.6562E+04	.2456E+00	.3778E+00	.4645E+00
633	.3304E+04	.2136E+04	.7300E+04	.2935E+00	.4515E+00	.5457E+00
634	.2515E+04	.2377E+04	.7891E+04	.3206E+00	.4932E+00	.5957E+00
635	.1463E+05	.2862E+04	.7630E+04	.1365E-01	.2100E-01	.3297E-01
636	.1222E+05	.3436E+04	.8524E+04	.1619E-01	.2184E-01	.3364E-01
637	.3838E+04	.3319E+04	.9853E+04	.6805E-01	.1047E+00	.1538E+00
638	.3142E+04	.3242E+04	.1107E+05	.7754E-01	.1193E+00	.1754E+00
639	.2448E+04	.3156E+04	.1209E+05	.8563E-01	.1317E+00	.1914E+00
640	.2029E+04	.2157E+03	.5735E+03	.1937E+00	.2980E+00	.4342E+00

641	.3563E+04	.4896E+03	.1561E+04	.1932E+00	.2972E+00	.5151E+00
642	.3092E+04	.8033E+03	.2585E+04	.3170E+00	.4876E+00	.7327E+00
643	.2940E+04	.1063E+04	.3371E+04	.4102E+00	.6311E+00	.8749E+00
644	.2524E+04	.1220E+04	.4079E+04	.4834E+00	.7638E+00	.9928E+00
645	.2239E+04	.1319E+04	.4821E+04	.6000E+00	.9230E+00	.1195E+01
646	.4757E+04	.1412E+04	.5648E+04	.1917E+00	.2949E+00	.3886E+00
647	.3678E+04	.1551E+04	.6266E+04	.2465E+00	.3793E+00	.4720E+00
648	.2827E+04	.1734E+04	.7003E+04	.2933E+00	.4513E+00	.5517E+00
649	.2065E+04	.1895E+04	.7602E+04	.3209E+00	.4937E+00	.6018E+00
650	.1514E+05	.2476E+04	.7323E+04	.1322E-01	.2034E-01	.3300E-01
651	.1377E+05	.2540E+04	.8078E+04	.1432E-01	.2204E-01	.3428E-01
652	.4070E+04	.2813E+04	.9552E+04	.6591E-01	.1014E+00	.1504E+00
653	.3368E+04	.2932E+04	.1085E+05	.7587E-01	.1167E+00	.1732E+00
654	.2916E+04	.3135E+04	.1204E+05	.8526E-01	.1312E+00	.1910E+00
655	.1288E+04	.9827E+02	.3374E+03	.1835E+00	.2823E+00	.3787E+00
656	.2749E+04	.3496E+03	.9575E+03	.1773E+00	.2728E+00	.4280E+00
657	.2789E+04	.7058E+03	.2093E+04	.2798E+00	.4305E+00	.6455E+00
658	.2528E+04	.1009E+04	.3077E+04	.4184E+00	.6436E+00	.8683E+00
659	.2047E+04	.1214E+04	.3912E+04	.5287E+00	.8134E+00	.1043E+01
660	.1785E+04	.1424E+04	.4719E+04	.6685E+00	.9977E+00	.1269E+01
661	.4005E+04	.1457E+04	.5138E+04	.1924E+00	.2960E+00	.3931E+00
662	.3111E+04	.1575E+04	.5940E+04	.2438E+00	.3750E+00	.4758E+00
663	.2319E+04	.1698E+04	.6666E+04	.2900E+00	.4462E+00	.5579E+00
664	.1888E+04	.1857E+04	.7319E+04	.3211E+00	.4940E+00	.6139E+00
665	.1660E+05	.1937E+04	.7587E+04	.1544E-01	.2375E-01	.3473E-01
666	.1819E+04	.2338E+03	.4714E+03	.1596E+00	.2456E+00	.3394E+00
667	.2633E+04	.5224E+03	.1556E+04	.2073E+00	.3189E+00	.4925E+00
668	.2254E+04	.7964E+03	.2551E+04	.3833E+00	.5897E+00	.7860E+00
669	.2108E+04	.1070E+04	.3566E+04	.5431E+00	.8356E+00	.1052E+01
670	.1068E+04	.1376E+04	.4685E+04	.7848E+00	.1207E+01	.1480E+01
671	.3311E+04	.1292E+04	.5106E+04	.2009E+00	.3091E+00	.3980E+00
672	.2531E+04	.1428E+04	.5588E+04	.2369E+00	.3645E+00	.4729E+00
673	.1988E+04	.1522E+04	.6357E+04	.2867E+00	.4411E+00	.5656E+00
674	.1477E+04	.1556E+04	.6997E+04	.3187E+00	.4904E+00	.6267E+00
675	.1482E+05	.2465E+04	.6898E+04	.1392E-01	.2141E-01	.3350E-01
676	.1183E+04	.7211E+02	.3431E+03	.1581E+00	.2433E+00	.3484E+00
677	.2235E+04	.3052E+03	.1138E+04	.1874E+00	.2883E+00	.4399E+00
678	.1999E+04	.4872E+03	.2255E+04	.3835E+00	.5900E+00	.7760E+00
679	.1989E+04	.5759E+03	.3211E+04	.5605E+00	.8624E+00	.1067E+01
680	.2635E+04	.8497E+03	.4625E+04	.9487E+00	.1460E+01	.1756E+01
681	.1338E+04	.1516E+04	.3593E+04	.1225E+01	.1884E+01	.2246E+01
682	.2872E+04	.1449E+04	.4766E+04	.1988E+00	.3059E+00	.3794E+00
683	.2258E+04	.1431E+04	.5243E+04	.2303E+00	.3544E+00	.4673E+00
684	.1781E+04	.1506E+04	.6016E+04	.2842E+00	.4372E+00	.5750E+00
685	.1557E+04	.1672E+04	.6665E+04	.3172E+00	.4880E+00	.6449E+00
686	.1380E+05	.1719E+04	.6976E+04	.1611E-01	.2171E-01	.3300E-01
687	.1371E+05	.1927E+04	.7898E+04	.1537E-01	.2364E-01	.3539E-01
688	.3637E+04	.2157E+04	.9547E+04	.6619E-01	.1018E+00	.1486E+00
689	.3276E+04	.2379E+04	.1084E+05	.7606E-01	.1170E+00	.1722E+00
690	.2930E+04	.2504E+04	.1208E+05	.8574E-01	.1319E+00	.1909E+00
691	.1669E+04	.5085E+02	.7543E+03	.1759E+00	.2706E+00	.3909E+00
692	.1546E+04	.2395E+03	.1935E+04	.3487E+00	.5365E+00	.7013E+00
693	.1488E+04	.4313E+03	.2871E+04	.4886E+00	.7517E+00	.9316E+00
694	.6432E+03	.3254E+03	.3584E+04	.1327E+01	.2042E+01	.2422E+01
695	.2072E+04	.5627E+03	.6616E+04	.2041E+00	.3140E+00	.3805E+00
696	.1948E+04	.7857E+03	.5012E+04	.2321E+00	.3571E+00	.4723E+00
697	.1605E+04	.9208E+03	.5702E+04	.2782E+00	.4279E+00	.5815E+00
698	.1240E+04	.1029E+04	.6389E+04	.3156E+00	.4855E+00	.6601E+00
699	.1349E+05	.1112E+04	.7403E+04	.1514E-01	.2330E-01	.3342E-01
700	.1132E+04	.4184E+02	.7112E+03	.1470E+00	.2262E+00	.3307E+00
701	.1007E+04	.1103E+03	.1747E+04	.3197E+00	.4918E+00	.6496E+00
702	.1000E+04	.1978E+03	.2791E+04	.4660E+00	.7169E+00	.8942E+00
703	.3757E+03	.2835E+03	.3645E+04	.1626E+01	.2190E+01	.2592E+01
704	.1811E+04	.2310E+03	.4189E+04	.2032E+00	.3126E+00	.3803E+00
705	.1679E+04	.4055E+03	.4770E+04	.2278E+00	.3504E+00	.4684E+00
706	.1411E+04	.5589E+03	.5426E+04	.2662E+00	.4095E+00	.5759E+00

707	.1045E+04	.6860E+03	.6115E+04	.3058E+00	.4705E+00	.6601E+00
708	.1388E+05	.1311E+04	.6309E+04	.1612E-01	.2172E-01	.3242E-01
709	.6469E+03	.9613E+02	.6834E+03	.1084E+00	.1671E+00	.2433E+00
710	.7000E+03	.2873E+03	.1710E+04	.2766E+00	.4255E+00	.5607E+00
711	.6971E+03	.4233E+03	.2581E+04	.4402E+00	.6772E+00	.8454E+00
712	.4806E+03	.5196E+03	.3584E+04	.1433E+01	.2205E+01	.2606E+01
713	.1666E+04	.6589E+03	.6049E+04	.2045E+00	.3146E+00	.3817E+00
714	.1506E+04	.7773E+03	.4619E+04	.2311E+00	.3555E+00	.4752E+00
715	.1265E+04	.9177E+03	.5277E+04	.2637E+00	.4056E+00	.5781E+00
716	.1008E+04	.1019E+04	.5871E+04	.2970E+00	.4569E+00	.6587E+00
717	.1292E+05	.1091E+04	.6523E+04	.1393E-01	.2143E-01	.3186E-01
718	.1262E+05	.1720E+04	.7781E+04	.1546E-01	.2378E-01	.3522E-01
719	.3311E+04	.1779E+04	.9554E+04	.6651E-01	.1023E+00	.1472E+00
720	.3079E+04	.1890E+04	.1089E+05	.7675E-01	.1181E+00	.1719E+00
721	.2970E+04	.2011E+04	.1216E+05	.8679E-01	.1335E+00	.1916E+00
722	.8958E+03	.3922E+03	.5443E+03	.1437E+00	.2210E+00	.3062E+00
723	.1016E+04	.3978E+03	.1314E+04	.2769E+00	.4259E+00	.5475E+00
724	.1055E+04	.6659E+03	.2261E+04	.3988E+00	.6135E+00	.7716E+00
725	.8371E+03	.9711E+03	.3283E+04	.1445E+01	.2223E+01	.2633E+01
726	.1503E+04	.1141E+04	.3831E+04	.2144E+00	.3299E+00	.3958E+00
727	.1341E+04	.1272E+04	.4453E+04	.2478E+00	.3813E+00	.4995E+00
728	.1111E+04	.1402E+04	.5128E+04	.2805E+00	.4315E+00	.6019E+00
729	.1055E+04	.1503E+04	.5678E+04	.3008E+00	.4627E+00	.6705E+00
730	.1192E+05	.1759E+04	.6599E+04	.1388E-01	.2136E-01	.3141E-01
731	.1230E+05	.1304E+04	.7866E+04	.1564E-01	.2406E-01	.3519E-01
732	.3243E+04	.1488E+04	.9521E+04	.6646E-01	.1022E+00	.1465E+00
733	.3262E+04	.1619E+04	.1092E+05	.7729E-01	.1189E+00	.1722E+00
734	.3202E+04	.1723E+04	.1223E+05	.8772E-01	.1349E+00	.1927E+00
735	.1325E+04	.5384E+03	.8248E+03	.3610E+00	.5554E+00	.7007E+00
736	.1717E+04	.6817E+03	.1631E+04	.3354E+00	.5160E+00	.6617E+00
737	.8791E+03	.8986E+03	.2859E+04	.1470E+01	.2262E+01	.2703E+01
738	.1352E+04	.1111E+04	.3652E+04	.2302E+00	.3542E+00	.4220E+00
739	.1194E+04	.1217E+04	.4346E+04	.2698E+00	.4151E+00	.5307E+00
740	.9898E+03	.1321E+04	.5003E+04	.3021E+00	.4648E+00	.6314E+00
741	.9362E+03	.1440E+04	.5588E+04	.3185E+00	.4899E+00	.6905E+00
742	.1118E+05	.1054E+04	.6260E+04	.1264E-01	.1945E-01	.2933E-01
743	.1467E+04	.1974E+03	.1081E+04	.2101E+00	.3232E+00	.4528E+00
744	.5896E+03	.4382E+03	.2531E+04	.1432E+01	.2203E+01	.2674E+01
745	.1221E+04	.6092E+03	.3436E+04	.2248E+00	.3459E+00	.4168E+00
746	.1052E+04	.7462E+03	.4256E+04	.2776E+00	.4271E+00	.5432E+00
747	.8741E+03	.8562E+03	.4951E+04	.3127E+00	.4810E+00	.6457E+00
748	.7560E+03	.9389E+03	.5533E+04	.3315E+00	.5100E+00	.7062E+00
749	.1095E+05	.9059E+03	.6892E+04	.1334E-01	.2052E-01	.2994E-01
750	.1011E+04	.7707E+02	.8667E+03	.1456E+00	.2240E+00	.3374E+00
751	.2760E+03	.1987E+03	.2335E+04	.1369E+01	.2106E+01	.2608E+01
752	.1034E+04	.2775E+03	.3275E+04	.2151E+00	.3309E+00	.4004E+00
753	.8717E+03	.3416E+03	.4160E+04	.2794E+00	.4299E+00	.5474E+00
754	.7430E+03	.6275E+03	.4911E+04	.3189E+00	.4907E+00	.6543E+00
755	.5916E+03	.5145E+03	.5491E+04	.3391E+00	.5217E+00	.7164E+00
756	.1080E+05	.7164E+03	.6430E+04	.1281E-01	.1971E-01	.2897E-01
757	.1157E+05	.9763E+03	.7817E+04	.1531E-01	.2356E-01	.3453E-01
758	.3325E+04	.9860E+03	.9409E+04	.6573E-01	.1011E+00	.1455E+00
759	.3662E+04	.1114E+04	.1088E+05	.7728E-01	.1189E+00	.1722E+00
760	.3880E+04	.1213E+04	.1228E+05	.8864E-01	.1364E+00	.1939E+00
761	.7156E+03	.2673E+02	.8362E+03	.1567E+00	.2411E+00	.3376E+00
762	.1820E+03	.1121E+03	.2303E+04	.1362E+01	.2096E+01	.2626E+01
763	.7958E+03	.1664E+03	.3205E+04	.2217E+00	.3410E+00	.4073E+00
764	.6730E+03	.2373E+03	.4152E+04	.2902E+00	.4464E+00	.5616E+00
765	.5768E+03	.2732E+03	.4929E+04	.3290E+00	.5061E+00	.6673E+00
766	.4454E+03	.2763E+03	.5520E+04	.3477E+00	.5350E+00	.7261E+00
767	.9666E+04	.6089E+03	.6694E+04	.1224E-01	.1884E-01	.2708E-01
768	.1126E+05	.5261E+03	.7650E+04	.1473E-01	.2266E-01	.3293E-01
769	.3467E+04	.6934E+03	.9306E+04	.6484E-01	.9973E-01	.1437E+00
770	.4361E+04	.7907E+03	.1066E+05	.7567E-01	.1164E+00	.1705E+00
771	.4743E+04	.1113E+04	.1212E+05	.8815E-01	.1356E+00	.1943E+00
772	.5990E+03	.5255E+02	.8297E+03	.1651E+00	.2540E+00	.3446E+00

773	.1493E+03	.9810E+02	.2305E+04	.1615E+01	.2177E+01	.2717E+01
774	.6373E+03	.1639E+03	.3232E+04	.2322E+00	.3572E+00	.4205E+00
775	.5125E+03	.2169E+03	.4185E+04	.3043E+00	.4682E+00	.5802E+00
776	.4166E+03	.2582E+03	.4994E+04	.3422E+00	.5265E+00	.6834E+00
777	.3226E+03	.2721E+03	.5616E+04	.3612E+00	.5556E+00	.7610E+00
778	.8561E+04	.3181E+03	.6758E+04	.1215E-01	.1870E-01	.2570E-01
779	.1032E+05	.4391E+03	.8081E+04	.1681E-01	.2278E-01	.3168E-01
780	.3445E+04	.8605E+03	.9548E+04	.6633E-01	.1021E+00	.1430E+00
781	.3949E+04	.1062E+04	.1058E+05	.7442E-01	.1145E+00	.1675E+00
782	.6960E+04	.1824E+04	.1102E+05	.7943E-01	.1222E+00	.1879E+00

## **APPENDIX C**

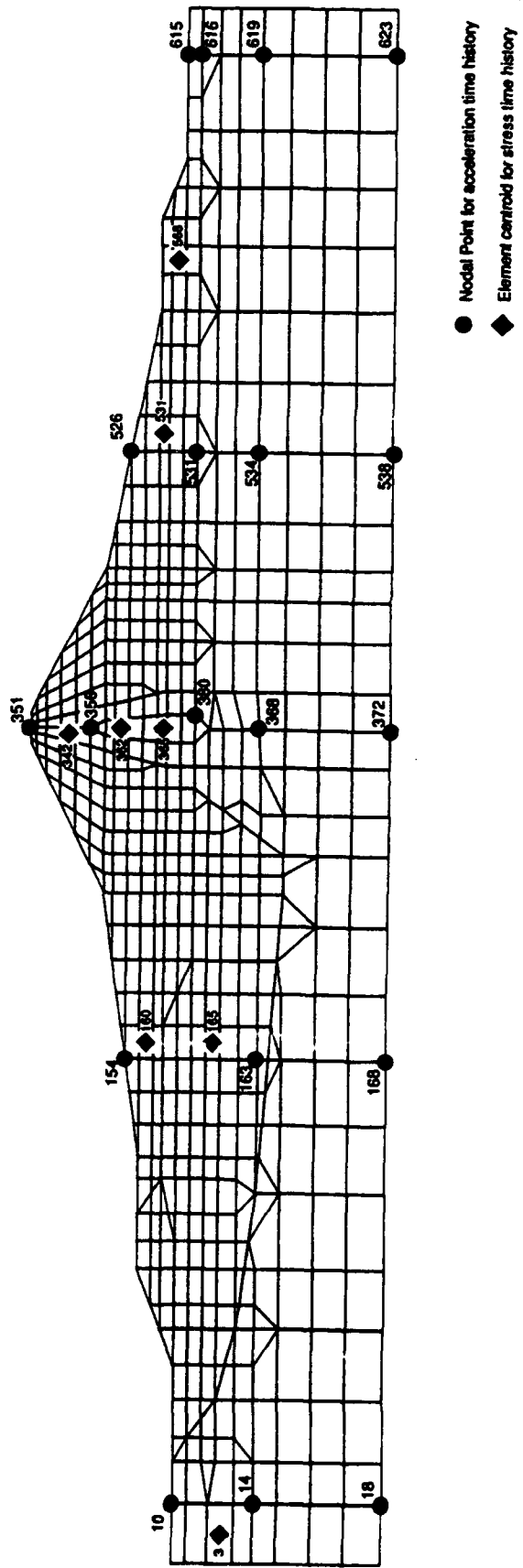


**Figure C-1.** Location of nodal points and element centroids in section B8 for time history output

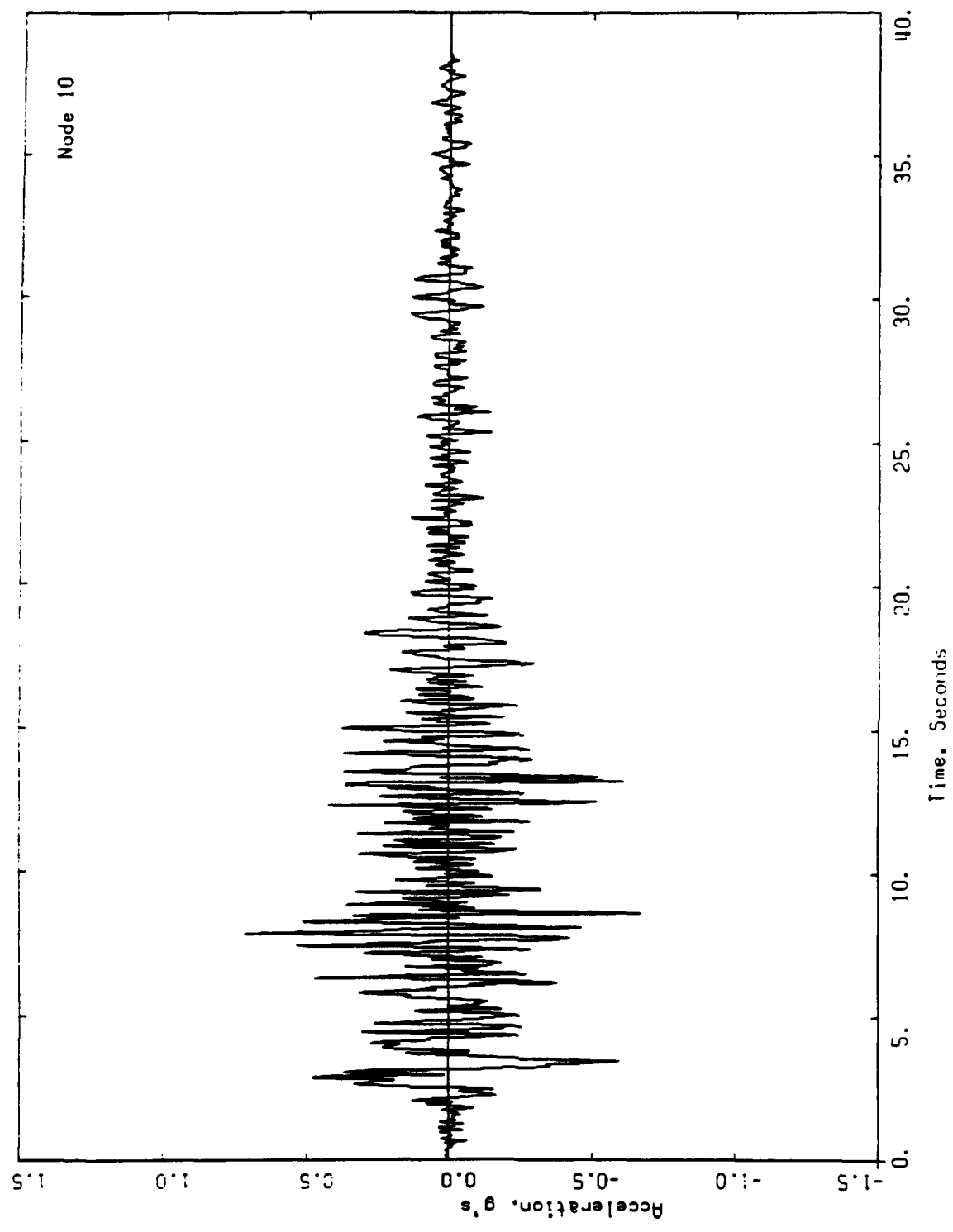


Figure C-2. Acceleration time history at nodal point 10

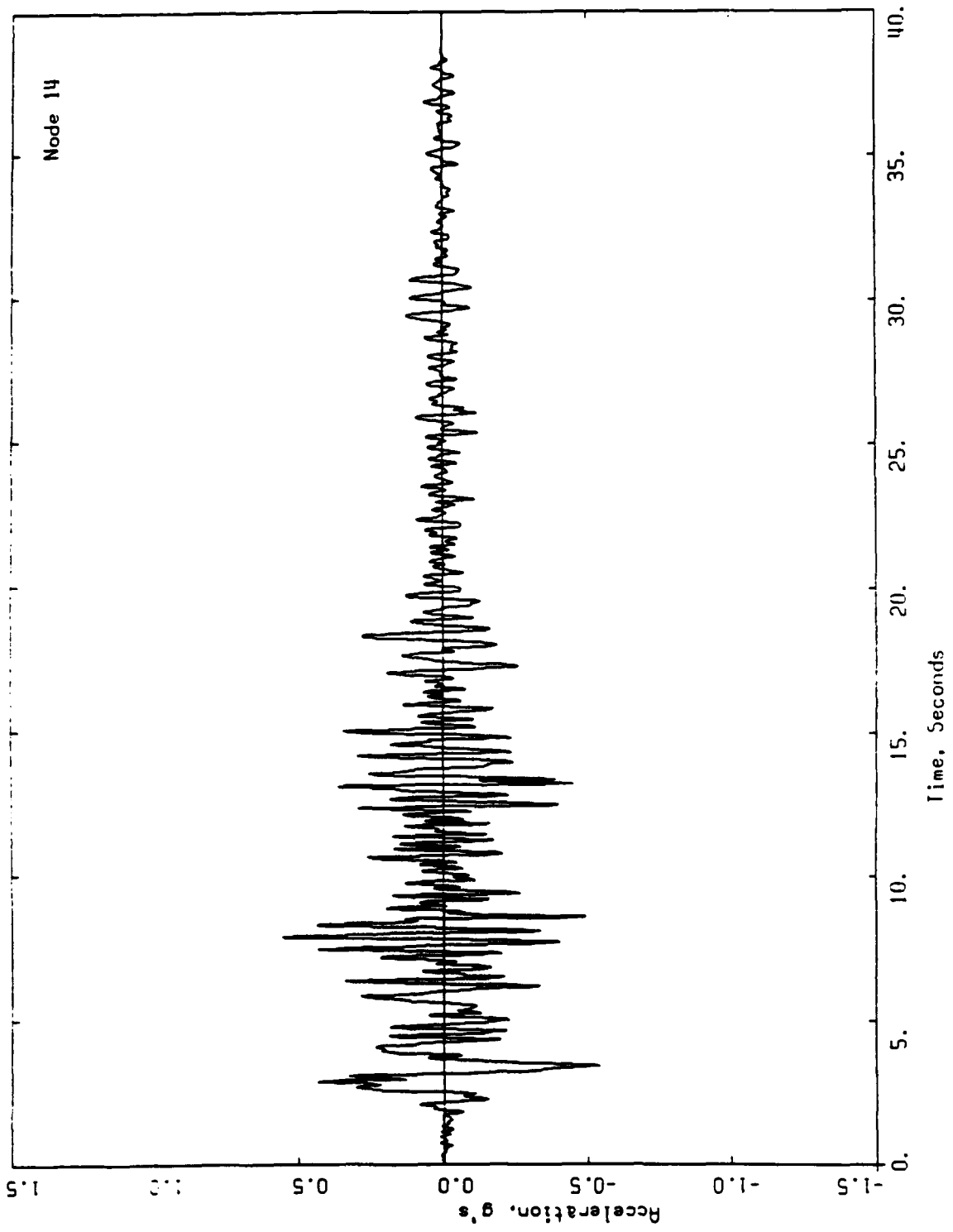


Figure C-3. Acceleration time history at nodal point 14

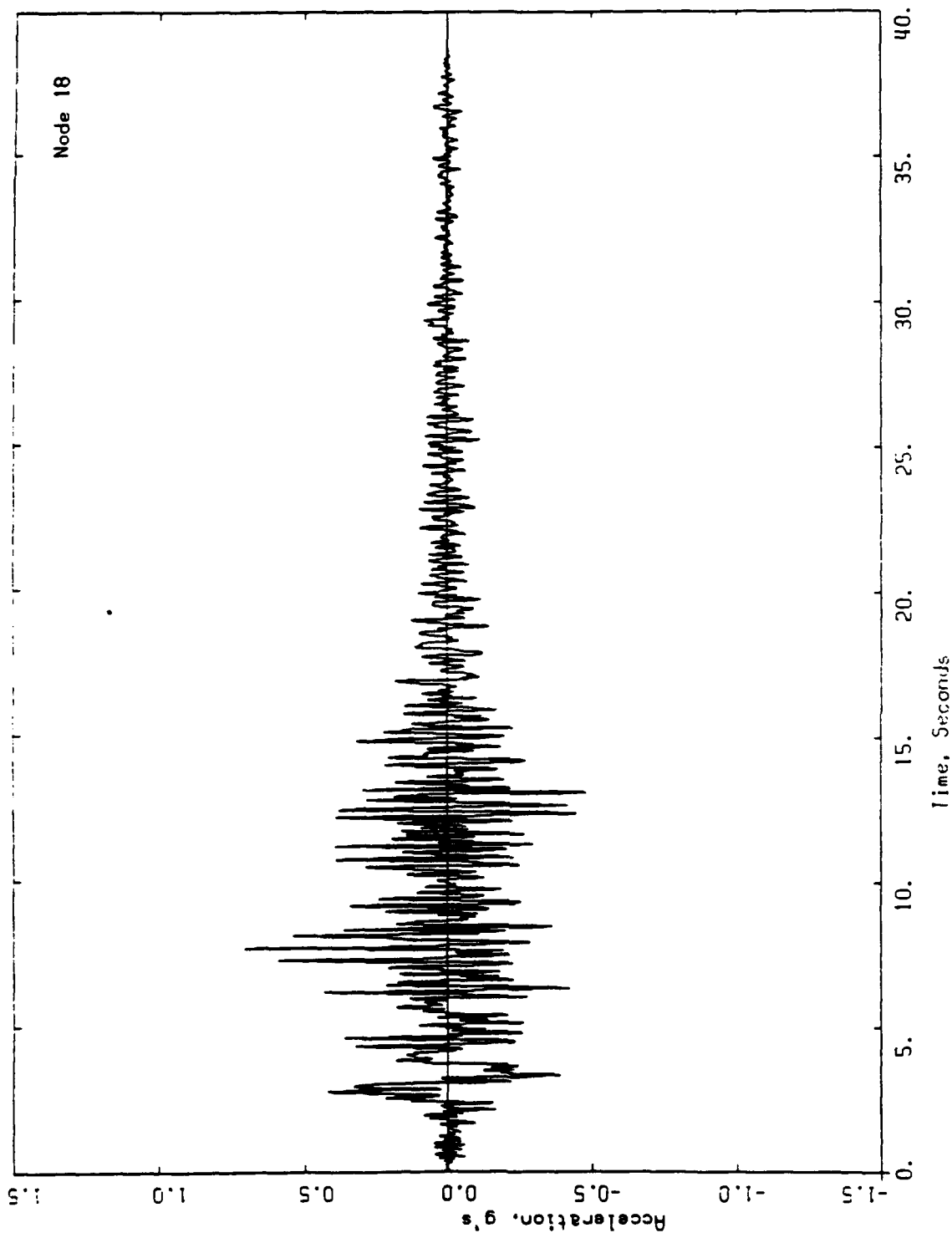


Figure C-4. Acceleration time history at nodal point 18

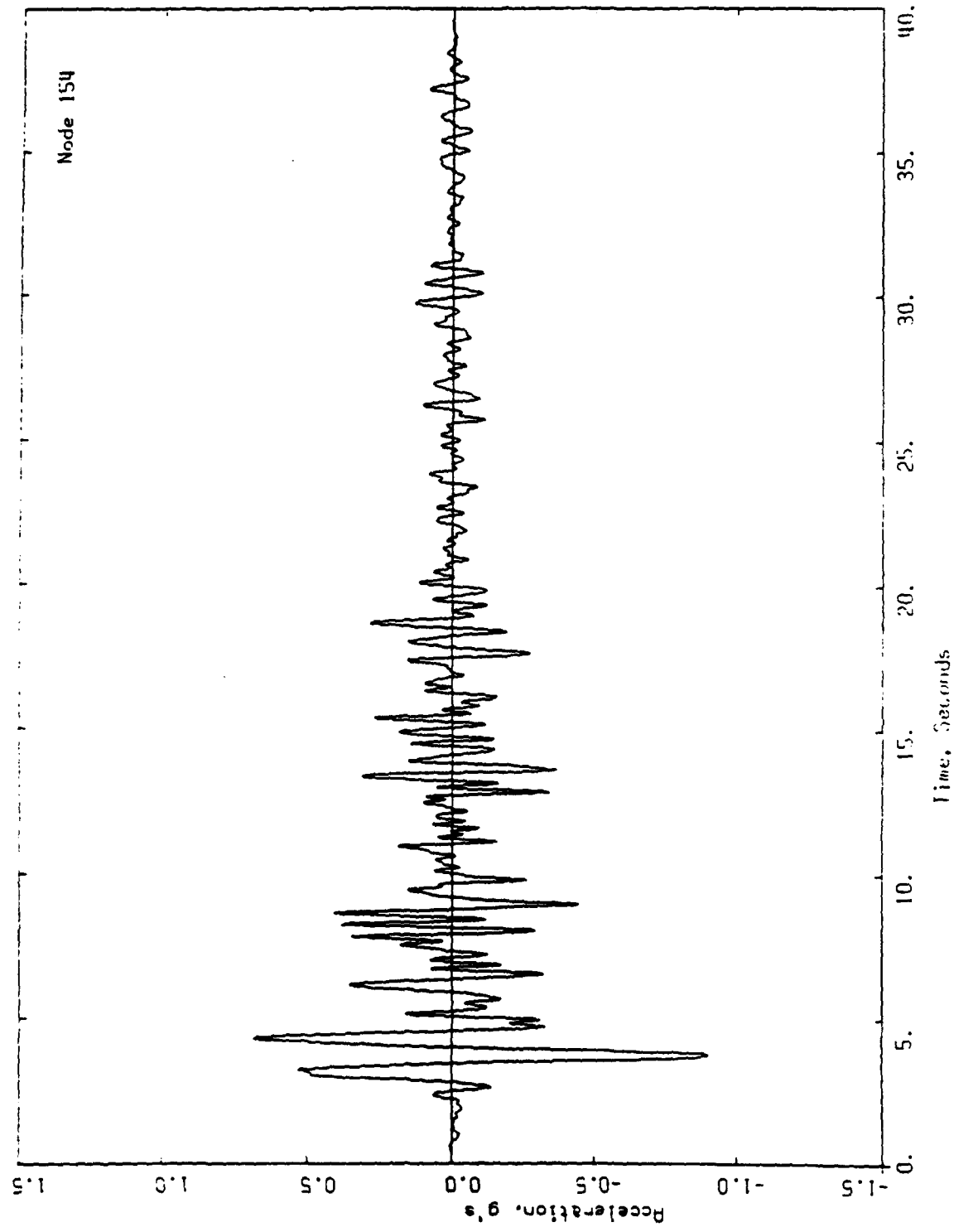


Figure C-5. Acceleration time history at nodal point 154

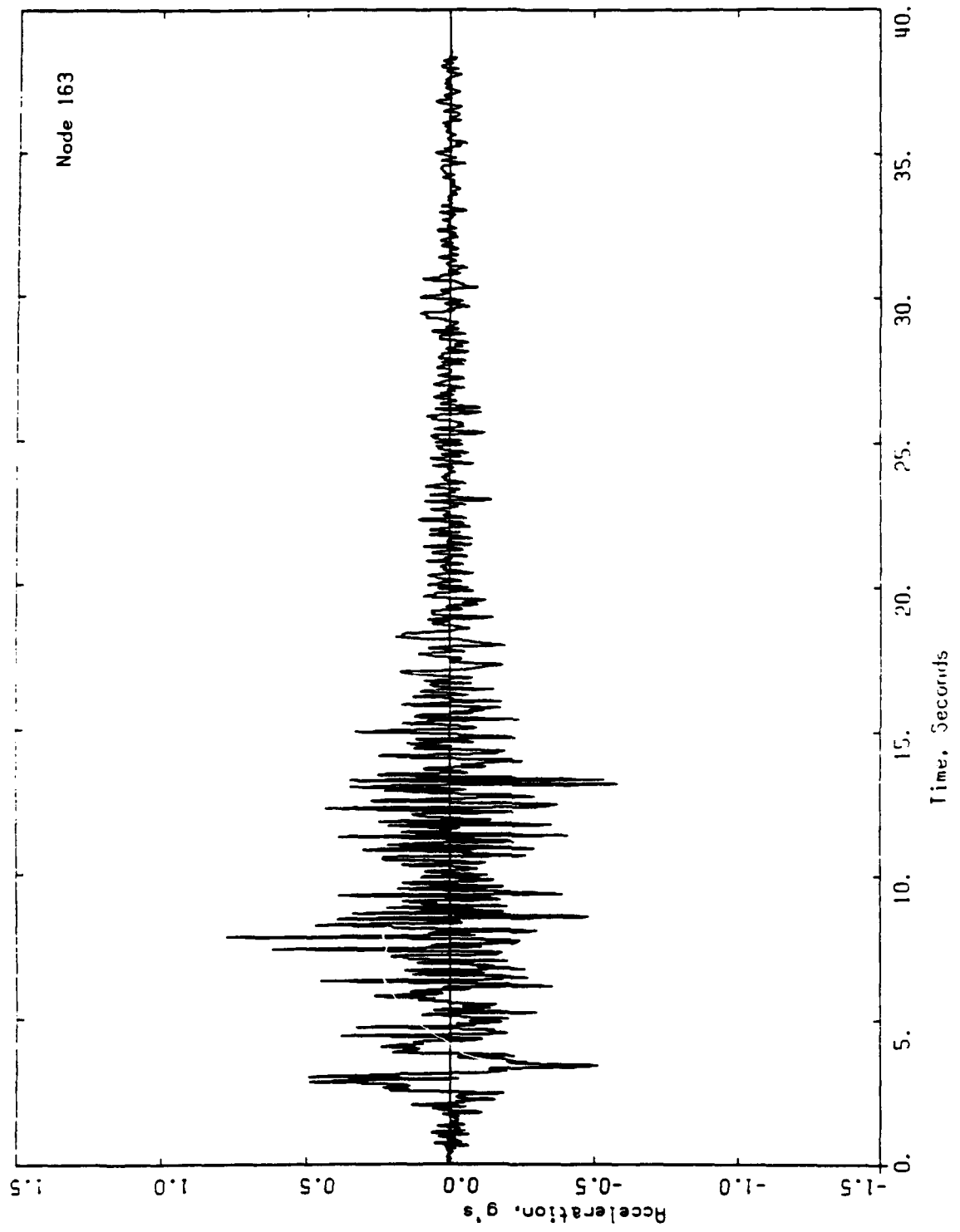


Figure C-6. Acceleration time history at nodal point 163

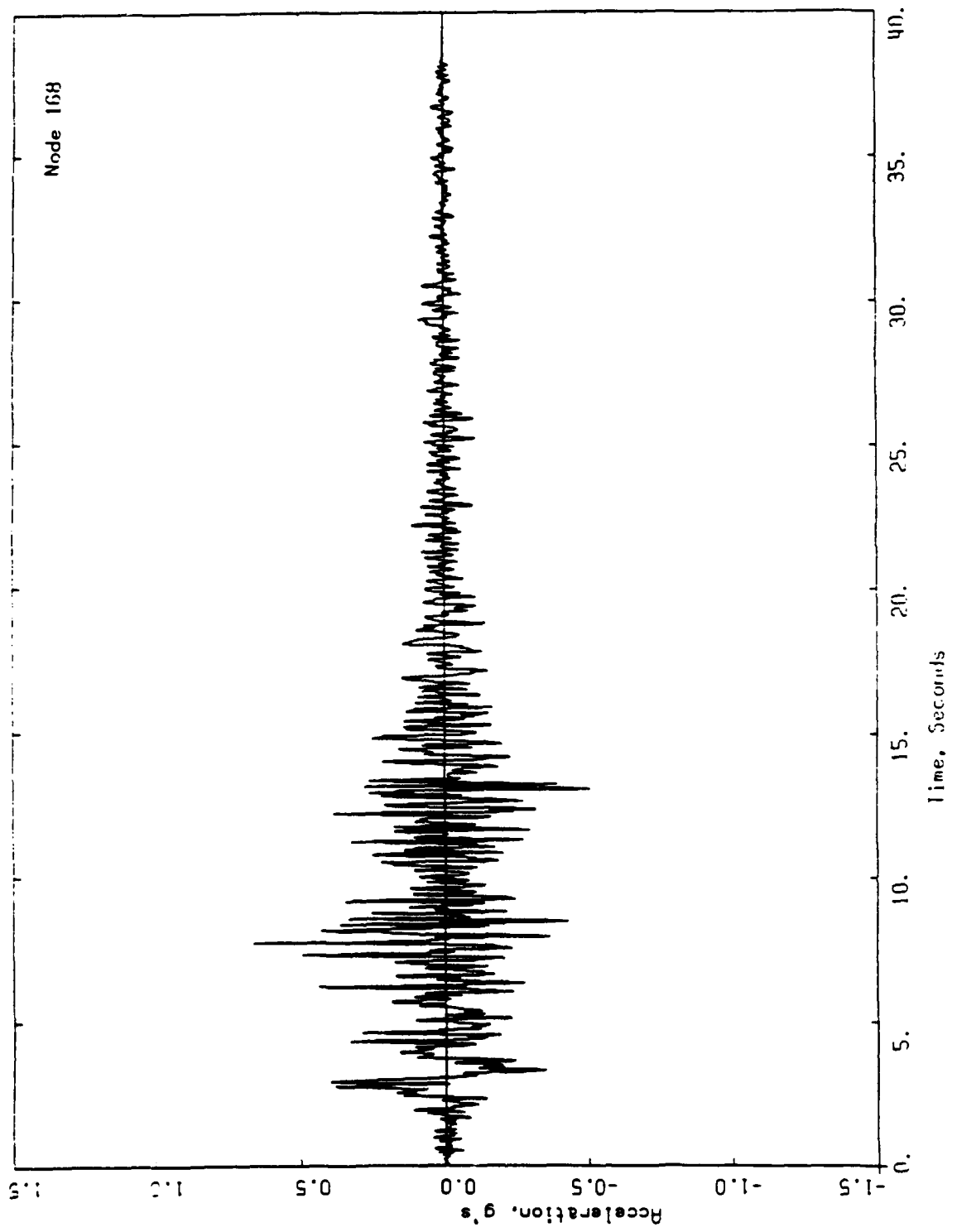


Figure C-7. Acceleration time history at nodal point 168

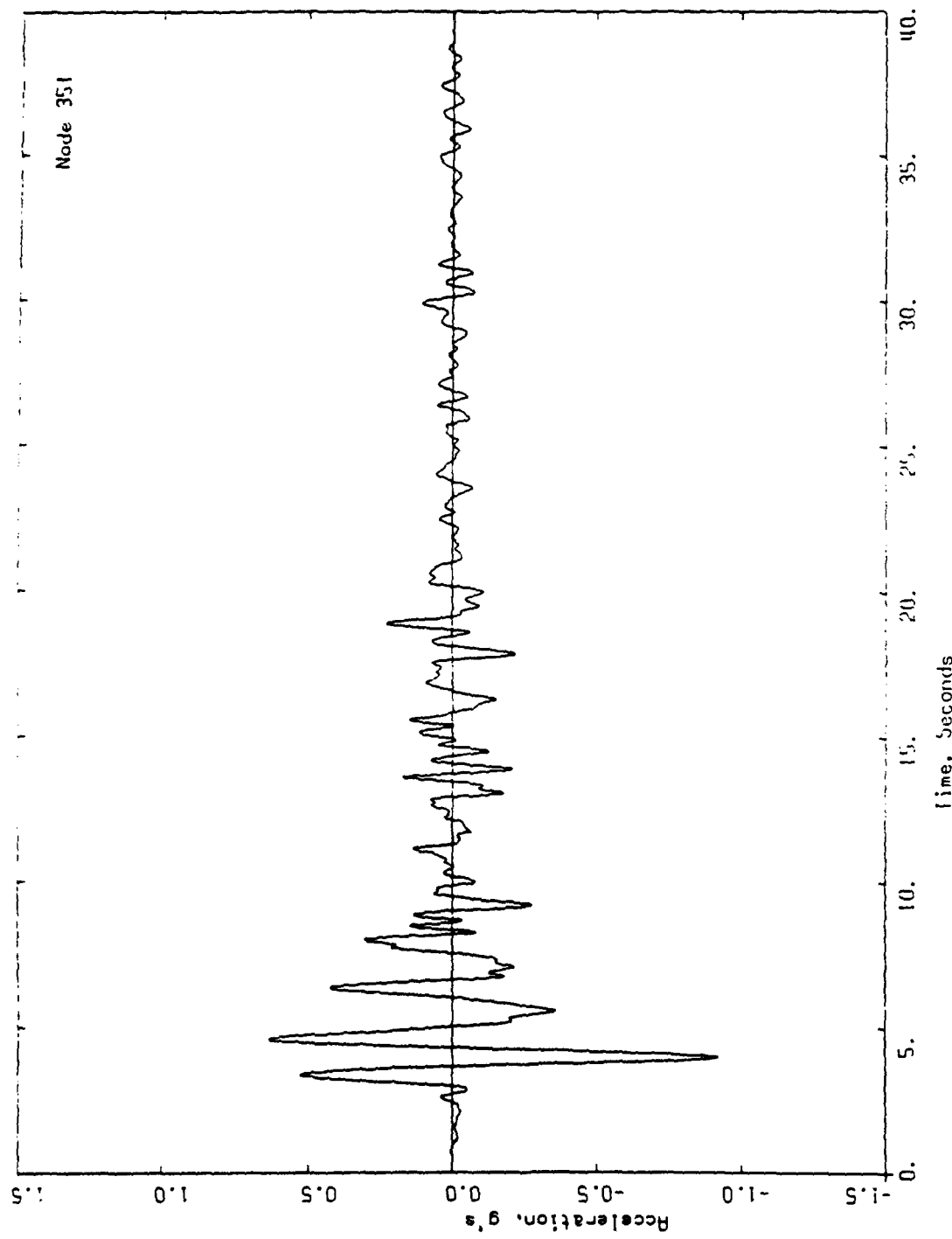


Figure C-8. Acceleration time history at nodal point 351

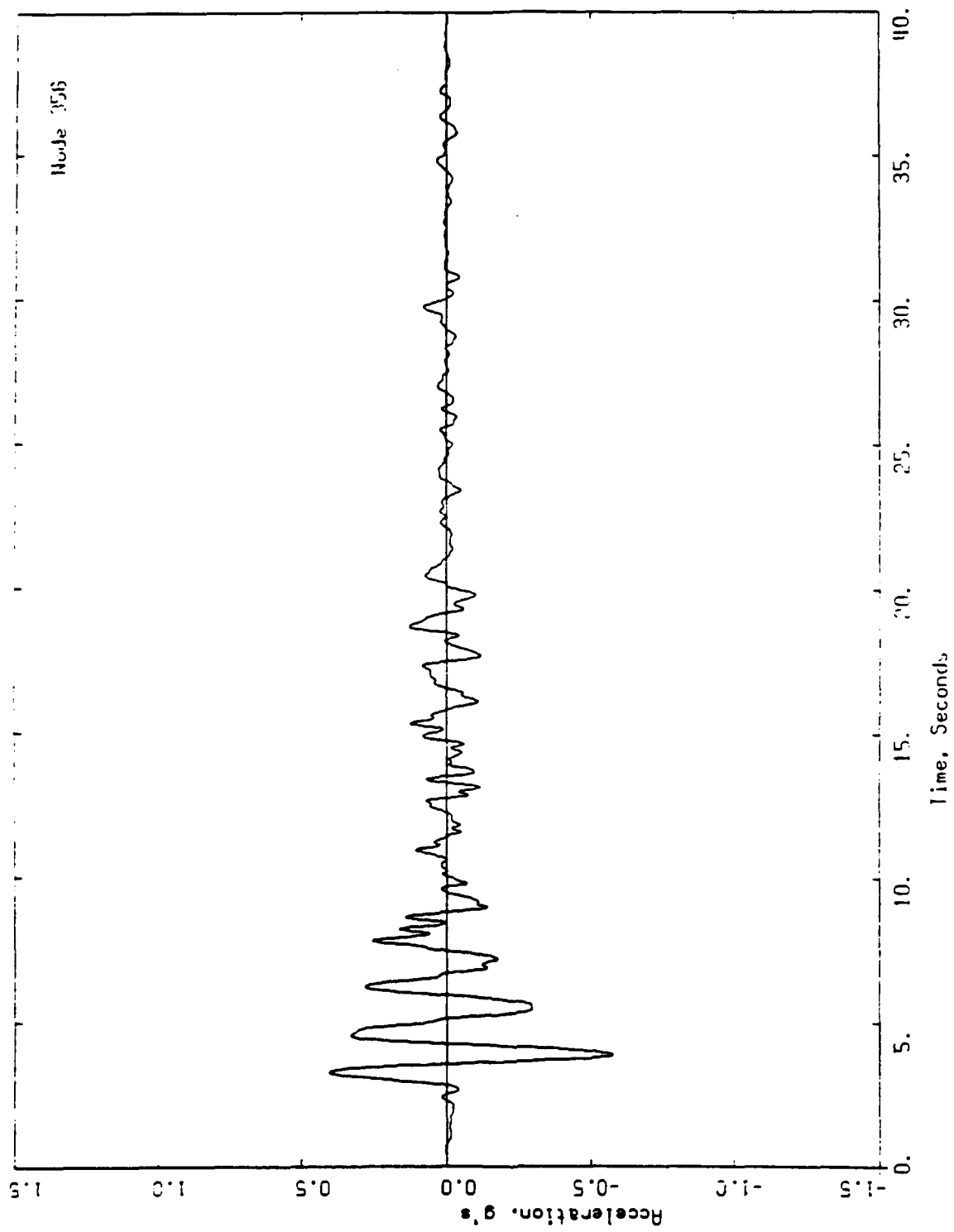


Figure C-9. Acceleration time history at nodal point 356

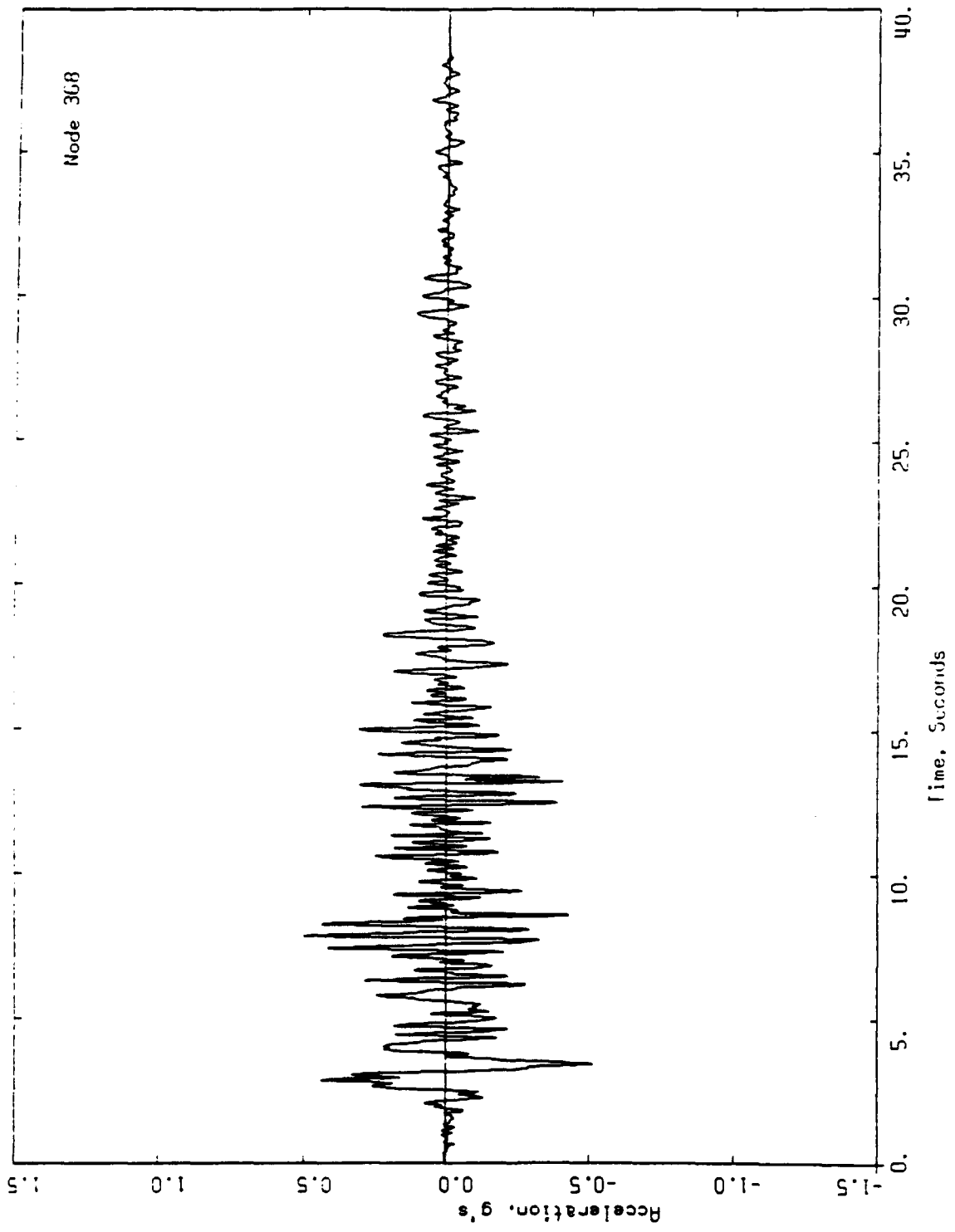


Figure C-10. Acceleration time history at nodal point 368

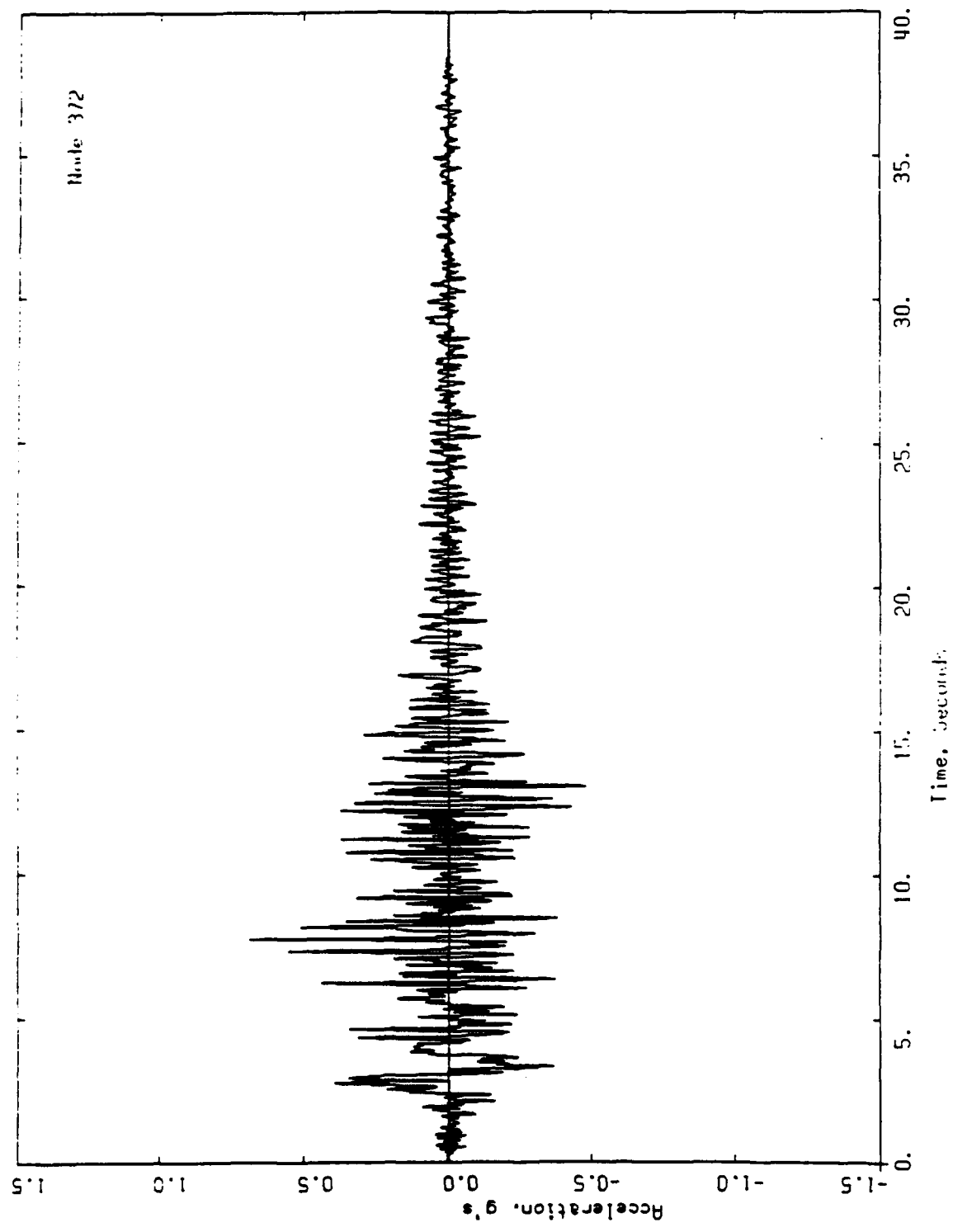


Figure C-11. Acceleration time history at nodal point 372

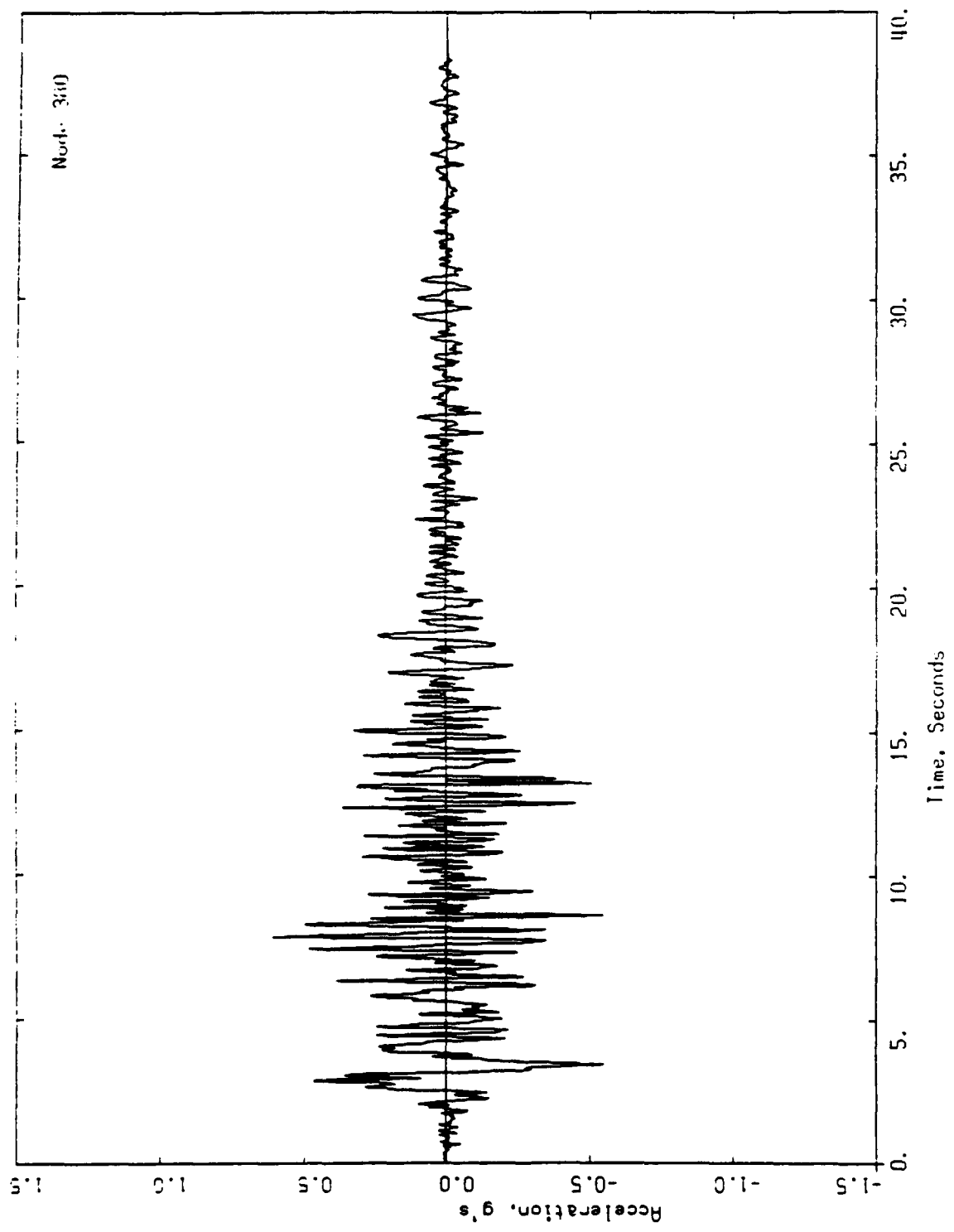


Figure C-12. Acceleration time history at nodal point 360

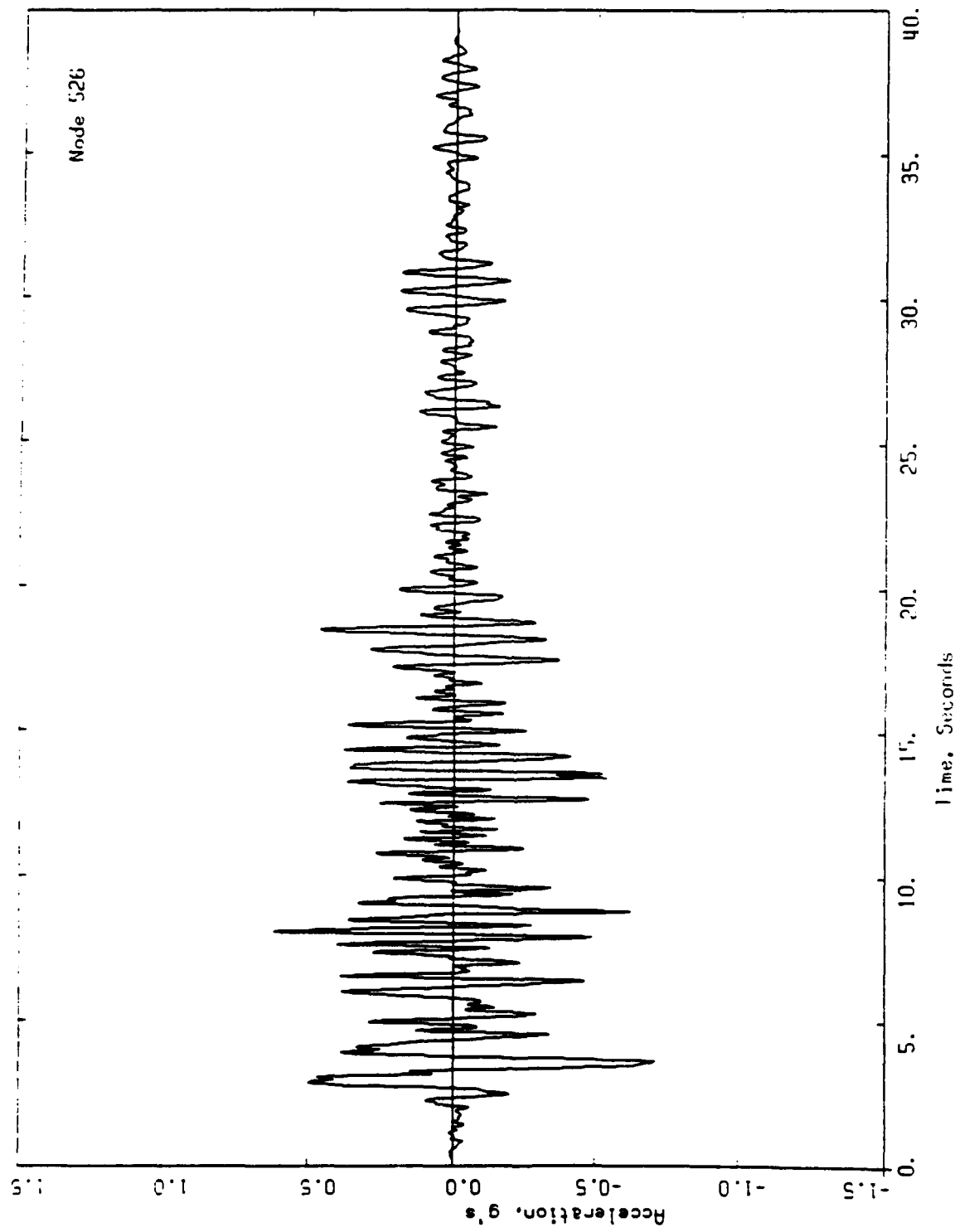


Figure C-13. Acceleration time history at nodal point 526

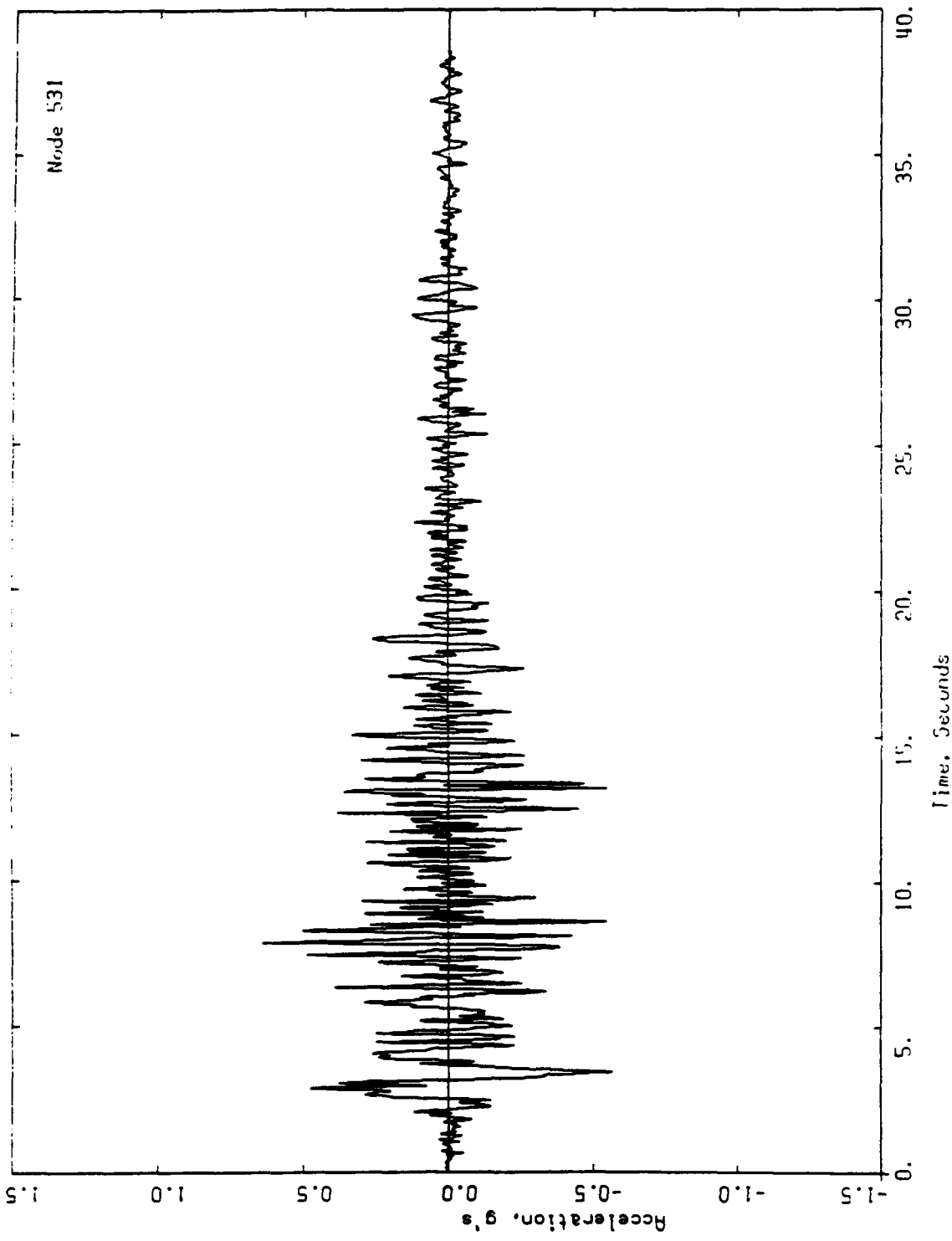


Figure C-14. Acceleration time history at nodal point 531

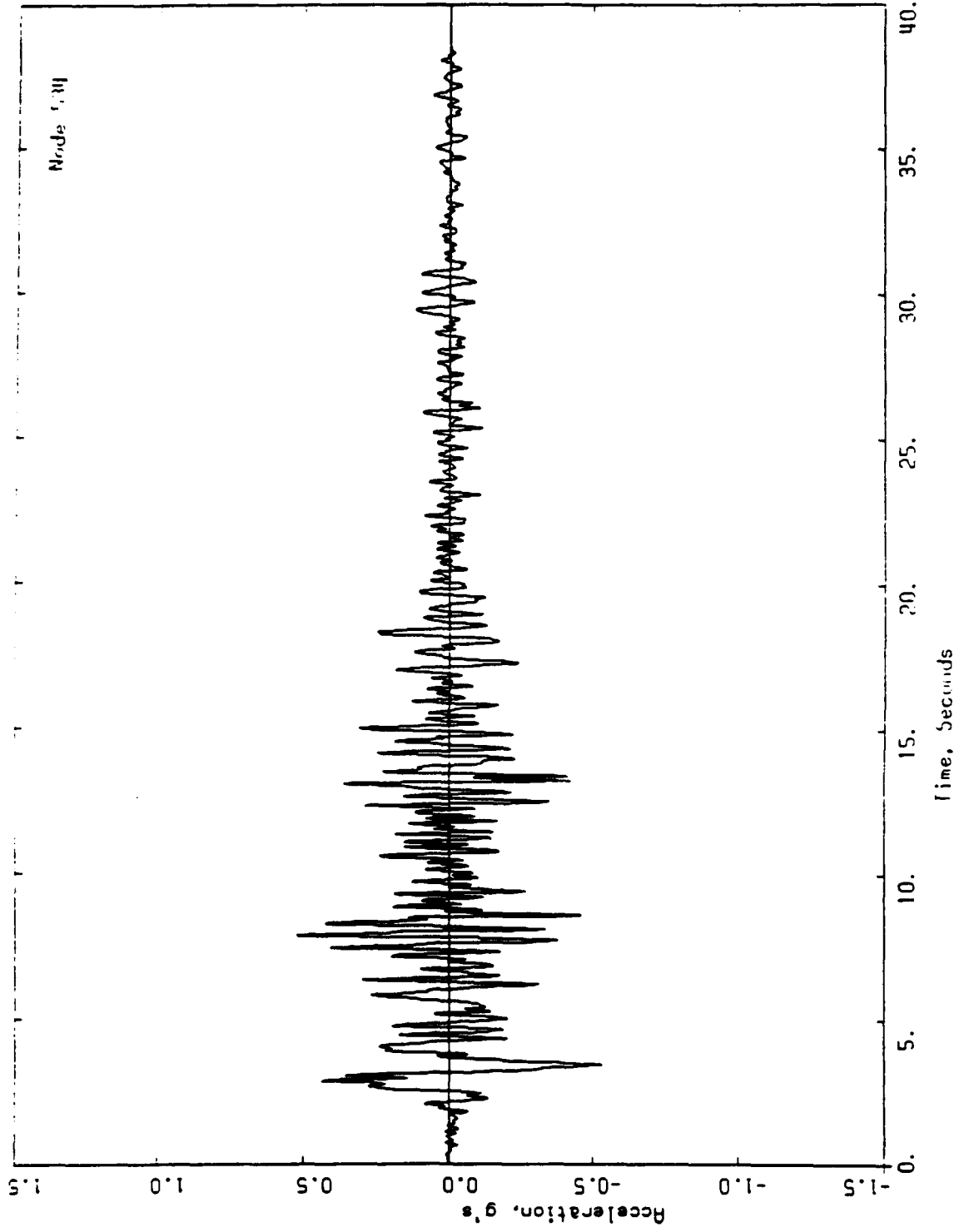


Figure C-15. Acceleration time history at nodal point 534

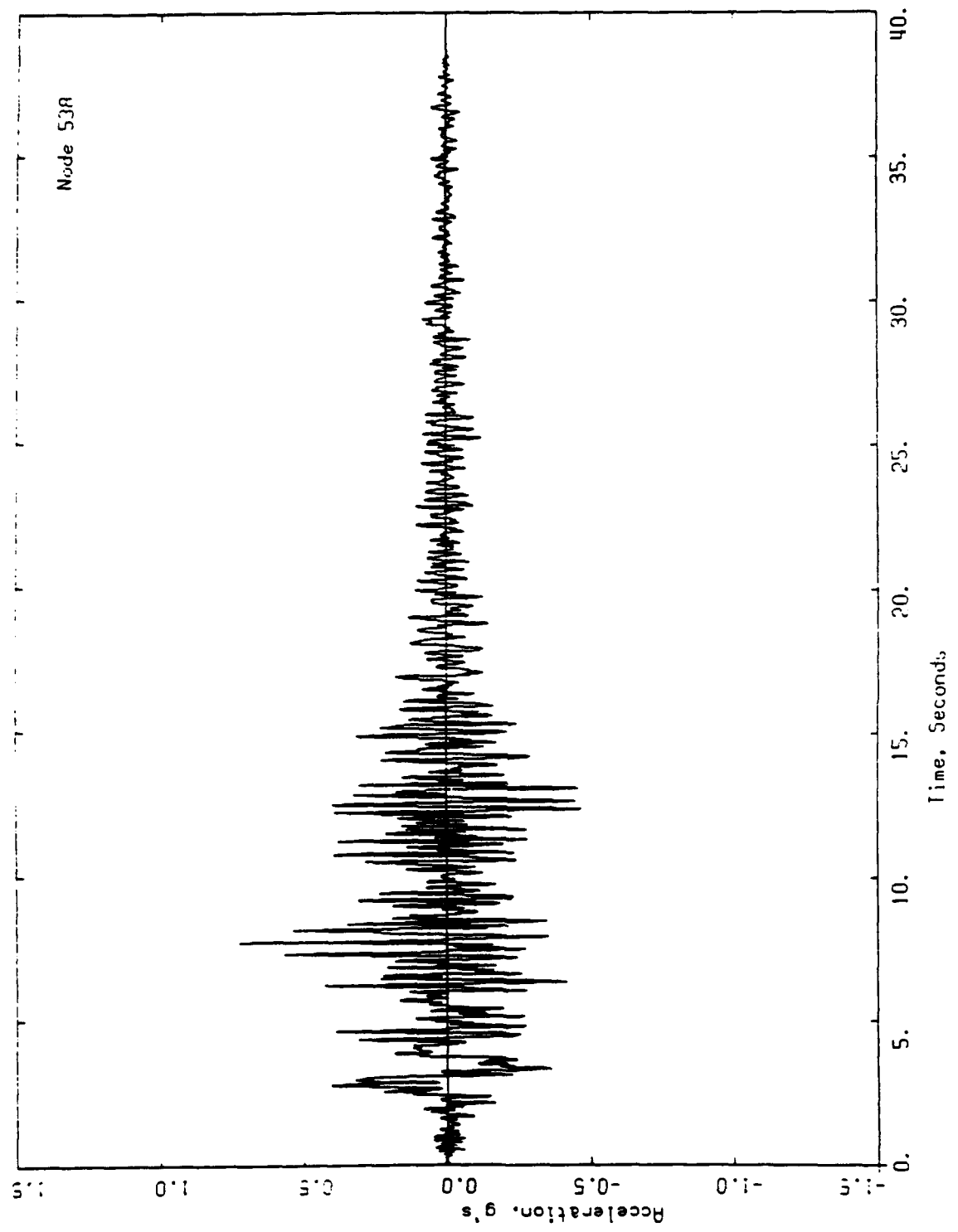


Figure C-16. Acceleration time history at nodal point 538

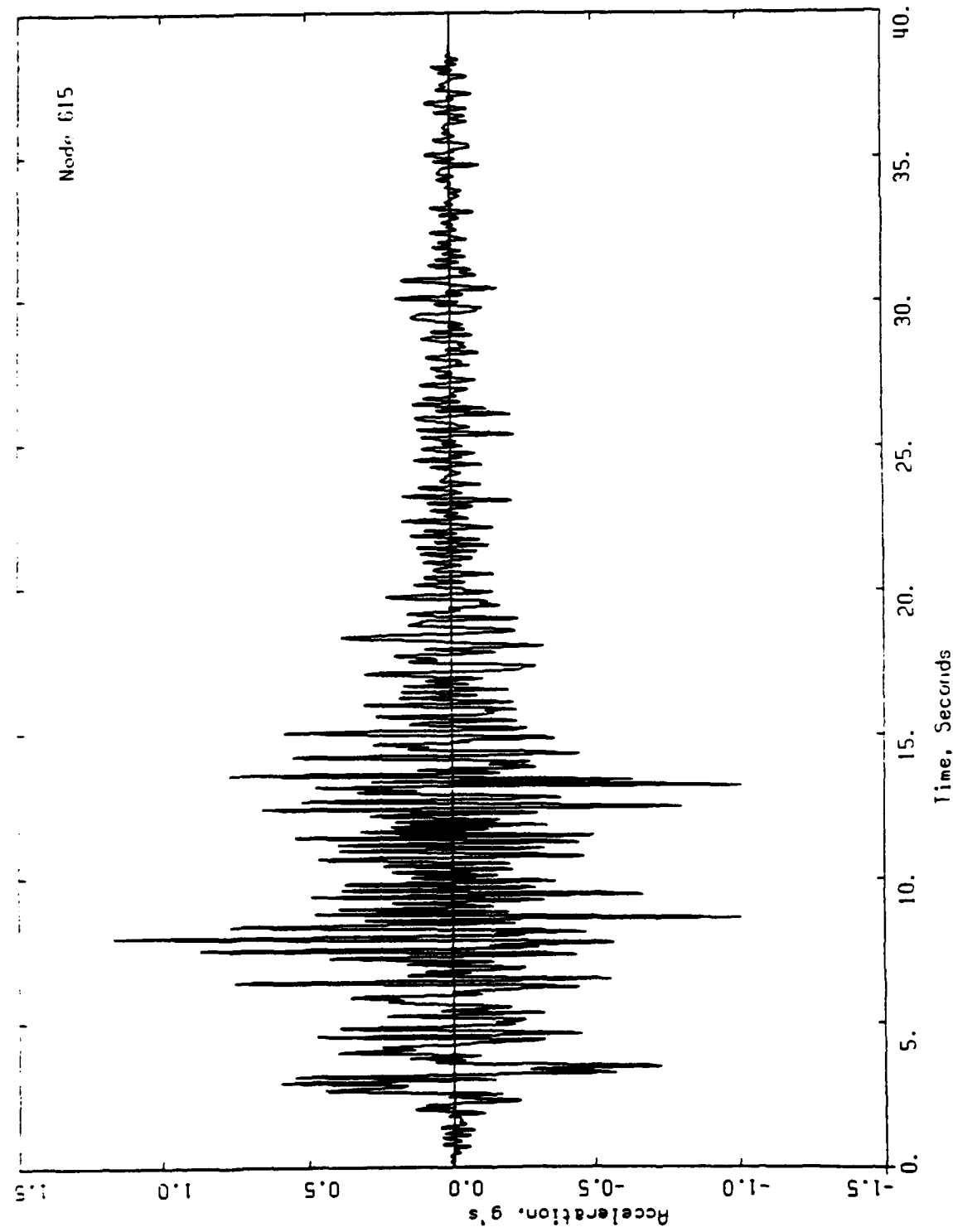


Figure C-17. Acceleration time history at nodal point 615

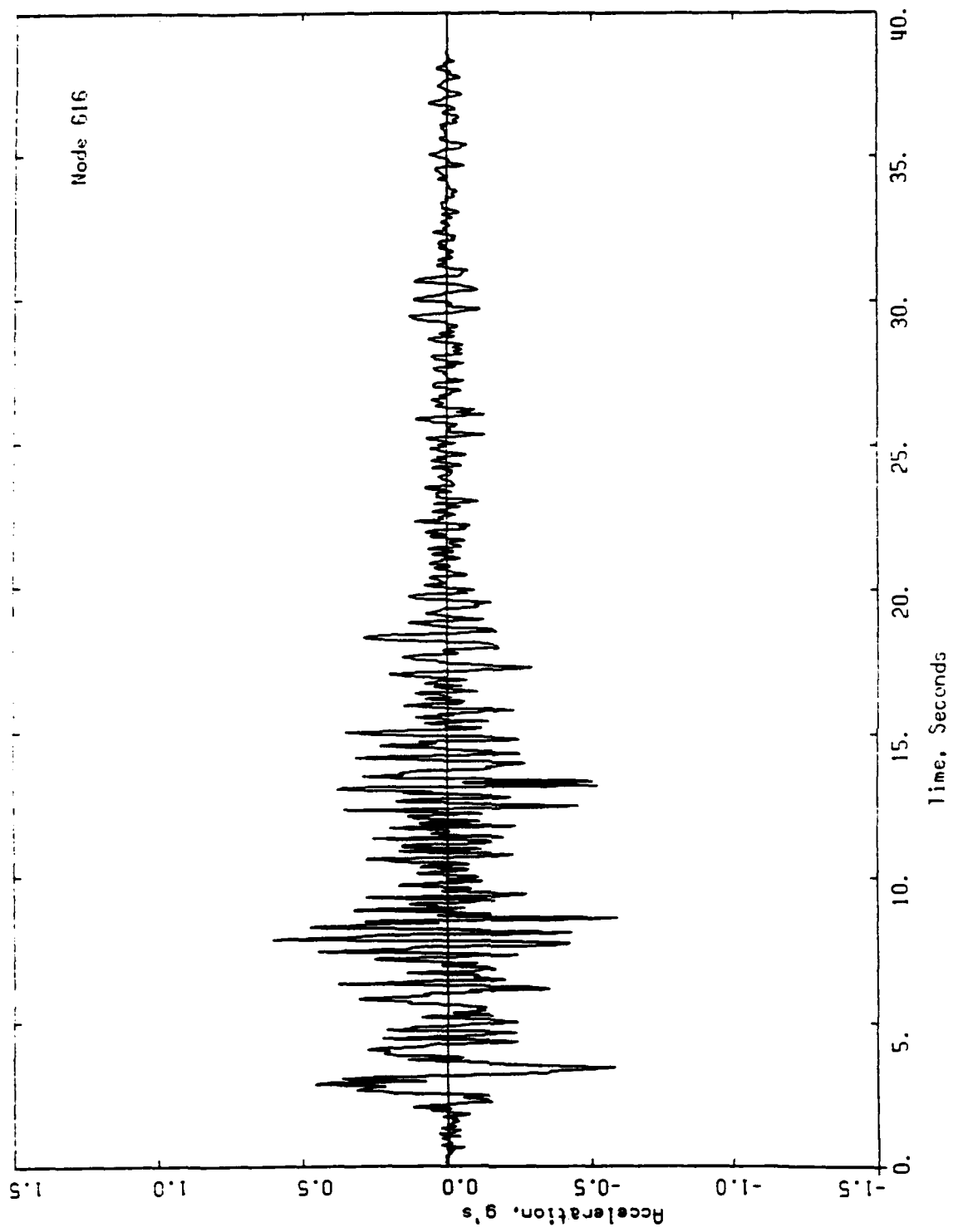


Figure C-18. Acceleration time history at nodal point 616

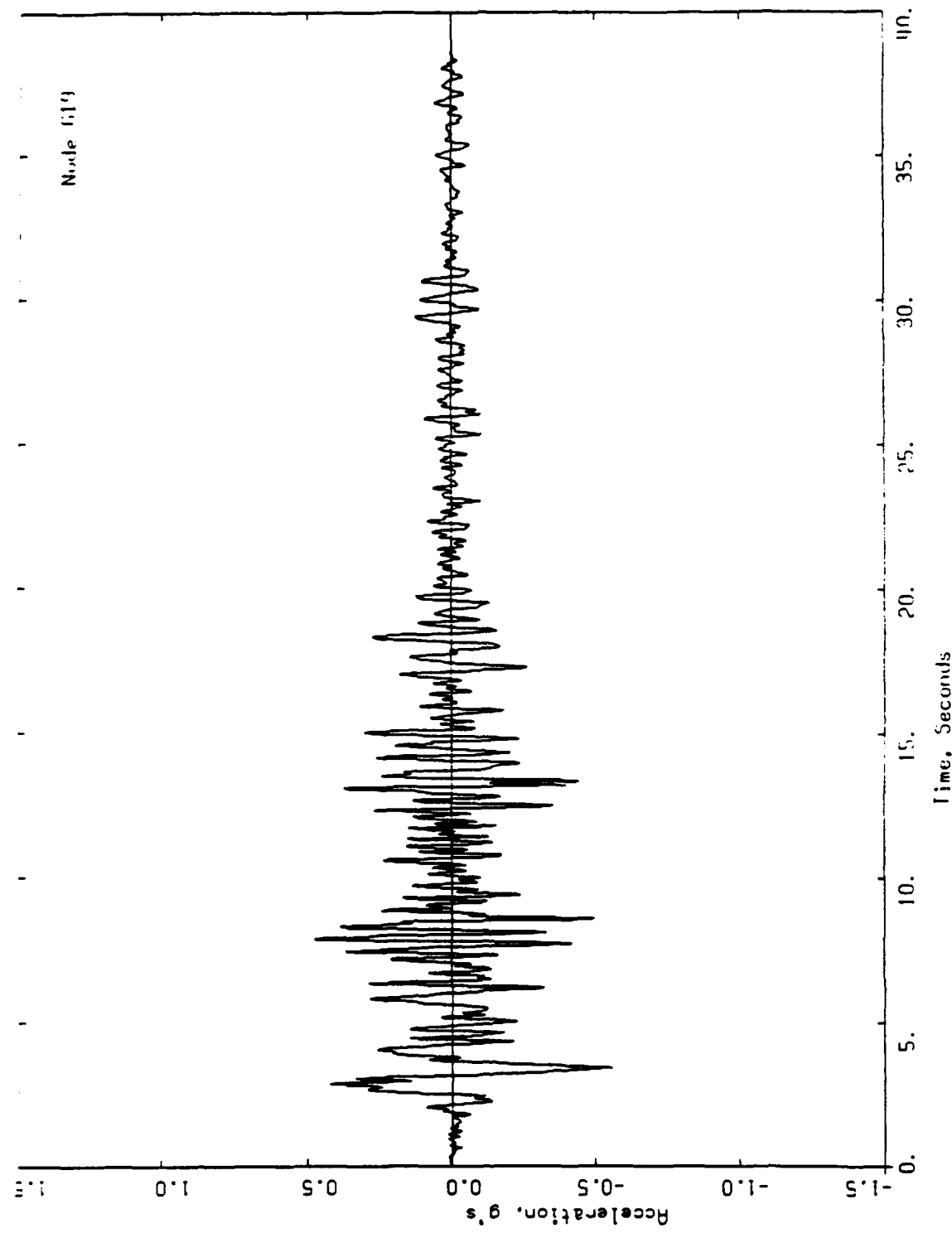


Figure C-19. Acceleration time history at nodal point 619

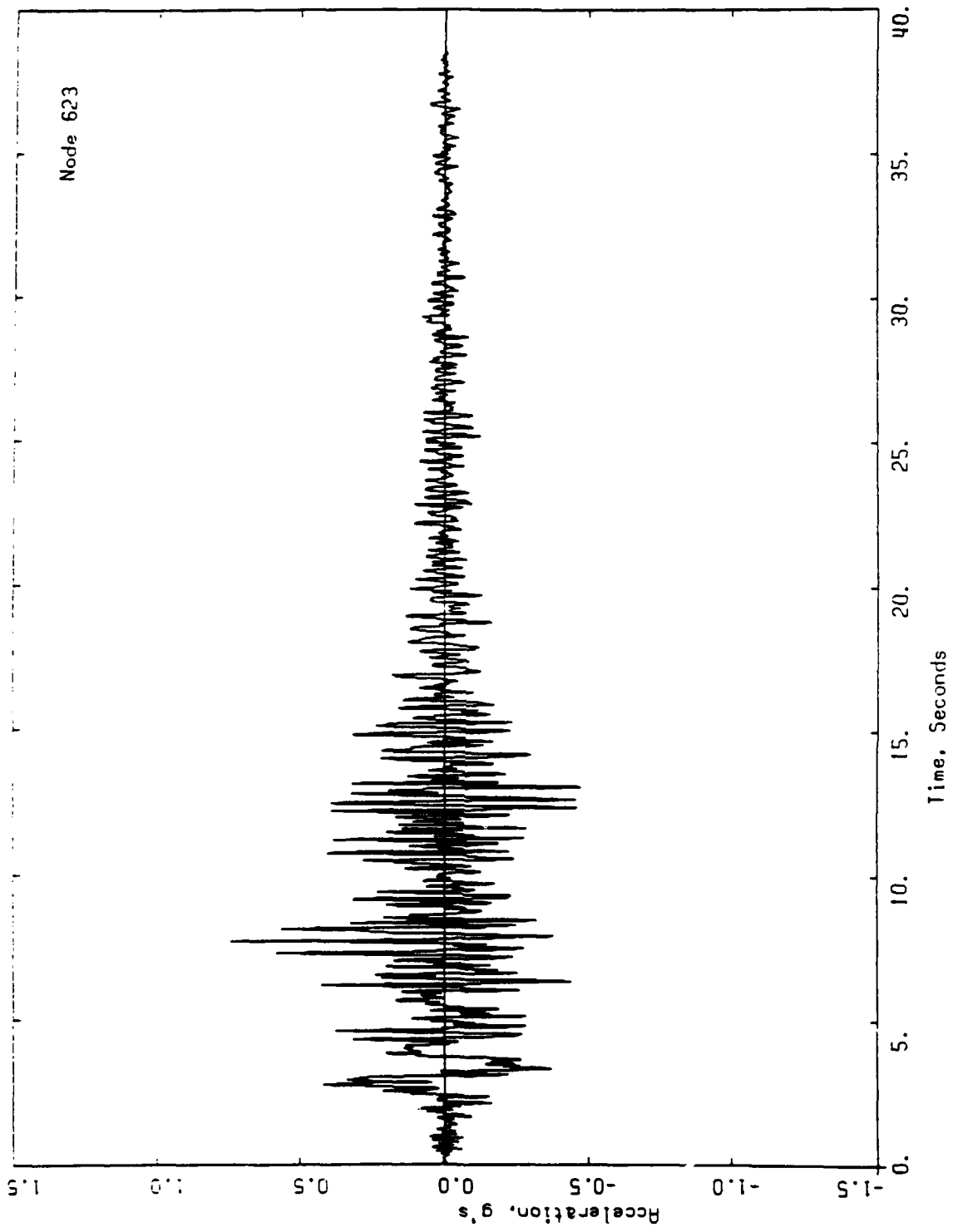


Figure C-20. Acceleration time history at node 1 point 623

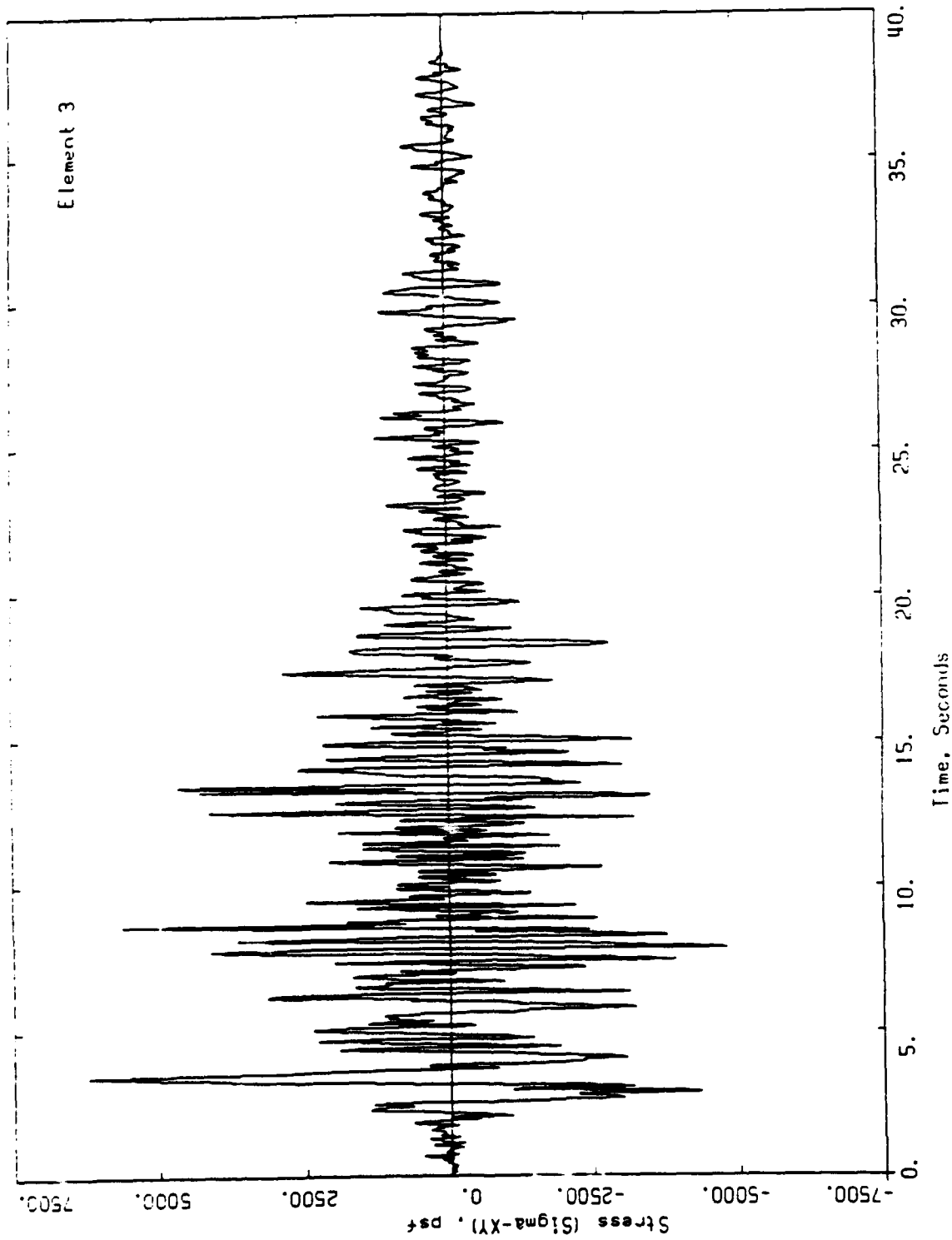


Figure C-21. Time history of horizontal shear stress in element 3

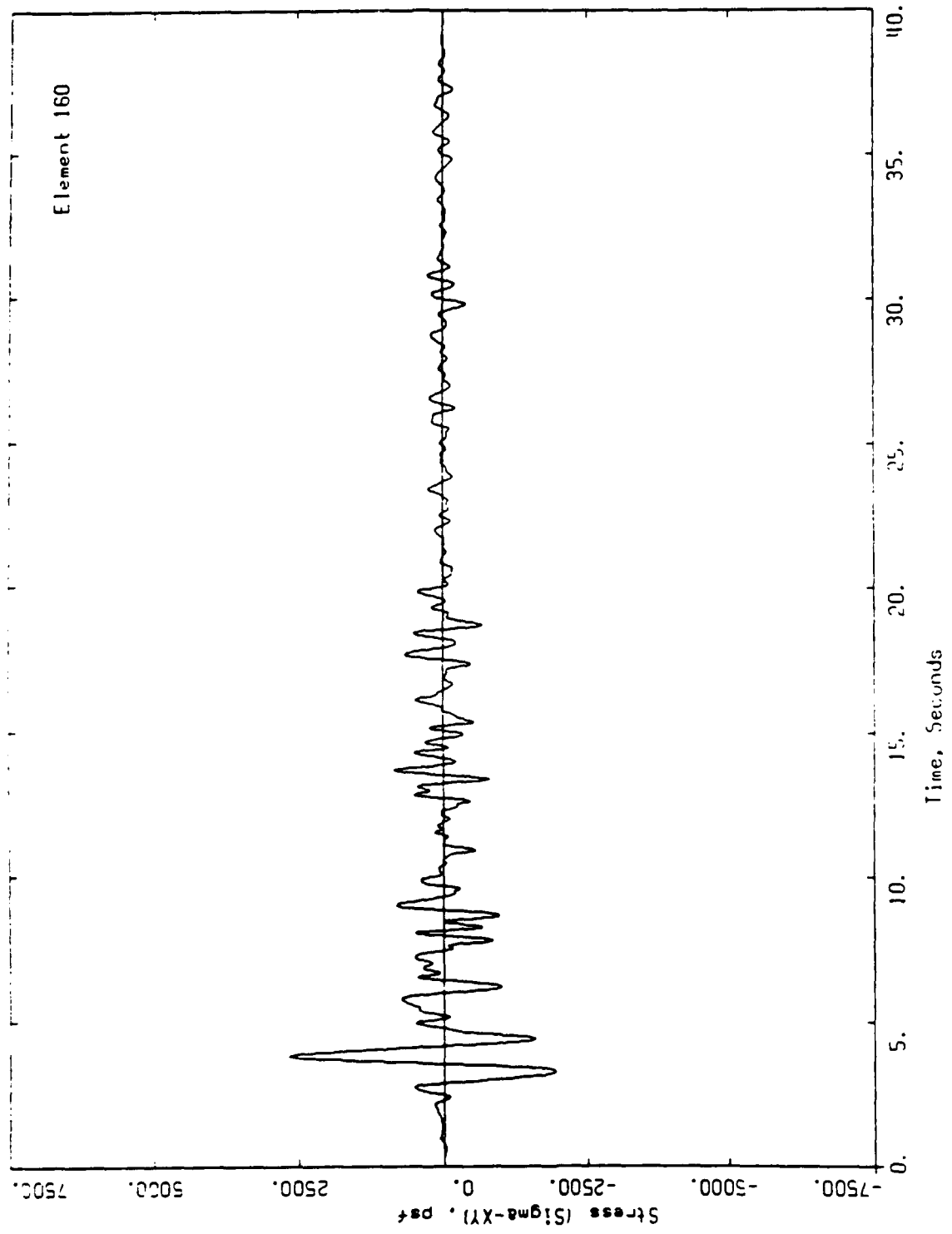


Figure C-22. Time history of horizontal shear stress in element 160

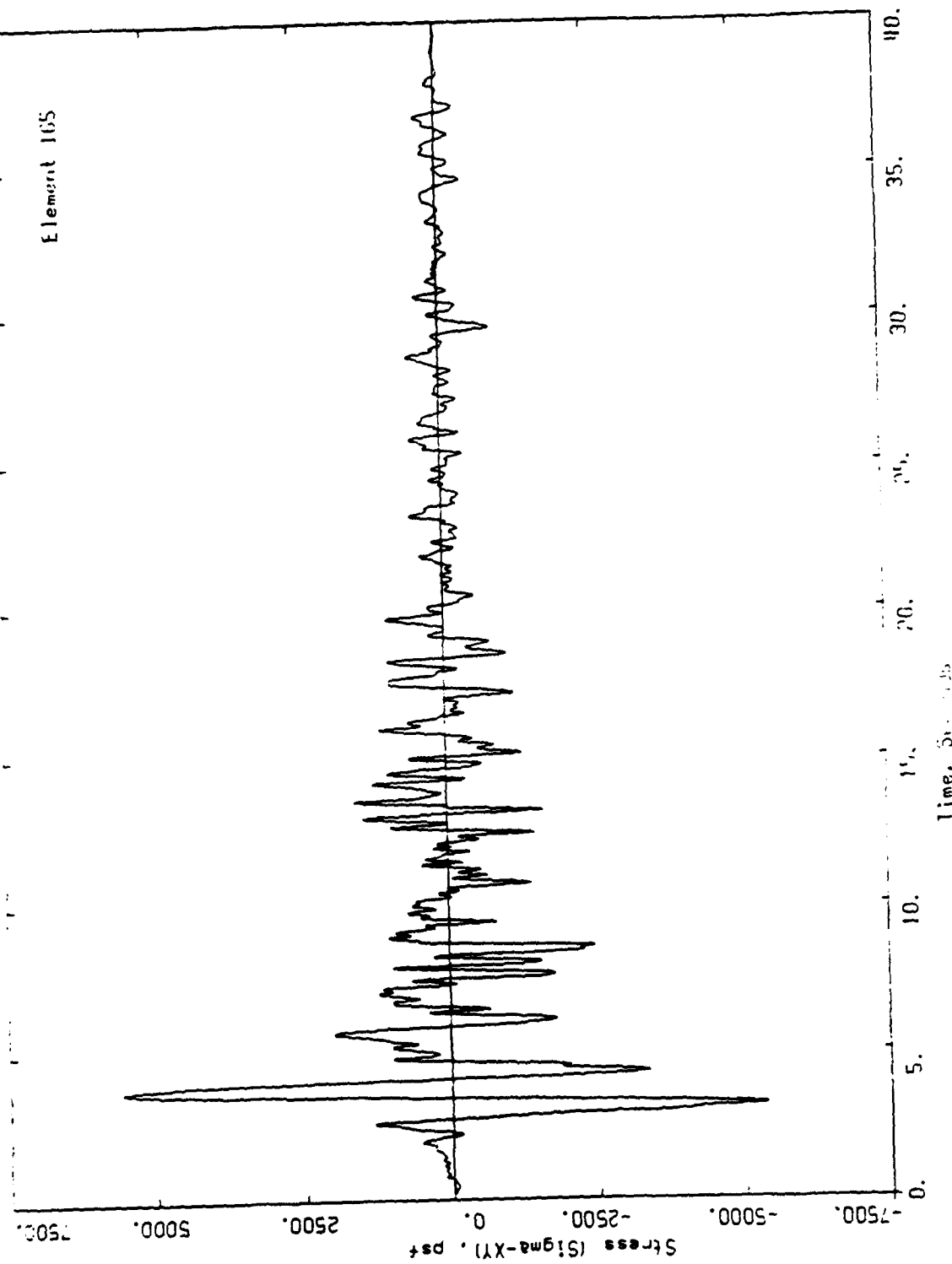


Figure C-23. Time history of horizontal shear stress in element 165

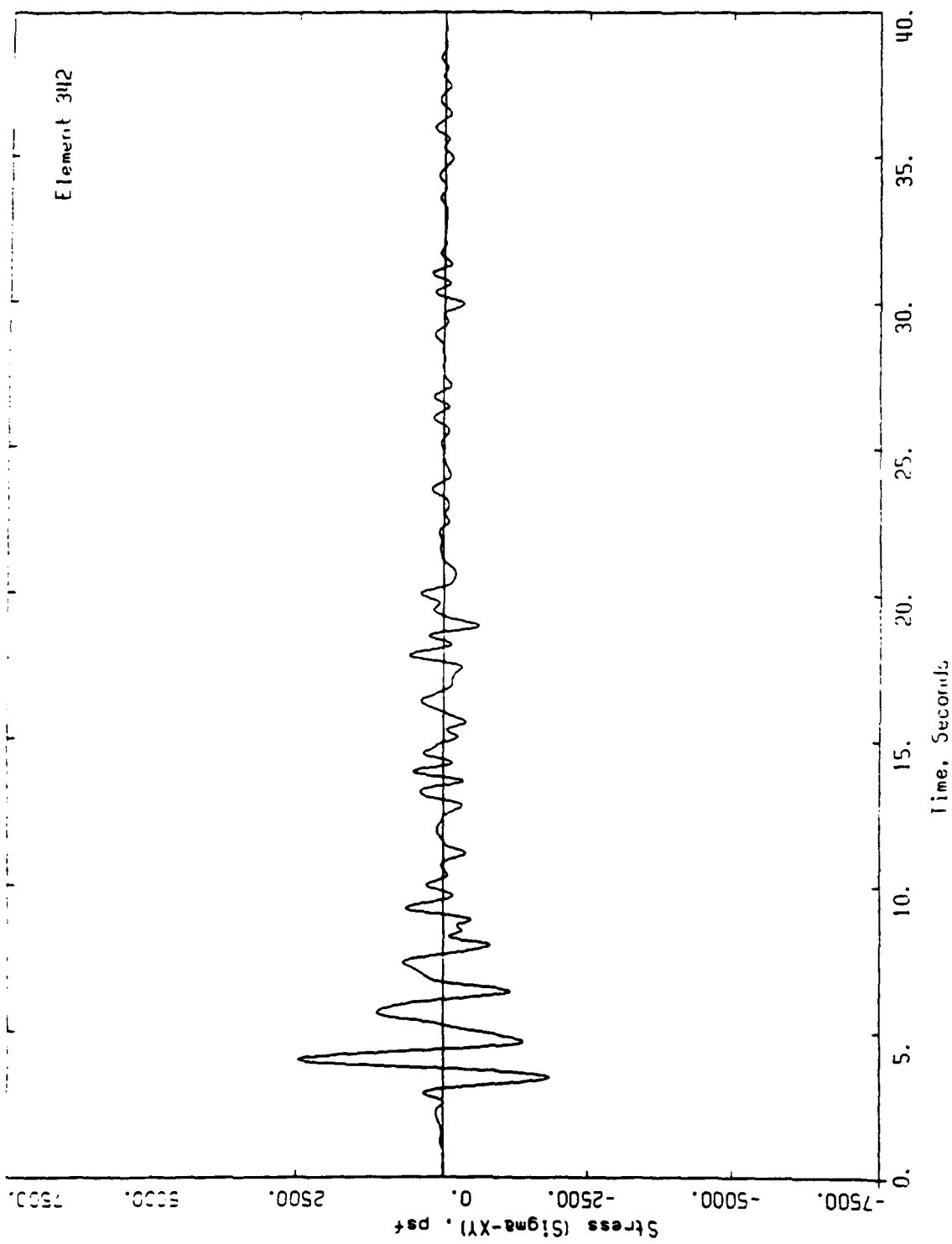


Figure C-24. Time history of horizontal shear stress in element 342

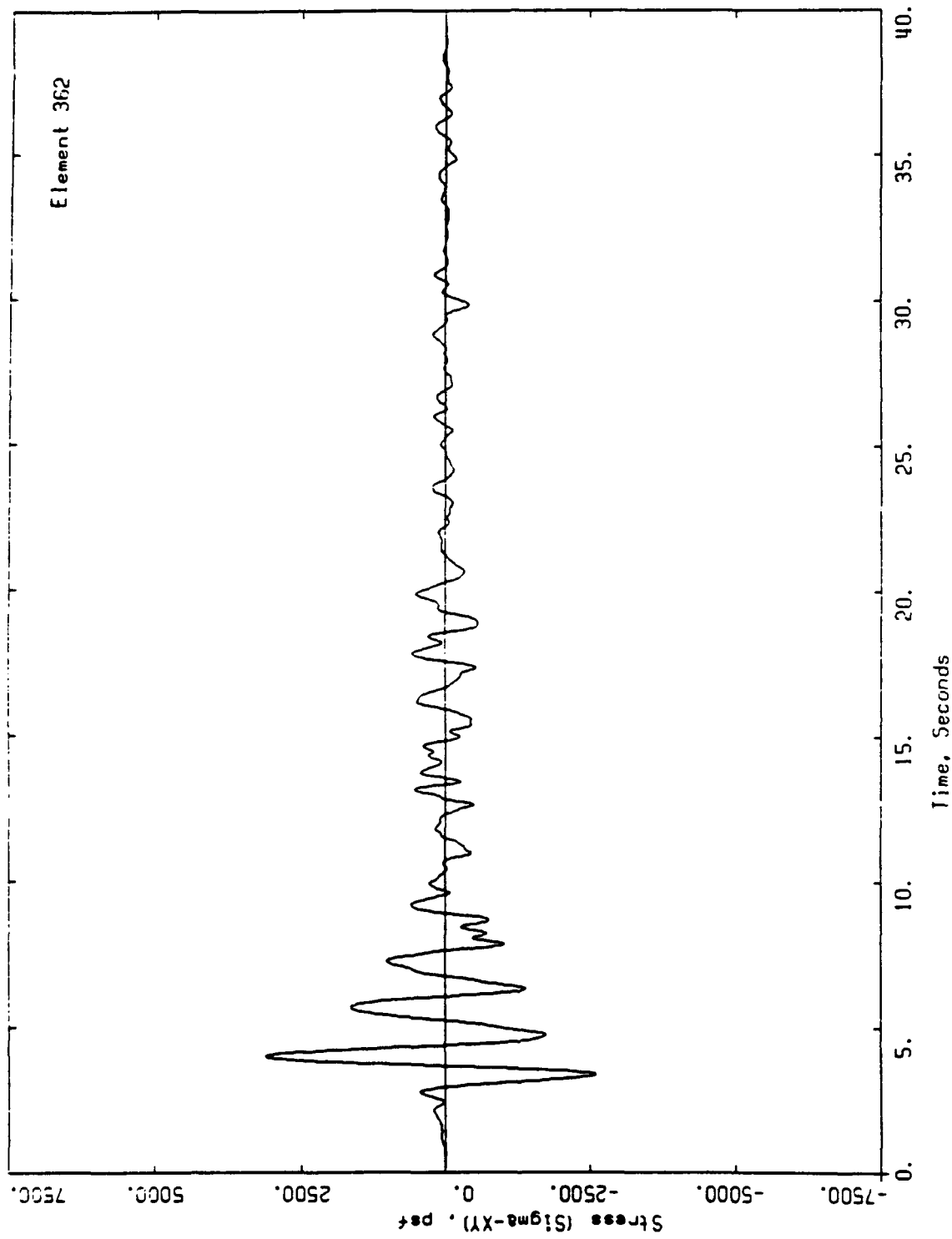


Figure C-25. Time history of horizontal shear stress in element 362

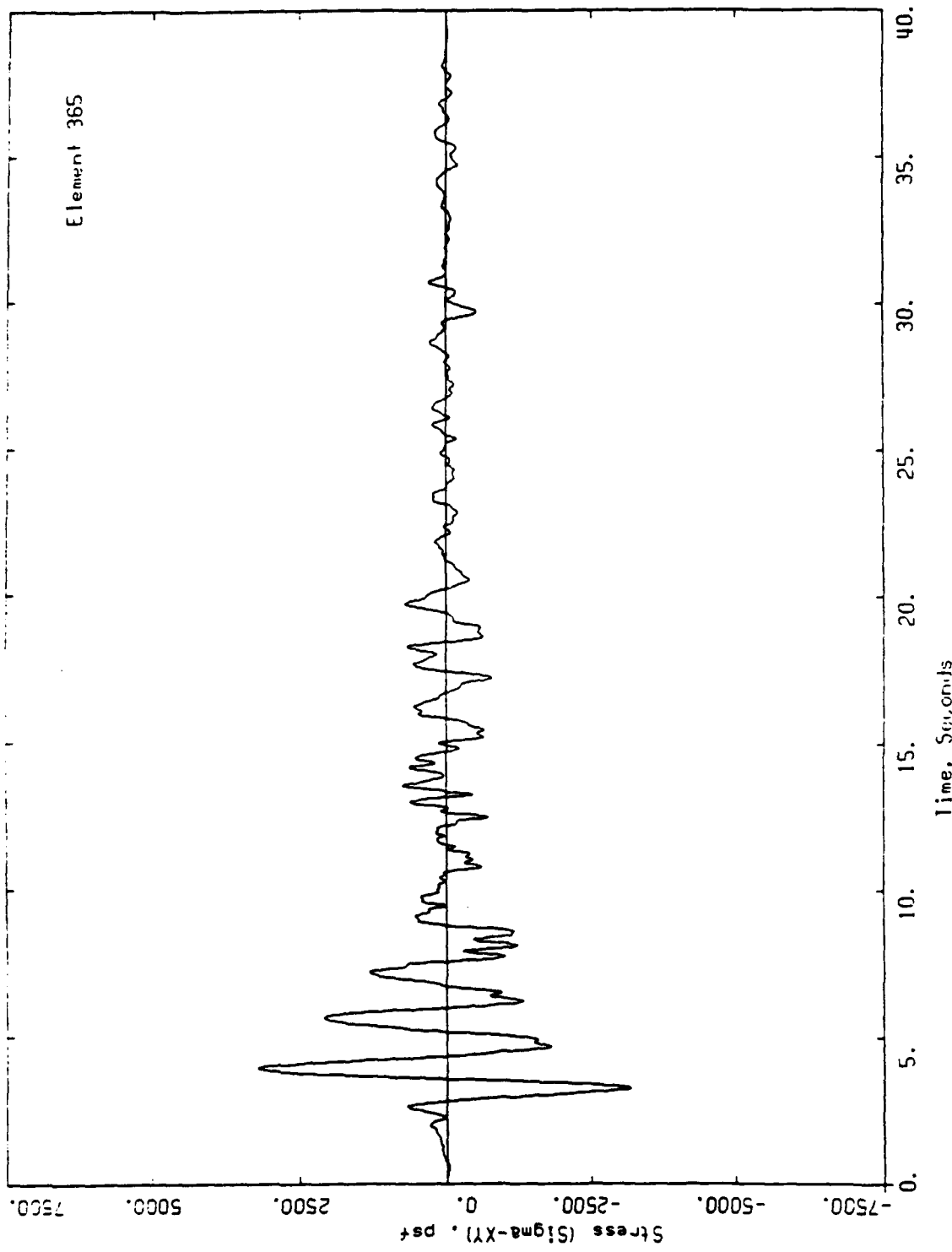


Figure C-26. Time history of horizontal shear stress in element 365

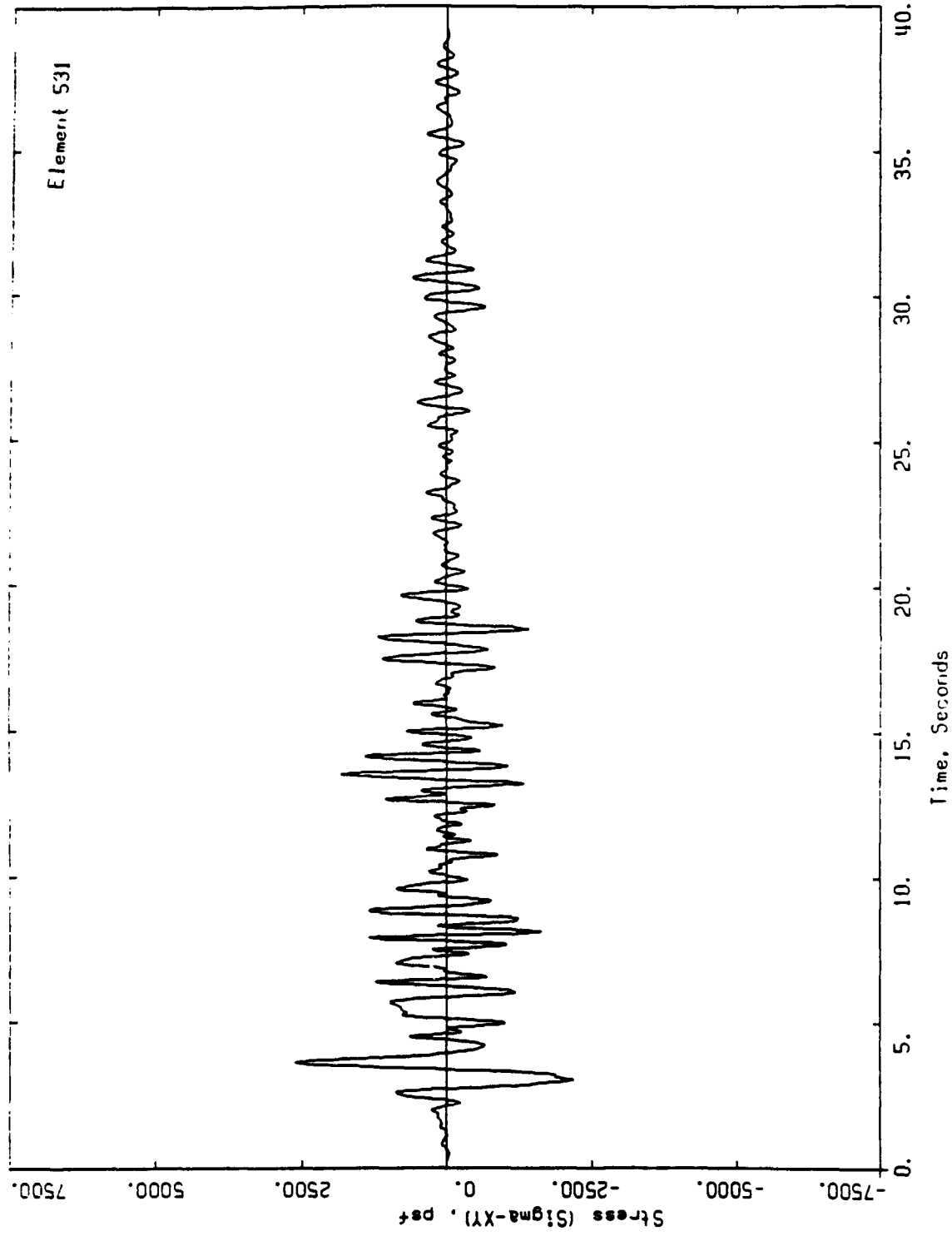


Figure C-27. Time history of horizontal shear stress in element 531

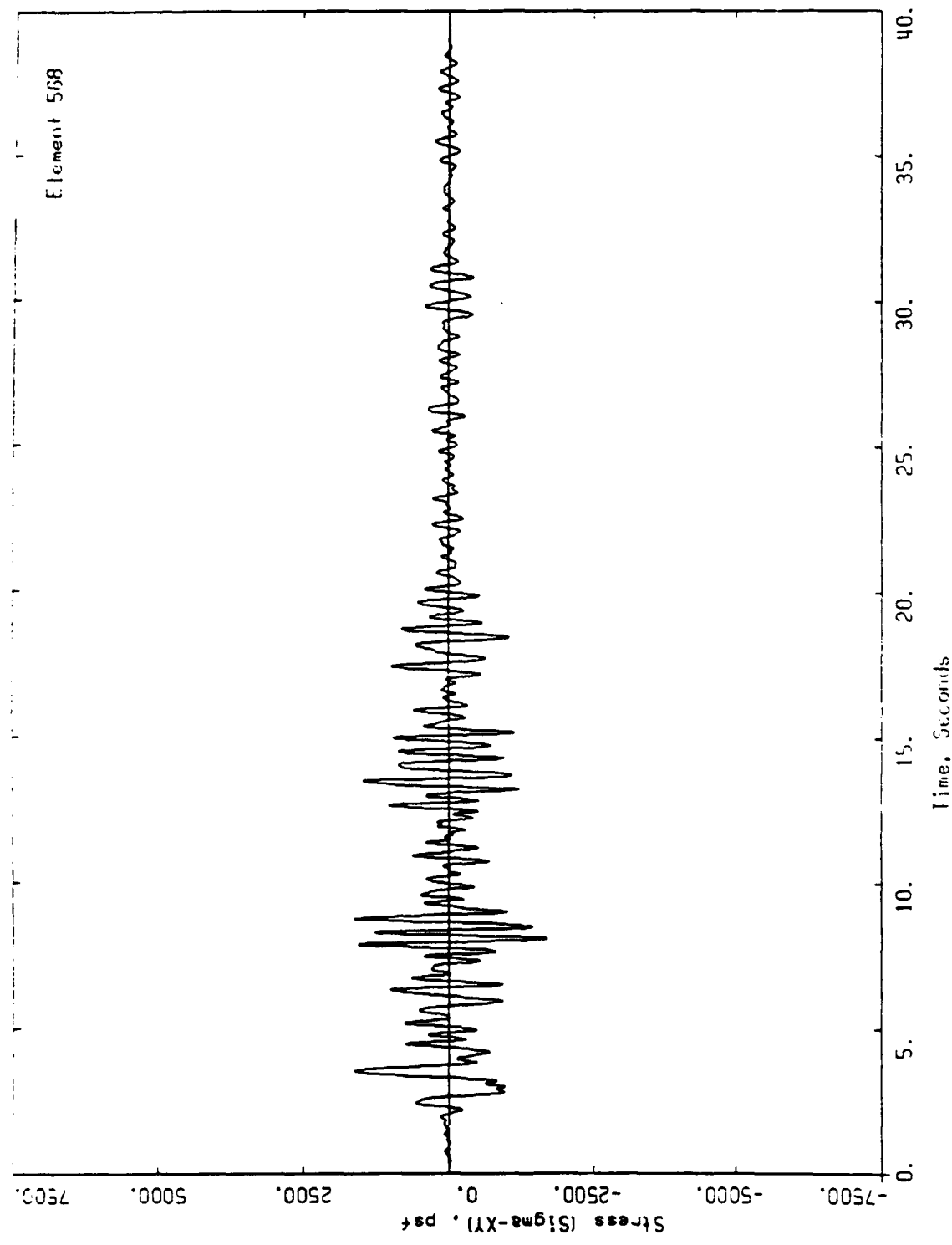


Figure C-28. Time history of horizontal shear stress in element 568

**APPENDIX D**

①

1	8	19	24	35	46	55	55	75	32	
2		10	20	20	25	35	47	58	78	33
		11	21	28	27	37	49	57	80	34
3		12	22	29	38	39	49	59	81	35
4		13	29	30	43	51	60	70	82	36
5		14	31		61	52	51	71	84	
6		15	32		42			72		37
7		16	33		43			73		38
8		17	34		44			74		39

(2)

52	75	82	93	95	101	103	110	121	135	149	150	152	171	197	205	215			
53	75	83	101	103	102	109	111	122	135	149	151	173	188	205	219				
54	77	80	91	102	109		111	122	135	149	152	174	192	207	220				
55	79	82	94	104		109	112	123	137	151	153	175	191	209	221				
56	79	83	93	105		109	113	124	138	152	154	177	193	209	222				
57	80	84	94	105		109	114	125	138	153	155	179	194	210	223				
58	81	85	95	107		109	115	126	143	154	155	179	195	211	224				
59	82	86	95	109		109	115	127	141	155	167	189	195	212	225				
60	83		96	109		115	115	127	141	155	167	189	195	212	225				
70	83		96	109		115	115	127	141	155	167	189	195	212	225				
71	94		97	115		115	129	129	142	155	153	191	197	213	225				
72	95			130			143	143	157	155	159	192	199	214	227				
73	96			131			145	145		154		192	200						
74	97			132			149	149		155		195		201					

(3)

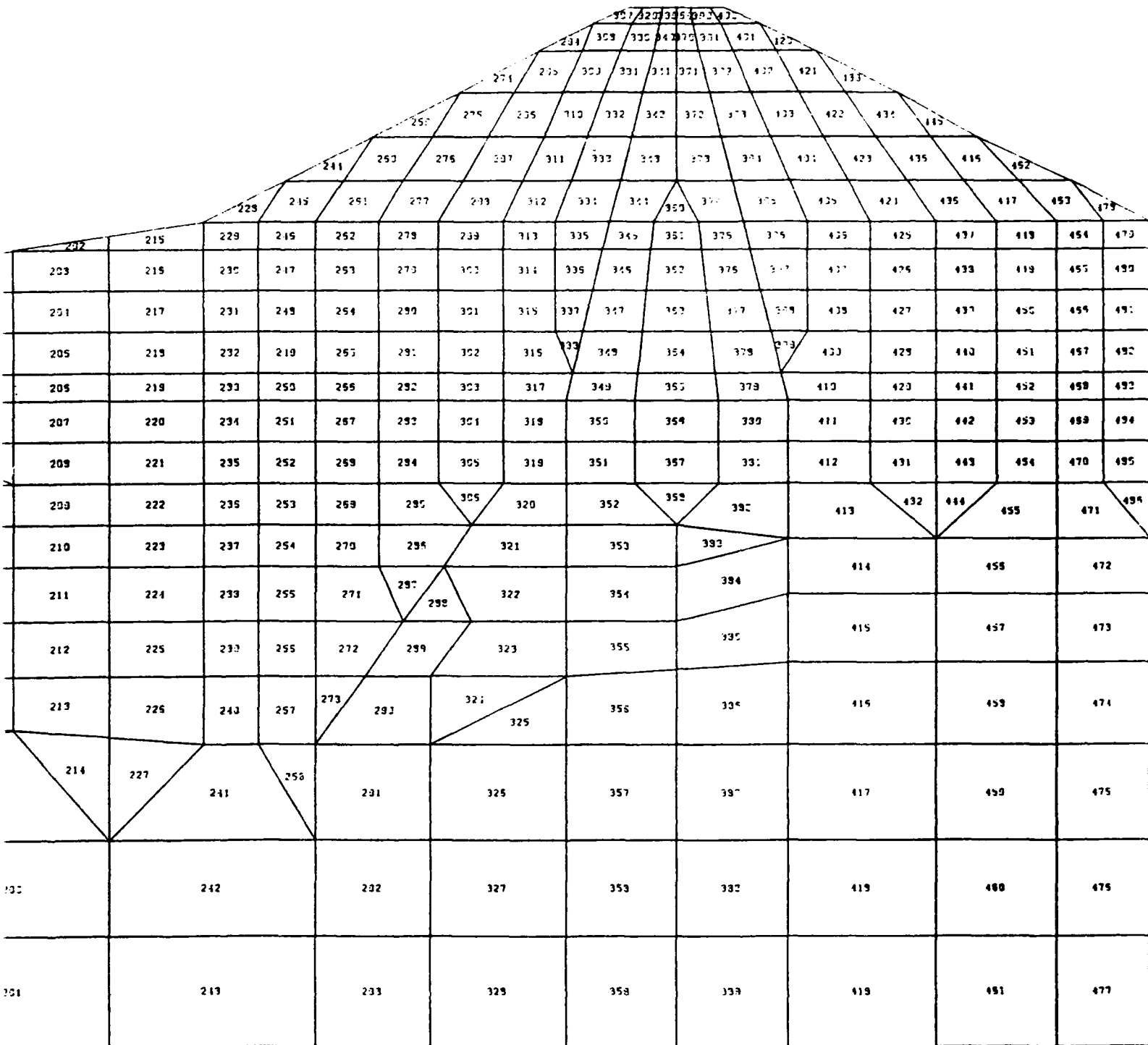


Figure D-1. Element numbering of dynamic finite element mesh for section BB

(4)

452															
417	453	473													
419	454	470	497	495											
419	455	490	493	495	503	522									
450	456	491	499	497	510	523	520	535							
451	457	492	490	499	511	524	530	535	547	553					
452	458	493	491	499	512	525	531	537	549	553	553	553	557		
453	459	494	492	502	513	526	532	539	549	550	554	552			
454	470	495	493	501	514	527	539	533	550	551	555	558			
455	471	496	491	502	515	529	536	540	551	552	559	570			
455	472		503		515		541		552		571				
457	473		501		517		542		553		572				
453	474		505		513		541		554		573				
459	475		505		519		541		555		574				
460	476		507		520		545		555		575				
451	477		509		521		545		557		576				

(5)

552	557	572	537					
554	559	573	532	531				
555	559	573	533	532	531	592	513	512
2	556	570	590	500	533	595	503	511
								513
	571	591		505		501		514
	572	582		517		595		515
	573	593		509		595		516
	574	534		519		527		517
	575	595		503		593		519
	576	536		501		593		518

2/11-292

\*\*\*\*\*  
 TABLE D-1  
 SUMMARY OF SHEAR STRAIN AND STRESS  
 SECTION BB'  
\*\*\*\*\*

SOLID ELEMENTS

MAXIMUM SHEAR STRAIN COMPUTED FROM ITS TIME HISTORY

COMPARISON BETWEEN MAXIMUM SHEAR STRAINS

ELEM.	SIG-X	SIG-Y	SIG-XY	EFF. SHEAR STRN	TIME DOMAIN PERCENT	FREQ DOMAIN PERCENT
	LB/FT**2	LB/FT**2	LB/FT**2	PERCENT		
1	.6775E+04	.2044E+03	.1124E+04	.4924E-02	.7575E-02	.1126E-01
2	.7344E+04	.3598E+03	.3487E+04	.6497E-02	.9995E-02	.1777E-01
3	.9224E+04	.1024E+04	.6195E+04	.1041E-01	.1601E-01	.2769E-01
4	.1131E+05	.1545E+04	.8170E+04	.1415E-01	.2177E-01	.3574E-01
5	.2913E+04	.1882E+04	.9717E+04	.6749E-01	.1038E+00	.1522E+00
6	.3145E+04	.2170E+04	.1127E+05	.7981E-01	.1228E+00	.1796E+00
7	.4001E+04	.2306E+04	.1227E+05	.8805E-01	.1355E+00	.1980E+00
8	.8202E+04	.2434E+04	.1278E+05	.9382E-01	.1443E+00	.2128E+00
9	.5428E+04	.2343E+03	.1490E+04	.4259E-02	.6552E-02	.9215E-02
10	.7254E+04	.6307E+03	.3548E+04	.6668E-02	.1026E-01	.1756E-01
11	.8366E+04	.7653E+03	.5586E+04	.1038E-01	.1597E-01	.2667E-01
12	.1033E+05	.1248E+04	.6120E+04	.1120E-01	.1724E-01	.2991E-01
13	.1350E+05	.1428E+04	.7889E+04	.1423E-01	.2190E-01	.3751E-01
14	.3535E+04	.1890E+04	.9475E+04	.6594E-01	.1014E+00	.1495E+00
15	.3808E+04	.2131E+04	.1103E+05	.7845E-01	.1207E+00	.1757E+00
16	.4961E+04	.2203E+04	.1218E+05	.8813E-01	.1356E+00	.1949E+00
17	.6168E+04	.2698E+04	.1356E+05	.1004E+00	.1545E+00	.2135E+00
18	.1900E+04	.5368E+03	.7567E+03	.2292E+00	.3526E+00	.5148E+00
19	.5766E+04	.7655E+03	.1343E+04	.4116E-02	.6332E-02	.8095E-02
20	.6970E+04	.8953E+03	.4616E+04	.7496E-02	.1153E-01	.1891E-01
21	.9296E+04	.1115E+04	.5478E+04	.1047E-01	.1611E-01	.2685E-01
22	.1240E+05	.1039E+04	.6373E+04	.1245E-01	.1916E-01	.3315E-01
23	.1405E+05	.1707E+04	.7119E+04	.1334E-01	.2052E-01	.3721E-01
24	.2958E+04	.2332E+03	.5492E+03	.2691E+00	.3833E+00	.5379E+00
25	.4706E+04	.1379E+04	.1303E+04	.2709E+00	.4168E+00	.5794E+00
26	.8385E+04	.2946E+04	.5417E+04	.8502E-02	.1308E-01	.2089E-01
27	.6961E+04	.1813E+04	.1697E+04	.2480E+00	.3816E+00	.5216E+00
28	.1254E+05	.3667E+04	.8182E+04	.1436E-01	.2209E-01	.3581E-01
29	.1496E+05	.1538E+04	.7657E+04	.1456E-01	.2239E-01	.3825E-01
30	.1650E+05	.1764E+04	.7992E+04	.1559E-01	.2398E-01	.4021E-01
31	.4331E+04	.2184E+04	.9459E+04	.6619E-01	.1018E+00	.1463E+00
32	.4551E+04	.2430E+04	.1101E+05	.7876E-01	.1212E+00	.1717E+00
33	.4630E+04	.3198E+04	.1242E+05	.9035E-01	.1390E+00	.1924E+00
34	.5224E+04	.3604E+04	.1380E+05	.1018E+00	.1565E+00	.2104E+00
35	.3750E+04	.4466E+03	.9658E+03	.3371E+00	.5136E+00	.6853E+00
36	.5271E+04	.8168E+03	.2207E+04	.3328E+00	.5119E+00	.6916E+00
37	.5301E+04	.1095E+04	.2778E+04	.2852E+00	.4388E+00	.5900E+00
38	.4595E+04	.1358E+04	.3804E+04	.3331E+00	.5125E+00	.6823E+00
39	.2267E+05	.4242E+04	.9548E+04	.2022E-01	.3111E-01	.5281E-01
40	.1955E+05	.2308E+04	.9166E+04	.1811E-01	.2787E-01	.4647E-01
41	.6193E+04	.3053E+04	.1000E+05	.7079E-01	.1035E+00	.1509E+00
42	.5373E+04	.3055E+04	.1138E+05	.8198E-01	.1261E+00	.1723E+00
43	.4899E+04	.3855E+04	.1266E+05	.9218E-01	.1413E+00	.1908E+00
44	.4564E+04	.4482E+04	.1391E+05	.1021E+00	.1570E+00	.2072E+00
45	.1742E+04	.5801E+03	.1258E+04	.8195E+00	.1261E+01	.1518E+01
46	.5364E+04	.9940E+03	.2005E+04	.4224E+00	.6498E+00	.8069E+00

47	.5681E+04	.1325E+04	.3088E+04	.3761E+00	.5786E+00	.7394E+00
48	.5602E+04	.1758E+04	.3852E+04	.3454E+00	.5314E+00	.6879E+00
49	.5811E+04	.2281E+04	.6476E+04	.3320E+00	.5107E+00	.6656E+00
50	.2674E+05	.2816E+04	.9868E+04	.2306E-01	.3548E-01	.5954E-01
51	.2543E+05	.3572E+04	.9680E+04	.2114E-01	.3253E-01	.5472E-01
52	.6487E+04	.2597E+04	.1016E+05	.7249E-01	.1115E+00	.1506E+00
53	.1723E+04	.6250E+03	.1021E+04	.7589E+00	.1168E+01	.1423E+01
54	.2441E+04	.7699E+03	.2106E+04	.8457E+00	.1301E+01	.1583E+01
55	.5272E+04	.9834E+03	.3217E+04	.4467E+00	.6873E+00	.8391E+00
56	.5511E+04	.1428E+04	.3861E+04	.4073E+00	.6266E+00	.7807E+00
57	.5379E+04	.1715E+04	.4436E+04	.3785E+00	.5822E+00	.7369E+00
58	.4832E+04	.1796E+04	.4936E+04	.3418E+00	.5258E+00	.6756E+00
59	.4282E+04	.2188E+04	.5006E+04	.3382E+00	.5203E+00	.6692E+00
60	.2895E+05	.3730E+04	.1003E+05	.2438E-01	.3752E-01	.6090E-01
61	.8098E+04	.3327E+04	.1034E+05	.7408E-01	.1160E+00	.1547E+00
62	.1472E+04	.4967E+03	.7630E+03	.4101E+00	.6310E+00	.8243E+00
63	.1765E+04	.3581E+03	.1802E+04	.6671E+00	.1026E+01	.1308E+01
64	.2095E+04	.5704E+03	.2925E+04	.8606E+00	.1324E+01	.1624E+01
65	.4661E+04	.6929E+03	.3762E+04	.4494E+00	.6914E+00	.8371E+00
66	.4829E+04	.8522E+03	.4446E+04	.4311E+00	.6632E+00	.8066E+00
67	.4761E+04	.1073E+04	.4942E+04	.4003E+00	.6159E+00	.7602E+00
68	.4479E+04	.1368E+04	.5384E+04	.3642E+00	.5603E+00	.7061E+00
69	.4143E+04	.1372E+04	.6061E+04	.3511E+00	.5401E+00	.6902E+00
70	.2968E+05	.1142E+04	.9209E+04	.2490E-01	.3831E-01	.6171E-01
71	.7657E+04	.2668E+04	.1062E+05	.7729E-01	.1189E+00	.1568E+00
72	.7167E+04	.2962E+04	.1148E+05	.8343E-01	.1284E+00	.1702E+00
73	.5815E+04	.3611E+04	.1269E+05	.9227E-01	.1420E+00	.1867E+00
74	.4490E+04	.4357E+04	.1387E+05	.1013E+00	.1559E+00	.2033E+00
75	.7412E+03	.3086E+03	.1059E+04	.3511E+00	.5402E+00	.7163E+00
76	.1173E+04	.6349E+03	.2375E+04	.6616E+00	.1018E+01	.1285E+01
77	.1377E+04	.7795E+03	.3288E+04	.8562E+00	.1317E+01	.1593E+01
78	.3882E+04	.8378E+03	.4332E+04	.4680E+00	.7200E+00	.8565E+00
79	.4085E+04	.8230E+03	.4939E+04	.4579E+00	.7044E+00	.8401E+00
80	.4083E+04	.7882E+03	.5451E+04	.4308E+00	.6628E+00	.8038E+00
81	.3810E+04	.8015E+03	.5805E+04	.3922E+00	.6034E+00	.7507E+00
82	.3514E+04	.1083E+04	.5340E+04	.3500E+00	.5384E+00	.6867E+00
83	.3406E+05	.4389E+04	.1133E+05	.2649E-01	.4075E-01	.6713E-01
84	.1026E+05	.1988E+04	.1005E+05	.7574E-01	.1165E+00	.1501E+00
85	.8502E+04	.2629E+04	.1105E+05	.8030E-01	.1235E+00	.1591E+00
86	.6470E+04	.2867E+04	.1267E+05	.9168E-01	.1411E+00	.1805E+00
87	.5162E+04	.3223E+04	.1394E+05	.1015E+00	.1561E+00	.2003E+00
88	.9460E+03	.2124E+03	.1183E+04	.3086E+00	.4748E+00	.6304E+00
89	.9255E+03	.5010E+03	.2493E+04	.6437E+00	.9903E+00	.1228E+01
90	.9378E+03	.7475E+03	.3473E+04	.8184E+00	.1259E+01	.1511E+01
91	.3316E+04	.7591E+03	.4566E+04	.4972E+00	.7650E+00	.9046E+00
92	.3258E+04	.9354E+03	.4615E+04	.4614E+00	.7099E+00	.8358E+00
93	.3369E+04	.1066E+04	.5201E+04	.4546E+00	.6993E+00	.8265E+00
94	.3474E+04	.1073E+04	.5568E+04	.4305E+00	.6623E+00	.7966E+00
95	.3329E+04	.1058E+04	.6120E+04	.3990E+00	.6139E+00	.7600E+00
96	.3836E+04	.1195E+04	.7046E+04	.3314E+00	.5098E+00	.6462E+00
97	.1333E+05	.2627E+04	.8847E+04	.6909E-01	.1063E+00	.1448E+00
98	.1190E+04	.1831E+03	.9265E+03	.3739E+00	.5752E+00	.7769E+00
99	.1254E+04	.3372E+03	.1309E+04	.2986E+00	.4594E+00	.6197E+00
100	.1672E+04	.5429E+03	.2407E+04	.9082E+00	.1397E+01	.1688E+01
101	.1183E+04	.5099E+03	.2983E+04	.7021E+00	.1080E+01	.1312E+01
102	.1125E+04	.6153E+03	.3274E+04	.8529E+00	.1312E+01	.1571E+01
103	.2229E+04	.7433E+03	.3953E+04	.4606E+00	.7086E+00	.8395E+00
104	.2619E+04	.9783E+03	.4808E+04	.4615E+00	.7101E+00	.8325E+00
105	.2728E+04	.1120E+04	.5358E+04	.4597E+00	.7073E+00	.8326E+00
106	.2958E+04	.1212E+04	.5875E+04	.4400E+00	.6769E+00	.8092E+00
107	.2973E+04	.1188E+04	.6139E+04	.4214E+00	.6483E+00	.7958E+00
108	.4141E+04	.1303E+04	.6362E+04	.3353E+00	.5159E+00	.6555E+00
109	.1470E+04	.1392E+03	.1091E+04	.5101E+00	.7848E+00	.1019E+01
110	.1003E+04	.3002E+03	.2495E+04	.1081E+01	.1664E+01	.1969E+01
111	.2747E+04	.5920E+03	.4055E+04	.4432E+00	.6818E+00	.8150E+00
112	.2722E+04	.7625E+03	.4740E+04	.4699E+00	.7230E+00	.8478E+00

113	.2814E+04	.9915E+03	.5673E+04	.4653E+00	.7158E+00	.8390E+00
114	.2715E+04	.1094E+04	.5920E+04	.4347E+00	.6688E+00	.7963E+00
115	.2907E+04	.1179E+04	.6516E+04	.4138E+00	.6366E+00	.7777E+00
116	.3000E+04	.1321E+04	.6734E+04	.3481E+00	.5355E+00	.6784E+00
117	.2441E+04	.1367E+04	.6861E+04	.3816E+00	.5871E+00	.7403E+00
118	.9043E+04	.1890E+04	.8626E+04	.6682E-01	.1028E+00	.1388E+00
119	.9876E+03	.1731E+03	.3559E+03	.5057E+00	.7781E+00	.9300E+00
120	.1777E+04	.2048E+03	.1415E+04	.6220E+00	.9569E+00	.1212E+01
121	.1180E+04	.3180E+03	.2752E+04	.1205E+01	.1853E+01	.2154E+01
122	.3155E+04	.4084E+03	.3961E+04	.3859E+00	.5938E+00	.7174E+00
123	.2986E+04	.5608E+03	.4938E+04	.4425E+00	.6808E+00	.8033E+00
124	.2776E+04	.7939E+03	.5617E+04	.4524E+00	.6960E+00	.8210E+00
125	.2843E+04	.1038E+04	.6115E+04	.4210E+00	.6478E+00	.7743E+00
126	.2715E+04	.1220E+04	.6343E+04	.3979E+00	.6121E+00	.7517E+00
127	.2537E+04	.1397E+04	.6452E+04	.3607E+00	.5549E+00	.7036E+00
128	.2259E+04	.1467E+04	.7058E+04	.3778E+00	.5812E+00	.7248E+00
129	.8143E+04	.2496E+04	.8105E+04	.5688E-01	.8750E-01	.1173E+00
130	.7212E+04	.2512E+04	.1028E+05	.7360E-01	.1132E+00	.1456E+00
131	.6038E+04	.2882E+04	.1240E+05	.8901E-01	.1369E+00	.1742E+00
132	.5386E+04	.3076E+04	.1398E+05	.1015E+00	.1561E+00	.1990E+00
133	.1582E+04	.2287E+03	.6352E+03	.5193E+00	.7990E+00	.9962E+00
134	.1839E+04	.2934E+03	.1947E+04	.8042E+00	.1237E+01	.1515E+01
135	.1292E+04	.4740E+03	.3145E+04	.1304E+01	.2006E+01	.2314E+01
136	.3366E+04	.6664E+03	.4071E+04	.3810E+00	.5861E+00	.7112E+00
137	.3063E+04	.7873E+03	.4897E+04	.4197E+00	.6456E+00	.7727E+00
138	.2896E+04	.1024E+04	.5615E+04	.4249E+00	.6536E+00	.7828E+00
139	.2693E+04	.1232E+04	.5898E+04	.3975E+00	.6116E+00	.7420E+00
140	.2493E+04	.1439E+04	.6207E+04	.3695E+00	.5685E+00	.7077E+00
141	.2337E+04	.1638E+04	.6581E+04	.3595E+00	.5530E+00	.6939E+00
142	.2321E+04	.1764E+04	.7049E+04	.3719E+00	.5721E+00	.7051E+00
143	.4959E+04	.1642E+04	.7676E+04	.5224E-01	.8036E-01	.1079E+00
144	.4963E+04	.2503E+04	.9049E+04	.6277E-01	.9658E-01	.1299E+00
145	.4471E+04	.2974E+04	.1163E+05	.8231E-01	.1266E+00	.1655E+00
146	.4976E+04	.3307E+04	.1378E+05	.9953E-01	.1531E+00	.1967E+00
147	.1853E+04	.2741E+03	.9246E+03	.5030E+00	.7739E+00	.1046E+01
148	.1786E+04	.3980E+03	.2356E+04	.9447E+00	.1453E+01	.1759E+01
149	.1388E+04	.6151E+03	.3485E+04	.1364E+01	.2098E+01	.2421E+01
150	.3415E+04	.7783E+03	.4346E+04	.4105E+00	.6316E+00	.7679E+00
151	.3234E+04	.1220E+04	.5046E+04	.4251E+00	.6540E+00	.7911E+00
152	.2993E+04	.1321E+04	.5512E+04	.4089E+00	.6290E+00	.7659E+00
153	.2777E+04	.1422E+04	.5806E+04	.3791E+00	.5832E+00	.7191E+00
154	.2478E+04	.1574E+04	.6034E+04	.3444E+00	.5299E+00	.6711E+00
155	.2125E+04	.1737E+04	.6532E+04	.3435E+00	.5285E+00	.6602E+00
156	.2106E+04	.1871E+04	.7025E+04	.3547E+00	.5456E+00	.6684E+00
157	.5730E+04	.3384E+04	.7389E+04	.4984E-01	.7667E-01	.1016E+00
158	.1067E+04	.2627E+03	.2803E+03	.4421E+00	.6801E+00	.8724E+00
159	.2265E+04	.2875E+03	.1231E+04	.4613E+00	.7097E+00	.1059E+01
160	.1899E+04	.5563E+03	.2659E+04	.9705E+00	.1493E+01	.1823E+01
161	.1354E+04	.5721E+03	.3742E+04	.1363E+01	.2097E+01	.2452E+01
162	.3622E+04	.1243E+04	.4870E+04	.4632E+00	.7126E+00	.8689E+00
163	.3468E+04	.1097E+04	.5205E+04	.4195E+00	.6454E+00	.7911E+00
164	.3392E+04	.1375E+04	.5373E+04	.3871E+00	.5955E+00	.7396E+00
165	.3215E+04	.1476E+04	.5587E+04	.3468E+00	.5335E+00	.6737E+00
166	.2790E+04	.1526E+04	.5868E+04	.3163E+00	.4867E+00	.6254E+00
167	.2161E+04	.1726E+04	.6381E+04	.3187E+00	.4904E+00	.6129E+00
168	.1898E+04	.1899E+04	.6887E+04	.3301E+00	.5079E+00	.6222E+00
169	.3760E+04	.2179E+04	.7512E+04	.5054E-01	.7775E-01	.1025E+00
170	.1539E+04	.1986E+03	.4402E+03	.4300E+00	.6615E+00	.9006E+00
171	.2638E+04	.4529E+03	.1602E+04	.4776E+00	.7348E+00	.1143E+01
172	.2296E+04	.8300E+03	.2913E+04	.9372E+00	.1442E+01	.1793E+01
173	.2435E+04	.1246E+04	.3762E+04	.1217E+01	.1872E+01	.2256E+01
174	.4143E+04	.2284E+04	.3549E+04	.8097E+00	.1246E+01	.1607E+01
175	.3502E+04	.8373E+03	.5623E+04	.5296E+00	.8147E+00	.9860E+00
176	.4008E+04	.1137E+04	.5617E+04	.4435E+00	.6823E+00	.8506E+00
177	.4045E+04	.1102E+04	.5397E+04	.3671E+00	.5647E+00	.7140E+00
178	.3884E+04	.1217E+04	.5383E+04	.3141E+00	.4833E+00	.6290E+00

179	.3367E+04	.1533E+04	.5812E+04	.2952E+00	.4542E+00	.5825E+00
180	.2566E+04	.1860E+04	.6223E+04	.2893E+00	.4450E+00	.5592E+00
181	.1871E+04	.2028E+04	.6650E+04	.2985E+00	.4593E+00	.5661E+00
182	.4044E+04	.2792E+04	.6594E+04	.4334E-01	.6667E-01	.9360E-01
183	.3614E+04	.2665E+04	.8167E+04	.5517E-01	.8488E-01	.1206E+00
184	.3374E+04	.3167E+04	.1102E+05	.7708E-01	.1186E+00	.1607E+00
185	.4392E+04	.3456E+04	.1368E+05	.9859E-01	.1517E+00	.1964E+00
186	.1876E+04	.2758E+03	.7374E+03	.4692E+00	.7219E+00	.1055E+01
187	.3060E+04	.6985E+03	.2042E+04	.6102E+00	.9387E+00	.1380E+01
188	.2845E+04	.1101E+04	.3179E+04	.9588E+00	.1475E+01	.1875E+01
189	.2904E+04	.1300E+04	.3782E+04	.1061E+01	.1632E+01	.2040E+01
190	.3097E+04	.1048E+04	.3864E+04	.8566E+00	.1318E+01	.1710E+01
191	.4630E+04	.3074E+04	.3710E+04	.6340E+00	.9754E+00	.1347E+01
192	.5140E+04	.1022E+04	.5863E+04	.4782E+00	.7357E+00	.9248E+00
193	.5353E+04	.1291E+04	.3058E+04	.3416E+00	.5255E+00	.6816E+00
194	.4598E+04	.1686E+04	.5468E+04	.2982E+00	.4588E+00	.6087E+00
195	.3856E+04	.2057E+04	.5841E+04	.2834E+00	.4361E+00	.5624E+00
196	.3019E+04	.2374E+04	.6148E+04	.2638E+00	.4059E+00	.5168E+00
197	.2163E+04	.2628E+04	.6554E+04	.2655E+00	.4084E+00	.5119E+00
198	.6487E+04	.3296E+04	.7066E+04	.4692E-01	.7219E-01	.1041E+00
199	.4681E+04	.2511E+04	.8219E+04	.5628E-01	.8659E-01	.1241E+00
200	.4605E+04	.3274E+04	.1140E+05	.8096E-01	.1245E+00	.1707E+00
201	.3817E+04	.3868E+04	.1415E+05	.1026E+00	.1579E+00	.2029E+00
202	.5536E+03	.4192E+03	.2049E+03	.5757E+00	.8857E+00	.1154E+01
203	.2583E+04	.5258E+03	.1108E+04	.5458E+00	.8397E+00	.1270E+01
204	.3528E+04	.1101E+04	.2401E+04	.6964E+00	.1071E+01	.1569E+01
205	.3358E+04	.1472E+04	.3337E+04	.9352E+00	.1439E+01	.1898E+01
206	.3365E+04	.1614E+04	.3808E+04	.9576E+00	.1473E+01	.1929E+01
207	.3566E+04	.1943E+04	.4002E+04	.8652E+00	.1331E+01	.1787E+01
208	.3031E+04	.1511E+04	.4098E+04	.7179E+00	.1104E+01	.1501E+01
209	.5688E+04	.2256E+04	.4864E+04	.2851E+00	.4386E+00	.6051E+00
210	.5074E+04	.2627E+04	.5405E+04	.2841E+00	.4370E+00	.5850E+00
211	.4456E+04	.2934E+04	.5740E+04	.2655E+00	.4085E+00	.5351E+00
212	.3415E+04	.3196E+04	.5956E+04	.2307E+00	.3549E+00	.4624E+00
213	.2483E+04	.3296E+04	.6300E+04	.2164E+00	.3330E+00	.4280E+00
214	.6384E+04	.4614E+04	.7713E+04	.5680E-01	.8739E-01	.1305E+00
215	.1789E+04	.5335E+03	.7128E+03	.9566E+00	.1472E+01	.2008E+01
216	.3634E+04	.1065E+04	.1817E+04	.7397E+00	.1138E+01	.1744E+01
217	.3869E+04	.1673E+04	.2842E+04	.8602E+00	.1323E+01	.1897E+01
218	.3643E+04	.2256E+04	.3512E+04	.1002E+01	.1542E+01	.2080E+01
219	.3561E+04	.2731E+04	.3866E+04	.9876E+00	.1519E+01	.2043E+01
220	.3532E+04	.3115E+04	.4067E+04	.9071E+00	.1396E+01	.1884E+01
221	.3652E+04	.3811E+04	.4175E+04	.8041E+00	.1237E+01	.1682E+01
222	.5351E+04	.4030E+04	.5122E+04	.3074E+00	.4729E+00	.6493E+00
223	.5243E+04	.4174E+04	.5423E+04	.2991E+00	.4601E+00	.6212E+00
224	.4992E+04	.4192E+04	.5547E+04	.2570E+00	.3953E+00	.5276E+00
225	.4054E+04	.4117E+04	.5605E+04	.2014E+00	.3098E+00	.4183E+00
226	.2692E+04	.4167E+04	.5827E+04	.1696E+00	.2609E+00	.3552E+00
227	.9259E+04	.3661E+04	.9598E+04	.7220E-01	.1111E+00	.1582E+00
228	.2186E+04	.5841E+03	.1048E+04	.1049E+01	.1614E+01	.2053E+01
229	.2732E+04	.1083E+04	.1716E+04	.1146E+01	.1762E+01	.2336E+01
230	.4121E+04	.1980E+04	.2753E+04	.8023E+00	.1234E+01	.1763E+01
231	.3832E+04	.2853E+04	.3690E+04	.7609E+00	.1171E+01	.1653E+01
232	.3503E+04	.3719E+04	.4358E+04	.8177E+00	.1258E+01	.1706E+01
233	.3380E+04	.4290E+04	.4709E+04	.8010E+00	.1232E+01	.1666E+01
234	.3333E+04	.4782E+04	.4928E+04	.7513E+00	.1156E+01	.1573E+01
235	.3535E+04	.5333E+04	.5243E+04	.6492E+00	.9988E+00	.1399E+01
236	.5184E+04	.5761E+04	.6788E+04	.2786E+00	.4286E+00	.5904E+00
237	.5520E+04	.5673E+04	.5016E+04	.2797E+00	.4303E+00	.5820E+00
238	.5526E+04	.5130E+04	.4948E+04	.2288E+00	.3520E+00	.4784E+00
239	.4726E+04	.4744E+04	.4897E+04	.1692E+00	.2602E+00	.3636E+00
240	.3019E+04	.4284E+04	.5072E+04	.1256E+00	.1932E+00	.2859E+00
241	.6663E+04	.3546E+04	.1170E+05	.8755E-01	.1347E+00	.1855E+00
242	.5089E+04	.5516E+04	.1347E+05	.9721E-01	.1496E+00	.1992E+00
243	.3089E+04	.5639E+04	.1502E+05	.1095E+00	.1685E+00	.2145E+00
244	.1517E+04	.4887E+03	.1117E+04	.7198E+00	.1107E+01	.1375E+01

245	.2604E+04	.1281E+04	.1892E+04	.8020E+00	.1234E+01	.1602E+01
246	.3398E+04	.2295E+04	.2947E+04	.1018E+01	.1566E+01	.2100E+01
247	.3776E+04	.3072E+04	.3468E+04	.8404E+00	.1293E+01	.1776E+01
248	.3536E+04	.3888E+04	.4111E+04	.8326E+00	.1281E+01	.1733E+01
249	.3148E+04	.4381E+04	.4623E+04	.8615E+00	.1325E+01	.1781E+01
250	.3003E+04	.4692E+04	.4921E+04	.8372E+00	.1288E+01	.1744E+01
251	.3068E+04	.4958E+04	.5109E+04	.7578E+00	.1166E+01	.1616E+01
252	.3226E+04	.5151E+04	.5227E+04	.6284E+00	.9667E+00	.1385E+01
253	.5532E+04	.5406E+04	.5112E+04	.2958E+00	.4550E+00	.6292E+00
254	.5860E+04	.5150E+04	.4707E+04	.2626E+00	.4040E+00	.5479E+00
255	.6102E+04	.4889E+04	.4496E+04	.2001E+00	.3078E+00	.4235E+00
256	.5171E+04	.4641E+04	.4473E+04	.1432E+00	.2204E+00	.3167E+00
257	.2864E+04	.4167E+04	.4041E+04	.9481E-01	.1459E+00	.2273E+00
258	.2514E+05	.1853E+05	.1517E+05	.1137E+00	.1750E+00	.2402E+00
259	.1245E+04	.4762E+03	.9501E+03	.4522E+00	.6957E+00	.8789E+00
260	.2030E+04	.1220E+04	.1935E+04	.5958E+00	.9166E+00	.1173E+01
261	.3002E+04	.2153E+04	.3174E+04	.7054E+00	.1085E+01	.1415E+01
262	.2960E+04	.2778E+04	.3510E+04	.9900E+00	.1523E+01	.2003E+01
263	.3219E+04	.3550E+04	.4113E+04	.8834E+00	.1359E+01	.1806E+01
264	.2916E+04	.4204E+04	.4488E+04	.8509E+00	.1309E+01	.1742E+01
265	.2688E+04	.4725E+04	.4831E+04	.8346E+00	.1284E+01	.1727E+01
266	.2633E+04	.5011E+04	.5037E+04	.7881E+00	.1212E+01	.1667E+01
267	.2816E+04	.5209E+04	.5127E+04	.7056E+00	.1085E+01	.1545E+01
268	.3476E+04	.5336E+04	.5411E+04	.6380E+00	.9815E+00	.1403E+01
269	.5675E+04	.4878E+04	.4680E+04	.3170E+00	.4877E+00	.6731E+00
270	.6943E+04	.5733E+04	.4590E+04	.2529E+00	.3891E+00	.5289E+00
271	.7109E+04	.5165E+04	.3160E+04	.1473E+00	.2266E+00	.3171E+00
272	.6581E+04	.5074E+04	.2815E+04	.8036E-01	.1236E+00	.2009E+00
273	.4879E+04	.5118E+04	.3381E+04	.8304E-01	.1278E+00	.1743E+00
274	.1273E+04	.1107E+04	.6136E+03	.1032E+00	.1587E+00	.2198E+00
275	.1347E+04	.1134E+04	.1920E+04	.3876E+00	.5964E+00	.7455E+00
276	.2051E+04	.2101E+04	.3175E+04	.5684E+00	.8745E+00	.1101E+01
277	.2251E+04	.2612E+04	.3677E+04	.6350E+00	.9769E+00	.1256E+01
278	.2418E+04	.3202E+04	.4279E+04	.9409E+00	.1448E+01	.1871E+01
279	.2361E+04	.3659E+04	.4493E+04	.8838E+00	.1360E+01	.1770E+01
280	.2194E+04	.4227E+04	.4837E+04	.8339E+00	.1283E+01	.1692E+01
281	.2198E+04	.4653E+04	.4996E+04	.7741E+00	.1191E+01	.1619E+01
282	.2237E+04	.4934E+04	.5106E+04	.7098E+00	.1092E+01	.1536E+01
283	.2651E+04	.5155E+04	.5307E+04	.6401E+00	.9847E+00	.1442E+01
284	.3322E+04	.5391E+04	.5664E+04	.6355E+00	.9778E+00	.1386E+01
285	.9919E+04	.5586E+04	.4536E+04	.2934E+00	.4514E+00	.6154E+00
286	.9977E+04	.3931E+04	.1710E+04	.1927E+00	.2964E+00	.4016E+00
287	.1120E+05	.5595E+04	.1468E+04	.1230E+00	.1893E+00	.2659E+00
288	.3714E+04	.7953E+04	.8167E+04	.1297E-01	.1995E+01	.3322E+01
289	.7167E+04	.7433E+04	.1510E+05	.2444E-01	.3760E-01	.5406E-01
290	.2054E+05	.1129E+05	.2264E+05	.3925E-01	.6039E-01	.8310E-01
291	.6474E+04	.6005E+04	.1225E+05	.8758E-01	.1347E+00	.1789E+00
292	.3345E+04	.5153E+04	.1254E+05	.8933E-01	.1376E+00	.1819E+00
293	.2996E+04	.5606E+04	.1395E+05	.1008E+00	.1551E+00	.2007E+00
294	.8947E+03	.1206E+04	.6385E+03	.9777E-01	.1504E+00	.2027E+00
295	.1007E+04	.9842E+03	.1538E+04	.1866E+00	.2871E+00	.3490E+00
296	.1284E+04	.2160E+04	.2826E+04	.4442E+00	.6833E+00	.8345E+00
297	.1221E+04	.2491E+04	.3599E+04	.6125E+00	.9423E+00	.1165E+01
298	.1353E+04	.2989E+04	.4264E+04	.6390E+00	.9830E+00	.1239E+01
299	.1505E+04	.3180E+04	.4462E+04	.9283E+00	.1428E+01	.1821E+01
300	.1463E+04	.3560E+04	.4793E+04	.8720E+00	.1342E+01	.1728E+01
301	.1513E+04	.3842E+04	.4948E+04	.742E+00	.1222E+01	.1614E+01
302	.1640E+04	.4067E+04	.5162E+04	.6945E+00	.1068E+01	.1479E+01
303	.1831E+04	.4224E+04	.5328E+04	.6391E+00	.9833E+00	.1421E+01
304	.2133E+04	.4326E+04	.5565E+04	.6161E+00	.9479E+00	.1389E+01
305	.4001E+04	.4005E+04	.5844E+04	.7585E+00	.1167E+01	.1610E+01
306	.1436E+05	.5782E+04	.1377E+04	.3173E+00	.4882E+00	.6605E+00
307	.6818E+03	.9137E+03	.3142E+03	.8574E-01	.1319E+00	.1931E+00
308	.8503E+03	.6199E+03	.1612E+04	.1918E+00	.2951E+00	.3537E+00
309	.9671E+03	.2125E+04	.2664E+04	.4018E+00	.6181E+00	.7344E+00
310	.6519E+03	.2843E+04	.3408E+04	.6467E+00	.9949E+00	.1193E+01

311	.6613E+03	.3512E+04	.4100E+04	.7312E+00	.1125E+01	.1365E+01
312	.7425E+03	.3561E+04	.4368E+04	.6931E+00	.1066E+01	.1318E+01
313	.8191E+03	.3612E+04	.4682E+04	.9200E+00	.1415E+01	.1783E+01
314	.8910E+03	.3655E+04	.4680E+04	.8072E+00	.1242E+01	.1593E+01
315	.1040E+04	.3765E+04	.4893E+04	.6892E+00	.1060E+01	.1409E+01
316	.1139E+04	.3689E+04	.4890E+04	.5474E+00	.8421E+00	.1187E+01
317	.1159E+04	.3026E+04	.4823E+04	.4617E+00	.7104E+00	.1069E+01
318	.1656E+04	.1978E+04	.5615E+04	.5480E+00	.8431E+00	.1197E+01
319	.1471E+04	.1655E+04	.7100E+04	.8548E+00	.1315E+01	.1757E+01
320	.1494E+05	.3232E+04	.5475E+04	.1521E-01	.2340E-01	.3474E-01
321	.6934E+04	.3311E+04	.5729E+04	.1076E-01	.1655E-01	.2445E-01
322	.5508E+04	.3205E+04	.8769E+04	.1369E-01	.2106E-01	.3138E-01
323	.1598E+05	.3268E+04	.1294E+05	.2397E-01	.3687E-01	.4886E-01
324	.2139E+05	.4687E+04	.2162E+05	.3957E-01	.6087E-01	.7943E-01
325	.4157E+04	.4553E+04	.8266E+04	.5585E-01	.8592E-01	.1151E+00
326	.2301E+04	.2257E+04	.1242E+05	.8853E-01	.1362E+00	.1782E+00
327	.3200E+04	.3266E+04	.1303E+05	.9373E-01	.1442E+00	.1870E+00
328	.3681E+04	.3707E+04	.1420E+05	.1032E+00	.1588E+00	.2043E+00
329	.1403E+04	.1335E+03	.6932E+03	.1249E+00	.1921E+00	.2474E+00
330	.1306E+04	.1461E+04	.2748E+04	.5062E+00	.7788E+00	.9336E+00
331	.3881E+03	.2720E+04	.3541E+04	.7658E+00	.1178E+01	.1403E+01
332	.8430E+03	.3704E+04	.3957E+04	.9447E+00	.1453E+01	.1730E+01
333	.1446E+04	.4030E+04	.4323E+04	.9537E+00	.1667E+01	.1761E+01
334	.1816E+04	.4681E+04	.4486E+04	.8667E+00	.1330E+01	.1617E+01
335	.1226E+04	.4019E+04	.4423E+04	.9496E+00	.1461E+01	.1819E+01
336	.1201E+04	.3938E+04	.4640E+04	.7911E+00	.1217E+01	.1563E+01
337	.7592E+03	.3644E+04	.4648E+04	.6432E+00	.9896E+00	.1338E+01
338	.1207E+04	.2954E+04	.4648E+04	.4967E+00	.7642E+00	.1123E+01
339	.1664E+04	.3567E+03	.2244E+04	.1389E+01	.2137E+01	.2636E+01
340	.1084E+04	.6507E+03	.2147E+04	.2080E+01	.3200E+01	.3893E+01
341	.1758E+04	.1090E+04	.2344E+04	.2025E+01	.3115E+01	.3804E+01
342	.2576E+04	.1189E+04	.2468E+04	.1981E+01	.3047E+01	.3731E+01
343	.2512E+04	.7971E+03	.2621E+04	.1796E+01	.2763E+01	.3413E+01
344	.3986E+04	.2332E+04	.2770E+04	.1595E+01	.2453E+01	.3087E+01
345	.2432E+04	.1175E+04	.3069E+04	.1590E+01	.2446E+01	.3130E+01
346	.2051E+04	.1116E+04	.2914E+04	.1369E+01	.2106E+01	.2779E+01
347	.1755E+04	.1202E+04	.2974E+04	.1168E+01	.1797E+01	.2452E+01
348	.1426E+04	.1437E+04	.2928E+04	.9815E+00	.1510E+01	.2130E+01
349	.1488E+04	.1776E+04	.3056E+04	.8192E+00	.1260E+01	.1840E+01
350	.1002E+04	.1196E+04	.3145E+04	.8411E+00	.1294E+01	.1822E+01
351	.2804E+04	.3346E+04	.3567E+04	.1008E+01	.1550E+01	.2085E+01
352	.1255E+05	.2748E+04	.7417E+04	.1387E-01	.2134E-01	.3054E-01
353	.7530E+04	.1415E+04	.9108E+04	.1478E-01	.2274E-01	.3358E-01
354	.9187E+04	.1663E+04	.1060E+05	.1768E-01	.2720E-01	.3960E-01
355	.1609E+05	.1185E+04	.1275E+05	.2405E-01	.3700E-01	.4895E-01
356	.2509E+04	.1841E+04	.1033E+05	.7223E-01	.1111E+00	.1469E+00
357	.2329E+04	.1531E+04	.1319E+05	.9489E-01	.1460E+00	.1902E+00
358	.2362E+04	.1730E+04	.1421E+05	.1035E+00	.1592E+00	.2059E+00
359	.3644E+04	.1953E+04	.1496E+05	.1097E+00	.1688E+00	.2152E+00
360	.2998E+04	.1537E+04	.2816E+04	.1579E+01	.2429E+01	.3015E+01
361	.3452E+04	.9820E+03	.2881E+04	.1470E+01	.2261E+01	.2852E+01
362	.2843E+04	.1390E+04	.3111E+04	.1261E+01	.1940E+01	.2505E+01
363	.2247E+04	.1539E+04	.3065E+04	.1058E+01	.1628E+01	.2164E+01
364	.1862E+04	.1687E+04	.3238E+04	.8837E+00	.1360E+01	.1875E+01
365	.1510E+04	.1681E+04	.3219E+04	.7165E+00	.1102E+01	.1581E+01
366	.1169E+04	.1695E+04	.3509E+04	.7166E+00	.1102E+01	.1544E+01
367	.1138E+04	.1441E+04	.3798E+04	.9623E+00	.1481E+01	.1971E+01
368	.9019E+04	.3479E+04	.5813E+04	.1255E-01	.1930E-01	.2773E-01
369	.2611E+04	.3974E+03	.1557E+04	.9410E+00	.1448E+01	.1836E+01
370	.7520E+03	.3395E+03	.1732E+04	.1339E+01	.2060E+01	.2605E+01
371	.2480E+04	.5623E+03	.1963E+04	.1514E+01	.2329E+01	.2888E+01
372	.3697E+04	.9129E+03	.2443E+04	.1742E+01	.2680E+01	.3298E+01
373	.4656E+04	.1252E+04	.2755E+04	.1775E+01	.2730E+01	.3370E+01
374	.3904E+04	.1202E+04	.2998E+04	.1745E+01	.2684E+01	.3348E+01
375	.4262E+04	.1653E+04	.3289E+04	.1600E+01	.2462E+01	.3124E+01
376	.3476E+04	.2103E+04	.3243E+04	.1467E+01	.2257E+01	.2932E+01

377	.2803E+04	.2752E+04	.3285E+04	.1244E+01	.1913E+01	.2563E+01
378	.2121E+04	.2873E+04	.3216E+04	.1029E+01	.1583E+01	.2207E+01
379	.2031E+04	.3131E+04	.3686E+04	.8150E+00	.1254E+01	.1833E+01
380	.1882E+04	.2554E+04	.3614E+04	.8253E+00	.1270E+01	.1781E+01
381	.3023E+04	.4967E+04	.6131E+04	.8661E+00	.1332E+01	.1751E+01
382	.7278E+04	.4269E+04	.7067E+04	.1244E+01	.1914E+01	.2994E+01
383	.1034E+05	.1472E+04	.9636E+04	.1538E+01	.2366E+01	.3782E+01
384	.1039E+05	.1956E+04	.1010E+05	.1713E+01	.2635E+01	.4037E+01
385	.1361E+05	.1197E+04	.1109E+05	.2064E+01	.3175E+01	.4439E+01
386	.2982E+04	.1580E+04	.1126E+05	.7952E+01	.1223E+00	.1604E+00
387	.2524E+04	.1458E+04	.1331E+05	.9590E+01	.1475E+00	.1914E+00
388	.2313E+04	.1569E+04	.1447E+05	.1054E+00	.1622E+00	.2100E+00
389	.2736E+04	.1543E+04	.1520E+05	.1115E+00	.1716E+00	.2193E+00
390	.2209E+04	.1627E+03	.5091E+03	.3902E+00	.6003E+00	.7422E+00
391	.6200E+03	.1160E+04	.7151E+03	.5617E+01	.8642E+01	.1436E+00
392	.3299E+04	.1994E+04	.1718E+04	.1686E+00	.2594E+00	.3630E+00
393	.4342E+04	.2947E+04	.2811E+04	.3436E+00	.5286E+00	.6815E+00
394	.5180E+04	.3826E+04	.3386E+04	.4273E+00	.6578E+00	.8431E+00
395	.5647E+04	.4850E+04	.3603E+04	.4239E+00	.6521E+00	.8502E+00
396	.5328E+04	.6397E+04	.3400E+04	.4051E+00	.6233E+00	.8190E+00
397	.3797E+04	.6978E+04	.3733E+04	.4352E+00	.6696E+00	.9297E+00
398	.3699E+04	.7330E+04	.4076E+04	.4115E+00	.6331E+00	.9190E+00
399	.2725E+04	.9321E+04	.4489E+04	.4134E+00	.6361E+00	.9553E+00
400	.7059E+03	.3248E+03	.5050E+03	.2287E+00	.3518E+00	.4555E+00
401	.8302E+03	.3560E+03	.2963E+03	.3190E+01	.4908E+01	.9109E+01
402	.2999E+04	.9674E+03	.1575E+04	.2609E+00	.4013E+00	.4806E+00
403	.4682E+04	.1345E+04	.3087E+04	.4895E+00	.7530E+00	.9097E+00
404	.6283E+04	.1436E+04	.4093E+04	.5456E+00	.8394E+00	.1046E+01
405	.6949E+04	.1212E+04	.4445E+04	.4986E+00	.7671E+00	.9929E+00
406	.6926E+04	.1300E+04	.6633E+04	.4275E+00	.6576E+00	.8881E+00
407	.4518E+04	.1967E+04	.4508E+04	.4323E+00	.6651E+00	.9628E+00
408	.3901E+04	.2735E+04	.4969E+04	.3776E+00	.5810E+00	.8787E+00
409	.2984E+04	.3733E+04	.5582E+04	.3683E+00	.5666E+00	.8265E+00
410	.2372E+04	.4809E+04	.5807E+04	.4185E+00	.6439E+00	.9103E+00
411	.1421E+04	.5533E+04	.6963E+04	.5238E+00	.8059E+00	.1090E+01
412	.9804E+03	.4576E+04	.7767E+04	.5973E+00	.9189E+00	.1172E+01
413	.1071E+05	.3545E+04	.6861E+04	.1211E+01	.1864E+01	.2783E+01
414	.1210E+05	.1343E+04	.9289E+04	.1623E+01	.2498E+01	.3452E+01
415	.1234E+05	.1245E+04	.1074E+05	.1874E+01	.2883E+01	.3898E+01
416	.3073E+04	.1364E+04	.1163E+05	.8248E+01	.1269E+00	.1626E+00
417	.2942E+04	.1638E+04	.1345E+05	.9701E+01	.1492E+00	.1922E+00
418	.2607E+04	.1670E+04	.1449E+05	.1055E+00	.1623E+00	.2103E+00
419	.2249E+04	.1624E+04	.1528E+05	.1119E+00	.1721E+00	.2214E+00
420	.1357E+04	.4713E+03	.3521E+03	.9049E+01	.1392E+00	.2511E+00
421	.2688E+04	.5188E+03	.1886E+04	.3912E+00	.6018E+00	.7104E+00
422	.5270E+04	.6708E+03	.3539E+04	.6173E+00	.9498E+00	.1136E+01
423	.6519E+04	.9289E+03	.4212E+04	.6485E+00	.9977E+00	.1236E+01
424	.7755E+04	.1642E+04	.4953E+04	.5843E+00	.8989E+00	.1157E+01
425	.7693E+04	.1639E+04	.4938E+04	.4891E+00	.7525E+00	.1010E+01
426	.5486E+04	.1523E+04	.4997E+04	.5110E+00	.7862E+00	.1130E+01
427	.4540E+04	.1348E+04	.5257E+04	.4542E+00	.6987E+00	.1015E+01
428	.3447E+04	.1150E+04	.5960E+04	.4779E+00	.7353E+00	.1020E+01
429	.2524E+04	.1092E+04	.6821E+04	.5342E+00	.8219E+00	.1104E+01
430	.1537E+04	.1111E+04	.7135E+04	.5616E+00	.8641E+00	.1124E+01
431	.1055E+04	.1241E+04	.7644E+04	.5475E+00	.8424E+00	.1061E+01
432	.1411E+05	.1340E+04	.7479E+04	.1281E+01	.1970E+01	.2999E+01
433	.2085E+04	.1184E+03	.1258E+04	.6712E+00	.1033E+01	.1214E+01
434	.4301E+04	.1285E+04	.2747E+04	.7830E+00	.1205E+01	.1440E+01
435	.6777E+04	.1840E+04	.4199E+04	.7680E+00	.1182E+01	.1461E+01
436	.7381E+04	.2212E+04	.4472E+04	.6582E+00	.1013E+01	.1299E+01
437	.8294E+04	.2712E+04	.5025E+04	.5337E+00	.8211E+00	.1089E+01
438	.6009E+04	.2901E+04	.4897E+04	.5550E+00	.8539E+00	.1207E+01
439	.5272E+04	.3072E+04	.5175E+04	.4608E+00	.7089E+00	.1035E+01
440	.3838E+04	.3153E+04	.5718E+04	.4879E+00	.7506E+00	.1048E+01
441	.2965E+04	.3291E+04	.6238E+04	.5230E+00	.8047E+00	.1089E+01
442	.2360E+04	.3472E+04	.6886E+04	.5444E+00	.8376E+00	.1100E+01

443	.2066E+04	.3519E+04	.7205E+04	.5468E+00	.8412E+00	.1068E+01
444	.1704E+05	.2973E+04	.7052E+04	.1215E-01	.1870E-01	.3146E-01
445	.2540E+04	.3071E+03	.1602E+04	.1057E+01	.1627E+01	.1946E+01
446	.4975E+04	.1374E+04	.2694E+04	.8574E+00	.1319E+01	.1642E+01
447	.7088E+04	.1818E+04	.4047E+04	.6972E+00	.1073E+01	.1383E+01
448	.7797E+04	.2541E+04	.4087E+04	.5437E+00	.8364E+00	.1112E+01
449	.6325E+04	.3012E+04	.4525E+04	.5570E+00	.8569E+00	.1205E+01
450	.5703E+04	.3409E+04	.4758E+04	.4437E+00	.6826E+00	.1004E+01
451	.4335E+04	.3785E+04	.5327E+04	.4722E+00	.7265E+00	.1022E+01
452	.3402E+04	.4052E+04	.5896E+04	.5128E+00	.7889E+00	.1077E+01
453	.2903E+04	.4245E+04	.6411E+04	.5364E+00	.8252E+00	.1092E+01
454	.2710E+04	.4426E+04	.6977E+04	.5483E+00	.8436E+00	.1079E+01
455	.1769E+05	.4134E+04	.7125E+04	.1269E-01	.1952E-01	.3078E-01
456	.1397E+05	.2833E+04	.8684E+04	.1510E-01	.2323E-01	.3107E-01
457	.1093E+05	.2185E+04	.1038E+05	.1726E-01	.2655E-01	.3466E-01
458	.3465E+04	.2104E+04	.1163E+05	.8228E-01	.1266E+00	.1613E+00
459	.3067E+04	.2119E+04	.1326E+05	.9538E-01	.1467E+00	.1892E+00
460	.2743E+04	.2061E+04	.1429E+05	.1037E+00	.1596E+00	.2084E+00
461	.2445E+04	.2110E+04	.1516E+05	.1108E+00	.1704E+00	.2217E+00
462	.2861E+04	.5153E+03	.1889E+04	.8855E+00	.1362E+01	.1709E+01
463	.4926E+04	.1368E+04	.2397E+04	.6441E+00	.9909E+00	.1299E+01
464	.7654E+04	.2036E+04	.3609E+04	.5169E+00	.7952E+00	.1063E+01
465	.6032E+04	.2543E+04	.3760E+04	.5148E+00	.7920E+00	.1121E+01
466	.5993E+04	.3244E+04	.4271E+04	.4021E+00	.6186E+00	.9221E+00
467	.6614E+04	.3714E+04	.4897E+04	.4350E+00	.6692E+00	.9494E+00
468	.3635E+04	.4080E+04	.5456E+04	.4908E+00	.7551E+00	.1037E+01
469	.3206E+04	.4425E+04	.6164E+04	.5346E+00	.8225E+00	.1094E+01
470	.2902E+04	.4565E+04	.6770E+04	.5526E+00	.8502E+00	.1094E+01
471	.2033E+05	.5367E+04	.6211E+04	.1254E-01	.1930E-01	.3222E-01
472	.1572E+05	.4260E+04	.7641E+04	.1361E-01	.2094E-01	.3075E-01
473	.1046E+05	.3245E+04	.9574E+04	.1562E-01	.2403E-01	.3219E-01
474	.3651E+04	.2863E+04	.1127E+05	.7933E-01	.1220E+00	.1579E+00
475	.3180E+04	.2714E+04	.1296E+05	.9285E-01	.1428E+00	.1864E+00
476	.2793E+04	.2734E+04	.1403E+05	.1016E+00	.1562E+00	.2064E+00
477	.2516E+04	.2814E+04	.1503E+05	.1096E+00	.1687E+00	.2218E+00
478	.3132E+04	.5792E+03	.1658E+04	.6593E+00	.1014E+01	.1341E+01
479	.5606E+04	.1166E+04	.2326E+04	.5389E+00	.8290E+00	.1110E+01
480	.6081E+04	.1977E+04	.3096E+04	.4706E+00	.7240E+00	.1026E+01
481	.5882E+04	.2675E+04	.3653E+04	.3453E+00	.5312E+00	.8088E+00
482	.4768E+04	.3403E+04	.4366E+04	.3692E+00	.5680E+00	.8206E+00
483	.3746E+04	.3967E+04	.4940E+04	.4269E+00	.6567E+00	.9128E+00
484	.3107E+04	.4483E+04	.5660E+04	.4881E+00	.7509E+00	.1008E+01
485	.3080E+04	.5224E+04	.6775E+04	.5501E+00	.8463E+00	.1096E+01
486	.2324E+05	.4251E+04	.5955E+04	.1633E-01	.2513E-01	.3780E-01
487	.3410E+04	.7111E+03	.1134E+04	.6483E+00	.9974E+00	.1361E+01
488	.5272E+04	.1223E+04	.2148E+04	.5396E+00	.8302E+00	.1208E+01
489	.5578E+04	.1857E+04	.3047E+04	.4386E+00	.6748E+00	.1049E+01
490	.4696E+04	.2327E+04	.3711E+04	.4595E+00	.7070E+00	.1047E+01
491	.3750E+04	.2667E+04	.4167E+04	.5139E+00	.7907E+00	.1117E+01
492	.3026E+04	.3007E+04	.4606E+04	.5703E+00	.8774E+00	.1188E+01
493	.2426E+04	.3439E+04	.5104E+04	.6153E+00	.9467E+00	.1230E+01
494	.2322E+05	.4457E+04	.6484E+04	.1651E-01	.2541E-01	.3957E-01
495	.1343E+04	.2578E+03	.3666E+03	.4425E+00	.6808E+00	.9221E+00
496	.3700E+04	.3862E+03	.1171E+04	.3792E+00	.5834E+00	.8674E+00
497	.4809E+04	.9130E+03	.2177E+04	.3322E+00	.5111E+00	.8513E+00
498	.4362E+04	.1371E+04	.3074E+04	.3660E+00	.5631E+00	.8927E+00
499	.3584E+04	.1674E+04	.3702E+04	.4247E+00	.6534E+00	.9666E+00
500	.2790E+04	.1969E+04	.4264E+04	.5035E+00	.7746E+00	.1076E+01
501	.1947E+04	.2208E+04	.5016E+04	.5929E+00	.9121E+00	.1194E+01
502	.2076E+05	.3473E+04	.6182E+04	.1617E-01	.2180E-01	.3508E-01
503	.1681E+05	.3739E+04	.6806E+04	.1267E-01	.1918E-01	.3245E-01
504	.1163E+05	.3265E+04	.8736E+04	.1426E-01	.2194E-01	.3226E-01
505	.4078E+04	.3132E+04	.1076E+05	.7527E-01	.1158E+00	.1544E+00
506	.3357E+04	.3134E+04	.1254E+05	.8945E-01	.1376E+00	.1833E+00
507	.2920E+04	.3230E+04	.1372E+05	.9896E-01	.1523E+00	.2042E+00
508	.2715E+04	.3304E+04	.1490E+05	.1085E+00	.1670E+00	.2217E+00

509	.2257E+04	.1974E+03	.6940E+03	.2593E+00	.3989E+00	.5993E+00
510	.3863E+04	.4280E+03	.1684E+04	.2332E+00	.3588E+00	.6344E+00
511	.3508E+04	.7056E+03	.2600E+04	.2937E+00	.4519E+00	.7731E+00
512	.3060E+04	.9622E+03	.3271E+04	.3674E+00	.5652E+00	.8950E+00
513	.2365E+04	.1202E+04	.39u5E+04	.4587E+00	.7056E+00	.1042E+01
514	.1530E+04	.1516E+04	.4682E+04	.3550E+00	.8538E+00	.1159E+01
515	.1927E+05	.2084E+04	.5051E+04	.1399E-01	.2152E-01	.3375E-01
516	.1676E+05	.2343E+04	.5998E+04	.1204E-01	.1853E-01	.3207E-01
517	.1358E+05	.2772E+04	.7783E+04	.1334E-01	.2053E-01	.3269E-01
518	.6516E+04	.3016E+04	.1017E+05	.7068E-01	.1087E+00	.1503E+00
519	.3630E+04	.3159E+04	.1200E+05	.8511E-01	.1309E+00	.1799E+00
520	.3160E+04	.3401E+04	.1330E+05	.9556E-01	.1470E+00	.2017E+00
521	.2992E+04	.3560E+04	.1465E+05	.1065E+00	.1639E+00	.2209E+00
522	.1133E+04	.1516E+03	.4021E+03	.2064E+00	.3176E+00	.4882E+00
523	.2730E+04	.3296E+03	.1187E+04	.1851E+00	.2848E+00	.5044E+00
524	.2609E+04	.6523E+03	.2209E+04	.2730E+00	.4200E+00	.7042E+00
525	.2279E+04	.8892E+03	.2978E+04	.3706E+00	.5701E+00	.8790E+00
526	.1803E+04	.1078E+04	.3662E+04	.4596E+00	.7070E+00	.1037E+01
527	.1202E+04	.1221E+04	.4325E+04	.5221E+00	.8033E+00	.1145E+01
528	.1902E+05	.1641E+04	.5776E+04	.1472E-01	.2265E-01	.3552E-01
529	.1788E+04	.2266E+03	.7318E+03	.1685E+00	.2592E+00	.4368E+00
530	.2157E+04	.5495E+03	.1767E+04	.2341E+00	.3601E+00	.6068E+00
531	.1758E+04	.8276E+03	.2613E+04	.3615E+00	.5562E+00	.8504E+00
532	.1404E+04	.1015E+04	.3368E+04	.4652E+00	.7157E+00	.1036E+01
533	.9662E+03	.1155E+04	.4098E+04	.5610E+00	.8323E+00	.1157E+01
534	.1763E+05	.1992E+04	.4260E+04	.1393E-01	.2144E-01	.3364E-01
535	.1031E+04	.1486E+03	.3736E+03	.1688E+00	.2597E+00	.4124E+00
536	.1853E+04	.3752E+03	.1218E+04	.1914E+00	.2944E+00	.5045E+00
537	.1519E+04	.6824E+03	.2159E+04	.3525E+00	.5116E+00	.7925E+00
538	.1226E+04	.9125E+03	.3012E+04	.4534E+00	.6975E+00	.1018E+01
539	.8376E+03	.1044E+04	.3837E+04	.5514E+00	.8483E+00	.1175E+01
540	.1626E+05	.1172E+04	.4963E+04	.1226E-01	.1886E-01	.3070E-01
541	.1539E+05	.1669E+04	.5721E+04	.1182E-01	.1818E-01	.3108E-01
542	.1420E+05	.2091E+04	.7432E+04	.1307E-01	.2011E-01	.3346E-01
543	.4369E+04	.2394E+04	.9770E+04	.6765E-01	.1041E+00	.1481E+00
544	.3661E+04	.2708E+04	.1161E+05	.8207E-01	.1263E+00	.1781E+00
545	.3146E+04	.2983E+04	.1305E+05	.9358E-01	.1440E+00	.2005E+00
546	.2949E+04	.3203E+04	.1450E+05	.1054E+00	.1621E+00	.2208E+00
547	.1458E+04	.2265E+03	.7464E+03	.1736E+00	.2671E+00	.4465E+00
548	.1513E+04	.4790E+03	.1634E+04	.2757E+00	.4241E+00	.6780E+00
549	.1165E+04	.7353E+03	.2586E+04	.4207E+00	.6472E+00	.9695E+00
550	.7638E+03	.8903E+03	.3512E+04	.5664E+00	.8406E+00	.1187E+01
551	.1422E+05	.1274E+04	.4493E+04	.1135E-01	.1746E-01	.2884E-01
552	.1414E+05	.1159E+04	.5687E+04	.1126E-01	.1732E-01	.2994E-01
553	.1381E+05	.1473E+04	.7334E+04	.1285E-01	.1978E-01	.3382E-01
554	.3767E+04	.1737E+04	.9534E+04	.6594E-01	.1014E+00	.1474E+00
555	.3322E+04	.2012E+04	.1140E+05	.8057E-01	.1240E+00	.1779E+00
556	.2923E+04	.2277E+04	.1294E+05	.9297E-01	.1430E+00	.2009E+00
557	.2595E+04	.2470E+04	.1450E+05	.1055E+00	.1624E+00	.2214E+00
558	.9479E+03	.1580E+03	.3883E+03	.1806E+00	.2779E+00	.4465E+00
559	.1504E+04	.2567E+03	.1006E+04	.1958E+00	.3013E+00	.5203E+00
560	.1039E+04	.4369E+03	.2127E+04	.3777E+00	.5810E+00	.9174E+00
561	.6385E+03	.5763E+03	.3193E+04	.5344E+00	.8222E+00	.1210E+01
562	.1376E+05	.7737E+03	.4140E+04	.1043E-01	.1604E-01	.2735E-01
563	.1083E+04	.2450E+02	.5495E+03	.1218E+00	.1874E+00	.3823E+00
564	.8566E+03	.1297E+03	.1770E+04	.3334E+00	.5129E+00	.8844E+00
565	.4659E+03	.2662E+03	.2921E+04	.5095E+00	.7839E+00	.1225E+01
566	.1291E+05	.1064E+04	.3866E+04	.1020E-01	.1569E-01	.2621E-01
567	.7248E+03	.5181E+02	.5729E+03	.1117E+00	.1718E+00	.3387E+00
568	.5876E+03	.6370E+02	.1692E+04	.3231E+00	.4970E+00	.8966E+00
569	.3490E+03	.1106E+03	.2780E+04	.4738E+00	.7290E+00	.1206E+01
570	.1262E+05	.6446E+03	.3944E+04	.9562E-02	.1471E-01	.2499E-01
571	.1282E+05	.8014E+03	.5210E+04	.1029E-01	.1583E-01	.2809E-01
572	.1333E+05	.1032E+04	.6993E+04	.1220E-01	.1878E-01	.3332E-01
573	.3557E+04	.1219E+04	.9311E+04	.6433E-01	.9898E-01	.1469E+00
574	.3404E+04	.1424E+04	.1125E+05	.7963E-01	.1225E+00	.1782E+00

575	.3223E+04	.1612E+04	.1291E+05	.9309E-01	.1432E+00	.201.
576	.3038E+04	.1787E+04	.1458E+05	.1066E+00	.1639E+00	.2225E-01
577	.5771E+03	.5636E+02	.6496E+03	.1403E+00	.2158E+00	.3916E+00
578	.7989E+03	.2289E+03	.1674E+04	.3156E+00	.4855E+00	.8592E+00
579	.5866E+03	.4753E+03	.2367E+04	.4277E+00	.6579E+00	.1111E+01
580	.1195E+05	.1319E+04	.3629E+04	.9086E-02	.1398E-01	.2331E-01
581	.1233E+05	.1110E+04	.4663E+04	.9636E-02	.1683E-01	.2630E-01
582	.1266E+05	.1055E+04	.6643E+04	.1178E-01	.1813E-01	.3251E-01
583	.3372E+04	.1124E+04	.9135E+04	.6313E-01	.9712E-01	.1465E+00
584	.3660E+04	.1191E+04	.1115E+05	.7918E-01	.1218E+00	.1786E+00
585	.3447E+04	.1261E+04	.1291E+05	.9350E-01	.1438E+00	.2027E+00
586	.3371E+04	.1389E+04	.1468E+05	.1078E+00	.1659E+00	.2239E+00
587	.9916E+03	.3902E+03	.4945E+03	.2347E+00	.3612E+00	.5811E+00
588	.1408E+04	.5657E+03	.1323E+04	.2944E+00	.4529E+00	.7968E+00
589	.1023E+04	.9421E+03	.2195E+04	.3691E+00	.5678E+00	.9512E+00
590	.1179E+05	.8161E+03	.2183E+04	.8562E-02	.1317E-01	.2068E-01
591	.1040E+04	.5026E+03	.7658E+03	.2919E+00	.4491E+00	.7731E+00
592	.1142E+04	.7294E+03	.1450E+04	.2785E+00	.4284E+00	.6849E+00
593	.1138E+05	.1134E+04	.3623E+04	.8484E-02	.1305E-01	.2159E-01
594	.4251E+03	.1376E+03	.9504E+03	.1845E+00	.2838E+00	.4482E+00
595	.1100E+05	.9689E+03	.2497E+04	.8157E-02	.1255E-01	.2018E-01
596	.1141E+05	.1226E+04	.4714E+04	.8972E-02	.1380E-01	.2501E-01
597	.1196E+05	.1065E+04	.6751E+04	.1178E-01	.1812E-01	.3174E-01
598	.3259E+04	.1143E+04	.9085E+04	.6277E-01	.9657E-01	.1466E+00
599	.3549E+04	.1271E+04	.1108E+05	.7882E-01	.1213E+00	.1790E+00
600	.3743E+04	.1301E+04	.1284E+05	.9328E-01	.1435E+00	.2033E+00
601	.3836E+04	.1244E+04	.1474E+05	.1088E+00	.1674E+00	.2253E+00
602	.1370E+03	.5714E+02	.9167E+03	.1932E+00	.2973E+00	.4240E+00
603	.9585E+04	.3071E+03	.2721E+04	.7609E-02	.1171E-01	.1896E-01
604	.1036E+05	.4337E+03	.4498E+04	.8202E-02	.1262E-01	.2319E-01
605	.1115E+05	.7802E+03	.6717E+04	.1139E-01	.1753E-01	.3014E-01
606	.3174E+04	.9974E+03	.9069E+04	.6246E-01	.9609E-01	.1460E+00
607	.3455E+04	.1134E+04	.1099E+05	.7784E-01	.1198E+00	.1785E+00
608	.4210E+04	.1241E+04	.1252E+05	.9056E-01	.1393E+00	.2020E+00
609	.4825E+04	.1188E+04	.1443E+05	.1069E+00	.1645E+00	.2245E+00
610	.7660E+02	.4684E+02	.9394E+03	.2063F+00	.3173E+00	.4425E+00
611	.9139E+04	.4925E+03	.2081E+04	.6758E-02	.1040E-01	.1748E-01
612	.6621E+02	.2427E+02	.9486E+03	.2036E+00	.3133E+00	.4387E+00
613	.8258E+04	.2452E+03	.2546E+04	.6645E-02	.9915E-02	.1721E-01
614	.9385E+04	.1750E+03	.4739E+04	.7907E-02	.1217E-01	.2224E-01
615	.1051E+05	.4636E+03	.7003E+04	.1170E-01	.1800E-01	.2923E-01
616	.3036E+04	.7208E+03	.9215E+04	.6341E-01	.9755E-01	.1660E+00
617	.3060E+04	.9614E+03	.1104E+05	.7782E-01	.1197E+00	.1780E+00
618	.3431E+04	.1119E+04	.1227E+05	.8779E-01	.1351E+00	.1995E+00
619	.7603E+04	.2486E+04	.1314E+05	.9642E-01	.1483E+00	.2173E+00

**APPENDIX E: PREDICTION OF THE SEISMIC RESPONSE OF THE RIRIE DAM  
USING SIMPLIFIED NONLINEAR SHEAR BEAM MODELS**  
**(Dakoulas 1989a)**

PREDICTION OF THE SEISMIC RESPONSE OF THE RIRIE DAM  
USING SIMPLIFIED NONLINEAR SHEAR BEAM MODELS

by Panos C. Dakoulas

Report to U. S. Army Engineer,  
Waterways Experiment Station

March 1989

Civil Engineering Department  
George Brown School of Engineering  
Rice University  
Houston, Texas

## TABLE OF CONTENTS

TABLE OF CONTENTS.	i
LIST OF FIGURES.	ii
LIST OF TABLES	vii
ABSTRACT	viii
1. INTRODUCTION.	1
2. MODELING OF RIRIE DAM	8
2.1 Geometry and Materials.	8
2.2 Shear Beam Models	9
2.2.1 Model 1	9
2.2.2 Model 2	18
2.2.3 Model 3	21
2.3 Fundamental Period of Ririe Dam	23
3. PARAMETRIC STUDIES.	27
3.1 Response of Ririe Dam Using Model 1	27
3.2 Response of Ririe Dam Using Model 2	53
3.3 Response of Ririe Dam Using Model 3	77
4. CONCLUSIONS	86
5. REFERENCES.	89
6. APPENDIX.	90

## LIST OF FIGURES

<b>Figure 1.1 Plan view of Ririe Dam . . . . .</b>	<b>2</b>
<b>Figure 1.2 Cross-section of Ririe Dam at the midsection . . . . .</b>	<b>3</b>
<b>Figure 1.3 Longitudinal section of Ririe Dam. . . . .</b>	<b>4</b>
<b>Figure 1.4 Hypothetical acceleration (provided by Prof. H. B. Seed) . . .</b>	<b>5</b>
<b>Figure 1.5 Hypothetical velocity (provided by Prof. H. B. Seed) . . . .</b>	<b>6</b>
<b>Figure 1.6 Acceleration response spectra of input motion (provided by Prof. H. B. Seed) . . . . .</b>	<b>7</b>
<b>Figure 2.1 Cross-section at midsection . . . . .</b>	<b>10</b>
<b>Figure 2.2 Longitudinal section . . . . .</b>	<b>11</b>
<b>Figure 2.3 Model 1: Dam and foundation layer in a rectangular canyon (a) perspective view, (b) longitudinal and cross-section, (c) stresses acting on infinitesimal bodies (Ref. 2) . . . .</b>	<b>13</b>
<b>Figure 2.4 Illustrative example of response of a dam on a foundation layer, using the piece-wise linear method: (a) average (within the dam) shear strain and equivalent sinusoidal amplitude versus time, (b) shear modulus degradation versus time, (c) damping ratio versus time . . . . .</b>	<b>15</b>
<b>Figure 2.5 Definition of outcrop rock and dam base motion . . . . .</b>	<b>17</b>
<b>Figure 2.6 Model 2: Dam cross-section and distribution of shear modulus with depth . . . . .</b>	<b>19</b>
<b>Figure 2.7 Typical comparison between cross accelerations obtained from linear analysis using consistent inhomogeneous shear beams and finite element models . . . . .</b>	<b>20</b>
<b>Figure 2.8 Model 3: Dam in a semi-cylindrical canyon, (a) perspec- tive view, (b) longitudinal section, (c) cross-section, (d) shear stresses acting on infinitesimal element . . . .</b>	<b>22</b>

<b>Figure 2.9</b> Corrected lateral horizontal accelerations recorded near midcrest during the 1983 Mount Borah earthquake, (a) time histories, (b) Fourier spectra. . . . .	24
<b>Figure 2.10</b> Corrected lateral horizontal accelerations recorded at the downstream during the 1983 Mount Borah earthquake, (a) time histories, (b) Fourier spectra. . . . .	25
<b>Figure 2.11</b> Corrected lateral horizontal accelerations recorded at the abutment during the 1983 Mount Borah earthquake, (a) time histories, (b) Fourier spectra. . . . .	26
<b>Figure 3.1</b> Hypothetical acceleration time history and Fourier spectra .	30
<b>Figure 3.2</b> Case 1: Distribution with depth of peak acceleration evaluated at midsection . . . . .	31
<b>Figure 3.3</b> Case 1: Crest acceleration time history and Fourier spectra evaluated at midsection . . . . .	32
<b>Figure 3.4</b> Case 1: Acceleration time history and Fourier spectra evaluated at depth = 39 ft. from the crest at midsection. .	33
<b>Figure 3.5</b> Case 1: Distribution with depth of peak displacements evaluated at midsection. . . . .	34
<b>Figure 3.6</b> Case 1: Distribution with depth of peak shear strains $\gamma_{yz}$ evaluated at midsection. . . . .	35
<b>Figure 3.7</b> Case 1: Distribution with depth of peak shear stresses $\tau_{yz}$ evaluated at midsection . . . . .	36
<b>Figure 3.8</b> Transfer function relating the acceleration amplitude at the dam base and at the outcrop rock . . . . .	39
<b>Figure 3.9</b> Acceleration time history and Fourier spectra at the dam base . . . . .	40

Figure 3.10 Case 2: Distribution with depth of peak acceleration evaluated at midsection . . . . .	41
Figure 3.11 Case 2: Crest acceleration time history and Fourier spectra evaluated at midsection . . . . .	42
Figure 3.12 Case 2: Distribution with depth of peak displacements evaluated at midsection . . . . .	43
Figure 3.13 Case 2: Distribution with depth of peak shear strains $\gamma_{yz}$ evaluated at midsection . . . . .	44
Figure 3.14 Case 2: Distribution with depth of peak shear stresses $\tau_{yz}$ evaluated at midsection . . . . .	45
Figure 3.15 Case 3: Distribution with depth of peak accelerations evaluated at midsection. . . . .	48
Figure 3.16 Case 3: Crest acceleration time history and Fourier spectra evaluated at midsection . . . . .	49
Figure 3.17 Case 3: Distribution with depth of peak displacements evaluated at midsection. . . . .	50
Figure 3.18 Case 3: Distribution with depth of peak shear strains $\gamma_{yz}$ evaluated at midsection . . . . .	51
Figure 3.19 Case 3: Distribution with depth of peak shear stresses $\tau_{yz}$ evaluated at midsection . . . . .	52
Figure 3.20 Case 4: Distribution with depth of peak accelerations . . .	55
Figure 3.21 Case 4: Crest acceleration time history and Fourier spectra . . . . .	56
Figure 3.22 Case 4: Distribution with depth of peak displacements . . .	57
Figure 3.23 Case 4: Distribution with depth of peak shear strains . . .	58
Figure 3.24 Case 5: Distribution with depth of peak accelerations . . .	61

Figure 3.25 Case 5: Crest acceleration time history and Fourier spectra. . . . .	62
Figure 3.26 Case 5: Distribution with depth of peak displacements. . . .	63
Figure 3.27 Case 5: Distribution with depth of peak shear strains $\gamma_{yz}$ . . . . .	64
Figure 3.28 Case 6: Distribution with depth of peak accelerations. . . .	67
Figure 3.29 Case 6: Crest acceleration time history and Fourier spectra. . . . .	68
Figure 3.30 Case 6: Distribution with depth of peak displacements. . . .	69
Figure 3.31 Case 6: Distribution with depth of peak shear strains. . . .	70
Figure 3.32 Case 7: Distribution with depth of peak accelerations. . . .	73
Figure 3.33 Case 7: Crest accelerations time history and Fourier spectra. . . . .	74
Figure 3.34 Case 7: Distribution with depth of peak displacements. . . .	75
Figure 3.35 Case 7: Distribution with depth of peak shear strains at the dam base . . . . .	76
Figure 3.36 Transfer function relating the acceleration amplitude at the dam base and at the outcrop rock for the case of a semi-cylindrical canyon. . . . .	80
Figure 3.37 Acceleration time history and Fourier spectra at the dam base . . . . .	81
Figure 3.38 Case 8: Distribution with depth of peak accelerations evaluated at midsection. . . . .	82
Figure 3.39 Case 8: Crest acceleration time history and Fourier spectra evaluated at midsection. . . . .	83
Figure 3.40 Case 8: Distribution with depth of peak displacements evaluated at midsection. . . . .	84

<b>Figure 3.41 Case 8: Distribution with depth of peak shear strains</b>	
$\gamma_{yz}$ evaluated at midsection . . . . .	85
<b>Figure 6.1 Case 2: Acceleration time histories at various elevations</b>	
within the dam . . . . .	91
<b>Figure 6.2 Case 2: Displacement time histories at various elevations</b>	
within the dam . . . . .	92
<b>Figure 6.3 Case 2: Shear strain time histories at various elevations</b>	
within the dam . . . . .	93

## LIST OF TABLES

<b>Table 2.1 Estimated Static and Dynamic Material Properties' for Ririe Dam (provided by Professor T. Stark and Professor H. B. Seed) . . . . .</b>	<b>12a</b>
<b>Table 3.1 Input Data for Case 1 . . . . .</b>	<b>28</b>
<b>Table 3.2 Input Data for Case 2 . . . . .</b>	<b>38</b>
<b>Table 3.3 Input Data for Case 3 . . . . .</b>	<b>47</b>
<b>Table 3.4 Input Data for Case 4 . . . . .</b>	<b>54</b>
<b>Table 3.5 Input Data for Case 5 . . . . .</b>	<b>60</b>
<b>Table 3.6 Input Data for Case 6 . . . . .</b>	<b>66</b>
<b>Table 3.7 Input Data for Case 7 . . . . .</b>	<b>72</b>
<b>Table 3.8 Input Data for Case 8 . . . . .</b>	<b>79</b>
<b>Table 4.1 Estimated Peak Response of Ririe Dam . . . . .</b>	<b>88</b>

## ABSTRACT

The objective of this work is to evaluate the response of Ririe Dam, Idaho, to a strong ground shaking by using three theoretical nonlinear shear beam models. The first model assumes that the dam rests on a foundation layer and idealizes the canyon with an equivalent rectangular shape. Soil stiffness is assumed to increase with depth within the dam, depending on the material type and confining stress. The nonlinearity is represented in a simple piece-wise linear scheme, in which the soil shear moduli and damping ratios within the dam and the layer are continuously updated at small time intervals during the analysis. The second model assumes plane strain conditions and no foundation layer, while the rest factors are treated as in the first model. The third model assumes that the canyon has a semi-cylindrical shape, the dam homogeneous, and is used only for equivalent linear analysis. All three models consider the effect of radiation damping. Results from eight analyses are presented selectively in the form of time histories and distributions with depth of peak accelerations, displacements, shear stains and shear stresses. The best estimates of the response indicate peak midcrest accelerations about 1.5 g but deamplification of the input acceleration for most of the dam body and its alluvial foundation.

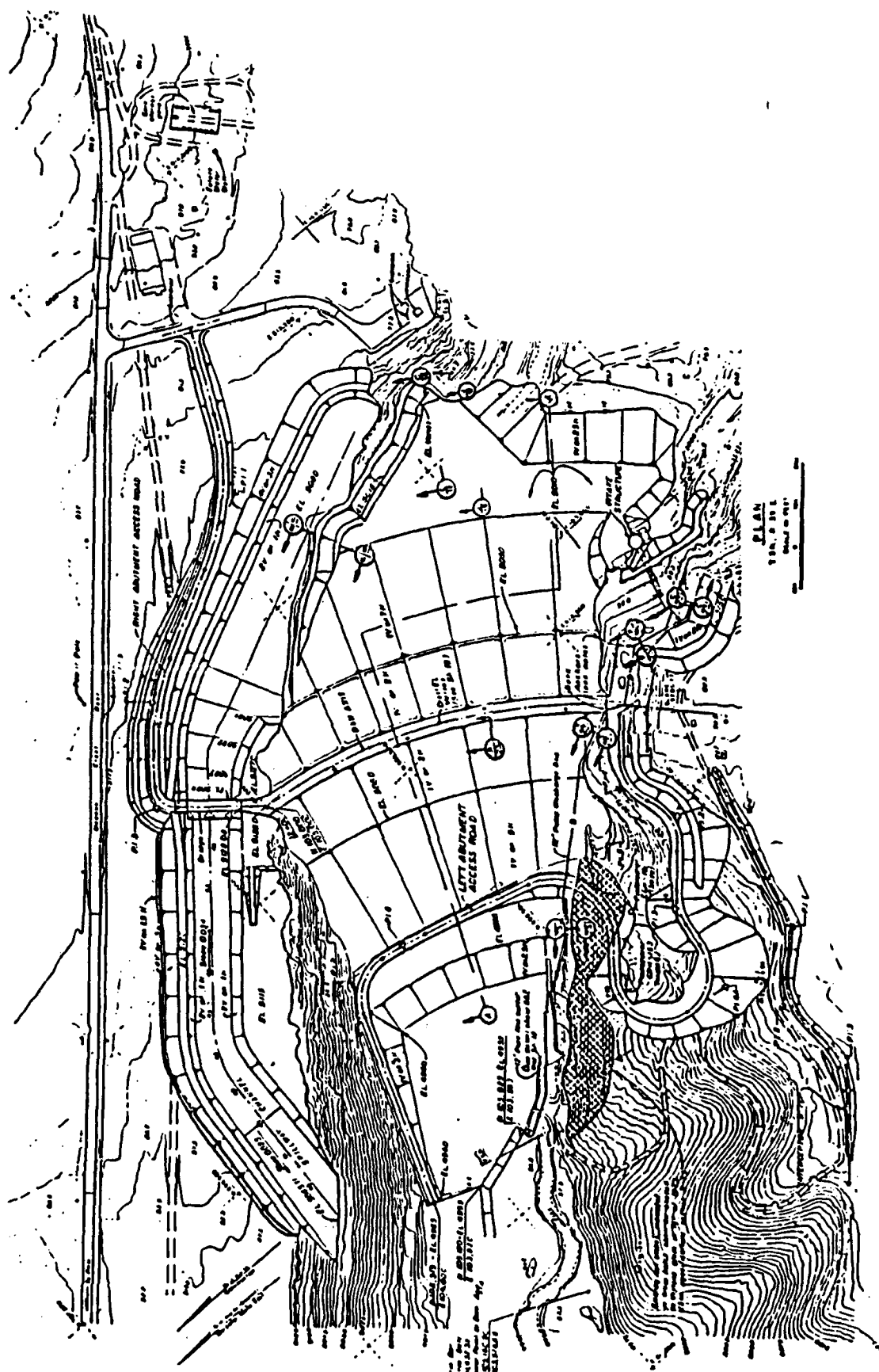
## 1. INTRODUCTION

The objective of this work is to evaluate the seismic response of the Ririe Dam, located in Southwestern Idaho, to an anticipated strong ground shaking. The Ririe Dam is about 178 ft. high and founded in a narrow canyon. Figs. 1.1, 1.2, and 1.3 show a plan view, a characteristic cross-section and a longitudinal section of the dam, respectively.

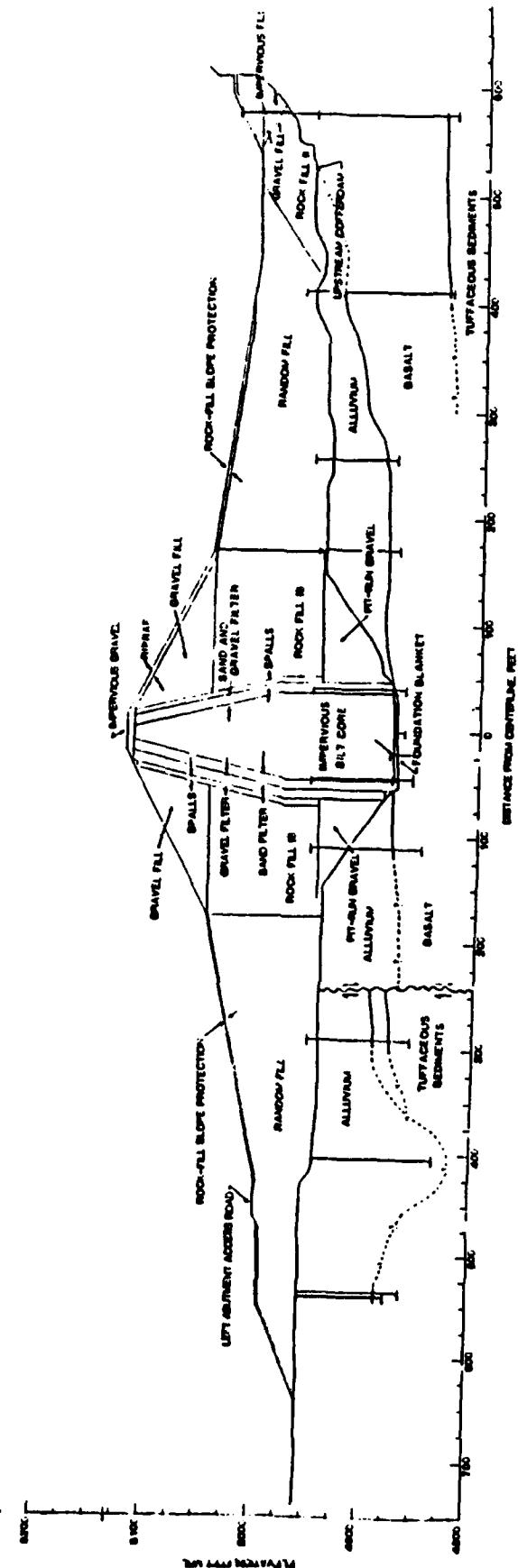
A study by E. L. Krinitzsky and J. B. Dunbar at WES (Ref. 1) suggests that a possible earthquake of magnitude  $7\frac{1}{2}$ , initiated along the faults in the Grand-Swan Valley at a distance of 4 to 10 km from the dam site, would result in a very strong ground shaking having the following characteristics:

- (a) Peak acceleration :  $1200 \text{ cm/s}^2$
- (b) Peak velocity :  $120 \text{ cm/s}$
- (c) Duration : 33 s

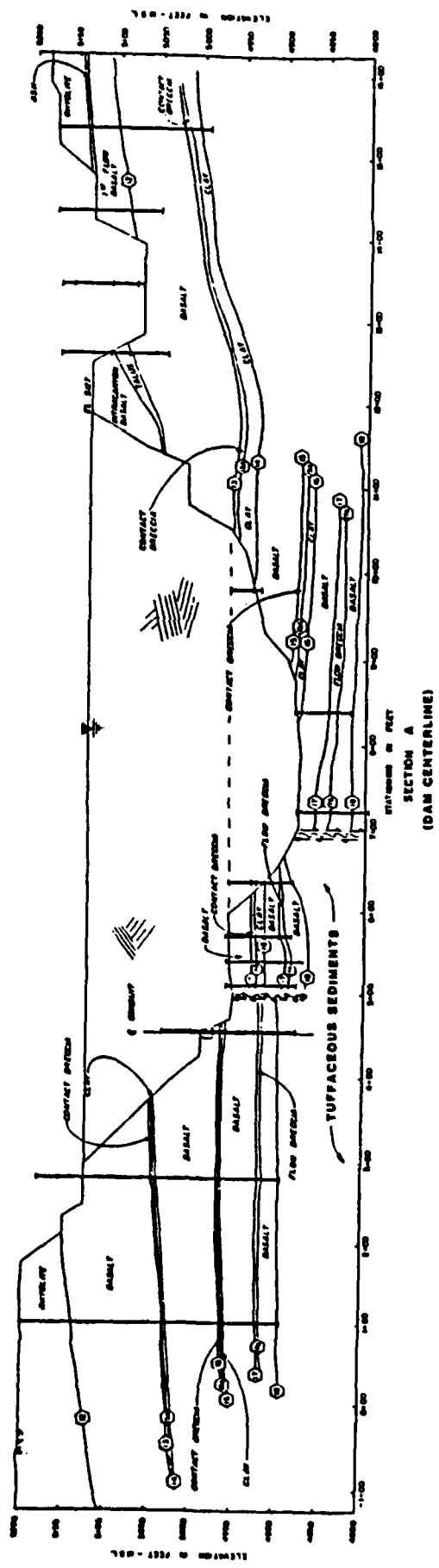
Professor H. Bolton Seed prepared a hypothetical motion consistent with the aforementioned characteristics by modifying the recorded Pacoima Dam motion during the 1971 San Fernando earthquake. The acceleration and velocity time histories are presented in Figures 1.4 and 1.5. The acceleration response spectra in Fig. 1.6 illustrate the severity of the expected earthquake shaking.



**Figure 1.1** Plan view of Ririe Dam



**Figure 1.2** Cross-section of Ririe Dam at the midsection



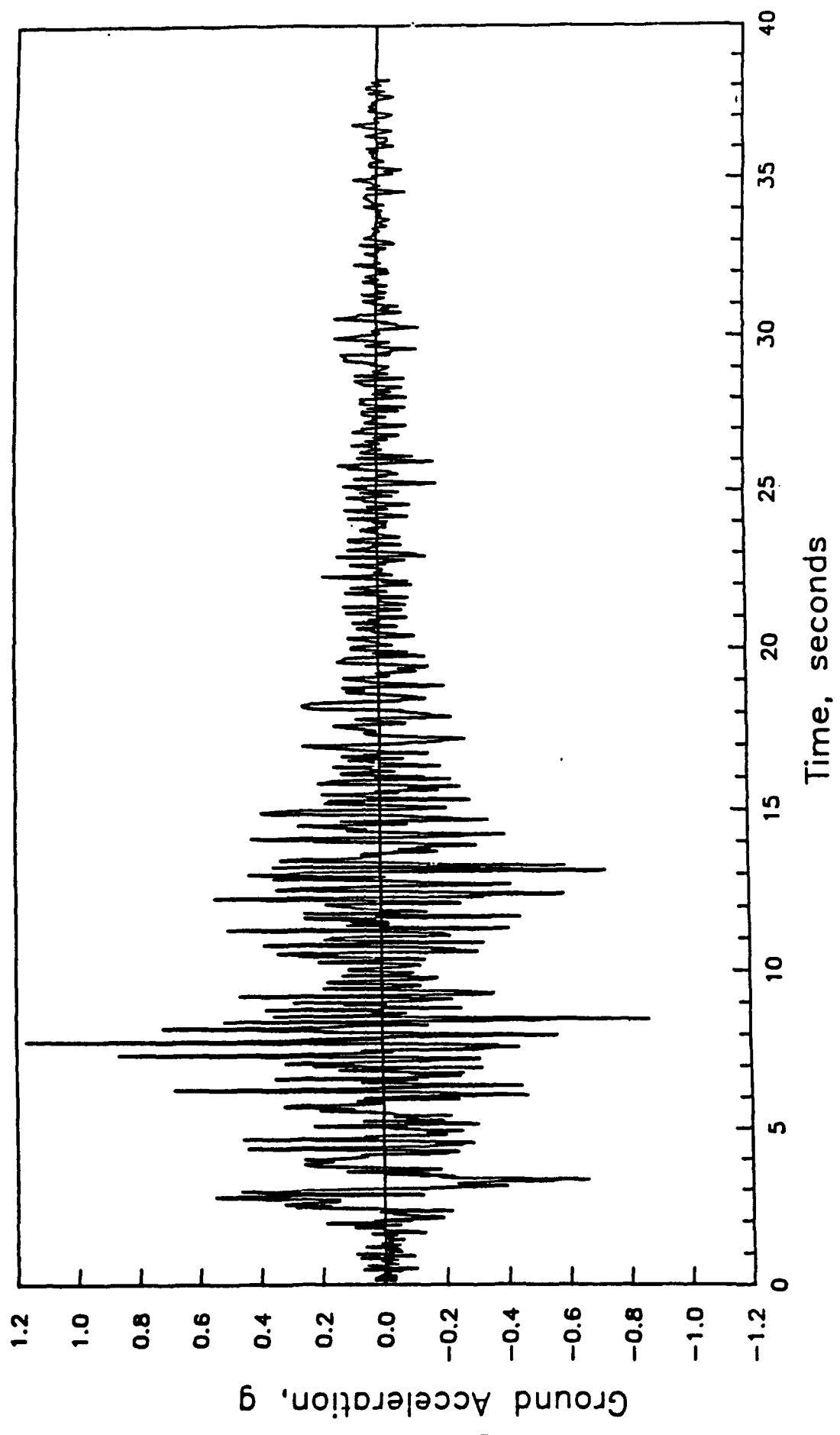


Figure 1.4 Hypothetical acceleration (provided by Prof. H. B. Seed)

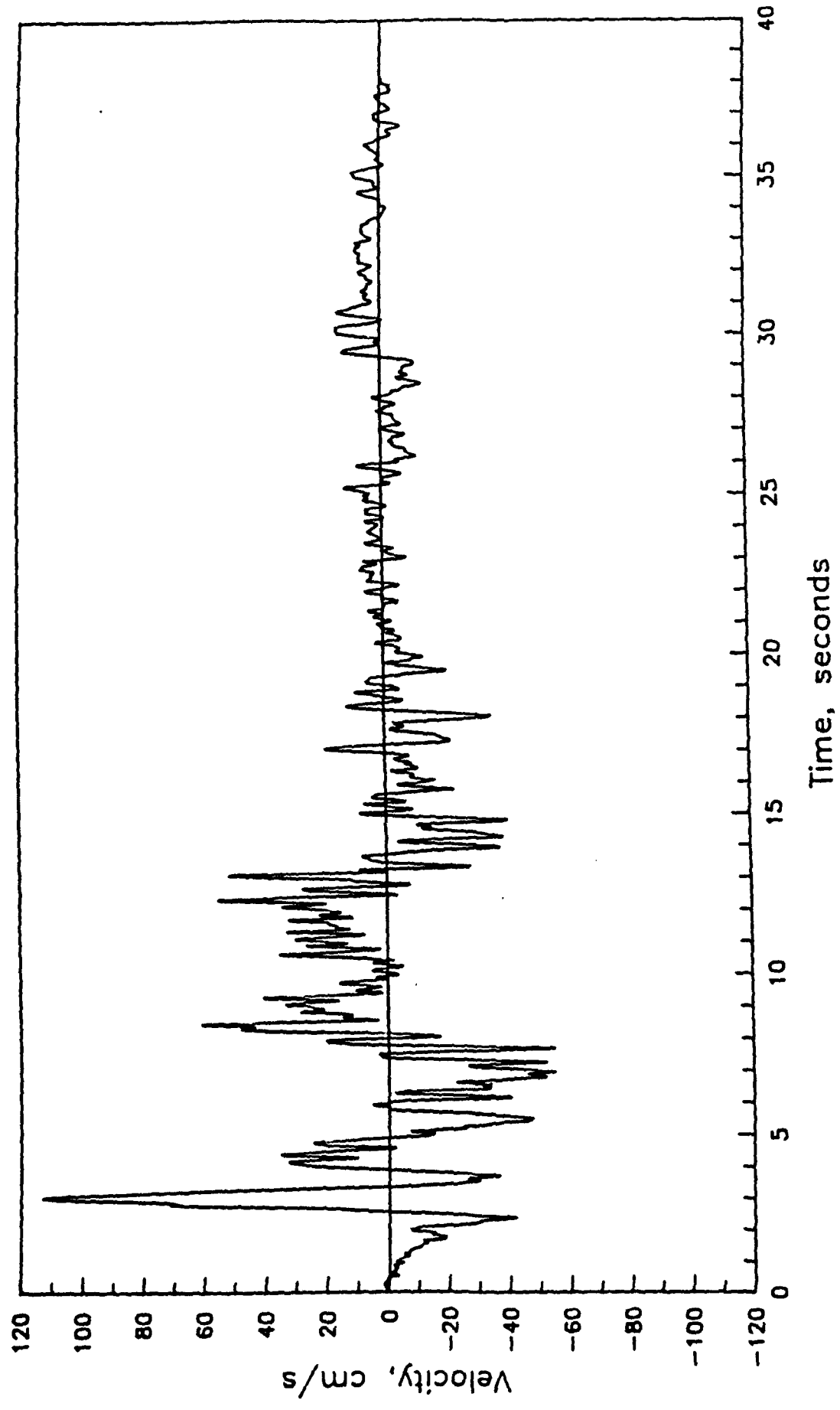


Figure 1.5 Hypothetical velocity (provided by Prof. H. B. Seed)

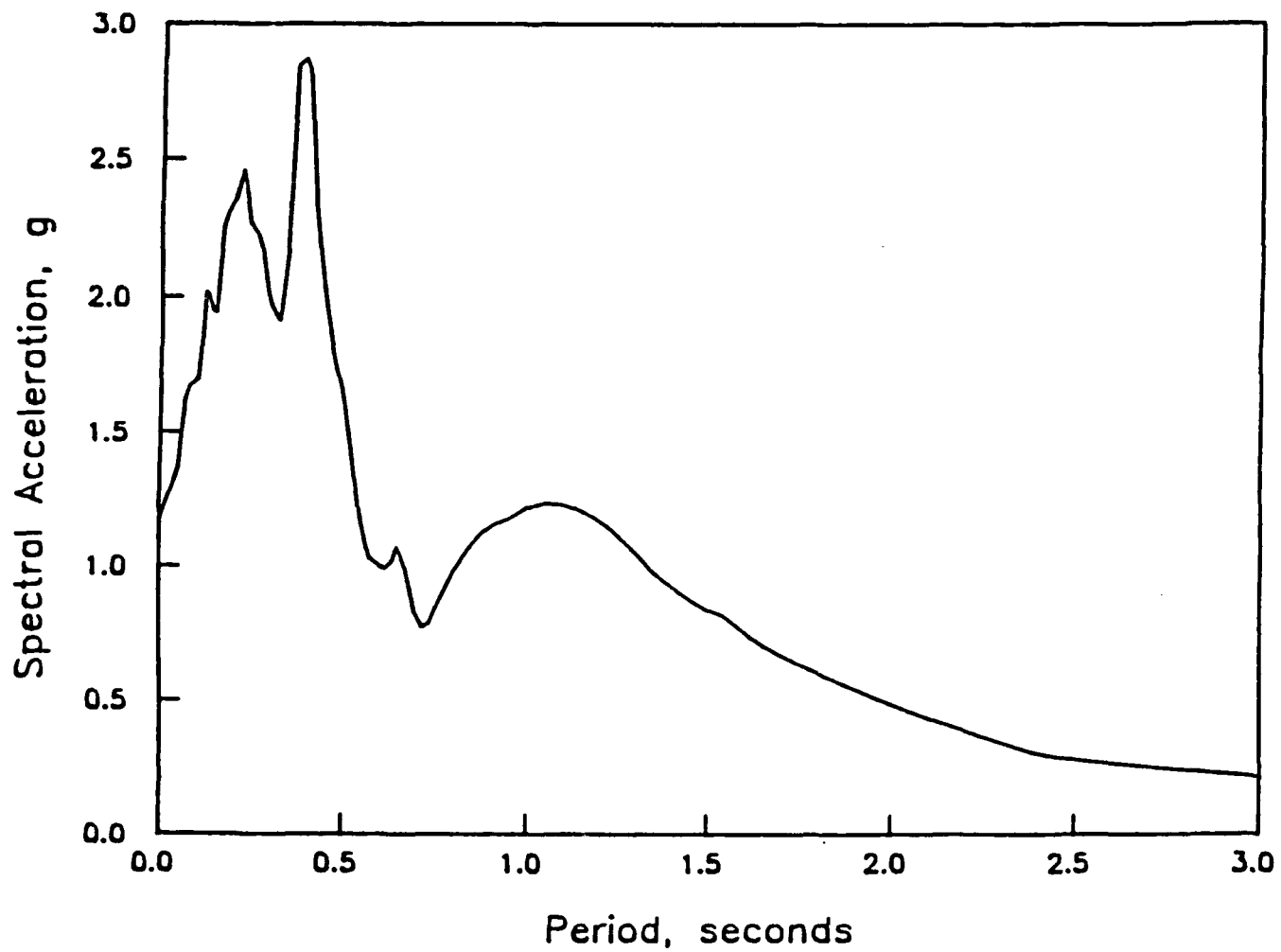


Figure 1.6 Acceleration response spectra of input motion (provided  
by Prof. H. B. Seed)

## 2. MODELING OF RIRIE DAM

### 2.1 Geometry and Materials

Modeling of the Ririe Dam is a fairly difficult undertaking because of the complex geometry of the dam canyon boundaries and slope surfaces, as well as the variability of the materials. This work attempts only a simplified modeling of the dam-canyon system to be used with closed-form shear beam type models for seismic analysis.

Figure 2.1 shows a typical cross-section located about the middle of the dam. The dam cross-section consists of:

- (a) an impervious silt core
- (b) a gravel fill
- (c) rock fill
- (d) random fill

As shown in the figure, the dam body consists of an upper part with slopes 1:2 and a height of 78 ft. and a lower part with variable and much flatter slopes and a thickness of 100 ft. The modeling was made by dividing the cross-section in smaller pieces and by computing the corresponding shear modulus of each piece as a function of its material type and the level of the confining effective stresses. Then the distribution with depth of an average (across the width of the dam) shear modulus was obtained. This distribution may be expressed as

$$G(z) = G_b (z/H)^m \quad (2.1)$$

where  $z$  = depth from the crest,  $H$  = height of the dam,  $m$  = inhomogeneity parameter and  $G_b$  is the shear modulus at the dam base.

The computation of the shear modulus of each piece of the dam body was made under the assumption that the water table within the dam section is as shown in Fig. 2.1. The material properties presented in Table 2.1 have been provided by Prof. T. Stark and Prof. H. Bolton Seed. Regarding the shear modulus  $k_2$  coefficient, the Seed/Stark estimates have been used in the following analyses.

Note that different values of shear moduli for each type of shear beam model have been used. The specific values are discussed in Chapter 3 describing the parametric analyses.

The dam body described above rests partly on basalt and partly on alluvium consisting of loose to dense sandy gravel, silts, and weakened basalt as shown in Fig. 2.2. As the depth of this alluvial deposit varies along the length of the dam, only an approximate equivalent modeling of its effect is possible. Finally, the alluvial deposit is underlain mainly by basalt, and in a smaller area by tuffaceous sediments.

## 2.2 Shear Beam Models

Three different types of shear beam models are used to account for the most important parameters influencing the response. A brief description of each model type is given below:

2.2.1 Model 1: This model represents the canyon with an equivalent rectangular shape and idealizes the dam as a triangular wedge lying on a soil foundation layer at the bottom of the canyon (Fig. 2.3). Although the canyon shape is idealized as a rectangle solely for mathematical convenience, in practice an "equivalent" rectangle offers a reasonable approximation. The dam consists of a hysteretic material with a constant mass

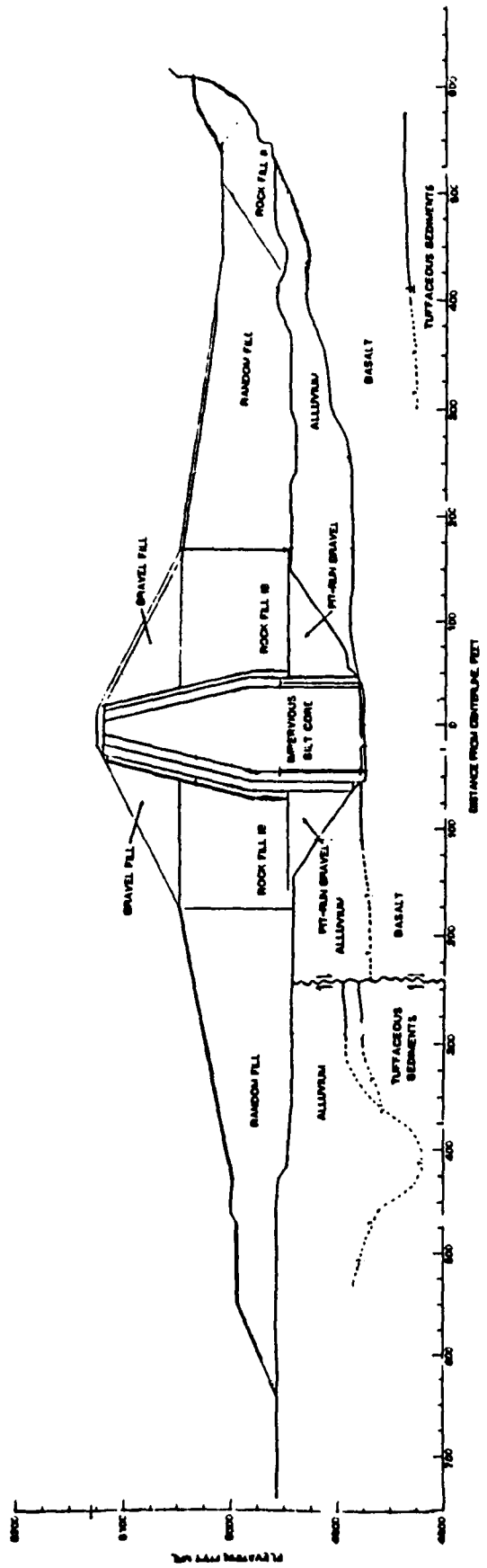


Figure 2.1 Cross-section at midsection

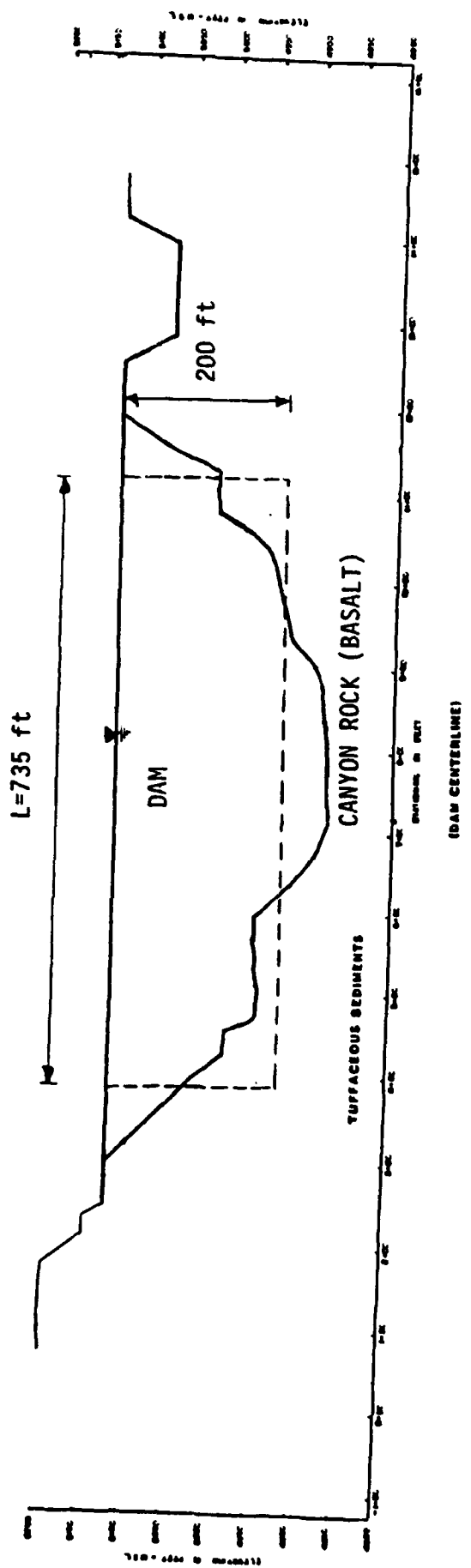


Figure 2.2 Longitudinal section

density,  $\rho_1$ , an average (across the width) shear modulus  $G(z) = G_b(z/H)^m$ , where  $z/H$  = normalized depth from the crest,  $G_b$  = the shear modulus at the dam base and  $m$  = the inhomogeneity parameter. The foundation layer consists of a uniform and hysteretic material with a constant mass density,  $\rho_2$ , a constant shear modulus,  $G_2$ , and a constant hysteretic damping ratio,  $\beta_2$ .

The seismic excitation consists exclusively of vertically propagating S-waves creating horizontal motions in the upstream-downstream direction. Moreover, the entire canyon is assumed to vibrate as a rigid body with identical (in both amplitude and phase) oscillations at each point along the interface at the base and at the two abutments.

The response of the dam and its foundation layer to the aforementioned type of seismic excitation is assumed to be only in horizontal lateral shear deformation with the horizontal lateral displacement,  $u$ , uniformly distributed across the width of the dam. This constitutes the basis for the classic "shear beam" models that have been used for seismic analysis of earth dams and soil deposits. Comparisons of results on seismic response obtained from detailed analyses of earth dams using consistent finite element and shear beam models have confirmed the validity of the above assumptions (Ref. 4-6). More details about Model 1 may be found in Reference 3.

Nonlinear Response: A piece-wise strain-compatible linear analysis is employed in order to take into account the nonlinear behavior of soil by ensuring the compatibility of soil shear moduli and damping ratios with the current magnitude of shear strains at every time  $t$  during the ground shaking. To this end, the root-mean-squared (rms) values of the shear

Material Location	Saturated/ Buoyant Unit Weight (pcf)	Moist Unit Weight (pcf)	Young's Modulus		Failure Loadings/ Unloading Exponent		Bulk Modulus K <sub>b</sub>	Effective Cohesion C <sub>e</sub>	Effective Friction Angle at 1 atm. I <sub>r</sub>	Reduction in Friction Angle		Measured Shear Modulus G <sub>o</sub>	Seed/Start Shear Modulus G <sub>s</sub>
			Young's Modulus	Young's Modulus	Failure Loadings/ Unloading Exponent	n				Per Log Cycle Change in Confining Stress	Static Stress Ratio		
Inspurious Silt core	125/63	120	780	0.48	0.6	520	0.3	0	35	5	0.45	30-100	55
Gravel Fill	145/83	135	1400	0.45	0.7	500	0.3	0	48	6	0.4	160-265	120
Rockfill	145/83	135	1000	0.45	0.7	500	0.3	0	48	6	0.4	100-150	120
Sand fill	140/78	130	700	0.45	0.7	255	0.3	0	45	6	0.4	75-110	85
Alluvium													
I.) Silt	120/58	112	425	0.5	0.7	205	0.3	0	33	6	0.45	55-110	50
II.) Loose Sandy Gravel	135/73	135	500	0.5	0.8	255	0.3	0	43	6	0.4	75-110	80
III.) Dense Sandy Gravel	144/82	144	1400	0.5	0.7	1300	0.3	0	48	6	0.4	135-250	100
IV.) Weathered Basalt/ Gravel	167/85	167	1600	0.5	0.7	1300	0.3	0	50	6	0.4	260-1000	150
Basalt	170/108	170	2000	0.4	0.7	1400	0.3	0	50	0	0.35	Shear Wave = 30000 fips	
Tuffaceous Sediments	155/73	155	1000	0.49	0.9	520	0.3	0	45	6	0.45	Shear Wave = 1600-2500 fips	

Table 2.1 Estimated Static and Dynamic Material Properties for Ririe Dam (provided by Professor T. Stark and Professor H. B. Seed)

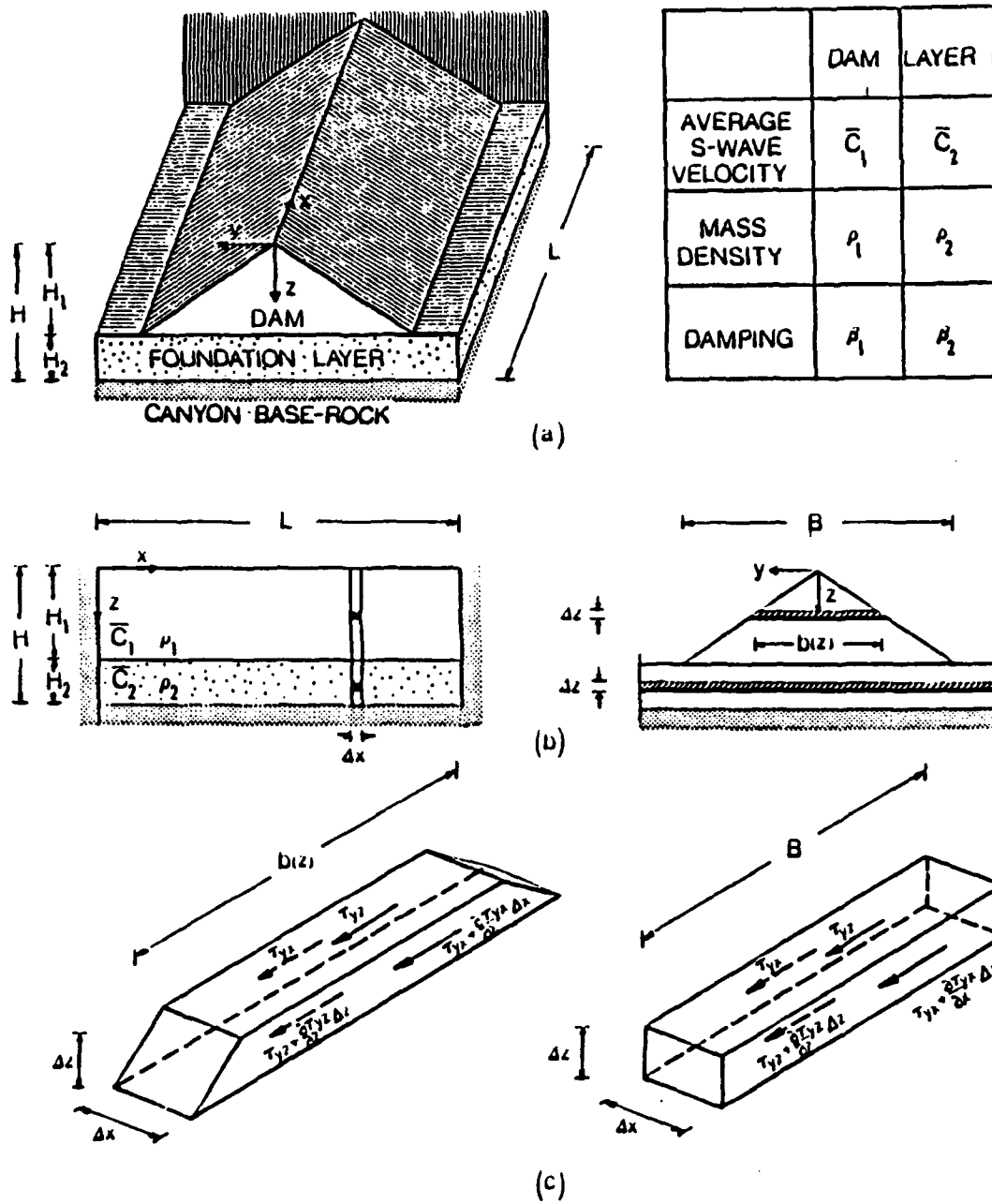


Figure 2.3 Model 1: Dam and foundation layer in a rectangular canyon  
 (a) perspective view, (b) longitudinal and cross-section,  
 (c) stresses acting on infinitesimal bodies (Ref. 2)

strain are computed over a time window equal to the fundamental period of the dam.

For the time interval  $\Delta t_i$ ,  $\gamma_{rms,i}$  is

$$\gamma_{rms,i}^2 = \frac{1}{\Delta t_i} \int_{t_i}^{t_{i+1}} \gamma^2(t) dt \quad (2.2)$$

An equivalent sinusoidal shear strain amplitude  $\gamma_{0,i} = \sqrt{2} \gamma_{rms,i}$  is obtained by equating shear strain energies. This value of  $\gamma_{0,i}$  is then used to read consistent values of shear moduli  $G_i$  and damping ratios  $\beta_i$  from existing experimental data by Seed et al (Ref. 9). Three iterations are usually sufficient for convergence for each time interval  $i$ . Fig. 2.4a gives an example of a shear strain time history,  $\gamma(t)$ , (representing an average shear strain along the height of the dam). Along with  $\gamma(t)$ , the amplitude of an equivalent sinusoidal shear strain  $\gamma_0 = \sqrt{2} \gamma_{rms}$  is also plotted with a dashed line. The corresponding variations of the normalized shear modulus,  $G(t)/G_0$ , and the damping ratio,  $\beta(t)$ , obtained iteratively to be compatible with the current value of  $\gamma_0(t)$  at each time,  $t$ , are also plotted in Figs. 2.4b and c. Note that as the level of shear strains within the dam may be quite different than those within the foundation layer, two sets of compatible  $\gamma_0(t)$ ,  $G(t)/G_0$  and  $\beta(t)$  are required, one for the dam and one for the foundation layer at each time,  $t$ . This means that the ratio of the shear modulus of the dam over the shear modulus of the layer,  $G_1(t)/G_2(t)$ , changes continuously during the excitation and new eigenvalues have to be computed for each time interval and each iteration within that interval. Despite that, the method is quite efficient. More details about the method may be found in Reference 8.

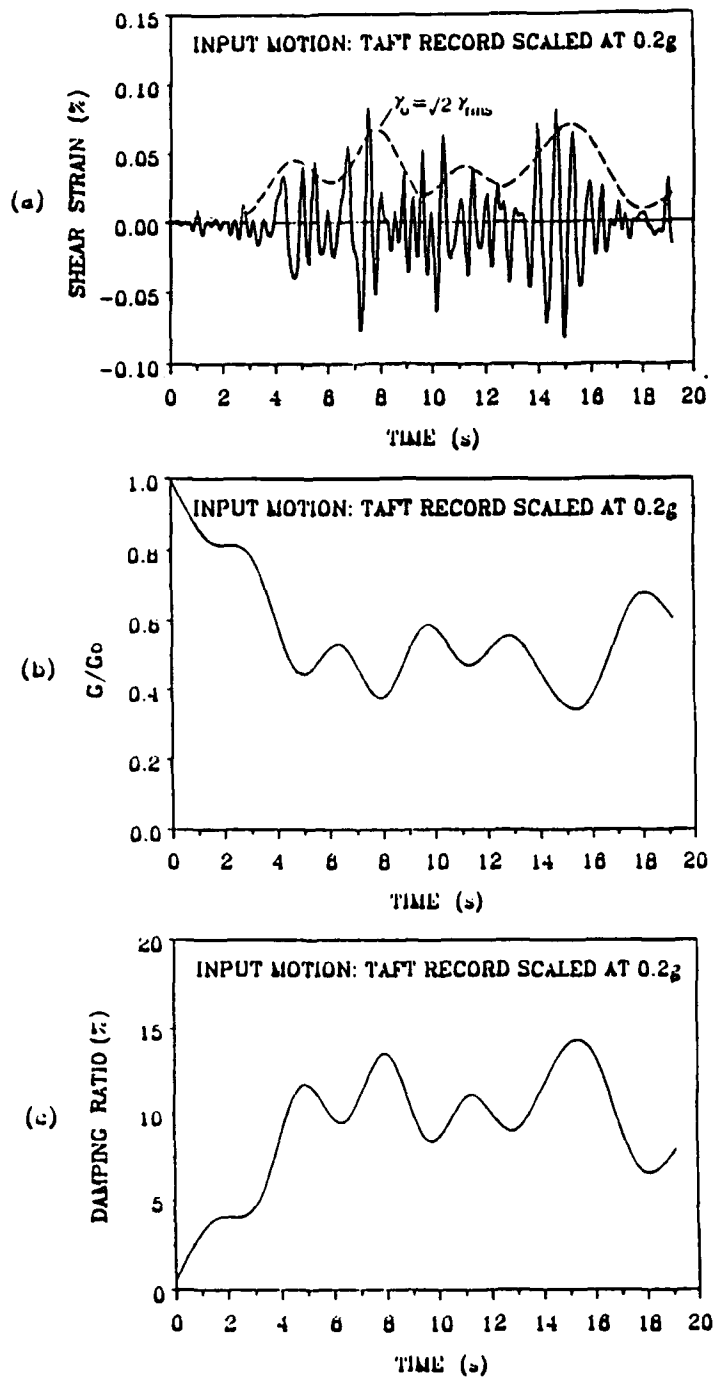


Figure 2.4 Illustrative example of response of a dam on a foundation layer, using the piece-wise linear method: (a) average (within the dam) shear strain and equivalent sinusoidal amplitude versus time, (b) shear modulus degradation versus time, (c) damping ratio versus time

Radiation Damping: The earthquake excitation recorded at an outcrop rock may be different from the actual ground shaking experienced at the dam base (see Fig. 2.5). The incoming seismic waves reflect on the free surfaces of the dam and return downwards, consuming part of their energy into strain energy. The frequency characteristics of these waves will be affected by the natural frequencies of the dam and the relative stiffness between the foundation rock and the dam soil. It is of interest to approximately simulate this dam-foundation interaction, often referred to as radiation or geometric damping. To this end, the standard soil amplification procedure (Ref. 12) is to:

1. Compute the discrete Fourier transform of the outcrop acceleration  $\ddot{u}_g(t)$ .
2. Multiply (the obtained transform) by the outcrop-base rock transfer function.
3. Compute the inverse discrete Fourier transform of the product, which is the needed acceleration  $\ddot{u}_b(t)$  at the dam base.

As the exact closed-form transfer function relating the acceleration at the dam base to the acceleration at the outcrop rock is not available for Model 1, it is approximated with that corresponding to a very long dam with similar fundamental frequency. In fact, this is the exact transfer function for Model 2 (plane strain) described below. For an inhomogeneous dam, this is given by

$$TF = \frac{J_q(a)}{J_q(a) + i\alpha J_{q+1}(a)} \quad (2.3)$$

$J_q(a)$  = Bessel function of first kind and order  $q$

$q = \frac{m}{2-m}$ ,  $m$  = inhomogeneity parameter

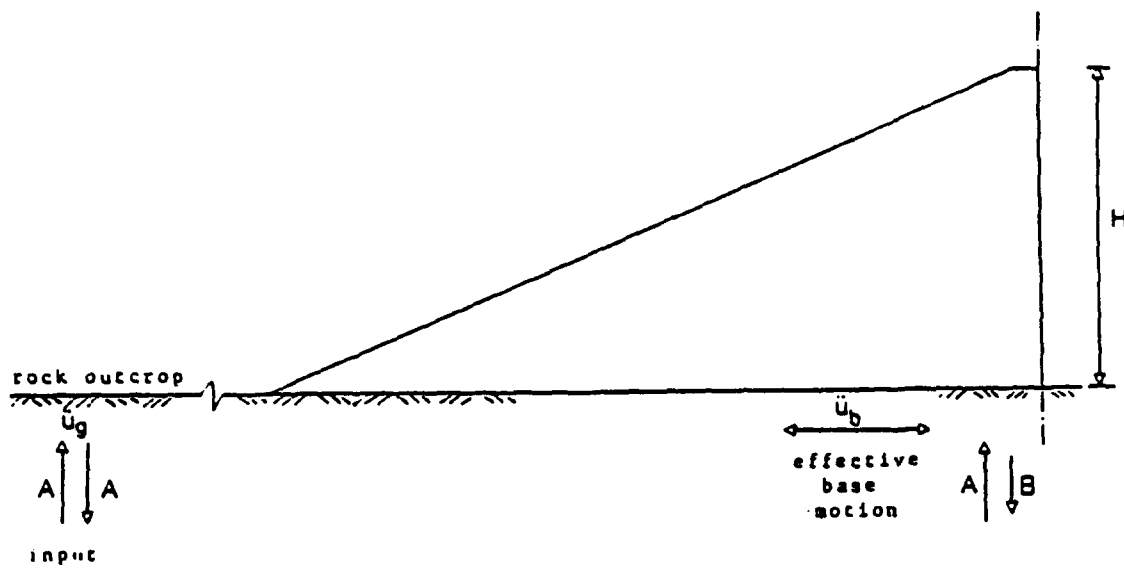


Figure 2.5 Definition of outcrop rock and dam base motion

$$a = \omega H(1 + q)/C_s^*$$

$\omega$  = frequency of vibration

H = height of the dam

$$C_s^*, C_r^* = C_{s,r}(1 + 2i\beta_{s,r})^{1/2} = \text{complex S-wave velocity of soil (s) and rock (r), respectively}$$

$\beta_s, \beta_r$  = hysteretic damping of soil and rock, respectively

$\rho_s, \rho_r$  = mass densities of soil and rock, respectively

$$\alpha = \frac{\rho_s C_s^*}{\rho_r C_r^*} = \text{impedance ratio.}$$

More information is in Ref. 10-11.

As the performed analyses are nonlinear, resulting into a continuous variation with time of  $C_s$ ,  $\alpha$ , and  $a$ , the above approach for modeling the radiation damping corresponds to equivalent average (in time) values of shear wave velocity. This approximation, however, poses no problem because the final effect of the radiation damping on the response was small.

2.2.2 Model 2: This model is used under the assumption that nonlinearity is more important than the narrowness of the canyon. The dam is idealized as an infinitely long truncated triangular shear beam (Fig. 2.6). The distribution with depth of the average (across the width) shear modulus,  $G(z)$ , is of the form  $G(z) = G_b(z/H)^m$ , where  $z/H$  = normalized depth from the crest,  $G_b$  = the shear modulus at the dam base, and  $m$  = inhomogeneity parameter. The response is assumed to take place only in shear mode. The model assumes a uniform distribution of horizontal lateral displacements and accelerations across the width of the dam. Shear stresses and shear strains represent average values (across the width). Fig. 2.7 shows a typical comparison of seismic acceleration time histories at the crest

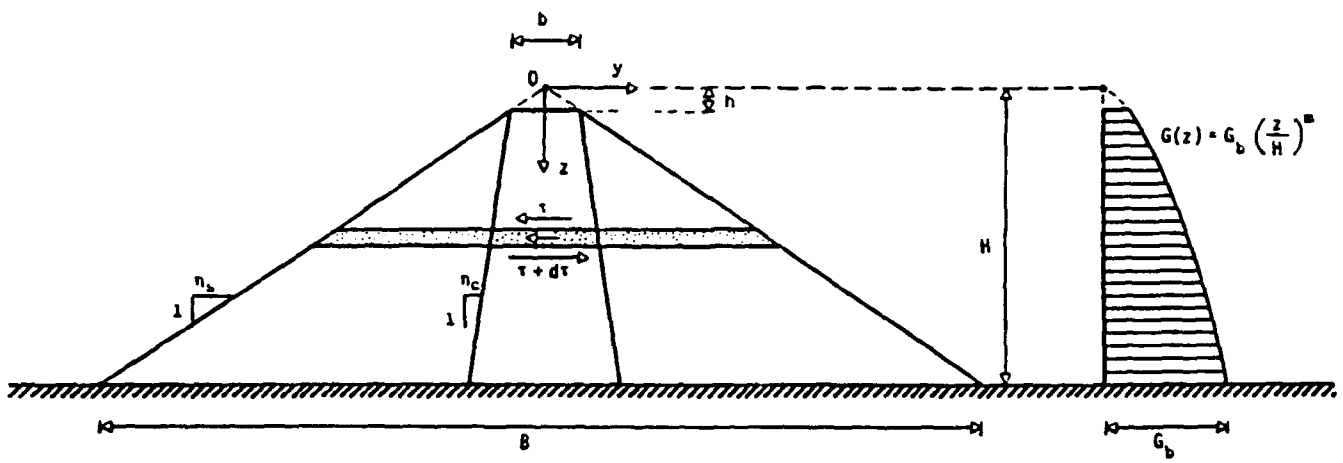


Figure 2.6 Model 2: Dam cross-section and distribution of shear modulus with depth

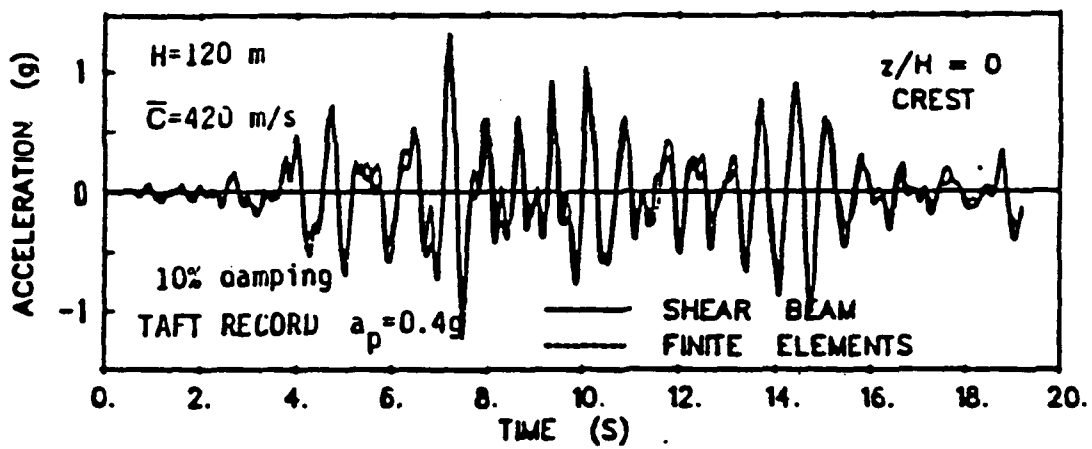
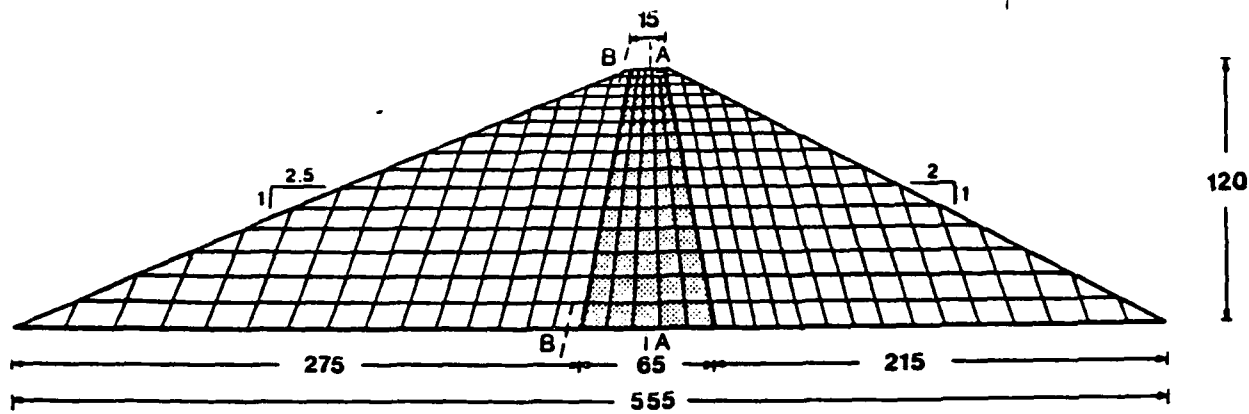


Figure 2.7 Typical comparison between cross accelerations obtained from linear analysis using consistent inhomogeneous shear beams and finite element models

of a 120 m dam (with an average shear wave velocity = 420 m/s and damping ratio = 10%) obtained for linear analyses using consistent inhomogeneous shear beam and finite element models. Nonlinear analysis is performed by using a piece-wise linear analysis with small time steps, as described above. The radiation damping is taken into account by considering the reflection of waves back to the baserock at the dam base, as discussed in the previous section.

2.2.3 Model 3: This model assumes that the canyon has a semi-cylindrical shape (Fig. 2.8). The dam is idealized as a triangular homogeneous shear wedge. In its present form the model may be used for equivalent linear analyses. The effect of radiation damping may be taken into account. The transfer function in this case is

$$TF = \frac{\sin a}{\sin a + i\alpha(\frac{\sin a}{a} - \cos a)}$$

where  $a = \frac{\omega R}{C_s^*}$

$\omega$  = frequency of vibration

R = radius of the semi-cylindrical canyon

$C_s^*, C_r^*$  = average S-wave velocity for soil and rock, respectively

$\rho_s, \rho_r$  = average mass densities for soil and rock, respectively

$$\alpha = \frac{\rho_s C_s^*}{\rho_r C_r^*} \text{ impedance ratio.}$$

Although in the case of the Ririe Dam the actual canyon geometry is not semi-cylindrical, it would be useful for the analysis to identify trends in the expected response by using this model to perform parametric studies.

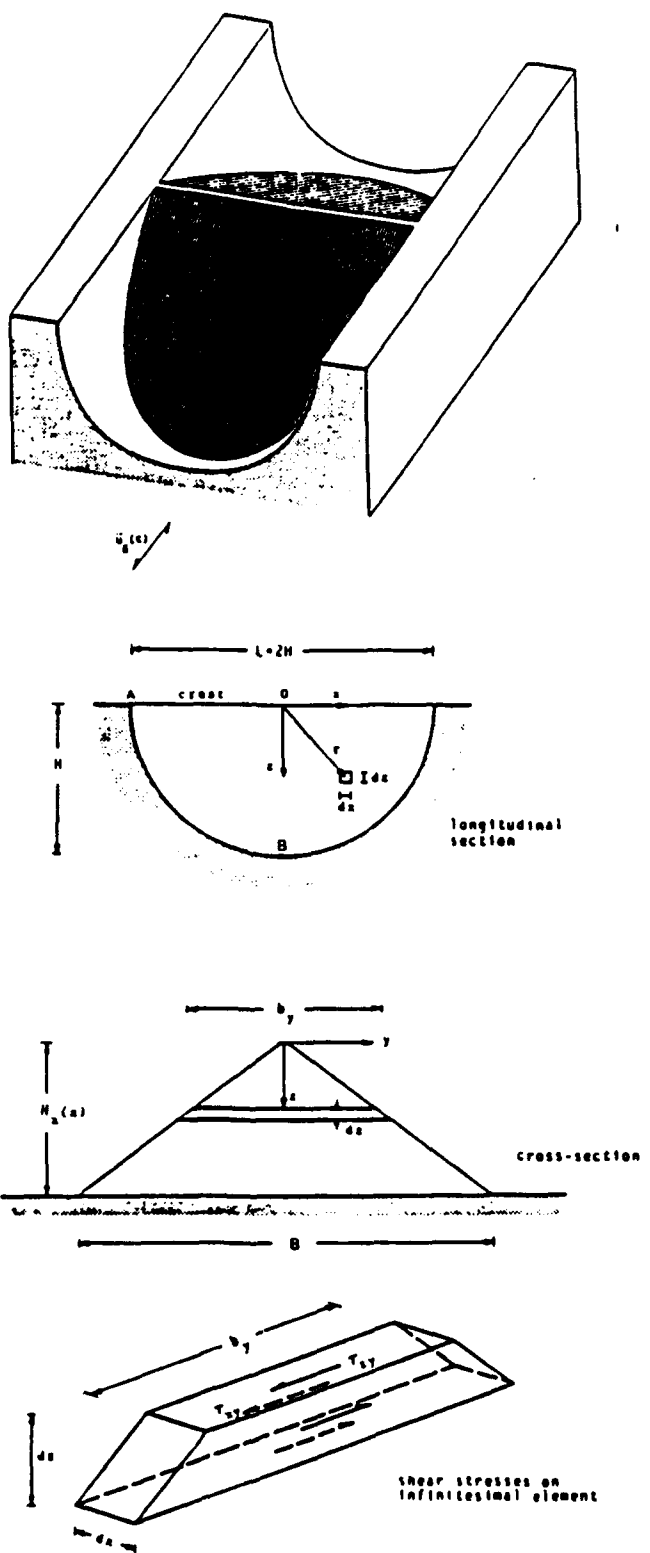


**Figure 2.8 Model 3: Dam in a semi-cylindrical canyon, (a) perspective view, (b) longitudinal section, (c) cross-section, (d) shear stresses acting on infinitesimal element**

### 2.3 Fundamental Period of Ririe Dam

An earthquake of Richter magnitude 6.9 with an epicenter west of Mount Borah shook Ririe Dam on October 23, 1983. The corrected lateral horizontal acceleration time histories and their corresponding Fourier spectra recorded at the crest, the downstream and the abutment are presented in Figs. 2.9-2.11, respectively.

Fig. 2.9 suggests that the fundamental period of Ririe dam is about 0.45 seconds. Note that the recorded accelerations at the downstream and the abutment are quite different from each other. This is natural considering that the canyon rock is not rigid, but flexible and inhomogeneous, characterized by joints, layers of softer soil and local geometric irregularities. Moreover, the acceleration time histories would vary from point to point along the dam-canyon interface even in the case of a homogeneous canyon with regular geometry, due to the dam-canyon interaction. In reality the recordings at the downstream and the abutment, measured near the surface, are expected to consist of accelerations larger than those at the middle of the dam base. Also, they may not represent the outcrop acceleration due to the influence of local conditions. The two accelerations records were used as base input motion in shear beam analyses, but the computed crest accelerations did not match well the recorded crest motion. The main reason for this discrepancy is that neither of the two records appears to represent the true outcrop excitation but instead they are influenced by local conditions.

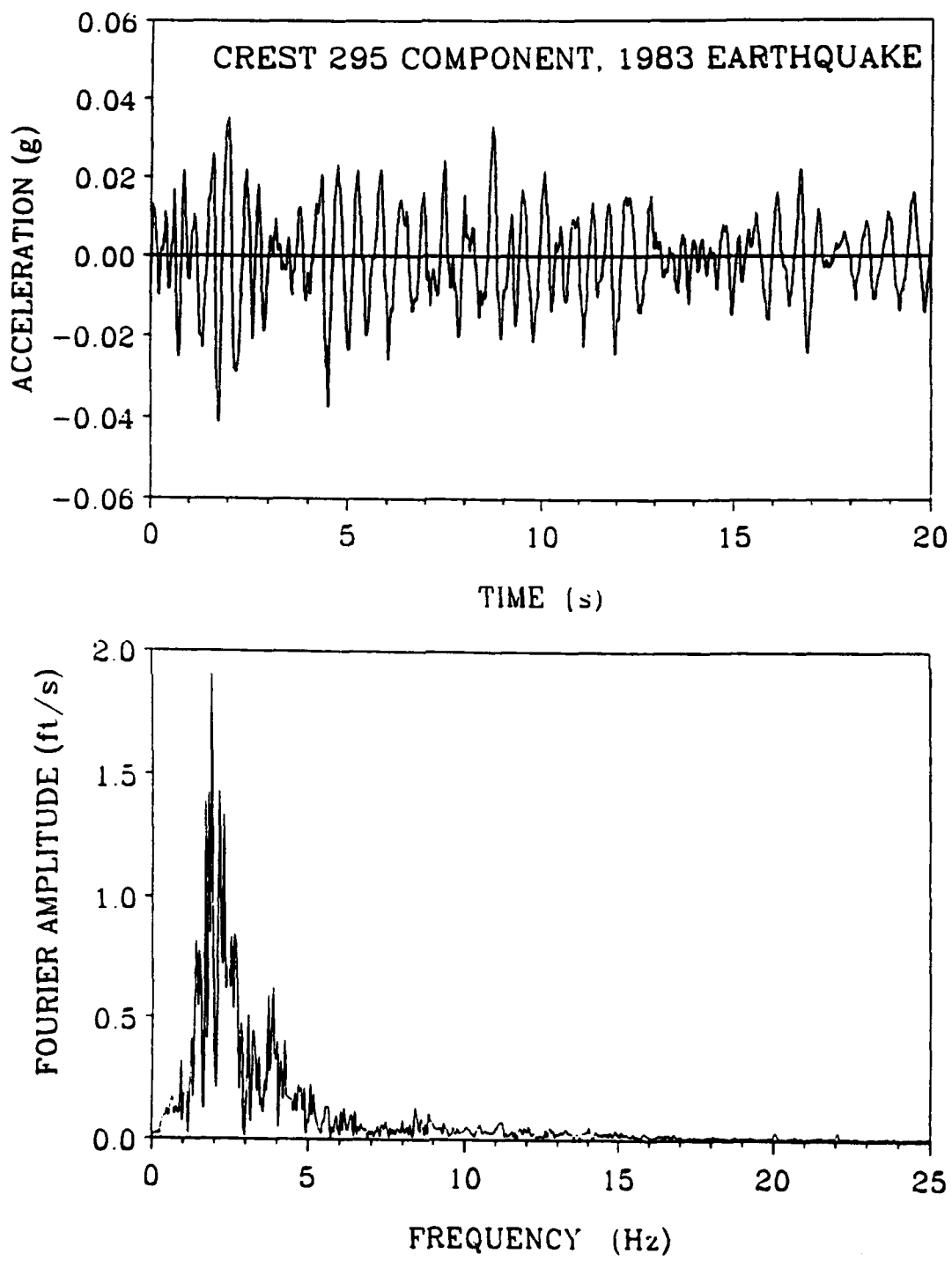


**Figure 2.9** Corrected lateral horizontal accelerations recorded near midcrest during the 1983 Mount Borah earthquake,  
 (a) time histories, (b) Fourier spectra

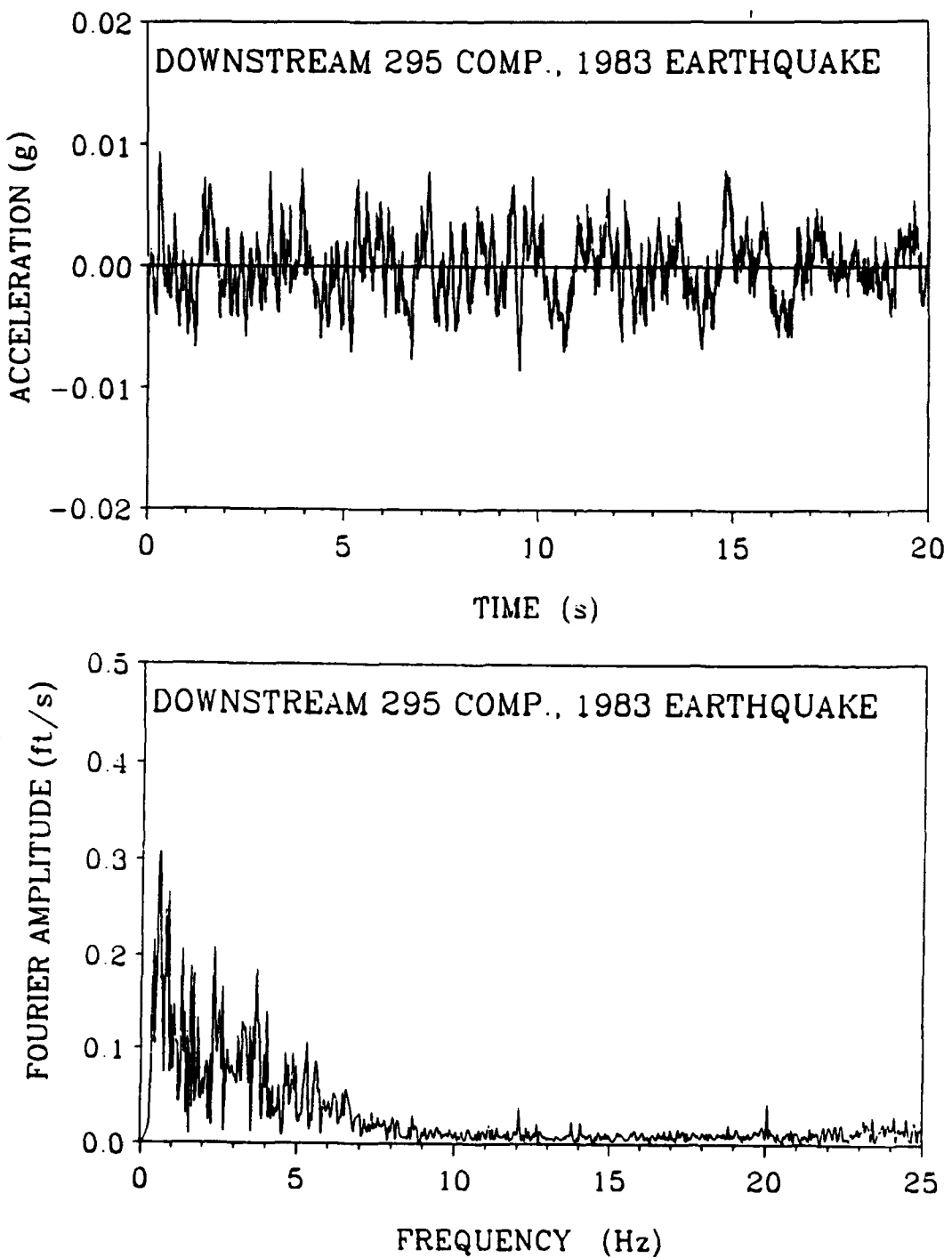


Figure 2.10 Corrected lateral horizontal accelerations recorded at the downstream during the 1983 Mount Borah earthquake,  
 (a) time histories, (b) Fourier spectra

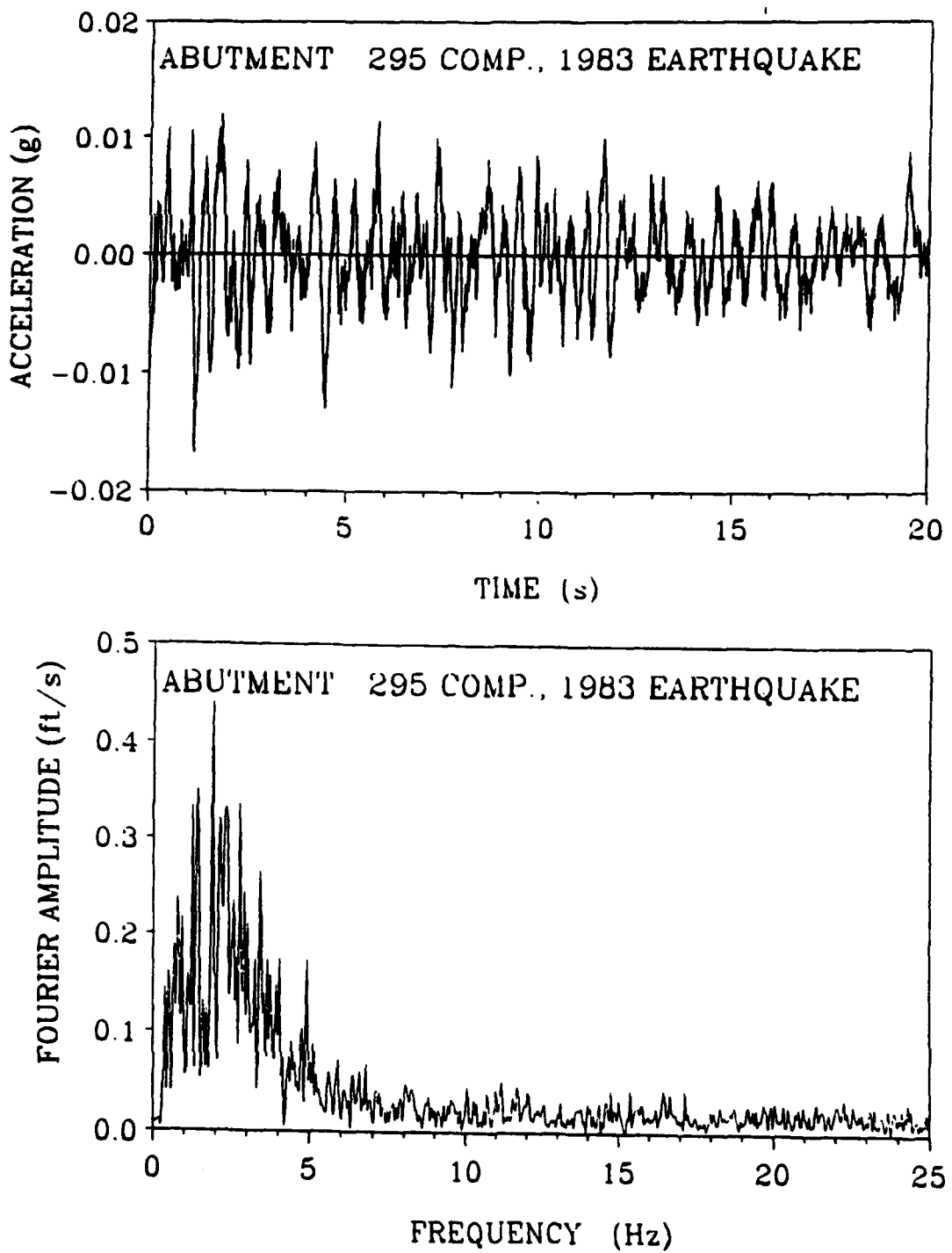


Figure 2.11 Corrected lateral horizontal accelerations recorded at the abutment during the 1983 Mount Borah earthquake,  
 (a) time histories, (b) Fourier spectra

### 3. PARAMETRIC STUDIES

By using the three models described in Section 2.2 combined with a range of values for the dam-canyon material and geometric characteristics, a series of seismic analyses has been performed in order to investigate a range for the expected response values. A selected number of the most important cases is presented in the following.

#### 3.1 Response of Ririe Dam Using Model 1

##### Case 1

The canyon is idealized with an equivalent rectangular shape of length  $L = 735$  ft. The significant flatness of the lower part of the dam body and the presence of the alluvial deposit covering a large part of the foundation area suggest that these two would respond in a way which is closer to the response of a foundation soil layer underlying the dam as shown in Fig. 2.3. Thus, in this case the dam body is considered to be only 78 ft. high and underlain by a 122 ft. foundation layer. The latter consists of 100 ft. from the lower part of the dam body and of an effective layer of 22 ft. from the alluvial deposit. The determination of the effective thickness of 22 ft. of the alluvial deposit was made by utilizing the best estimates for the computation of the shear moduli in each part within the dam and the foundation along with the criterion of a fundamental natural period of the dam-layer system about 0.45 seconds. The average S-wave velocities selected for the individual parts are presented in Table 3.1 which summarizes all the assumptions and input data for the analysis. The inhomogeneity parameter selected for the distribution of shear modulus with depth is  $m = 0.3$ .

### Case 1

Dam Idealization: Model 1

Type of Analysis: Nonlinear (piece-wise linear)

Dam Height:  $H_1 = 78$  ft. (23.77 m)

Dam Ave. S-wave Velocity:  $\bar{C}_1 = 1050$  ft/s (320 m/s)

Dam Ave. Mass Density:  $\rho_1 = 136$ pcf (2178 kg/m<sup>3</sup>)

Inhomogeneity Parameter:  $m = 0.3$

Layer Thickness:  $H_2 = 122$  ft. (37.19 m)

Layer Ave. s-wave Velocity:  $\bar{C}_2 = 1300$  ft/s (396.2 m/s)

Layer Ave. Mass Density:  $\rho_2 = 136$ pcf (2178 kg/m<sup>3</sup>)

Canyon Width:  $L = 735$  ft. (224 m)

Base: Rigid Rock (no radiation damping is considered)

Input Motion: Given Hypothetical Acceleration (peak acceleration = 1.17  
g, see Fig. 3.1)

Computed Fundamental Period:  $T_1 = 0.46$  s

Table 3.1 Input Data for Case 1

Figs. 3.2 plots the distribution versus depth of peak values of absolute accelerations computed at the midsection of the idealized dam and corresponding to different times during the earthquake shaking. Notice that the peak acceleration at crest is about 1.5 g, corresponding to an amplification of 1.28 of the input motion. It is very interesting to note that the peak of the input motion (at time  $t = 7.8$  s) is actually of much less importance than the acceleration pulse with a peak of about 0.65 g occurring from 2.5 to 5 seconds. In the lower part of the dam body, however, the acceleration is deamplified with amplification values as low as a 0.67.

Figs. 3.3-3.4 illustrate the acceleration time histories and their Fourier spectra at the crest ( $z = 0$ ) and at a depth  $z = 39$  ft. from the crest. As expected, comparison of the two figures shows that the high frequency content of the computed motion decreases significantly with depth. This is quite natural as the high-frequency "whip-lash" effect on any structure is observed only near its top.

Figs. 3.5-3.7 plot the distribution versus depth of peak values of relative displacements, shear strains  $\gamma_{yz}$  and shear stresses  $\tau_{yz}$  computed at the midsection of the idealized dam (see Fig. 2.3). Notice that significant shear strains up to 1% are computed within the lower part of the dam and the foundation layer. Such strains could potentially cause liquefaction of soil pockets within the alluvium that may consist of contractive silts and sands.

#### Case 2

Except of the assumption about the rigidity of the base rock, Case 2 is identical to Case 1. Here the base rock is assumed to be flexible with a constant S-wave velocity of  $C_r = 3000$  ft/s. By utilizing equation

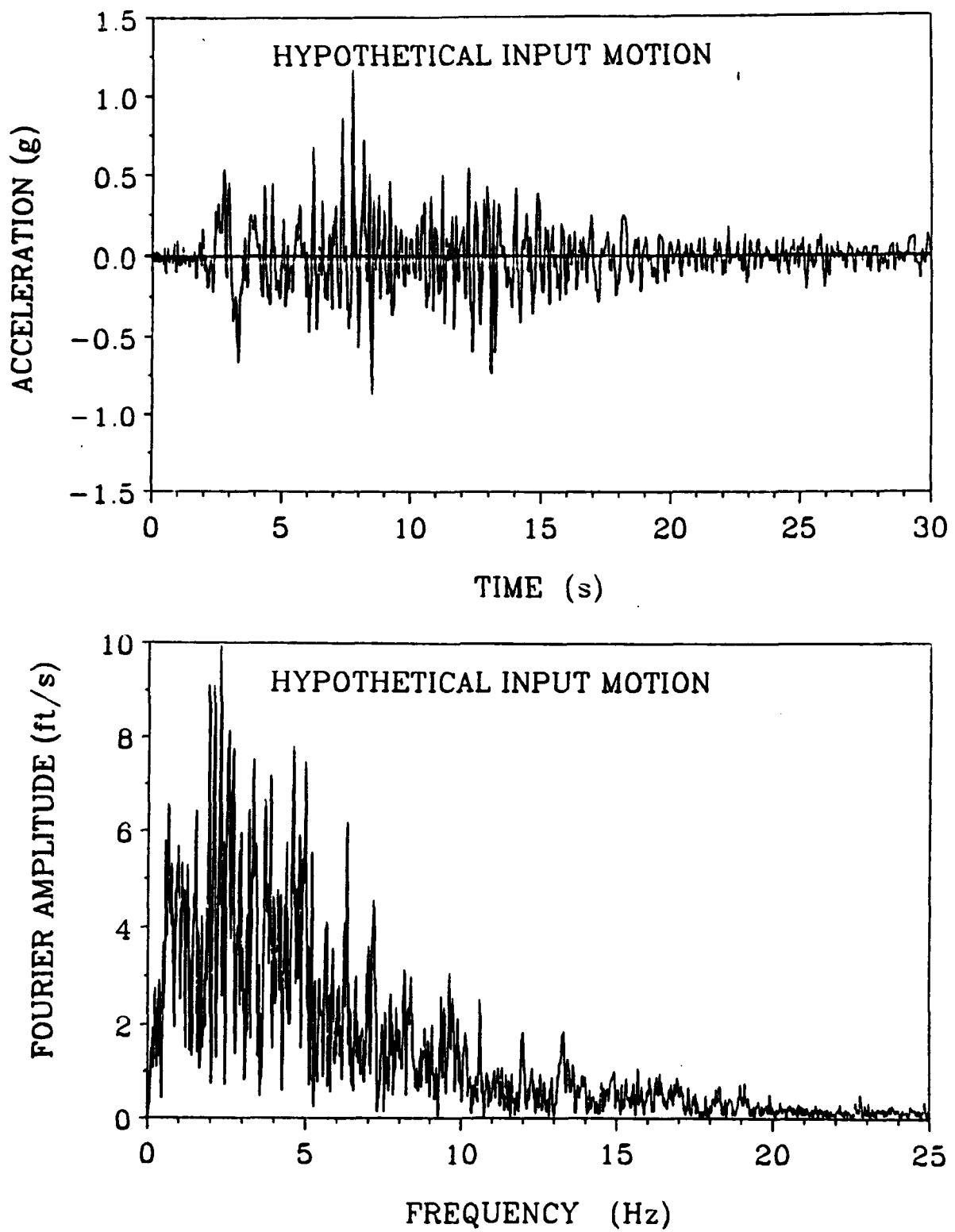
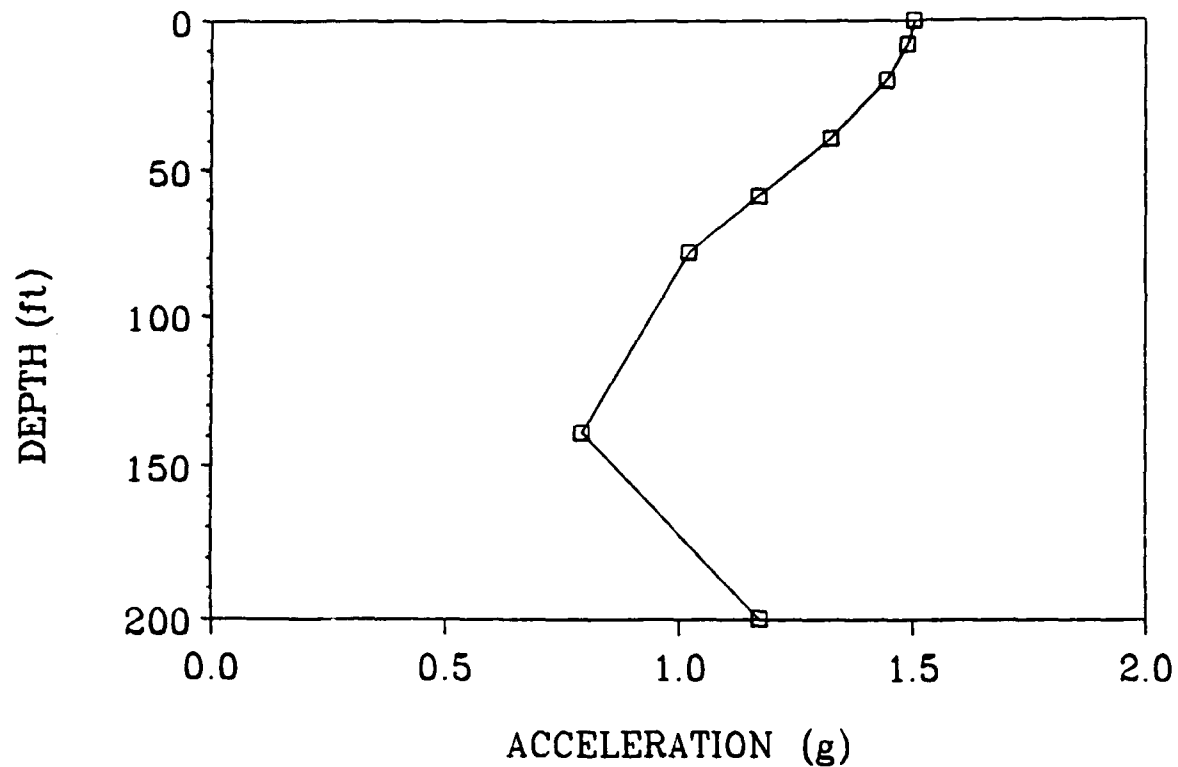


Figure 3.1 Hypothetical acceleration time history and Fourier spectra

### RESPONSE AT MIDSECTION



DAM :       $H_1 = 78 \text{ ft}$        $C_1 = 1050 \text{ ft/s}$   
LAYER :     $H_2 = 122 \text{ ft}$        $C_2 = 1300 \text{ ft/s}$   
CANYON :     $L = 735 \text{ ft}$

Figure 3.2 Case 1: Distribution with depth of peak acceleration evaluated at midsection

COMPUTED RESPONSE AT MIDCREST

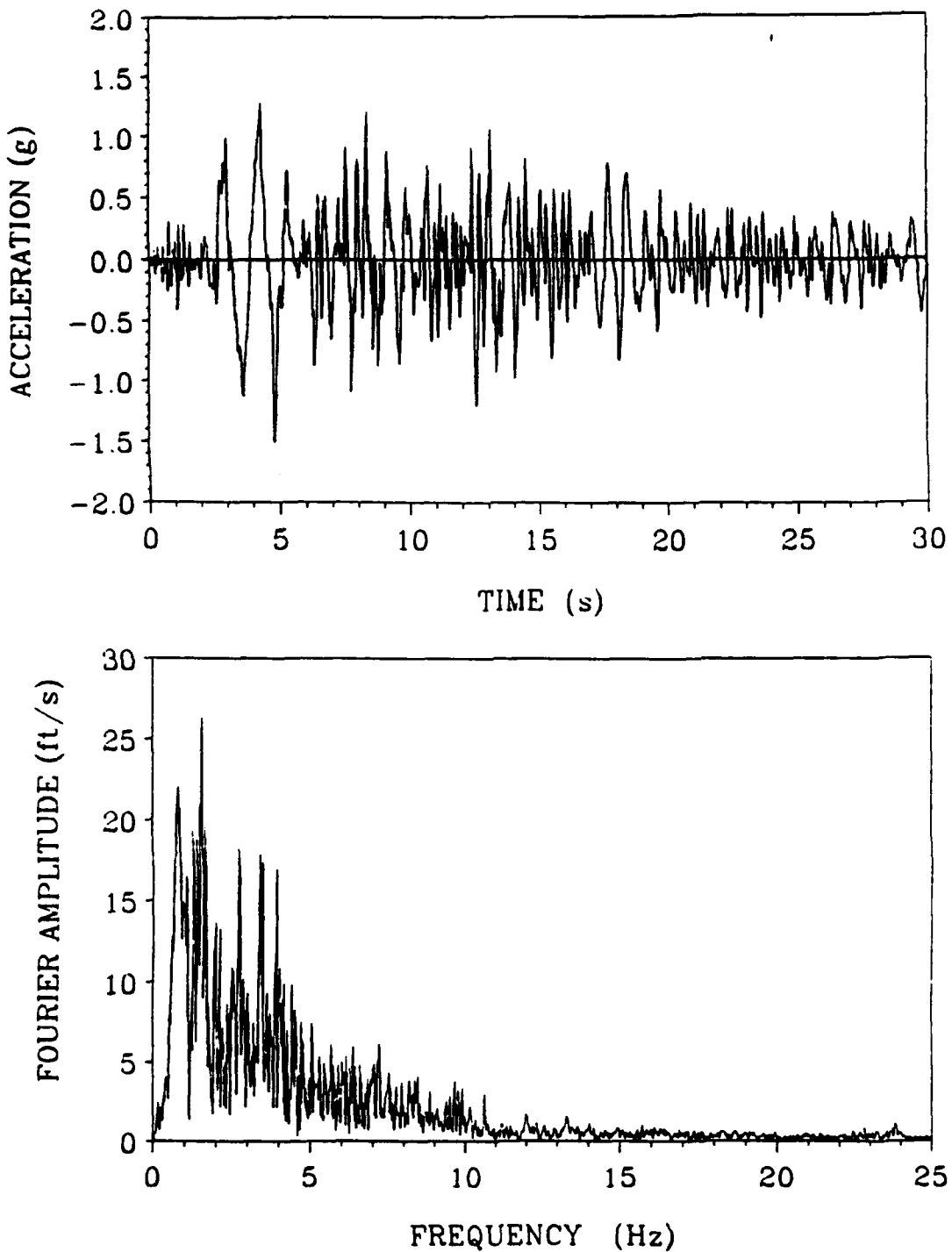


Figure 3.3 Case 1: Crest acceleration time history and Fourier spectra evaluated at midsection

COMPUTED RESPONSE AT DEPTH  $z = 39$  ft

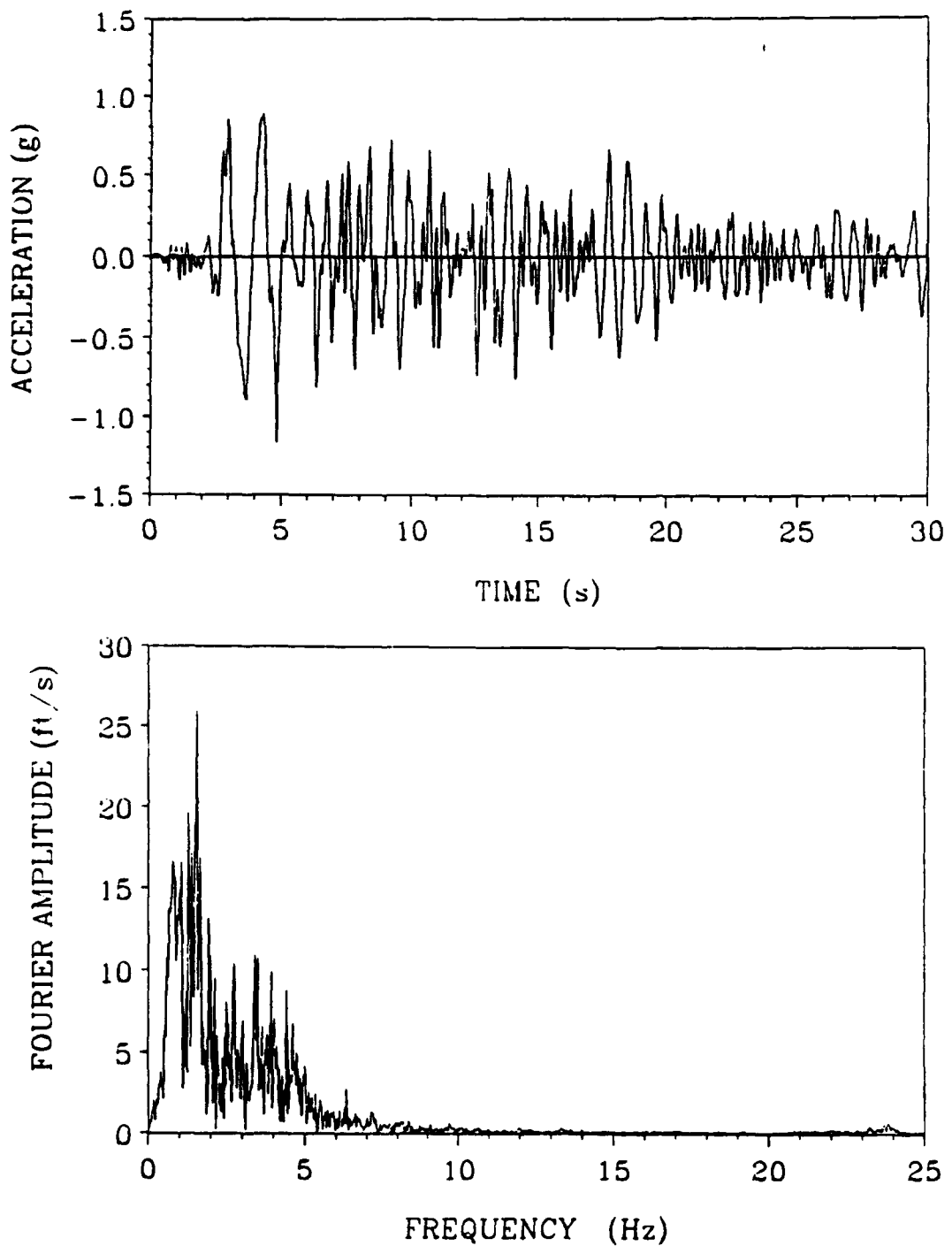
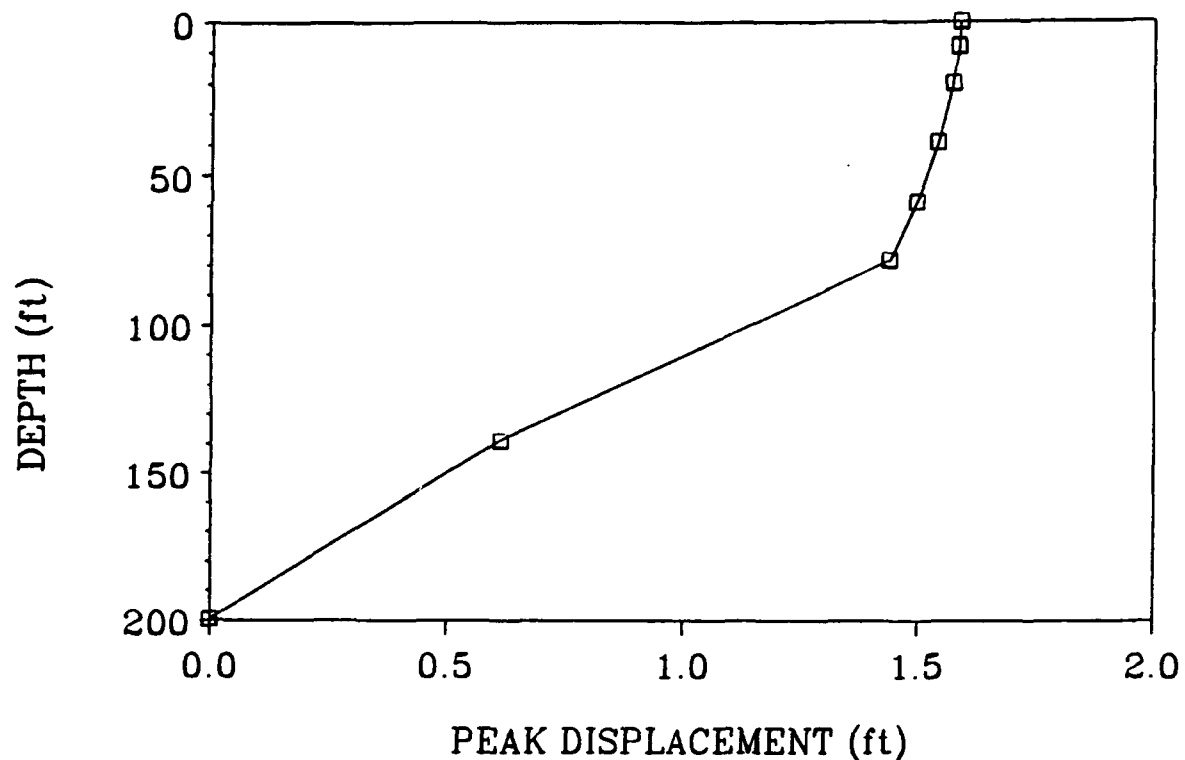


Figure 3.4 Case 1: Acceleration time history and Fourier spectra evaluated at depth = 39 ft. from the crest at midsection

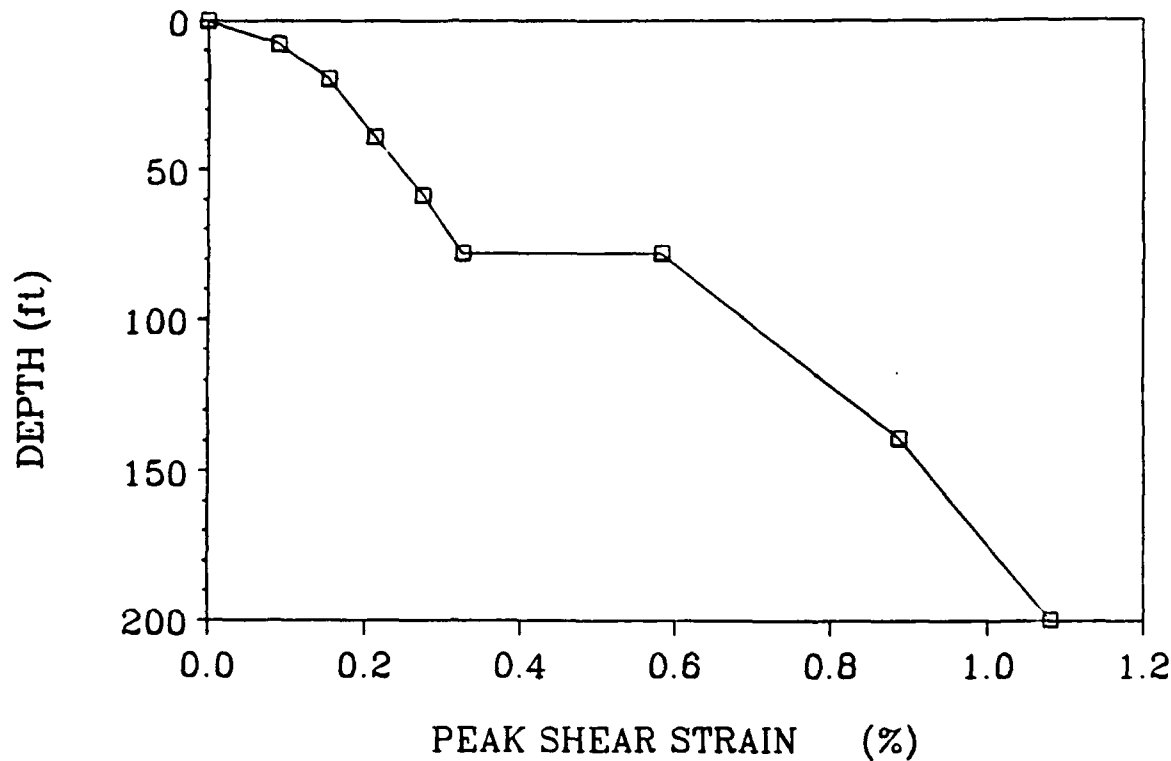
### RESPONSE AT MIDSECTION



DAM :       $H_1 = 78 \text{ ft}$        $C_1 = 1050 \text{ ft/s}$   
LAYER :     $H_2 = 122 \text{ ft}$        $C_2 = 1300 \text{ ft/s}$   
CANYON :     $L = 735 \text{ ft}$

Figure 3.5 Case 1: Distribution with depth of peak displacements evaluated at midsection

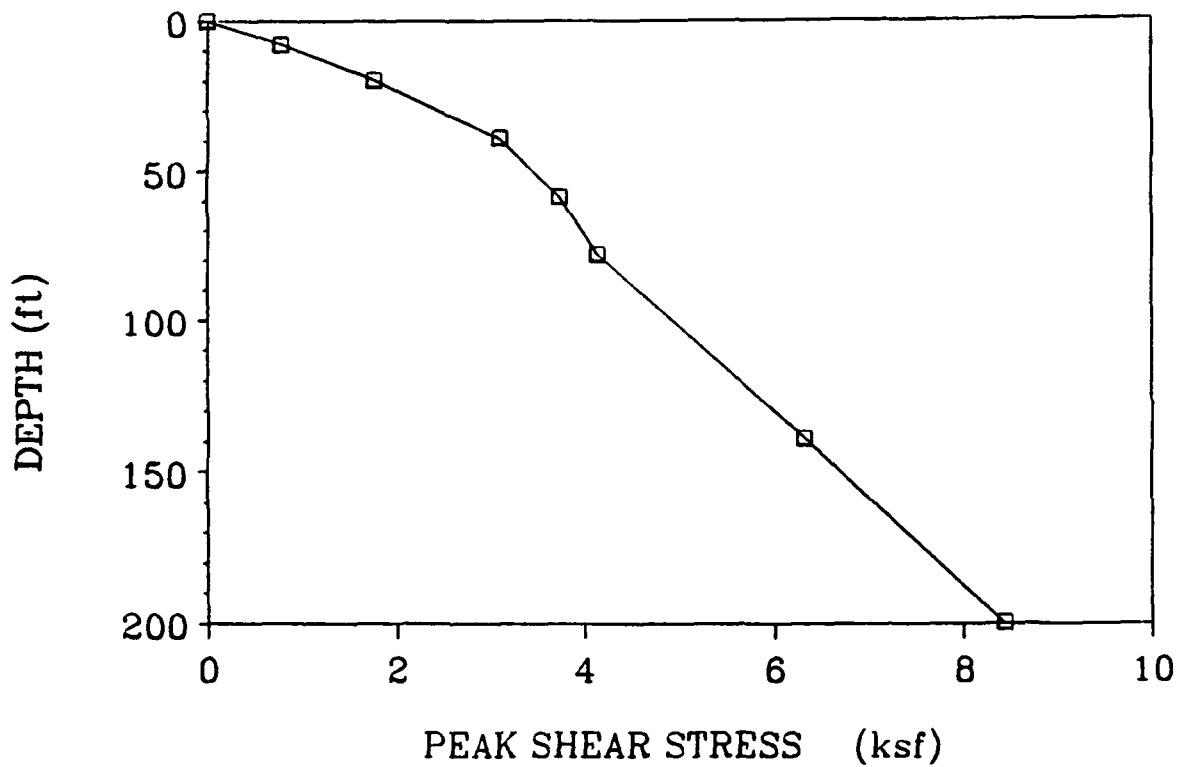
### RESPONSE AT MIDSECTION



DAM : H<sub>1</sub> = 78 ft C<sub>1</sub> = 1050 ft/s  
LAYER : H<sub>2</sub> = 122 ft C<sub>2</sub> = 1300 ft/s  
CANYON : L = 735 ft

Figure 3.6 Case 1: Distribution with depth of peak shear strains  
 $\gamma_{yz}$  evaluated at midsection

### RESPONSE AT MIDSECTION



DAM :       $H_1 = 78 \text{ ft}$        $C_1 = 1050 \text{ ft/s}$   
LAYER :     $H_2 = 122 \text{ ft}$        $C_2 = 1300 \text{ ft/s}$   
CANYON :     $L = 735 \text{ ft}$

Figure 3.7 Case 1: Distribution with depth of peak shear stresses  
 $\tau_{yz}$  evaluated at midsection

(2.3), the transfer function  $TF = \ddot{u}_b / \ddot{u}_g$  (where  $\ddot{u}_b$  = acceleration at the dam base and  $\ddot{u}_g$  = acceleration at the outcrop rock) is computed and plotted in Fig. 3.8. Assuming the given hypothetical acceleration as the outcrop motion, the resulting acceleration at the dam base is obtained with a peak value of 1.02 g (see Fig. 3.9). This now becomes the input motion for the nonlinear analysis using the shear beam model 1. Table 3.2 summarizes all the assumptions and input data for Case 2.

Fig. 3.10 plots peak accelerations versus depth computed at the mid-section, while Fig. 3.11 plots the crest acceleration time history and its Fourier spectra. A comparison with the results of Case 1 (Figs. 3.3-3.4) shows that, in this case, the effect of radiation damping on the amplitude and frequency content of the acceleration is indeed very small. However, there is about 25% decrease of crest displacements and about 20% decrease of shear strains near the base (see Figs. 3.12-3.14). Time histories of accelerations, relative displacements, shear strains  $\gamma_{yz}$  and shear stresses  $\tau_{yz}$  at various elevations at midsection from Case 2 are presented in the Appendix.

## Case 2

Dam Idealization: Model 1

Type of Analysis: Nonlinear (piece-wise linear)

Dam Height:  $H_1 = 78 \text{ ft. (23.77 m)}$

Dam Ave. S-wave Velocity:  $\bar{C}_1 = 1050 \text{ ft/s (320 m/s)}$

Dam Ave. Mass Density:  $\rho_1 = 136 \text{ pcf (2178 kg/m}^3\text{)}$

Inhomogeneity Parameter:  $m = 0.3$

Layer Thickness:  $H_2 = 122 \text{ ft. (37.19 m)}$

Layer Ave. S-wave Velocity:  $\bar{C}_2 = 1300 \text{ ft/s (396.2 m/s)}$

Layer Ave. Mass Density:  $\rho_2 = 136 \text{ pcf (2178 kg/m}^3\text{)}$

Canyon Width:  $L = 735 \text{ ft. (224 m)}$

Base Rock S-wave Velocity:  $C_r = 3000 \text{ ft/s (914 m/s)}$

Impedance Ratio:  $\alpha = 0.15$

Input Motion: the computed acceleration at the dam base in Fig. 3.9 (The outcrop rock motion is the given hypothetical acceleration in Fig. 3.1)

Computed Fundamental Period:  $T_1 = 0.46 \text{ s}$

Table 3.2 Input Data for Case 2

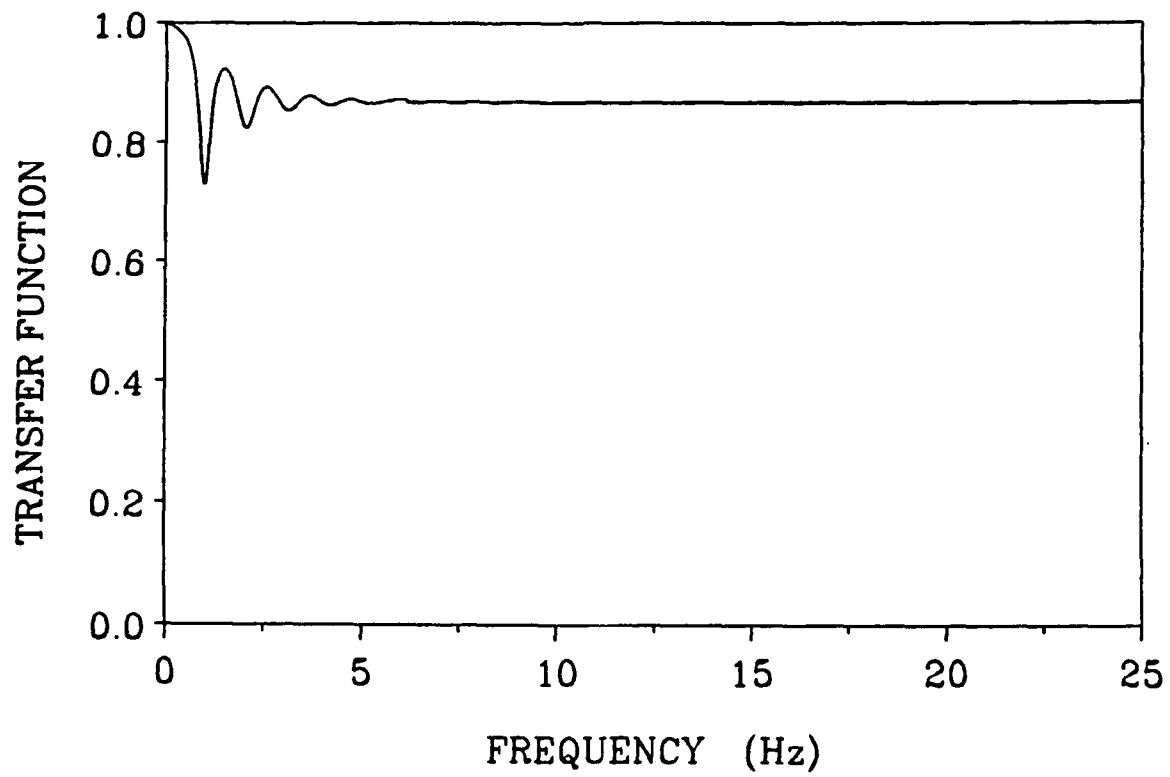


Figure 3.8 Transfer function relating the acceleration amplitude at the dam base and at the outcrop rock

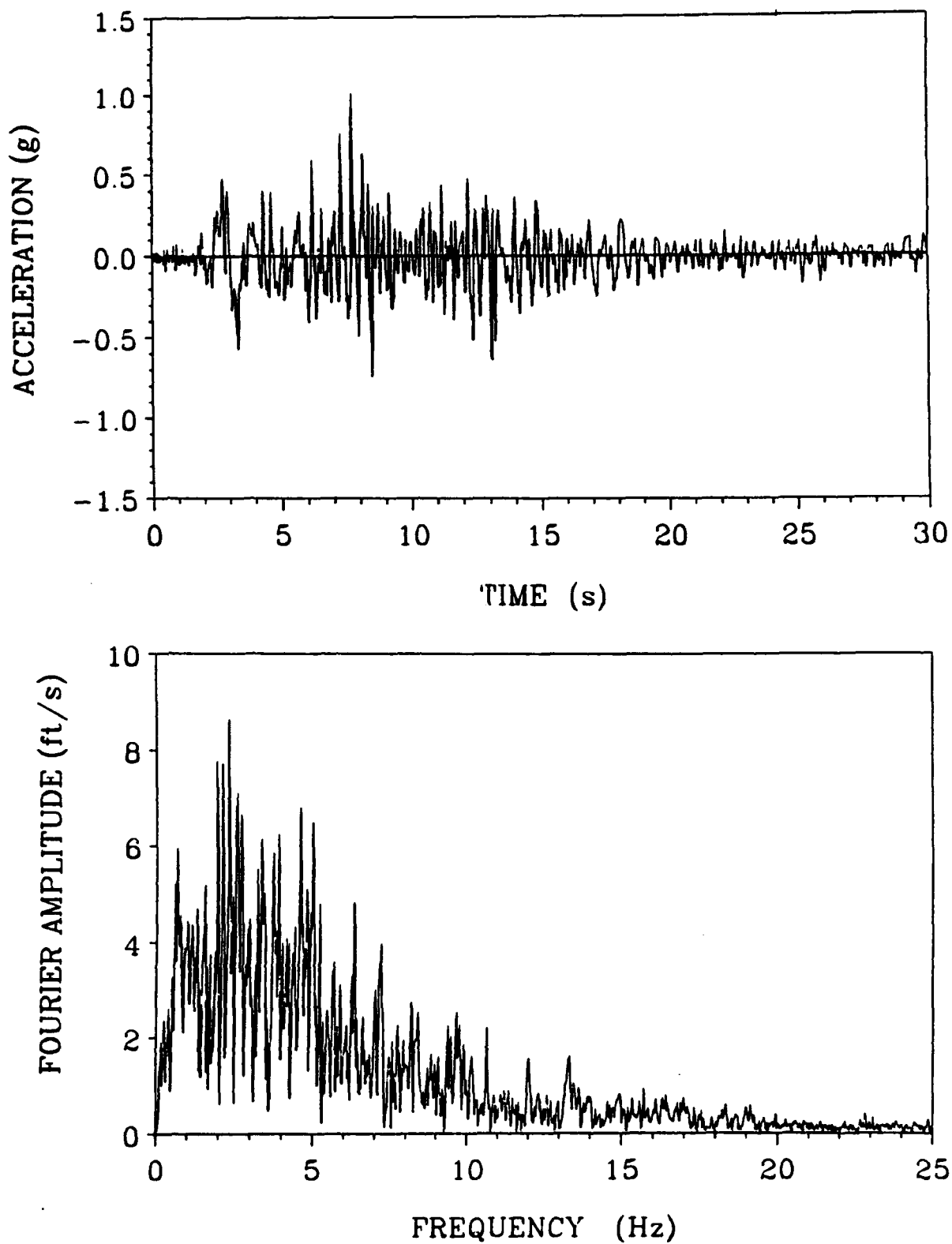
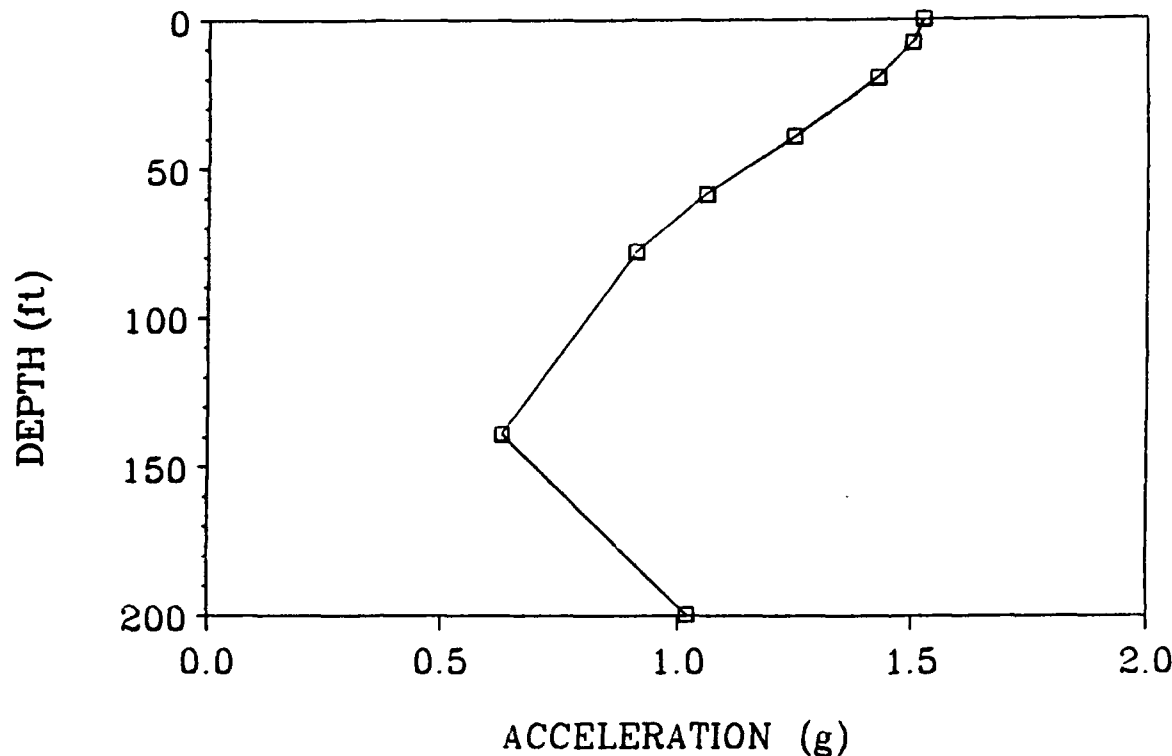


Figure 3.9 Acceleration time history and Fourier spectra at the dam base

### RESPONSE AT MIDSECTION



DAM :       $H_1 = 78 \text{ ft}$        $C_1 = 1050 \text{ ft/s}$   
LAYER :     $H_2 = 122 \text{ ft}$        $C_2 = 1300 \text{ ft/s}$   
CANYON :    $L = 735 \text{ ft}$

Figure 3.10 Case 2: Distribution with depth of peak acceleration evaluated at midsection

### COMPUTED RESPONSE AT MIDCREST

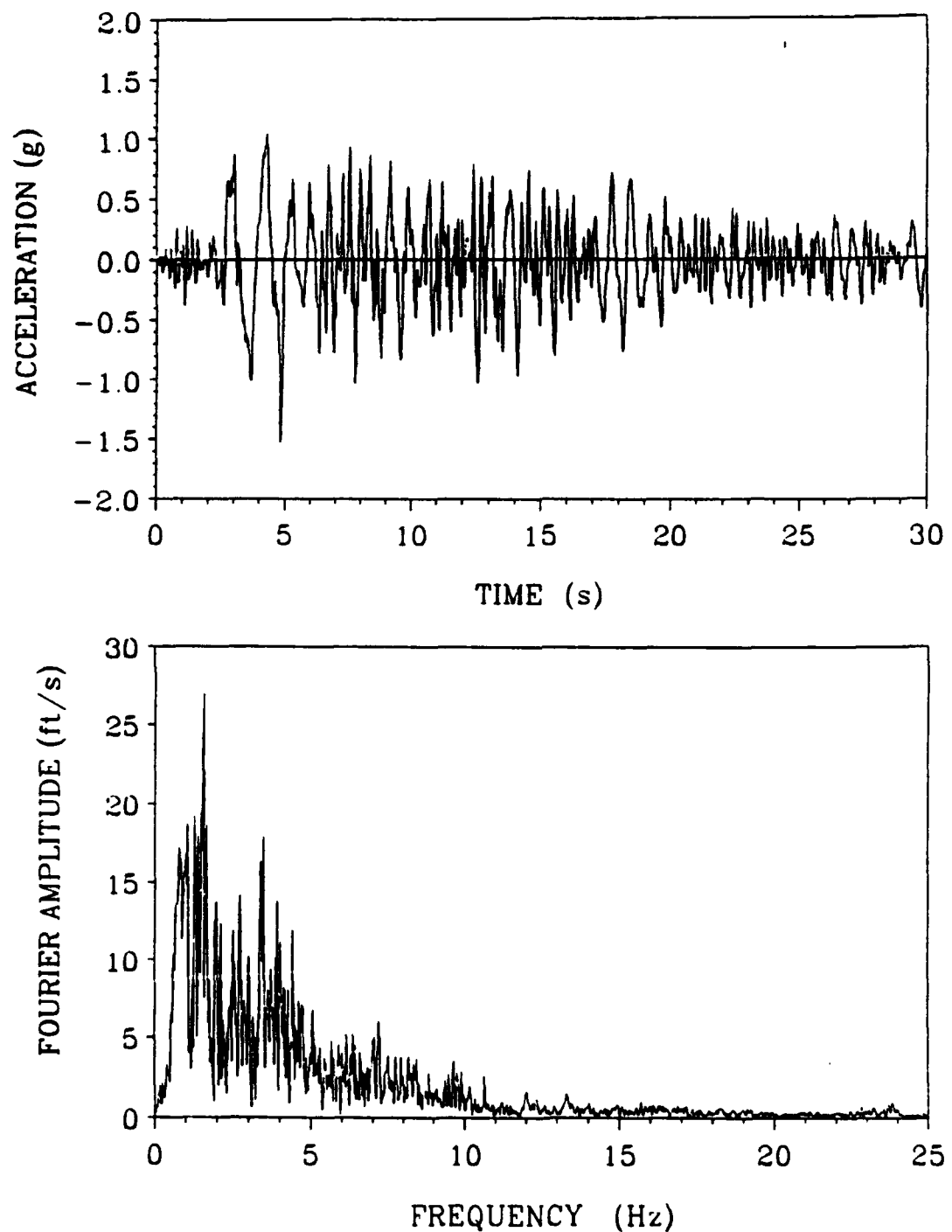
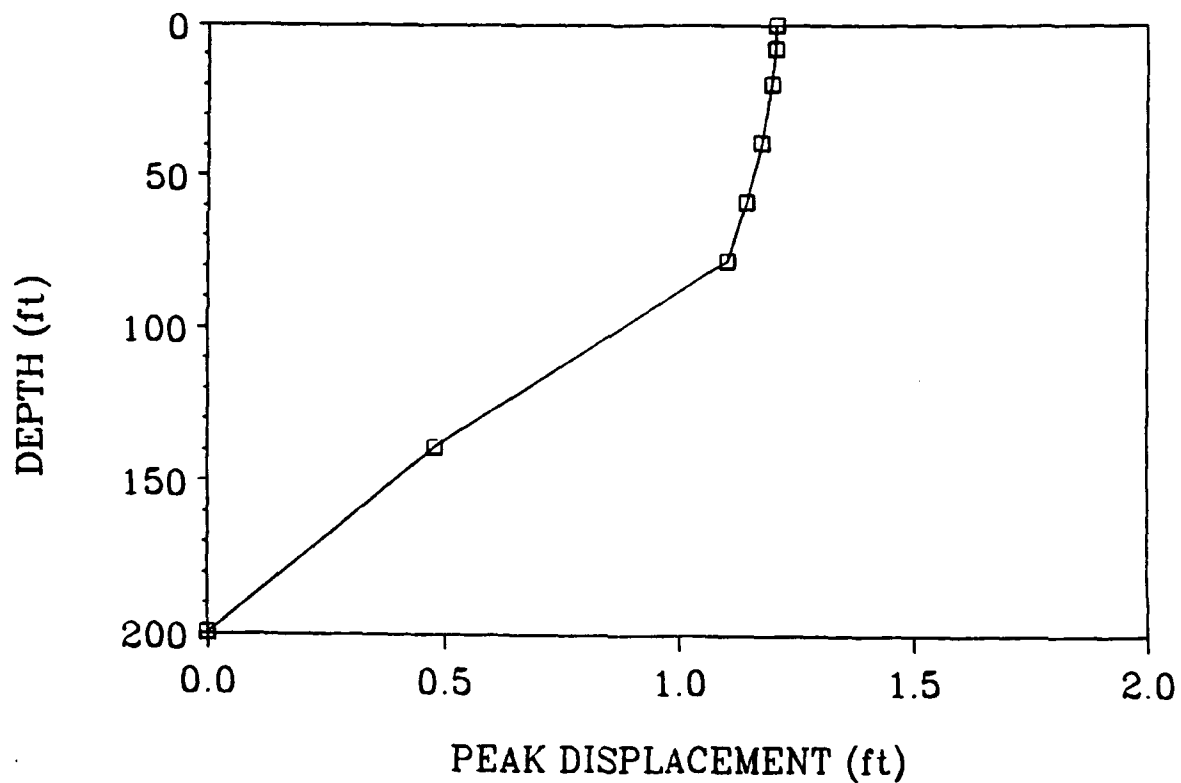


Figure 3.11 Case 2: Crest acceleration time history and Fourier spectra evaluated at midsection

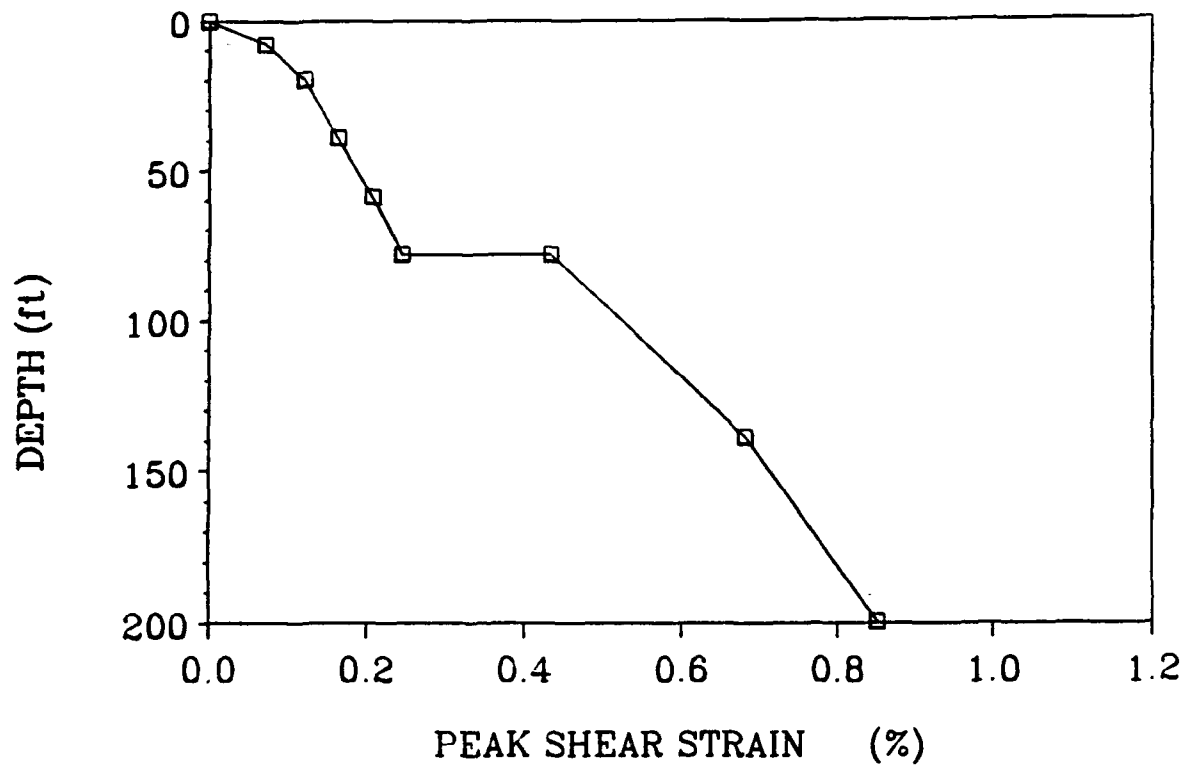
### RESPONSE AT MIDSECTION



DAM :       $H_1 = 78 \text{ ft}$        $C_1 = 1050 \text{ ft/s}$   
LAYER :     $H_2 = 122 \text{ ft}$        $C_2 = 1300 \text{ ft/s}$   
CANYON :     $L = 735 \text{ ft}$

Figure 3.12 Case 2: Distribution with depth of peak displacements evaluated at midsection

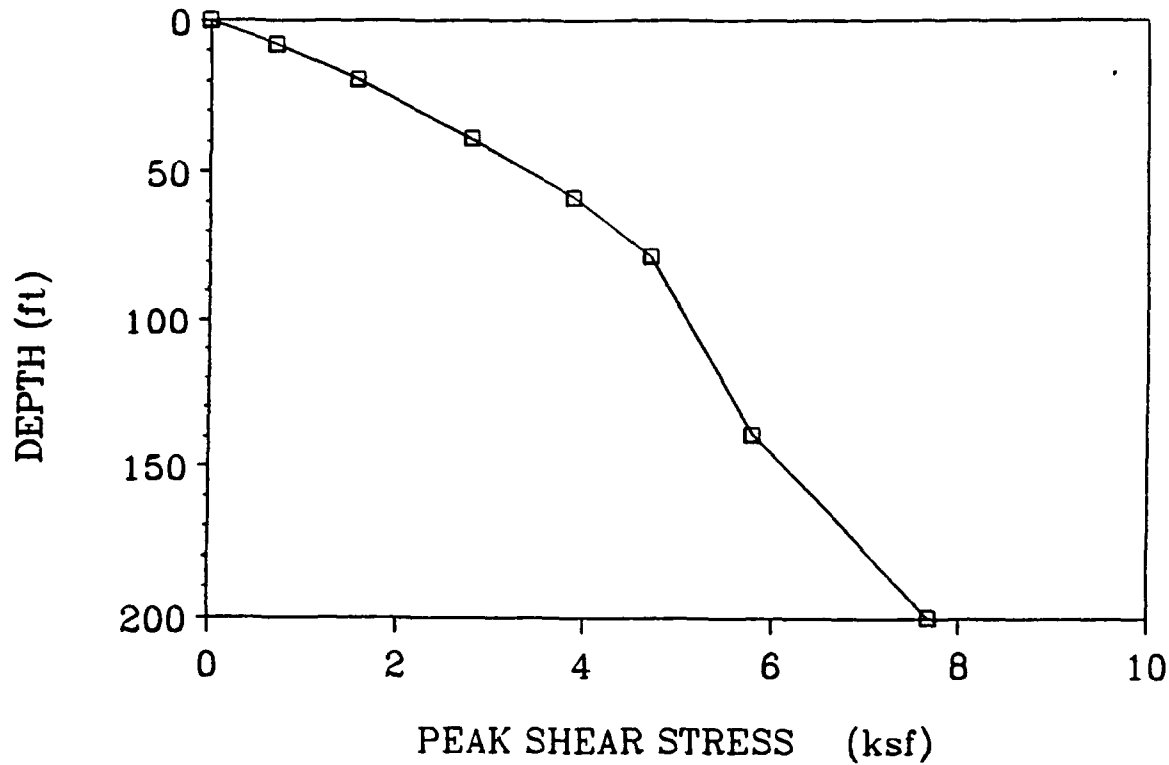
### RESPONSE AT MIDSECTION



DAM : H<sub>1</sub> = 78 ft C<sub>1</sub> = 1050 ft/s  
LAYER : H<sub>2</sub> = 122 ft C<sub>2</sub> = 1300 ft/s  
CANYON : L = 735 ft

Figure 3.13 Case 2: Distribution with depth of peak shear strains  
 $\gamma_{yz}$  evaluated at midsection

### RESPONSE AT MIDSECTION



DAM : H<sub>1</sub> = 78 ft C<sub>1</sub> = 1050 ft/s  
LAYER : H<sub>2</sub> = 122 ft C<sub>2</sub> = 1300 ft/s  
CANYON : L = 735 ft

Figure 3.14 Case 2: Distribution with depth of peak shear stresses  
 $\tau_{yz}$  evaluated at midsection

### Case 3

The previous two analyses assumed that the upper 78 ft. of the structure have the dynamic characteristics of an embankment dam, while the lower 100 ft. of the structure, because of the flatness of the slopes, would tend to respond in a way closer to that of a foundation layer. The present analysis extends the height of the dam by 40 ft., i.e.,  $H_1 = 78 + 40 = 118$  ft., while the thickness of the foundation layer becomes  $H_2 = 60 + 22 = 82$  ft. The base rock is assumed to be flexible. Table 3.3 summarizes all the assumptions and input data for Case 3.

Fig. 3.15 plots peak accelerations versus depth computed at the mid-section. Except for small variations, the response values are not very different from those computed in Cases 1 and 2 with a peak crest acceleration about 1.5 g. However, a closer look at the crest acceleration time histories (Fig. 3.16) suggests the following differences: (a) the peak response in Case 3 occurs at the moment of peak ground acceleration and not during the early low-frequency pulse as in Cases 1 and 2; (b) the acceleration response in Case 3 is richer in high-frequency motion than those of Cases 1 and 2. In addition, the peak displacements are smaller (Fig. 3.17) and the fundamental natural period is about 0.43 seconds. All the above indicate a "stiffer" dam-layer system compared to that in the previous two cases.

### Case 3

Dam Ideealization: Model 1

Type of Analysis: Nonlinear (piece-wise linear)

Dam Height:  $H_1 = 118$  ft. (35.96 in.)

Dam Ave. S-wave Velocity:  $\bar{C}_1 = 1102$  ft/s (336 m/s)

Dam Ave. Mass Density:  $\rho_1 = 136$  pcf (2178 kg/m<sup>3</sup>)

Inhomogeneity Parameter:  $m = 0.3$

Layer Thickness:  $H_2 = 82$  ft. (25.00 m)

Layer Ave. S-wave Velocity:  $C_2 = 1330$  ft/s (405 m/s)

Layer Ave. Mass Density:  $\rho_2 = 136$  pcf (2178 kg/m<sup>3</sup>)

Canyon Width:  $L = 735$  ft. (224 in.)

Base Rock S-wave Velocity:  $C_r = 3000$  ft/s (914 m/s)

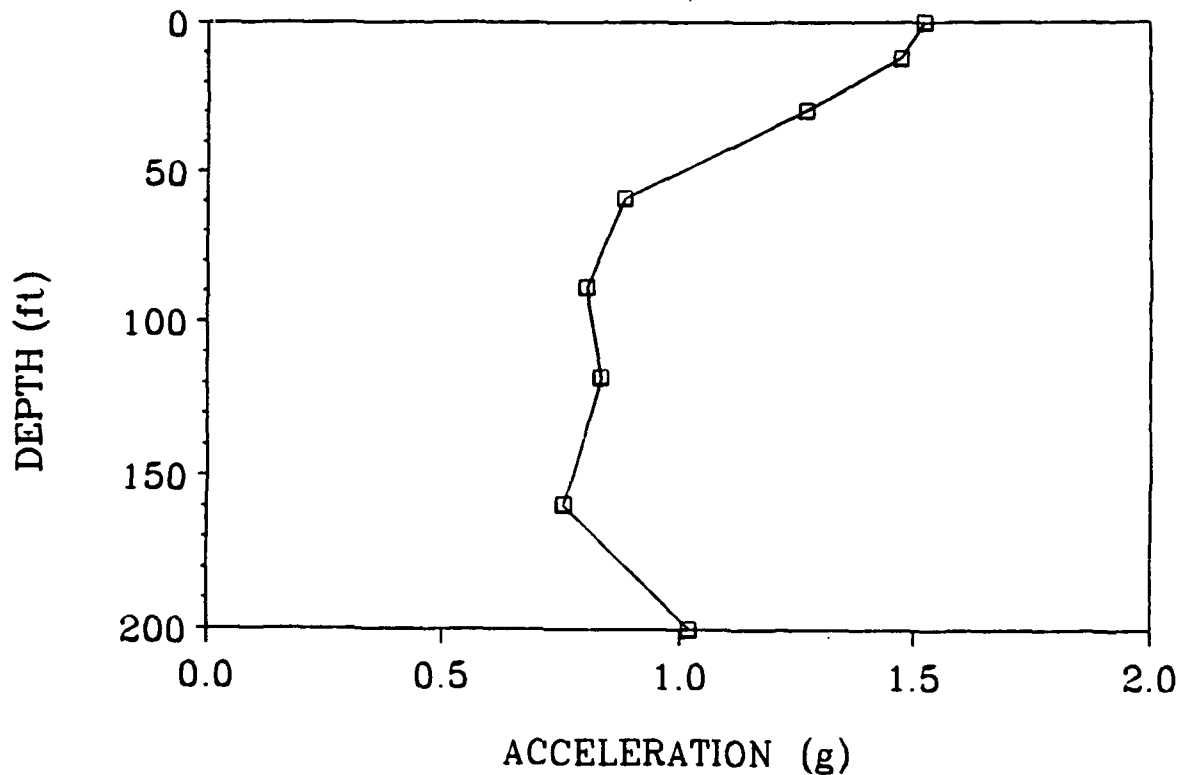
Impedance Ratio:  $\alpha = 0.15$

Input Motion: the computed acceleration at the dam base in Fig. 3.9 (the outcrop rock motion is the given hypothetical acceleration in Fig. 3.1)

Computed Fundamental Period:  $T_1 = 0.43$  s

Table 3.3 Input Data for Case 3

### RESPONSE AT MIDSECTION



DAM :  $H_1 = 118 \text{ ft}$        $C_1 = 1102 \text{ ft/s}$

LAYER :  $H_2 = 82 \text{ ft}$        $C_2 = 1330 \text{ ft/s}$

CANYON :  $L = 735 \text{ ft}$

Figure 3.15 Case 3: Distribution with depth of peak accelerations  
evaluated at midsection

### COMPUTED RESPONSE AT MIDCREST

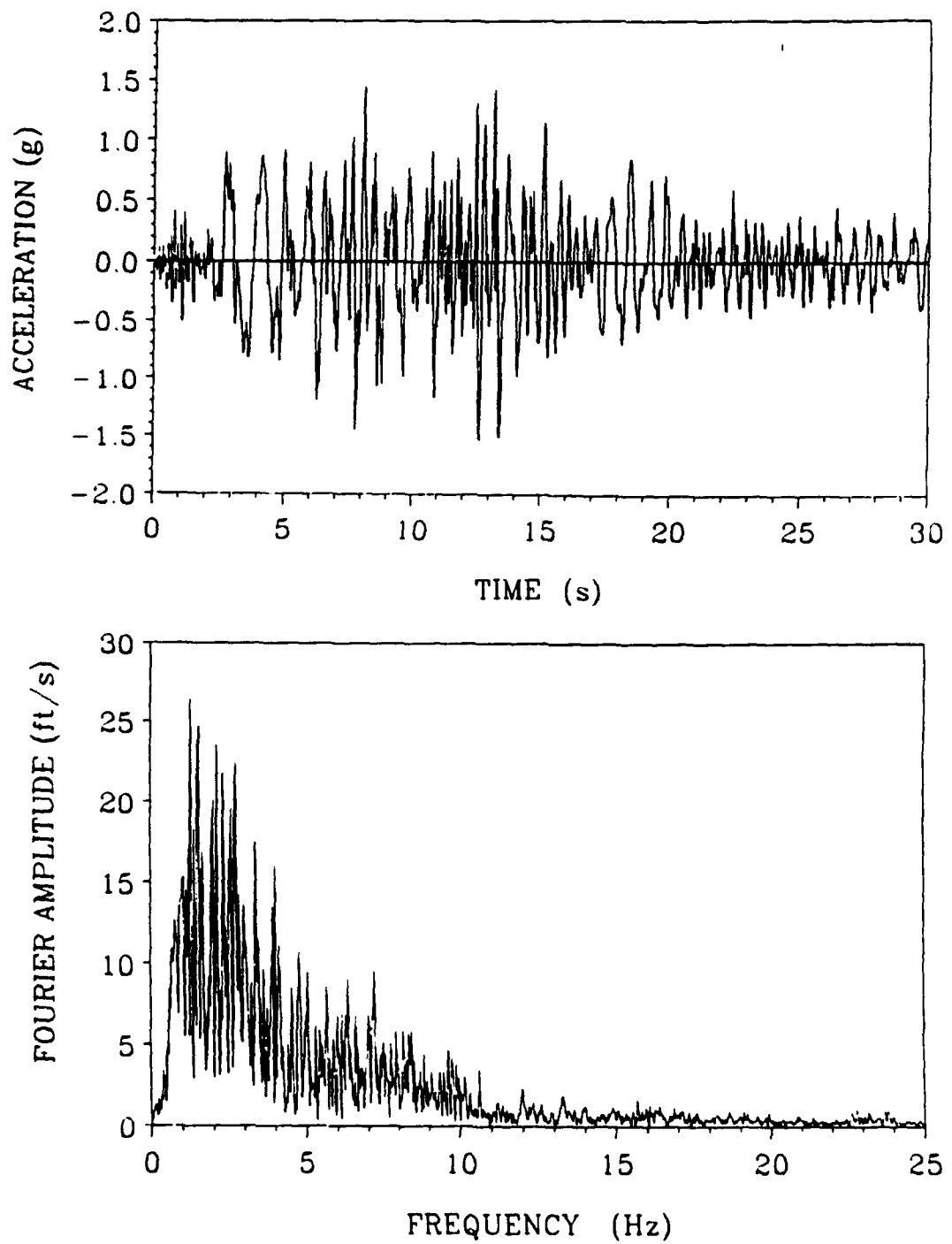
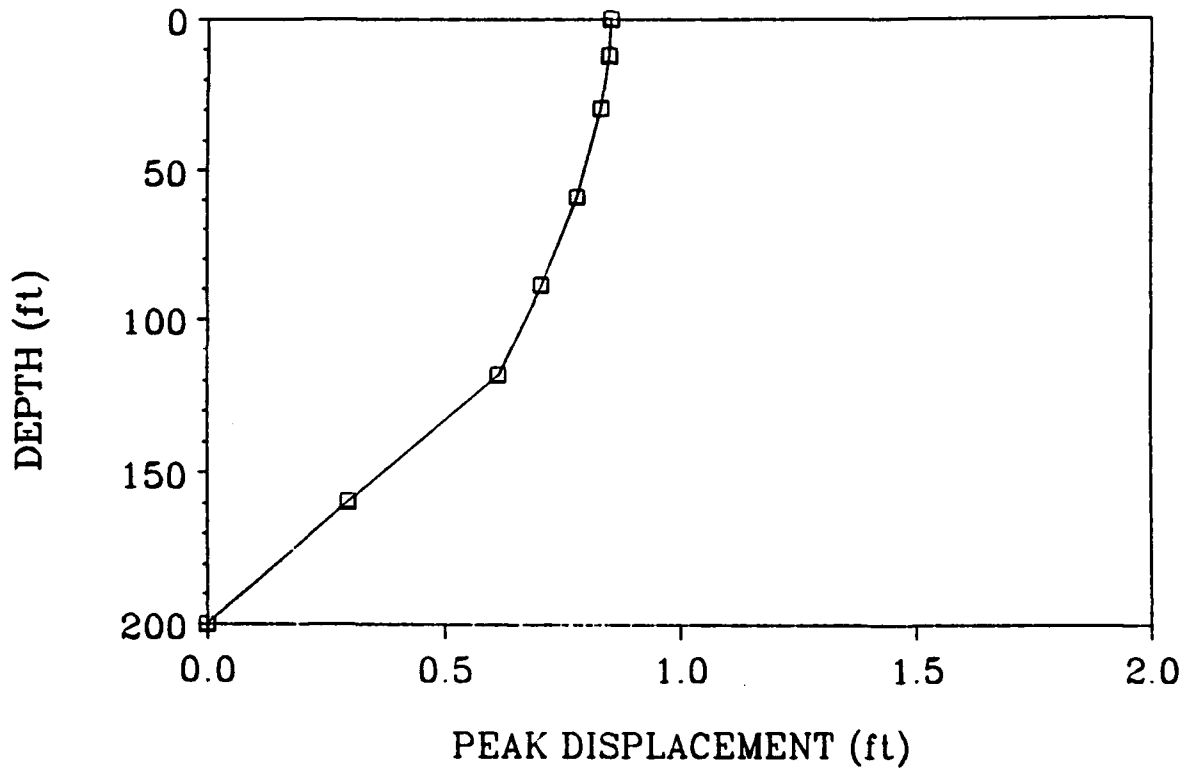


Figure 3.16 Case 3: Crest acceleration time history and Fourier spectra evaluated at midsection

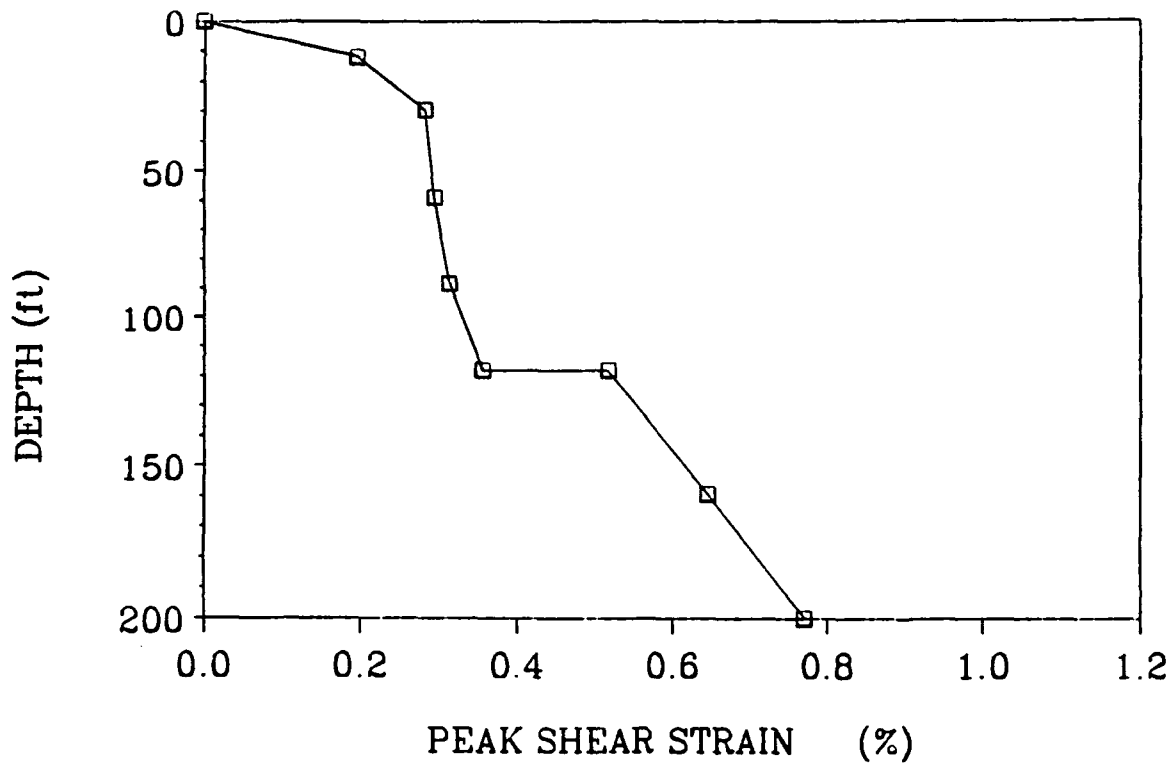
### RESPONSE AT MIDSECTION



DAM :       $H_1 = 118 \text{ ft}$        $C_1 = 1102 \text{ ft/s}$   
LAYER :     $H_2 = 82 \text{ ft}$        $C_2 = 1330 \text{ ft/s}$   
CANYON :    $L = 735 \text{ ft}$

Figure 3.17 Case 3: Distribution with depth of peak displacements evaluated at midsection

### RESPONSE AT MIDSECTION

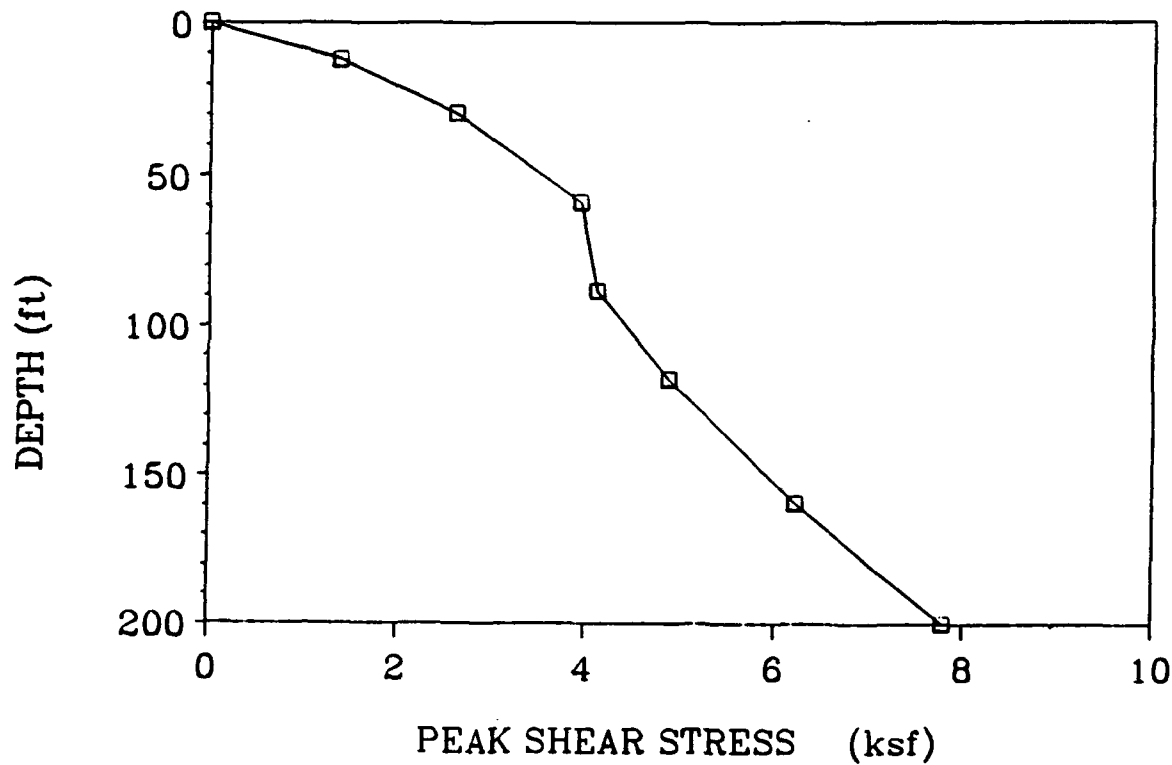


DAM :  $H_1 = 118 \text{ ft}$        $C_1 = 1102 \text{ ft/s}$   
LAYER :  $H_2 = 82 \text{ ft}$        $C_2 = 1330 \text{ ft/s}$   
CANYON :  $L = 735 \text{ ft}$

Figure 3.18 Case 3: Distribution with depth of peak shear strains

$\gamma_{yz}$  evaluated at midsection

### RESPONSE AT MIDSECTION



DAM : H<sub>1</sub> = 118 ft C<sub>1</sub> = 1102 ft/s  
LAYER : H<sub>2</sub> = 82 ft C<sub>2</sub> = 1330 ft/s  
CANYON : L = 735 ft

Figure 3.19 Case 3: Distribution with depth of peak shear stresses  
 $\tau_{yz}$  evaluated at midsection

### 3.2 Response of Ririe Dam Using Model 2

#### Case 4

This analysis assumes that the stiffening effect of the canyon is significantly reduced by the effects of the strongly nonlinear behavior of soil. Therefore, an infinitely long dam may be assumed (plane strain conditions). Even if this assumption is only approximate, the present analysis would provide some additional insight by extending the range of response values obtained from the previous analyses. The specific values regarding the material and geometric characteristics are given in Table 3.4. The computed fundamental period of the dam at small strains is 0.44 seconds.

The peak crest acceleration in Fig. 13.20 is 1.27 g (crest amplification = 1.04), while the peak accelerations within the rest of the dam body are lower with a minimum value of 0.66 g. Peak relative displacements and peak shear strains in Figs. 13.22 and 13.23, respectively, appear to be about 40% smaller than those in Case 1.

#### **Case 4**

**Dam Idealization: Model 2**

**Type of Analysis: Nonlinear (piece-wise linear)**

**Dam Height:  $H = 200 \text{ ft.} (60.96 \text{ ft.})$**

**Dam Ave. S-wave Velocity:  $C = 1245 \text{ ft/s} (380 \text{ m/s})$**

**Inhomogeneity Parameter:  $m = 0.3$**

**Dam Ave. Mass Density:  $\rho = 136 \text{pcf} (2178 \text{ kg/m}^3)$**

**Dam Length: Infinite (Plane Strain Conditions)**

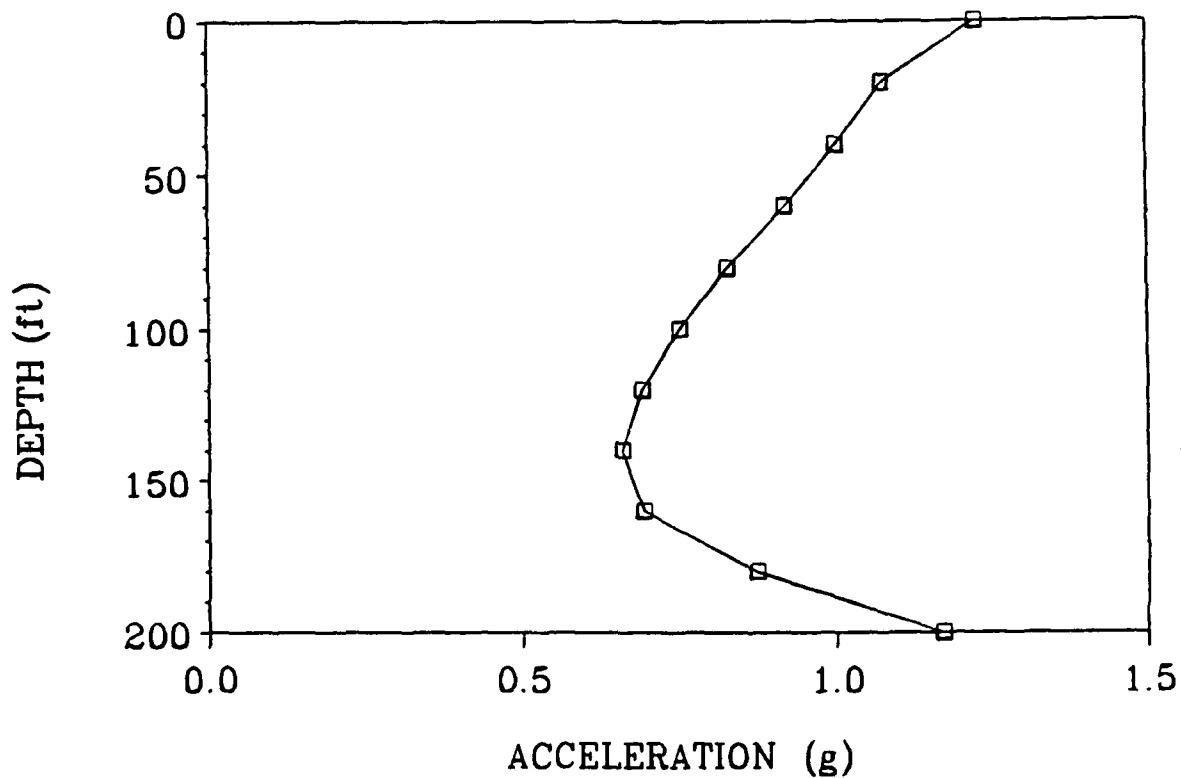
**Base: Rigid Rock**

**Input Motion: Given Hypothetical Acceleration (Fig. 3.1)**

**Computed Fundamental Period:  $T_1 = 0.44 \text{ s}$**

**Table 3.4 Input Data for Case 4**

### RESPONSE AT MIDSECTION



DAM : H<sub>1</sub> = 200 ft C<sub>1</sub> = 1245 ft/s

PLANE STRAIN ANALYSIS

Figure 3.20 Case 4: Distribution with depth of peak accelerations

COMPUTED RESPONSE AT MIDCREST

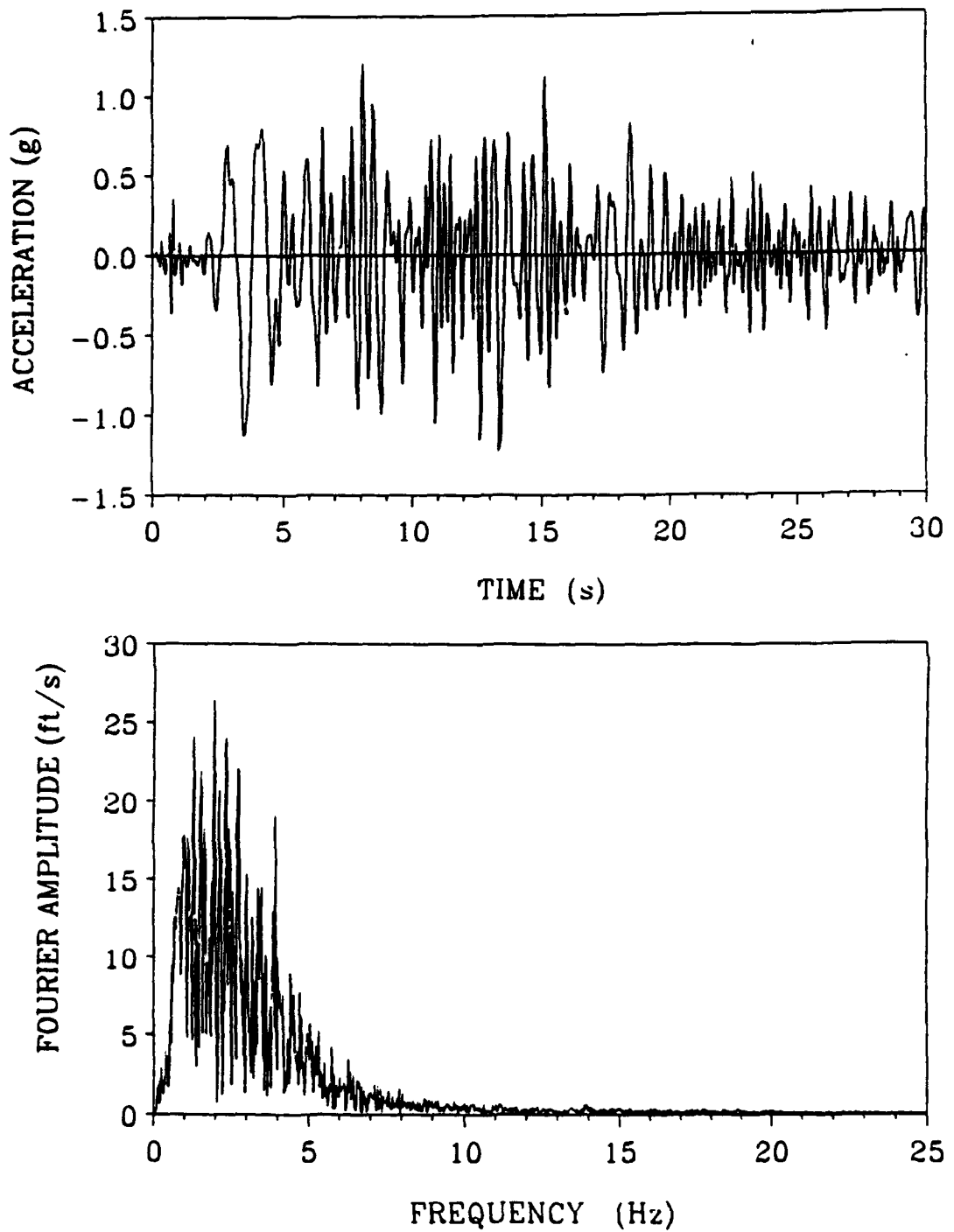
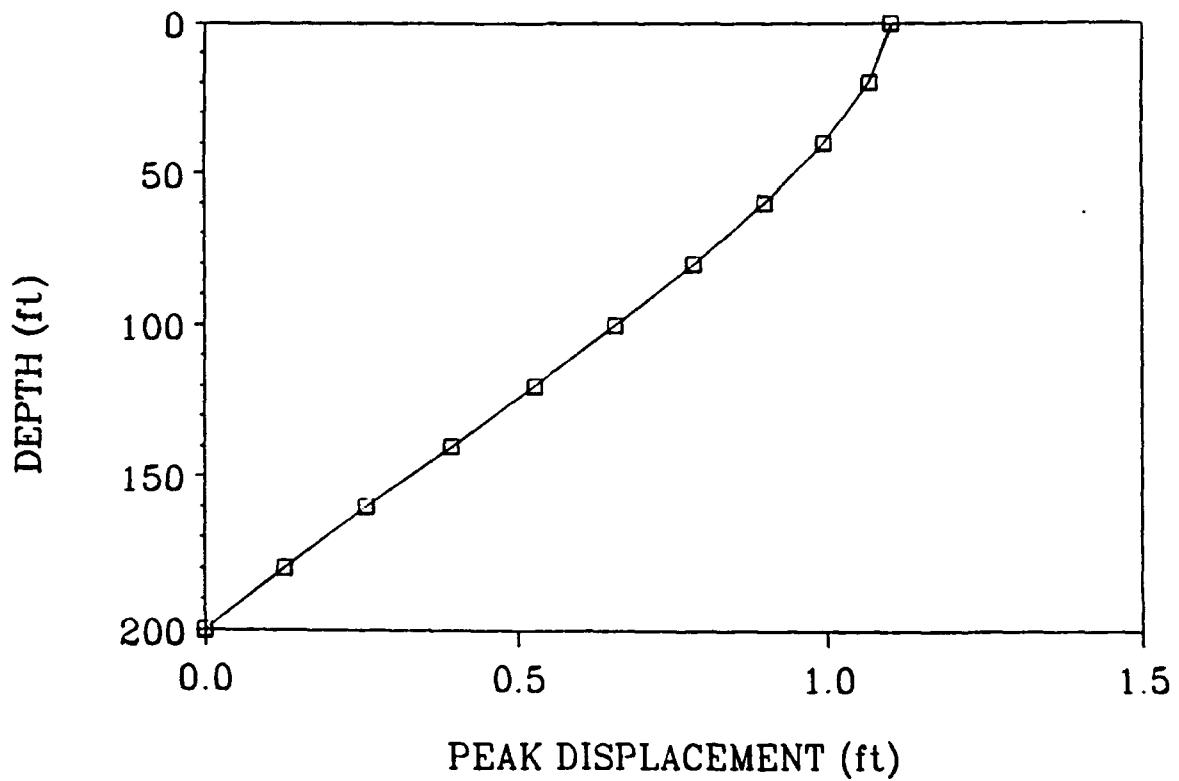


Figure 3.21 Case 4: Crest acceleration time history and Fourier spectra

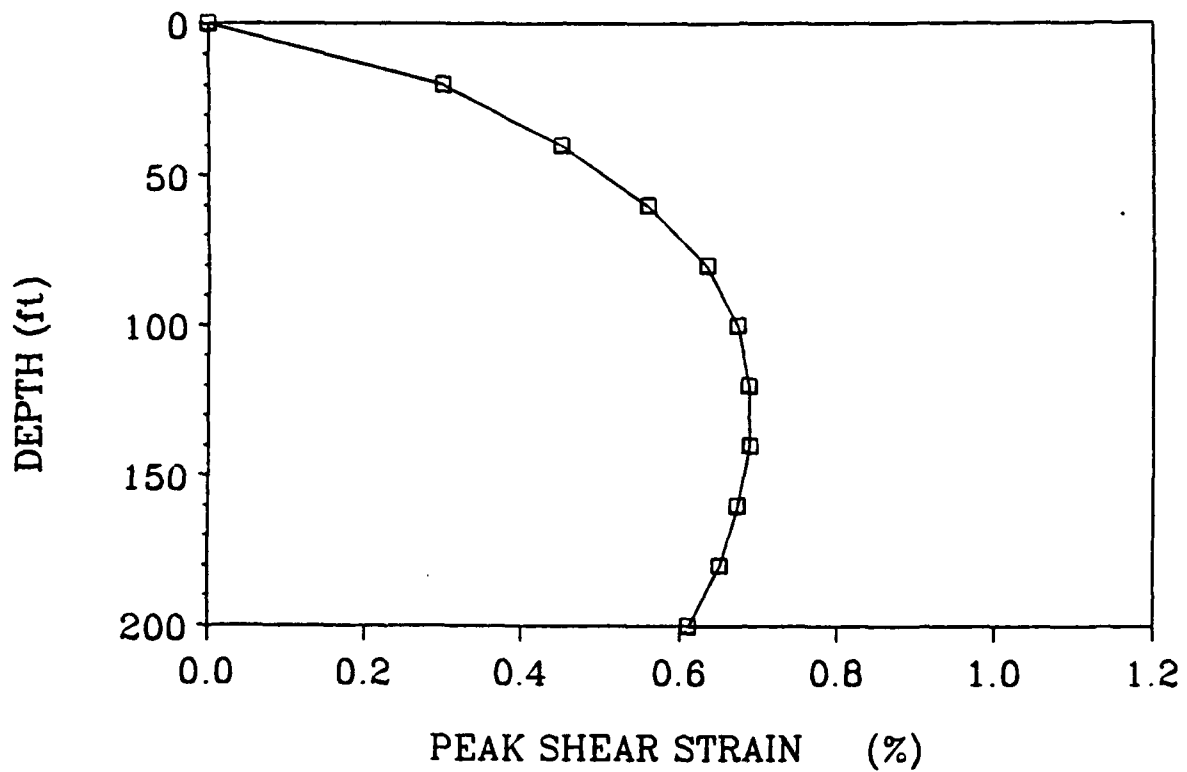
### RESPONSE AT MIDSECTION



DAM :       $H_1 = 200 \text{ ft}$        $C_1 = 1245 \text{ ft/s}$   
PLANE STRAIN ANALYSIS

Figure 3.22 Case 4: Distribution with depth of peak displacements

### RESPONSE AT MIDSECTION



DAM :  $H_1 = 200 \text{ ft}$   $C_1 = 1245 \text{ ft/s}$   
PLANE STRAIN ANALYSIS

Figure 3.23 Case 4: Distribution with depth of peak shear strains

### Case 5

Case 5 is identical to Case 4, except for the baserock which is now assumed to be flexible with a constant S-wave velocity of  $C_r = 3000$  ft/s. The base input motion is the acceleration record in Fig. 3.9. Table 3.5 summarizes all the assumptions and input data for Case 5.

The crest peak acceleration is 1.3 g which is a little higher than that in Case 4 due to resonance (Fig. 13.24-13.25). The peak displacements and shear strains, however, are affected by the radiation damping and decrease even further (see Figs. 13.26-13.27).

### Case 5

Dam Idealization: Model 2

Type of Analysis: Nonlinear (piece-wise linear)

Dam Height:  $H = 200$  ft. (60.90 ft.)

Dam Ave. S-wave Velocity:  $C = 1245$  ft/s (780 m/s)

Inhomogeneity Parameter:  $m = 0.3$

Dam Ave. Mass Density:  $\rho = 136$  pcf (2178 kg/m<sup>3</sup>)

Dam Length: Infinite (Plane Strain Conditions)

Base Rock S-wave Velocity:  $C_r = 3000$  ft/s (914 m/s)

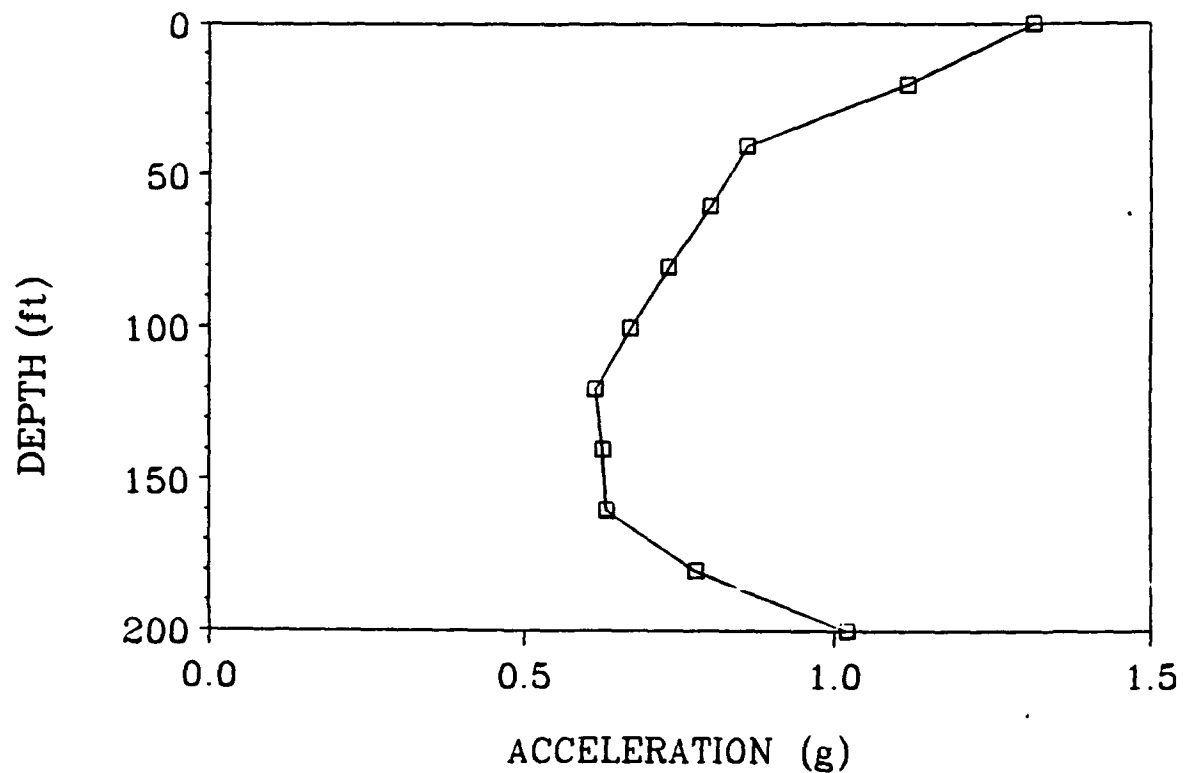
Impedance Ratio:  $\alpha = 0.15$

Input Motion: the computed acceleration at the dam base in Fig. 3.9 (The outcrop motion is the given hypothetical acceleration in Fig. 3.1)

Computed Fundamental Period:  $T_1 = 0.44$  s

Table 3.5 Input Data for Case 5

### RESPONSE AT MIDSECTION



DAM :             $H_1 = 200 \text{ ft}$              $C_1 = 1245 \text{ ft/s}$   
PLANE STRAIN ANALYSIS

Figure 3.24 Case 5: Distribution with depth of peak accelerations

COMPUTED RESPONSE AT MIDCREST

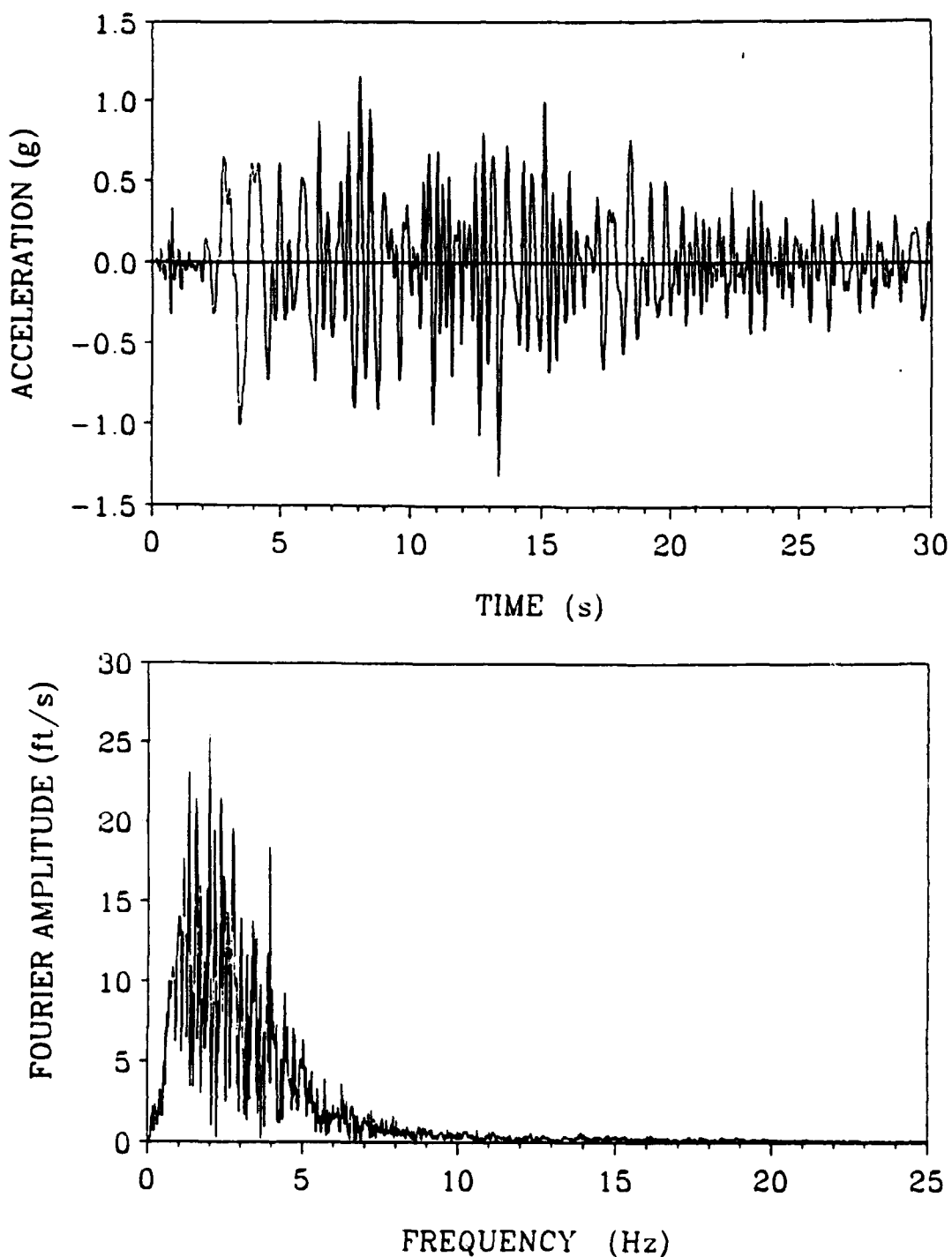
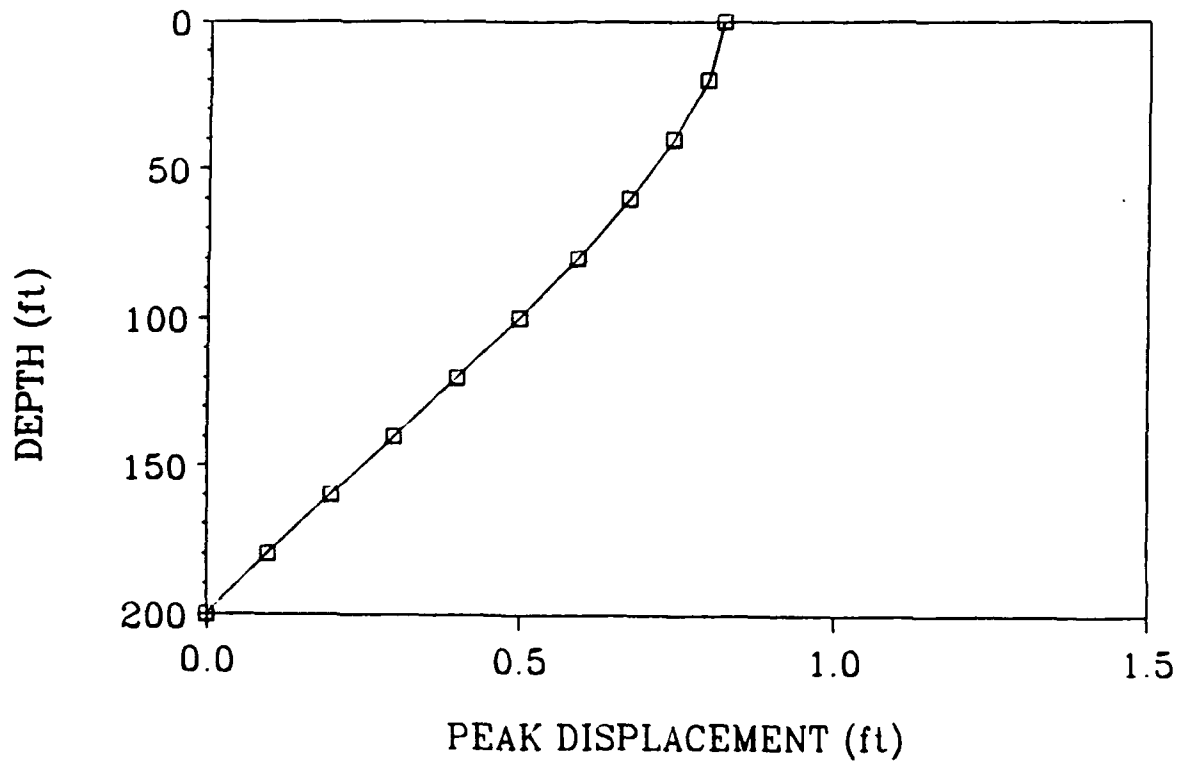


Figure 3.25 Case 5: Crest acceleration time history and Fourier

spectra

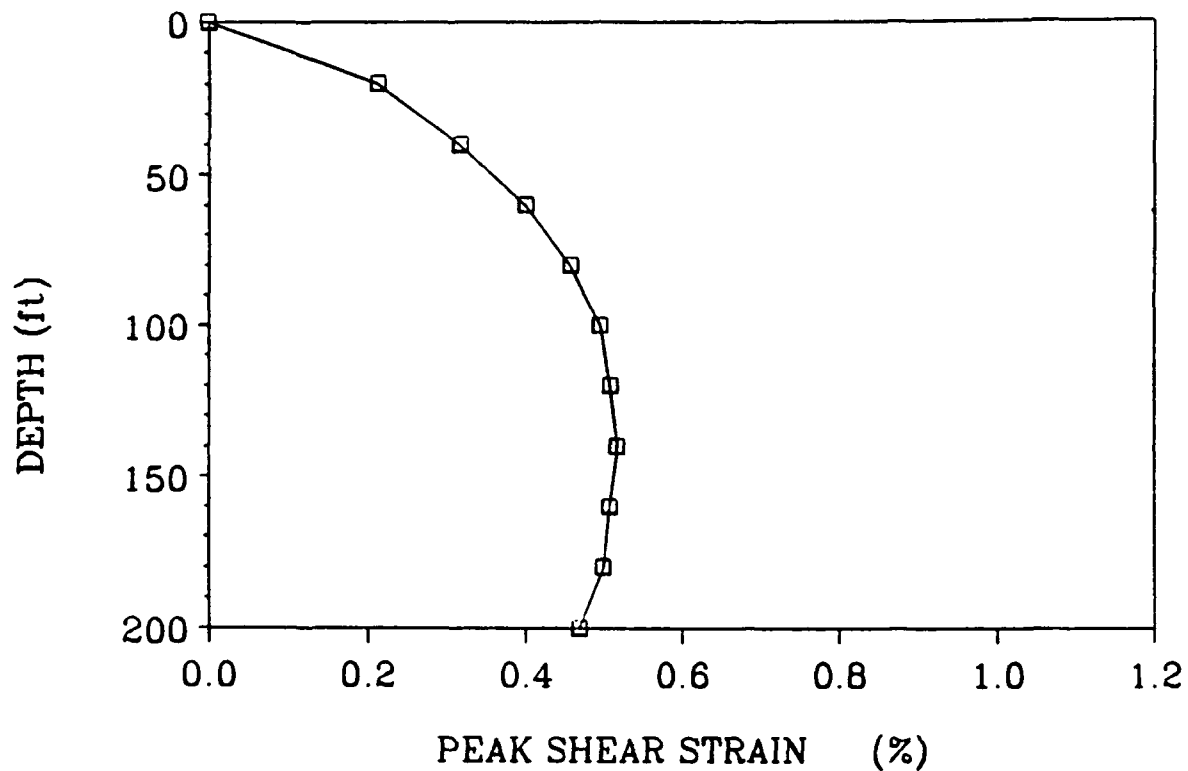
### RESPONSE AT MIDSECTION



DAM :       $H_1 = 200 \text{ ft}$        $C_1 = 1245 \text{ ft/s}$   
PLANE STRAIN ANALYSIS

Figure 3.26 Case 5: Distribution with depth of peak displacements

### RESPONSE AT MIDSECTION



DAM : H<sub>1</sub> = 200 ft C<sub>1</sub> = 1245 ft/s  
PLANE STRAIN ANALYSIS

Figure 3.27 Case 5: Distribution with depth of peak shear strains

### Case 6

Case 6 is identical to Case 5 except for the value of the inhomogeneity parameter which is now taken equal to  $m = 0.5$  (i.e.,  $G(z) = G_b (z/H)^{0.5}$ ). Table 3.6 summarizes all assumptions and input data for case 6.

The computed response values are quite consistent with those obtained in Cases 4 and 5 (see Figs. 13.28-13.31).

### **Case 6**

**Dam Idealization: Model 2**

**Type of Analysis: Nonlinear (piece-wise linear)**

**Dam Height:  $H = 200$  ft. (60.90 ft.)**

**Dam Ave. S-wave Velocity:  $C = 1245$  ft/s (780 m/s)**

**Inhomogeneity Parameter:  $m = 0.5$**

**Dam Ave. Mass Density:  $\rho = 136$  pcf (2178 kg/m<sup>3</sup>)**

**Dam Length: Infinite (Plane Strain Conditions)**

**Base Rock S-wave Velocity:  $C_r = 3000$  ft/s (914 m/s)**

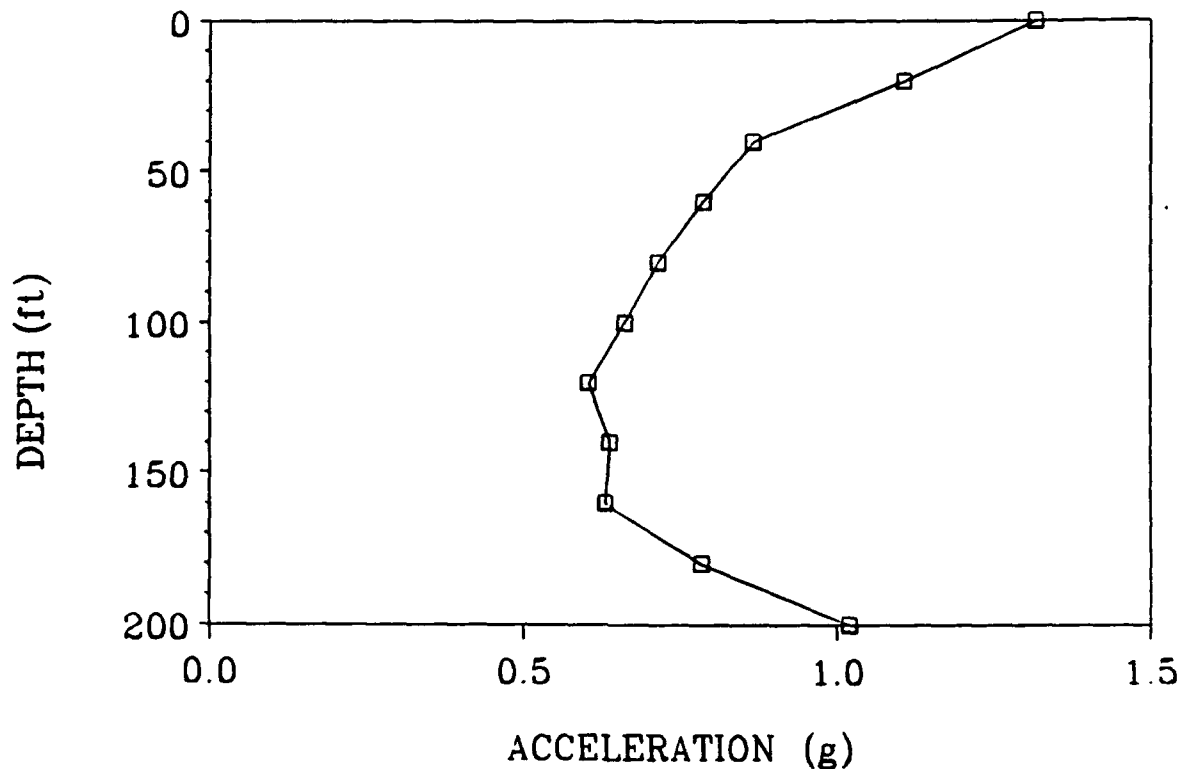
**Impedance Ratio:  $\alpha = 0.15$**

**Input Motion:** the computed acceleration at the dam base in Fig. 3.9 (The outcrop motion is the given hypothetical acceleration in Fig. 3.1)

**Computed Fundamental Period:  $T_1 = 0.43$  s**

**Table 3.5 Input Data for Case 6**

### RESPONSE AT MIDSECTION



DAM :  $H_1 = 200 \text{ ft}$   $C_1 = 1245 \text{ ft/s}$

PLANE STRAIN ANALYSIS

Figure 3.28 Case 6: Distribution with depth of peak accelerations

COMPUTED RESPONSE AT MIDCREST

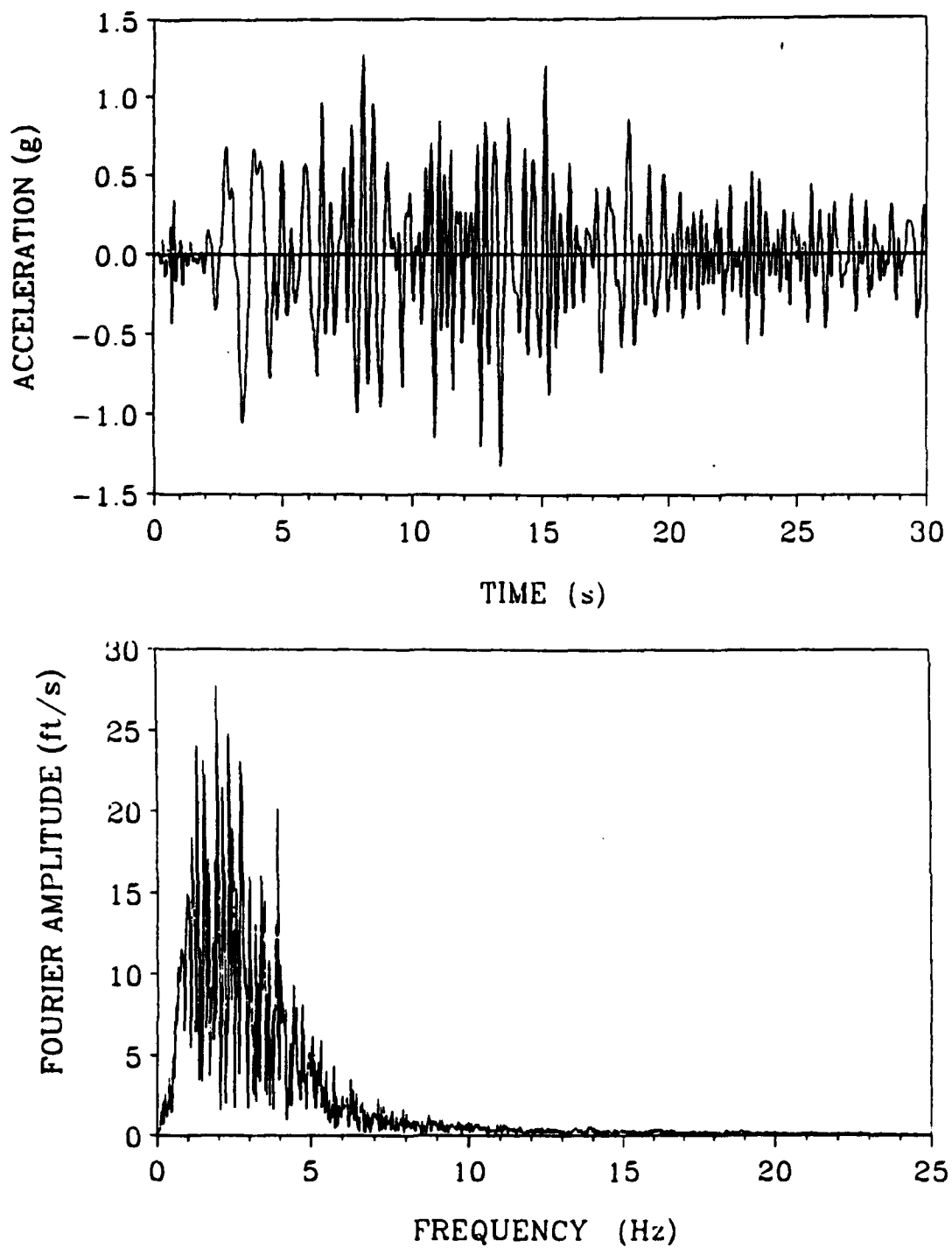
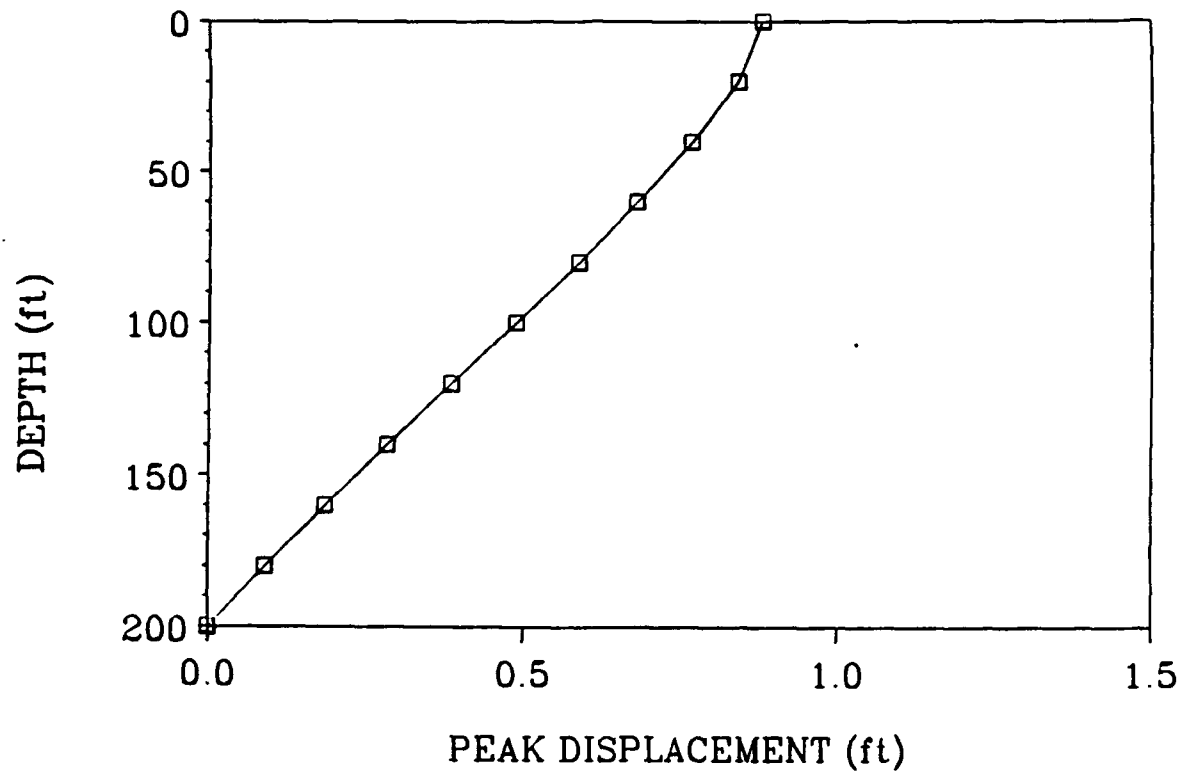


Figure 3.29 Case 6: Crest acceleration time history and Fourier spectra

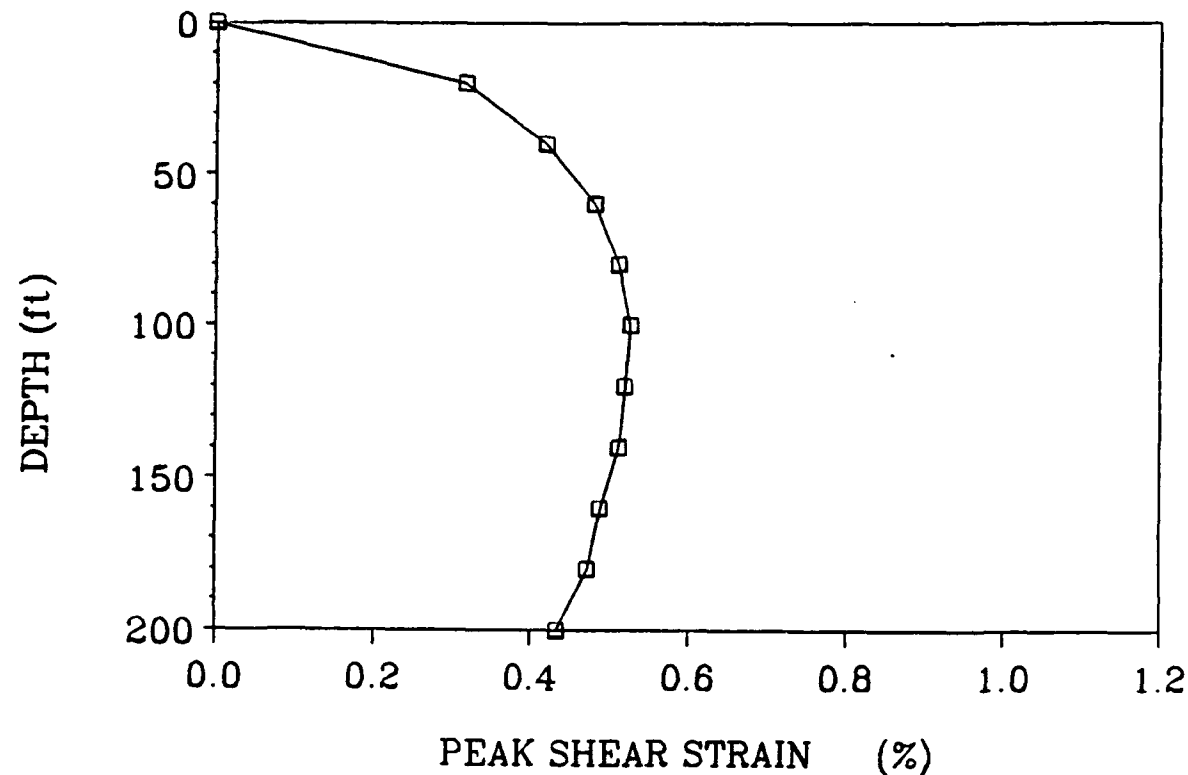
### RESPONSE AT MIDSECTION



DAM :  $H_1 = 200 \text{ ft}$   $C_1 = 1245 \text{ ft/s}$   
PLANE STRAIN ANALYSIS

Figure 3.30 Case 6: Distribution with depth of peak displacements

### RESPONSE AT MIDSECTION



DAM :  $H_1 = 200 \text{ ft}$   $C_1 = 1245 \text{ ft/s}$   
PLANE STRAIN ANALYSIS

Figure 3.31 Case 6: Distribution with depth of peak shear strains

### Case 7

Here the presence of the alluvium, which covers part of the foundation area, is ignored. Thus, the dam is assumed to be 178 ft. high. The base-rock is assumed to be flexible with  $C_r = 3000$  ft/s. Table 3.6 summarizes all the assumptions and input data for Case 5. As shown in the table, the computed fundamental period is now 0.40 seconds due to the "stiffening" of the structure caused by height decrease. Although this period differs from the period of 0.45 seconds observed during the 1983 earthquake, the analysis is performed to explore the sensitivity of the response to the assumptions.

Notice that the computed peak values of crest acceleration is 1.4 g, but in general the acceleration response is very consistent with that of the previous cases (Figs. 3.32-3.33). The peak displacements decrease even further with a value of crest about 0.6 ft., while the peak shear strains take an average value of about 0.4% (see Figs. 3.34 or 3.35).

### **Case 7**

**Dam Idealization: Model 2**

**Type of Analysis: Nonlinear (piece-wise linear)**

**Dam Height:  $H = 178 \text{ ft. (54.25 ft.)}$**

**Dam Ave. S-wave Velocity:  $C = 1210 \text{ ft/s (369 m/s)}$**

**Inhomogeneity Parameter:  $m = 0.3$**

**Dam Ave. Mass Density:  $\rho = 136 \text{pcf (2178 kg/m}^3\text{)}$**

**Dam Length: Infinite (Plane Strain Conditions)**

**Base Rock S-wave Velocity:  $C_r = 3000 \text{ ft/s (914 m/s)}$**

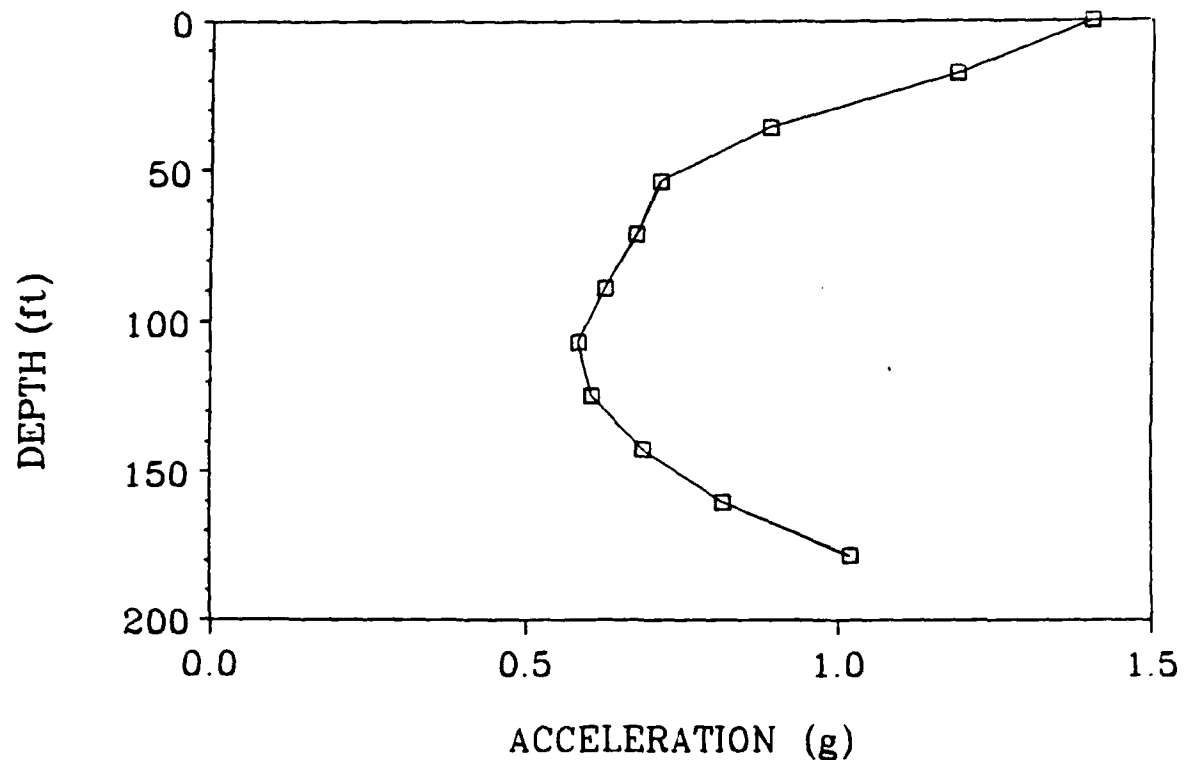
**Impedance Ratio:  $\alpha = 0.15$**

**Input Motion: The computed acceleration at the dam base in Fig. 3.9 (The outcrop motion is the given hypothetical acceleration in Fig. 3.1)**

**Computed Fundamental Period:  $T_1 = 0.40 \text{ s}$**

**Table 3.6 Input Data for Case 7**

### RESPONSE AT MIDSECTION



DAM :       $H_1 = 178 \text{ ft}$        $C_1 = 1210 \text{ ft/s}$   
PLANE STRAIN ANALYSIS

Figure 3.32 Case 7: Distribution with depth of peak accelerations

COMPUTED RESPONSE AT MIDCREST

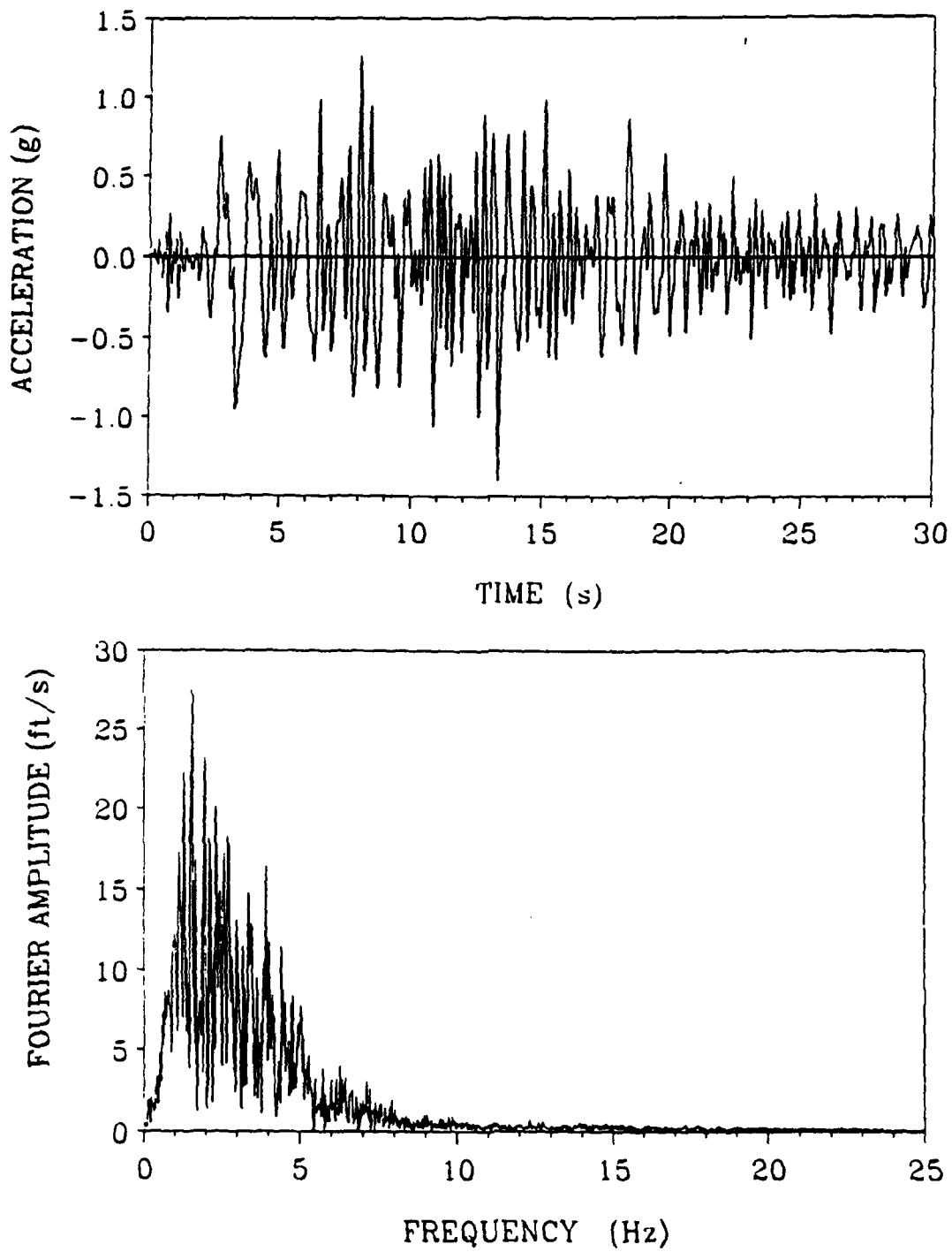
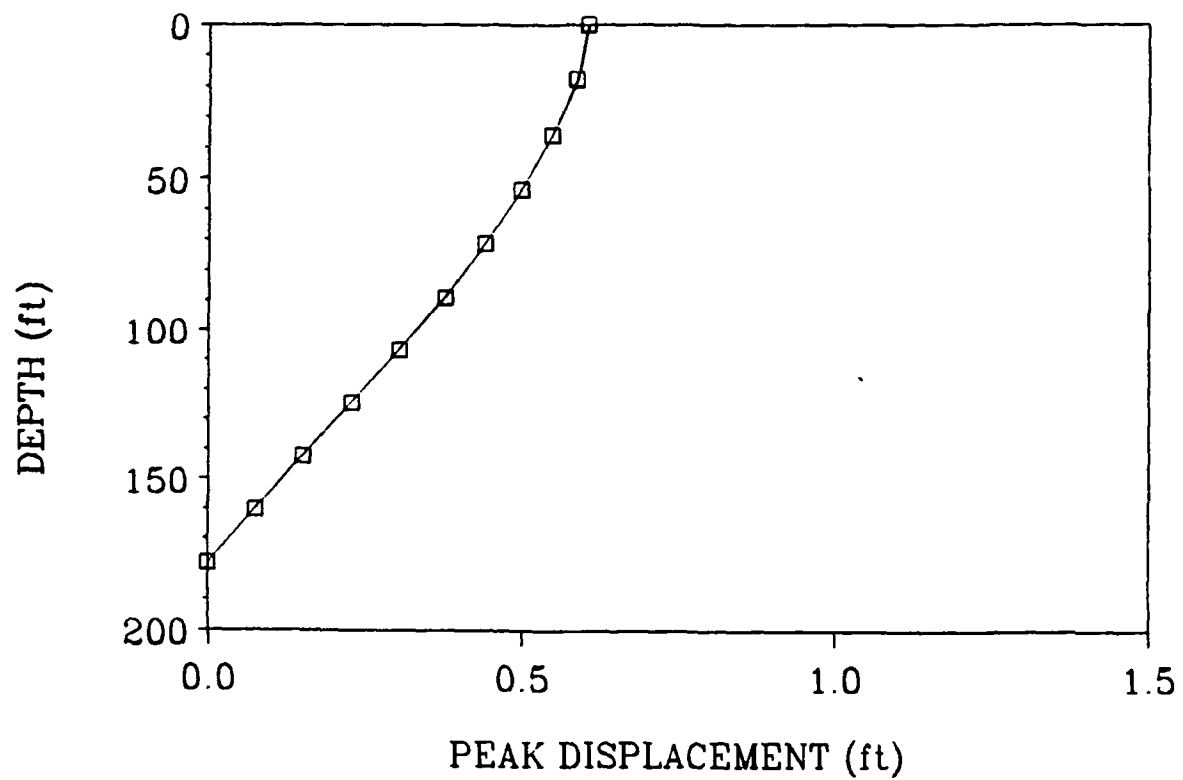


Figure 3.33 Case 7: Crest accelerations time history and Fourier spectra

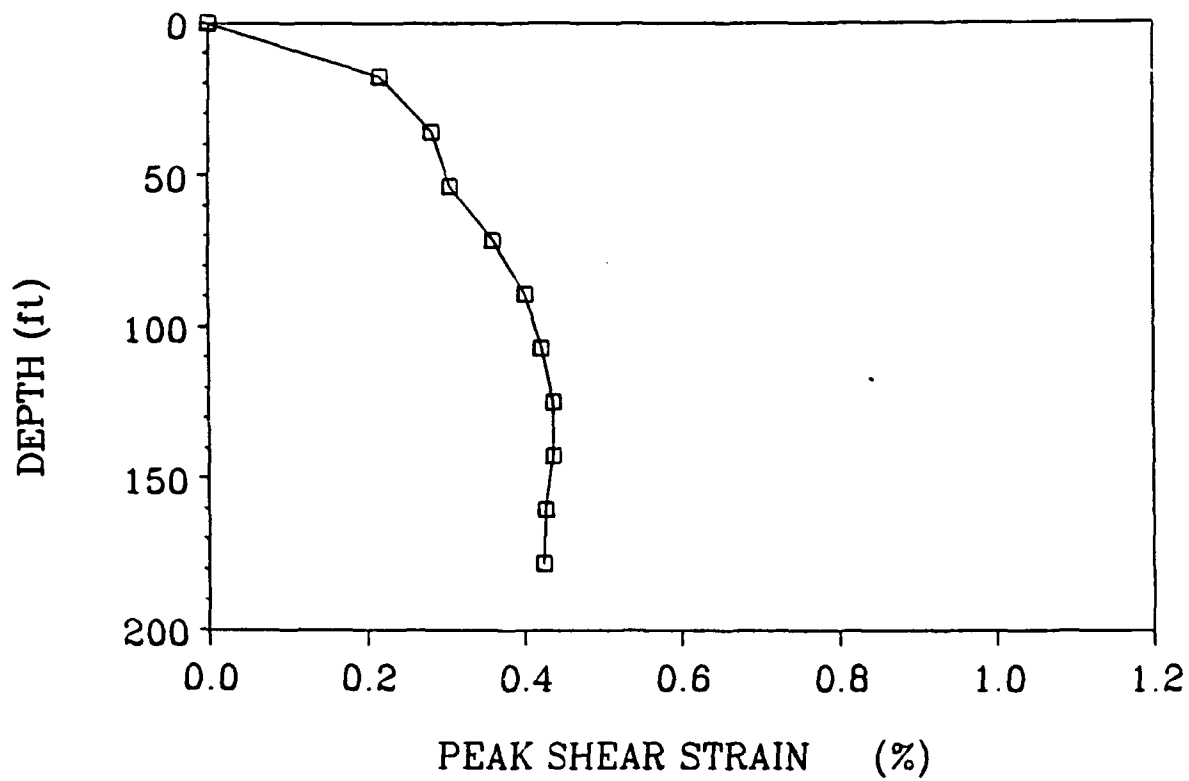
### RESPONSE AT MIDSECTION



DAM :  $H_1 = 178 \text{ ft}$   $C_1 = 1210 \text{ ft/s}$   
PLANE STRAIN ANALYSIS

Figure 3.34 Case 7: Distribution with depth of peak displacements

### RESPONSE AT MIDSECTION



DAM :  $H_1 = 178 \text{ ft}$   $C_1 = 1210 \text{ ft/s}$   
PLANE STRAIN ANALYSIS

Figure 3.35 Case 7: Distribution with depth of peak shear strains at the dam base

### 3.3 Response of Ririe Dam Using Model 3

#### Case 8

Although the idealization of the dam and the canyon using Model 3 is only approximate, the analysis is useful in showing the sensitivity of the response to the various assumptions. Indeed, a number of analyses have been performed to demonstrate the effect of the assumed height and average S-wave velocity of the dam. The results indicated an acceleration response consistently higher than that obtained with Models 1 and 2. Only one from those analyses is presented here, corresponding to the closest idealization of the dam-canyon system.

In this, the semi-cylindrical canyon has a radius of  $R = 262$  ft., while the average S-wave velocity of the dam is  $C = 1210$  ft/s. This results in a computed fundamental period of the dam about 0.43 seconds. The base rock is assumed again flexible with  $C_r = 3000$  ft/s. The corresponding transfer function for the semi-cylindrical canyon shape is plotted in Fig. 3.36 while the computed acceleration time history at the dam base and its Fourier spectra are shown in Fig. 3.37. As Model 3 does not allow nonlinear analysis, the presented results were obtained from equivalent linear analysis.

Fig. 3.38 plots peak accelerations with depth computed at the midsection. Notice a significant increase to about 2 g of the crest accelerations, which is roughly consistent to all the analyses using Model 3 (and in some cases, is even higher). The crest acceleration time histories and their Fourier spectra indicate a larger participation of higher frequencies (Fig. 3.39). These high accelerations occur only near the crest and it appears they are due mainly to a wave-focusing effect due to the

semi-cylindrical canyon shape. However, the actual canyon shape would result in crest acceleration values smaller than those computed for the semi-cylindrical canyon shape. The peak accelerations within the dam body are found significantly less ranging from 1.17 to 1.55 g, corresponding to amplification of 1 to 1.36. The peak displacements at the crest are found about 1.3 ft. (Fig. 13.40) while the peak shear strains have a maximum of 0.68% (Fig. 13.41).

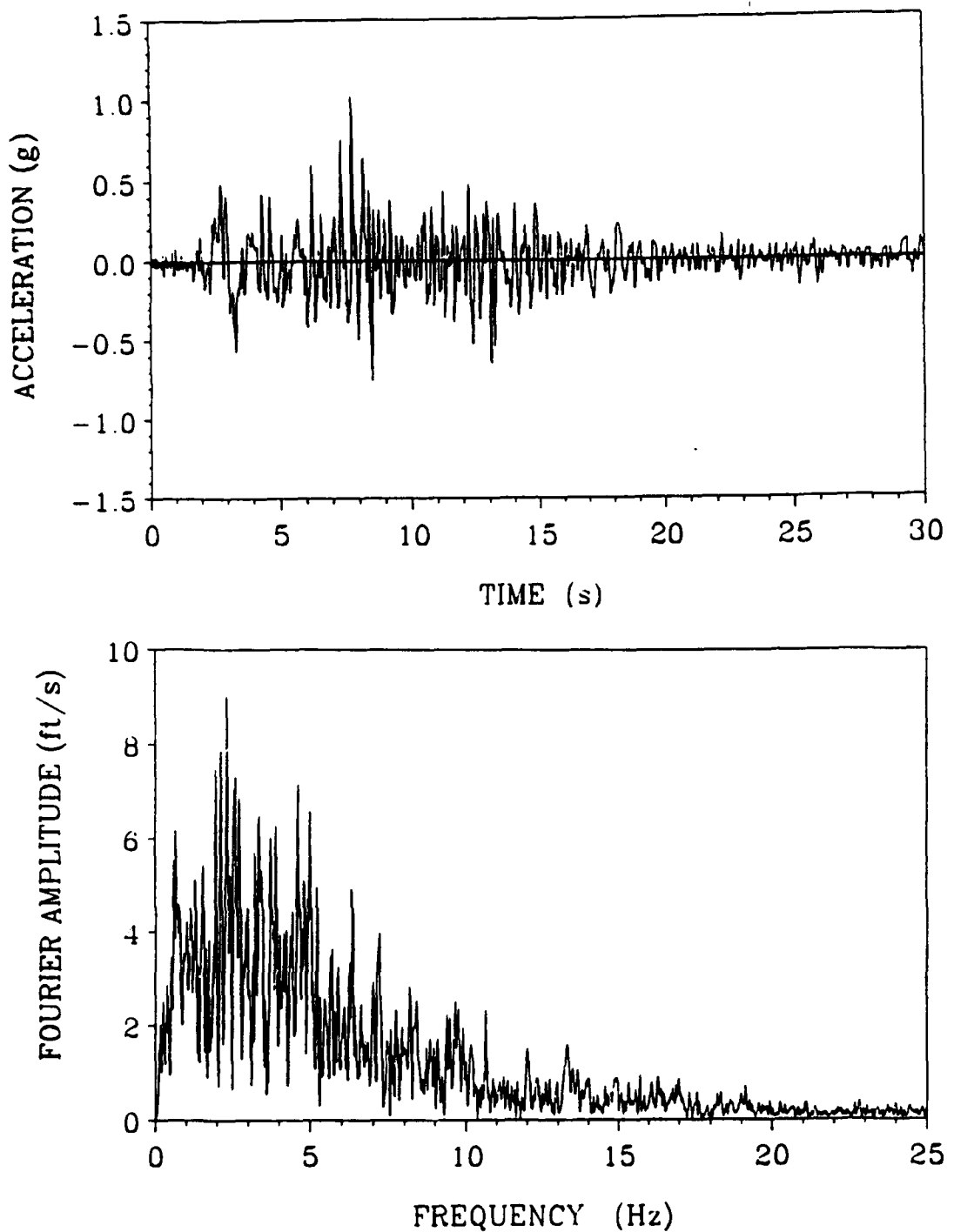
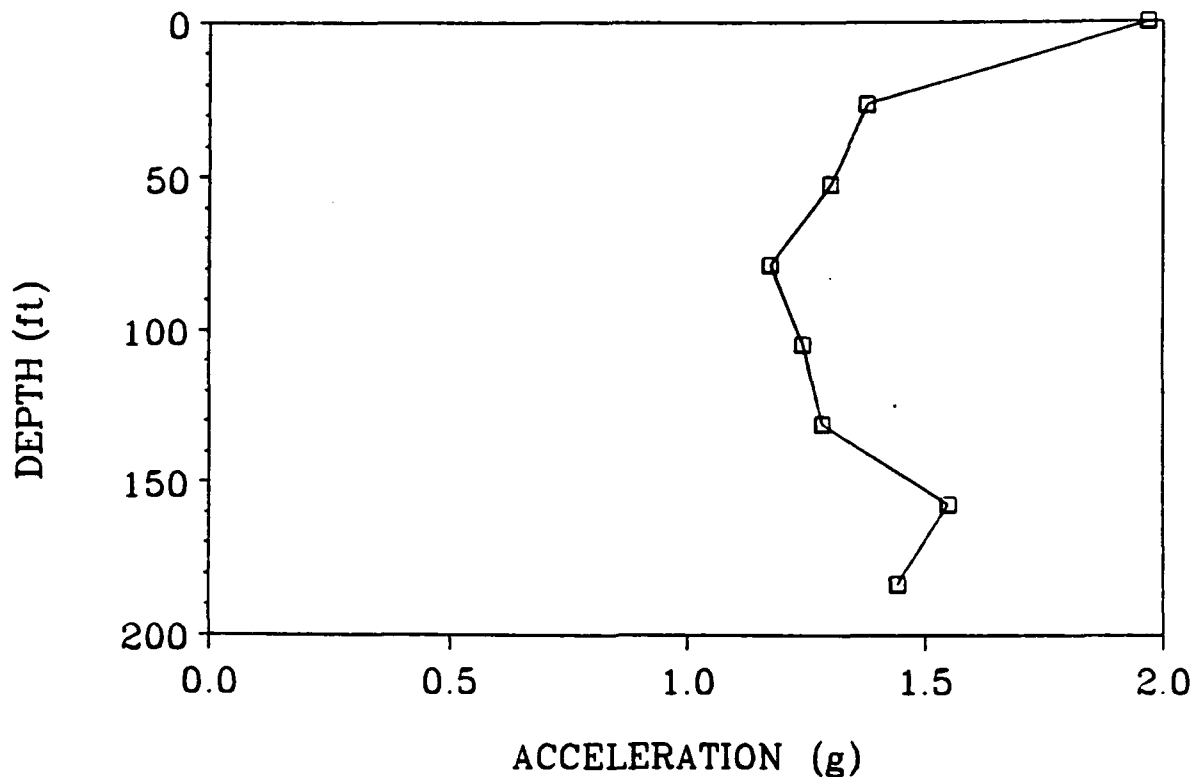


Figure 3.37 Acceleration time history and Fourier spectra at the dam

### RESPONSE AT MIDSECTION



DAM :  $H_1 = 262 \text{ ft}$   $C_1 = 1210 \text{ ft/s}$   
SEMI-CYLINDRICAL CANYON SHAPE

Figure 3.38 Case 8: Distribution with depth of peak accelerations evaluated at midsection

### **Case 8**

**Dam Idealization: Model 3**

**Type of Analysis: Equivalent Linear**

**Dam Height:  $H = 262$  ft. (80 m)**

**Dam Ave. S-wave Velocity:  $C = 1210$  ft/s (369 m/s)**

**Inhomogeneity Parameter:  $m = 0$  ( $m > 0$  is not possible)**

**Dam Mass Density:  $\rho = 136$  pcf (2178 kg/m<sup>3</sup>)**

**Base Rock S-wave Velocity:  $C_r = 3000$  ft/s (914 m/s)**

**Impedance Ratio:  $\alpha = 0.15$**

**Input Motion:** The computed acceleration at the dam base in Fig. 13.37 (The outcrop motion is the given hypothetical acceleration in Fig. 3.1).

**Computed Fundamental Period:  $T_1 = 0.43$  s**

**Table 3.7 Input Data for Case 8**

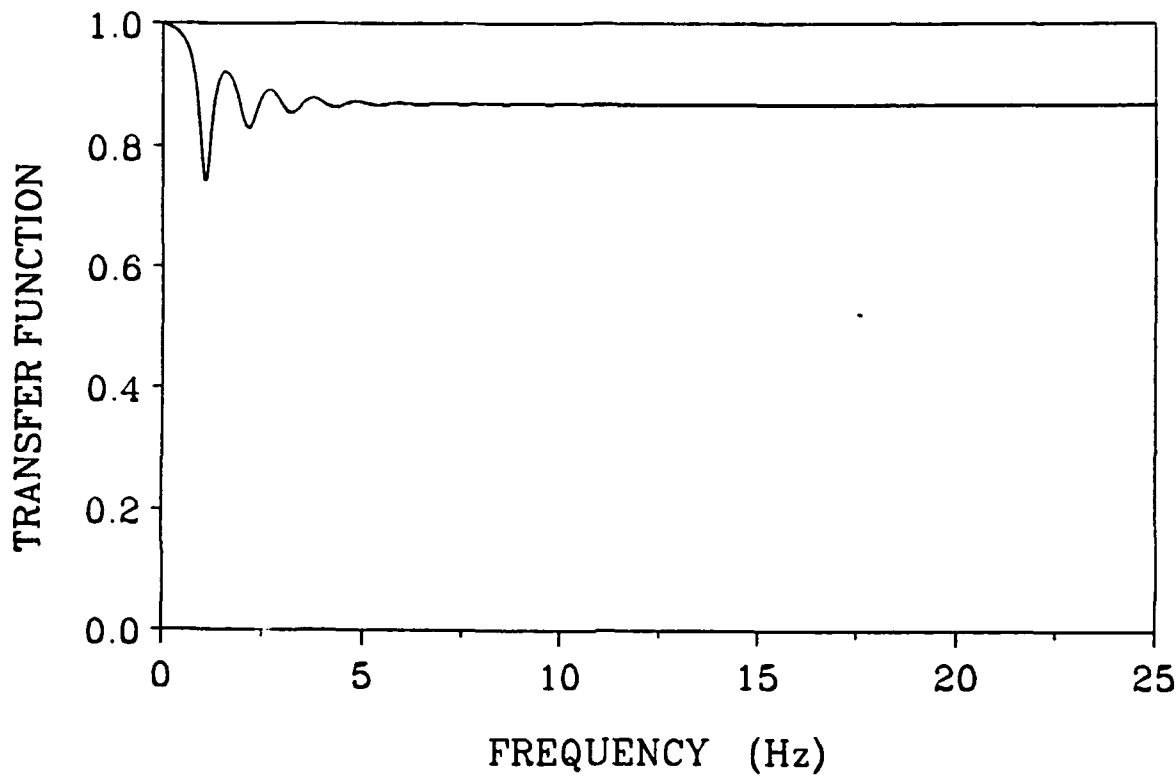


**Figure 3.36** Transfer function relating the acceleration amplitude at the dam base and at the outcrop rock for the case of a semi-cylindrical canyon

COMPUTED RESPONSE AT MIDCREST

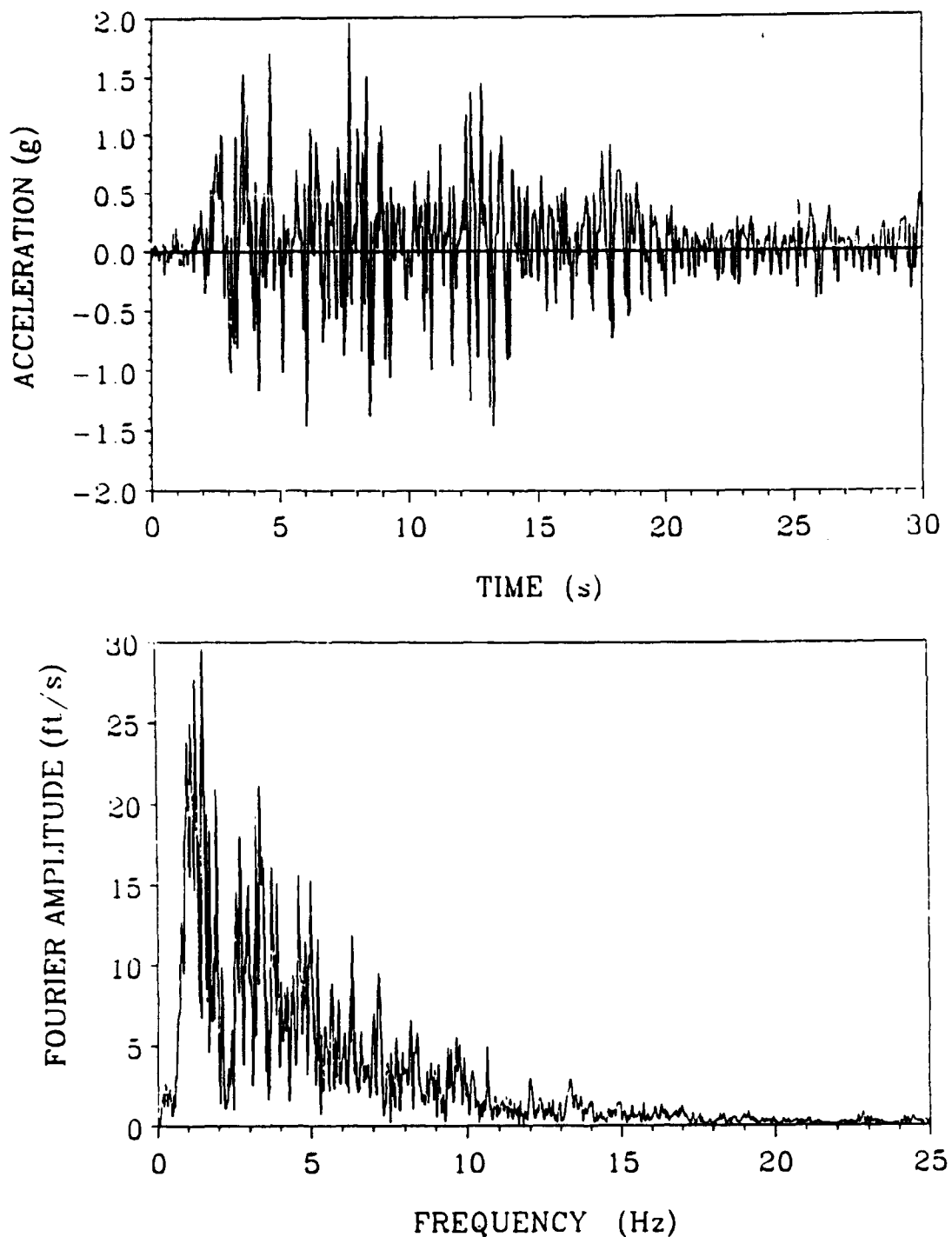
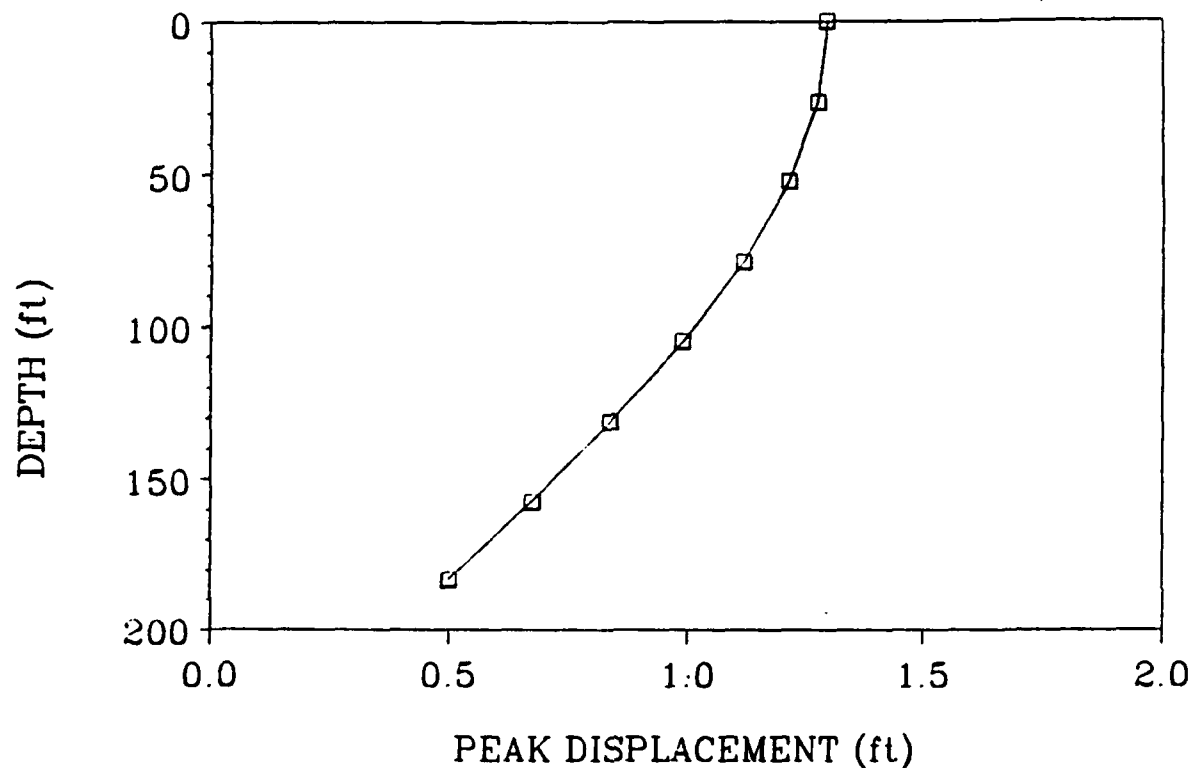


Figure 3.39 Case 8: Crest acceleration time history and Fourier spectra evaluated at midsection

### RESPONSE AT MIDSECTION

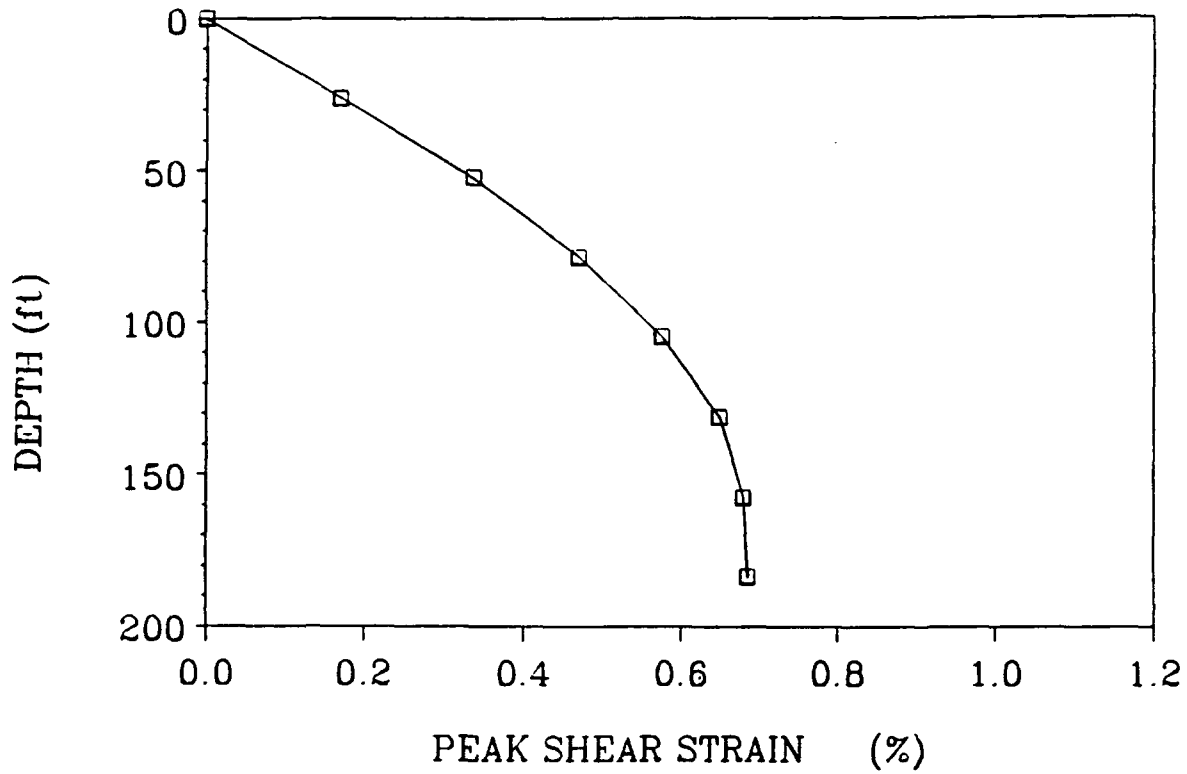


DAM : H<sub>1</sub> = 262 ft C<sub>1</sub> = 1210 ft/s

SEMI-CYLINDRICAL CANYON SHAPE

Figure 3.40 Case 8: Distribution with depth of peak displacements evaluated at midsection

### RESPONSE AT MIDSECTION



DAM : H<sub>1</sub> = 262 ft C<sub>1</sub> = 1210 ft/s

SEMI-CYLINDRICAL CANYON SHAPE

Figure 3.41 Case 8: Distribution with depth of peak shear strains

$\gamma_{yz}$  evaluated at midsection

#### 4. CONCLUSIONS

A series of linear and equivalent linear analyses of the Ririe Dam have been performed using three different shear beam models with a variety of assumptions regarding the material and geometric characteristics of the dam-canyon system. The eight most representative of those analyses were presented in Chapter 3. By considering the results of all analyses, including those not presented in this report, the following conclusions may be drawn.

1. Among the three used models, it appears the Model 1 is the best fit to represent the dynamic characteristics of the Ririe dam-canyon system. Moreover, Cases 2 and 3 (or an intermediate of those two) are likely to represent closer the actual characteristics of the system response.
2. The computed response from Cases 2 and 3 yielded
  - (a) peak crest accelerations about 1.5 g
  - (b) acceleration amplification values ranging from 1 to 1.5 g in the upper 50 ft. of the dam and from 1 to 0.67 within the lower dam body and foundation layer
  - (c) peak crest displacements about 1.2 ft. and
  - (d) peak shear strains about 0.8% at the lower part of the dam body and the alluvium.
3. The high response values presented above are understandable considering the severity of the earthquake motion. Indeed, if the natural period of the dam is  $T_1 \approx 0.45$  seconds, the acceleration

response spectra in Fig. 1.6 suggest that a significant number of modes (including the fundamental) is excited to accelerations ranging from 2 to 3 g. The dramatic reduction of soil stiffness and the resulting increase of the natural periods, leads to crest accelerations about 1.5 g, while for about 75-80% of the dam the peak acceleration is equal or less than the peak input acceleration (1.17 g).

4. The peak shear strains developed within the alluvium deposit range from 0.35 to 0.9 percent for all the cases examined. Of course, these peak shear strains by far exceed the threshold strains for the development of excess pore water pressures. Such threshold strains are given by M. H. Haynes-Griffin (Ref. 13) for gravel and R. Dobry (Ref. 14) for sand.
5. It should be noted that the use of the nonlinear shear beam models for the seismic analysis of earth dams subjected to extremely severe ground shakings (as the record in Figs. 1.4-1.6) has been subjected to limited testing. Comparisons of nonlinear shear beam response and elastoplastic finite element response (using the Pacoima record and a rough F.E. discretization) gave good agreement in peak response values and fair agreement in frequency characteristics (Ref. 11). However, more evidence is required for the performance of the shear beam under such severe ground shakings, and therefore, in such cases, the results should be used with caution.

Peak Response	"Best" Estimate	Response Range From Eight Analyses
Crest Acceleration	1.5 g	1.5 g - 2 g
Crest Relative Displacement	1.2 ft.	0.5 - 1.6 ft.
Maximum Shear Strains	0.85%	0.35% - 0.90%

Table 4.1 Estimated Peak Response of Ririe Dam

## REFERENCES

1. Krinitzsky, E.L. and Dunbar, J.B., "Geological and Seismological Evaluation of Earthquake Hazards at Ririe Dam, Idaho," WES Report.
2. Chang, F.K., "Analysis of Strong-Motion Data from the Mount Borah, Idaho, Earthquake of 28 October 1983," Miscellaneous Paper GL-85-12, WES, Corps of Engineers, Vicksburg, Mississippi.
3. Dakoulas, P., "Nonlinear Response of Dams Founded on Alluvial Deposits in Narrow Canyons," Journal of Soil Dynamics and Earthquake Engineering, 1989, (in press).
4. Dakoulas, P. and Gazetas, G., "A Class of Inhomogeneous Shear Models for Seismic Response of Dams and Embankments," Journal of Soil Dynamics and Earthquake Engineering, 1985, 4(4), 166-182.
5. Dakoulas, P. and Gazetas, G., "Shear Strains and Seismic Coefficients for Dams and Embankments," Journal of Soil Dynamics and Earthquake Engineering, 1986, 5(2), 75-83.
6. Gazetas, G., "Seismic Response of Earth Dams: Some Recent Developments" Journal of Soil Dynamics and Earthquake Engineering, 1987, 6(1), 2-47.
7. Dakoulas, P. and Gazetas, G., "Seismic Shear Vibration of Embankment Dams in Semi-Cylindrical Valleys," Journal of Earthquake Engineering and Structural Dynamics, 1986, 14, 19-40.
8. Dakoulas, P. and Gazetas, G., "Nonlinear Seismic Response of Embankment Dams," Proceedings of the 2nd International Conference on Soil Dynamics and Earthquake Engineering, Springer-Verlag, 1985, 5, 29-43.
9. Seed, H.B., Wong, R.T., Idriss, I.M., and Tokimatsu, K., "Moduli and Damping Ratios for Dynamic Analysis of Cohesionless Soils," Report No. UCB/EERC-84/14, University of California, Berkeley, California, 1984.
10. Dakoulas, P. and Gazetas, G., "Vibration Characteristics of Dams in Narrow Canyons," Journal of Geotechnical Engineering Division, ASCE, 1987, 113(8), 899-904.
11. Dakoulas, P., "Contributions to Seismic Analysis of Earth Dams and Embankments," Doctoral Thesis, Rensselaer Polytechnic Institute, Troy, New York, 1985.
12. Roesset, J., "Soil Amplification of Earthquakes, Numerical Methods in Geotechnical Engineering," Ed. by Desai and Christian, McGraw-Hill, 1977.

13. Hynes-Griffin, M.H., "Pore Pressure Generation Characteristics of Gravel Under Undrained Cyclic Loading," Doctoral Thesis, University of California, Berkeley, 1988.
14. Dobry, R., Ladd, R.S., Yokel, F.Y., Chung, R.M., Powell, D., "Prediction of Pore Water Pressure Buildup and Liquefaction of Sands During Earthquakes by the Cyclic Strain Method," National Bureau of Standards Building Science Series 138, U. S. Department of Commerce, 1982.

**APPENDIX**  
**Response Time Histories from Case 2**

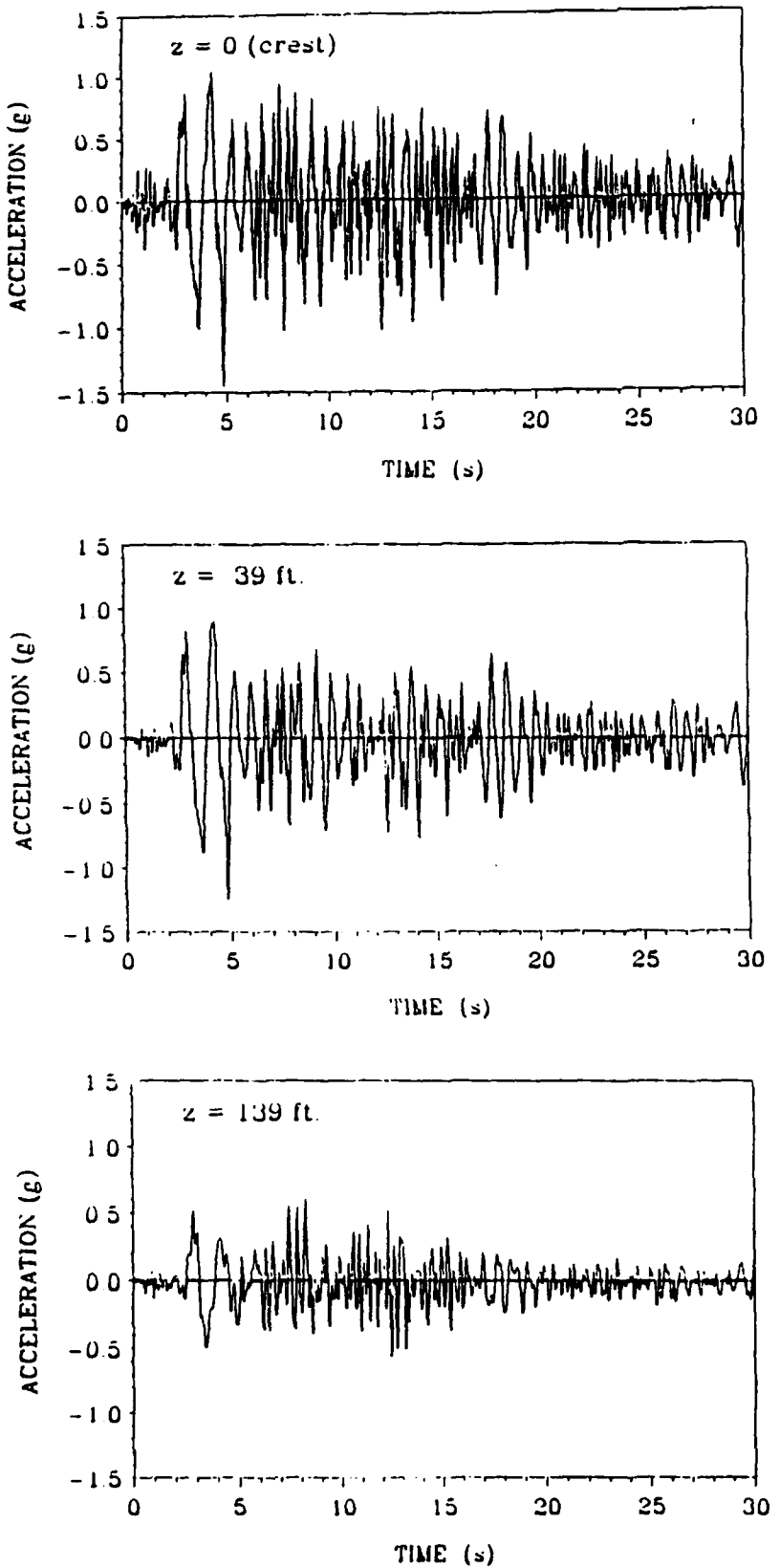


Figure 6.1 Case 2: Acceleration time histories at various elevations  
within the dam

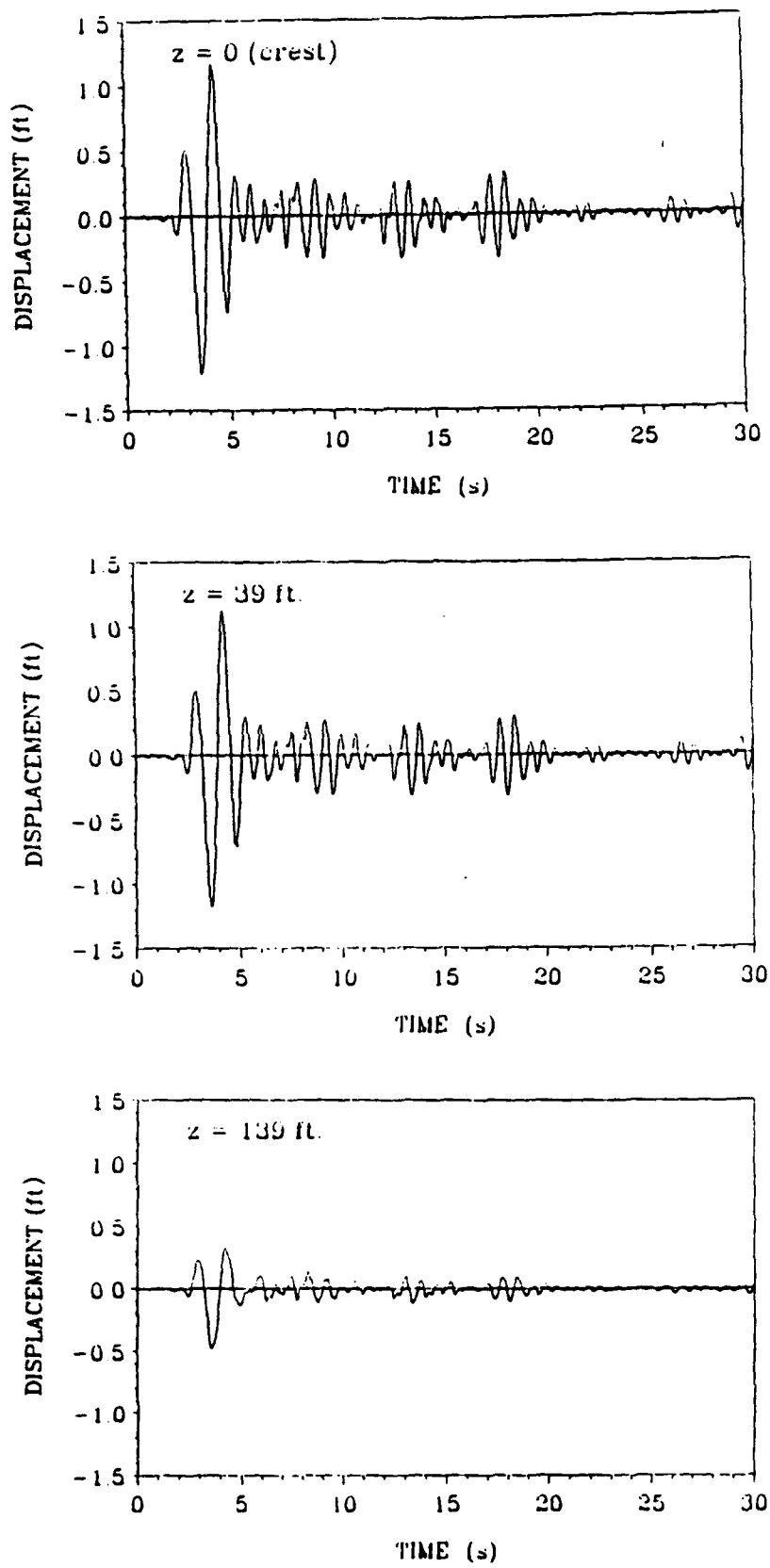


Figure 6.2 Case 2: Displacement time histories at various elevations  
within the dam 92

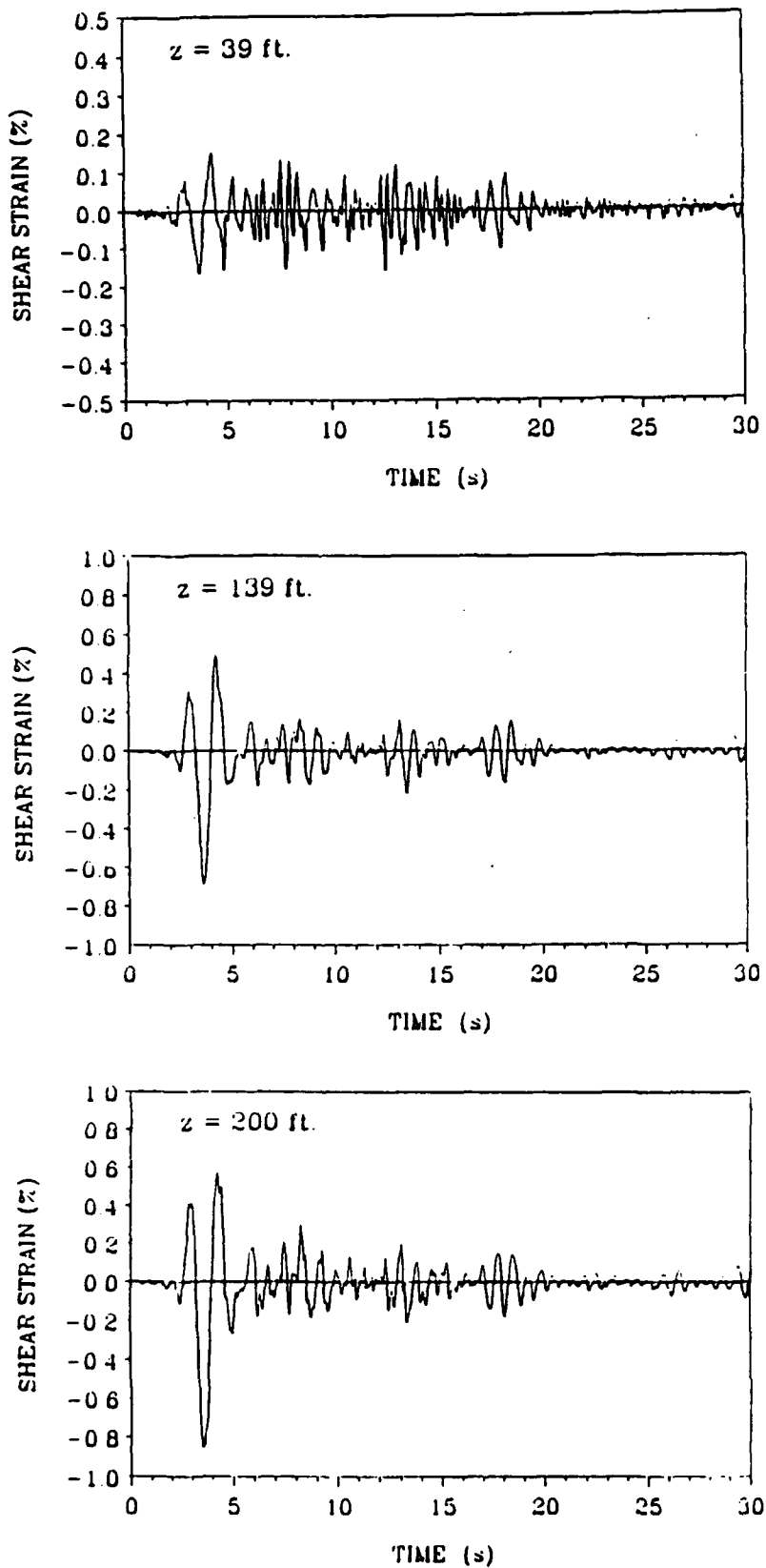


Figure 6.3 Case 2: Shear strain time histories at various elevations